THE COMPOUNDING OF SHORT FIBRE REINFORCED THERMOPLASTIC COMPOSITES

A thesis submitted for the degree of Doctor of Philosophy

by

Paul David Shipton

Department of Materials Technology, Brunel University

July 1988

Brunel University
Department of Materials Technology
Uxbridge, Middlesex, UB8 3PH

Paul David Shipton

The Compounding of Short Fibre Reinforced Thermoplastic Composites

Ph. D. Degree

1988

ABSTRACT

It is generally accepted that the mechanical properties of short fibre reinforced thermoplastics do not correspond with the high mechanical properties of fibres used to reinforce them.

A study is made into the methods of compounding reinforcing fibres into thermoplastics to produce short fibre reinforced thermoplastics of enhanced properties.

The initial method chosen for investigation is the twin screw extrusion compounding process. Variables such as fibre feeding arrangement and extrusion screw design are found to be factors influencing the properties of carbon and glass reinforced nylon 6,6. Use is made of computer programs to predict properties, assess compound quality and estimate fibre-matrix bond strength.

Investigations indicate that the presence of reinforcing fibres with enhanced lengths does not result in the predicted property increases. The reasons for this shortfall are believed to lie in unfavourable fibre orientation in injection mouldings and the reduced strain to break of these materials.

Short Kevlar reinforced thermoplastics are compounded and their mechanical properties assessed. The reasons for the poor mechanical properties for these materials are identified as a poor bond strength between fibre and matrix, the formation of points of weakness within the fibres by the compounding and moulding processes and the coiled arrangement of fibres present in injection mouldings.

A method suitable for the routine assessment of fibre-matrix bond strength is used to examine combinations of fibre and thermoplastic matrix. A comparison is made of the values derived from this method with values calculated from stress-strain curves of injection mouldings. This allows an understanding of the nature of the fibre-matrix bond yielded by compounding and injection moulding steps.

A description is given of a novel method designed to overcome the limitations of conventional compounding routes to produce long fibre reinforced injection moulding feedstock. Further work is necessary before this method is a feasible production technique.

Abstract

It is generally accepted that the mechanical properties of short fibre reinforced thermoplastics do not correspond with the high mechanical properties of fibres used to reinforce them.

A study is made into the methods of compounding reinforcing fibres into thermoplastics to produce short fibre reinforced thermoplastics of enhanced properties.

The initial method chosen for investigation is the twin screw extrusion compounding process. Variables such as fibre feeding arrangement and extrusion screw design are found to be factors influencing the properties of carbon and glass reinforced nylon 6,6. Use is made of computer programs to predict properties, assess compound quality and estimate fibre-matrix bond strength.

Investigations indicate that the presence of reinforcing fibres with enhanced lengths does not result in the predicted property increases. The reasons for this shortfall are believed to lie in unfavourable fibre orientation in injection mouldings and the reduced strain to break of these materials.

Short Kevlar reinforced thermoplastics are compounded and their mechanical properties assessed. The reasons for the poor mechanical properties for these materials are identified as a poor bond strength between fibre and matrix, the formation of points of weakness within the fibres by the compounding and moulding processes and the coiled arrangement of fibres present in injection mouldings.

A method suitable for the routine assessment of fibre-matrix bond strength is used to examine combinations of fibre and thermoplastic matrix. A comparison is made of the values derived from this method with values calculated from stress-strain curves of injection mouldings. This allows an understanding of the nature of the fibre-matrix bond yielded by compounding and injection moulding steps.

A description is given of a novel method designed to overcome the limitations of conventional compounding routes to produce long fibre reinforced injection moulding feedstock. Further work is necessary before this method is a feasible production technique.

Wer Immer Strebend sich bemuht, den Konnen

Wir erlosen

Whosoever unceasingly strives upward ...

him can we save.

GOETHE

The Compounding of Short Fibre Reinforced Thermoplastic Composites

Chapter 4 **Results**

1.1 The Problems Associated with the Incorporation of Short Fibres into Thermoplastics

Thermoplastics containing short fibres were first introduced with the intention of offering a new range of materials with intermediate properties between high tonnage commodity plastics and the sophisticated continuous fibre composites well established in the aerospace industry. The increase in stiffness and strength compared with the parent thermoplastic was modest but sufficient to establish the class of material in lightly stressed applications.

Short fibre reinforced thermoplastics are now well established engineering materials and are now used to fabricate many articles traditionally produced from metals.

The production of components is normally carried out in two stages; compounding of the polymer followed by injection moulding. Direct attempts to injection mould fibre/polymer blends can lead to problems of poor surface finish, high differential shrinkage and variable strength due to the presence of undispersed bundles in the finished article.

It has become apparent that the detailed procedures used for compounding have a marked effect on the properties of the moulded component, and work has been directed towards a more fundamental understanding and subsequent control of the factors which determine the desired properties.

The major variables for influencing the performance of short fibre reinforced thermoplastics are the adhesion between fibre and matrix, the length of the fibres and fibre orientation.

Care is required in the compounding operation to produce an adequate dispersion of bundles while preventing significant fibre attrition.

The selection of the appropriate compounding technology is consequently dependent on the requirements of fibre length and degree of dispersion of the fibres throughout the matrix. The most common method of compounding involves the use of a single or twin-screw extruder to mix chopped fibres and matrix and produce an extrudate which can be subsequently pelletized to give feedstock for injection moulding.

This research is centred on the development of compounding extrusion techniques that

allow more effective utilization of the properties of high performance reinforcing fibres. This area of investigation is vital if the mechanical properties of fibre reinforced thermoplastics are to be enhanced compared with currently available products.

1.2 Review of Adopted Approach to Produce High Performance Short Fibre Reinforced Thermoplastics

Three basic approaches were used in this study to produce high performance short fibre reinforced thermoplastics. The first approach was to compound inherently brittle glass and carbon fibres into thermoplastics in such a way that fibre length was retained. After considering the available literature, the starting point for this approach was the use of a twin screw extruder where fibres could be added to a premelted matrix. The first three experiments, based on a small laboratory twin screw extruder, determined the most important factors that influenced the fibre length distribution of short brittle fibre reinforced thermoplastics. The three subsequent series of experiments, which were performed on a full scale production twin screw compounding system, utilized the knowledge gained in the initial three experiments. A wide range of compounding arrangements were investigated and detailed characterisation procedures were carried out on the materials produced. An optimum screw configuration for producing carbon fibre reinforced nylon 6,6 was derived.

The second approach adopted was to compound Kevlar 49, an inherently tough fibre into thermoplastics. Although Kevlar 49 is flexible and abrasion resistant, its tensile properties rank close to carbon and glass. Because of its non brittle properties, it was thought that this fibre could be incorporated into a thermoplastic with a substantial proportion of its fibre length retained. As little work had been previously carried out on the incorporation of Kevlar into thermoplastics, the starting point for this approach was single screw compounding. The limitations however in single screw compounding were quickly realised. Successful compounding was eventually achieved using the production scale twin-screw compounding system.

The third approach adopted was to employ a novel technique in which the limitations which became evident in the first two approaches would be overcome. The technique adopted was a

specially designed crosshead die.

1.3 Outline of Thesis Structure

This chapter includes a brief review of composite theory relevant to this study. The literature survey, Chapter 2, starts with a concise discussion of the nature of composite materials and endeavours to outline the characteristics of the reinforcing fibres used in this study. An attempt is made to review critically the current understanding of the compounding of short fibres into thermoplastics. In the survey, conclusions are made and literature concerning a selected technique, twin screw extrusion is presented. The literature survey concludes with an examination of the computational methods that have been used to assess the effectiveness of compounding techniques.

Chapter 3 firstly reviews the materials used in this thesis, describes the machines used for compounding and the conditions used for the moulding of the materials. The techniques employed to assess the materials are detailed, these include fibre length properties, mechanical testing, scanning electron microscopy and the analysis and prediction of material properties by computer programmes. The final part of Chapter 3 describes in detail the compounding experiments performed.

Chapter 4 presents firstly the experimental results for the preliminary investigations based on a small scale laboratory twin-screw extruder. In the following section the results are discussed. Results are then presented for compounding glass and carbon fibre into nylon 66 on a production scale twin-screw compounder of greater power and output, these results are then discussed. The second part of Chapter 4 is based on the results and subsequent discussion of Kevlar reinforced thermoplastics. A single screw extruder and a twin-screw compounder were used to incorporate Kevlar fibres into thermoplastic matrices.

From a practical point of view composite materials in addition to being stiff and strong must also be reasonably resistant to impact loading. The final part of Chapter 4 presents and discusses the impact properties of some of the materials produced in the compounding experi-

ments. The impact properties of short fibre Kevlar reinforced thermoplastics were measured in an attempt to rank them against conventional glass reinforced thermoplastics. For selected glass reinforced nylon 6,6 compounds the contribution to fracture energy G_c by fibre pull-out was estimated and compared with measured values.

Chapter 5 describes the techniques used for the determination of critical length of fibres in short fibre reinforced thermoplastics. The chapter is divided into four sections to describe fully the technique and present the results.

Chapter 6 presents a description of a novel technique developed for the production of fibre reinforced thermoplastics using a specially designed crosshead die.

The concluding chapter, Chapter 7, seeks to draw together the findings gathered throughout the study and make recommendations for future investigations.

1.4 Aims and Objectives

(i) Using selected types of compounding machinery, to investigate the limitations of compounding brittle types of fibre such as glass and carbon into thermoplastics and suggest compounding arrangements that may be used to produce mouldings with enhanced properties.

(ii) To investigate methods of compounding Kevlar 49, a tough fibre with good mechanical properties, into thermoplastics and examine the salient properties of the resulting composites.

(iii) To examine the properties of the bond between selected thermoplastics and reinforcing fibres and develop methods for assessing the effectiveness of the bond.

(iv) On the basis of the findings made, to develop an alternative compounding operation which would overcome any difficulties found with conventional techniques.

1.5 Reinforcement Theory

The prediction of the mechanical properties of a fully aligned long fibre reinforced composite is a difficult mathematical problem, particularly when the load is not applied along the fibre

axis. To perform the same exercise in a short fibre reinforced composite is even more difficult. The fibres can not be regarded as infinitely long and in addition a real moulded component exhibits a very complex fibre orientation distribution. Any realistic reinforcement theory has to include the effect of fibre length distribution and a distribution of fibre orientations with respect to the applied load. While the stiffness of short fibre reinforced thermoplastics has received the most attention and can be predicted fairly accurately, properties such as strength and toughness are difficult to predict even for continuous fibre composites. The corresponding problem with short fibre reinforced thermoplastics has not received much attention.

1.5.1 The Stiffness and Strength of Continuous Fibre Composites

The simplest type of fibrous composite is one with straight parallel isotropic and homogeneous fibres in a isotropic homogeneous matrix. Here the mechanical properties of the composite can be explained simply in terms of the mechanical properties of fibre and matrix[1]. When a load is applied parallel to the fibres, effectively little load is carried by the matrix. The principal purpose of the matrix is to bind the fibres together. For long fibres, stress is constant over the whole length of the fibres. This idealised composite is the starting point for all theories of reinforcement. When a load is applied parallel to the fibres, the load is distributed in proportion to the relative volume fractions of the fibre and matrix, the composite's mechanical properties in this direction can be described by The Rule of Mixtures. If we assume the fibres and matrix behave elastically and are perfectly bonded to each other and consider what happens when a strain ε is applied uniformly in the fibre direction (Figure 1), the total force will be the sum of the forces in the fibre and matrix.

The Young's modulus of the composite E_c in the fibre direction is:-

$$E_c = V_f E_f + (1 - V_f) E_m \qquad (1)$$

where

V_f = volume fraction of fibres

E_f = Young's Modulus of fibres

E_m = Young's Modulus of matrix

The tensile strength of the composite σ_{uc} is given by:-

$$\sigma_{uc}=\sigma_{uf}V_f+\sigma'_m(1-V_f) \quad (2)$$

where

σ_{uf} = ultimate strength of fibre

σ'_m = stress in matrix at the ultimate strain of the fibres

Whereas equation 1 only holds true for stiffness with their components in the elastic state equation 2 may still be used with the matrix in the plastic state. However in practice the strength of a continuous fibre reinforced composite rarely approaches the value given by the equation. Whereas stiffness can be predicted for such a system fairly accurately by the rule of mixtures, strength is a difficult quantity to predict using the rule of mixtures even for such an idealised system.

1.5.2 The Stiffness and Strength of Short Fibre Reinforced Thermoplastics

In the case of discontinous fibre composites the only continuous phase is the matrix phase so the load is transferred to the stiff fibre via shear stresses at the interface.

For the purpose of this survey, a short fibre reinforced material is one in which the fibres have an aspect ratio (length:diameter) of between 10 and 1000[2]. To consider the stiffness and strength of a discontinuous fibre composite we need to take into account how stress is transferred to or from the fibre.

Five theories[3] have been presented on the longitudinal stress distribution along the fibre matrix interface. Four of these have considered both the fibre and matrix in the elastic state the fifth has considered the matrix in a plastic state. These are reviewed briefly in Figure 2a and b.

Composite materials are commonly used in the range of stresses between the very low stresses at which the Cox theory can be used, and the failure stresses described by the failure theories. The incompatibility of the assumptions needed for the modulus expression and those needed for the strength expression received attention by Piggot[9]. Piggot extended earlier theories of reinforcement and estimated the effect on the stress-strain curve of factors such as friction

between fibre and matrix, residual and shrinkage stresses. Unfortunately little data exists on these parameters so there is little empirical evidence to substantiate his theory.

In this thesis it was decided to use the Cox analysis to predict tensile stiffness, as at low levels of strain where tensile stiffness is meaured, the thermoplastic matrix at the interface between the fibre and matrix could be expected to behave elastically and not yield or debond from the fibre. The Kelly-Tyson analysis was used to predict properties such as interfacial shear strength and ultimate tensile strength at higher values of strain where the matrix was likely to have yielded and plastic deformation could take place at points along the interface.

Each of the chosen analyses will now be discussed in more depth.

The Cox Shear Analysis

The main assumptions made by Cox are:-

(i) A round fibre is surrounded by a cylindrical matrix as shown in Figure 3.

(ii) The transfer of load from the matrix to the fibre depends on the difference between the actual displacement of a point on the interface and displacement than would exist if the fibre were absent.

(iii) A perfect bond exists between fibre and matrix.

(iv) There is no load transfer through the ends of the fibre.

With reference to Figure 3 consider a fibre of length l and radius r embedded in a matrix. We assume that the matrix as a whole is strained homogeneously by the application of a load applied parallel to the fibre axis. Since the shear stress τ at the fibre-matrix interface will vary along the fibre, so also will the tensile stress in the fibre. Considering a small element of the fibre length δx, the net tensile load δF across this element must be balanced by the shear force at the interface i.e.

$$\delta F = \tau\, 2\, \pi\, r\, \delta\, x \text{ or } \frac{dF}{dx} = 2\pi\, r\, \tau \qquad (3)$$

when $\delta x \rightarrow 0$

Since the assumption has been made that the matrix and fibres are strained elastically, then $\tau \alpha \gamma$ where γ is the shear strain developed at the fibre-matrix interface. Furthermore, γ can reasonably be expected to be proportional to the difference in elastic displacement u in the fibre at some point x from one end and the elastic displacement v of the matrix at the same point, if the fibre were absent. Hence we may write:-

$$\frac{dF}{dx}=H(u-v) \qquad (4)$$

where H is a constant for a particular composite.

From Hooke's Law

$$F=E_fA_f\frac{du}{dx} \qquad (5)$$

where E_f = Young's modulus of the fibre A_f = Area of cross-section of a fibre

Differentiating equation (4) with respect to x we have:-

$$\frac{d^2F}{dx^2}=H\left[\frac{du}{dx}-\frac{dv}{dx}\right]$$

but $\frac{du}{dx}=\frac{F}{E_fA_f}$ from equation (5), while $\frac{dv}{dx}=\varepsilon$, the strain in the matrix.

hence $\frac{d^2F}{dx^2}=H\left[\frac{F}{E_fA_f}-\varepsilon\right]$

This second order differential equation has a solution of the form:-

$$F=E_fA_f\,\varepsilon+B\sinh\beta x+C\cosh\beta x$$

where $\beta=\left[\frac{H}{E_fA_f}\right]^{\frac{1}{2}}$ and B and C are constants of integration, whose values are determined by two boundary conditions. These are that no loads are transferred across the end faces of a fibre i.e. $F=0$ at $x=0$ and $x=l$. We then obtain for the distribution of tensile stress along the fibre:-

$$\sigma_f=\frac{F}{A_f}=E_f\varepsilon\left[1-\frac{\cosh\beta(l/2-x)}{\cosh\beta l/2}\right]$$

From this result, the average tensile stress developed in the fibre can be easily evaluated and is given by:-

$$\bar{\sigma}_f = E_f \varepsilon \left[1 - \frac{\tanh \beta l/2}{\beta l/2} \right]$$

The average longitudinal stress in a composite containing a volume fraction of fibres V_f can then be calculated as a weighted average of the stresses developed separately in the fibre and matrix i.e.:-

$$\sigma_c = V_f \bar{\sigma}_f + (1-V_f)\sigma_m$$

where σ_m is the stress developed in the matrix.

since $\sigma_m = E_m \varepsilon$, where E_m = Young's modulus of the matrix

$$\sigma_c = V_f E_f \varepsilon \left[1 - \frac{\tanh \beta l/2}{\beta l/2} \right] + (1 - V_f) E_m \varepsilon$$

The effective longitudinal modulus of the composite is given by:-

$$E_c = \frac{\sigma_c}{\varepsilon} = V_f E_f \left[\frac{1 - \tanh \beta l/2}{\beta l/2} \right] + (1-V_f)E_m \qquad (6)$$

If the mean centre-to-centre separation of the fibres normal to their length is R then Cox showed that:-

$$H = \frac{2\pi G_m}{\log_e \left[\frac{R}{r} \right]}$$

If it is assumed the fibres are arranged hexagonally the volume fraction of fibres:-

$$V_f = \frac{2\pi r^2}{\sqrt{3} R^2}$$

The largest value of interfacial shear stress occurs at the ends and is zero in the middle. The main source of error in the analysis is the manner in which the shear stress is assumed to decay around individual fibres. The Cox analysis ignores interactions between adjacent fibres. Using finite element analysis, Chen[10] showed that due to the discontinuity of neighbouring fibres in discontinuous fibre composites, the portion of fibre adjacent to a neighbouring fibre end must be under greater stress than it would be in the continuous case. This concept was denoted the perturbation effect and cannot be predicted by the Cox shear lag analysis. Tyson and Davis[11] showed using a

two dimensional photoelastic model the existence of high shear stresses near fibre ends, which peak to values greater than these predicted by shear lag theory. The existence of these high stresses at fibre ends was also confirmed by Chen and Lavengood[12] by a finite element analysis. The artificial model of fibre packing in the Cox model also becomes more difficult when extended to non aligned fibres.

Figures 4 to 7 show the dependence of predicted stiffness on average fibre length for the four types of composite material produced in this thesis.

The Kelly Tyson Analysis

Whenever a thermoplastic is loaded in tension, if the applied load exceeds a certain value the material shows a yield point. When a thermoplastic is used as a matrix material for a short fibre reinforced thermoplastics the shear stresses developed towards the end of the fibres can exceed the shear strength of the matrix τ_m. The effect is to limit the maximum shear strength at the fibre interface to τ_m. Whereas in the Cox analysis the variation of tensile stress towards the fibre ends is strictly non linear, the presence of a constant shear strength τ_m will lead to a simple linear increase in tensile stress from the ends of the fibre until a constant tensile stress of $E_f \varepsilon$ is reached. In composites containing very short fibres the shear stress induced at the fibre-matrix interface will cause failure at the interface before the maximum stress in the fibre reaches the fibre failure stress, while in composites containing longer fibres the fibre failure stress will be reached first and failure will occur by fibre breakage. There thus exists a 'critical fibre length' (l_c) where the fibre failure stress and shear failure stress are reached simultaneously. It can be shown that this is given by

$$l_c = \frac{\sigma_{uf} d}{2\tau_u} \qquad (7)$$

where

σ_{uf} ═══ fibre strength

d ═══ fibre diameter

τ_u ═══ interfacial shear strength

The variation of tensile stress with fibre length according to this analysis is shown in Figure 8 for a fibre (a) less than (b) equal to and (c) greater than the critical length.

If $\bar{\sigma}_f$ is the average stress carried by the fibre

$$\bar{\sigma}_f = \left[1 - \frac{l_c}{2l} \right] \sigma_{uf} \text{ for } l > l_c$$

$$\sigma_{uc} = \sigma_{uf} V_f \left[1 - \frac{l_c}{2l} \right] + (1 - V_f)\sigma'_m$$

where σ'_m = stress in the matrix at the ultimate strain of the fibres. However if the fibres are shorter than l_c the maximum fibre stress is only $2\tau_u l/d$ and the mean strength will be half of this. The composite strength will be

$$\sigma_{uc} = \left[\frac{\tau_u l}{d} \right] V_f + (1 - V_f)\sigma'_m$$

On the basis of this theory even if the ratio of $\frac{l}{l_c}$ is as low as 10 then 95% of the strength obtained with continuous fibres can be obtained with aligned discontinuous fibres[13].

In all the short fibre reinforced thermoplastics considered in this study, however, there are distributions of fibre lengths. Then it is necessary to sum the contributions arising from the fibres of sub critical and super critical length to give an equation of the form advocated by Nielson and Chen[14]. For aligned fibres:-

$$\sigma_{uc} = \sum_i \frac{\tau_u l_i V_{fi}}{d} + \sum_j \sigma_{uf} V_{fj} \left[1 - \frac{l_c}{2l_j} \right] + (1 - V_f)\sigma'_m \qquad (8)$$

As was the case of the Cox shear lag analysis, the main error inherent in the Kelly-Tyson analysis is the neglection of fibre-fibre interaction. In a study directed at predicting the tensile strength of discontinuous aligned composites, Riley[15] concluded that due to the concentration of stress that occurs at a fibre end which must be taken up by surrounding fibres, discontinuous composites will never achieve strengths greater than 6/7 of the continuous fibre strength.

1.5.3 The Stiffness and Strength of Partially Aligned Composites

The description of the theory so far has been concerned with the mechanical properties of uniaxially aligned short fibre composites. In moulded composites however, fibres are seldom aligned, so some provision must be made in the theoretical analyses to allow for partially orientated systems.

The prediction of stiffness of partially orientated composites has been approached by a number of investigators. Krenchel[16] and Cox[4] evaluated the relative efficiency of fibres in each orientation followed by an averaging procedure for the whole composite. In his approach, Krenchel adopted an orientation efficiency factor of reinforcement η_o to allow for reduction of reinforcement of fibres lying at an angle θ to the stress axis. In the general case of transverse isotropy Krenchel proposed that η_o could the form

$$\eta_o = \sum_n a_n \, \mathrm{Cos}^4 \, \theta_n$$

where $\sum_n a_n = 1$, a_n is the volume fraction of fibres lying at an angle θ_n to the stress axis and n is the number of angular intervals into which the fibre orientation is divided.

Since in the case of this study we are concerned with short fibres the total efficiency factor

$$\eta = \eta_o \eta_l \text{ where } \eta_l = 1 - \frac{\tanh \beta l/2}{\beta l/2}$$

if the Cox analysis is used.

The total stiffness of the composite is then given by:-

$$E_c = \eta_o \, \eta_l \, V_f E_f + (1 - V_f) \, Em$$

Jerina et al[17] predicted stiffness by treating the composite as an assembly of plies. The stiffness of each layer is predicted or measured experimentally and the stiffness of the plies are summed to give the stiffness of the composite, this method is reported to be comparatively straight forward to apply.

In the prediction of stiffness by Brody and Ward[18], the composite is regarded as an aggregate of sub-units, each sub-unit possessing the elastic properties of a reinforced composite in

which fibres are continuous and fully aligned. Involved algebra is required to obtain upper and lower bounds for composite elastic constants.

As in the case with stiffness, the strength of an aligned short fibre composite decreases as the angle between the fibre axis and loading direction increases. The prediction of strength anistropy requires a failure criterion. There are two criterion that have received wide spread attention. Stowell and Liu[19] invoke a maximum stress criterion and define three failure mechanisms. For stresses directed along or at small angles θ to the fibre axis, failure will be controlled by fibre strength. At larger angles the dominant failure made will be due to shear processes. At very large θ, approaching 90° the mode will change again to one of transverse failure either in the matrix or at the interface.

These may be expressed mathematically as follows:-

$\sigma_u\theta = \sigma_{uc}\,\mathrm{Sec}^2\,\theta$

for fibre tensile failure

$\sigma_u\theta = 2\tau_{uc}\mathrm{cosec}2\theta$ for shear failure

parallel to the fibres

$\sigma_u\theta = \sigma_{ut}\mathrm{cosec}^2\theta$ for tensile

failure normal to the fibres

$\sigma_u\theta$ is the composite strength at an angle θ to the fibres, σ_{uc} and σ_{ut} are the strengths of the uniaxially aligned composite with and normal to the fibres, and τ_{uc} is the in-plane composite shear strength. An alternative failure criterion found to fit strength data for short fibre composites is due to Hill[20] and Azzi and Tsai[21]. They used a maximum distortional energy based on the Von Mises criterion.

The approach adopted by Krenchel for predicting stiffness can also be applied to obtain an estimate of the strength of a composite containing misaligned fibres. Lees[22] integrated the Stowell-Liu equations over all angles for the special case where the fibres were random in plane

to give the following equations for the average strength of the composite

$$<\sigma_{uc}> = 2\frac{\tau_{uc}}{\pi}\left[\,2+\log_e\left[\frac{\sigma_{uc}\sigma_{ut}}{\tau_{uc}^2}\right]\right]$$

as before τ_{uc} is the composite shear strength and σ_{ut} is the transverse strength of the uniaxially aligned composite.

Using a similar approach to Lees, Chen[23] suggests that the predictive equation should be

$$<\sigma_{uc}> = \frac{2\tau_{uc}}{\pi}\left[\,2+\log_e\left[\frac{\sum \sigma_{uc}\sigma'_m}{\tau_{uc}^2}\right]\right]$$

where $\sum$ is a strength efficiency factor that relates the strength of an undirectional short fibre composite to the rule of mixtures prediction.

The factors discussed in this review affecting the strength of a glass reinforced nylon are displayed schematically in Figure 9.

1.5.4 The Toughness of Discontinuous Fibre Composities

Few materials are selected for a structural use on the basis of one property alone, usually a balance of properties of strength, stiffness and toughness are required. Toughness however is even more difficult to predict than stiffness and strength. For many composites the conditions that lead to high stiffness and strength also result in low elongation to break, so that the toughness of a material can vary quite unpredictably[24].

Much effort has been devoted to defining parameters which relate applied stress, the size of an existing crack and sample geometry to allow toughness or resistance to crack propagation to be defined in the same way that a modulus can be used to define toughness. One is via an energy approach G_c, the other by a stress intensity factor K_c.

Via an Energy Approach

When a body is stressed, energy is stored in the material as strain energy. If a crack extends, some of the energy is released. By equating the energy released to that absorbed in plastic deformation and creating new fracture surfaces, it is possible to derive a 'strain energy release

rate', G_c, which should be constant at failure. The general solution for calculating G_c, which is applicable to any loading system is:-

$$G_c=\frac{P_f^2}{2B}\frac{dc}{da}$$

where P_f is the applied load at failure, B is the thickness, a is the crack length and dC/da is the change in compliance C (1/stiffness), with respect to crack length increase, da.

For many modes of loading with axisymmetric cracks, presuming a linear stress-strain curve where the stored energy is $1/2\sigma_c\varepsilon$ which can often be assumed to be correct for plastics, G_c can be calculated as:

$$G_c=\frac{\pi\sigma_{uc}^2 a}{E}$$

where 2a = crack length, where σ_{uc} is the failure stress and E the material modulus. (Note that $G_c=2\alpha$, where α is the "Griffith" surface energy).

Via a Stress Intensity Factor K_c

By consideration of the detailed stress field at the tip of a sharp crack, it has been shown that the degree of stress intensification can be more precisely defined by a parameter K - known as the stress intensity factor. For a crack in a thin plate under tension (where the crack dimensions are small compared with overall plate dimensions) K is given by

$$K=\sigma\sqrt{\pi a}$$

where σ is the applied stress and 2a the crack length. It is postulated that there is a critical value, K_c, at the onset of cracking given by:

$$K_c=\sigma_{uc}\sqrt{\pi a}$$

where σ_{uc} is the gross failure stress. The value of K_c is referred to as the fracture toughness. Although the above outline is correct, it is simplistic. Frequently the crack dimensions and "correction factors", Y, have to be used to account for finite plate effects.

The symbol K_I is used to denote opening mode (mode I) fracture in which the crack is opening normally under tensile stress. Mode II refers to shear stresses acting parallel to the direction

of crack propagation, and mode III refers to shear stresses acting parallel to the crack tip. As neither modes II or III have received significant attention in the polymer literature, these mode of stressing are not considered in this thesis.

In the past before the introduction of instrumented impact testers, assessments of toughness have been based on estimates of work of fracture using Charpy or Izod tests. These measure the amount of energy absorbed from a swinging pendulum striker. The tests however are not easily related to conditions which may be encountered in service.

The value of G_c for a fibrous composite is very often much higher than can be accounted for by adding the contributions of the matrix and the fibre. Much argument has centred on the interactions between these two components responsible for this large increase. Cook and Gordon[25], in their now classic crack blunting mechanism, suggest crack insensitivity may be produced by providing an interface parallel to the fibres which is weak in tension.

Theories perhaps more relevant to short fibre composites include that of Outwater and Murphy[26] who argued the energy required to debond a fibre from the matrix is the predominant energy governing the total fracture energy. This theory is supported by McGarry and Mandel[27] and Beaumont and Phillips[28]. Cottrell[29] obtained a relationship that the fracture energy produced by fibre pull out (U) was related to fibre length by the following expression:-

$$U \alpha l^2 \text{ when } l < l_c$$

$$U \alpha \frac{1}{l} \text{ when } l > l_c$$

$$U = U_{max} \text{ when } l = l_c$$

Such a variation is found for discontinuous fibres by Cooper and Kelly[30] and Cooper[31] using discontinuous flawed fibres and Helfet and Harris[32] using chopped wires in a polyester resin. Kelly presents an analysis[33] which suggests the work of fibre pullout is always greater than that of debonding. It seems likely that neither is predominant for all composites but the largest contributer depends on fibre and matrix type and fibre surface treatment[34,35].

Rule of mixtures model for a unidirectional composite

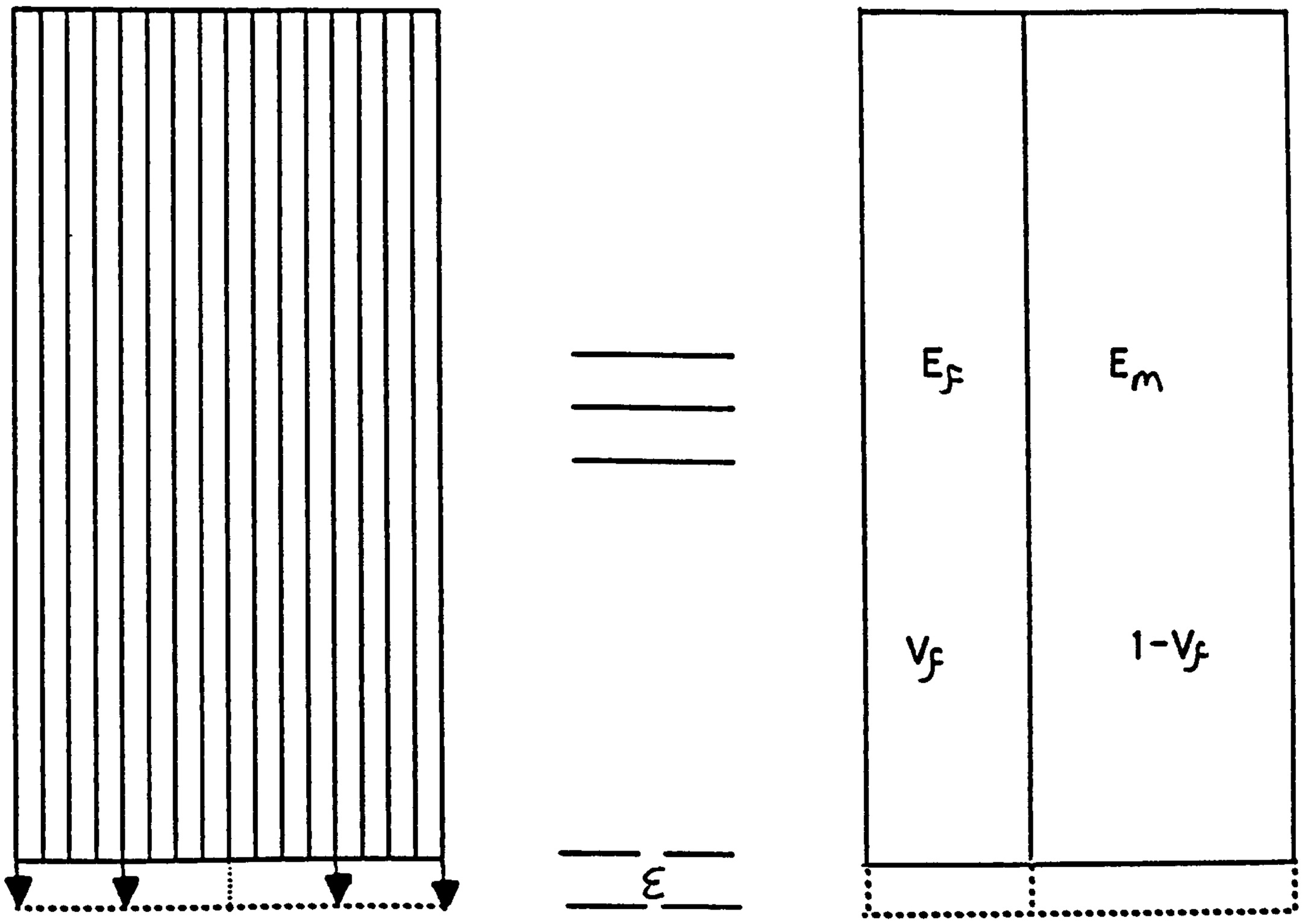

Figure 1

Theoretical solutions of the isolated fibre in a matrix

H. L. COX 1952

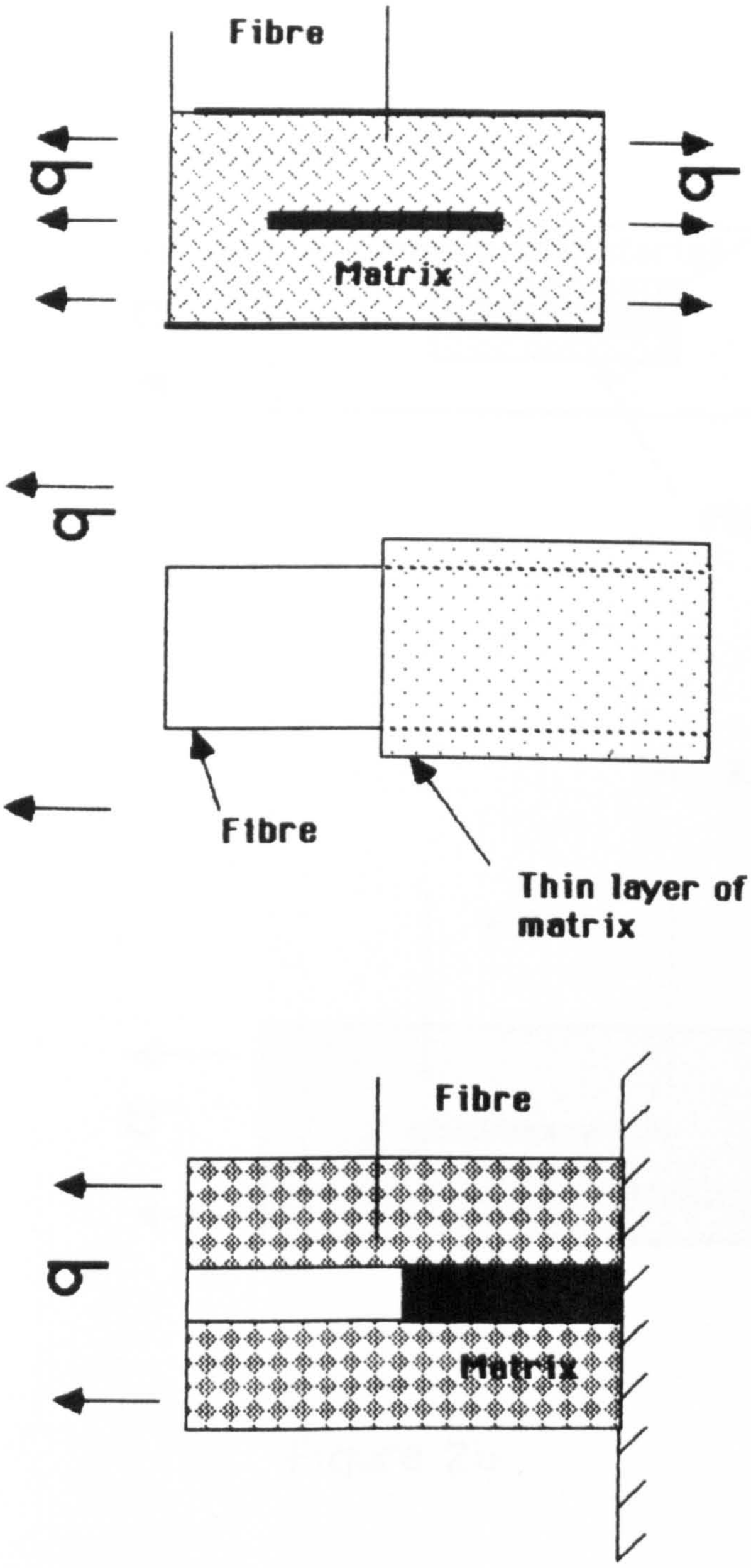

Considers an elastic fibre completely bonded into an elastic matrix which is subjected to uniform strain along the direction of the fibre axis.
There is no load transferred through the ends of the fibre.

J. O. OUTWATER 1956

Theory involves a film of negligible thickness which shrinks on to the fibre reinforcement. This film does not deflect in shear.

Once the initial adhesive bond is broken the resin slides off of the fibre and the frictional force between resin and fibre enables further load to be transferred to the fibre as the strain on the composite is increased.

N. F DOW 1963

Axial load is supplied to a cylindrical matrix containir fully bonded elastic fibre. No matrix is present at the end of the fibre .The solution implies that the initially straight lines remain straight after deformation.
Two and three Dimensional configurations have been analysed

Figure 2a

Theoretical solutions of the isolated fibre
in a matrix continued

W. B. ROSEN 1964

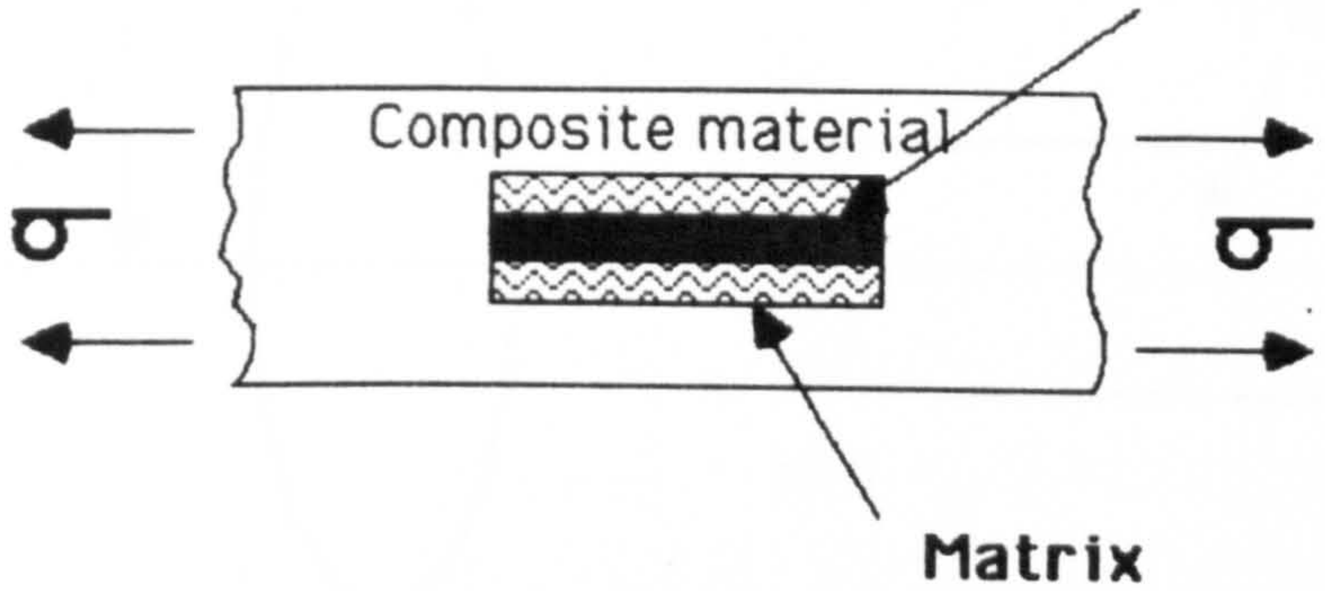

Modification of Dows theory. Fibre surrounded by a material having average properties of the composite. The fibre and average material only carry tensile stresses and the matrix only carries shear stresses.

A. KELLY and W. R. TYSON 1965

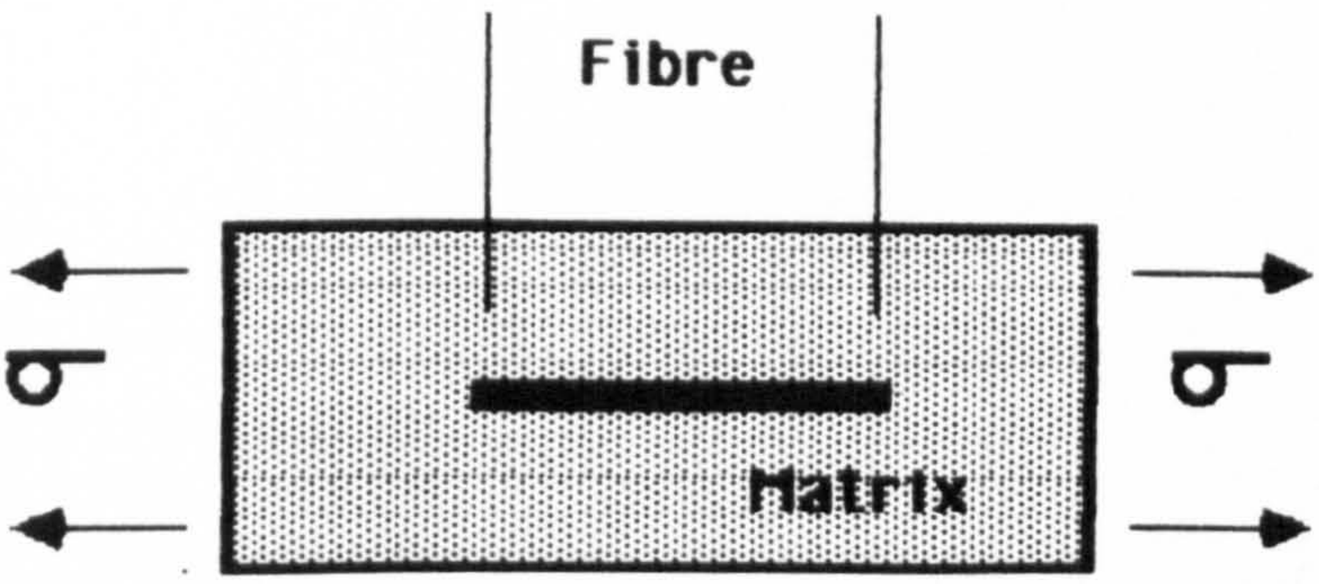

Model consists of a elastic fibre in a plastic matrix. The plastic matrix flows when the shear stress reaches an critical value.

Figure 2b

The definitions of symbols used in The Cox Shear Lag Analysis

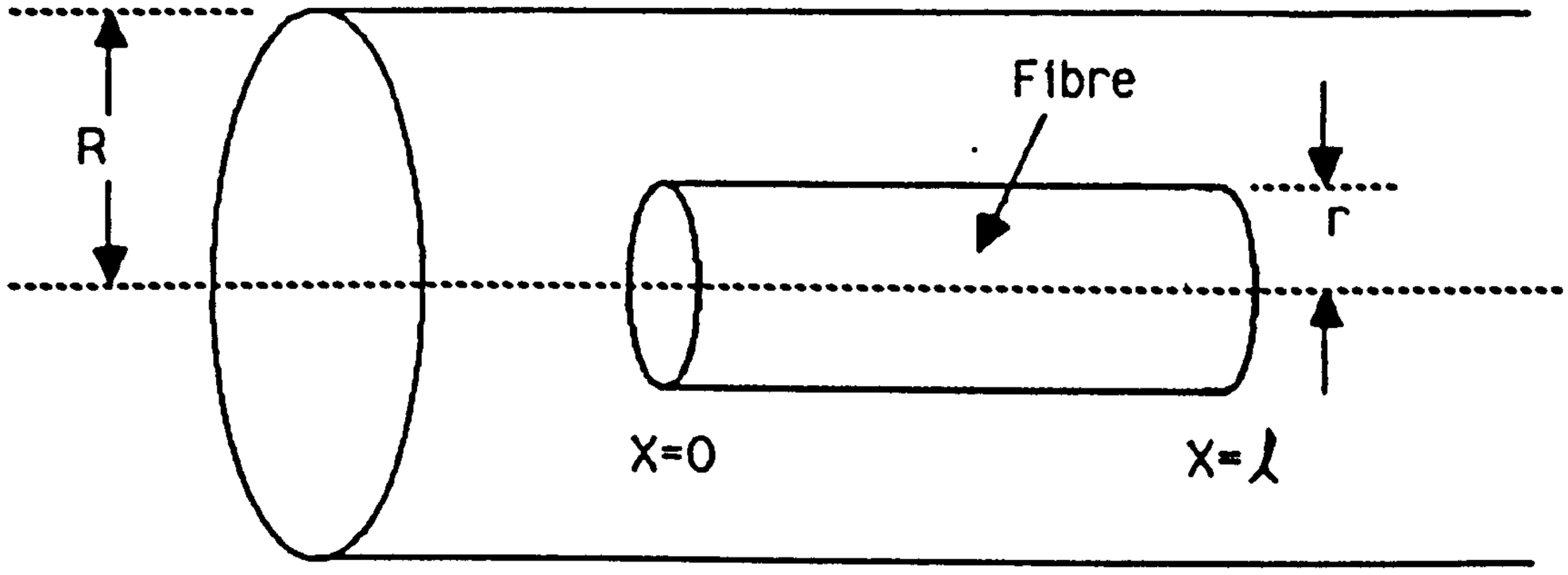

Figure 3

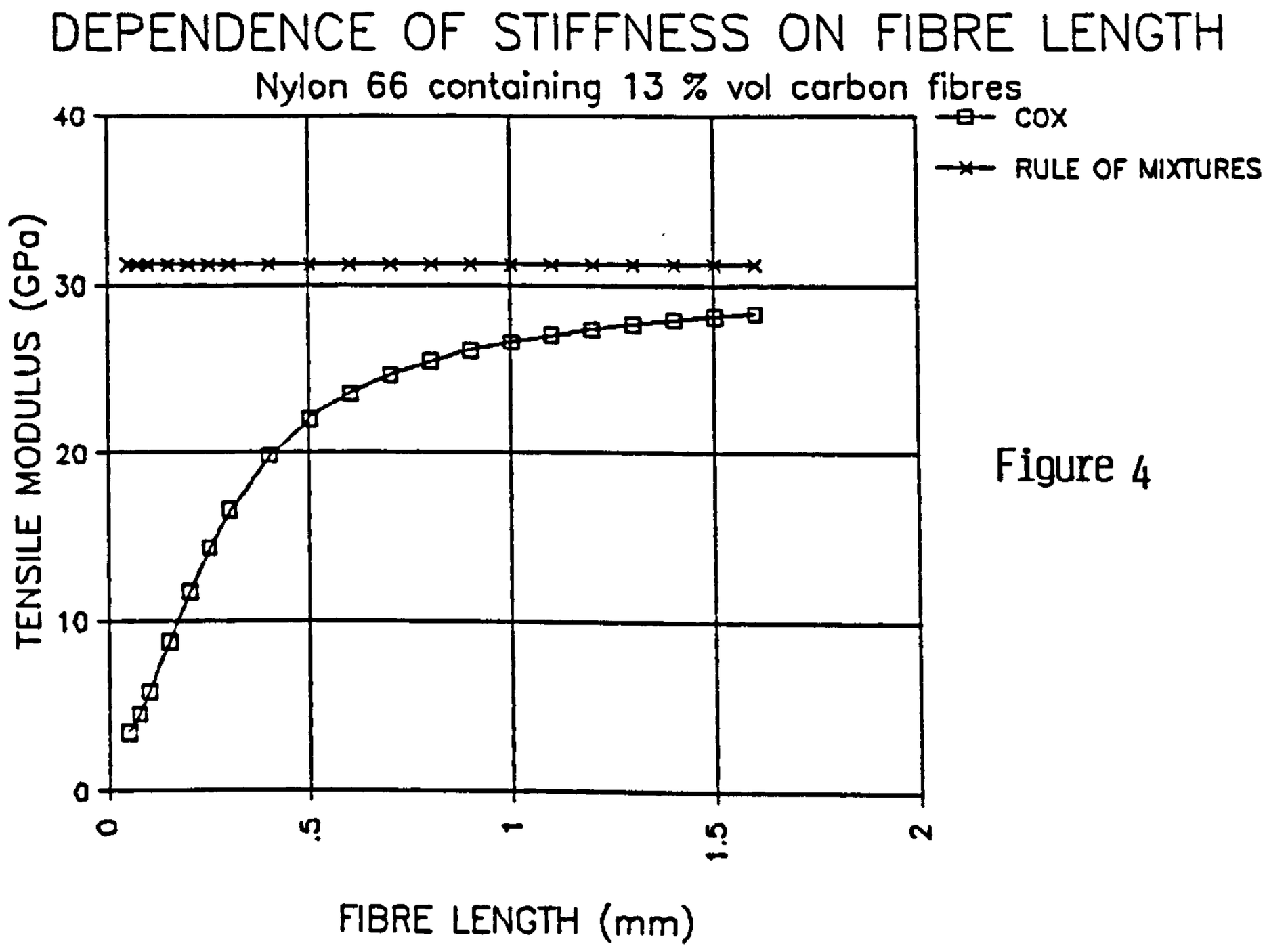

Figure 4

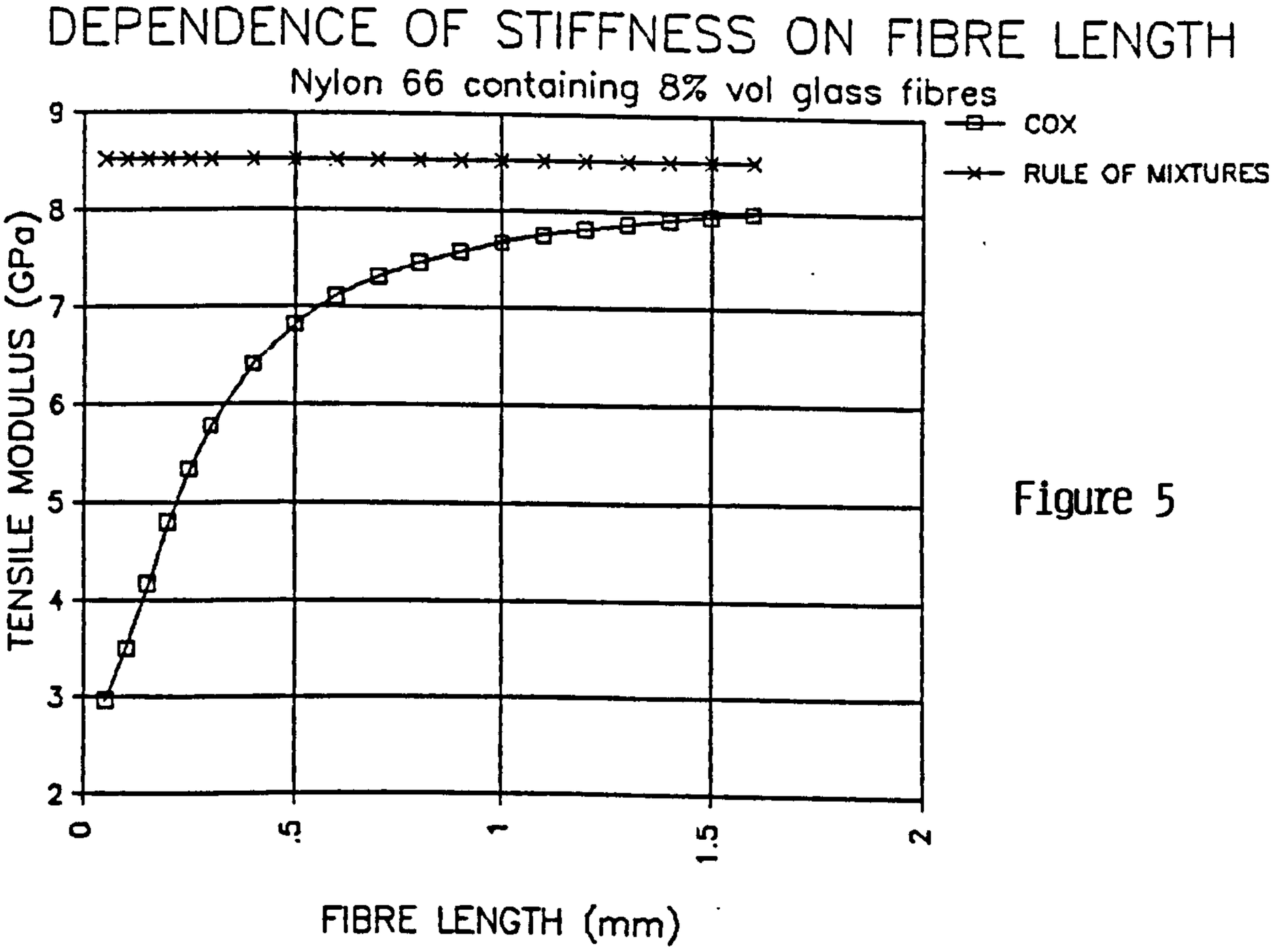

Figure 5

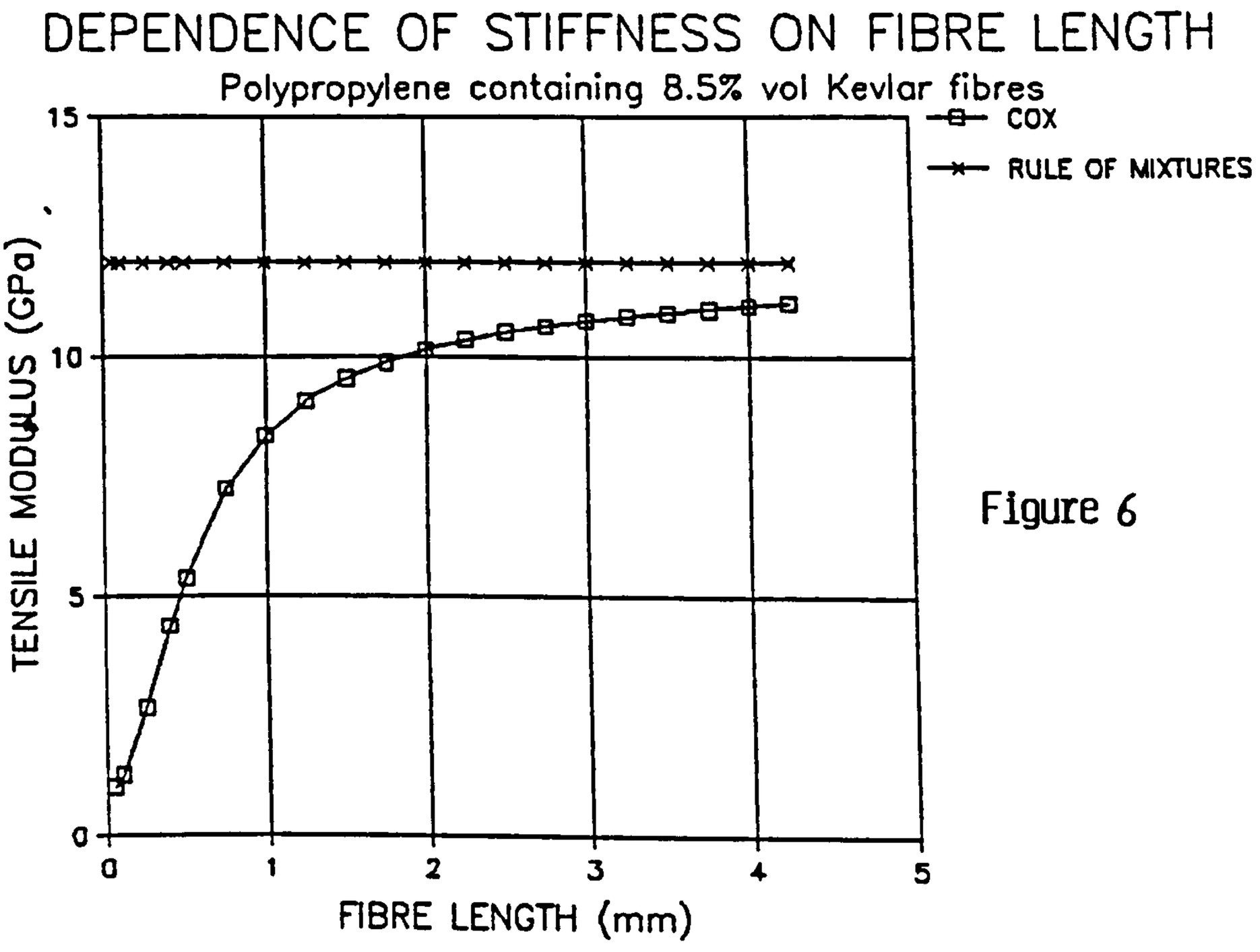

Figure 6

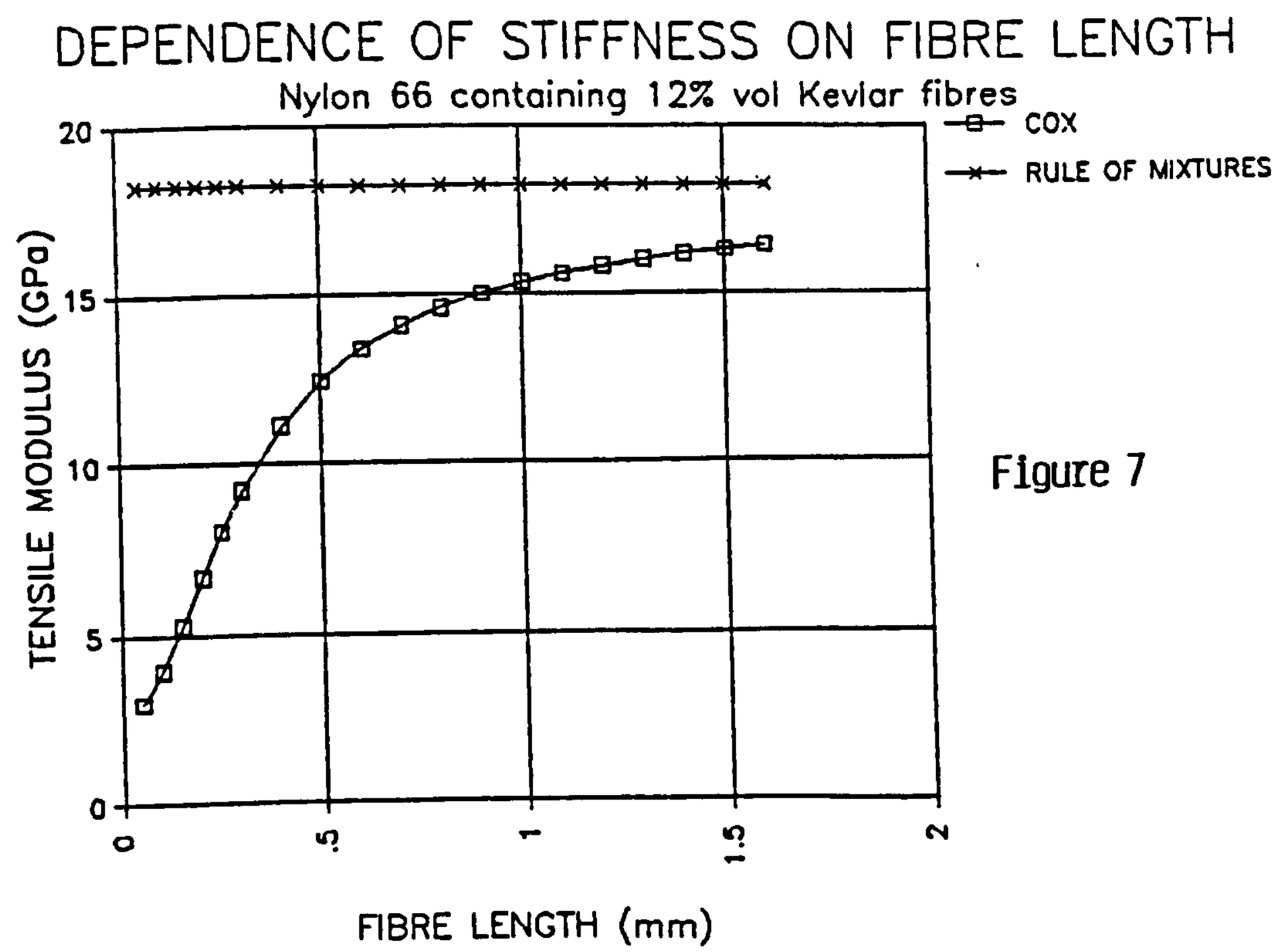

Figure 7

The variation of tensile stress along a fibre
according to Kelly and Tyson

Figure 8

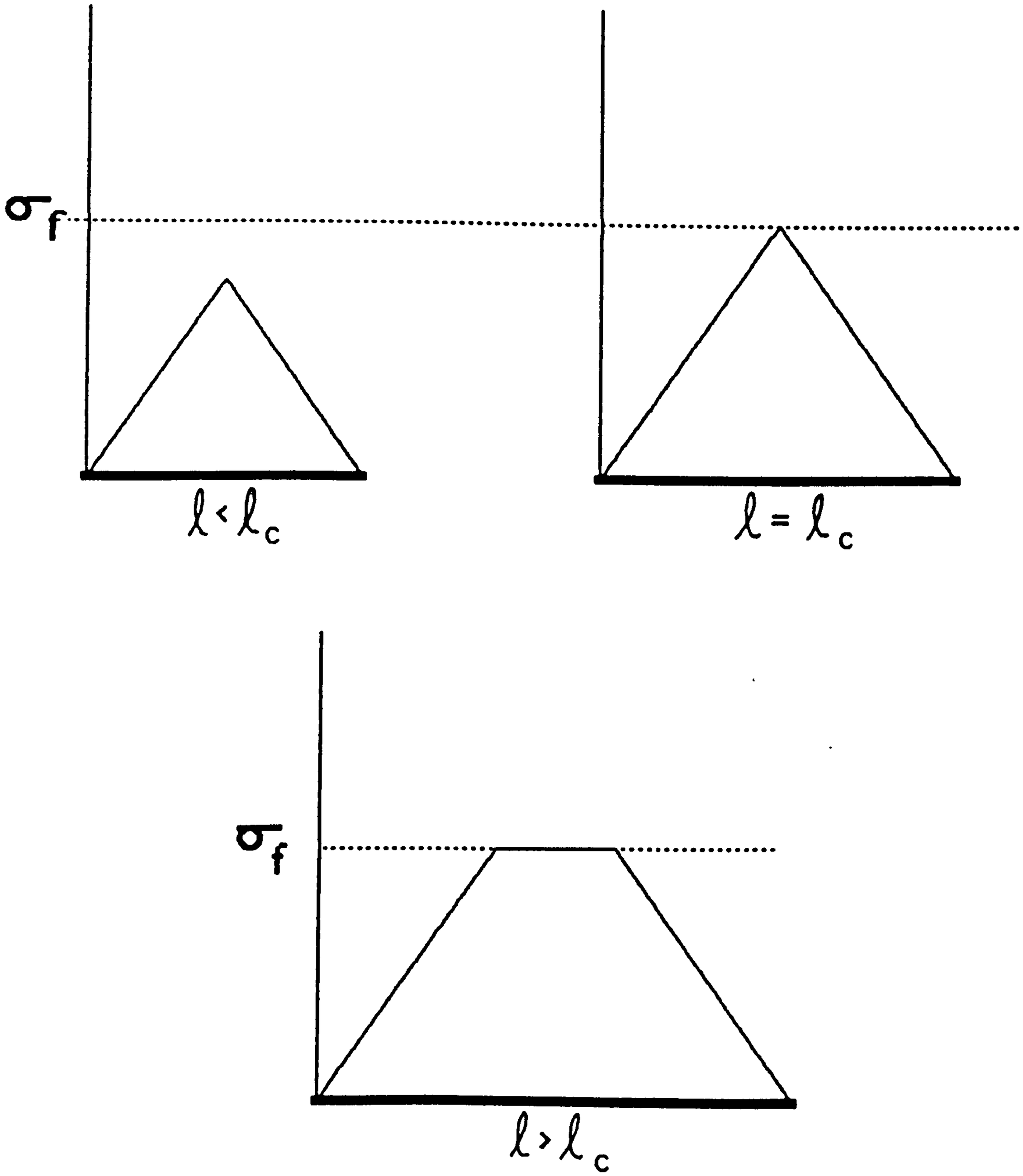

Factors influencing the strength of composites

Glass reinforced nylon 66.

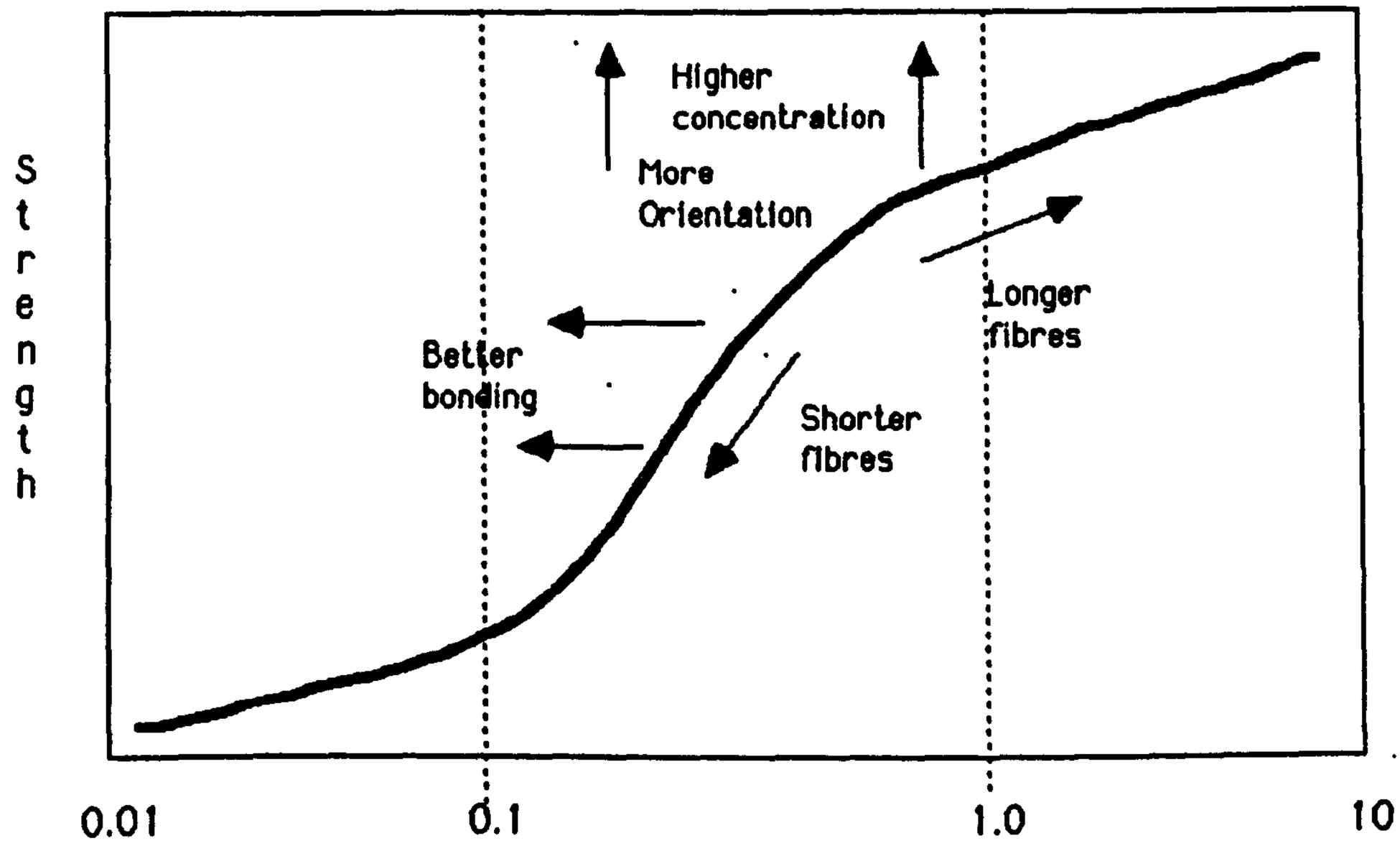

Figure 9

2.1 Composite Materials

A precise definition of a composite material is difficult to formulate. According to the Encyclopedia of Polymer Science and Technology[36] composites can be defined as combinations of materials differing in composition or form on a macroscopic scale and having constituents that retain their identities and do not dissolve or otherwise completely merge into each other. This definition is not strictly accurate as it includes some materials not often considered to be composites. Also some combinations may be thought of as composite structures rather than composite materials, the dividing line is not sharp and differences in opinion do exist. Within this definition examples of composite materials can be identified, from straw filled mud bricks to ceramic whisker filled epoxy used in space shuttles.

Within the last 35 years there has been a rapid growth in the use of all types of plastics. These materials have found an ever widening use in structural applications, where plastics containing reinforcing additives have become well established.

Parratt[1] and Maxwell[37] attempted to list the principal benefits of reinforcement over conventional bulk materials.

1. Higher specific strength
2. Higher specific stiffness
3. Enhanced heat deflection temperature
4. Better dimensional stability
5. Better impact and shock resistance
6. Better creep strength
7. Better fatigue strength
8. Control of thermal conductivity and electrical conductivity possible

Thermoplastics containing short fibres were first introduced on to the market with the intention of producing a new range of materials with intermediate properties between the high tonnage commodity plastics and the sophisticated continuous fibre reinforced composites well established

in the aerospace Industry. The increase in stiffness and strength compared with the parent thermoplastic was modest but sufficient to establish this class of material in lightly stressed applications.

Virtually all common thermoplastics can be reinforced. The widest variety of materials are reinforced with glass fibre. The earliest commercial source for these materials was the Fibrefill process by which production of reinforced polystyrene was started in 1955[31]. Applications included land mines, which required high stiffness and strength but non metallic properties to escape detection devices.

When discussing fibre reinforcement of thermoplastics it is worthwhile to recognise the difference between crystalline and amorphous polymers. The amorphous engineering materials (notably polycarbonate, ABS and polyphenylene oxide) are valued for their low shrinkage and good impact strength, but their fatigue and chemical behaviour can be suspect in common environmental conditions. Crystalline plastics are much more affected by temperature but this deterioration is corrected very positively by reinforcement. Data presented in Table 1 is taken from a publication by Maxwell[37] indicates the benefits of reinforcement possible by the incorporation of 30% glass fibres. The requirements of structural and mechanical components are more likely to be met by crystalline thermoplastics.

During the last few years there has been some significant advances in the development of very high melting point thermoplastics for example, Polyethersulphones (Amorphous). Polyetheretherketones (Crystalline) together with a gradual reduction in costs of specialised fibres such as carbon. Materials manufacturers are now combining engineering thermoplastics with more expensive fibres to produce a new range of products. There still is however research required into the fabrication technology necessary to optimise the mechanical properties of these high application temperature short fibre reinforced thermoplastics.

2.2 Reinforcing Fibres

This survey attempts to review briefly the background of the reinforcing fibres used in this

study and outline some of their salient properties.

2.2.1 Carbon Fibres

Carbon fibres had been known for nearly a century when Thomas Edison first used them as filaments for incandescent lamps. These were produced from the carbonisation of bamboo and rayon. This use for carbon fibre was abandoned after the development of tungsten fibres.

The present activities in the development and use of carbon fibres stems from the work carried out in the late 1950's early 1960's in America, Britain and Japan. In America work was initiated on Rayon based carbon fibres and led to Union Carbide's introduction of the Thornel carbon fibres.

At approximately the same time Shindu[38] in Japan and Watt[39] and his co-workers in Britain working independently successfully prepared carbon fibres from polyacrylonitrile (P.A.N.). These carbon fibres had relatively low strength but high modulus. The mechanical properties of these P.A.N. based carbon fibres were further enhanced by carrying out certain oxidative treatments under stress.

The stages in the current production method of P.A.N. based carbon fibre is shown in Figure 10. The P.A.N. fibre is first subjected to oxidisation in air at 200-300°c. During this process the fibre is stretched to obtain carbon fibres of a high quality level. Oxidation will lead to the formation of a ladder polymer consisting of condensed and partly hydrogenated pyridine rings. The subsequent treatment in an inert atmosphere serves to remove hydrogen and nitrogen. Temperatures between 1000 and 1300°C produce fibres having high strength (type II) while additional heat treatment at temperatures between 2000 and 3000°C produce graphite fibres having a very high tensile modulus of elasticity (type I). To improve adhesion to the matrix the fibres are sometimes subjected to an oxidative surface treatment and then provided with a finish. The variation of strength and stiffness found with graphitisation temperature is shown in Figure 11.

Figure 12 based on values taken from Hull[40] compares the specific properties of the fibres used in this study. From the data it is apparent that the specific modulus of carbon fibre is five

times greater than glass and approximately twice that of Kevlar. Table 2 presents a general comparison of the properties of the reinforcing fibres.

Although carbon fibre reinforced thermoplastics are at least an order of magnitude more expensive than the majority of conventional moulding compounds their physical properties make them uniquely attractive in some engineering applications. The area in which the material has progressed significantly is in the replacement of aluminium and zinc castings, where due to the complex shape and extensive post machining required on the casting the injection moulded thermoplastic can compete effectively. Some properties of short fibre reinforced thermoplastics compared with metals[41] are shown in Table 3.

In 1984 the world assumption of P.A.N. carbon fibre was estimated to be 2, 500 tonnes per annum. The demand is expected to grow at a rate of 40 to 60% per annum[42] and reach 10,000 tonnes by 1990. Carbon fibre reinforced thermoplastics account for a modest proportion of the demand at present with about 14% of total production.

2.2.2 Glass

Fibre glass was first produced as a decoration for Syrian and Egyptian glass ornaments. French and German commercial glass blowers produced glass fibres using very crude winding machines in the early to middle 1700's.

The present day fibre glass industry resulted when two American glass companies instituted a joint research effort to find methods of producing glass in an economical manner. Continuous filaments were produced from a heated platinum box containing a multiplicity of orifices instead of a single hole which their predecessors had used. A diagrammatic representation of the fibre glass forming scheme, the Owens-Corning manufacturing process[43] is shown in Figure 13. Continuous filaments are produced by melting the raw materials in a reservoir which feeds the molten glass into a series of platinum bushings, each of which has several hundred holes in its base. The glass flows downwards on to drums at speeds of several thousand metres per minute. Sizes are usually added to the filaments before they are gathered into a strand the resulting "cakes" are

then dried in an oven before being produced into a roving.

E glass (E for electrical) is the most commonly used glass because it has good strength, stiffness, electrical and weathering properties. This is the type of glass used in this study. C glass (C for corrosion) is more expensive and has lower strength properties but a higher resistance to chemical corrosion. S glass is more expensive than E glass but has higher tensile strength and is more temperature resistant.

The strength of glass fibre is strongly dependent on processing conditions and testing environment. From available literature[44] the most important factor determining the ultimate strength of the glass is the damage which the fibres sustain when they rub together during processing. The application of a size coating helps to minimise this damage. Current production of glass fibres worldwide has been estimated at over half a million tonnes.

2.2.3 Kevlar

The most commercially successful organic fibre developed to date is that of the trade name Kevlar produced by the Du Pont company. (The term Aramid is an approved term to denote this class of fibre). Kevlar was developed at Delaware in America in the mid to late 1960's. Initial work was centred on polyparabenzamide[45] but due to a development in spinning technology was switched to poly para phenylene terephthalamide (P.P.T.A). Kevlar fibres are produced by spinning P.P.T.A. - sulphuric acid dopes from 80°C into a 1°C water coagulation bath. The interior of the fibre crystallizes whereas the exterior cools rapidly to form a non crystalline skin. Subsequent treatment includes neutralising the acid washing and drying. After drying the fibres have a modulus of 65 GPa and are referred to as Kevlar 29, these fibres are sometimes used in car tyres. Further treatment at 550°C for a few seconds under stress produces more perfect alignment of the macromolecules and doubles the fibre modulus to form Kevlar 49 fibres. The type preferred for high performance composite materials and used in this study.

One of the first models of the ultra structure of Kevlar was proposed by Dobb et al[46,47]. It consisted of a system of radially arranged sheets regularly pleated along their axis. A schematic

diagram taken from their 1980 publication[48] is shown in Figure 14. A later model that may explain mechanical properties more readily was that of Li, Allard and Bigelow[49]. They proposed a model where the core of the fibre is characterised by a layered structure with layers stacked perpendicular to the fibre axis. The layers are composed of a rod like crystallites with an average diameter of 50 nm and a length that is dependent on molecular weight. The crystallites in each layer are closely packed with their axis in the tangential direction and hydrogen bonds aligned almost in the radial direction of the fibre. Some crystallites extend through two or more layers and this strengthens the fibre along the fibre axis. A schematic diagram of this structure is shown in Figure 15.

Unfortunately the Kevlar variants are reported as having poor compressional properties[50]. The ratio of tensile to compressive strengths of undirectional epoxy composites containing carbon, glass and Kevlar 49 are 1.1 and 1.9 and 5.0 respectively. Greenwood and Rose[51] have shown that this property of Kevlar composites is due primarily to the low compressive yield strength of the fibres themselves, not the matrix component. On subjecting the fibres to an elastica loop test they observed buckled areas in the fibres followed by non Hookean elastic behaviour. Dobb et al[52] investigating with a number of mechanical and structural techniques confirmed the results of Greenwood and Rose and suggested a mechanism where band formation occurs which leads ultimately to buckling and weakening. They proposed that the rigid chain system of such fibres cannot accommodate any compression by a gradual change in chain direction, this leads to complete chain rupture or permanent deformation.

Dobb et al and Greenwood and Rose conclude that the weak compressional properties are due to weak Van der Waals forces and hydrogen bonds between crystal chains.

The stress strain curves for the fibres used in this study in their pristine condition are shown schematically in Figure 16.

2.3 Compounding

2.3.1 Introduction

The term compounding has been used in recent years to describe a wide range of operations[53] which can be classified into material combining processes, material separation processes and processes for altering the macromolecule. Throughout this work compounding can be taken to mean the incorporation or mixing of fibres into a plastics material prior to the moulding of a component in order to give certain specific properties.

Mixing was defined concisely by Moore[54] as a process in which two or more materials initially separate are interspersed in space with one another. Tadmor and Gogos[55] define a mixture as "the state formed by a complex of two or more ingredients which do not bear a fixed proportion to one another and which however comingled, are conceived as retaining in separate existance". Mixing is defined by them "as the operation that is intended to reduce the non-uniformity of the mixture". They discuss the basic types of motion involved in mixing and state that convection or bulk diffusion is the dominant mixing mechanism in high viscosity polymer melts. Strictly speaking mixing involves only the alteration of the initial distributions of the components in space, and the particles of the components are assumed not to extend any physical force on each other. With fibre bundles this assumption is often not justified, interparticle forces cause the formation of fibre aggregates which must be filamentised if mixing is to be complete. Mixing of thermoplastics with other materials like fibres involve true mixing and dispersion.

Folkes[24] lists the following requirements for the compounding operation:-

(a) The fibres have to be wetted-out i.e. each fibre must be totally enclosed by the matrix.

(b) The fibres should be uniformly dispersed throughout the matrix with an absence of undispersed fibre bundles, which might otherwise lead to variable strength of the composite.

(c) The fibres should be sufficiently long to ensure an effective transfer of stress from the matrix to the fibres.

As mentioned in Chapter 1 attempts to injection mould dry blends of polymer and fibre directly can lead to problems in component quality so a separate compounding operation is usually required to produce a feed stock that can be moulded satisfactorily.

From the review on the dependence of composite properties on fibre length it is clear that a very important factor that influences product properties is the fibre length distribution produced by the compounding operation. The quantitative measurement of fibre length distribution therefore features prominently in compounding and injection moulding investigations.

Most if not all previous work on the effect of compounding on component properties has been based on brittle fibres, typically glass or carbon. Discussion of the compounding of a tough type of fibre (Kevlar fibres) will be deferred to the end of this chapter.

By far the most popular method of compounding involves the single or twin screw extruder to mixed chopped fibres and matrix and produce a continuous extrudate. As mentioned previously this technique produces very significant fibre breakage that occurs along the screw(s). There is however a more fundamental problem when mixing a high volume fraction of fibres into a matrix; the maximum possible packing of randomly orientated fibres. The maximum packing of discontinuous fibres were discussed by Parratt[1] and Charrier[56]; increasing the volume fraction beyond the natural packing density results in the undesirable breakage of fibre and/or the formation of bundles. Mileswski[57] and Gibson[58] give the following approximate relationship between maximum fibre volume fraction V max, and the aspect ratio for discontinuous fibres in three dimensional random orientation:

$$V\,max = 4\,\frac{D}{L}$$

where

D = Diameter of fibre

L = Length of fibre

To produce pellets containing a large volume fraction of long fibres different approaches to extrusion compounding are needed. Such techniques rely on the fact fibres are required to be parallel to be efficiently packed. Parratt states that a realistic packing limit is 70% in this configuration. The most widely used technique to produce the above arrangement is by the continuous coating of a fibre matrix by a crosshead extruder followed by pelletizing[13,59,60]. This method produces pellets containing fibres of a well defined length, although some breakage is

still inevitable in the chopping process. Disadvantages of this process include the potentially inadequate penetration of the polymer into the fibre, slow production rate and excessive moulding machine wear[61].

This technique has been developed further in this thesis, but discussion is deferred to Chapter 6.

Baer[62] describes a novel way of producing pellets by in situ polymerisation. The fibre is introduced and wetted by monomer before polymerisation is allowed to take place. Baer used short glass fibres in Styrene-Acrylonitrile (S.A.N.). By careful control of the polymerisation it was found that the glass strands align themselves in a parallel array completely embedded in the polymeric matrix. Hollingsworth and Sims[63] produced by in situ polymerisation of fibres in caprolactam but found the mechanical properties obtained were somewhat lower than those obtained by the incorporation of fibres into nylon 6 melts. This was thought to be due to the situ polymerised nylon having a lower molecular weight or fibre bundles not being completely dispersed in the low viscosity caprolactam melt. They suggest however such a technique offers a simple and convenient means of forming intricate parts.

The literature reviewed in the following three sections refer to melt compounding operations and knowledge gained by subsequent moulding operations. The review will be divided into the following sections: Melt compounding other than extrusion, Extrusion melt compounding and injection moulding. From these three sections, compounding conditions required to produce fibre reinforced thermoplastics with optimum fibre length distribution will be recommended.

2.3.2 Melt Compounding Other Than Extrusion

Hollingsworth and Sims[63] published one of the first papers concerning the breakdown of the fibre lengths during processing. Compounding a series of fibre types in thermoplastics using an oil heated Banbury internal mixer, they discovered a significant reduction in aspect ratio. In the case of carbon it was reduced from 300 to 24.

Stade[64] worked with a continuous kneading compounding machine in which reciprocating

movement was superimposed on the rotation of a high shear kneading screw. It was found that glass fibres added while the polymer was molten, using a second stage arrangement gave a more gentle treatment resulting in less fibre breakage. Generally high melt temperatures, low screw speeds and low fibre concentrations helped to maintain fibre length.

2.3.3 Extrusion Melt Compounding

The most comprehensive study of extrusion compounding of a short fibre reinforced thermoplastic using a single screw extruder has been published by Lunt and Shortall[65,66]. The work undertaken was based on glass fibre reinforced nylon 66.

In their first publication[65] they noticed that a modest increase in barrel temperature increased fibre length by up to 25%. A reduction in die size from 4mm to 3mm resulted in a decrease in fibre length, but a decrease in die size from 3mm to 2mm and 1.5mm rather surprisingly showed an increase in the amount of undispersed bundles and hence longer fibre lengths, an effect they attributed somewhat vaguely to variations in mixing during the extrusion process. They observed that for each die size increasing the screw speed caused an increase in the extent of fibre degradation. On increasing the glass content, initially there was an increase in fibre degradation, but as the glass fibre content was increased to a level greater than 30%, the fibre length was found to increase. Folkes[24] attributed this latter effect to a large proportion of the material being immobile. Lunt and Shortall conclude that the differences in the properties of the final injection moulded composites were greater than can be attributed to the difference in fibre length alone and suggest other factors such as tensile strength of the processed fibre, interfacial shear strength or specific fibre orientation may be important.

In Lunt and Shortall's second publication[66] they examined sections taken from screw channels and found the major source of fibre degradation occurring in the melting region of the extrusion process. They described a commonly observed melting mechanism[67] shown schematically in Figure 17 and observed fibre degradation occurring at the interface between the solid bed and the melt film. They suggest that undispersed fibres may be present in the melt pool if the melting process occurs primarily by conduction and not shear stress, a situation that would tend to occur

at a low screw speed. They conclude by stating that useful increases in residual fibre lengths are unlikely to be achieved if the fibres are introduced prior to the melting stage and alternative processes in which the fibres are introduced into the molten polymer would appear to offer the ideal solution.

Folkes and Stuart[68] studied the incorporation of carbon fibres into nylon 66. In the absence of a die, samples showed little fibre orientation and poor dispersion. In the presence of a die, increased fibre degradation was observed. It was suggested that this effect can be attributed to increased back pressure that alters the flow profile in the extruder. They also found that on increasing the rear feed zone temperature by 30°C, average fibre length increased by 20%. On increasing the temperatures of all zones an average fibre length increase 45% was observed. On examination of samples removed from screw channels, they sited the feed zone to be the primary zone for fibre degradation. It was suggested that by raising feed zone temperature melting occurred earlier, reducing the crushing action subjected to the fibres by unmelted nylon pellets.

Kashfi[69] has examined the fibre length distribution in glass filled polypropylene at various points along the screw in a single screw extruder. The data produced showed the die produced a significant amount of fibre degradation. An increase in screw speed was found to reduce the average fibre length.

2.3.4 Injection Moulding

In the total processing operation, the final step is the moulding of the compounded pellets. There is plainly little purpose in producing pellets with a high fraction of long fibres if they are only to be subsequently highly degraded by injection moulding. In addition the first stage of an injection moulding cycle involves extrusion. Knowledge gained from publications based on injection moulding may also be relevant to the extrusion operation.

Murphy[70] in 1965 published one of the earliest papers on the injection moulding of fibre reinforced thermoplastic materials. Using a plunger machine there was observed to be a minimum filling pressure required to produce reproducible mouldings. Although no explanation

is given it was also noted that higher cylinder temperatures could improve physical properties. It was suggested that to improve the dispersion of the fibres high filling pressures and dispersion plates could be utilized. No comment is made however at the effect of such measures on fibre length.

Moulding glass reinforced nylon 6,6 with a preplasticising injection moulding machine, Filbert[71] found decreasing rear zone temperature reduced the average fibre length. Increasing the back pressure had a similar effect. Results also show that fibre breakage was closely related to the peripheral speed of the screw. Increasing screw speed was found to reduce average fibre length. Yang, Farris and Chien[72] studied the effect of regrind on the tensile strength of glass reinforced nylon 6,6, they observed a uniform decrease in tensile strength with number of mouldings. This was attributed to the cumulative breakage of fibre length through mechanical working. It was suggested that critical length could be varied with different coupling agents applied to the fibre surface. A model was derived that suggested that when fibre content is high the tensile strength decreases appreciably with increasing critical length.

2.3.5 Conclusions from Reviewed Literature

From this brief review we can conclude that to enable fibres to make the maximum contribution to enhance composite properties, fibre length must be maintained by:

1. Addition of the fibres while the material is molten.
2. Maintaining processing temperature as high as degradation allows.
3. Permitting only low screw speeds on extrusion and injection moulding.
4. Allowing the lowest possible back pressures either when injection on by the die on extrusion.

From available literature covering a variety of melt compounding techniques, it would seem that the best way to incorporate these factors in a compounding operation would be by the adoption of a twin screw extrusion compounding route. This technique will be reviewed in the following section.

2.3.6 Twin Screw Extrusion

The twin screw extruder would seem to be the best compounder in which fibres could be introduced into polymer melt for the following reasons:

(i) There is much more versatility in the feeding arrangement of the polymer and the fibre. There is the possibility of introducing fibres either continuous or chopped at some point along the barrel when the polymer is already molten.

(ii) The twin screw extruder relies on the action of its screws to produce mixing. Depending on whether the extruder screws are co or counter rotating the material is either continuously branched and joined repeatedly or subjected to calendering, compression and shearing each time it passes the intermeshing point. Single screw extruders rely on the development of high die pressures.

(iii) There is an improvement in dispersion by the mixing action.

(iv) Less wear takes place in the working parts of the extruder as a result of addition of fibres to molten polymer.

2.3.6.1 Twin Screw Extruder Processing

The main difference between single and twin screw extruders is the mechanism of conveying. In single screw extruders conveying is based on frictional forces in the melt conveying zone - drag flow. Although drag flow is present in some types, twin screw extruders are usually designed to have a high degree of positive conveying.

Based on the investigations of a wide number of types of twin screw extruder designs, authors have suggested the following benefits can be obtained by the positive nature of conveying in a twin screw extruder:

(i) A more homogeneous product[73,74]. This is a result of a narrow residence time distribution. Nearly all particles have spent the same amount of time travelling through the barrel, subjected to the same degree of heat and work.

(ii) Effective mixing action[76,77,78]. This can have a major influence in types and levels of additives used. The improved wetting and dispersion obtained with multiscrew extruders has allowed a reduction in the amount of additives used e.g. stabilizers, antioxidants and lubricants, which can lead to products with superior final properties. The mixing action also allows higher concentrations of fillers or reinforcing fibres to be added.

(iii) Better control of devolatization[73] with proper screw design, it is relatively easy to expose large areas of the screws to a devolatilizing opening and keep this opening from being clogged by surging polymer - a well known problem with single screw machines in devolatilizing service. Also, it is possible with twin screw machines to have a number of devolatilizing ports with a rapid sequence of decompression for devolatilizing followed by compression.

(iv) A wide processing viscosity range[76,78,79]. Twin screw extruders can handle viscosities from a few centipoise to a million centipoise.

(v) The requirement of less ancillary equipment[74]. The superior intake capabilities of a twin screw system often eliminate the need for crammer feeders and other expensive devices. Usually twin screw extruders require considerably less space than single screw units of similar output. In many cases twin screws are more easily removed than their single screw counterparts, so if screw changes or cleaning becomes necessary, maintenance costs and down time are reduced.

(vi) Ability to operate with large cross section dies[74,75,77]. Single screw machines are dependent particularly for any mixing action on the development of high back pressures. Thus with dies of large cross section difficulties are encountered in achieving such pressures.

(vii) Self cleaning action[73,74,78]. Twin screw extruders can be designed with self wiping screw profiles.

(viii) Less waste of energy[75]. Twin screw extruders can be designed as polytropic machines in which the mechanical work does not supply the total energy, but only part of it and where additional energy is supplied by heaters. Single screw extruders are commonly autogenous

in nature. Mechanical work increases the temperature of the molten polymer higher than the extrusion temperature. Cooling systems therefore have to be devised to transfer heat out of the melt. With the twin screw system there is also generally better temperature control and heat transfer.

(ix) Down stream metering[53,74,80]. Steady and uniform conveying throughout the system allows down stream metering of other materials into partially filled flights for safer intake.

(x) Surge free discharge[73]. This stems from the fact that melt travel is little affected by pressure and viscosity.

It is worth noting that this list includes generalisations, processing characteristics are very dependant on different types of machine construction and specific screw designs.

2.3.6.2 Characteristics of Twin Screw Extruders

Four[81] different types of twin screw extruder can be found on the market today. The screws can operate in the same or opposite directions (co-rotating or counter-rotating extruders). Although varying degrees of intermeshing are possible either type of screw operation can be generally described as intermeshing or non-intermeshing.

Non intermeshing extruders can be regarded more or less as two single screw machines with some internal action. With intermeshing screws the process fluid is displaced positively from hopper to die in C-shaped chambers which are moved by the screw rotation.

For counter-rotating systems the direction of rotation can be either inward or outward. To allow as much material as possible to be fed, it is usual for the screws to turn outwards at the top and inwards at the bottom.

The literature is often poorly differentiated with regard to these four possible geometries, which can be a serious problem as even among themselves twin screw extruders can be as different from another as they are from single screw machines[83]. The benefits and draw backs of co or counter-rotating geometries seems to have been a controversial issue for forty years. The benefits and draw backs have been published in a number of publications[73,75,82,83,84,85]. Some of

the arguments used seem to be based on personal bias rather than objective scientific analysis. The complexity of flows that take place in twin screw extruders is the main reason that there has been little success in establishing a valid description of their operation or performance, the development of successful machine being a result of empirical knowledge with efficient constructional engineering[84]. Janssen even calls twin screw extruder technology an art!

The intermeshing corotating extruders can be further subdivided into low and high speed machines[84], these are much different in design operational characteristics and applications. The low speed extruders have a closely fitted flight and channel profile, therefore they have a high degree of positive conveying characteristics and run at low speeds (generally 10-20 rpm). These machines are used primarily in profile extrusion applications.

The high speed corotating extruders generally have self wiping characteristics. However this does not mean the flights close off opposite channels. In fact in these designs, there is considerably opportunity for the material to leak back from one screw channel into a channel of the opposite screw. Thus these machines have a low degree of positive conveying. The geometry allows these extruders to run at high speeds.

The intermeshing counter-rotating extruders can be further sub-divided into conical and cylindrical extruders[84]. Conical extruders have the advantage of reduced shear rates towards the die and more space to incorporate thrust bearings. They are however more difficult to manufacture, cannot take advantage of reduced shear rates towards the die and are not able to take advantage of the design flexibility in combining different screw elements[75,86] in the "building block" principle[80]. Counter-rotating extruders allow a maximum sealing of the screw channels so the maximum degree of positive conveying can be achieved with intermeshing counter-rotating twin scre extruders.

When considering the incorporation of fibres using a twin screw extruder an important question is: Which type or screw rotation ensures the best mixing? Ferns[53] argued in favour of co-rotating screws on two grounds: Firstly because of their operating principle, counter-rotating screws must have a certain minimum gap between screws and so therefore cannot be fully

intermeshing, as fully intermeshing screws are required for self cleaning action the screws cannot be self cleaning. In the co-rotating twin screw extruder, the material in the screw groove is transferred to the groove of another screw when passing the intermeshing point, the screws can be fully intermeshed and so self cleaning. Second the material is subjected to higher temperature and hence less temperature control in counter-rotating screws than in a co-rotating arrangement. In the latter a greater proportion of the material is in contact with the cooling surface of the barrel, and the high peak temperature which prevails as material passes between counter-rotating screws is avoided.

Ranwedaal's[84] analysis concludes that the co-rotating extruder is quite effective in its distributive mixing capability because of the large shear rates and frequent re-orientation of the material. The counter-rotating extruder is more effective in its dispersive mixing capacity. This is thought to be due to the local higher stresses the material is exposed to when it is drawn through the intermeshing region. Based on these results one would expect the co-rotating to be better suited to melt blending operations. Where as the counter-rotating would be better suited where solid fillers have to be dispersed in a polymer matrix.

2.4 The Compounding of Short Fibre Kevlar Fibre into Thermoplastics

If the properties of Kevlar 49 are compared to other reinforcing fibres that are currently well established in short fibre reinforced thermoplastics, Kevlar 49 would seem to have potentially very promising future.

Properties for epoxy impregnated continuous Kevlar fibre are well proven and in many cases superior than S glass epoxy systems[87]. However Kevlar reinforced thermoplastics are generally accepted to be at an early stage of development[88]. Most of the work to date having been performed on small scale preparations of such composites.

Kevlar fibre is ductile in the sense that it can be bent through a small radius without breaking, this is in complete contrast to glass and carbon fibre which fail in a brittle fashion. The brittle fracture behaviour of carbon fibre has been demonstrated by the successful application of the

Griffith equation to it[89].

It was observed by Bader and Bowyer[90] that the fracture strength of short fibre reinforced thermoplastics are controlled by the fracture strain of the fibre, and it was suggested that this could be substantially increased if fibres that withstood higher strains were employed. Kevlar fibres having better properties of strength than glass yet a higher strain to break than carbon or glass would appear to offer excellent prospects in improving strength properties. The combination of Kevlar fibre with glass or carbon in a two species hybrid short fibre composite should be more attractive than the combination of carbon and glass, since values for tensile modulus and elongation at break of Kevlar 49 fibre are compromised between those of carbon and glass. The load and its effect on strain would be expected to be better distributed between fibres. Kevlar and carbon may be considered more compatible than glass and carbon due to their similar coefficients of expansion, resulting in a lower level of internal stresses produced during composite fabrication.

Blumentritt et al[91,92] in a study to develop data on a variety of short fibre reinforced thermoplastics matrices, incorporated 3/8" chopped unsized Kevlar 49 fibres into a number of thermoplastic materials. Powdered resin was mixed with fibres in a V shaped dry blender and subsequently compression moulded with fibres orientated in one or two dimensions. Random in plane and undirectional composites were found to have a very good mechanical properties. The tensile properties of the composites produced are shown in Table 4. From the measure of the stress-strain curve area, Kevlar composites appeared to be tougher than corresponding inorganic fibre composites. In a later publications[93] the fracture surfaces of the composites produced above were described. Good adhesion between Kevlar and polyethylene was observed. Favre and Merienne[94] however using fibre pullout tests found the adhesion between Kevlar and an epoxide and Kevlar and a polycarbonate to be as low as 4 and 11 MPa respectively.

In an attempt to improve the dispersion of discontinuous Kevlar fibres in polyethylene and ionomer, Takayanagi et al[95] modified the fibre surface of Kevlar fibre using a metalation reaction in dimethyl sulphoxide to provide the surface with functional groups such as the - octadecyl group, carboxymethyl group, and acrylonitrile. Treated fibres had a rougher surface than untreated fibres. Composites based on carboxymethyl modified Kevlar were found to have superior mechanical properties than those based on unmodified Kevlar.

More recently Therberge et al[96] stated the use of Kevlar fibres in thermoplastics has been slow to develop because surface energy of the fibre does not allow facile wetting at the interface and the unique compressions failure made of the fibres does not allow shear intensive mixing. Kevlar fibres are evaluated as reinforcing fibres in nylon, polyester, polycarbonate, polyphenylene sulphide, polypropylene and polystyrene resins. It was observed that only in the case of nylon was a significant degree of property enhancement achieved. Aramid fibre reinforced thermoplastics were found to yield isotropic mechanical and thermal properties, low isotropic mould shrinkage, improved wear abrasion resistance and improved temperature deformation resistance. No explanation was given for these isotropic mechanical and thermal properties and no information was revealed about the compounding route.

One potentially important area for the exploitation of Kevlar short fibre reinforced thermoplastics that has not been investigated is the potential of these tough fibres to enhance impact strength.

Handcox and Wells[97] included in their list of methods of improving impact properties of carbon fibre reinforced materials the inclusion of a percentage of fibres such as Kevlar which as mentioned earlier has a higher strain to break carbon fibre. Another suggestion made by the authors was the ue of duplex fibres which consisted of an outer sheaf which could bond well to the matrix and an inner fibre that when pulled from the outer sheaf could expend a considerable amount of energy. The structure of Kevlar as reviewed in Section 2.2.4 consists of an amorphous skin surrounding crystalline fibres many offer the possibility of this energy absorbing mechanism.

From the available literature it is clear that much work is necessary to exploit these promising materials.

2.5 Methods to Evaluate the Effect of Compounding Technology on the Stress Transfer Interface of Short Fibre Reinforced Thermoplastics

Much attention has been given to the manner in which composite properties are dictated by fibre and matrix properties, and also fibre length and orientation. An additional factor that affects composite properties is the nature of the stress transfer interface between the fibre and matrix. In order to fully evaluate the efficiency of a compounding process it is necessary to evaluate the effectiveness of the stress transfer interface. Most computational techniques that have been developed to assess this property have taken into consideration test bar fibre length distributions in conjunction with a model that describes composite behaviour. The method adopted by Bader and Bowyer[98], McNally et al[99] and Lunt and Shortall[66] utilise the Kelly-Tyson elastic fibre, plastic matrix model described in Chapter 1. For the case of misaligned short fibres according to the model the theoretical strength of the composite can be expressed as:-

$$\sigma_{uc} = Z \sum_{i}^{l_i<l_c} \frac{\tau_u l_i V_{fi}}{d} + \sum_{j}^{l_j>l_c} \sigma_{uf} V_{fj} \left(1-\frac{l_c}{2l_j}\right) + (1-V_f)\sigma'_m \qquad (9)$$

where

τ_u = interfacial shear strength

V_{fi} or V_{fj} = Volume fraction of fibres of length i or j

σ_{uc} = tensile strength or composite

σ_{uf} = strength of fibres

σ'_m = stress carried by matrix at fibre failure strain

l = fibre length

l_c = critical fibre length

Z = orientation parameter

V_f = total volume fraction

This is similar to equation 8 but the coefficient Z has been added which is the orientation factor.

This has a value equal to or less than 1.

Bader and Bowyer devised a method to calculate interfacial shear strength using mechanical property data and a measure of fibre length distribution. They used the definition of critical length in its broadest sense and suggested that at any value of composite strain there is a critical length fibre. The shape of a stress strain graph for an elastic fibre reinforced plastic matrix being a result of fibres progressively becoming sub-critical. In their method two values of strain are selected e_1, and e_2, such that $e_2=2e_1$. The ratio of the loads at these two strains are obtained from the stress-strain graph. An assumed value of τ_u, the interfacial shear strength, is selected and corresponding "critical lengths" at strains e_1 and e_2 are calculated. Using the measured fibre length distributions for the tensile bars, the ratio of the loads carried by the fibres at strains e_1 and e_2 are calculated by the use of the following equation:-

$$\sigma_e = \sum^{l_i<l_c} \frac{\tau_u l_i V_{fi}}{d} + \sum^{l_j>l_c} E_{fe}\left(1-\frac{E_f e r}{2 l_j \tau_u}\right)V_{fj}+(1-V_f)\sigma_{me} \qquad (10)$$

where

σ_e = Load at strain e

V_{fi} or V_{fj} = Volume fraction of fibres length i or j

σ_{me} = Stress in matrix at strain e

l_c = "Critical length of fibre" at strain e

The value of the calculated ratio is compared with the ratio measured from the stress-strain graph. The interfacial shear strength τ_u is adjusted and hence l_{e1} and l_{e2} modified until the two ratios are the same. The value of τ_u was assumed to be the final correct value. The critical length l_c can be calculated using the equation 4.

It is important to realise that the term "critical length" at a specific composite strain is not the same as the widely recognised term of critical length that exists only at the composite failure strain.

McNally et al[99] used an alternative approach to calculate interfacial shear strength. They used equations that approximated to equation 9 as expressions for both tensile strength σ_{uc} and

composite tensile modulus E_c. The orientation factor for modulus was denoted as D and for strength as D^1. On the basis of strength and modulus anisotropy data they suggested D and D^1 have very similar values. Using experimentally measured values of σ_{uc} and E_c together with the fibre length distribution and an assumed value of τ_u. Values of D and D^1 were calculated. This process was repeated for different values of τ_u until the calculated values converged. The corresponding value of was then taken to be the interfacial shear strength.

Another method used by McNally et al to assess compound quality was the designation of a stress transfer interface efficiency parameter for stiffness and strength. Here using the value of τ_u calculated above, the average stresses for the fibres present in the compounded product were calculated by the use of the Kelly-Tyson model for the tensile strength at the ultimate strain of the composite; and at a small strain for stiffness. These values were divided by a summation of stresses obtainable if the fibres were undamaged at each strain.

Lunt and Shortall[66] assuming an interfacial shear strength used equation 9 to calculate composite strength with an assumed value of the orientation factor and a measured estimate of fibre length in the manufactured composite.

They divided this value by the calculated value of strength that would have been achieved if the fibres had retained their initial length. The value of this fraction was the reinforcing efficiency f.

Perhaps the simplest method of assessing compounding techniques was suggested by Hollingsworth and Sims[63] who simply used a fibre utilization efficiency value which has observed value of composite stiffness divided by the calculated value based on the rule of mixtures.

The manufacturing of carbon fibre

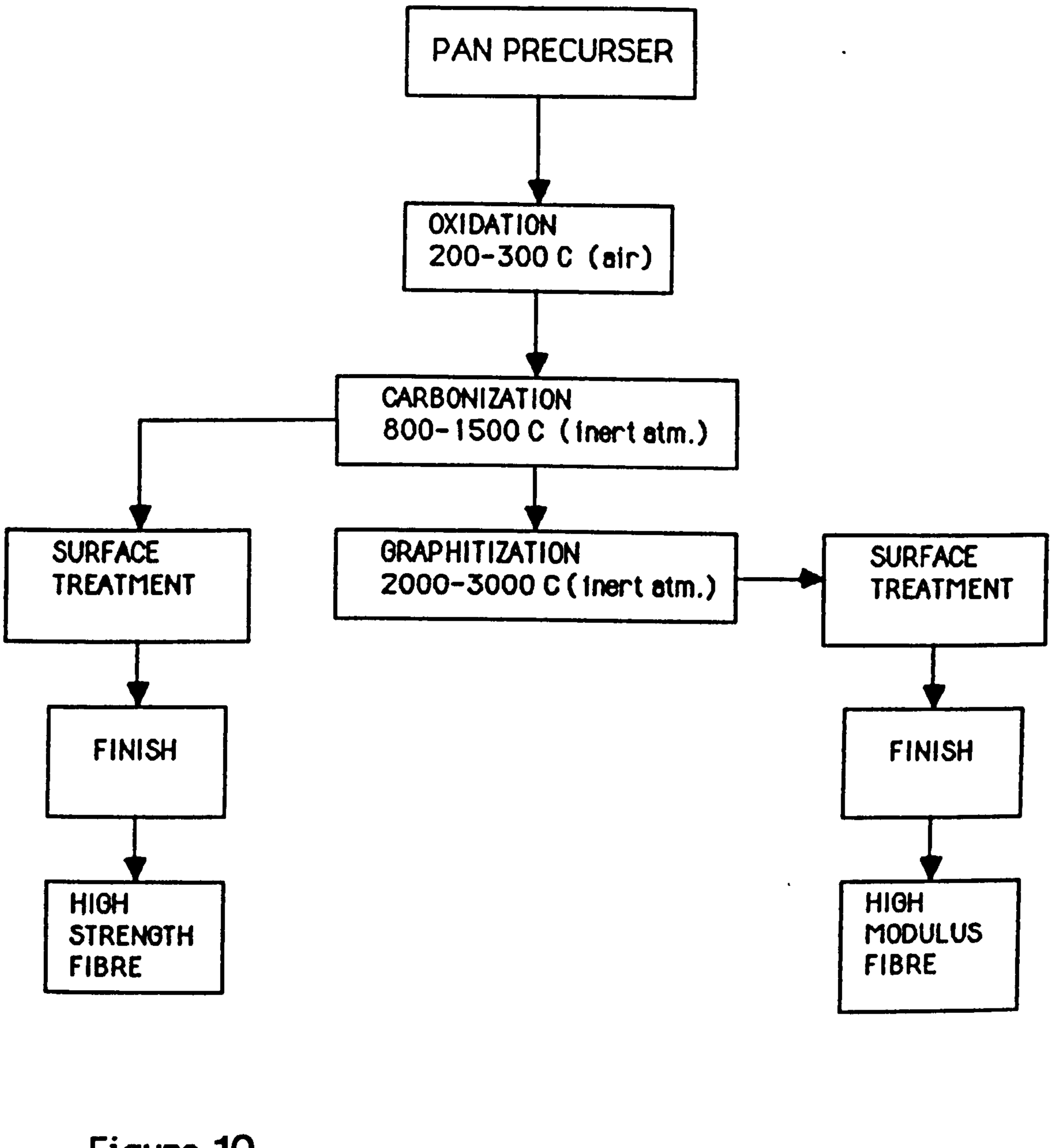

Figure 10

The influence of heat treatment on the tensile strength and Youngs modulus of carbon fibres produced from a PAN precursor

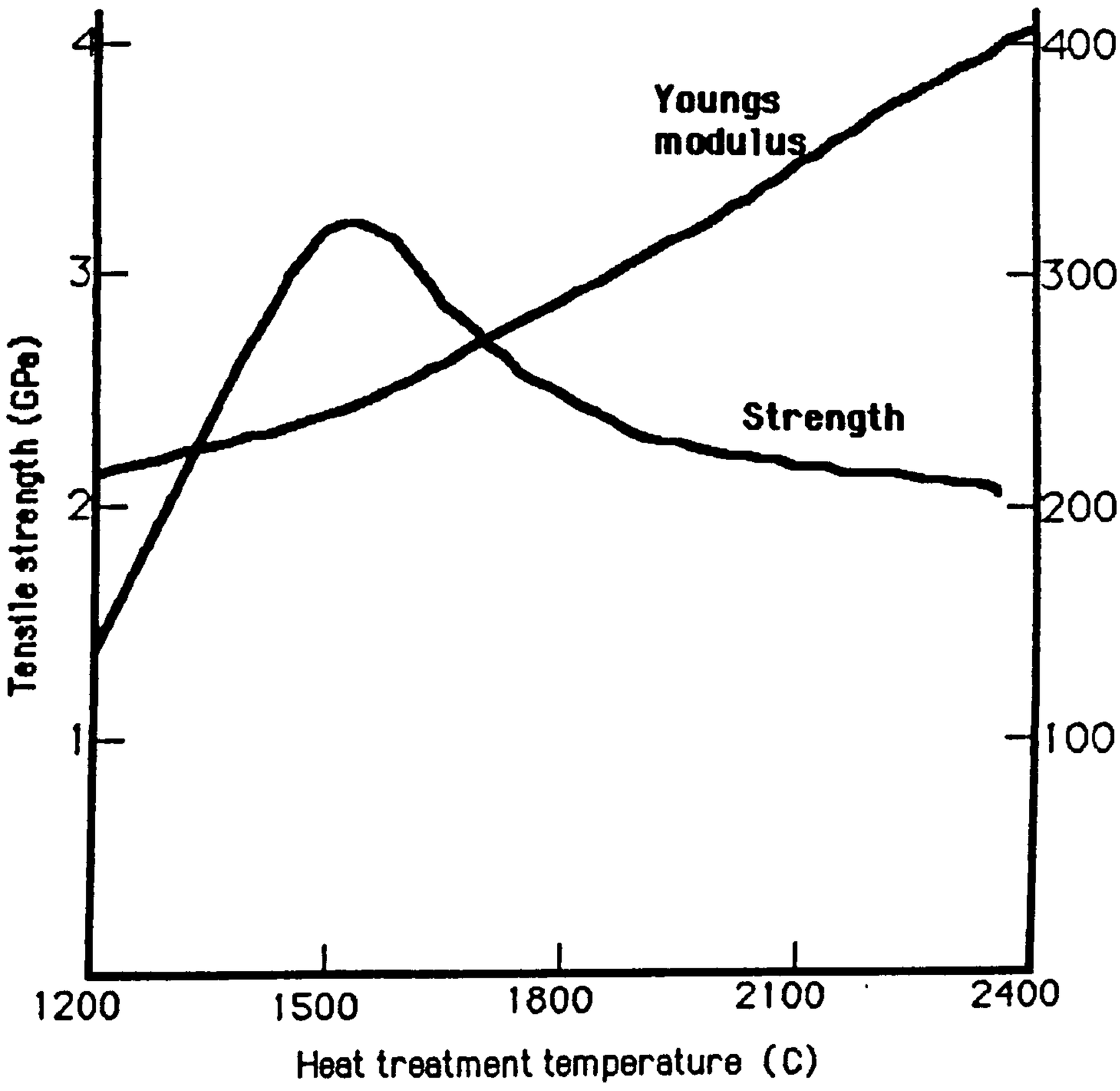

Figure 11

Specific properties of reinforcing fibres

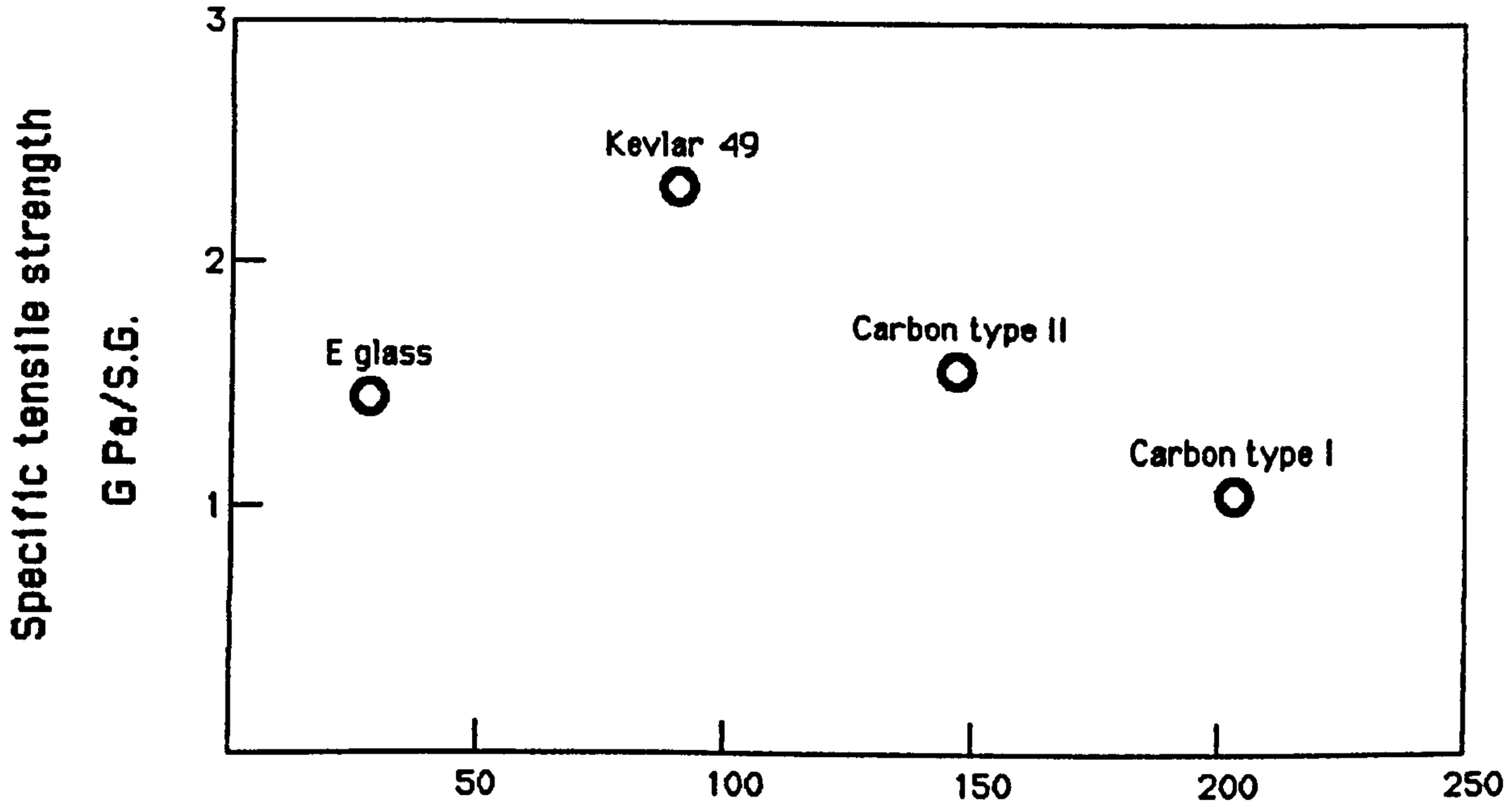

Figure 12

Diagrammatic representation of glass forming scheme

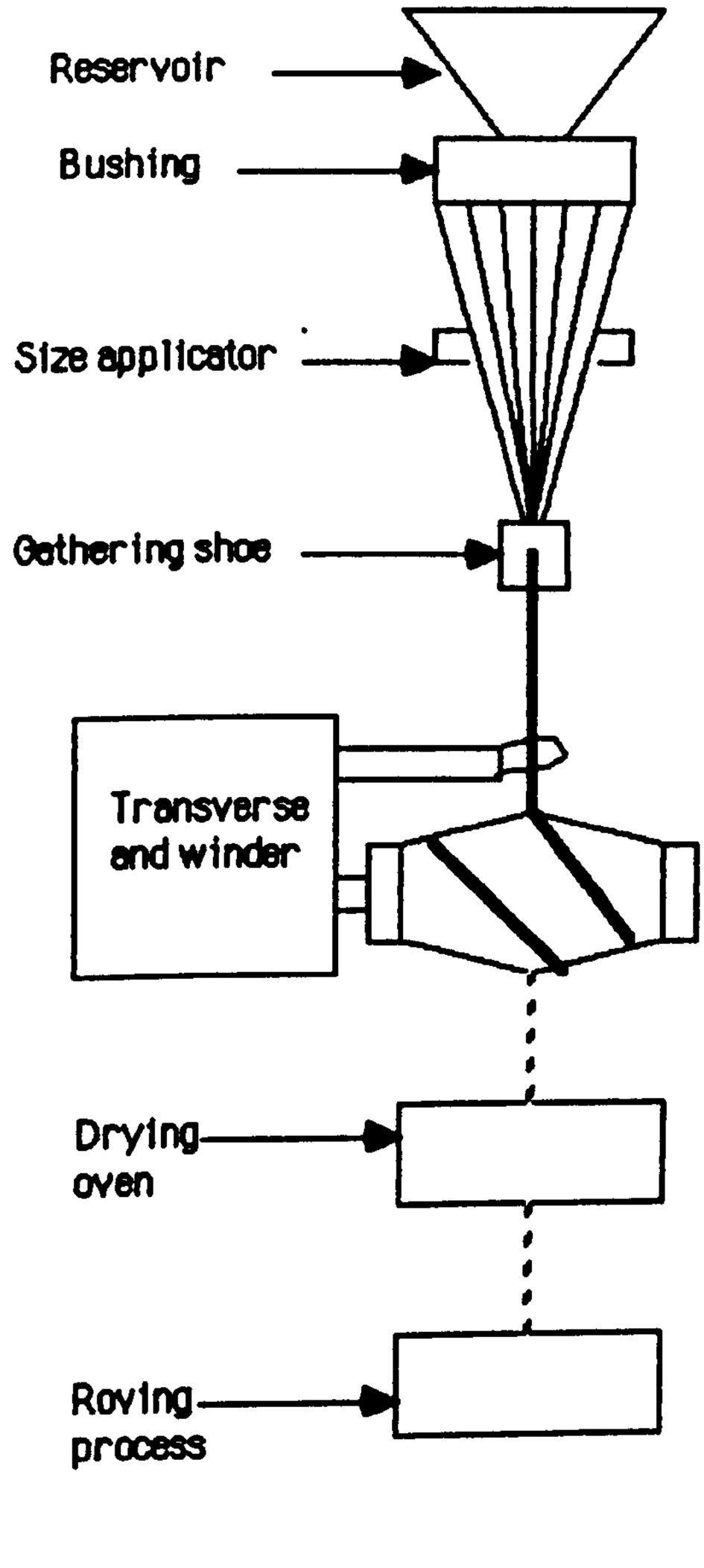

Figure 13

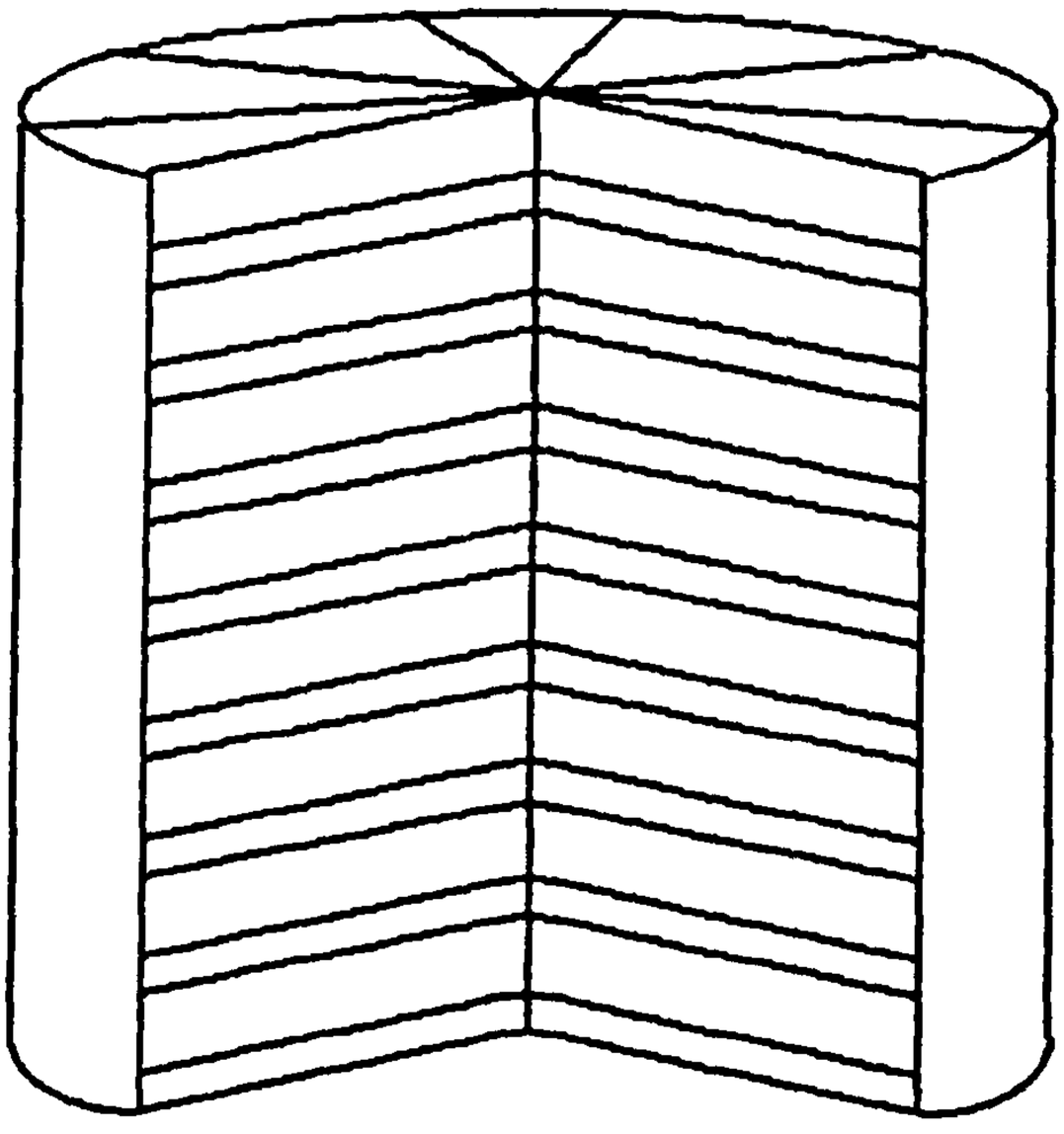

Schematic representation of the structure of aromatic polyamide fibres

Figure 14

(From Dobb,Johnson & Saville 1980)

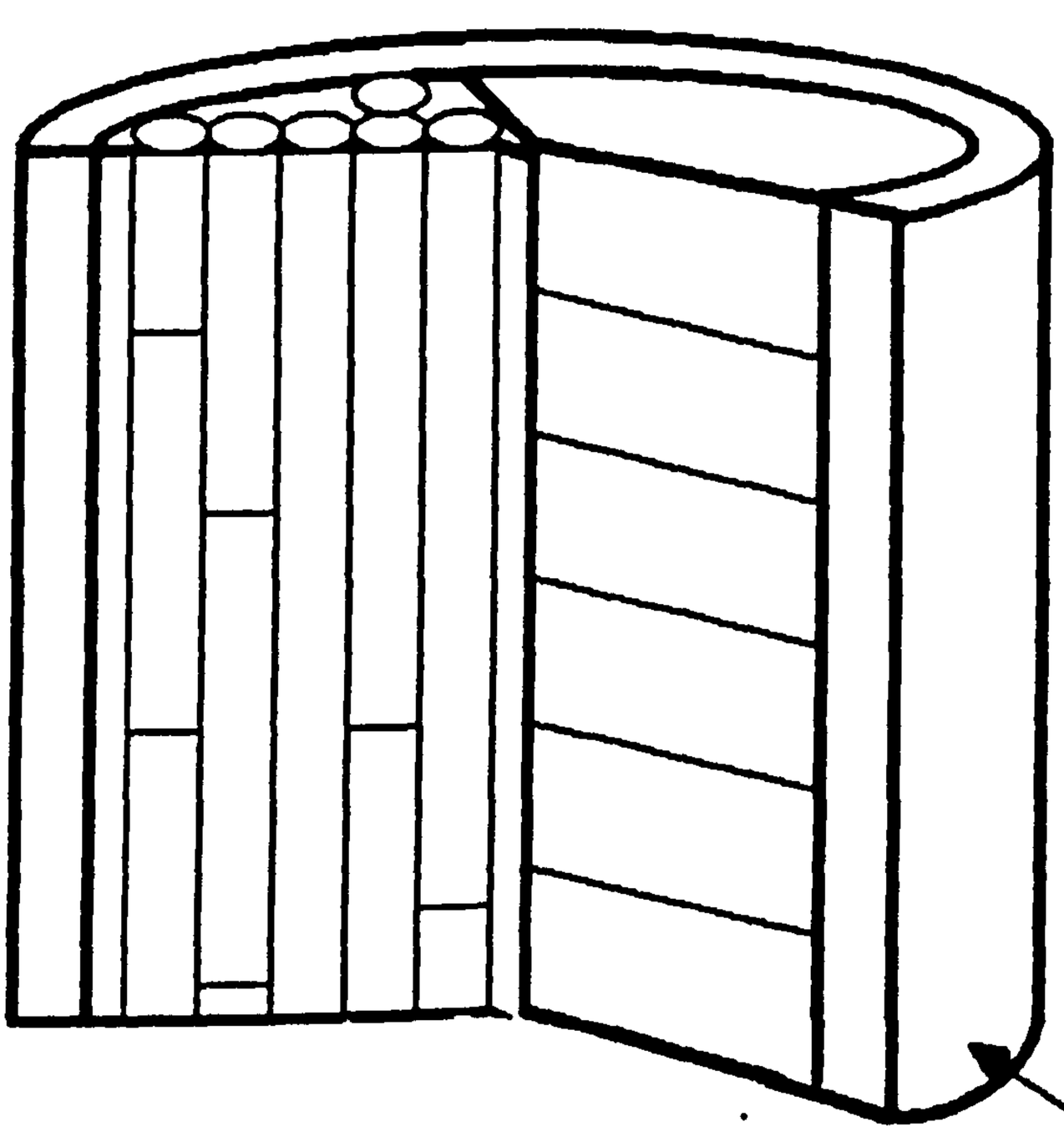

Schematic representation of the structure of aromatic polyamide fibres

Figure 15

(From Li,Allard & Bigelow 1983)

Stress-Strain curves of fibres used in this study

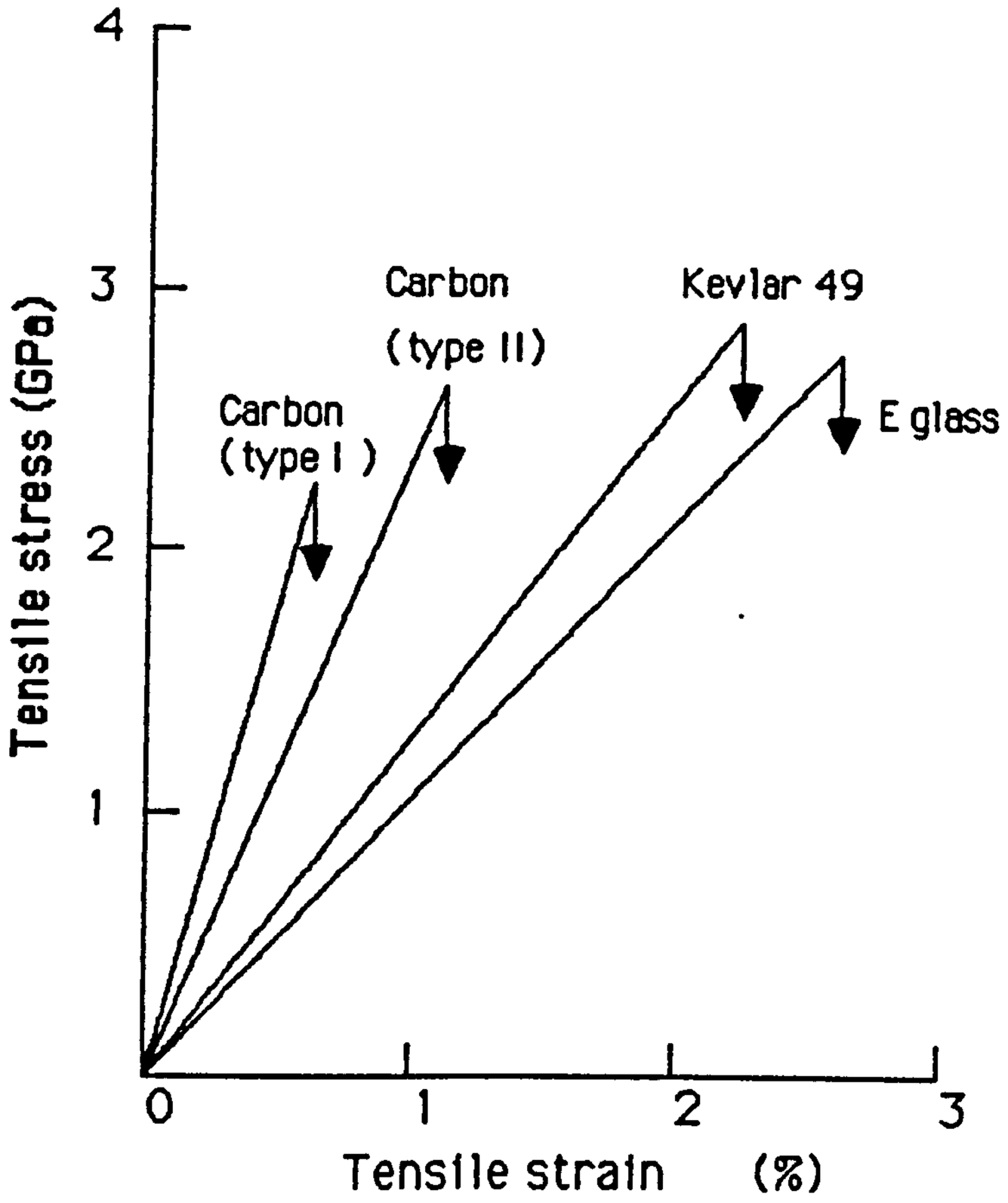

Figure 16

Conventional single screw compounding extruder flig
cross section

Figure 17

The Gays TS40 DV-L twin screw extruder

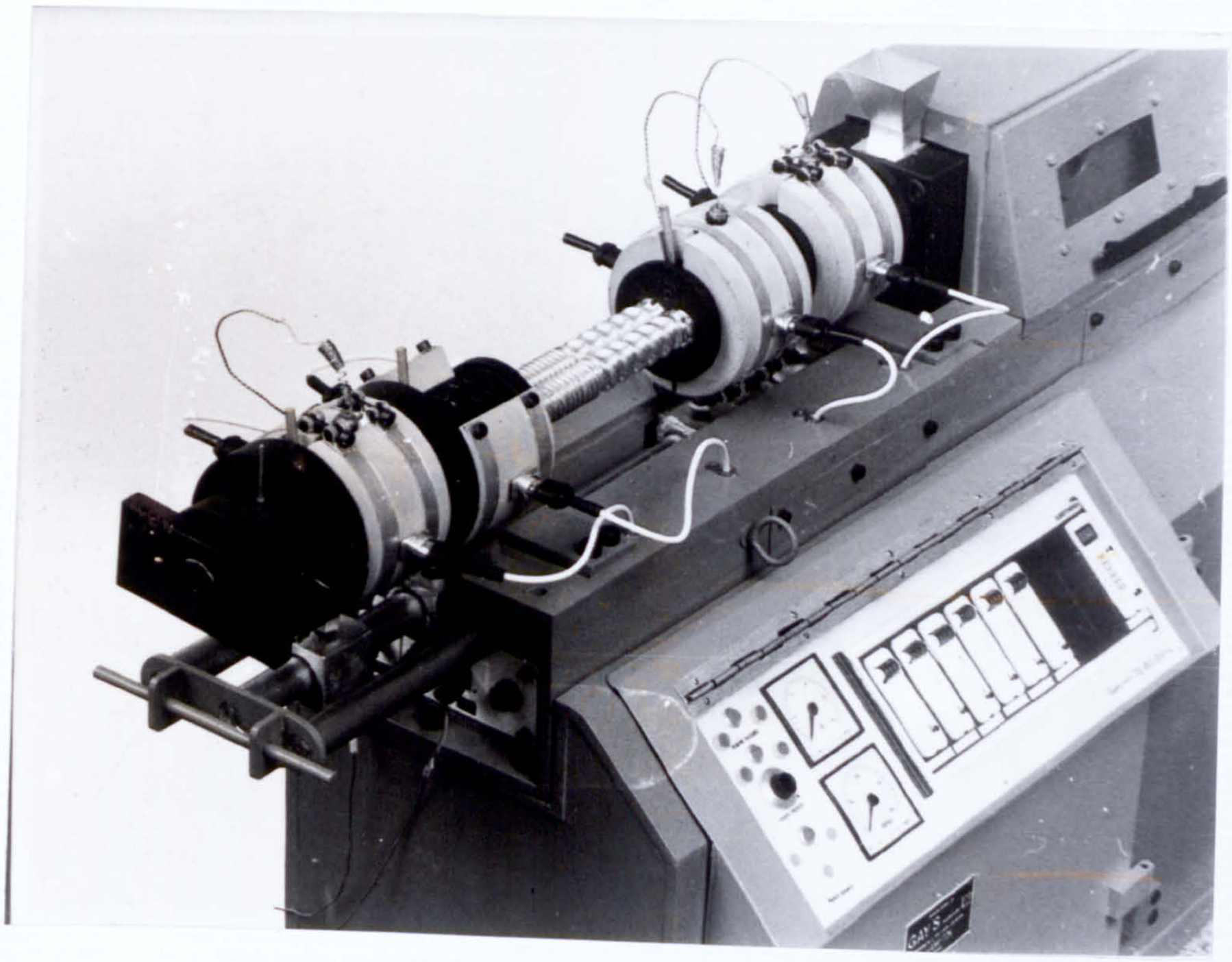

Figure 18

Screw configurations possible for the Gays twin-screw extruder with the 17:1 LID ratio variant

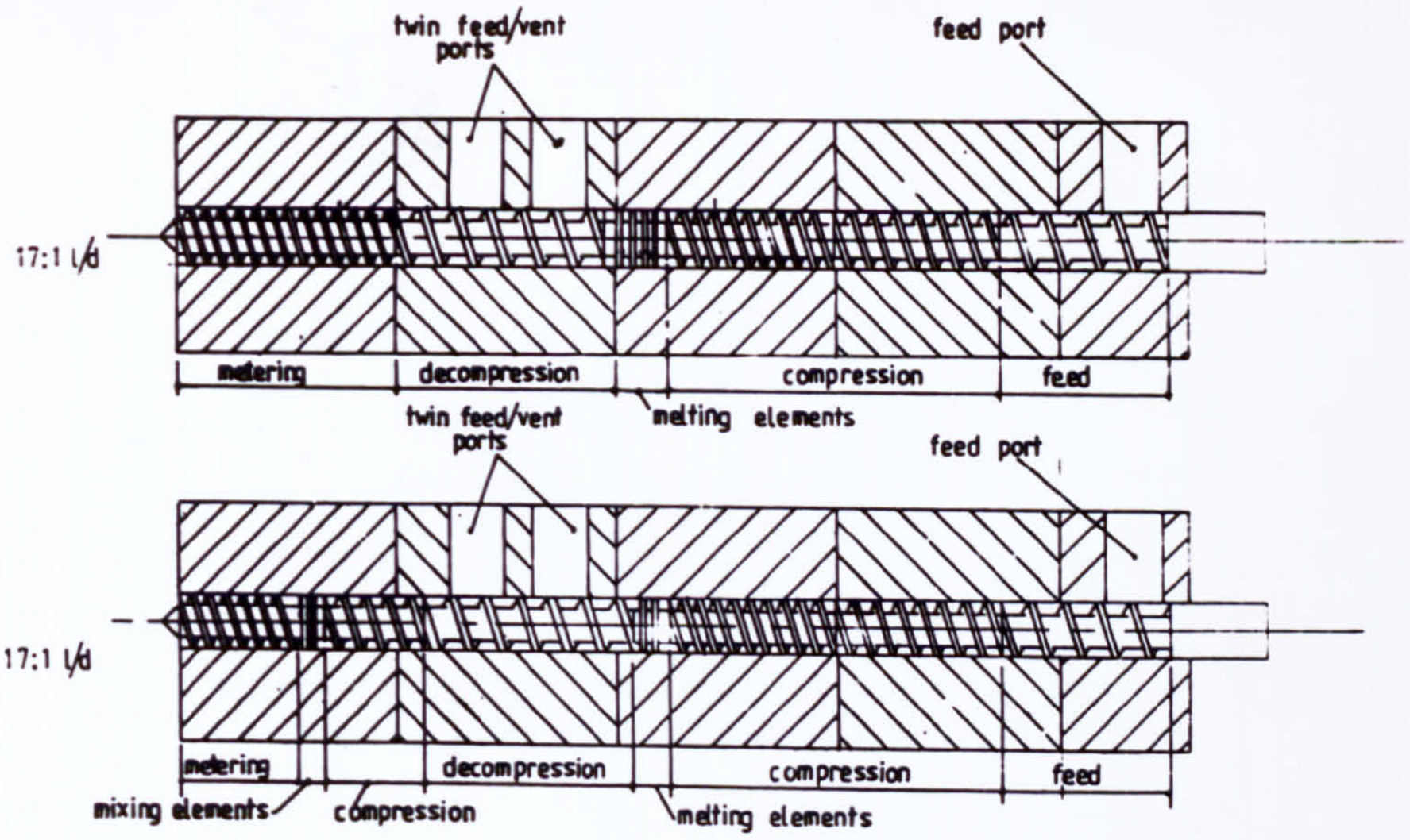

Figure 19

The design features of the Baker Perkins MPC/V50 twin screw compounder

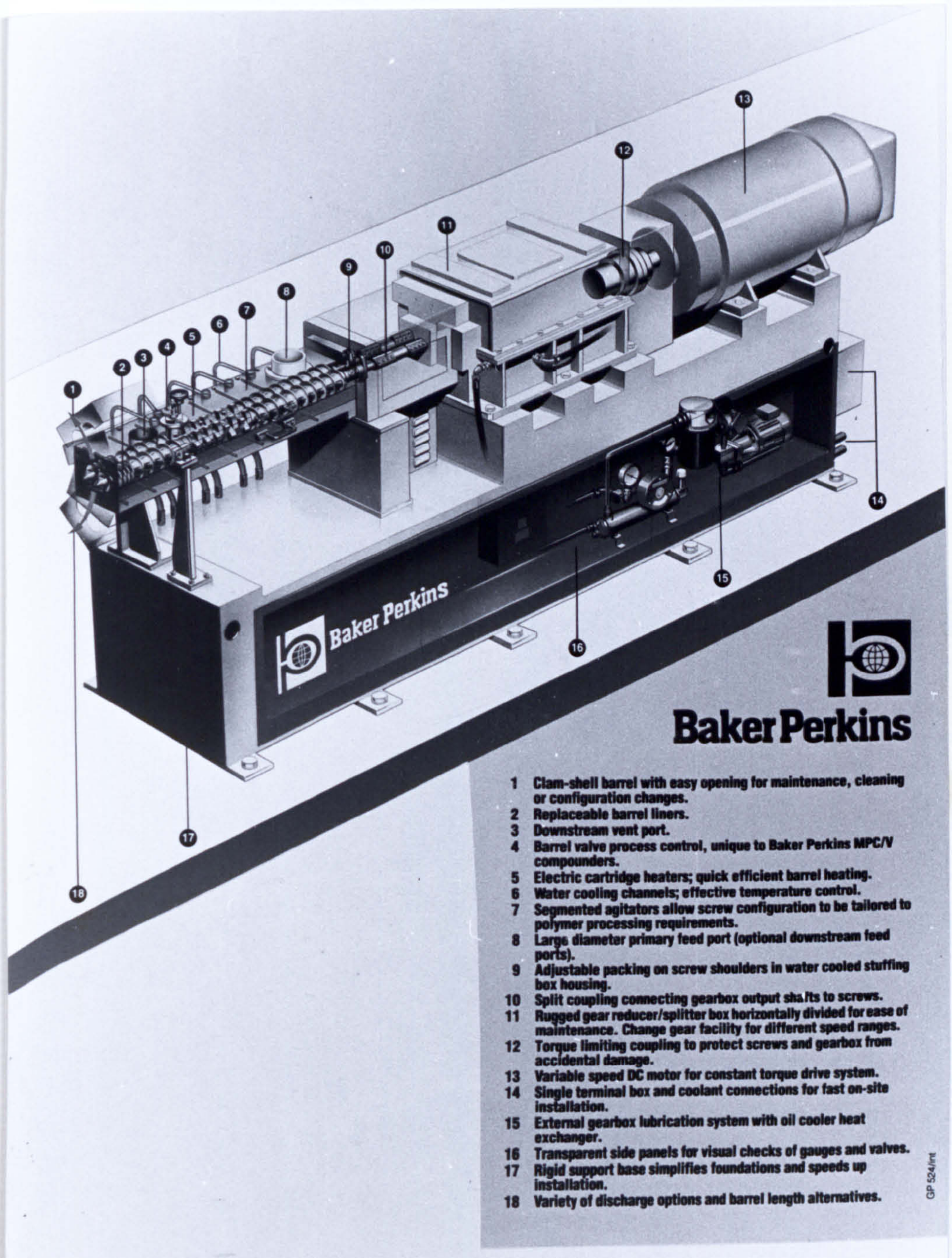

Figure 20

The barrel valve feature of the Baker Perkins MPC/V50 twin screw compounder

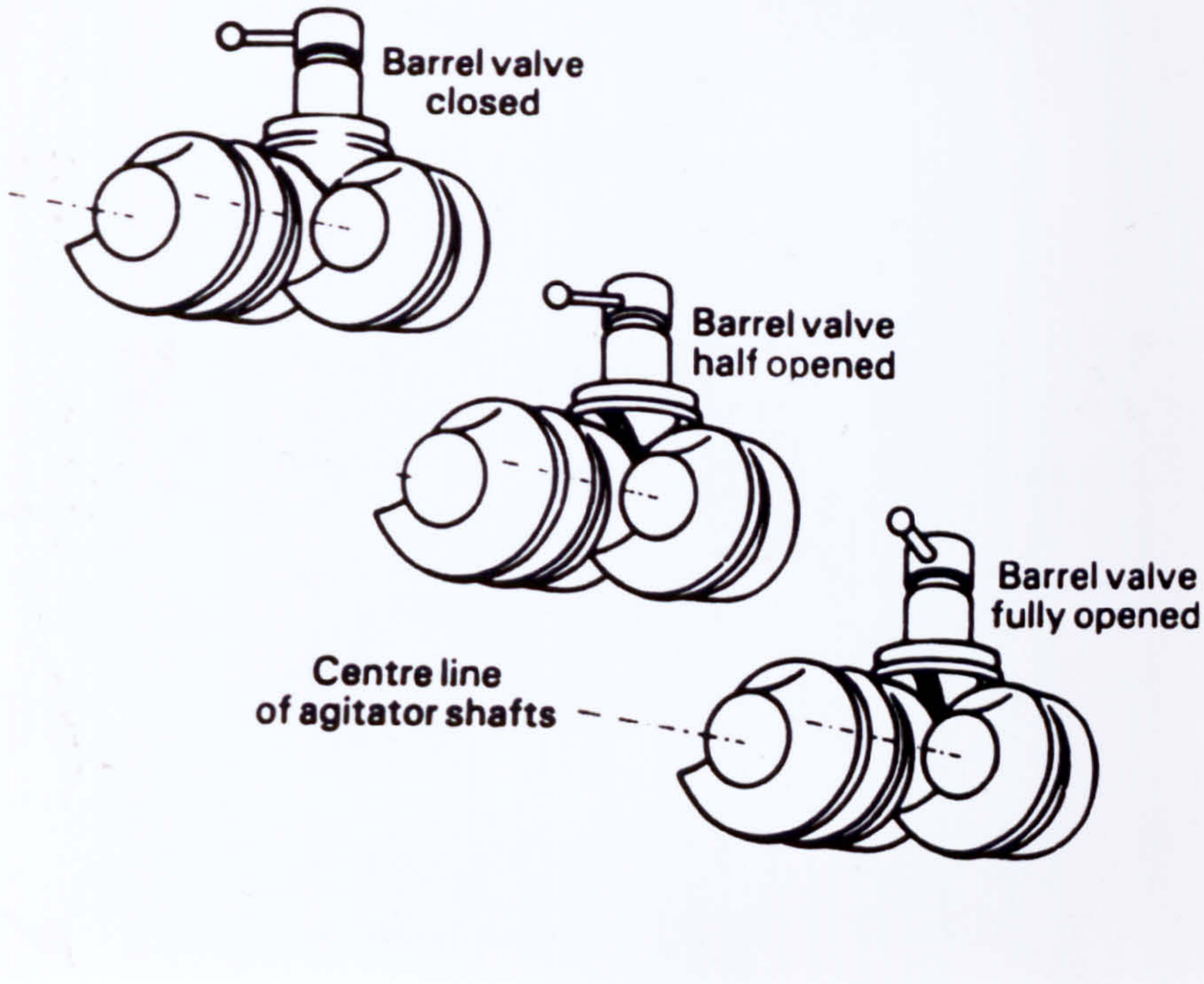

Figure 21

The configuration of crosshead extruder located at the end of the MPC/V twin screw compounder

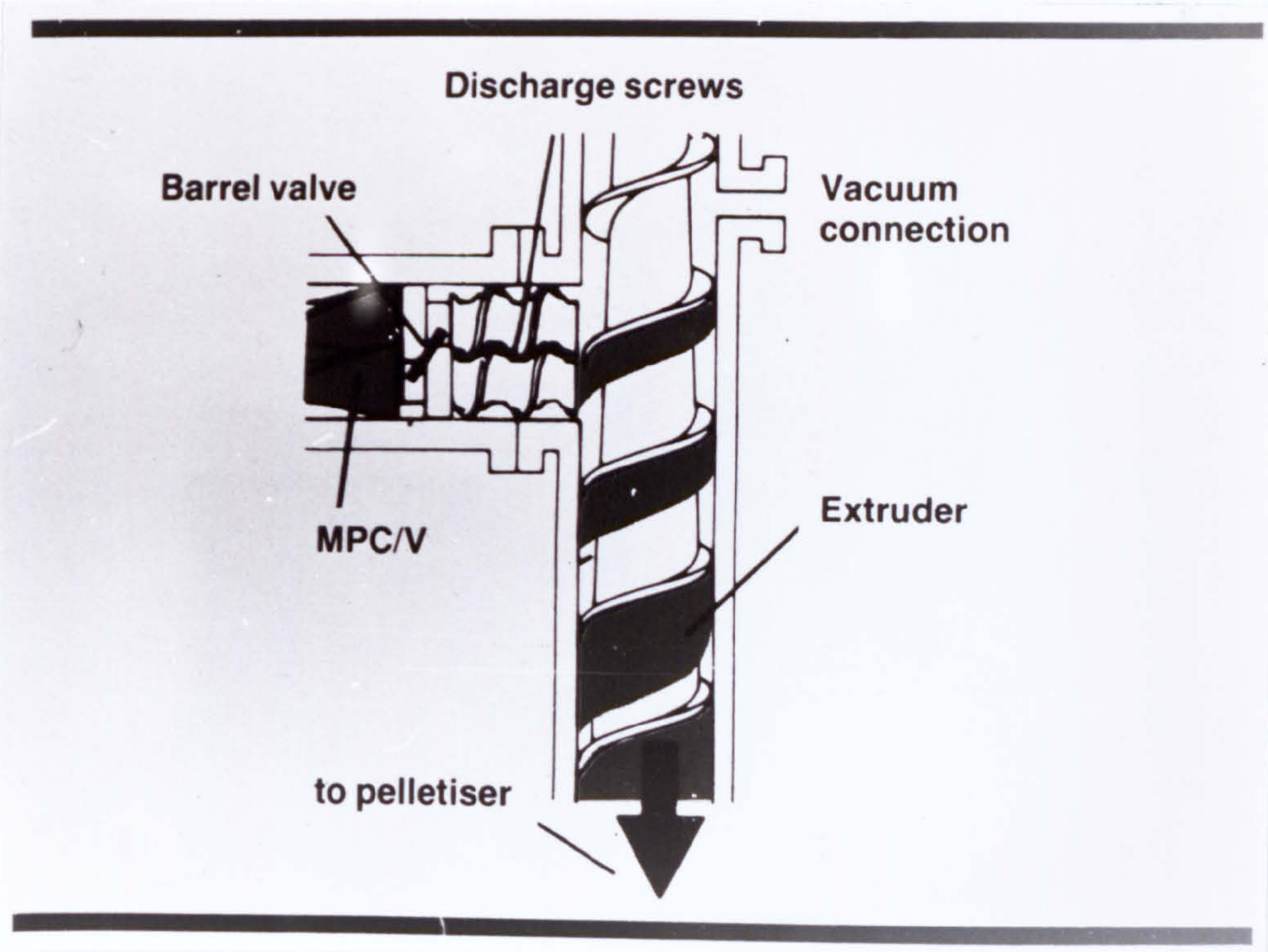

Figure 22

Crystalline and amorphous thermoplastics. Benefits of reinforcement with 30 % glass fibres

	Heat distortion temperature		Tensile strength	
	Actual C.	Enhancement C.	Actual (MPa)	Enhancement (MPa)
Crystalline				
Nylon 66	248	+153	180	+100
PEEK	300	+145	175	+75
PBT	210	+145	135	+75
Nylon 6	212	+137	160	+100
Polypropylene	148	+87	86	+51
Acetal	164	+58	140	+72
Amorphous				
PES	216	+15	145	+55
Modified PPO	145	+15	125	+59
Polycarbonate	140	+10	120	+56
ABS	100	+10	90	+40

(From Maxwell 1983)

Table 1

Typical Quoted Properties of Carbon, Glass and Kevlar Fibres at 20 C

Property	Units	Carbon (PAN) Type 1	Carbon (PAN) Type 11	E-glass	Kevlar 49
Diameter	um	7.0-9.7	7.6-8.6	8-14	11.9
Density	gcm^{-3}	1.95	1.75	2.56	1.45
Youngs Modulus	(GPa)	390	250	76	125
Tensile Strength	(MPa)	2.2	2.7	1.4-2.5	2.8-3.6
Elongation to Fracture	%	0.5	1.0	1.8-3.2	2.2-2.8
Coefficient of Thermal Expansion (0-100C)	$10^{-6}\ C^{-1}$	-0.5to-1.2 (parallel) 7-12 (radial)	-0.1to-0.5 (parallel) 7-12 (radial)	4.9	-2 (parallel) 59 (radial)
Thermal Conductivity	$WM^{-1}\ C^{-1}$	105	24	1.04	0.04

TABLE 2

PROPERTIES OF SHORT FIBRE REINFORCED THERMOPLASTICS COMPARED WITH METALS

		METALS		SHORT FIBRE REINFORCED THERMOPLASTICS (NYLON)		
PROPERTY	UNITS	TYPICAL MILD STEEL (BS220M07)	AL	UNFILLED	30% GLASS	30% CARBON
SPECIFIC GRAVITY	g/cm^{-3}	7.8	2.8	1.14	1.37	1.28
TENSILE STRENGTH	MPa	500	200	81	179	241
FLEXURAL STRENGTH	MPa	-	121	103	262	351
YOUNG'S MODULUS	GPa	210	69	2.8	9	20
TENSILE ELONGATION	%	25	8	10	3-4	3-4
TENSILE STRESS AT 0.2% STRAIN	MPa	300	110	6	20	50

TABLE 3

Tensile properties of fibre reinforced thermoplastics

Matrix	Reinforcement	Orientation	Tensile strength MPa	Tensile modulus GPa	Stress/ Strain curve area
Poly-ethylene	Glass	Random in plane	42.1	3.41	0.43
		Unidirectional	142.7	9.45	1.4
	Kevlar 49	Random in plane	73.8	5.16	1.06
		Unidirectional	131.7	10.6	1.71
	Graphite	Random in plane	58.61	6.66	0.28
		Unidirectional	110.3	19.31	0.45
Poly-carbonate	Glass	Random in plane	61.36	3.94	0.66
		Unidirectional	114.4	7.52	1.23
	Kevlar 49	Random in plane	115.8	5.06	1.94
		Unidirectional	163.4	9.79	1.83
	Graphite	Random in plane	68.95	8.55	0.33
		Unidirectional	176.5	12.62	1.03

Table 4 (From: Blumentritt,B.F. ,VU,B.T and Cooper,S.L.1975)

3.1 Materials

3.1.1 Matrix Systems

Two types of thermoplastic matrices were used in this study.

(a) Maranyl A 100 nylon 6,6, manufactured by Imperial Chemical Industries. The manufacturer's published physical properties are shown in Table 5. As this material absorbs water it was used immediately from an unopened bag or dried overnight at 90°C under vacuum.

(b) Propathene GW 522 M polypropylene homopolymer manufactured by Imperial Chemical Industries. This was a powder grade, manufacturers published physical properties are shown in Table 6.

3.1.2 Precompounded Materials

(a) Maranyl A 190, a 33% by weight glass reinforced nylon 6,6, manufactured by Imperial Chemical Industries using a processing route which results in glass fibres in the compound being comparatively short with an average fibre length of approximately 0.3mm. Manufacturer's properties are shown in Table 7.

(b) Verton AG 1030, a 30% by weight glass reinforced nylon 6,6 manufactured by Imperial Chemical Industries using a special process which allows long fibre lengths to be retained. Manufacturer's properties are shown in Table 7.

(c) Propathene HW60 GR20 and HW60 GR30 20% and 30% respectively glass reinforced polypropylene manufactured by Imperial Chemical Industries. Manufacturer's properties are shown on Table 8.

(d) RG20, a 20% carbon fibre reinforced nylon 6,6 manufactured by Hysol Grafil. Manufacturer's properties are shown in Table 9.

3.1.3 Reinforcing Fibres

Carbon

In the studies undertaken both continuous and chopped fibres were used. The chopped material used was Hysol Grafil's XAS, chopped to an approximate length of 6mm, and having a polyamide size. The continuous material used was epoxy sized Grafil XAS fibre. Manufacturer's properties for chopped and continuous fibres are shown in Table 10.

Glass Fibres

Fibreglass chopped and continuous fibres manufactured by Pilkingtons were used. The chopped fibres were previously cut to a nominal length of 6mm. Both fibre types were coated with a size containing a silane coupling agent to aid handling and coupling to the matrix, manufacturer's properties for the glass fibres are shown in Table 11.

Kevlar 49

Untreated Kevlar 49 fibres were used in chopped (6mm) and continuous form. Measured properties of the fibres supplied by their manufacturer Du Pont are shown in Table 12. Before use all fibres were dried in an oven overnight at 80°C under vacuum.

3.2 Compounding Extruders

3.2.1 Gay's TS40 - DV-L Twin Screw Extruder

This is a corotating intermeshing type and was manufactured by Gay's (Hampton) Ltd but is now manufactured by Betol Machinery Ltd in the BTS series. The Gay's machine is shown in Figure 18. The screw sections, are made in short modular sections and are located on central shafts using keys. A variable screw geometry may be assembled to suit a particular compounding task.

The barrel, also manufactured on a modular principle, consists of 3 main sections together with a water cooled feedblock and a twin port devolatilization section that serves both for the venting of volatile matter or if required incorporation of additives.

Several combinations for screw and barrel assemblies are available, a 21:1 L/D variant has provision for additive feeding and/or venting at two positions along the barrel, for the work in this study however the standard 17:1 L/D ratio was used. Figure 19 shows two possible screw configurations which can be used with the 17:1 L/D ratio variant. Each barrel section is heated by split cast in aluminium bands which are also cored to allow liquid cooling and connected to an Eurotherm 600 series proportional temperature control with solid state switching. One of the extruder's special features is a barrel withdraw facility, in which the full weight of the barrel assembly is supported on three hardened shafts accommodated on three hardened races.

The main drive consists of a constant torque 5.5 kw (7½ hp) d-c shunt wound electric motor, this is coupled to a shaft mounted gear box with a speed reduction of 13:1 and the resulting torque divided by a secondary gear box with a ratio of 1.73:1 to the screw shafts.

A summary of specifications for the twin screw extruder is given on Table 13.

3.2.2 Baker Perkins MPC/V50 Compounding System

In the twin-screw compounder twin agitators co-rotate within a figure of 8 shaped barrel. Agitators are made entirely of slip-on elements, so positions and types of elements can be adjusted for various compounding purposes. Two L/D ratios are available 10:1 and 13:1, the "clam shell" opening barrel with some of its features is illustrated in Figure 20 and its specifications given in Table 14.

An important feature of the machine are the barrel valves, these are simple vane valves in the saddle section of the machine that can be used to control the filled length within each mixing section. They permit the regulation of energy input into the product. A barrel valve is illustrated in Figure 21. The features of the compounder screw elements used in this study are listed in Table 15.

To allow the pressure in the compounder to be reduced and maintain closer control over the subsequent pelletizing operation a single screw extruder can be mounted on the end at the compounder. This in effect separates the compounding and extrusion functions, this configuration is

illustrated in Figure 22. The specifications for the crosshead extruder are listed in Table 16.

Compounding in the twin screw compounder was usually executed in two stages, firstly the polymer was melted, this took place up to the first step of orifice plugs. The orifice plugs together with the barrel value ensured complete melting had taken place and regulated the flow of material. In many experiments the fibres were then added to the melt in the mixing section and mixed until the second set of orifice plugs and barrel valve. The second set of orifice plugs and barrel valve were important to ensure that an air tight seal was maintained, when a vacuum was applied to the melt. The compounder was then discharged using camel back screw elements through a die or into the crosshead extruder.

The important variable with all the experiments performed with the Baker Perkins compounder was the design of the mixing section, which was thought to influence fibre length.

3.2.2 Reifenhauser Single Screw Extruder

This machine was used to compound the initial Kevlar/polypropylene compounds. The extruder was fitted with a general purpose screw of length 61cm and diameter 2.54cm. The flight depth was 1.5-2mm. The barrel was electrically heated, using Ether and West thermostatic controls. The rear three heaters were built in separate band heaters were used to control the die temperature. Specifications and extrusion conditions are listed in Table 17.

3.3 Injection Moulding

All test samples were moulded using a Sandretto 6GV-5 injection moulding machine. Unless otherwise stated the conditions used to mould all material in this study are listed in Table 18.

In order to retain the maximum possible fibre lengths in the moulded component care was taken in the selection of injection moulding parameters. The minimum back pressure (plasticisation counter pressure) was maintained that allowed good dispersion. Screw speed was moderate to reduce damage in the feed zone to unmelted pellets. Injection speed and injection pressure were kept as low as possible while still producing a part of acceptable density and surface quality.

The moulds used were single gated. The dimensions of the tensile bar and 3mm thick plaque mouldings are shown in Figures 23 and 26 respectively.

3.4 Fibre Extraction

3.4.1 The Extraction of Carbon Fibres from Nylon 6,6

The extraction process was carried out in the following manner. An accurately preweighed sample of composite material was placed in a long neck reaction flask. Wearing gloves and eye protection, 35cc of 5M sulphuric acid was added. The flask and its contents were then placed in an electrical heating jacket and heated until the acid was fuming. Hydrogen peroxide of 50 weight % concentration was then added in droplets to minimise the violence of the reaction. Between 20 and 25ml was required. The exotherm of the reaction caused the mixture to continue to boil, but gentle heating after the exotherm, was sometimes required to ensure the nylon was completely digested.

The fibres were then diluted in a large beaker and neutralised liquid decanted and fibres washed thoroughly with distilled water. This was followed by drying thoroughly at 100°C for 2 hours and cooling in a desiccator. The fibres were then reweighed in order to calculate weight fraction and volume fraction. The formula used to calculate volume fraction is shown in Appendix 1. Fibre length analysis was then performed as described in section 3.5.

As a control check, quantities of powdered nylon 66 and chopped fibres were subjected to the above extraction method. No change in fibre length was observed comparing fibre length before and after the extraction of nylon.

3.4.2 The Extraction of Glass from Nylon 6,6 or Polypropylene

Preweighed samples were placed in crucibles and the resin content of the composites removed by heating in a muffle furnace for 8 hours at 550°C. To prevent damage to the glass, the samples were allowed to heat up gradually from room temperature. After cooling in a desiccator the residual glass contents were reweighed to allow weight and volume fractions to be deter-

mined. Fibre lengths were then analysed as described in section 3.5.

As a control check for this method a small quantity of fibres were heated and cooled repeatedly and fibre length analysed, no change in fibre length was observed.

3.4.3 Extraction of Kevlar 49 Fibres from Polypropylene

Preweighed samples were refluxed in xylene for 2 days. Saturated xylene was changed for fresh every 8 hours. Fibres were then dried on filter paper in a hot air oven for 2 hours and cooled in a desiccator. They were finally reweighed and their lengths analysed as described in section 3.5.

3.5 Fibre Length Determinations

Fibres were recovered from composite samples 1cm x 1cm for moulded test pieces, samples not shorter than 2cm long for extrudate or approximately 1 gram of pellets.

Recovered fibres were emptied into a large beaker containing microscope slides, water and a small amount of detergent to reduce surface tension. Dispersion of the fibres was obtained in the case of carbon and glass by plaoing the beaker in an ultrasonic bath for 30 seconds. The detergent solution was then removed from the beaker by pipette, with fibres on one side the slides were removed from the beaker and dried in an oven.

Composite photomicrographs of fibres were then taken from various points around the slides using a Reichert-Jung Microstar 110 transmission optical microscope with camera at a magnification of 50x. For glass and carbon it was possible to obtain reproducible fibre length distributions by counting between 500 and 750 fibres. For Kevlar not less than 100 fibres were measured for each distribution.

Measurement of fibre length and subsequent statistical analysis was achieved using a VIDS II computer image analysis system. Fibres were measured from composite photomicrographs by a Calcomp digitizing tablet connected to a computer via a serial interface. The VIDS II two dot measurement program was used for the measurement of straight brittle fibres, a cursor employed in combination with the digitizing tablet was used to simply locate the ends of the fibres. For

Kevlar 49 fibre length measurements the VID II linear measurement program was utilized, here the cursor was used to draw along the fibres.

Throughout this study two values of average fibre length are used, weight average and number average. Both are quoted in literature and both have different meanings (Table 19). The weight average fibre length value may be thought of as more useful since each full fibre is weighted equally. Number average values were obtained from the VIDS II computer image analysis system, weight average values were calculated from the statistical analysis given by the system using an Apricot F1 personal computer. The Apricot computer was also employed to plot histograms of fibre distributions and derive volume fractions for the prediction and assessment of compound properties.

3.6 Mechanical Testing

3.6.1 Tensile Properties

All tensile testing was performed on injection moulded single gated tensile bars (A.S.T.M. D638 - 77a type 1). Approximate dimensions are given in Figure 23. In recognising the importance of moisture uptake all samples were stored in a controlled atmosphere of 23°C and 50% relative humidity for a minimum of two weeks prior to testing.

Testing was carried out on an Instron (TT-C) universal testing machine. An extensometer was attached to test pieces to indicate strain accurately throughout the tensile test. No less than five specimens were tested of each type of material. Testing was in general accordance to A.S.T.M. D638 - 77a however, results given in this study for tensile modulus of elasticity are values recorded at a specified strain, this was thought by the Author to be less subject to error than extending the sometimes short initial elastic portion of the stress-strain curve.

The grips used to hold the specimen were slightly serrated to prevent slippage, highly serrated grips were found to act as stress concentrators and produce premature failure.

3.6.2 Flexural Properties

Injection moulded specimens as described in section 3.6.1 were used. Specimens were conditioned in a controlled atmosphere of 23°C and 50% relative humidity for a minimum of two weeks prior to testing. Tests were performed in accordance to A.S.T.M. D790.

A simple three point loading system was attached to the Instron universal testing machine, to allow the measurement of flexural properties. A length span of 50mm was used to ensure the specimens were deformed in flexure and not shear. A deformation rate of 1.3mm/min was used for all tests. Specimens were deformed until the recorded plot of force against deflection showed the first deviation from linearity. The modulus of elasticity in flexure was determined by drawing a tangent to the straight line portion of the load deflection curve using:-

$$E_B = \frac{S^3 M}{4BW^3} \qquad (11)$$

E_B = Modulus of elasticity in bending ($N/m^{2)}$

S = Support Span, (m)

B = Width of beam tested (m)

W = Depth of beam tested (m)

M = Slope of tangent to the initial straight line portion of the load deflection curve.

The flexural strength is equal to the maximum stress in the outer fibres at the moment of break and was calculated by the following equation:-

$$\sigma_s = \frac{P\,S}{B\,W^2}$$

σ_s = Flexural Strength ($N/m^{2)}$

P = Load at moment of break (N)

Symbols for B, W and S have the same meaning as in Equation 11.

3.6.3 Impact Properties

Measurements of impact properties were performed using a Davenport R.P.D. instrumented falling weight impact tester. Unlike conventional impact test equipment which yields only the energy required to break a specimen, an instrumented device provides detailed forces vs time or distance curves of the impact process. Conventional impact test equipment includes the Izod test (A.S.T.M. D256, ISO R - 180) and the Charpy (A.S.T.M. D256, DIN 53453, ISO R - 179). These tests are most useful for ranking materials in order of increasing toughness but it is not uncommon to find that different tests rank the same set of materials in different orders. For a standard falling weight test the energy to break a sample or drop height required to produce an agreed 50% failure of all samples is usually recorded. The instrumental technique requires fewer test specimens than conventional testing apparatus and allows the various failure types to be detected, this was especially relevant as in this study were mixed failure modes were found to occur.

A schematic description of the instrumented impact tester is shown in Figure 24. Impact energy is transferred to a specimen by the free but guided fall of an impactor nose coupled to a

force transducer. Available energy is determined from m.g.h. and the impact velocity determined from $\sqrt{2.g.h.}$ when m = impacted mass g = acceleration due to gravity and h = impact height. Details of the machine's operation and specifications can be found elsewhere[100].

Two types of specimen were tested to obtain an overall measure of impact properties; a bar cut from a tensile specimen and a 3mm thick plaque, specimen dimensions together with testing arrangements and conditions are shown for the bar and plaque in Figures 25 and 26 respectively. Energy vs distance, force vs distance and force vs time data was recorded for each sample tested. A minimum of ten samples for each material type were tested.

On selected glass reinforced nylon material measurements of G_c were estimated using a notched sample cut from a tensile bar. Specimen dimensions, testing arrangement, testing conditions and the meaning of symbols used are shown in Figure 27. The formula used to calculate G_c is derived by Bucknall[102] by combining linear elastic fracture mechanics with the stress in the outer fibre in a three point bending specimen. The formulae used in the deviation are shown below.

Stress intensity factor $K = Y (a)^{½}$

Where Y = correction factor (To account for finite plane effects)

$$\text{Fracture toughness } K_c = \frac{EG_c}{(1-v^2)}$$

where v = Poisson ratio of the material

a = depth of notch

For three point bend Charpy impact test piece, stress in outer fibre which contains a crack

$$\sigma_{SI} = \frac{3\,PS}{3\,BW^2}$$

(P = Load)

Symbols for B, W and S have the same meaning as in Equation 11.

In the instrumented tests used, the yield force or peak force P was measured directly. In the standard type of test where only the impact energy I is measured, it is necessary to derive G_c from I.

As

$$I=BWZ\,G_c$$

Symbols for B and W have the same meaning as in equation 11.

If the approximation $Y^2=\pi$ is used Z is given by

$$Z=\frac{1}{2}\frac{a}{W}+\frac{1}{18}\frac{S}{a}$$

Using the values of peak force and impact energy recorded two independent values of G_c were derived and the results compared.

An estimation of the contribution to G_c from the pull-out energy of fibres at or below their critical length was made for the compounds tested. The estimation was based on an analysis shown in Appendix 2.

A computer program which utilized fibre length distributions was employed to calculate values of G_c using the calculated value of interfacial shear strength.

3.7 Scanning Electron Microscopy

The fracture surfaces were observed in this study using a Cambridge S250 scanning electron microscope. Details of the instrument and modes of operation have been described elsewhere[103].

Samples were mounted on aluminium stubs using double sided sticky tape. To ensure electrical contact, silver paint was applied in one corner between the stub and sample and a thin layer of gold coated on to the specimen using a Polaron E5000 Splutter coater. Samples were placed in the splutter coater and a vacuum applied, the system was then purged with argon gas for one minute, after purging the samples were splutter coated with gold for two minutes to produce an even coating. Images were recorded from the microscope on Ilford FP4 film developed under

standard conditions.

Photomicrographs were examined to determine modes of failure of composing and fibres and the degree of interfacial adhesion between fibre and matrix.

3.8 Prediction of Composite Properties and Assessment of Compounding Techniques

Computer programs for the prediction of theoretical composite properties and assessment of compounding techniques were written using Commodore EBM model 4032 and Apricot F1 personal computers. Table 20 presents a summary of the methods used. Most techniques required an accurate measurement of fibre length distribution.

A possible source of error in the techniques was the derivation of fibre volume fraction for the calculations. In this study the fibre length distributions are expressed as histograms of weight % of recovered fibres against fibre length. In order to convert the distribution of weight % into volume fraction for each fibre length group the mid point length of each group was selected, the volume of this represented length was calculated and multiplied by the number of fibres within its group this value was then divided by the total volume fraction.

3.9 Investigations of Transcrystallinity

A study was made of transcrystallinity produced around pristine fibres and to a limited extent around fibres present in injection mouldings.

In the case of pristine fibres, a small amount of powdered polymer was placed on a microscope slide, to remove all residual crystallinity it was heated for 15-30 minutes above its melting point. With nylon it was necessary to minimise degradation by excluding air. This was done by circling the polymer with a small amount of silicone fluid and placing a coverslip over it. With the polymer melted the coverslip was pressed down to seal out air and reduce the thickness of the polymer. The slide was then rapidly transferred to a Reichert hot stage microscope maintained at the crystallising temperature. When crystallisation had reached its desired state as observed through the polarising microscope the specimen was quenched in water.

The preparation of uniform sections from injection mouldings proved to be difficult, nylon based composites were found not to cut in a satisfactory manner with a sledge microtone, polypropylene based composites were found to be easier to prepare. Thin sections were examined by a polarising microscope and attempts were made to induce crystallinity around processed fibres over a range of crystallisation temperatures in a manner similar as described for pristine fibres.

3.10 Experiments Performed Compounding Carbon and Glass (Brittle Fibres) into Thermoplastics

3.10.1 Introduction

Initial compounding experiments were based on the Gay's TS 40 DV-L twin screw extruder, but due to a combination of an insufficiently large feed port and inadequate power to compound high volume fraction materials and alternative compounder was sought. The Baker Perkins MPC/V50 was found to provide the necessary degree of flexibility and size to enable a thorough examination to be made of processing route. Table 21 presents a summary of the experiments performed with glass and carbon fibres.

3.10.2 Experiments based on the TS40 DV-L Twin Screw Extruder

For the three experiments performed, nylon 6,6 was used as the matrix. Carbon fibres were fed midstream after the nylon had melted. All electrical equipment in the vicinity was covered to prevent electrical short circuits.

The first experiment, denoted BRITTLE 1 investigated the nature of fibre breakdown along the screw by the shock cooling of the extruder whilst running. The extruder was run for five minutes until equilibrium conditions were maintained, stopped using the emergency button, heating turned off and cooling applied. A hydraulic jack was used to assist the removal of the barrel. Samples of nylon 6,6/carbon fibre were removed from points along the screw and fibre lengths characterised using the method described in Sections 3.4 and 3.5. The compounding configuration and processing conditions are shown in Figure 28.

As it was found from experiment BRITTLE 1 that a major hurdle for fibre length survival was the transition between screw sections of different pitches, experiment BRITTLE 2 was designed to investigate the effects of utilizing metering screws with different pitches. Chopped and continuous fibres were used fed mistream. Fibre length distributions and mechanical properties were evaluated. The compounding configuration and processing conditions are shown in Figure 29.

The third experiment denoted BRITTLE 3 was concerned with the effects of both converting extruded strands into feed stock suitable for injection moulding and die design on fibre length properties. The compounding configuration and processing conditions are shown in Figure 30. These were derived from experiments BRITTLE 1 and 2 and thought to be the best for the preservation of fibre length. Two dies were utilized of completely different design and flow geometry, they are shown in Figure 31 and 32.

One was 6mm rod die the other an adjustable slit die. Two slit die settings were used 3 and 4.4mm. Three machines for converting extruded strands into pellets were employed. A Cumberland 5x7 granulator, a Broyeurs Malanguers L100 granulator and a Cumberland 6" pelletiser.

Finally using the compounding arrangement for experiment BRITTLE 3, the effect on fibre length distribution, if a second fibre species is present was investigated. A 33% glass reinforced nylon 6,6 was used as the matrix The resulting fibre lengths of the carbon fibre in the extruded hybrid were evaluated.

3.10.3 Experiments Based on the Baker Perkins MPC/V50 Compounding System

Due to limitations of fibre incorporation found with the Gay's TS40 DV-L twin screw extruder as described previously, further investigations on brittle fibres were based on the Baker Perkins MPV/V50 compounding extruder system. Many screw configurations were assessed but for the purposes of this study the results based on three will be presented.

The first experiment BRITTLE 4 was comprehensive analysis of the capabilities of the compounding machine to produce high quality feed stock of carbon and glass fibre reinforced

nylon 6,6. The compounding systems and processing conditions illustrated in Figure 33. The materials and compounding arrangements are listed in Table 22 for carbon fibre compounds and 23 for glass fibre compounds.

The second experiment BRITTLE 5 was performed using continuous glass fibre with the compounder in its 10:1 length to diameter ratio. The minimum number of paddles were used in the mixing section to ensure enough fibre breakdown for the production of a uniform strand. The compounding configuration and processing conditions are shown in Figure 34.

Experiment BRITTLE 6 employed what was considered to be the optimum evolved extruder screw configuration for the incorporation of carbon fibres into nylon 6,6. Here the mixing paddles in the mixing section were substituted by 3 inch feed screws. The configuration allowed the possibility of a vacuum being applied to the melt. Chopped carbon fibre was used and a range of screw speeds and volume fractions were evaluated. The compounding configuration is shown in Figure 35 and the arrangements in Table 24.

Other screw configurations were investigated that indicated that replacing the second orifice plug by an extended feed screw allowed the production of carbon fibre compounds with number average fibre lengths of up to 800 μm. The absence of a second orifice plug however ruled out the possibility of applying a steady vacuum to the melt.

3.11 Experiments Performed Compounding Kevlar 49 (Ductile Fibre) into Thermoplastics

3.11.1 Introduction

The experiments performed incorporating a ductile fibre, Kevlar 49, into a thermoplastic can be subdivided into those based on the Reifenhauser single screw extruder and those which utilize the Baker Perkins MPC/V50 compounder for the compounding operation. A summary of the experiments performed are listed in Table 25.

3.11.2 Investigations based on the Reifenhauser Single Screw Extruder

The specification for the extruder used and the extrusion conditions are presented on Table

17. Premixes were prepared by mixing preweighed quantities of fibre and powdered polypropylene in an Henschel mixer for 1 minute. These mixes were fed into the feed hopper of the extruder. A wooden guide stick was used to ensure the feeding rate of the mixture remained constant. The first experiment, KEVLAR 1 attempted to investigate the basic properties of the materials produced, examining the effect of screw speed and volume fraction.

Because of the poor properties of materials produced in KEVLAR 1, the experiment was repeated only adding a titanate coupling agent in various concentrations to improve bonding and/or wetting of the Kevlar fibre by the polypropylene matrix.

Titinate coupling agents have been found to act as molecular bridges between substrates. They are not limited to an inorganic filler and a organic polymer matrix. Monte and Sugarman[104] found a significant increase in properties on addition of a titinate coupling agent to a Kevlar-epoxy composite. It was thought that titinates react with free protons provided by the Kevlar fibre surface, a significant reduction in viscosity occurred. Viscosity reduction was thought to be a result of the introduction of organic monomolecular layers on the surface of the fibre.

In this study isopropyl triisostearoyl titinate coded KRTTS and manufactured by Kenrich Petrochemicals was chosen as a type that would be compatible with both Kevlar 49 and polypropylene.

Experimental procedure was carried out in the same way as KEVLAR 1. The titinate was dispersed in a small quantity of Hexane and added as a liquid into the Henschel mixer in the mixing stage. Various concentrations of titinate were used, the concentration being based on the percentage of weight of the fibre used in each compound. Extrusion was carried out using the same conditions as described for KEVLAR 1.

3.11.3 Investigations Based on the Baker Perkins MPC/V50 Compounder

Because of poor dispersion and hence poor mechanical properties obtained from both experiments KEVLAR 1 and 2, it was decided to attempt to compound Kevlar into polypropylene using the Baker Perkins MPC/V50 Compounder.

A wide range of screw configurations were tried, the problems found when attempting to incorporate Kevlar using this machine were numerous. Because of its tough nature, screws were unable to break up continuous rovings of Kevlar added midstream, the fibre simply wrapped itself around the screws. Attempts to add chopped fibres to an aggressive screw configuration resulted in the breakage of compounder mixing paddles.

The final successful screw configuration is shown in Figure 36, the incorporation of Kevlar into polypropylene by the Baker Perkins Compounder is designated experiment KEVLAR 3. The front barrel valve was removed and chopped fibres were fed midstream into the melt on to continuous helix paddles. The barrel valve orifice was filled with chopped Kevlar fibres and an even feed rate maintained by introducing the fibres into the melt with a wooden guide stick. The amount of fibres taken up was controlled by the compounder screw speed, the matrix was starve fed at a constant rate. Because the front barrel valve and its associated orifice plugs were not present it was difficult to maintain a consistent barrel vacuum. The experiment was repeated using a nylon 6,6 matrix and denoted as KEVLAR 4, compounding conditions are shown on Figure 37.

Specimen dimensions for tensile testing

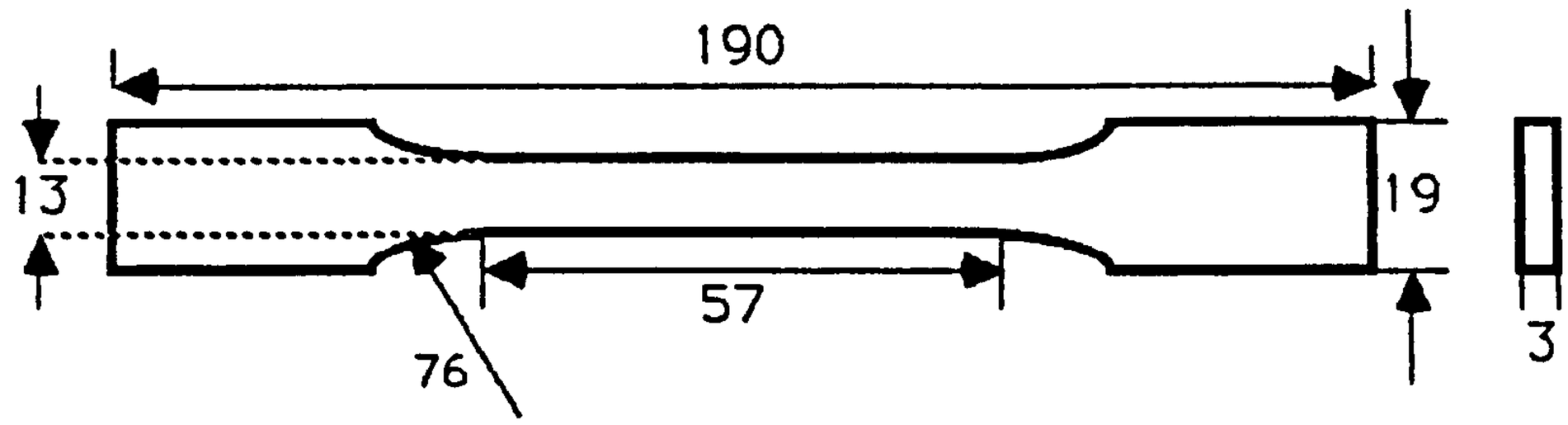

Dimensions in mm.

Figure 23

Schematic description of instrumented impact test

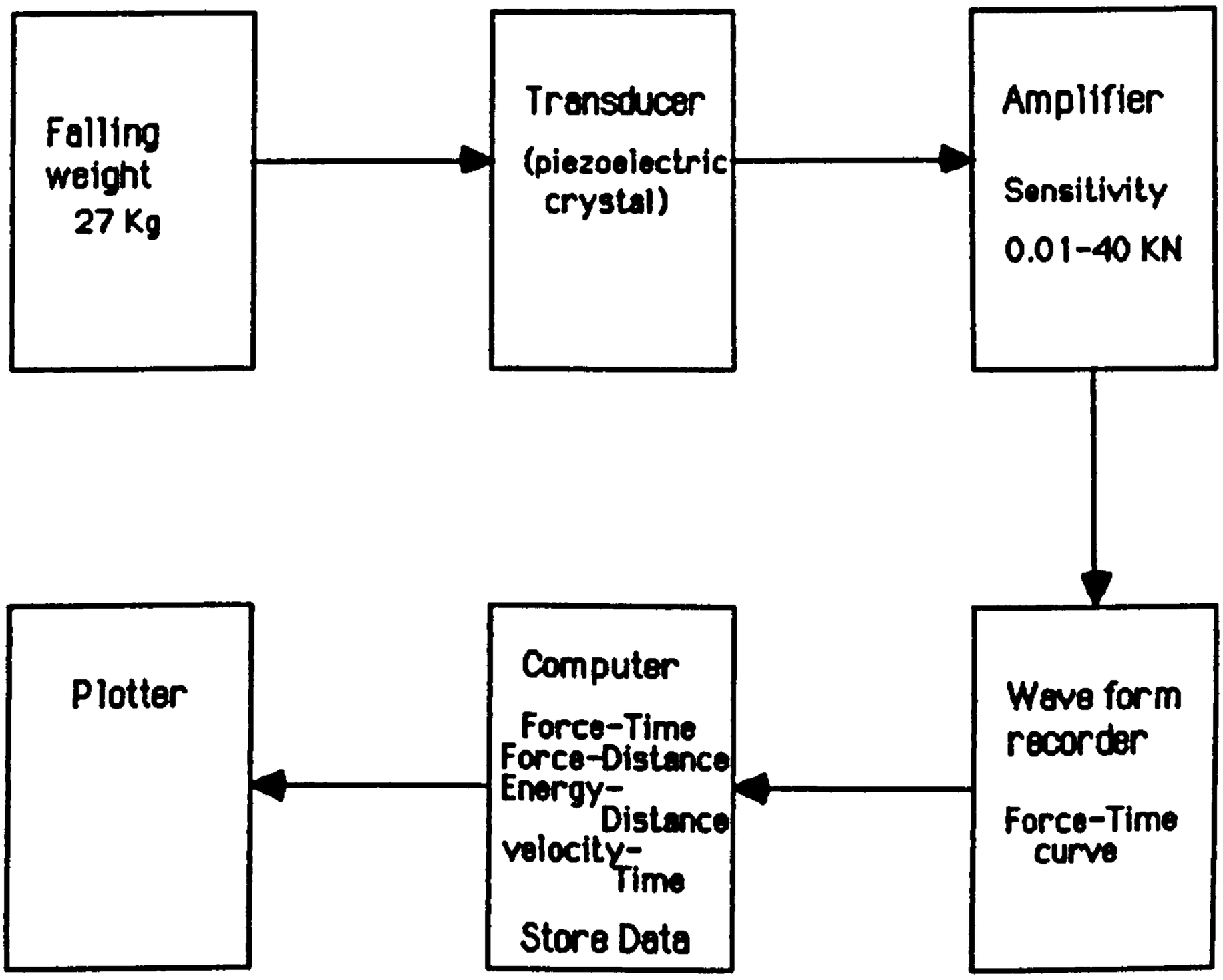

Figure 24

Sample and conditions for Impact properties (bar)

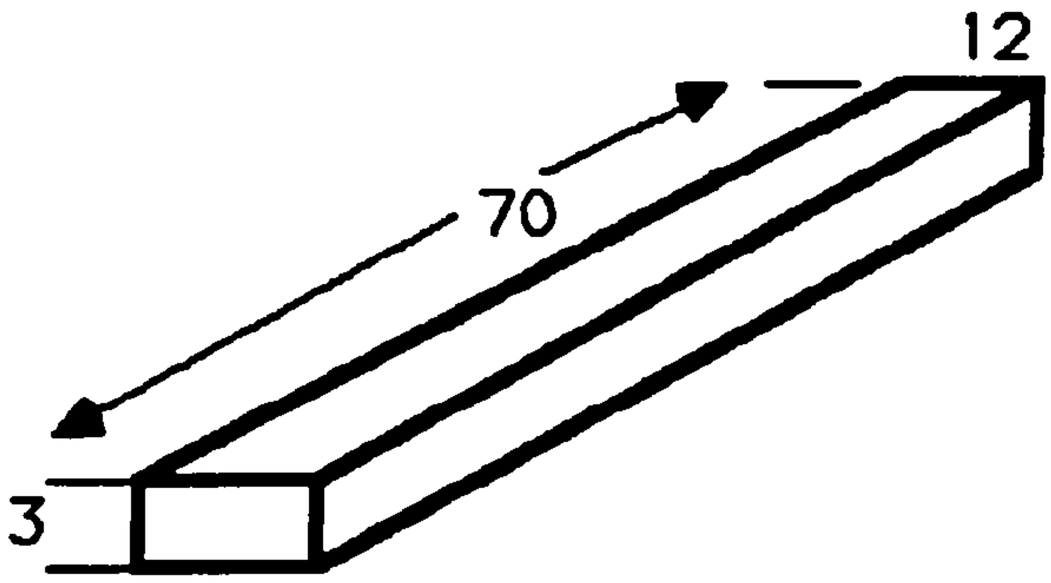

Dimensions in mm

Testing conditions

Temperature	23 C
Impact weight	27 Kg
impact velocity	2 M/S
Oclilloscope sweep time	20 mS
Full scale deflection of range	0.5 KN

Dimensions of impact tup head

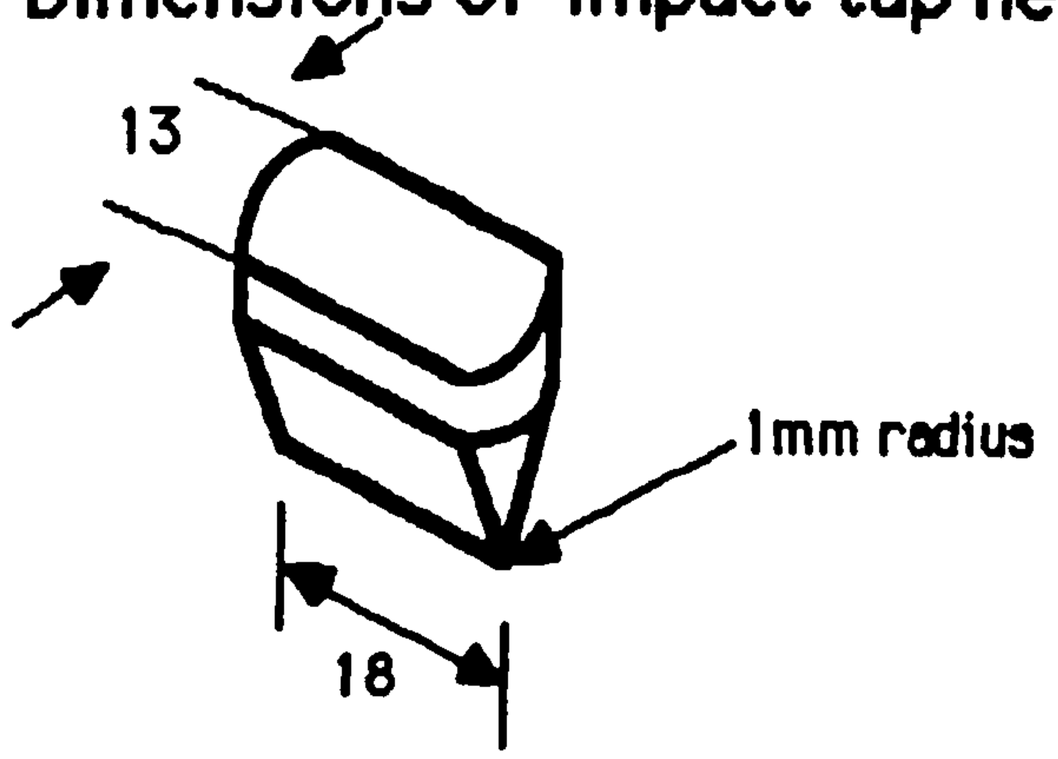

Impact load method

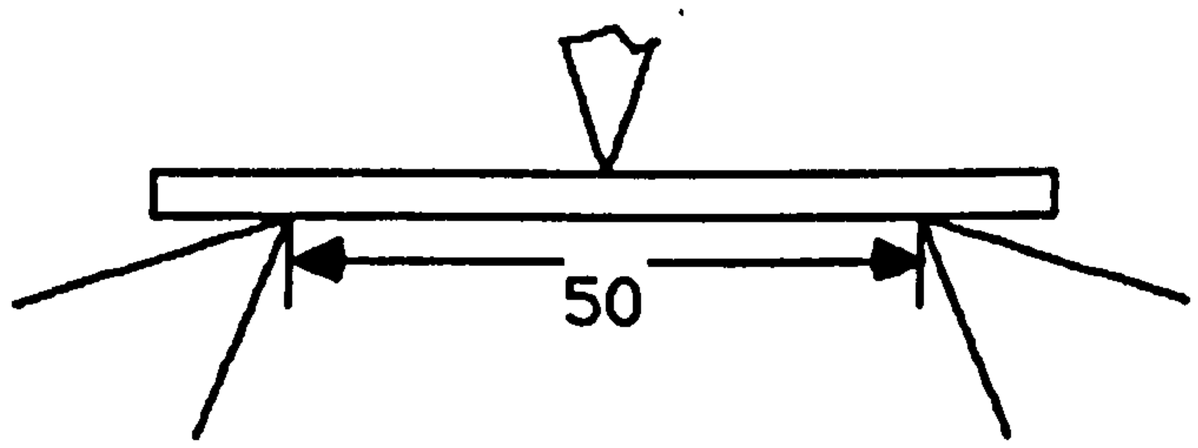

Figure 25

Sample and conditions for Impact properties (plaques)

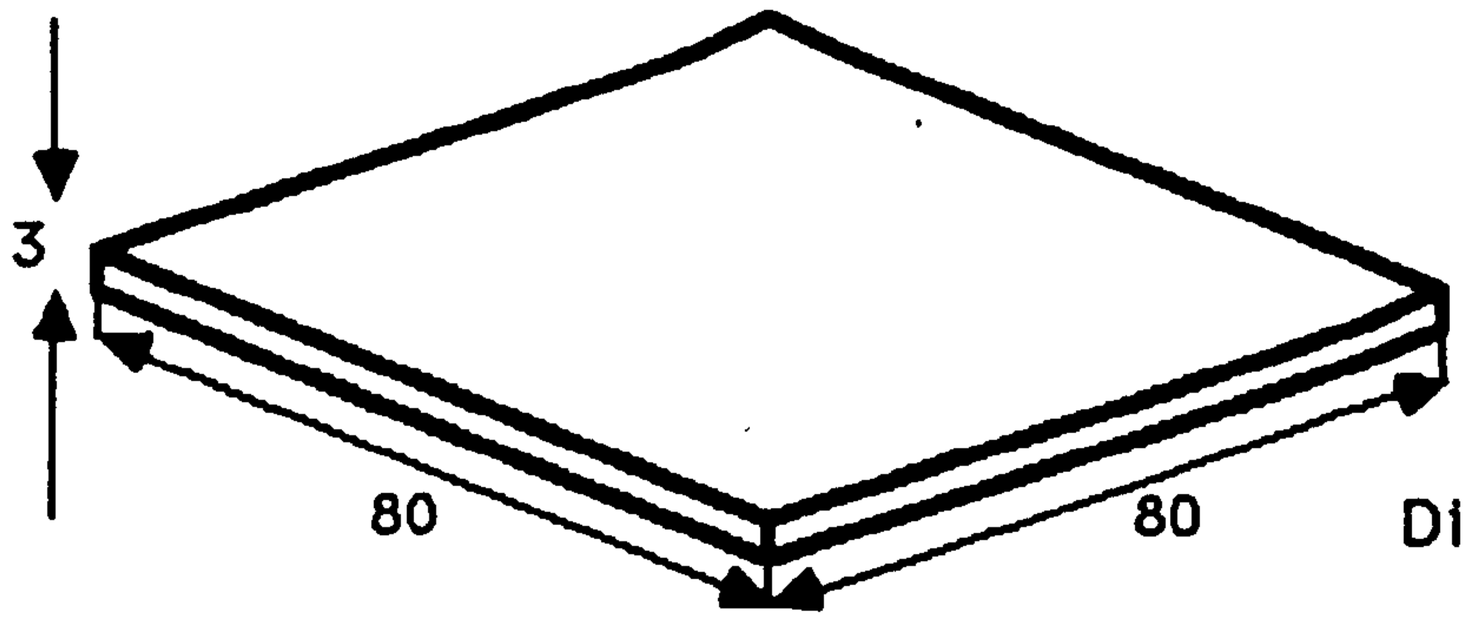

Dimensions in mm

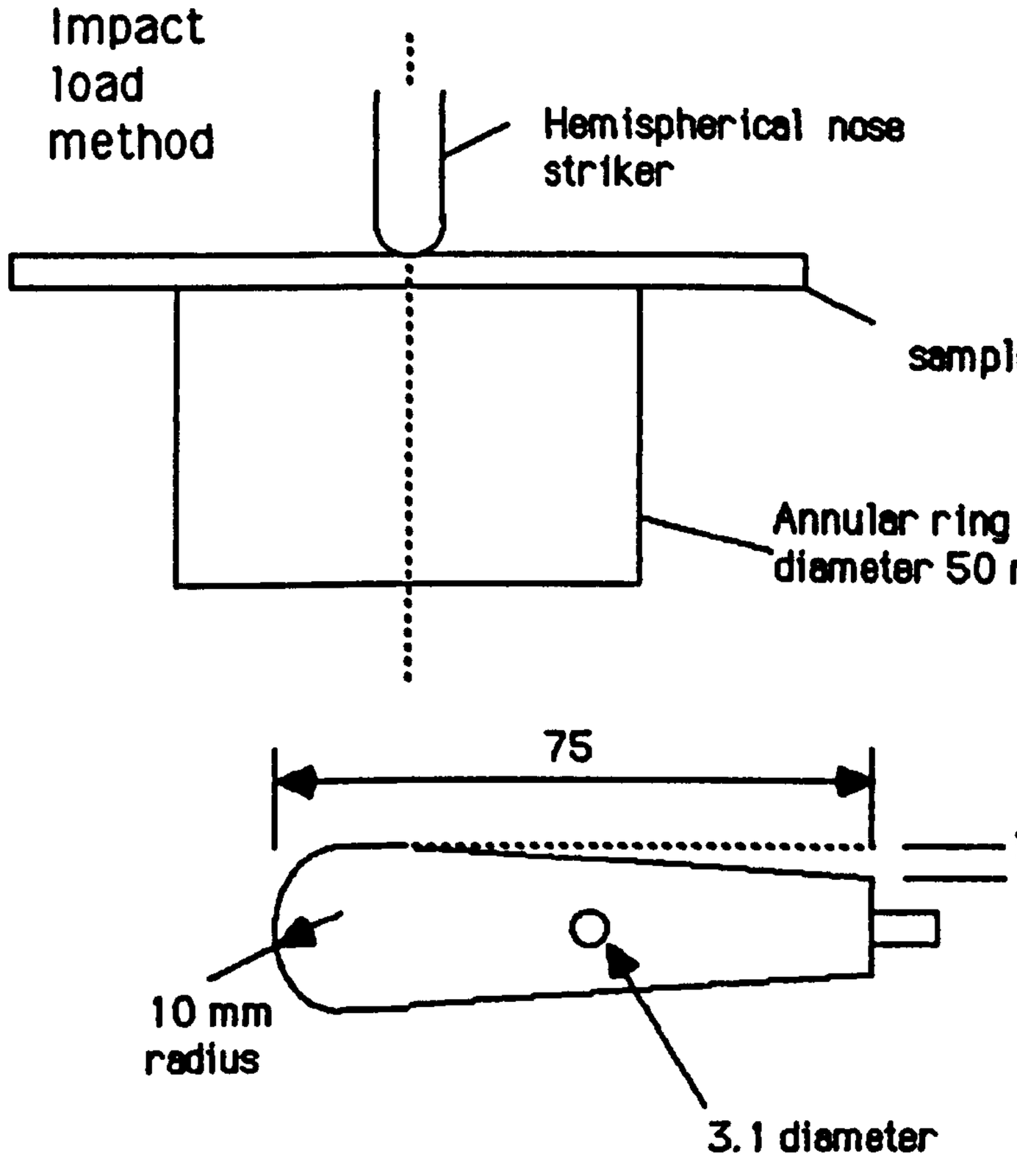

Testing conditions

Temperature:	23 C
Impact weight:	27 Kg
Impact velocity	3 M/S
Ocilloscope sweep time	5 mS
Full scale deflection of range	2KN

Dimensions of impact tup used.

Figure 26

Sample and conditions for G measurement

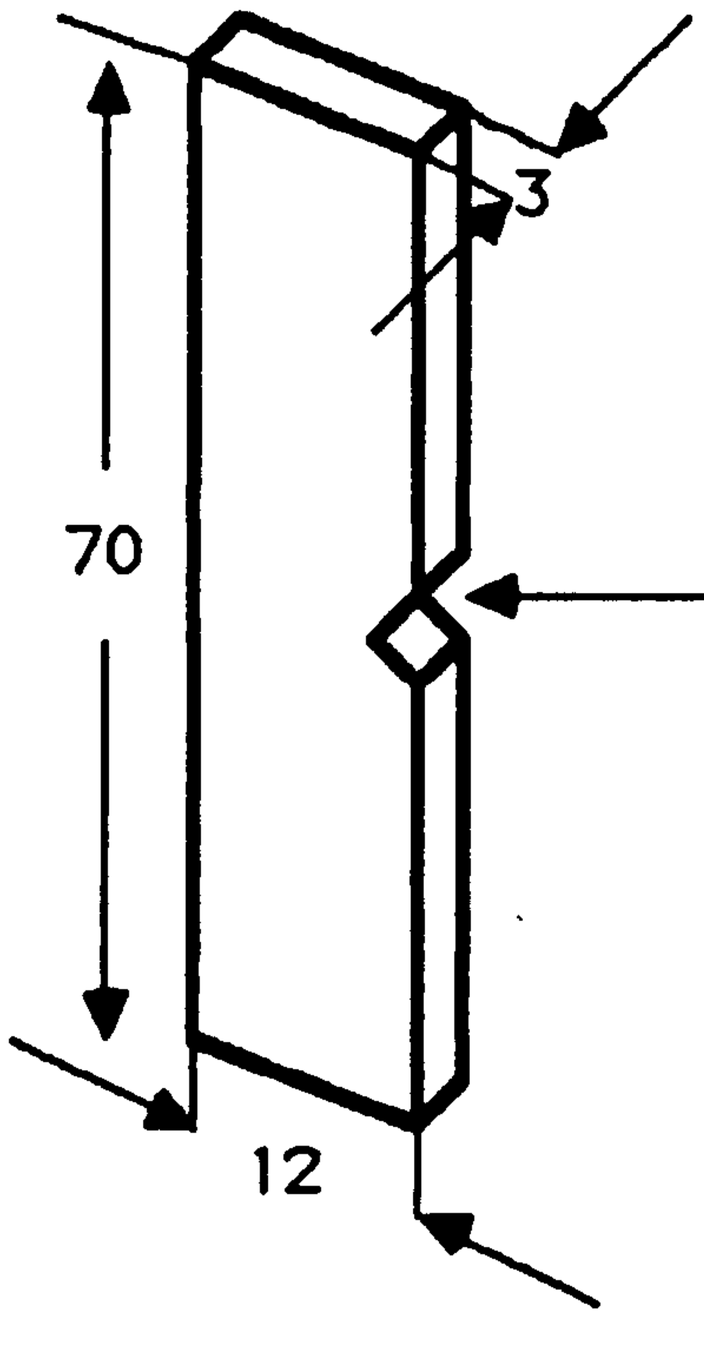

Dimensions in mm.

Testing Conditions

Temperature	23 C
Impact weight	27 Kg
Impact velocity	2 M/S
Ocilloscope sweep time	5 mS
Full scale deflection of range	0.5 KN

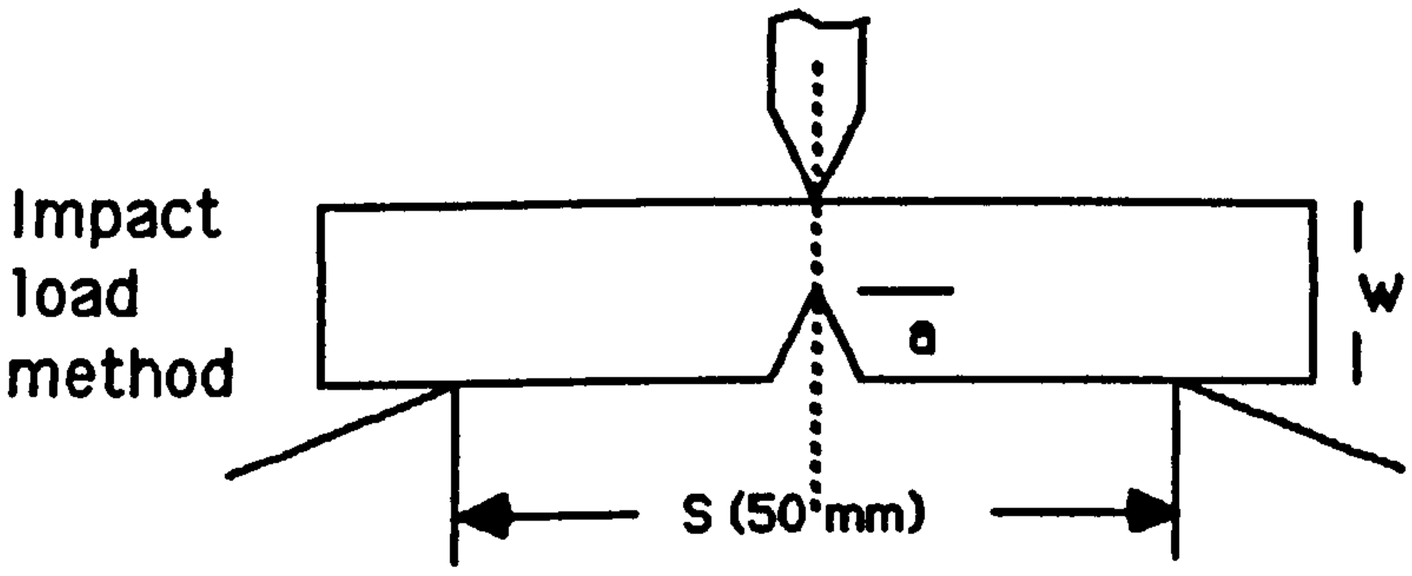

Crack has width B

$$G_c = \frac{9\, S^2 a Y^2 (1-\nu)}{4 B^2 W E} P_f$$

poisson ratio

P_f = peek force recorded

Y = geometric parameter

(geometric parameter calculated from Brown and Screwley 1966)

Figure 27

Experiment BRITTLE 1

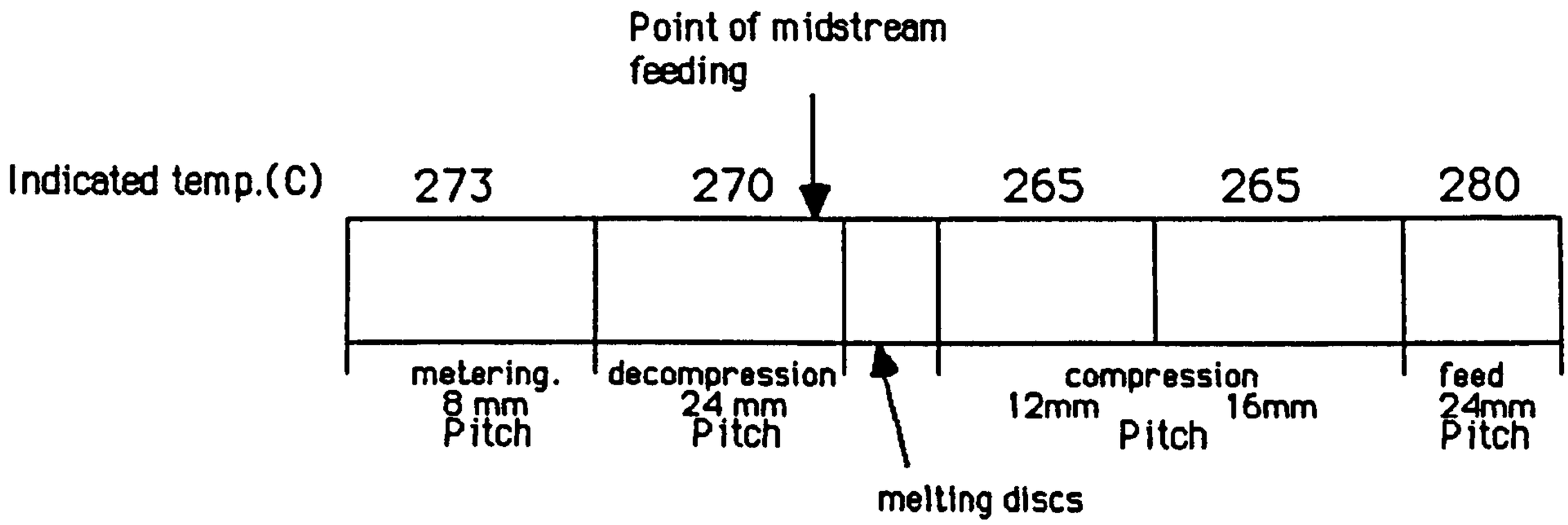

Materials: Nylon 66.
continuous XAS carbon fibre epoxy sized.

Screw speed 100 RPM
Die Not used

Granulator Not used.

Continuous fibres self feeding.

	Nylon and carbon
Current (amps)	14
Power (kW)	2.50

Figure 28

Experiment BRITTLE 2

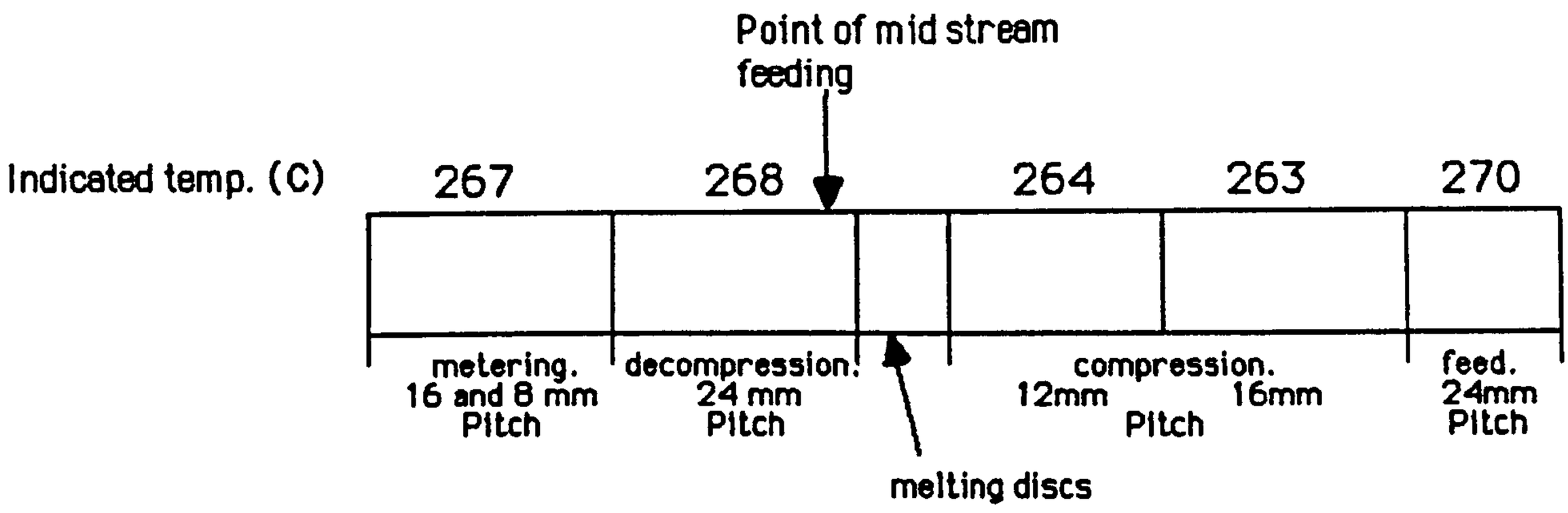

Materials: Nylon 66.
continuous and chopped XAS 3mm carbon fibre epoxy sized.

Screw speed 100 RPM

Die 6mm round (set 262 C)

Output 7.6 Kg/hour

Granulator Cumberland 5X7.

Chopped fibres added by hand.
Continuous fibres self feeding.

	Empty	Nylon only	Nylon and carbon
Power (kW)	0.5	1.9	2.52
Current (amps)	5	9	15

Figure 29

Experiment BRITTLE 3

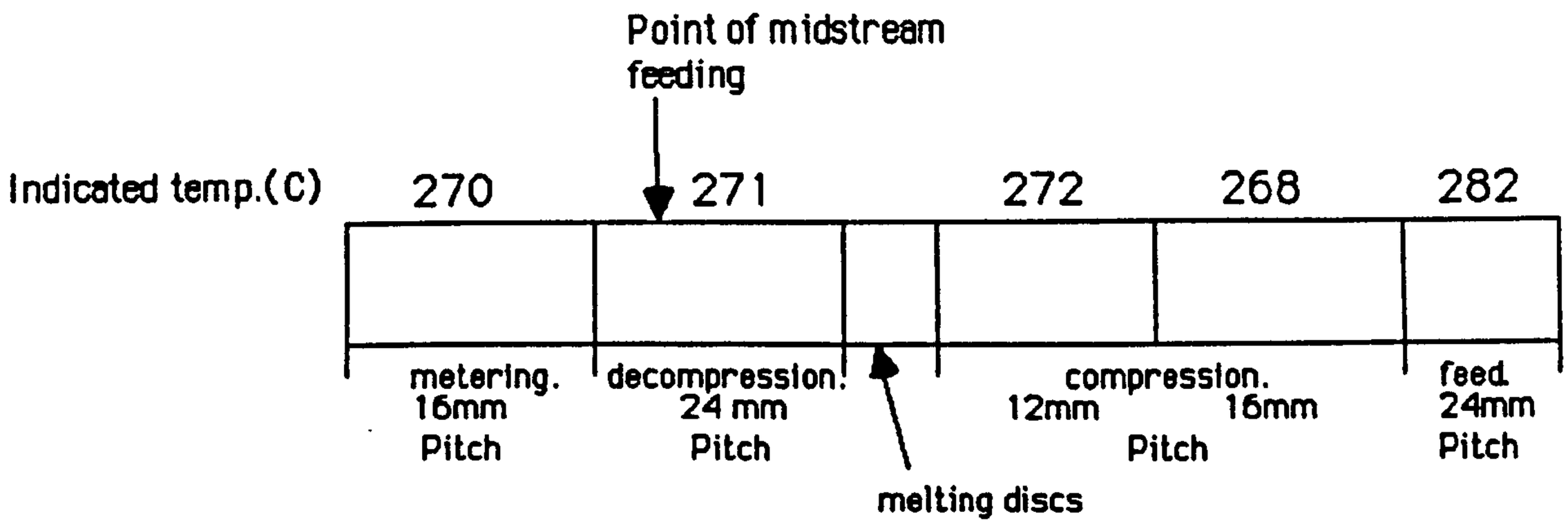

Materials: Nylon 66. Nylon 66./33% glass.
Continuous XAS carbon fibre epoxy sized.

Screw speed 100 RPM.

Feed stock for injection moulder produced by :

Cumberland 5X7.Granulator.
Broyeurs Malangeurs L100. Granulator.
Cumberland 6"Pelletiser.

Continuous fibres self feeding.

	Nylon and carbon
Power (kW)	2.50
Current (amps)	14

Dies: 6mm round (set 275 C)
3mm slit die (set 275 C)
4.4mm slit die (set 275 C)

Output 7.2 Kg/hour

Figure 30

The adjustable slit die

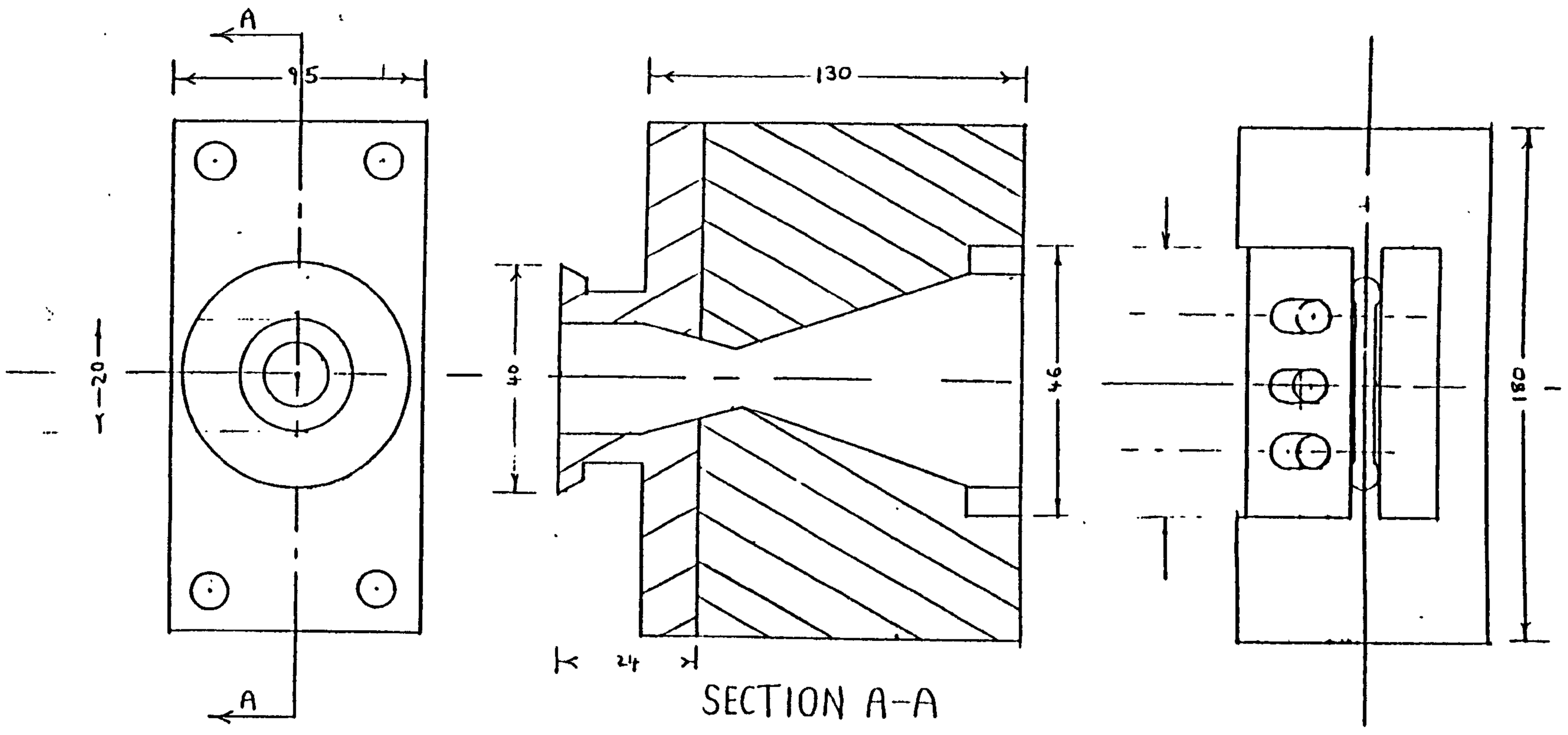

SCALE:- HALF SIZE

Figure 31

The 6mm rod die

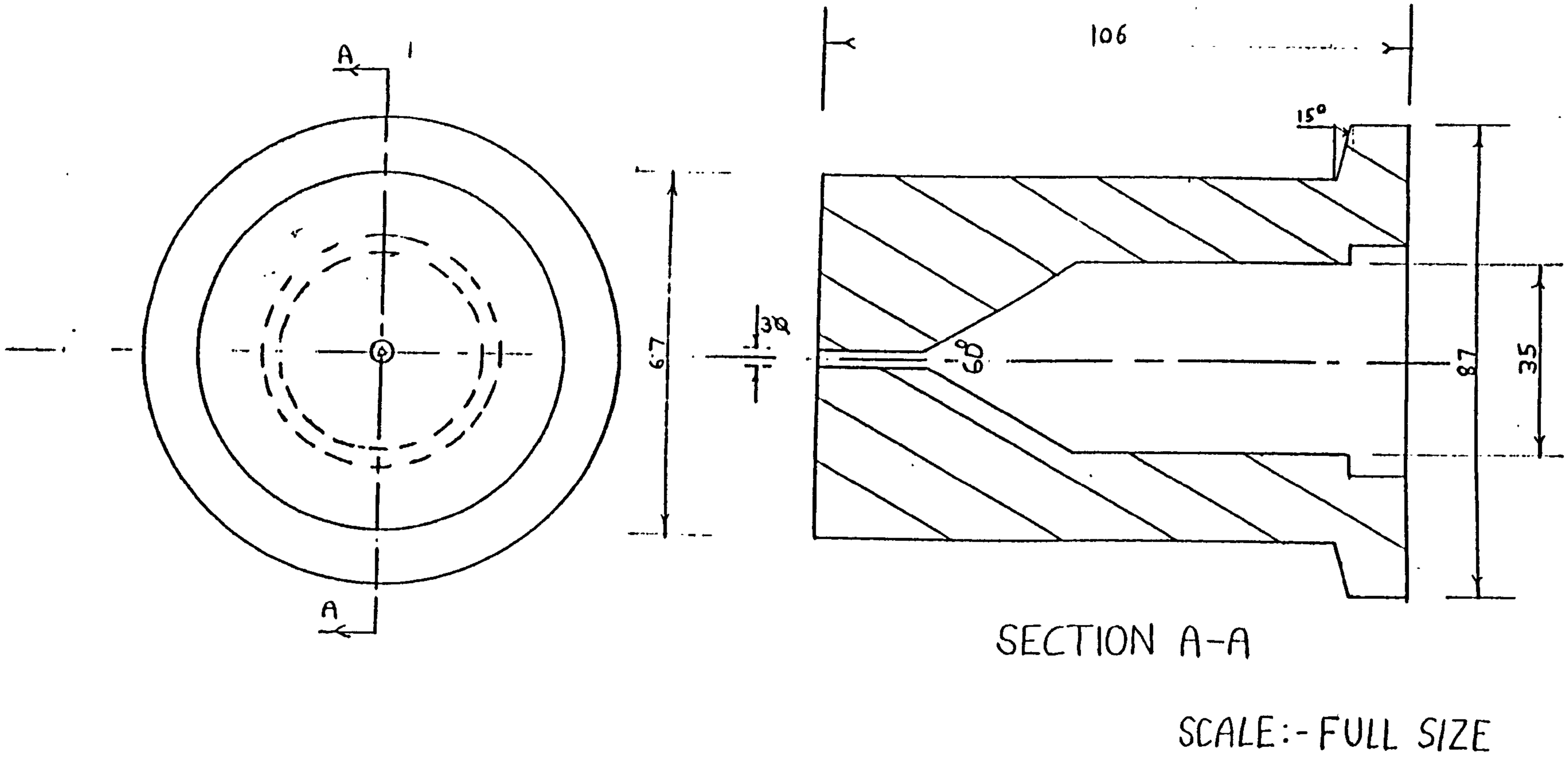

Figure 32

Experiment BRITTLE 4

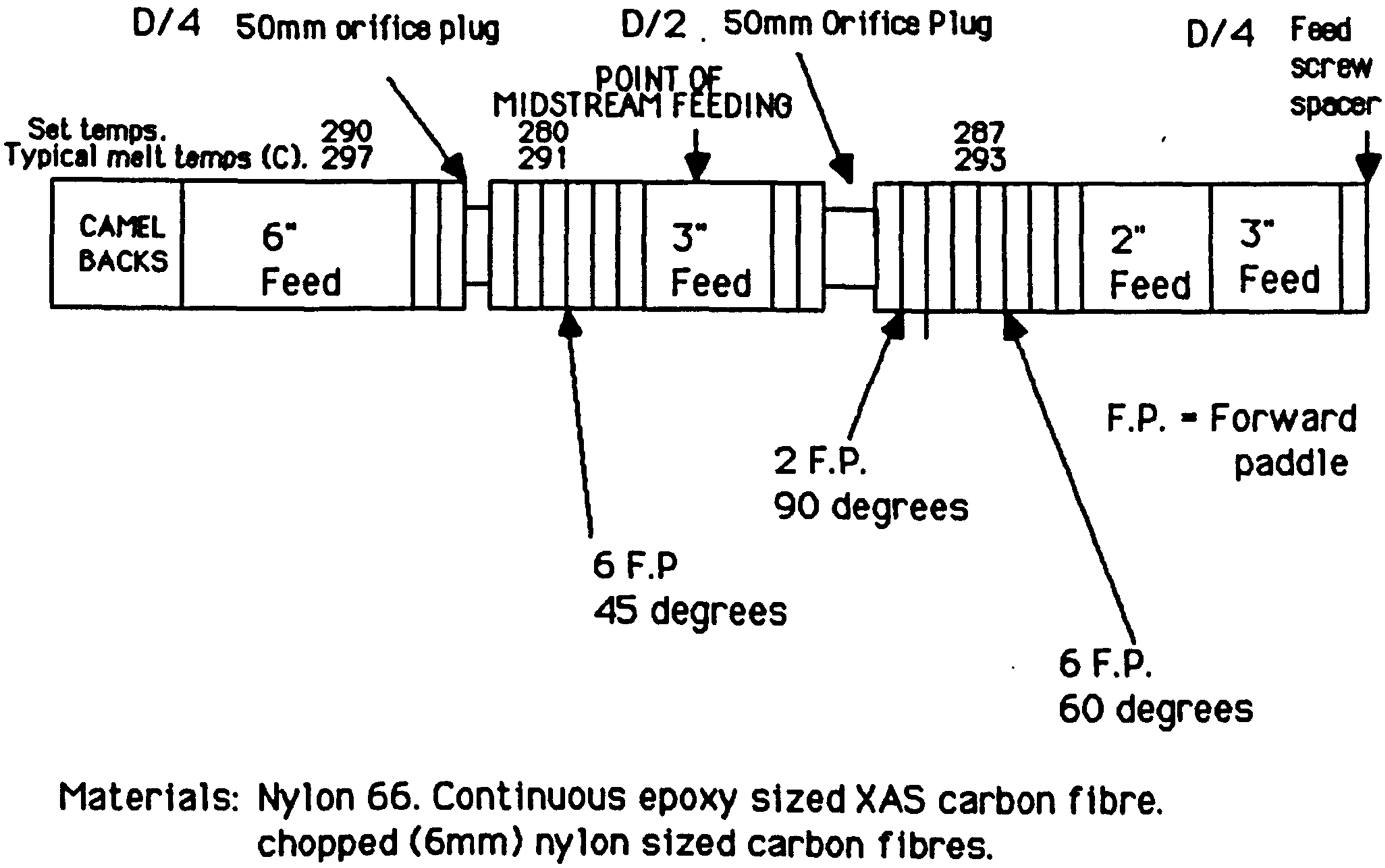

Materials: Nylon 66. Continuous epoxy sized XAS carbon fibre.
chopped (6mm) nylon sized carbon fibres.
Chopped (6mm) glass fibres.

Screw speed: 500 RPM.

L:D ratio: 13:1

Die: strand 4*4 holes.

Output: 27-54 Kg/hour.

Pelletiser: Conair Jetro 8*8 strand.

Torque: 90-105 %

Machine ran with and without Crosshead extruder.

Crosshead extruder conditions

	Melt	Feed	
Temp (C)	299	299	283

Screw speed: 40-60 RPM.

Torque 12-14 %

Figure 33

Experiment BRITTLE 5

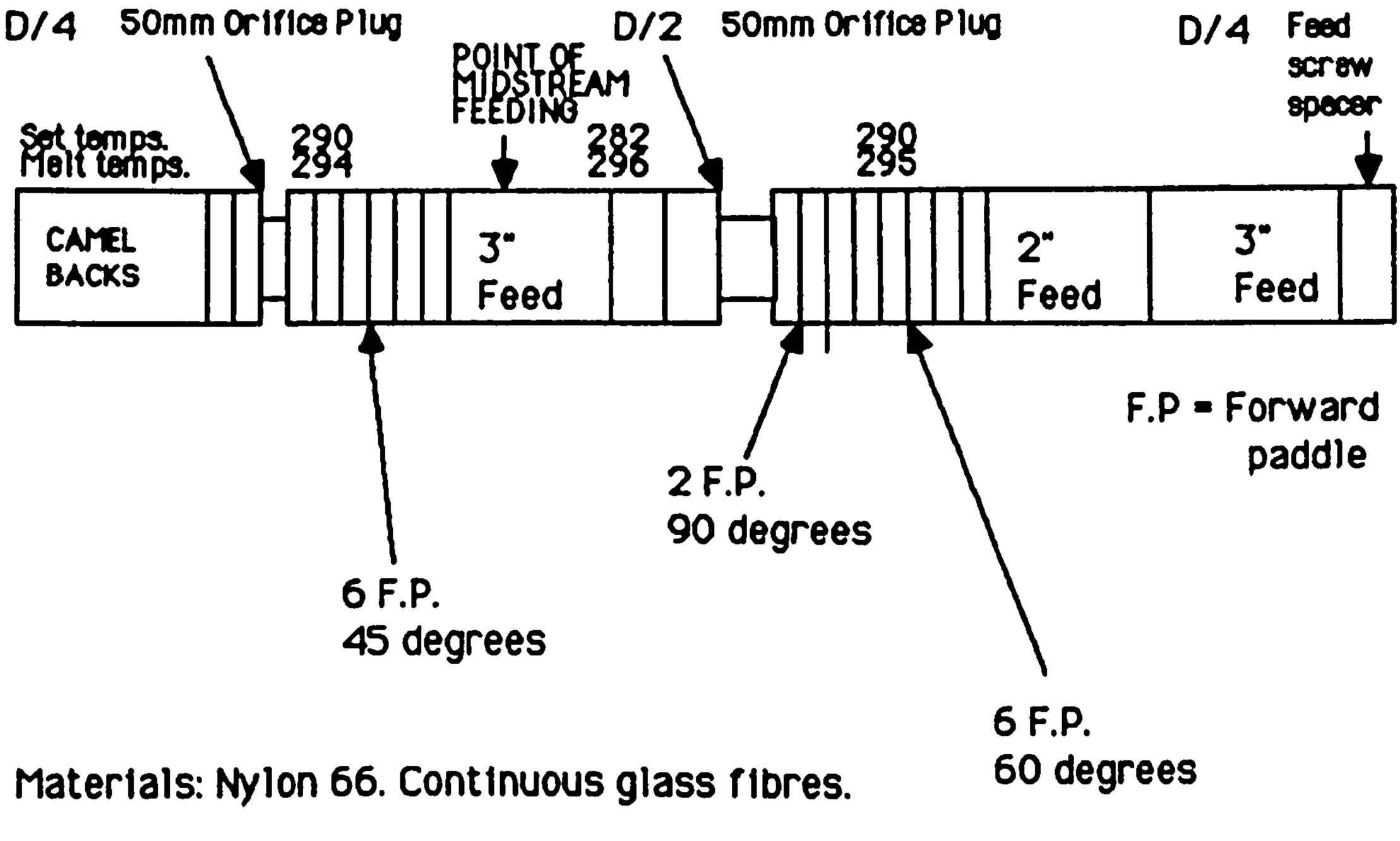

Materials: Nylon 66. Continuous glass fibres.

Screw speed: 300 RPM

L:D ratio: 10:1

Machine ran without crosshead extruder.

Die: strand 4*4 holes.

Pelletiser : Conair Jetto 8*8 strand.

Torque: 80-95 %.

Figure 34

Experiment BRITTLE 6

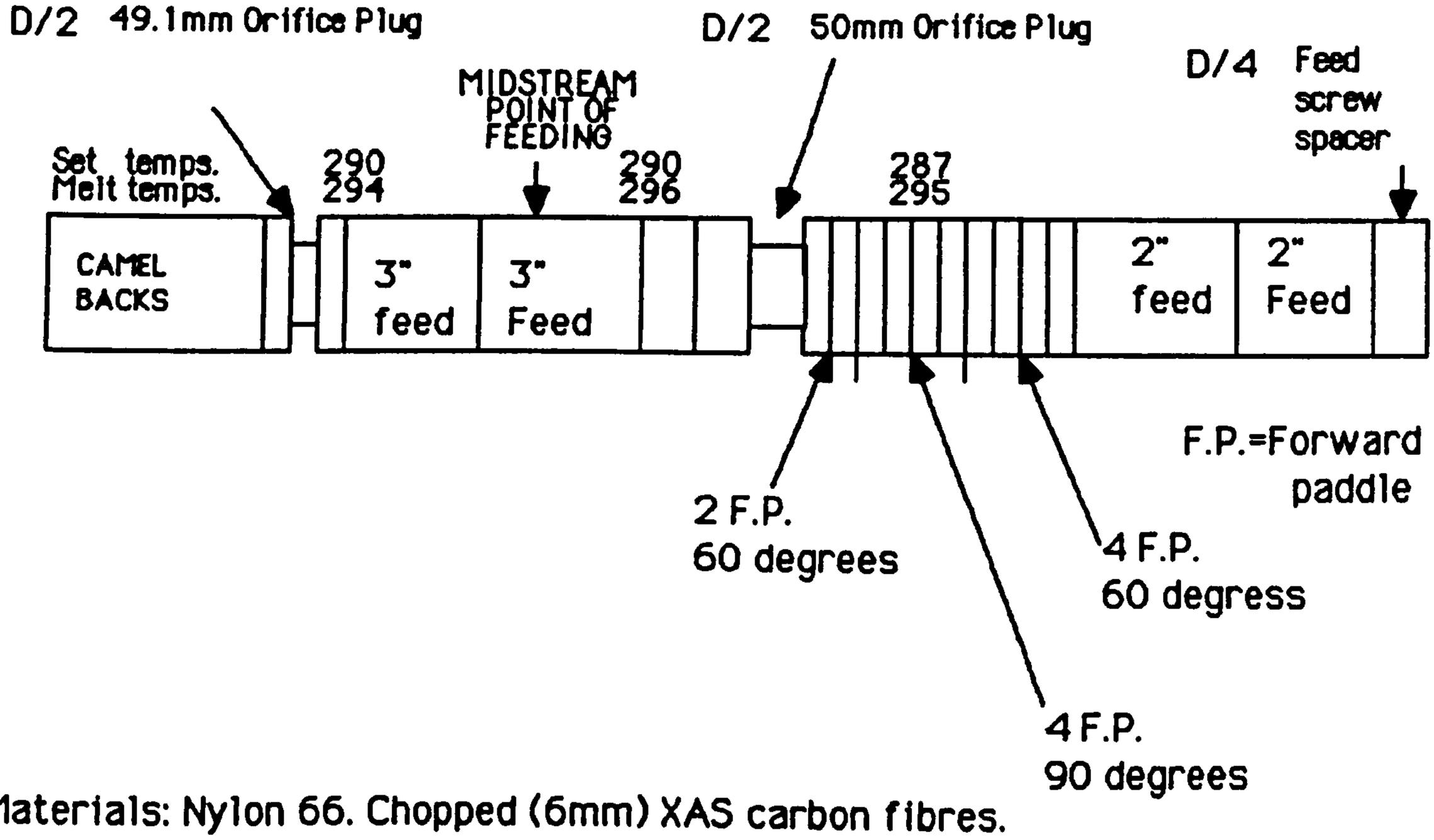

Materials: Nylon 66. Chopped (6mm) XAS carbon fibres.

Screw speed: Various

L:D ratio: 10:1

Die: 6mm dia rod

Pelletiser : Cumberland 6"

Torque: 80-95 %.

Machine ran with crosshead extruder.

Figure 35

Experiment KEVLAR 3

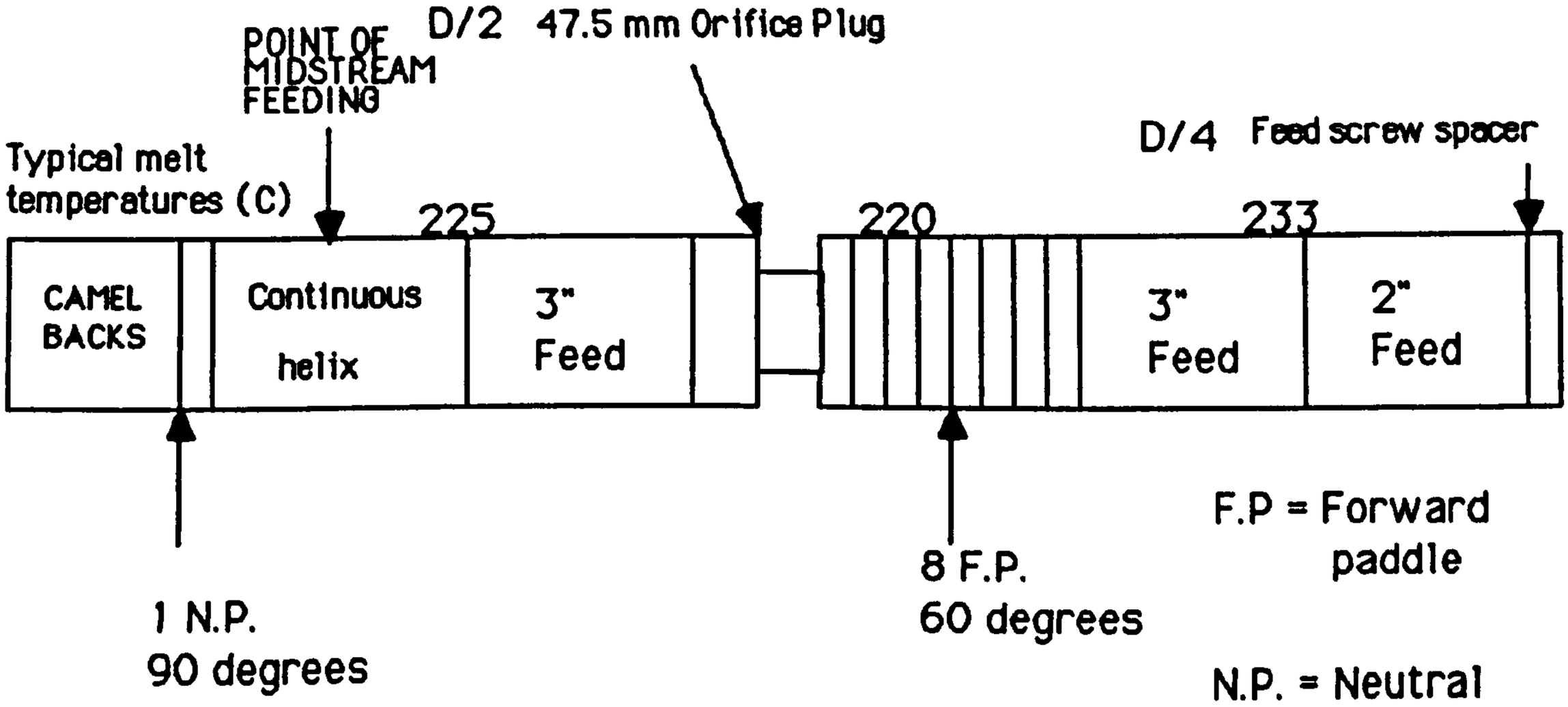

Materials: Polypropylene GW522M. Chopped 6mm Kevlar 49

Screw speeds: 135 and 270 RPM

L:D ratio 10:1

Die: 6mm rod

Pelletiser: Cumberland 6"

Machine ran without crosshead extruder

Die head pressure:
@ 135 RPM 160-200 PSI
@ 270 RPM 200-230 PSI

Torque: @ 135 RPM 19-20 %
@ 270 RPM 19-21 %

Output
@ 135 RPM 3.6 Kg/hr
@ 270 RPM 3.57 Kg/hr

Figure 36

Experiment KEVLAR 4

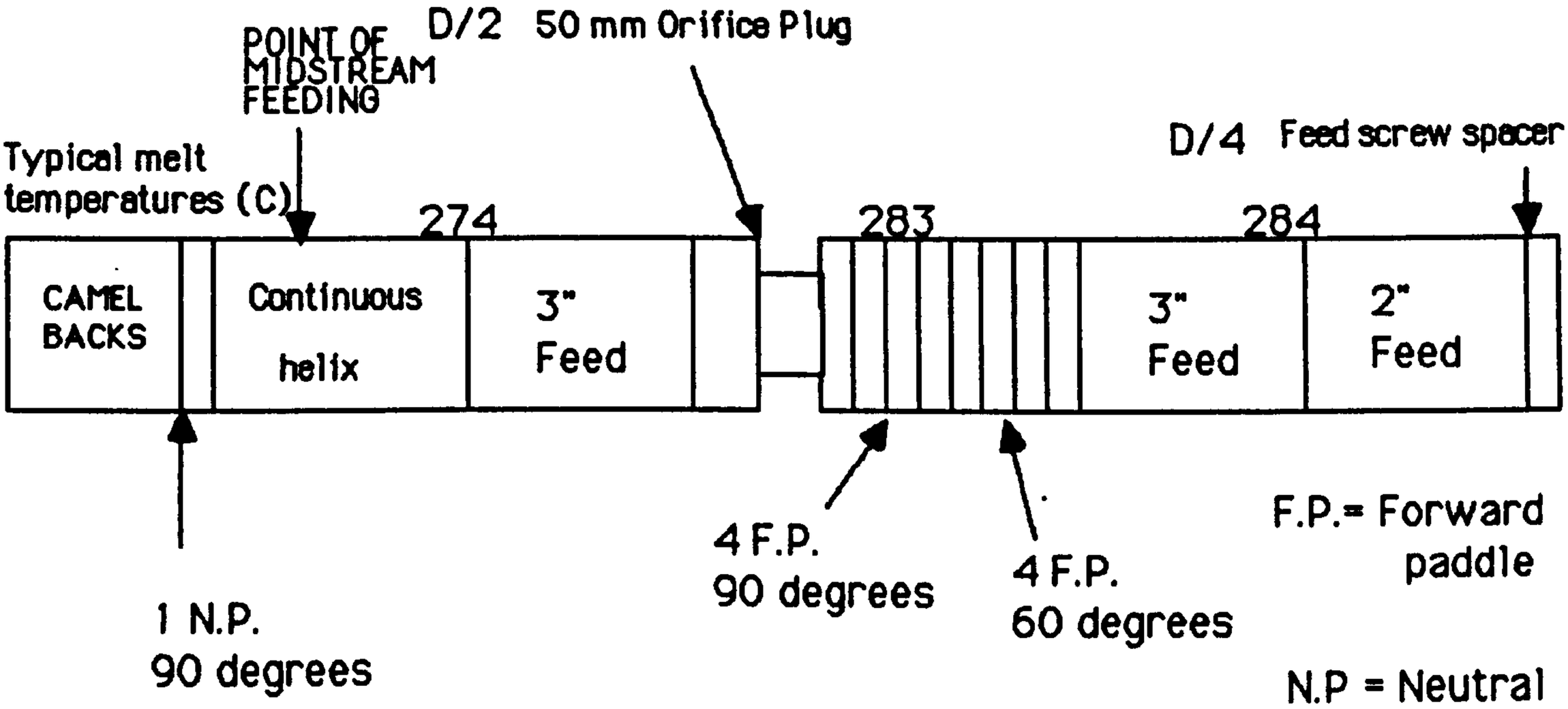

Materials: Nylon 66. A100. Chopped 6mm Kevlar 49

Screw speeds: 135 and 270 RPM

Machine ran without crosshead extruder.

L:D ratio 10:1

Die: 6mm rod

Pelletiser: Cumberland 6"

Torque: 35-37 %

Output 12.4 Kg/hr

Figure 37

Nylon 66. A100

Property	ASTM	Units		
Density	D792	g/cm3		1.14
Tensile strength	D638	MPa	@23 C	81
			@40 C	59.8
			@80 C	40
			@110 C	32
Elongation		%		10
Flexural modulus	D790	GPa		2.8
Flexural strength		MPa		103
Shear strength	D732	MPa		66
Izod impact strength (notch @23 C)	D256	J/m		48

Table 5

Polypropylene GW522M

Property	ASTM	Units	
Melt flow index	____	190 C/10 Kg	22
Density	D792	g/cm3	0.905
Tensile yield stress	D638-77a	MPa	34.5
Flexural modulus	D790	GPa	1.72
Izod impact strength (notch @23 C)	D256	J/m	45

Table 6

Glass reinforced nylon 66.

Property	ASTM	Units		A190	CG1090 (Verton)
Density	D792	g/cm3		1.39	1.37
Glass content		Wt %		33	30
Tensile strength	D638	MPa	@23 C	159	195
Elongation		%		3	4
Flexural modulus	D790	GPa		7.8	10
Sheer strength	D732	MPa		93	--
Izod impact strength (notch @23 C)	D256	J/m		90	--

Table 7

Glass reinforced polypropylene

Property	ASTM	Units	HW60GR20	HW60GR30
Glass content	____	% weight	20	30
Melt flow index	____	230 C/2.16Kg	4	4
Density	D792	g/cm3	1.04	1.12
Tensile yield stress	D638-77a	MPa	72.4	86.4
Flexural modulus	D790	GPa	4.96	6.2
Izod impact strength (notch @23 C)	D256	J/m	70	—
	(BS 2782		91	101)

Table 8

Carbon fibre reinforced nylon RG 20

Property	ASTM	Units	
Density	D792	g/cm3	1.34
Tensile strength	D638	MPa @23	193
Elongation	____	%	3-4
Flexural modulus	D790	GPa	16.5
Flexural strength	____	MPa	298
Sheer strength	D732	MPa	82
Izod impact strength (notch @23 C)	D256	J/m	59

Table 9

Fibre properties HYSOL GRAFIL XA-S carbon fibre

		6mm chopped polyamide sized	Continuous epoxy sized
Tensile strength (GPa)	min. 2.30		3.10*
Tensile modulus (GPa)	min. 185 average 220		235*
Elongation %		1.31	1.30
Density	(g/cm3)	1.79	1.79

* Impregnated tow test

Table 10

Fibre properties E-Glass

Tensile strength	(GPa)	3.
Tensile modulus	(GPa)	70
Elongation at break	(%)	2.5
Density	(g/cm3)	2.56
Diameter	(um)	12-13

Table 11

Fibre properties Kevlar 49

Tensile strength	(GPa)	2.760
Tensile modulus	(GPa)	131
Elongation at break	(%)	2.4
Density	(g/cm3)	1.45
Diameter	(um)	12

Table 12

Specifications for TS40-DV-L twin screw extruder

Screw diameter	40 mm.
Centre distance	35 mm.
Direction of screw rotation	Corotating.
Flight pitch	Feed 24 mm, Compression 12 and 16 mm, Devolatilization 24 mm and Metering 8,12, or 16 mm. 4 adjustable mixing/melting elements on each screw.
L/D ratio	17:1 (from front of feed port) on standard version.
Screw speed	10 to 200 RPM.
Main drive	5.5-KW d-c motor with base speed of 1500 RPM.
Total installed power	15.5 kW.
Output	Up to 30 Kg/hour depending on raw materials and die configuration.
Special features	Interchangeable screw and barrel geometry. Rapid-barrel-withdrawal assembly Cast-aluminum heaters cored for liquid cooling. Provision for melt temperature/pressure instrumentation.

Table 13

Specifications for MPC/V50 twin screw compounder

Barrel	Clam shell design,horizontally split. Electrically heated,water cooled.
Rotor speed	600 RPM with mechanical over torque protection.
Drive	18 kW.
Agitator coflguration	Side-by-side.
Feed ports	One top entry, one side entry.
Agitator rotors	50mm diameter Double lobed , self wiping, co-rotating.
L/D ratio	10:1 standard version, also 13:1 avalible.
Output	50-60 Kg/hour (engineering thermoplastics)
Special features	The machine is equipped with two barrel valves. The agitators are fully segmented construction and are made of nitrided hardened steel. Agitator parts include feed screws, mixing paddles, continuous helix screw and camel-back discharge screws

Table 14

The features of Baker Perkins screw elements

Element	Function	Comments
Mixing Paddles	melt feed materials and disperse additves.	Slip on segment lens shaped agitators. Five way keyways are reversible which gives a total of seven different positions. The paddles can be in a "forwarding configuration" when the offset paddle from the previous up-stream paddle is less than 90 degrees clockwise. If angle is 90 or 0 degrees the paddles are neutral i.e. no forwarding movement. If angle is greater than 90 degrees, paddles are reversing i.e retarding flow.
Feed Screw	Convey feed materials to mixing section and allow entry for side feed materials.	Helical section with equal lead to bore diameter. Of various lengths.
Continuous Helix	Gently fold in fillers or secondary feeds to a molten matrix.	Helical section with lead equal to six bore diameters.
Orifice Plugs	To restrict material flow causing melt back up.	Cylinderical discs. Variable diameter. D/2 and D/4 thicknesses avalible.

Forwarding capacity of paddles	Reversing		Neutral	Forwarding	
Off set angle (degrees)	-45	-60	90	45	30

Table 15

The features of Baker Perkins screw elements (continued)

Element	Function	Comments
Camel Back Discharge Screws	Provides a bearing support on outboard end of rotor and generates pressure for extrusion. When a vacuum is applied they expose the maximum amount of polymer to vacuum.	Single lead wide land discharge screw.
Barrel Valve	Allows control of polymer melt flow.	Used in conjuction with a pair of orifice plugs. The barrel valve provides a variable restriction causing a back up in flow in the mixing section of the barrel.

Table 15

Specifications for MPC/V50 crosshead extruder

Barrel	75 mm, electrically heated and water cooled.
Rotor speed	0-150 RPM variable speed drive.
Drive	7.5 kW.
L/D ratio	8:1.
Screw	Drilled for circulating temperature control fluid.

Table 16

Specifications for Reifenhauser single screw extruder.

Barrel: 30 mm diameter , electrically heated.

Screw speed: 0-120 RPM.

L/D ratio: 24:1

Screw: General purpose screw used.

Die: 6mm rod.

Extrusion conditions used for polypropylene/Kevlar 49 composites

	Indicated temperature (C)
Feed.	185
Middle.	190
Die.	230

Table 17

Sandretto 6GV-5 injection moulding conditions

Screw speed (RPM).	120
Plasticisation counter pressure (MPa).	4
Shot volume (cc).	10-37 (depending on mould)
1st injection pressure (MPa).	115
2nd injection pressure (MPa).	89
3rd injection pressure (MPa).	64
Injection speed (secs.).	20

	Nylon 66.	P.P.
Forward zone set temperature (C).	300	180
Middle zone set temperature (C).	290	185
Supply zone set temperature (C).	260	210
Nozzle set temperature (C).	310	220

P.P = Polypropylene

Table 18

Averages in common use

Mean	Formula	Physical meaning
Number average	$\frac{\sum f_i l_i}{\sum f_i}$	Gives measure of fibre end density.
Weight average	$\frac{\sum f_i l_i^2}{\sum f_i l_i}$	Gives better measure of proportion of long fibres in distribution.

Table 19

Assessment of compound quality Table 20

Property	Source	Comments
Interfacial Shear Strength	Bowyer and Bader [98]	Computer programme based on curve fitting method described in Section 2.5.
(Computer program Appendix 3)		
Stress Transfer interface Efficiency (Strength)	Mc Nally et al [99]	Computer programme that divides the contribution to stress at failure by sub and super critical fibres by the summation of stresses obtained if all fibres were undamaged to give efficiency ratio. Described in Section 2.5.
(Computer program Appendix 4)		
Stress Transfer interface Efficiency (Modulus)	"	As above but assesses contributions to stress at a specific value of strain. Described in Section 2.5
(Computer program Appendix 5)		
Orientation Parameter	Kelly and Tyson [8]	Using the value of interfacial shear strength calculated above and knowledge of the strain at break the composite theoretical strength can be computed assuming an orientation parameter of 1 (Z in eq. 9). The measured strength divided by the computed value gives a ratio which is an estimate of overall fibre orientation.
(Computer program Appendix 6)		

Prediction of composite properties

Stiffness	Cox [4]	Calculation based on F.L.D of injection mouldings. Assumes perfect hexagonal arr angement of fibres.
(Computer program Appendix 7)		
"	Rule of Mixtures	Calculation based on volume fraction.
(Computer program Appendix 8)		

Glass and carbon fibre based compounding experiments

Experiment designation	Compounding machine	Fibre	Matrix	Variables	Tests performed
BRITTLE 1	Gays TS40 DV-L	Carbon XAS continuous	Nylon 66. A100	_____	Fibre length break down along screw.
BRITTLE 2	Gays TS40 DV-L	Carbon XAS chopped & continuous	Nylon 66. A100	Metering screw pitch. Feeding form.	Fibre length. Tensile props.
BRITTLE 3	Gays TS40 DV-L	Carbon XAS continuous.	Nylon 66. A100. Glass filled A190	Die shape & size. Granulation/ pelletisation procedure.	Fibre length.
BRITTLE 4	Baker Perkins MPC/V50 with and without crosshead extruder.	Carbon XAS chopped & continuous. Glass chopped.	Nylon A100	Feeding form. Feeding place. Machine settings. Granulation/ pelletisation.	Fibre length. Tensile props. Impact props. (estimation of Gc) Flex. mod. Interfacial shear strength.
BRITTLE 5	Baker Perkins MPC/V50 without crosshead extruder. Different screw configuration to BRITTLE 4.	Glass continuous.	Nylon A100	_____	Fibre length. Tensile props. Flex mod. Impact props. (estimation of Gc) Interfacial shear strength.
BRITTLE 6	Baker Perkins MPC/V50 With crosshead extruder (Optimum screw configuration).	Carbon XAS chopped.	Nylon A100	Screw speed. Weight fraction.	Fibre length. Tensile props. Flex. mod. Interfacial shear strength.

Table 21

Experiment BRITTLE 4 compounding variables.

Carbon fibre reinforced nylon 66.

	Compounds					
	C1	C2	C3	C4	C5	C6
Configuration						
Direct compounder	✓	✓	✓			
With crosshead extruder				✓	✓	✓
Front barrel valve						
Fully open	✓	✓		✓		✓
Fully closed			✓		✓	
Feeding form						
Chopped carbon	✓	✓				✓
Continuous tow			✓	✓	✓	
Fibre feeding point						
Midstream	✓		✓	✓	✓	
As premix with nylon 66. granules		✓				✓

Table 22

Experiment BRITTLE 4 Compounding variables.
Glass fibre reinforced nylon 66.

	Compounds					
	G1	G2	G3	G4	G5	G6
Configuration						
Direct compounder	✓	✓	✓			
With crosshead extruder				✓	✓	✓
Front barrel valve						
Fully open	✓		✓	✓		✓
Fully closed		✓			✓	
Feeding form						
Chopped glass	✓	✓	✓	✓	✓	✓
Continuous tow						
Fibre feeding point						
Midstream		✓	✓	✓	✓	
As premix with nylon 66. granules	✓					✓

Table 23

Experiment BRITTLE 6 compounding variables.

Carbon fibre reinforced nylon 66.

	Compounds						
	C7	C8	C9	C10	C11	C12	C13
Compounder screw speed (RPM)	300	300	300	300	275	325	380
Configuration							
Direct compounder							
With crosshead extruder	✓	✓	✓	✓	✓	✓	✓
Front barrel valve							
Fully open	✓	✓	✓	✓	✓	✓	✓
Fully closed							
Feeding form							
Chopped carbon	✓	✓	✓	✓	✓	✓	✓
Continuous tow							
Fibre feeding point							
Midstream	✓	✓	✓	✓	✓	✓	✓
As premix with nylon 66. granules							

Table 24

Kevlar 49 fibre based compounding experiments

Experiment designation	Compounding machine	Matrix	Variables	Tests performed on injection moulded samples
KEVLAR 1	Reifenhauser	Polypropylene GW 522M	Screw speed. Fibre content .	Fibre length. Tensile props. Impact props.
KEVLAR 2	Reifenhauser	Polypropylene GW 522M	Titinate coupling agent content. Screw speed. Fibre content	Tensile props. Impact props.
KEVLAR 3	Baker Perkins MPC/V50	Polypropylene GW522M	Fibre content	Fibre length. Tensile props. Impact props Flexural mod.
KEVLAR 4	Baker Perkins MPC/V50	Nylon A100	Fibre content	Tensile Props. Impact props. Flex. mod. Anisotropy measurement.

Table 25

4.1 EXPERIMENTS PERFORMED COMPOUNDING BRITTLE FIBRE IN THE GAY'S TS40-DV-L TWIN SCREW EXTRUDER

4.1.1 Experiment BRITTLE 1

The location of the points along the screws where samples were removed for fibre length analysis are shown in Figure 38. Figure 39 is a photograph of the screw configuration investigated, samples from the front part of the 8mm pitch screws, having been previously removed. Figures 40 to 49 show the fibre length distributions measured for each point along the screws.

On addition of the continuous fibre tow, the fibre tow was immediately broken down into bundles approximately 10 to 15mm long. In doing this a small proportion of debris (discrete fibres, less than 1mm in length) were produced. As the fibres moved towards the die the length of the bundles gradually reduced and the total proportion of bundles in the material was lowered. As the flights were not full at this stage it was possible for fibre bundles to wrap around the screws without being significantly reduced in length. At the transition between the 24 and 8mm pitch screws all fibre bundles were found to disappear. After this point only fibre debris was present. After the first few turns of the 8mm metering screws, fibre length reduced to a level that remained constant for the last seven turns of the metering screws. The die appeared to reduce fibre length by approximately 40 μm. A summary of the fibre length characteristics found along the screws are shown in Table 26.

4.1.2 Experiment BRITTLE 2

Figures 50, 51, 52 and 53 show the extruded fibre length distributions for the 16mm pitch metering screw (tow feed), 16mm pitch metering screw (chopped feed), 8mm pitch metering screw (tow feed) and 8mm pitch metering screw (chopped feed) respectively. Figures 54, 55, 56 and 57 show the fibre length distributions present in injection moulded test bars for each of the above respective compounding arrangements.

Fibre length properties are summarised on Table 27 along with the results of mechanical tests performed. The mechanical properties are compared with that of a commercial material,

(Hysol Grafil 20 weight per cent carbon fibre reinforced nylon 6,6, RG20) using a property index value. The definition of the property index is also shown in Table 27.

From the results it is clear that fibre length is best preserved by a combination of a large metering screw pitch and a continuous fibre feed. The mechanical properties reflect the improvement in fibre length that are obtained with such a compounding arrangement.

Polished samples of sections taken from mouldings revealed that the fibres were well dispersed with the complete absence of fibre bundles for each feeding and metering screw configuration employed.

4.1.3 Experiment BRITTLE 3

The fibre length distributions for the extrudate from the 6mm rod, 3mm slit and 4.4mm slit dies are shown in Figures 58, 59 and 60 respectively. The fibre length properties are summarised on the top of Table 28.

The rod die was found to produce fibres of the greatest length. The slit die set at 3mm was found to allow longer fibres to survive that when it was set at 4.4mm. Figures 61 and 62 are photographs taken from the rod die extrudate and the 4.4mm slit die extrudate respectively. In the case of the rod extrudate the fibres seem to be more aligned in the flow direction which would reduce fibre-fibre interaction.

Figures 63, 64 and 65 show the fibre length distribution of the 6mm diameter rod after being reduced into pellets by the Cumberland 5x7 granulator, the Broyeurs Melangeurs L100 granulator and the Cumberland 6" pelletiser respectively. The fibre length properties are summarised on Table 28. The operation of converting strands into material suitable for injection moulding significantly reduced fibre length. It was possible that in some machines the cutting action, instead of cutting cleanly through the stands, smashed them, shattering fibres throughout their length.

A comparison of the effects of granulating and injection moulding on fibre length are also shown in Table 28. A compound produced using the 4.4mm slit die was granulated using the

Cumberland 5x7 granulator then subsequently injection moulded into ASTM D638 Tensile test bars. Figure 66 compares the fibre length distribution of the granulated and injection moulded material.

The fibre length distribution of carbon fibres which were compounded with a second fibre species, glass is shown in Figure 67. Fibre length properties are again summarised on Table 28. The presence of glass fibre clearly produced a considerable reduction in the length of the carbon fibres.

4.1.4 Discussion

The compounding arrangements employed in experiments BRITTLE 1, 2 and 3 allowed the addition of carbon fibre whilst the polymer was in molten state. This is an arrangement described by Lunt and Shortall[66] as offering the ideal solution to the problem of fibre degradation that was found occuring in the melting region of the conventional single screw extruder compounding process. It is clear however that in this "ideal" compounding arrangement still results in a high level of fibre degradation.

The flows that took place within the extruder used were complex. Investigations to assess the flow of material between and within the screw channels were undertaken by direct examination of material extracted from the screws after shock cooling the melt. In the decompression and metering sections material was transported from one screw channel to another in a figure of eight fashion. At the intermeshing region a significant portion of flow was split into two streams. This subjected the material to successive division and mergings. The number of successive mergings is dependent on the pitch of the screws, the route being less winding for larger pitch screws. Additional leakage flows observed included material passing between the channel of one screw and the flight land of another and melt flowing between the ends of the screw flights and the barrel wall. Although these clearances were small, high shear stresses were thought to be developed in these regions, these would cause significant fibre degradation. The flows that take place in the twin screw extruder are quite different to those found by other investigators[60,61,63,64] for single screw extruders, where discrete pockets of material are melted and the melt is not significantly

rearranged.

From the pattern of results for experiment BRITTLE 1 it is clear that on entering the extruder carbon fibre tow was not immediately filamentised but the action of the screws broke the two into bundles and a small proportion of carbon fibre debris (fibre less than 1mm). These bundles progressively reduced in length as they were moved down the screws towards the die. In reducing in length an increasing amount of carbon fibre debris was produced. It can be envisaged that fibre-fibre interaction was limited to the outside fibres in the bundles so fibre degradation took place gradually. The bundles disappeared at the transition to the metering screw section, to produce only carbon fibre debris. After a few screw pitch sections of the metering screw however, fibre length did not change significantly before the die. This would seem to indicate that once the fibres were well dispersed, discrete and at length characteristic of the screw pitch, the mixing action had little further effect on fibre degradation. This suggests fibre-fibre interaction was the significant cause of fibre breakage.

The last point of fibre breakage in the extrusion process occurred as the fibres passed through the die. Here fibres were forced to rotate from a previously misaligned direction to the flow direction. As the fibres were well wetted at this point, fibre-fibre interaction may be expected to play a minor role in length degradation. It is likely here that viscous loading by the polymer in the bulk state would cause fibre bending that could lead to fibre fracture. For this source of fibre breakage, an increase in the viscosity of the melt or an increase in shear rate as material passes through the die is likely to increase fibre breakage.

Experiment BRITTLE 2 investigated the influence of metering screw pitch and feeding form. The longest fibre length materials were produced using 16mm pitch metering screws in combination with continuous fibre tow. It would seem that the final extruded length distribution of carbon fibre fed as tow was wider than that which was fed as chopped fibre. The advantage in fibre length gained however was significantly reduced by the operations of converting the strands into feed stock pellets and injection moulding. It can be imagined that the path for material moving around larger pitch metering screws was less torturous than it would be for material moving

around shorter pitch flights, reducing the tendency for fibre-fibre interaction.

Although it is understood that the volume fraction of fibre present will effect the length of fibre in a compound, perhaps a more meaningful way of displaying mechanical data of compounds with different volume fractions of fibres is a property index relative to a fibre content as shown in Table 27.

The effect on fibre length of converting extrudate or strand into material suitable for injection moulding is clearly shown in experiment BRITTLE 3. It would seem that the granulators used; the Cumberland 5x7 and Broyeurs Malangeurs L100 reduced fibre length more significantly than the Cumberland 6" pelletiser. Figure 70 shows the much simplified designs of both the Cumberland 5x7 granulator and Cumberland 6" pelletiser. In the case of the pelletiser the knife produces a simple slicing action on the strands. In the case of the granulator strands of extrudate are added from the top and broken down by the steep angled rotor cutter until short enough to fall through a screen. It can be envisaged that the rotor may have to slice a piece of material many times before it is small enough, producing many fractured surfaces and applying shock. This shock could shatter brittle fibres within the material. It would seem likely that any wear that occurred on the pelletiser knives or granulator rotors would blunt the cutting edges and so produce a smashing action instead of the desired cutting action.

Die design was found to have a noteworthy effect on fibre length. The 6mm rod die was found to produce the least fibre breakage, in the case of the slit die, reducing the die width from 4.4 to 3mm yielded longer fibre lengths. Figures 61 and 62 reveal the orientation of the fibres produced by the rod and 4.4mm slit die respectively. Fibres present in the 4.4mm slit die material were less aligned in the flow direction. It was thought that fibres orientated parallel to the flow direction were less likely to be broken passing through the die than those transverse to the flow direction. The increase in fibre length that became apparent when the width of the die was reduced is difficult to explain. A possible reason may be the nature of converging flow that occurred within the die. In converging flow, an extensional flow is superimposed upon a shearing flow. As the angle of converging flows increased the extensional flow component becomes more

prominent. Although it was not possible to expose the effect in extruded sections by microscopic examination, it would seem likely that reducing the die width increased the ratio of extensional flow, producing a slightly higher proportion of fibres orientated parallel to the flow direction. Hence the fibres were more able to survive without being reduced in length on passing through the die. Lunt and Shortall[65] using a single screw extruder to produce glass reinforced nylon 6,6 found that when the diameter of the die was reduced from 4 to 3mm, fibre length was found to effectively increase. This was thought to be a result of the lowering in the amount of undispersed strands produced, an effect attributed to an increase in distributive mixing without a significant increase in dispersive mixing.

For carbon fibre, the advantages of using continuous tow as the feeding form for the compounding operation are numerous. It is more economical to use continuous tow as the fibre does not have to undergo a chopping operation or be heavily sized to prevent chopped fibres fluffing up on handling. With no size present the matrix can make contact directly to the chemically activated carbon fibre surface. If the fibre has been sized a low molecular weight coating may remain on its surface in the moulded component; this could limit the stress transfer efficiency between the fibre and matrix. Alternatively, the size migrates from the fibre surface to dilute the matrix and hence lower its mechanical properties.

4.2 Experiments Performed Compounding Brittle Fibres in the Baker Perkins Compounding System

4.2.1 Experiment BRITTLE 4

Fibre breakage during pelletisation was minimized as far as possible in this and subsequent experiments by the use of the Cumberland 6" Pelletiser as discussed previously. Figures 69 and 70 show the fibre length distributions for typical glass and carbon reinforced nylon 6,6 compounds before and after pelletising.

The fibre length distributions of the extruded carbon fibre reinforced material prior to pelletisation and of the injection moulded carbon fibre reinforced material are shown on Figures 71

to 78. Those of glass materials are shown on Figures 79 to 84. Tables 29 and 30 present a complete summary of fibre length characteristics together with mechanical properties of injection mouldings, predicted mechanical properties and values used to assess compound quality for the carbon and glass reinforced materials respectively. In the case of the carbon reinforced compounds, for comparison purposes, the results measured for a commercially available carbon fibre reinforced nylon 6,6, Hysol Grafil's RG20, are included. The fibre length distribution for RG20 is shown in Figure 85.

A volume fraction of 12% of carbon fibres in nylon 6,6 is approximately equal to weight fraction of 20%, a volume fraction of 8.5% of glass fibres in nylon 6,6 is approximately equal to a weight fraction of 20%.

From the overall results for carbon fibre it was apparent that for all compounding configurations used, the fibre lengths are below the 1mm needed to produce optimum stiffness properties, (See Figure 4). The greatest influence on fibre length was found to be the location of the feeding point. Compounds C2 and C6 fed as the premix with nylon granules had an average extruded fibre length approximately half of the fibres added midstream. The use of a crosshead extruder in combination with the twin screw compounder seemed to have no significant influence on fibre length. The front barrel valve which acted to provide a restriction to molten material as it moved towards the die also seemed to have little influence on fibre length. One concludes that the fibres are broken down to an equilibrium value on passing through the six, 45 degree forward paddles. The mixing section had a temperature rise of approximately 10°C above the barrel set temperature indicating that heat generating mixing took place. In all cases, the fibres were relatively short but well dispersed, the pelletising and injection moulding processes only reduced fibre length slightly. Compound C1 had a slight improvement in fibre length over the commercially produced compound containing approximately the same volume fraction of fibres.

For the glass reinforced nylon compounds all fibre lengths were below the length required to obtain optimum stiffness properties. (See Figure 5). Comparing identical processing arrangements with carbon, glass fibres were found to survive to approximately twice the length. As was

the case with carbon fibres, the greatest influence on fibre length was found to be the location of the feeding point. The fibres fed as a premix with nylon had fibre lengths approximately 1/2 to 3/4 of the fibres fed midstream. Evidence showed that glass fibres incorporated using the compounder with the cross head extruder (compounds G4 and G5) survived to be slightly longer than fibres processed using the direct compounding configuration. The front barrel valve setting was found to have no significant effect on glass fibre length. The difference between extruded compounding and injection moulded fibre lengths were not as great as in the case of carbon. This effect may be related to the relative brittleness of carbon compared to glass.

The interfacial shear strengths of compounds produced were calculated from the stress-strain curves of injection moulded test bars tested in tension as described in Sections 2.5 and 3.8. For the carbon fibre reinforced nylons the values calculated were up to twice the value of the matrix shear yield strength. Curtis et al[105] encountered the same effect when estimating the interfacial shear strength of carbon fibre reinforced nylon by a similar method, a result that they did not explain. Table 31 shows the dependence of the estimated shear strength on the strains chosen for its calculation. It is clear that realistic estimations of interfacial shear strength are only possible where the stress-strain curve is essentially non-linear at strains above 1%. Here the fibre-matrix interface can be assumed to have changed from "Cox behaviour" where a perfect bond exists between the fibre and matrix while the matrix behaves elastically to "Kelly-Tyson behaviour" where the matrix behaves plastically. Estimates at high values of strain are invalid however as they are beyond the strain at break of the carbon fibre. From scanning microscopy of the fracture surface of carbon fibre reinforced nylon 6,6 (Section 4.2.4) it appeared that the interfacial shear strength between the fibre and matrix was very close or equal to the matrix shear yield strength. The stress-strain curve method for estimating the interfacial shear strength of Kevlar and glass reinforced thermoplastics worked successfully. It would seem the method is only applicable within the strain at break of the fibre when the interfacial shear strength is not close to the shear yield strength of the matrix. For the analysis of the compounding performance of carbon fibre reinforced nylon compounds, the value of the shear strength of the matrix was

interfacial shear strength. The values of interfacial shear strengths estimated from a stress-strain curve of an injection moulding serves to act as an overall average of the interfacial shear strength that exists between fibre and matrix in the injection moulding. Comparison of this value for different compounding routes allows an evaluation of compounding efficiency to be made.

For the glass reinforced materials, the use of a crosshead extruder seemed to have no significant effect on interfacial shear strength. The barrel valve setting was found to have influence when the compounder was used in its direct form; closing the barrel valve was found to increase interfacial shear strength by 4 MPa., an increase of 14%. The stress transfer interface efficiencies calculated allowed the combined effects of fibre length and interfacial shear strength on tensile strength and modulus to be quantitively assessed. It is clear from the results that the modulus stress transfer interface efficiencies were greater than the strength transfer interface efficiencies. This is not surprising if it is considered that particulate filler in many crystalline thermoplastics reinforce modulus not strength. The carbon fibre reinforced materials with the highest stress transfer efficiency for both tensile modulus and strength were those fed with continuous fibres midstream. No significant influence was made by the setting of the barrel valve or by the use of the crosshead extruder. These configurations, however, had the lowest volume fractions therefore reducing the fibre-fibre interaction. The stress transfer properties for compound C1 were clearly better than the commercially available compound.

Of the carbon fibre reinforced materials, it was clear that the compounds with the shortest fibre lengths C2 and C6 had the poorest mechanical properties and the highest strain to failure. The improvements in the mechanical properties produced by the longer fibres in compound C1 over the commercially produced compounds is exhibited in terms of tensile modulus not tensile strength. The poor tensile strengths were a result of lower strain to failure. Despite having a lower volume fraction, the tow fed compounds C3, C4 and C5 had lower strains to failure than the chopped fibre fed compounds. This may have been a result of longer fibre lengths. For glass reinforced materials the shortest fibre compounds were also found to have the poorest mechanical properties and the highest strains to failure.

For the tensile bars overall "fibre orientation ratios" were generally between 0.7 and 0.8, indicating a high degree of fibre alignment. For the carbon fibre reinforced materials, it was apparent that materials with shorter fibre lengths had a higher degree of fibre alignment in the testing direction than those of longer fibre length. This lowering of the degree of orientation could have been due to the longer fibres impeding each other. In the case of glass reinforced materials there was no apparent relationship between fibre orientation ratio and fibre length. The compound with the highest orientation ratio was found to have an intermediate fibre length.

The rule of mixtures estimate of tensile modulus was 2 to 3 times the value measured. A considerably more accurate estimation was based on the fibre length distribution using the Cox shear lag analysis. The Cox estimated value was slightly higher than the measured value probably as a result of imperfect fibre alignment and the errors inherent in the analysis discussed in Section 1.5.2.

4.2.2 Experiment BRITTLE 5

This experiment was designed to assess the properties of compounds containing the longest possible glass fibre lengths that could be successfully stranded. The minimum number of neutral and reversing paddles were incorporated in the compounder screw profile and the fibre was fed mid stream in the form of a tow.

Figure 86 shows the fibre length distribution of the glass reinforced nylon material which was extruded without a die or die adapter directly into the water bath. A significant proportion of fibres over 1mm were produced. A photograph of the screw profile after the experiment was complete is shown in Figure 87, long strands can be seen hanging from the mixing paddles. With the 6mm die in position, strands were extruded, pelletised using the Cumberland 6" pelletiser and injection moulded. Figure 88 presents the fibre length distributions after each process. Table 32 summarises the fibre length properties, lists the mechanical properties of injection moulded samples and presents values that assess compound quality.

The elongation at break was reduced compared with glass reinforced nylons of a similar

The elongation at break was reduced compared with glass reinforced nylons of a similar volume fraction in experiment BRITTLE 4. The values of the interfacial shear strength calculated from the stress-strain curves of injection moulded bars tested in tension were low compared to the matrix shear yield strength. It was likely that this reflected a low level of wetting and dispersion. Undispersed bundles, however were not apparent in injection mouldings. Although fibre lengths were comparatively long, stress transfer interface efficiencies were limited by the poor interfacial shear strength. It is interesting to note that the efficiencies were in some cases inferior to some of the shorter fibre length compounds produced in experiment BRITTLE 4. The difference between the Cox estimation of the tensile modulus and the measured estimation was again likely to be a reflection of the imperfect orientation of the fibres in the testing direction.

4.2.3 Experiment BRITTLE 6

The compounding configuration used is shown in Figure 35. Mixing paddles were not used for the incorporation of fibre into the melt. To allow the minimum possible fibre attrition, fibres were added directly on to feed screws. The smallest available orifice plug was used to provide the minimum possible restriction to the melt before moving on to the camel back discharge screws.

As in experiment BRITTLE 4, the pelletising operation was arranged so that the longest possible pellets that could be successfully injection moulded were produced. The fibre length distributions of the extruded and injection moulded materials are presented in Figures 89 to 95. Summarised values of the fibre length properties together with mechanical properties of injection moulded compounds and estimates of compounding efficiency are presented in Table 33. Compared with the fibre reinforced materials produced in Experiment BRITTLE 4, extruded fibre lengths were increased by up to 30%. However, on injection moulding the fibre lengths were found to have decreased marginally. Despite the small increase in fibre length obtained, the benefits in mechanical properties were apparent. The stress transfer efficiencies of compounds C8 proved superior to that of compound C1 produced in experiment BRITTLE 4, which contained a comparable volume fraction of fibres.

It would seem from the pattern of orientation results, that as fibre length was reduced but volume fraction increased, fibre orientation became more discernible. Compounds produced with lower fibre volume fractions had longer average fibre lengths than the low fibre volume fraction materials produced in experiment BRITTLE 4. Their poorer mechanical properties may be partly explained by lower fibre orientation ratios.

Figure 96 is a plot of percentage volume fraction against number average fibre length after the processing operations of extrusion compounds and injection moulding. The graphs show that the volume fraction did not significantly influence fibre length for extrusion compounding, but on injection moulding when the extrudate was remelted, an increased volume fraction produced shorter fibre lengths.

Figure 97 is a plot of compounder screw speed against average fibre length for extruded compound, the cross head extruder having been set at a constant screw speed of 90 RPM for each compounder screw speed used. A compounder screw speed of 380 RPM allowed the production of fibres with an average fibre length that was 10% longer than was produced at 275 or 450 RPM. The higher fibre degradation at a lower speed may be the result of reduced shear rate of the screws allowing a slightly higher viscosity of the melt at the point fibre is added to the compounder. This would cause extra viscous loading by the polymer which could lead to greater fibre breakage. The higher degradation at screw speeds above 380 RPM may be the result of increased melt pressure at the junction between the end of the twin screw compounder and the start of the cross head extruder.

4.2.4 Discussion

The discussion of the results of experiments BRITTLE 4, 5 and 6 are divided up under the headings of fibre length properties, mechanical properties, fibre orientation, and the examination of tensile fracture surfaces by electron microscopy.

Fibre Length Properties

The fibre length properties measured in this study were taken at random from each batch of extruded or injection moulded material. The length results therefore should be taken as typical values rather than overall averages.

Fibre lengths in injection moulded test bars were well below the lengths required to produce the optimum properties of stiffness and strength. Carbon fibres were generally found to be reduced in length more significantly than glass fibre. Except in the case of those with highly degraded fibre lengths, chopped fed glass fibre compounds had flatter and wider fibre length distributions than chopped fed carbon compounds produced by the same compounding arrangement.

Chopped fibre fed carbon fibre compounds appeared to have positively skewed length distributions i.e. the greatest proportion of fibres were of shorter length. Continuous tow fed carbon fibre materials had fibre length distributions that were flatter and wider. This may have been a result of a wider spectrum of fibre lengths produced when the continuous tow was initially broken up inside the compounder. The influence of input fibre length on final fibre length in moulded components was investigated by Schweizer[106] using a single screw extruder to compound glass fibres of different starting lengths into polypropylene and polybutylene terephthalate. On injection moulding it was found that final fibre length in injection moulded artefacts were essentially independent of input fibre lengths. It is likely however that the injection moulding process may have masked any relationship that may have existed between input and compounded fibre lengths.

Experiment BRITTLE 5 performed with continuous glass showed that it was possible to produce compounds with comparatively long fibre lengths, but demonstrated that this can be at the expense of good dispersion and poor interfacial shear strength. The last experiment based on brittle fibres: BRITTLE 6 revealed that by careful selection of screw configuration and processing conditions fibre length in extruded compounds can be optimised. The potential length of fibres in the moulded product were however restricted by the fibre attrition that occurred in the pelletising and injection moulding operations. It is likely that the breakage of fibres by the pelletising operation may be reduced by pelletising whilst the matrix is above its glass transition temperature. A

number of pelletisers are commercially available which pelletise molten polymer as it is extruded through a multi hole die, these are called die face pelletisers. There are three basic types of machine: the hot cut pelletiser, the under water pelletiser and the water ring pelletiser. These machines differ from each other in the way in which molten pellets are quench cooled. Hot cut and water ring pelletisers have been found to be best suited to pelletising high melting point polymers.

Mechanical Properties

Figure 98 presents graphs showing the stress-strain curves for injection moulded tensile bars of compounds C8, C6 and C1. It is evident that the ultimate strength of compound C8 reinforced with longer fibres than compounds C6 and C1 does not increase proportionately to the increase in stiffness observed at lower strains. The lower strain at fracture for the long fibre compound is not easy to explain, it could be initiated by fibre fracture leading to catastropic transfer of stress to surrounding matrix or fibres, or be initiated in the matrix by higher stress concentrations produced at the ends of the longer fibres. Bader and Bowyer[90] investigating glass and carbon fibre reinforced nylon found the strain at failure was indepenent of volume fraction. It was suggested therefore that failure was initiated by fibre failure. As shown in Table 34, it was found in this study that strain to failure was reduced as volume fraction increased so either of the two mechanisms above would seem likely. It would seem probable that higher volume fraction composites having more fibre ends would have a larger number of matrix cracks promoting failure at lower strains.

Compound G7 which had poor interfacial bonding in combination with long fibres had a significant reduction in its strain to break compared with better wetted shorter fibre compounds, see Figure 99. The reduction in interfacial shear strength may have made the stress concentration at fibre ends more important at initiating fracture than individual fibre fracture. The fibres may have been able to debond more readily from the matrix increasing the stress concentrating effect.

Curtis, Bader and Bailey[105] observed a reduction in strain at break as the volume fraction of carbon and glass fibre in nylon 6,6 was increased. However unlike in this study, moulding was

carried out over a temperature range of 270 to 305°C, depending on volume fraction, so the effect in this case could be explained by embrittlement caused by a change in morphology. In the same publication Curtis, Bader and Bailey using an acoustic emission monitoring technique measured acoustic count with specimen strain for a wide range of fibre reinforced samples under tension. The relationship between stress-strain curves and acoustic output was correlated. It was found that fractures were proceeded by a marked increase in acoustic emission. As fibre length distributions between strained and unstrained samples were not found to differ significantly, and fracture surfaces indicated good bonding, it was concluded that the source of acoustic emission was matrix cracking. In a later publication Bader and Collins[60] extended the possible sources of acoustic emission. With compounds produced in the absence of coupling agent and boiled in water, acoustic emission was drastically reduced giving virtually no output. As unfilled matrix gave no acoustic output it was concluded that the sources of noise were fibre debonding, brittle matrix cracking and fibre fracture.

The model proposed for failure in tensile by Curtis, Bader and Bailey was that as stress is increased on the material small cracks form at the fibre ends, initially at the longest aligned fibres that carry the highest stress, then at the shorter more aligned fibres, followed by the shorter more misaligned fibres. Final failure will occur when catastrophic crack propagation is initiated either by the formation of the first crack or when a critical accumulation of cracks are developed. The three stage behaviour of the stress-strain graph of short fibre reinforced nylon described by Curtis, Bader and Bowyer in the same publication was in this study found to be more distinct for carbon than glass reinforced nylon. The first stage, a quasi-elastic regime was applicable to strains of 0.4% for the shorter fibre reinforced compounds such as C6 and 0.65% for the longer fibre reinforced compounds such as C8. The second stage of the stress-strain graph described, is a parabolic relationship determined by the effect of more and more fibres becoming effectively subcritical as strain is increased. The third stage is a flattening out of the stress-strain curve produced by cracking debonding or fibre breakage. For the longer fibre compounds produced in this study the third stage was found to be very short probably as a result of high stress concentration at the ends

of the fibre causing early catastophic failure. The overall strain to failure in tensile of carbon fibre compounds containing relatively short fibres were found to be at least twice the strain to failure of single carbon fibres (1%). Glass reinforced compounds were found to have a similar strain to break as single glass fibres (3%). It is generally concluded that the fibre failure strain represents the upper limit of useful extension of these materials.

The flexural properties measured are characteristic of the non standard test piece employed and therefore can not be compared directly with standard data sheets. The values are useful for comparison purposes between compounds. Despite the non standard test pieces all the values measured for flexural strength were higher than those measured in tension. According to Turner[107] this has been found to be the case for many classes of material. The ratio of the two strengths is known as the rupture factor. Vincent[108] investigated reasons for this disparity with polymethylmethacrylate and suggested that part of the difference can be attributed to the way cracks grow under tension and flexure. It was proposed that in flexure cracks tend to begin in the tension face and elongate along the surface rather than penetrate into the test piece. Shallow cracks introduce a lower stress concentration than deep ones, so a higher stress has to be applied to cause failure. It would seem that flexural properties offer the best guide to the performance of materials in service.

The ability of the Cox shear lag model to predict the tensile modulus of short carbon and glass reinforced nylon mouldings indicated that at low strains the material behaved elastically and good bonding existed between the fibres and nylon. The success of the model to is important as it proves that providing the properties of the matrix and fibre are known and the fibre length distribution can be evaluated accurately, a realistic estimation of modulus can be determined. The division of the value of modulus obtained by the Cox estimate by the value estimated by the rule of mixtures would yield a modulus efficiency ratio that could be used to compare the efficiencies of various theoretical length distributions.

The interfacial shear strengths computed are useful to assess the average interfacial shear strength in a moulded test piece. The main reasons for the difference between the values com-

puted and the shear yield strength of the matrix were likely to be poor bonding and inadequate fibre wetting. It is also possible that some of the discrepancy could be accounted for by internal stresses developed at the interface during moulding and subsequent cooling of the mouldings.

Fibre Orientation

In order to achieve the maximum benefit in mechanical properties from increased fibre lengths and improved bonding in short fibre reinforced thermoplastics it is important that the fibres are aligned in the stressing direction. The effects of fibre orientation on the mechanical properties of short fibre reinforced thermoplastic composite materials has been demonstrated by a number of investigators. McNally[109] showed using glass reinforced polybutylene terphthalate, that stiffness is a very sensitive function of fibre orientation for small degrees of off axis loading. The influence of the stress axis-fibre axis angle on tensile strength was investigated by Lees[22] using aligned fibres in a range of thermoplastics. This property was found to decrease rapidly as the angle between the mean fibre direction and load exceeded 10-20%.

It is well known that during the injection moulding process fibres become orientated in a complex manner. Investigators[110] have shown that the orientation in an injection moulding varies through its thickness with a skin core layer structure. This has been found to produce marked anistropy in mechanical properties.

For all the experiments based on brittle fibres, the mouldings produced were single end gated tensile bars for which the calculated fibre orientation ratios were between 0.65 and 0.82 (1 = perfect alignment) this indicated pronounced overall fibre alignment. The differences in estimated orientation ratios may have due to variations in relative thicknesses of skin core ratios. Because of the high degree of fibre alignment which was present in the stressing direction, stiffness and strength values measured in this study from end gated tensile bars may be considered to be near the upper band of what is achievable in a practical component. In actual components weld lines, areas of flow spitting and abrupt changes in section are all likely to introduce severe discontinuties in fibre orientation.

Figure 100 shows the relationship between average fibre length and calculated orientation ratio for the carbon and glass reinforced nylon 6,6 tensile bars produced. Although there is no obvious pattern, there seems to be a tendency for longer fibre compounds to have less fibres orientated parallel to the tensile bar. This result is in contrast to Bader and Bowyer[98] and also Bader and Collins[60] who produced "long" and "short" glass and carbon fibre reinforced nylon 66 material using two different types of production method. They showed that "long" fibre compounds had greater fibre alignment parallel to the testing direction in injection moulded test pieces. Various investigators have shown that fibre orientation in injection mouldings is dependent on a wide range of factors. Bright, Crowson and Folkes[111] studied the effect of injection speed on fibre orientation in simple mouldings of glass reinforced polypropylene. It was found that fibre orientation particularly in the core of mouldings is dependent on injection speed. A high injection speed gave alignment of fibres transverse to the flow direction, while for very low injection speeds the fibres aligned parallel to the flow direction. Sanou, Chung and Cohen[112] found that fibre orientation was dependent on mould cavity thickness, fibre concentration and melt temperature. When flow was reasonably undirectional, as in the thinnest cavity that was investigated (1mm), the fibres remained essentially in the plane of flow with their axes either along the flow direction or perpendicular to it. For a thicker cavity (2.54mm), a proportion of fibres were found to be arranged in a parabolic profile across its thickness.

Fibre orientation produced by injection moulding seems to be influenced by a wide range of moulding parameters. The fibre orientation present in mouldings produced in this study are only typical for the processing conditions used. In principle fibre orientation could be controlled by the careful mould design and the careful selection of injection moulding conditions. Much work is clearly required to optimise these parameters for the injection moulding of short fibre reinforced thermoplastics with increased fibre length.

The Examination of Tensile Fracture Surfaces by Scanning Electron Microscopy

Much information about interfacial adhesion and modes of failure can be gained about a short fibre reinforced thermoplastic by the examination of its fracture surface by scanning

electron microscopy.

If the fibres present in the moulded test bar are above their critical fibre length, after the application of a tensile stress great enough to break the test piece, the fibres have been stressed to their ultimate breaking stress. When one fibre breaks other fibres immediately become overloaded and then also break, so that a flat tensile fracture spreads over the cross section. If in contrast the fibres are under their critical fibre length, they do not break but pull-out of their holes, high fibre pull-out is observed. When fibre lengths are approximately equal to the critical fibre length, once one fibre breaks, neighbours of fibres will not generally break in the same cross section. As the extra load is transferred over the distance of their transfer length, since their most high stressed region occurs towards the centres of their own lengths, the fibres will break at their own centres rather than a common cross sectional plane giving a rough appearance to the fracture surface.

Figure 101 shows the overall tensile fracture surface of one of the carbon fibre reinforced compounds produced in this study (compound C1). The overall fractuure surface appeared rough and the fracture surfaces of individual fibres appeared clean indicating the fibres were approximately equal in length to the critical fibre length. Figure 102 is a closer study of the fracture surface of compound C1. Wetting of the fibre by the matrix is indicated by the small contact angle formed on the fibres by the adhering matrix, a small contact angle which was apparent for a number of fibres indicated good wetting. A number of fibres appeared to be coated by a sheath of material. It was evident that the bond between the sheath and the matrix was less than the bond between the sheath and fibre.

The tensile fracture surface of a glass reinforced nylon 6,6 produced in this study (compound G4) is shown in Figure 103. The fracture surface is quite different to that of the carbon fibre reinforced nylon 6,6. There are a large number of holes indicating fibre pull-out. The overall matrix fracture surface appears flat, this indicates the crack moved through the material without considerable diversion caused by fibres. Overall evidence from the fracture surface would seem to indicate that the fibres were below their critical fibre lengths. Figure 104 is a

closer study of the fracture surface, the fibres appeared to be rough but there is no evidence of a sheath of polymer on fibre surfaces.

One explanation for the sheaves of polymer observed around carbon fibres in the fracture surface is that the fibres acted to nucleate a region of transcrystallinity. The strength of the bond at the interface between the fibre and sheath region was significant as less energy was required to pull-out the fibres with their sheaves from the matrix than to sever the strong chemical bonds between fibre and matrix, even allowing for the increased friction which may have to be overcome in pulling out irregular shaped sheaves from the bulk matrix.

A number of studies have been performed on the combination of nylon and reinforcing fibres with a view to investigate the nature of the interfacial morphology. Bessel, Hull and Shortall[113] and Bessel and Shortall[114] investigated the interfacial morphology and interfacial bond strength of nylon 6,6 at glass and carbon fibre surfaces. In their investigation they prepared uniaxially aligned fibreous composites by insitu anionic polymerisation of caprolactam directly on to fibres. It was found that the fibres nucleated directional crystallisation (columnar growth) of the nylon at the interface between the fibres and matrix. The amount and form of columnar growth was found to depend on the type of fibre and polymerisation conditions. Optical polarising microscopy revealed that the columnar structure consisted of an inner zone adjacent to the fibre with a speckled structure, and an outer zone with a fibrillar structure extending into the spherulictic matrix. For type I carbon fibres the width of the inner zone was greater than it was for type II fibres. The ability of glass fibres to nucleate columnar growth was considerably less pronounced than carbon fibres. It is interesting to note that on studying fracture surfaces of the carbon fibre reinforced variant by scanning electron microscopy Bessel and Shortall found that the width of the columnar crystalline layer was too great to pull-out as a sheath, so very little fibre pull-out was observed.

Burton and Folkes[115] investigated the interfacial morphology present in fibre reinforced nylon 6,6. Although in the case of carbon and Kevlar fibres significant columnar growth was produced using a hot stage microscope, sections cut from injection moulded components showed no

real evidence of columnar growth. A reason suggested for this effect was that the presence of pulverised fibre debris produced during the compounding and injection moulding processes could provide extensive counter nucleation and inhibit columnar growth.

Figures 105 and 106 show the columnar transcrystallinity produced around fibres in nylon 6,6 using a hot stage microscope. Figure 105 shows two high modulus (type I) carbon fibres and Figure 106 shows the glass fibres both types of fibre are in a nylon 6,6 matrix. From the photographs it is clear that the transcrystallinity around the glass fibres is more random with more nucleating sites, this results in a patchy appearance. As has been identified in the fracture surface studied in this investigation the presence of such transcrystallinity has an effect on fracture behaviour and so is likely to have an important effect on composite properties. This effect is more likely to be significant at higher volume fractions of fibre where columnar regions around adjacent fibres interleave and thereby modify the matrix as a whole. As compounds are developed with increased fibre length, less fibre debris will be present so the effect of any counter nucleation caused by fibre debris will be reduced, transcrystallinity around fibres will be more likely and its presence may play an important role in deciding composite mechanical properties.

4.3 Experiments Performed Compounding Kevlar fibres in the Reinfenhauser Single Screw Extruder

4.3.1 Experiment KEVLAR 1

The starting point for the investigation of the compounding of Kevlar fibre into thermoplastics was their incorporation in short 6mm length bundles into polypropylene using a single screw extruder. Screw speeds of 50 RPM (compound K1), 30 RPM (compounds K2 and K4 using different volume fractions) and 10 RPM (compound K3) were used. The fibre length distributions were measured using the VIDS II computer image analysis system, employing a linear measurement program. This program enabled the length measurement of bent fibres. Repeated checks of the fibre length distribution of one sample indicated that the measurement of at least one hundred fibres was required in order to ensure reproducibility. The fibre length distributions for the

extruded and injection moulded compounds are shown on Figures 107 to 110. Table 35 shows the volume fraction of Kevlar fibres present in each compound together with mechanical properties of injection mouldings produced from the compounds.

Fibres seemed to survive the compounding operation reasonably intact. However on examination of compounds by polarised light microscopy, faults were observed along the fibre lengths. The faults consisted of slip bands and large blackened spots, where gross deformation had taken place. These faults had the appearance of kinks and were found to occur at approximately regular intervals.

On injection moulding fibre lengths were found to decrease more significantly, the distance between kink faults was found to slightly decrease. Table 36 presents values for average fibre length and average distance between kink faults. Figure 111 shows a section removed from an injection moulded tensile bar observed in polarised light, slip bands and kink faults are discernable in the photograph. A close up of two link faults is shown on Figure 112. It is interesting to note from Table 36 that although the extruded compound K1 had the longest fibre lengths it also had the shortest distance between kink faults. The injection moulding process was found to equalise any previous differences that existed between fibre length properties on compounding.

The mechanical properties for each compound were measured on the best ten tensile bar test pieces available. Flexural strengths for the composites were not measured because at high deflections specimens slipped between the supports without any increase in load, physically meaningful results were therefore not obtained. All the mouldings produced displayed a low property profile. Interfacial shear strengths were calculated using tensile stress-strain curves employing the method described in Section 3.8. From these values the average orientation ratios were calculated as described in the same section. Tensile strengths were low relative to the unreinforced matrix for all the compounds tested. The best properties were achieved by the compound with the highest interfacial shear strength (K1). This material was compounded at the highest extruder screw speed used. The poor interfacial shear strengths were likely to be due to a combination of poor fibre-matrix bonding and poor fibre wet out. A cross section taken from a tensile

test piece displaying the poor level of dispersion found in compound K2 is shown in Figure 113. Fibre orientation values are well below those of conventional brittle fibre reinforced thermoplastics.

4.3.2 Experiment KEVLAR 2

In this experiment a single screw extruder was used to compound Kevlar into polyropylene as in experiment KEVLAR 1, but a titanate coupling agent was added in an attempt to improve the bonding and wetting between Kevlar and polypropylene. Some mechanical properties of injection moulded test pieces are displayed in Table 37. The property profile for the composites produced are again low. The best properties were again obtained by the compound prepared with the highest extruder screw speed (compound K7). If the mechanical properties of material prepared in this experiment are compared with properties of the untreated compounds produced in experiment KEVLAR 1, the addition of 1% titanate coupling agent was found to marginally improve properties. No further increase in properties were found by increasing the coupling agent concentration to 3%. At a 5% addition properties appeared to decrease.

The interfacial shear strength of the most promising compound, K7 was calculated using its stress-strain curve and volume fraction but employing the fibre length distribution of compound K1. The interfacial shear strength calculated was slightly improved over compound K1.

Discussion

The initial experiments KEVLAR 1 and KEVLAR 2 served to indicate some of the important problems involved in compounding Kevlar fibre into a thermoplastic. Because of Kevlar's inherent fluffy nature it cannot be fed easily into a compounding extruder but has to be carefully added by hand, a process that could prove hard to automate. Only a poor level of dispersion was achieved by using a conventional single screw extruder as the compounder. The poor level of dispersion produced variable mechanical properties. Compounding was likely to have been made more difficult by the comparative high viscosity of polypropylene. Figure 114 is a photomicrograph of the fracture surface of a tensile bar of compound K1 taken at the central section. Poor

bonding is evident between the polymer and Kevlar fibre.

Although fibres appeared to be long and potentially highly reinforcing, from the estimation of interfacial shear strength it was clear that a significant proportion were below the critical fibre length (about 6mm). The attempt to improve bonding by the use of a titanate coupling agent was not fully successful. Tensile properties were slightly raised but the examination of tensile fracture surfaces of titanate treated moulded test pieces by scanning electron microscopy revealed that like the untreated samples produced in experiment KEVLAR 1, fibres were poorly bonded to the matrix. The tensile stress-strain curves of titanate treated and untreated test moulded pieces containing Kevlar fibre of the same volume fraction are shown in Figure 115. The slight increase in mechanical properties may have been a result of the coupling agent lowering the melt viscosity of the polymer. This may have allowed slightly better wetting of the fibres and a reduction in micro voids.

The reduction in melt viscosity to aid fibre wetting has been exploited by other investigators; Pristavka et al[116] used an organic peroxide with a bifunctional silane to improve the bonding between glass fibres and polypropylene. The tensile strength property of the material was improved by more than 100%. It was suggested that the improvement in mechanical properties could have been partly due to the peroxide partially degrading the polypropylene, reducing its viscosity and so allowing it to better wet the fibres.

The appearance of pristine Kevlar 49 in the scanning electron microscope is of an essentially smooth cylinder. It is clear from the experiments that the use of shear intensive mixing to compound these fibres into polypropylene resulted in a marked change in their nature. Figure 111 indicates the presence of a wide range of faults in the processed fibre. These faults are most likely to be a result of Kevlar's well documented poor compressional properties[117].

The origin and mechanism of the formation of surface bands on compressed Kevlar fibres was investigated by the examination of fibres with various loop radii by Dobb, Johnson and Saville[118]. Figure 116 is a schematic diagram showing the various phases of deformation that have been identified. The first (step A) is the appearance of irregularly shaped narrow bands

lying 40-50 degrees to the fibre axis. With progressive deformation individual kink band domains appear to propagate inwardly from the skin towards the fibre axis. At the same time the wedge increases by further kinking of the molecular chains and kink bands are formed at a distance either side of the original feature (step B). When the single surface bands become regularly spaced cross bands start to form which intersect the original bands (step C). The wedge shaped region can accommodate further compression by lateral displacement towards the centre of the loop, and form large surface bands whose edges are characterised by abrupt changes in direction (step D). Any further compression leads to a progressive failure of the outer regions of the fibre (step E). Broken outer regions are present in the fibres shown in Figure 111 they are points in the fibres which are black and enlarged. For the purposes of this study these points along the fibres are termed "kink bands" or "kink faults" and the distance between them termed "kink lengths". Other faults present can be thought to be at an intermediate stage of band formation.

The introduction of kink bands in Kevlar fibres by processing has been observed by Czarnecki and White[119] who performed rheological investigations on Aramid reinforced melts. The fibres were dispersed using a combination of a two roll mill and a Brabender single screw extruder. After processing the fibres exhibited a series of bends or kinks which were likely to have been the same in nature as the kink faults identified in this study. It was observed that the distance between the faults was a constant value of about 100 μm independent of the extent of flow used for the rheological measurements. Based on an analysis of buckling by Forgacs and Mason[120] the bending failure of Aramid fibres was expected to occur in a flow field when the fibre length to diameter ratio is greater than 100:12.

The fibre properties for experiment KEVLAR 1 (Table 36), indicated that increasing the extruder screw speed slightly reduced the average kink length, the most significant reduction in kink length however was produced by the injection moulding operation. Despite increased fibre damage, material produced using the highest extruder screw speed was found to yield the highest mechanical properties. The reason for this was probably the improved wetting obtained at high shear rates. This is likely to have masked any change in fibre properties.

As kink faults can be thought of inhomogenous domains where severe disruption of molecular orientation is present, it would be expected that such regions have a much reduced tensile strength in comparison to undeformed regions. The loss of the mechanical properties of Kevlar that had undergone only a slight deformation was shown by De Teresa, Farris and Porter[121] who used a thermoplastic matrix to apply a small compressive strain to Kevlar fibres. They found the fibre surface yielded in a shear mode at less than 3% compressive strain. Compressed fibres exhibited approximately 20% loss in breaking stress and a large loss in initial modulus.

It is clear that to ensure the best properties of Kevlar short fibre reinforced thermoplastics, fibres should be incorporated with the minimum level of kink faults. Criteria for compounding efficiency cannot be based only on fibre length and interfacial shear strength, but should also take into consideration the damage caused to the fibre. One simple method of doing this would be to measure and analyse the distance between kink faults.

The opening experiments KEVLAR 1 and 2 have illuminated the problems facing the development of short fibre Kevlar reinforced thermoplastics. Based on these findings it was decided that the next stage of work on these materials would utilise an alternative compounding system in an attempt to achieve better dispersion.

4.4 Experiments Performed Compounding Kevlar Fibre Using The Baker Perkins Compounding System

4.4.1 Experiment KEVLAR 3

In this experiment the Baker Perkins compounding extruder was used to compound Kevlar in to polypropylene. As described in Section 3.11.3 the proportion of Kevlar in the polymer was controlled by varying the compounder screw speed. Figures 117 and 118 show the fibre length distributions of the compounded and injection moulded materials produced at the two screw speeds used. Table 38 summarises the length properties and lists the mechanical properties measured. For comparison purposes a E-glass reinforced polypropylene was compounded using the same screw configuration, the mechanical properties of this compound are also included in Table

38.

The high level of dispersion of Kevlar in an injection moulded test piece is evident in Figure 119, this is a photograph of a cross section at the mid point of a tensile test bar moulded from material K11. Despite the high level of dispersion achieved, the interfacial shear strengths calculated were not greatly improved over the materials produced in experiments KEVLAR 1 and 2. Comparing compounds of the same volume fraction, the mechanical properties of Kevlar reinforced polypropylene are approximately half that for glass reinforced polypropylene.

4.4.2 Experiment KEVLAR 4

Using the Baker Perkins compounder with the same screw configuraion as was used in experiment KEVLAR 3, nylon 6,6 was used in experiment KEVLAR 3, nylon 66 was used as the matrix in this experiment. Figure 120 is a photograph of the compounder screw configuration used. The temperatures and screw configuration used had successfully melted the polymer prior to the Kevlar fibre addition. The fibre was added over the continuous helix screw sections.

Table 39 lists some of the mechanical properties of injection moulded test pieces. For comparison purposes the properties of a glass reinforced compound produced using the same screw configuration are listed together with values for the unfilled matrix.

Because of the difficulties associated in separating Kevlar fibres from nylon, volume fractions of Kevlar present in the compounds were estimated from density measurements. Interfacial shear strength and average fibre orientation estimations were based on the fibre length distributions measured in experiment KEVLAR 3.

Interfacial shear strengths between Kevlar and nylon 6,6 were improved over those between Kevlar and polypropylene. The stiffening ability was also improved but the strength reinforcing capacity remained approximately the same.

Theberge et al[96] stated that one advantage of Kevlar short fibre reinforced thermoplastics is their ability to produce isotropic mould shrinkage properties. An additional property that may give these materials an advantage over short brittle fibre reinforced thermoplastics is greater

mechanical isotropy. An analysis based on 3mm thick injection moulded plaques of the same dimensions as that shown in Figure 26 was carried out. Figure 121 shows the complete double plaque as injection moulded. The mouldings were fed from a sprue in the centre. Sample sections cut from the plaque were numbered. Ultimate tensile strength, stiffness at 1% strain and strain at break were measured for both Kevlar and glass reinforced plaques, four mouldings of each material were used for the analysis. The results of the analysis are shown in Table 40. The mechanical properties of the glass reinforced nylon are more position dependent and hence more mechanically anisotropic than the Kevlar reinforced nylon. A difference as much as 36% in tensile modulus for different sample sections were measured for glass reinforced nylon, the difference for Kevlar reinforced material was only a maximum of 13%. When the testing temperature is increased, the glass reinforced material can be expected to increase mechanical anisotropy to a greater extent than Kevlar reinforced material as a decrease in matrix modulus will tend to make properties more fibre dependent.

4.4.3 Discussion

It was generally found from scanning electron micrographs of fracture surfaces that the twin screw compounded material contained fibres that were more damaged than their single screw compounded counterparts.

Figures 122 to 126 are photomicrographs of damaged Kevlar fibres in tensile fractured injection moulded test bars as observed by a scanning electron microscope. Figure 122 shows what was shown schematically in Figure 116 the presence of irregularly shaped double bands lying 45-60 degrees to the fibre axis. Figures 123, 124 and 125 show the tendency of the skin of Kevlar fibre to peel away and leave crystalline fibrils. It was noticed that the skin ribbons often coiled into helices indicating that periodic residual strains in the skin were present.

The end splitting nature of Kevlar fibre is shown in Figure 126. Such longditudinally splitting may be at first thought to be advantageous as desirable high aspect fibrils are produced. However literature indicates that once the skin of Kevlar is removed the remaining fibrils can fracture easily. Pruneda et al[122] considered the structure of Kevlar to be similar that proposed to

Li, Allard and Bigelow[49] (Figure 15). Cracks can propagate readily parallel to the fibres longditudinal axis because it requires only the rupture of hydrogen bonds. Failure transverse to the fibre direction could occur by two possible mechanisms; the crack may follow the original macromolecular chain ends in the fibre, or new chain ends may be produced under stress as a result of macromolecular chain scission. It was concluded that failure occurs by aggregates of adjacent macromolecular chain ends within the fibre that favour transferse crack propagation.

From this analysis it is clear that any damage that takes place to the amorphous skin during compounding will weaken the fibre. Once the skin is unravelled from the fibre the remaining crystalline core will fail easily with a low level of fracture energy by transverse crack propagation. It is evident that there is a limiting interfacial bond strength within a Kevlar fibre that exists between the skin and fibrils. It is possible that in a composite this limiting bond could be exceeded by a very good bond between matrix and skin. If such a composite were loaded, fibres could internally debond. On the basis of this approach it could be argued that a strong bond between thermoplastic matrix and Kevlar fibre is undesirable because of the potential damage to the fibre skin. Figure 127 is the fracture surface of an extruded rod section of Kevlar reinforced nylon 6,6 produced in Experiment KEVLAR 4. On the left hand side, skin is observed to be torn from the fibre showing the interfacial shear strength between the matrix and fibre is greater than the bond between skin and crystalline core of the fibre. This was not observed in experiment KEVLAR 3 for Kevlar fibre reinforced polypropylene.

The stiffness and strength properties for well dispersed Kevlar reinforced thermoplastics proved to have a low profile. Compared with the Kevlar reinforced polypropylenes produced in experiments KEVLAR 1 and 2 the tensile strength and modulus properties were increased marginally.

Figure 128 is a montage scanning electron photomicrograph of a fracture surface of a tensile specimen of injection moulded Kevlar reinforced polypropylene compound K11 taken on a scanning electron microscope. Very significant fibre pull-out is observed, fibres as long as 1mm being visible. Figure 129 is a scanning electron photomicrograph of the specimen at its corner

shown the bases of pulled out fibres. The fibre appeared to be very clean, confirming earlier observations of the poor bond between polypropylene and Kevlar. Figure 130 is a scanning electron photomicrograph of an area of the fracture surface of the same compound where the fibres were orientated at right angles to the testing direction. The fibres were found to simply debond.

The fracture surface of Kevlar reinforced nylon 6,6 is different to that of Kevlar reinforced polypropylene. Figure 131 is a scanning electron photomicrograph of the fracture surface of an injection moulded specimen of compound K13. Fibre pull-out is significantly reduced and the ends of the fibres appear to be broken. Where the fibres are orientated at right angles to the testing direction, bonding is sufficient to cause the fibres to fail longditudinally (see Figure 132).

Figure 133 shows plots of the stress transfer interface efficiencies against interfacial shear strength based on fibre length distributions, for the Kevlar reinforced components produced using the Baker Perkins compounder with screw speeds of 135 RPM assuming pristine fibre condition. To achieve the same efficiencies in tensile modulus and strength as glass and carbon fibre reinforced materials produced in this thesis an interfacial shear strength of at least 15 MPa would be required. This is twice as great as was achieved for the Kevlar reinforced nylon compounds. The interfacial shear strengths of Kevlar reinforced polypropylene and nylon materials were only 20 and 25% respectively that of the glass reinforced polymers produced in this thesis.

Eagles, Blumentritt and Cooper[123] used a single filament pull-out test to study the adhesion of Kevlar 49 fibres to thermoplastics. A number of the thermoplastic materials were tested, the Kevlar having a number of surface treatments. Test results allowed the measurements of two stress levels; the interfacial bond strength where adhesive forces between fibre matrix are overcome and, frictional shear strength which represents the slippage between fibre and matrix. The observed failure mode was frequently complex, in some cases cohesive failure of the fibre surface occurred during the test resulting in a thin layer of material being stripped from the fibre surface. The interfacial bond strength between Kevlar and polypropylene was measured as 8 MPa, between Kevlar and nylon it was measured as 45 MPa. The frictional shear strengths of Kevlar with polyethylene and nylon were found to be 1.4 and 2 MPa respectively. The tensile strengths

of discontinuous fibre reinforced thermoplastics correlated well with the frictional shear strengths measured in the single filament pull out test. It was thought however because of the problems of dispersion the bulk properties did not possess good tensile properties.

From observations of the fracture surfaces of Kevlar reinforced polypropylene and nylon in this study it is clear that tensile failure involves wide scale fibre pull-out. It is imagined that during the tensile failure process, fibres are at different stages of debonding and pull-out so the values obtained for interfacial shear strength serve as average values of the debonding and pull-out processes.

In their analysis of the mechanical properties of short Kevlar fibre reinforced thermoplastics Eagles, Blummentritt and Cooper[123] assumed the radial coefficient of expansion of the fibre to be approximately equal to the coefficient of expansion of the matrix materials. Figure 134 illustrates the coefficients of expansion of the radial and longitudinal dimensions for each of the fibres used in this thesis. Both Kevlar and carbon have negative longitudinal coefficients of expansion, so the fibres expand on cooling. Although Kevlar 49 has a higher radial coefficient of expansion than carbon or glass fibre, it still has approximately half the coefficient of expansion of a thermoplastic matrix, so on cooling from T_g to room temperature a limited amount of lateral compressive stress is impinged on the fibre. Because of its negative longitudinal expansion coefficient this compressive stress produces longitudal compression stress in the fibre, it is possible to estimate this stress. Assuming that the fibre is perfectly straight and perfect bonding exists between the fibre and the matrix, for a nylon 6,6 matrix:

Difference in temperature between T_g and room temperature	X	Difference in coefficients of expansion between fibre and matrix	= Strain at the interface
40°C		102×10^{-6}	4.08×10^{-6}
Strain at interface	X	Stiffness of matrix	= Stress at interface
4.08×10^{-3}		3×10^{9}GPa	12.2MPa

The presence of this compressive stress at the interface would explain the kinks found during the investigation of transcrystallinity of Kevlar in nylon using a hot stage microscope using the method described in Section 3.9. Here in the absence of any shear processing the shrinking stresses were sufficient to debond the skin of the fibre from its core. No such internal debonding effect was observed during investigations of the transcrystallinity of Kevlar in polypropylene. The result is significant as it shows the limitation in the interfacial shear strength between the skin and core of a Kevlar fibre. This observation consolidates the earlier point that even if good bonding between the matrix and skin were possible, mechanical properties would be limited by the absence of a good bond between the reinforcing crystalline core and its amorphous skin.

Outwater[5] proposed that frictional shear strength controls the strength of composites that fail by a fibre pull-out mechanism. His theory states that failure of such a composite is initiated by concentrated shear stresses at the fibre ends causing debonding first at the fibre end then along its length. After debonding fibre pull-out begins and the load is transmitted by frictional forces. According to Outwater the strain of the composite when debonding occurs (e_b) will be:

$$e_b = \frac{\sigma_{uc}}{E_f V_f}$$

where σ_{uc} = Tensile Strength of the composite

E_f = Young's Modulus of fibre

V_f = Volume fraction of fibre

According to this equation, Kevlar reinforced polypropylene will debond at 0.3% strain and Kevlar reinforced nylon will debond at 0.6% strain. After this point the tensile properties would be controlled by frictional pull-out.

It is interesting to note that by varying hydrostatic pressure around steel wires encapsulated in epoxy, Bowden[124] was able to vary the initial load necessary to break the bond between the wire and its matrix and subsequently control the frictional stress when the bond was broken. This demonstrates that residual compressive stresses are necessary for high interfacial shear strengths.

Piggot[9] extending earlier theories of reinforcement for short fibre reinforced composites showed that adhesion forces do not have a very marked effect on the stress-strain curves of

composites, much more important are the residual stresses. Piggot suggests that short fibre reinforced materials can only be used at high strains i.e. levels beyond the elastic limit, when the residual stresses are relatively large and compressive. In the case of Kevlar reinforced nylon although there is enough lateral residual compression stress to damage the fibres, there seems insufficient to grip the fibre while under load, so poor properties are observed at high strains.

The comparison of the mechanical properties of different sample sections cut from glass and Kevlar reinforced nylon plaques have served to indicate the more isotropic properties of short Kevlar fibre reinforced thermoplastics. Figure 135 is a photograph of a thin section of a moulding taken from a tensile test bar of Kevlar reinforced polypropylene compound K11. The location of the section in the moulding is shown in Figure 136. Fibres appear coiled and largely random in orientation. This fibre arrangement would account for the isotropic nature of mechanical properties. In such a fibre orientation however under load fibres of some orientations would be put in compression and hence severely weakened. The combination of a low proportion of fibres aligned in the testing direction and the need for coiled fibres to straighten before they can be load carrying also serve to explain the poor mechanical properties found.

Figures 137 and 138 show the dependence of predicted tensile strength on the interfacial shear strength of Kevlar reinforced nylon 66 and polypropylene respectively. The upper curves were predicted from the Kelly-Tyson model (Section 1.5.2) assuming random fibre orientation for straight Kevlar fibres (fibre orientation ratio 0.33). The bottom curve was predicted again using the Kelly-Tyson model but using the fibre orientation ratio calculated for the Kevlar reinforced injection mouldings produced (0.153 for polypropylene and 0.111 for nylon). From Figure 138 for Kevlar reinforced nylon it is evident that even if fibres were undamaged and the interfacial shear strength were as high as the shear strength of the matrix (34 MPa), the tensile strength would not be greater than 120 MPa.

From the results and observations presented it would appear that the strength and stiffness properties of short fibre reinforced thermoplastic are limited. It would seem that Kevlar fibres are best suited to applications where they can be used in their continuous form. An example could be

in continuous laminates which involve the minimum fibre degradation in their manufacture and where fibre orientation is fixed, here interfacial shear strength is not such a critical property.

The impact properties of short-fibre reinforced thermoplastics are considered separately in Section 4.5.

4.5 Impact Properties of Short Fibre Reinforced Thermoplastics

4.5.1 Impact Properties of Kevlar Reinforced Thermoplastics

The various types of features revealed by the force-deflection curve on using the falling weight impact tester are shown in Figure 139. For the purpose of this study three important features will be presented for the materials tested; stiffness, yield force and energy to fracture. As indicated in Section 3.6.3, two types of specimen were used to assess impact properties; a bar and a plaque. The impact velocity of the 27 kg tup was 2 metres/second for the bar and 3 metres/second for the plaque.

Table 41 presents impact data for the Kevlar reinforced polypropylene produced in experiment KEVLAR 1. Results presented are the average values for tests on ten samples. An indication of the extent of scatter is shown by the coefficient of variation of the fracture energy. The values were between 10 and 12%, which is relatively high for mechanical testing. Figure 140 a, b and c present typical examples of the force-deflection impact curves for bar samples. As the extrusion screw speed was raised and hence shear rate increased, the yield force was enhanced and the total distance over which the failure took place reduced. The material produced at a low shear rate behaved similarly to the unreinforced matrix. It would appear that for material produced at higher shear rates, where the fibre wet-out was slightly better, the ductility of the matrix was reduced but energy absorption was compensated by fibre related mechanisms. Large scale pull-out was observed on the fracture surfaces of impact tested bars. Figure 141 is a photomicrograph of the impact surface of a Kevlar reinforced polypropylene plaque of compound K1. For unfilled polypropylene bars, limited crack propagation did occur but a far larger proportion of the width was not fractured before the sample bent sufficiently to allow it to leave the test instrument.

Some average values taken from force deflection curves of titanate coupling agent treated materials produced in experiment KEVLAR 2 are shown in Table 42. Again there was a large coefficient of variation in the values of fracture energy. No improvement in impact properties were found compared to the materials produced in experiment in KEVLAR 1. On increasing the titinate coupling agent concentration, both the yield force and energy to fracture appeared to drop.

The average values for the impact properties of the materials produced in experiment KEVLAR 3 are shown in Table 43, both test bars and plaques were used to assess impact properties. The materials are compared with measured average values of commercially available glass reinforced polypropylenes; a 20% reinforced (ICI HW60GR20) and a 30% reinforced material (ICI HW60GR30). From the results, the higher stiffness of the glass reinforced materials was evident as was the higher yield force. The Kevlar reinforced impact bars had a coefficient of variation of the energy to fracture of less than 10%; this may have reflected the better dispersion achieved by the compounding method compared with the materials produced in experiments KEVLAR 1 and 2. The force-deflection curves for typical glass reinforced and unreinforced polypropylene plaques are shown on Figure 142. Figure 143 a and b show the force-deflection curves for the Kevlar reinforced polypropylene plaques produced in experiment KEVLAR 3. Although the energy to fracture is comparable between Kevlar and glass reinforced impact bars, tests on impact plaques showed that glass reinforced materials had greater energy absorbing properties. Unlike the bars, the plaque samples did not leave the test instrument, the indentor penetrated the disc.

It is interesting to note that the yield force for the glass reinforced polypropylene plaque was comparable with that of the unreinforced matrix, the significant part of the energy absorbing process occurring during crack propagation. The yield force for the Kevlar reinforced polypropylenes occurred at a lower force than that of the matrix polymer. This is followed again by an energy absorbing crack propagation process.

The plaque samples of glass and Kevlar reinforced polypropylene showed on testing a mixture of radial and circular fractures, sometimes being fractured into four pieces. Kevlar rein-

forced plaques were not completely fractured into many pieces, fibres near the compressive face tended to hold the sample together. Even with the naked eye the fracture surfaces of the samples showed considerable pull-out. Figure 144 is a scanning electron micrograph of the fracture surface of an impact tested Kevlar reinforced polypropylene plaque (compound K11).

The impact results for Kevlar reinforced nylon 6,6 produced in experiment KEVLAR 4 together with unreinforced nylon 6,6 and glass reinforced nylon 6,6 are presented in Table 44. Both impact bars and plaques were again used to assess impact properties. Figure 145 presents typical force deflection curves for nylon 6,6, Kevlar and glass reinforced. The lack of perfect linearity for the curve of the unreinforced nylon is likely to be the result of the change in the radius of contact of the impact tup on the plaque during the first stages of impact. For the unreinforced material the energy to yield (initiation energy) was sufficient to cause failure. Once the crack was initiated the propagation energy was insignificant and contributed to the material's impact strength. This type of impact resistance is rate and temperature dependent. The drop in the impact properties of compounder processed unreinforced nylon was thought to be a result of contamination which acted as a notch to initiate premature failure. Figure 146 is scanning electron photomicrograph of the impact fracture surface of a plaque of processed unreinforced nylon. Contamination is evident on the right hand edge which may have acted to initiate failure. The coefficient of variation for unreinforced materials were high, again reflecting notch sensitivity.

Figure 147 is a scanning electron micrograph of the fracture surfaces of impact tested Kevlar reinforced nylon (compound K13). Fibre pull-out lengths appear shorter than were the case for Kevlar reinforced polypropylene materials.

4.5.2 The Estimation and Prediction of Fracture Energy for Glass Reinforced Nylon

Table 45 presents the results for the estimation and calculation of G_c for selected glass reinforced nylon 66 compounds having significantly different fifbre length distributions. These were compounds G3, G6 and G7 produced in experiments BRITTLE 4 and 5, examples of force deflection curves for the compounds are shown in Figure 148. The method used for calculating G_c is shown in Appendix 2. Two values of G_c are presented on Table 45. One is derived from

the yield force (peak force) value. This may be considered as a lower bound estimation of fracture energy as it does not assume any energy is absorbed by the specimen after the yield force. The other value of G_c was derived from the total impact energy. This can be considered to be an upper bound estimation of G_c as the specimen includes the energy taken in throwing the specimen and in generating noise. The calculated value of G_c estimates the total energy absorbed by pull-out of fibres of length l_c and less, it does not take into account effects from fibre orientation or fibres having greater in length than l_c. Despite these limitations, the calculated values seemed to give a reasonable estimate of fracture energy. The values approximately equal to the average of the two values of G_c measured in the two different ways. The last column in Table 45 estimates the maximum possible value of G_c that would be possible if all fibre were perfectly aligned 90° to the crack direction and equal to the critical fibre length.

4.5.3 Discussion

Toughness has been defined as the measure of resistance to the energy required to break a material[125]. This is the energy under the stress-strain curve. Increased toughness can be achieved by raising either the tensile strength or elongation to break or both. In doing so the area under the stress-strain curve can be increased to its fullest extent. In practice however adding reinforcement to a plastic material results in one parameter increasing at the sacrifice of another.

The impact properties measured in this study for fibre reinforced thermoplastics relate only to energies required to initiate and propagate an impact failure in a specifically fabricated specimen, a fundamental property was not measured. Impact strength can be increased by the ability of fibres or other additives to stop cracks propagating, this can however have little effect on the area under the stress-strain curve. In other words a material with high impact properties need not be tough, but a tough material generally has high impact properties.

The instrumented impact testing technique used in this study provided a complete record of the load applied to the specimens during the entire impact event. It allowed the identification of fracture initiation and propagation. The first peak in a force-deflection curve corresponds to the

crack appearing, the initiation point. The energy absorbed at this point corresponds to the initiation energy. The second part of the curve corresponds to the multiple crack propagation from the initial failure to the effective edge of the specimen. When the crack reaches the edge the force falls to zero.

A feature of all impact test data is scatter, impact tests generally show higher levels of scatter than other tests. This problem is highlighted in fibre reinforced materials where different failure modes or fracture paths occur as a result of differences in dispersion, fibre orientation or differences in moulded in stresses. Throughout the impact study, the values of the coefficiences of variation were found to be high for the fracture energies measured.

When measurements of toughness are made on specimens without introducing notches, the failure mode as influenced by the fabrication method employed to make the specimen. As the purpose of this study is to relate both materials and processing methods to impact properties it is thought that this effect does not serve a major disadvantage.

As briefly reviewed in Section 1.5.4, many investigators including Outwater and Murphy[26], McGarry and Mandle[27] and Beaumont and Phillips[28] argued that the energy required to debond fibre from a matrix is the predominant energy governing the total fibre fracture energy. Cottrell[29] suggested that the highest values of toughness would be obtained from a short fibre reinforced composite material if it contained fibres that were slighly smaller than l_c and if l_c were as large as possible. The improvements in toughness when fibre had lengths equal to l_c were found by investigators when fibre were semi-ductile and set in a high shrinkage brittle thermosetting matrix. Cooper[31] incorporated flawed copper wires in plasticised epoxy, Helfet and Harris[32] used steel wires in a polyester resin.

Piggot[126] comprehensively reviewed the effect of fibre aspect ratio on the toughness of brittle thermosetting matrices. He concluded that the most important property to be considered in selecting fibre lengths for maximum toughness is fibre ductility. When incorporated into composites to maximise the fibre contribution to the work of fracture, ductile fibres that dissipate a large amount of internal energy should be as long as possible. For brittle and moderately ductile fibres

having uniform strengths, fibre pull-out effects make the maximum contribution to toughness, so to achieve moderate toughness the fibre length should not be greater than about ten times the critical length required for reinforcement.

The impact energies of all the Kevlar reinforced thermoplastics were low, generally lower than their glass reinforced counterparts and in a few cases lower than the unreinforced matrix. The impact fracture surfaces of the Kevlar reinforced compounds revealed considerable fibre pull-out. The critical fibre length however of Kevlar in polypropylene and nylon 6,6 is greater than 2 and 0.5mm respectively (Chapter 5) because there are few fibres as long as this observed, the appearance of these apparently high energy fracture surfaces is misleading. As a result of the poor bonding between fibres and matrix, the matrix can be detached very easily from the fibres and deform plastically. This leaves the fibres unable to introduce new mechanisms of energy absorption and act only as brittle inclusions in a ductile matrix.

When evaluating the potential for short fibre reinforced Kevlar materials in applications where surface finish is important a comparison between crack initiation energies is useful. Unfilled polypropylene and nylon were found to show no damage prior to fracture i.e. crack initiation energy is very near the fracture energy. Crack initiation energies were comparable between unfilled and glass filled materials, Kevlar reinforced materials were found however to have lower crack initiation energies than the unfilled polymer. Kevlar and glass reinforced thermoplastics are therefore no better and sometimes worse than unfilled polymers in applications where toughness is demanded in combination with good surface finish. Fibre filled composites absorb energy once permanent damage has occurred, short fibre incorporation is therefore most effective in localising damage that would otherwise be catastropic.

The toughness properties of the unreinforced matrix can be expected to deteriorate with decreasing test temperature. Friedrich[125] observed when testing the fracture toughness of glass reinforced polyethylene terephtalate that the more glass added the less pronounced was this effect. For higher glass loadings, values measured at low temperatures were even higher than those measured at room temperature. According to Friedrich this indicated that above a certain

percentage of fibre loading, low temperature embrittlement due to the matrix is not as effective as the toughening improving effects due to fibres. The latter were to some extent controlled by fibre-matrix bond strength that was enhanced with decreasing temperature. This effect was due to higher thermal contraction of the matrix compared to the fibres, thus a higher amount of energy for the initiation of fibre pull-out is required. This useful effect is less likely to occur in Kevlar-thermoplastic materials because of the similarity in the radial coefficient of expansion with the thermoplastic matrix (Section 4.4.3). Once the weak fibre-matrix bond is broken, again because of the similarity in coefficient of expansion values little resistance would be offered by frictional force between the resin and the smooth Kevlar fibre. Increasing the frictional force by mechanically or chemically keying between the fibre and matrix may result in the amorphous layer of the Kevlar fibre being stripped in the impact process. As discussed earlier in Section 4.4.3, once the amorphous skin is unravelled, the remaining crystalline core is likely to fail with a low level of fracture energy by transverse crack propagation.

In the same publication mentioned above Friedrich found on measuring the fracture toughness of thin walled injection moulded plaques that the value depended very much on the axis it was measured in relation to the dominant fibre orientation. It was found that cracks which moved perpendicular to fibres experienced more hinderence than cracks moving longditudinally in the dominant fibre orientation. This gave rise to fracture toughness anisotropy. If Figure 136 is considered which shows the relative random orientation of Kevlar fibres in an injection moulded bar, such fibre orientation would offer relatively isotropic toughness properties but less effective crack hindrance in one specific direction.

If the bond strength between Kevlar and a thermoplastic matrix could be increased without damaging the integrity of the fibre, the relatively high strain to failure and plastic nature of Kevlar could be utilised. Mandle et al[127] measured the fracture toughness of single edge notched glass and carbon reinforced thermoplastic injection moulded plaques. They showed that providing the fibres are adequately bonded to the matrix, cracks propagate primarily in a crack avoidance mode. The fracture toughness was predicted to be dependent on the matrix through ultimate tensile

strength and on fibre length. The radius of the cracking zone was found to be a similar size to the longest fibres present. Fracture energy was found to have the following dependence:

$$G_c=2\pi l_{f*}\sigma_{uc}/E$$

where σ_{uc} = ultimate tensile strength of the composite

l_{f*} = effective length of longer fibres

The fibre-matrix bond strength has a tendency to increase ultimate tensile strength and thus increase toughness.

The importance of a good bond for the toughening of ductile thermoplastics was stressed by Leach and Moore[128] who argued that compounds with poor interfacial bonds can have cracks propagating along the interface thus debonding the fibre from the matrix. Materials with a strong interfacial bond have cracks propagating through the matrix and thus high fracture toughness. Ramsteiner and Theysohn[129] stated that to have high impact strengths, short fibre reinforced thermoplastics should have an interfacial shear strength which are comparable to the shear strength of the matrix.

Many methods have been developed in order to impart high toughness properties to composites, these are however primarily directed towards brittle fibre reinforced thermosets and rely on suitably modifying the mechanical properties of the interface between the fibre and the matrix. Atkins[130] intermittently coated fibres with an appropriate viscous fluid such as polyurethane varnish. The coated regions where the interfacial bonding was weak serve to blunt the propagating cracks by the Cook-Gordon fracture mechanism and increase the pull-out length so the toughness can be increased. Some of the boron-epoxy composites did not suffer any strength loss and had a 400% increase in fracture toughness. Based on a similar ideal, Handcock and Wells[131] were able to improve the toughness of their carbon fibre epoxy composites by 100% with no sacrifice in the flexure strength by fully coating fibres with 1% silicone rubber. The viscous shear work during fibre pull-out was maximised by Sung et al[132] who used strain rate sensitive coatings of selected viscosity to increase the impact strength of glass-polyester resin composites.

It would seem that in contrast to fibre reinforced thermosets, increasing the impact strengths of short fibre reinforced ductile thermoplastics requires good interfacial bonding and the longest possible fibre lengths. These conditions would permit the maximum possibility for the convolution of cracks, the maximum utilisation of the ductility of the matrix and the employment of the toughness of the fibres themselves. The above combination of composite properties would not seem to be in conflict with those required for strength and stiffness. The efficiency of fibres in toughening thermoplastics may be increased in particulate filled compounds where matrix ductility is suppressed.

For the samples considered the calculated values of fracture energy G_c, based on the estimation of the total energy absorbed by the pullout of fibres of length l_c and below serves as a useful indication of fracture energy of glass reinforced thermoplastics. Providing the fibre length distribution, the mechanical properties of glass and the average interfacial shear strength of a composite are known a reasonable prediction of fracture energy for totally aligned fibres is possible.

Location of sample points along screws
for experiment BRITTLE 1

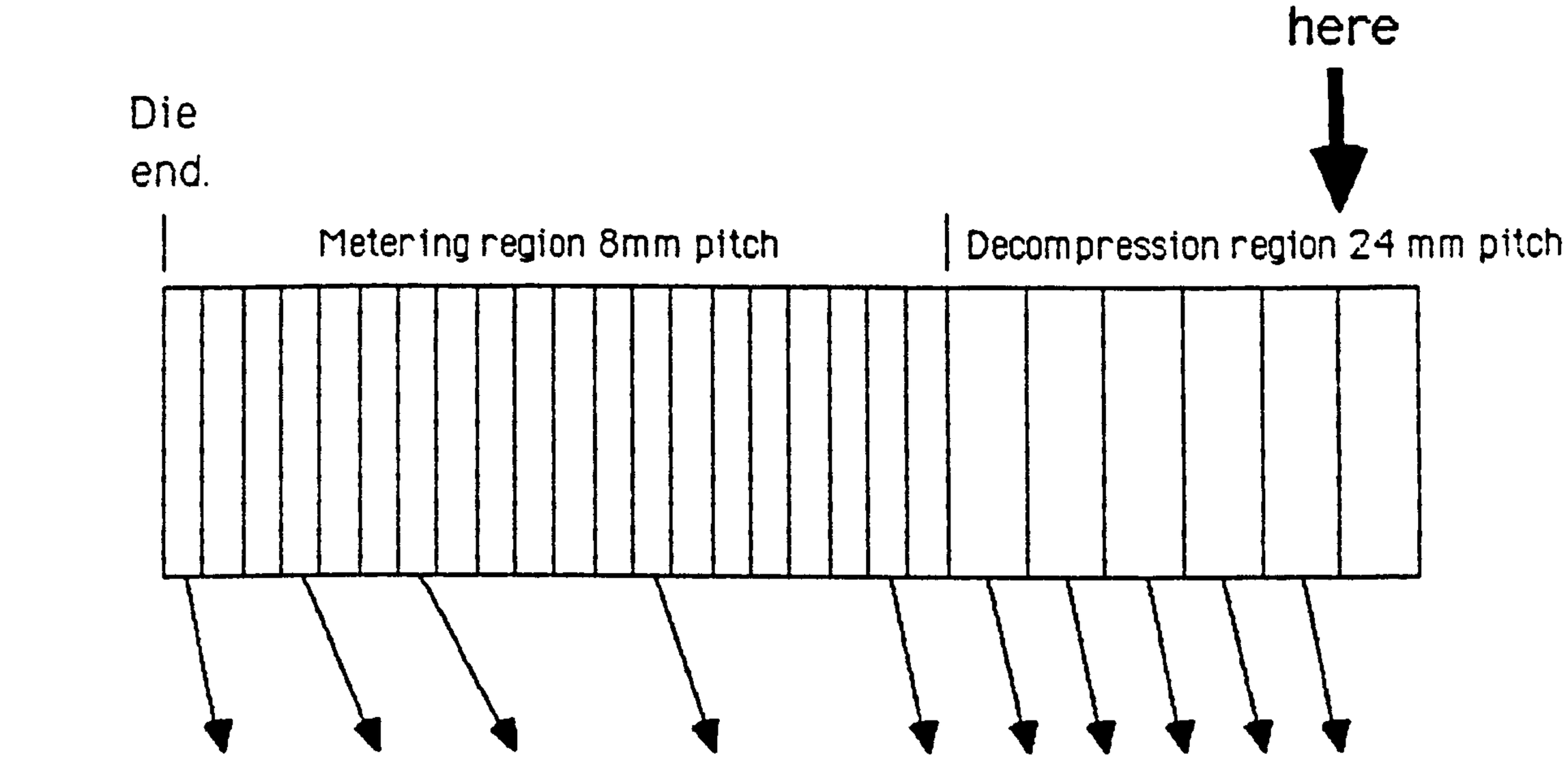

Figure 38

Screw profile used for experiment
BRITTLE 1

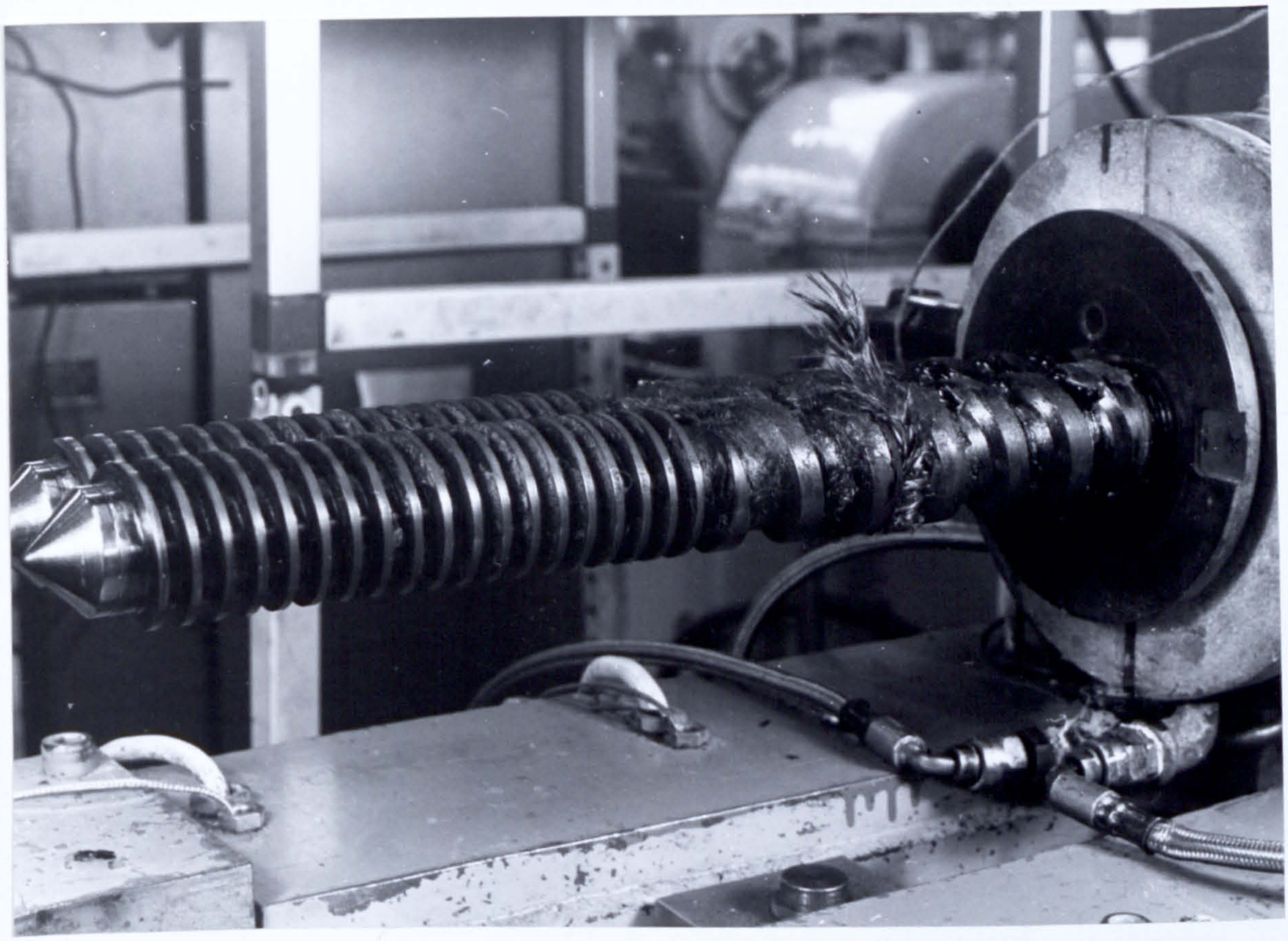

Figure 39

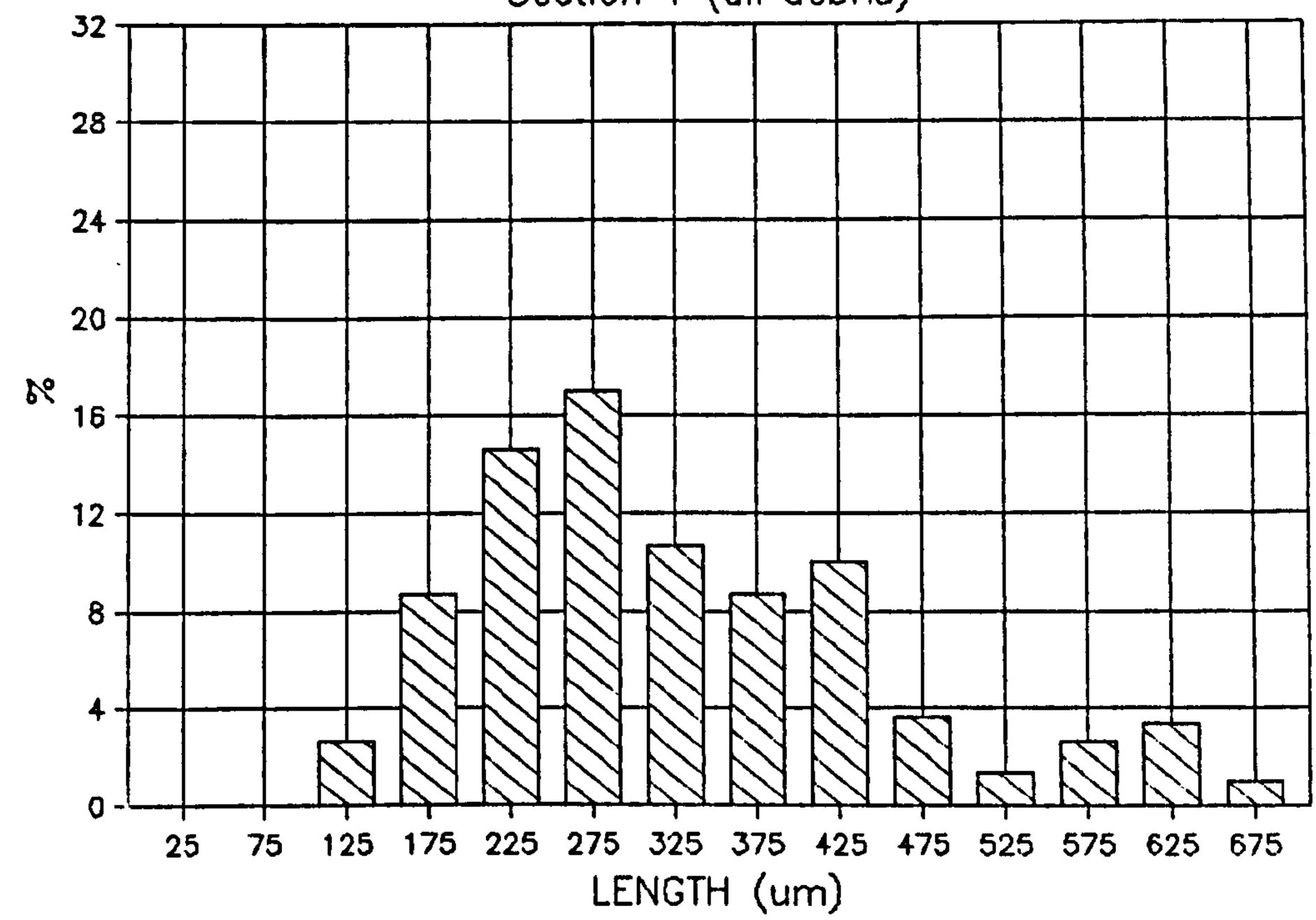

Figure 40

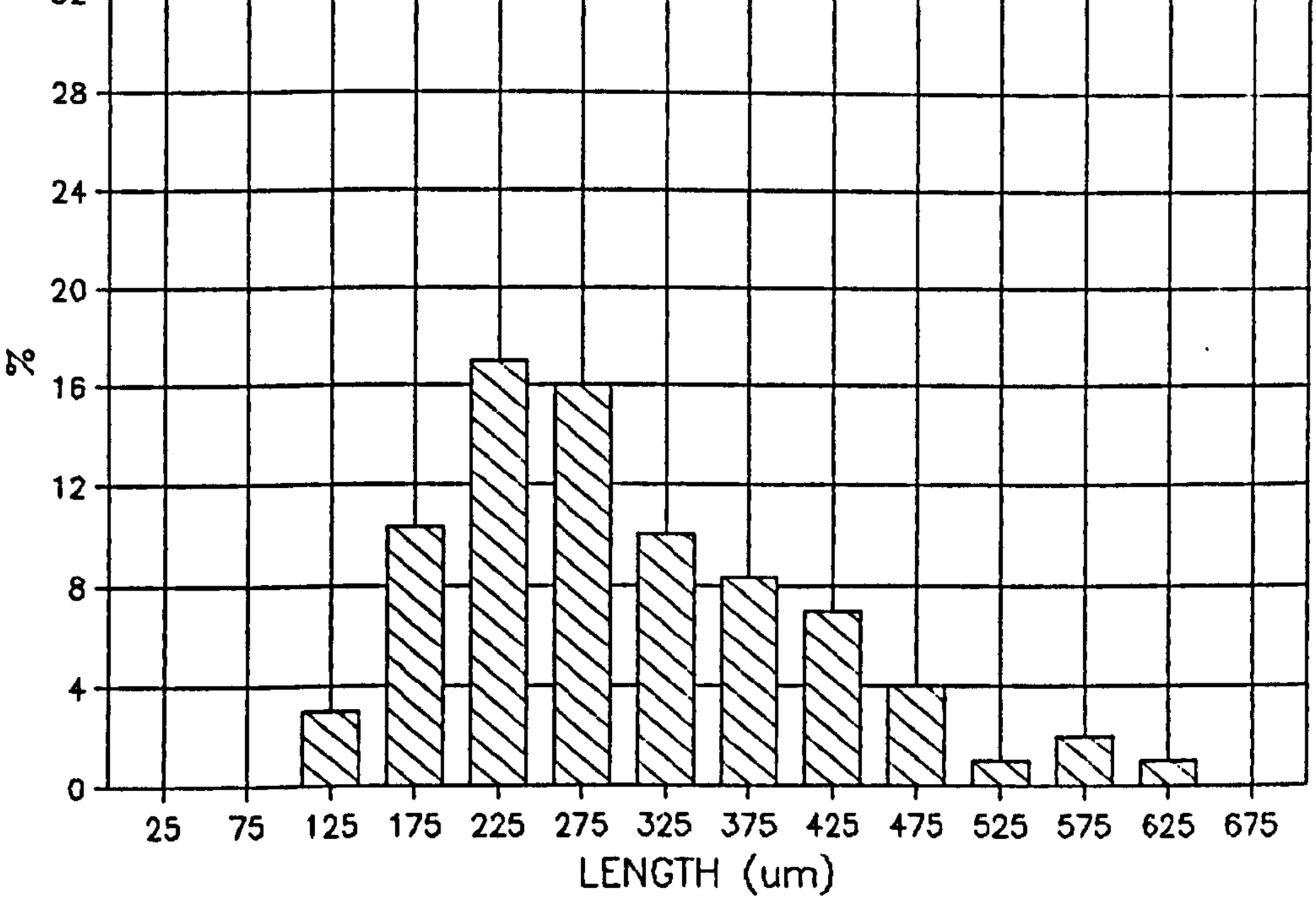

Figure 41

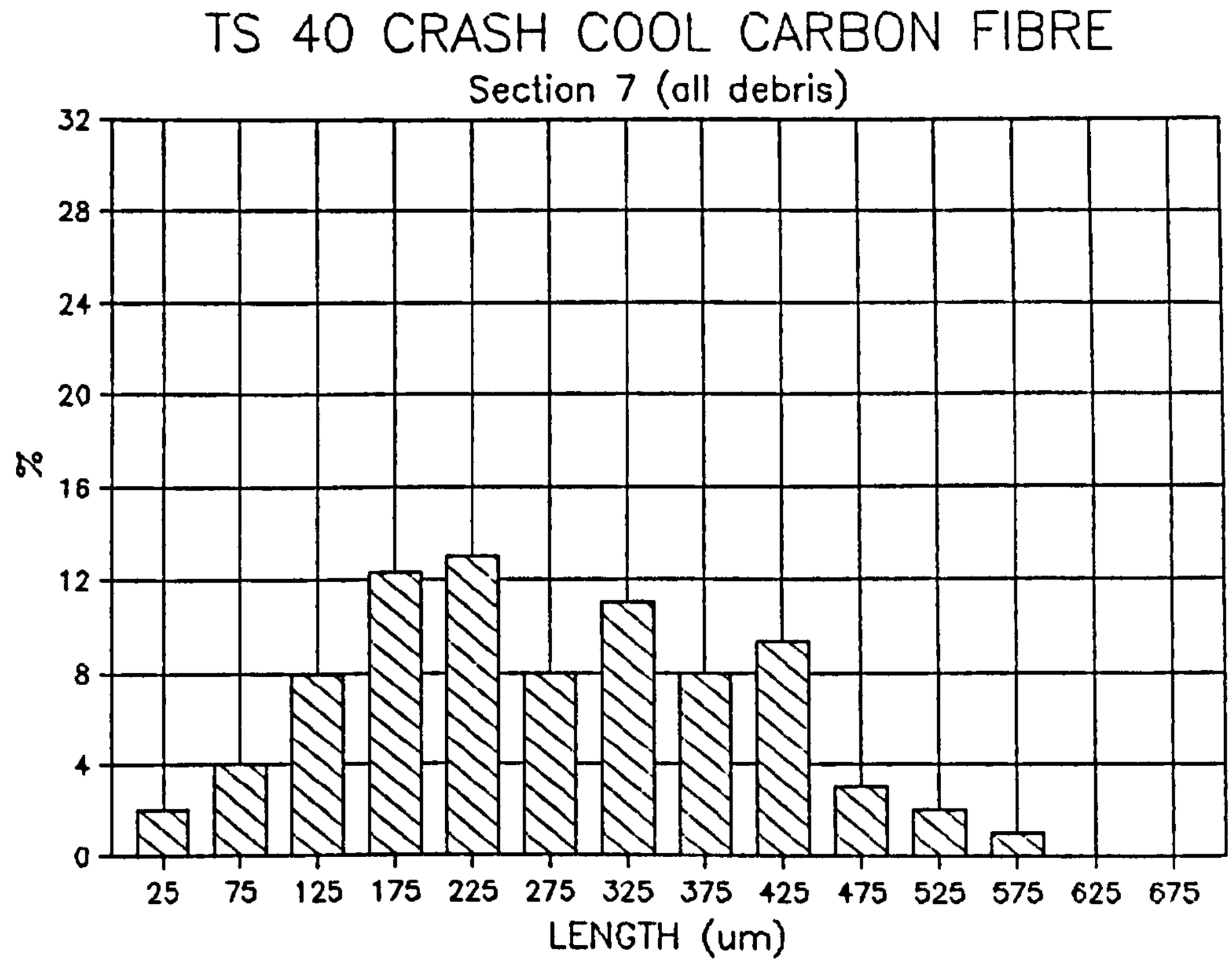

Figure 42

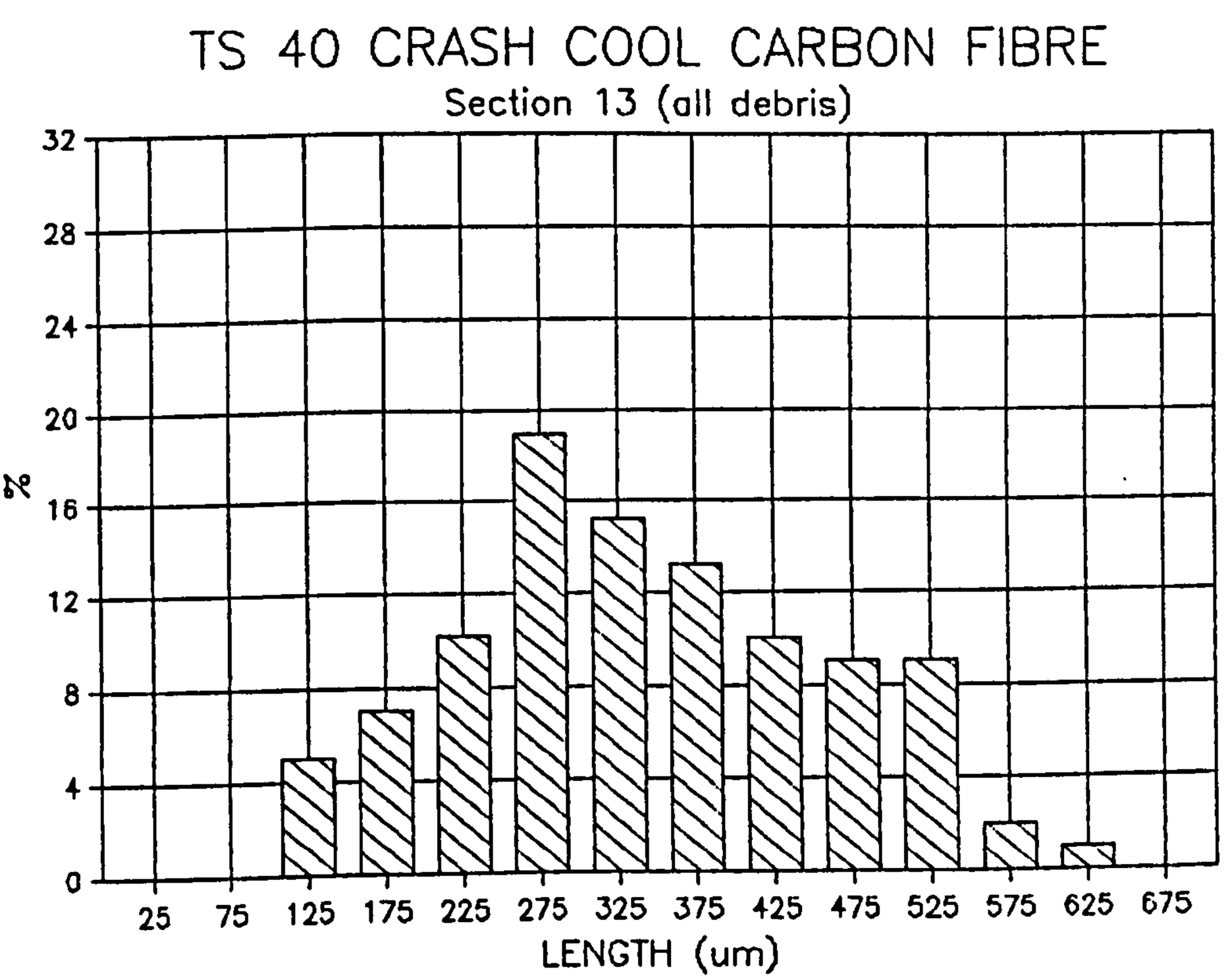

Figure 43

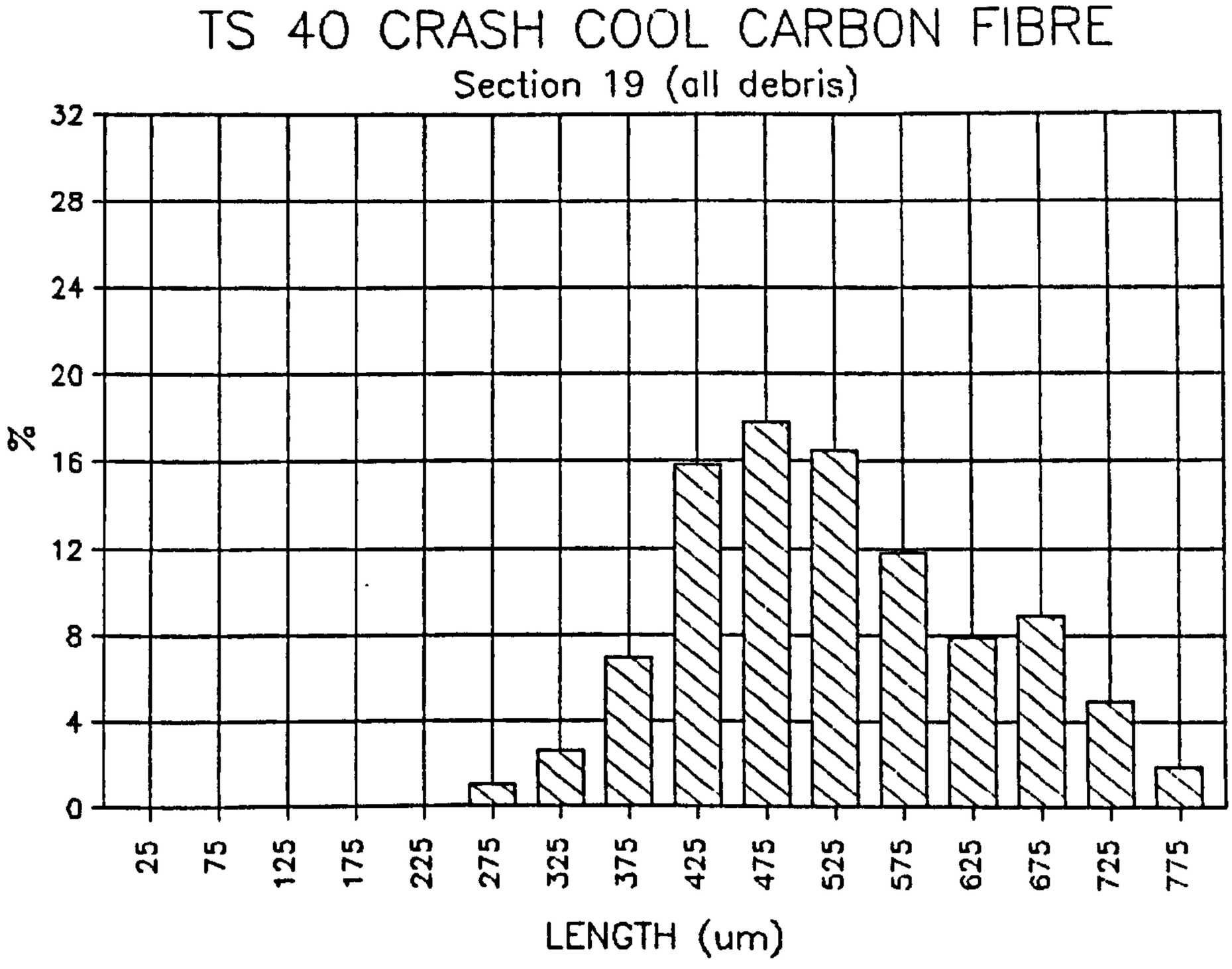
TS 40 CRASH COOL CARBON FIBRE
Section 19 (all debris)
%
32
28
24
20
16
12
8
4
0
25
75
125
175
225
275
325
375
425
475
525
575
625
675
725
775
LENGTH (um)

Figure 44

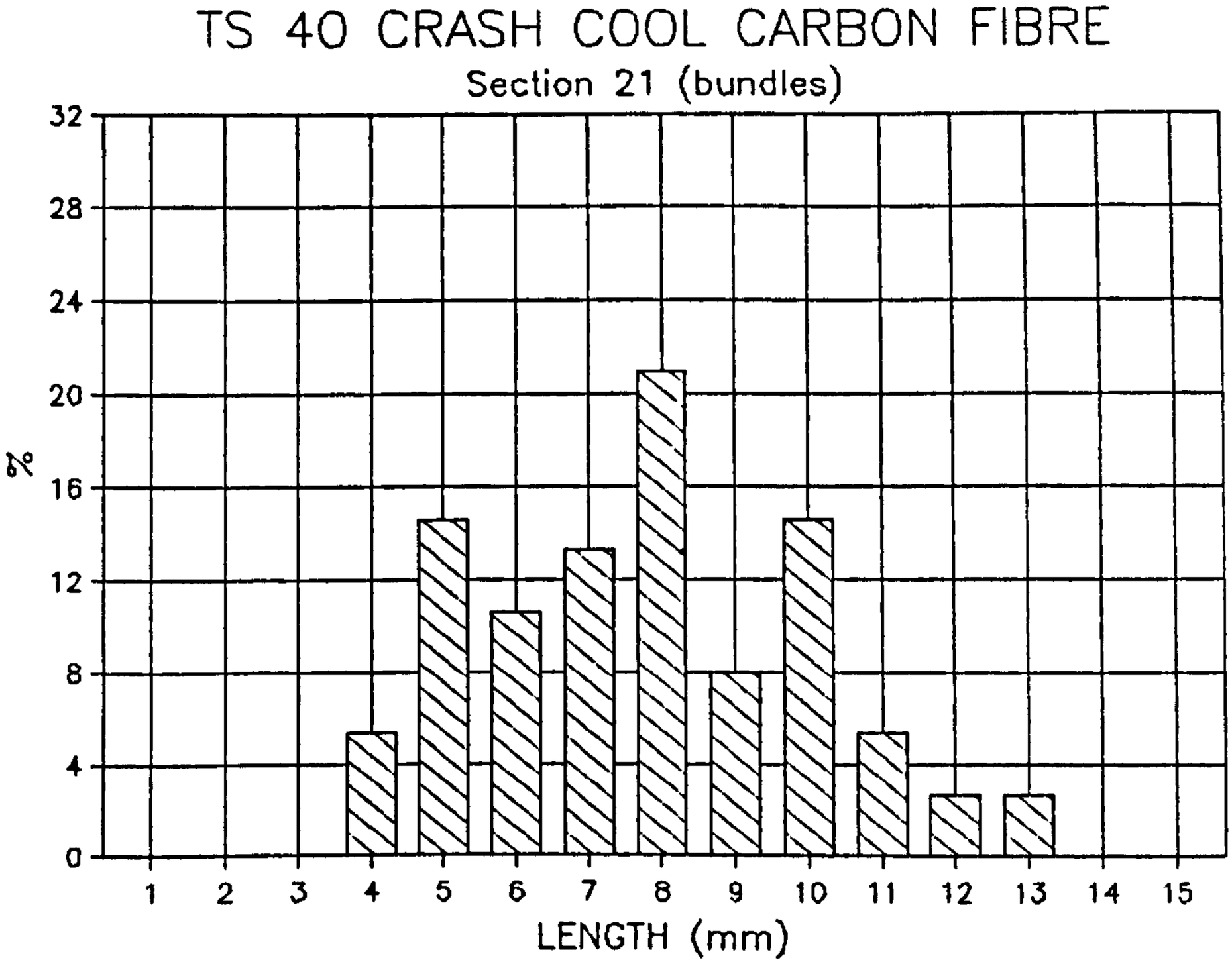
TS 40 CRASH COOL CARBON FIBRE
Section 21 (bundles)
32
28
24
20
16
12
8
4
0
%
1 2 3 4 5 6 7 8 9 10 11 12 13 14 15
LENGTH (mm)

Figure 45

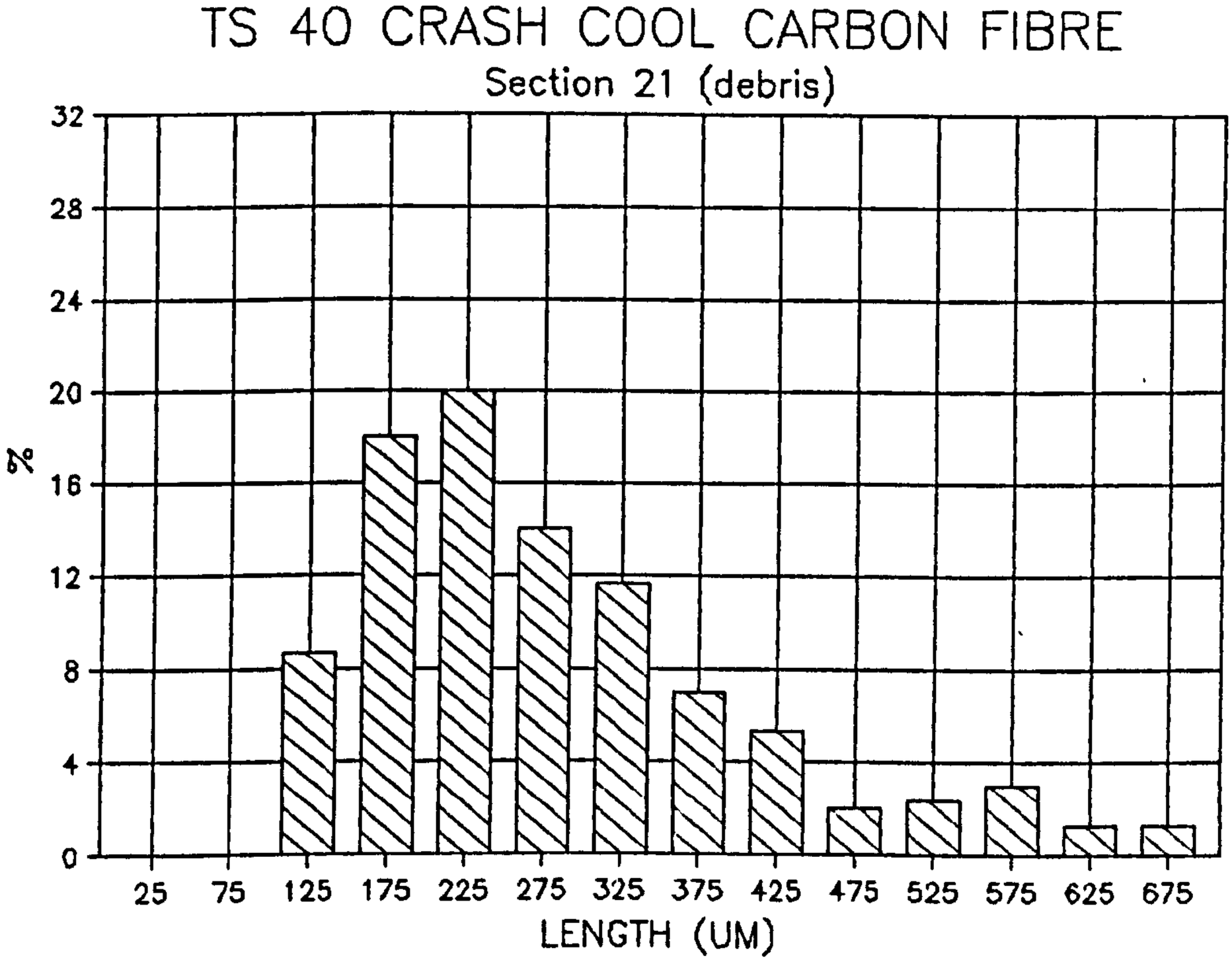
TS 40 CRASH COOL CARBON FIBRE
Section 21 (debris)
32
28
24
20
16
12
8
4
0
%
25 75 125 175 225 275 325 375 425 475 525 575 625 675
LENGTH (UM)

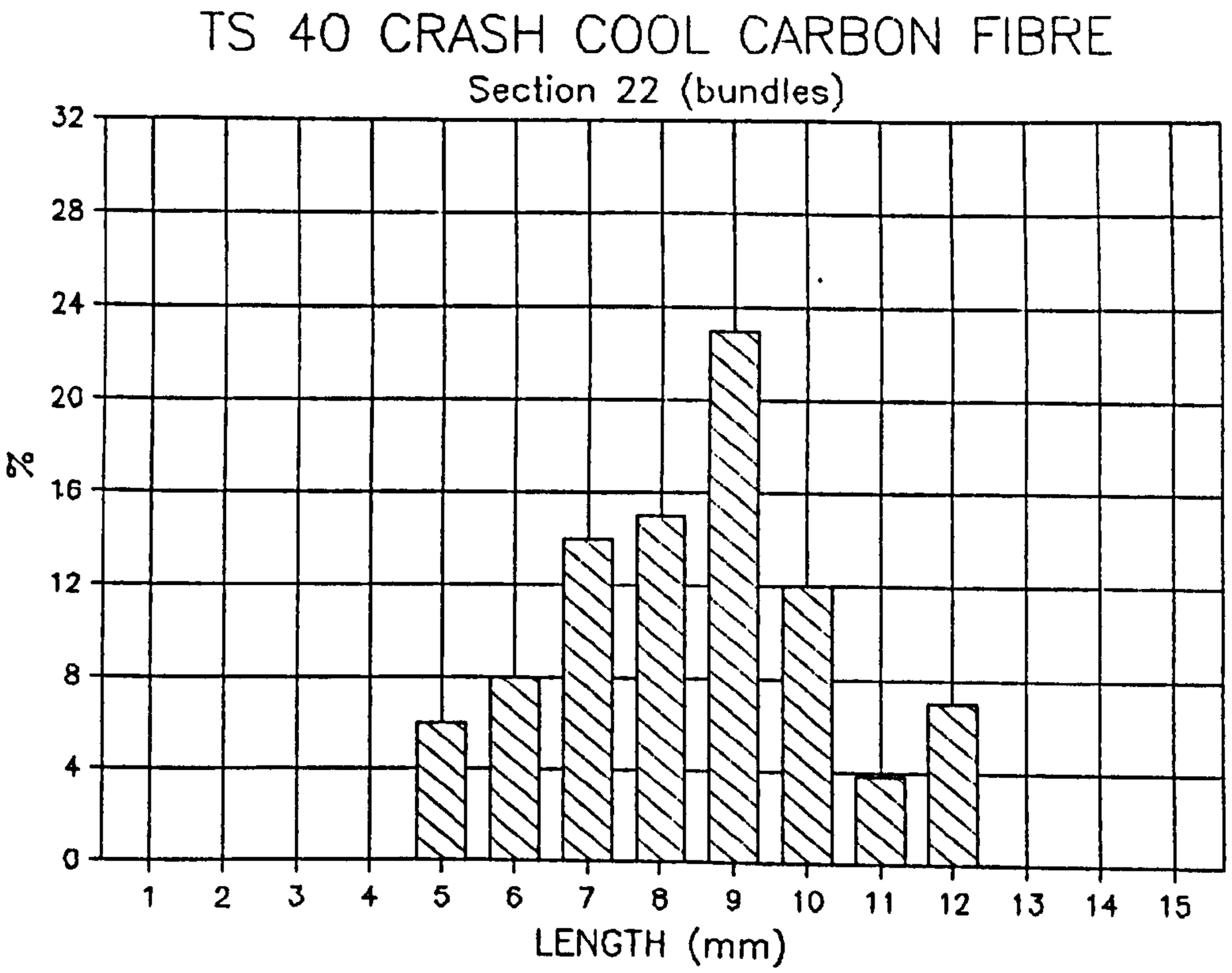
TS 40 CRASH COOL CARBON FIBRE
Section 22 (bundles)
%
32
28
24
20
16
12
8
4
0
1
2
3
4
5
6
7
8
9
10
11
12
13
14
15
LENGTH (mm)

Figure 46

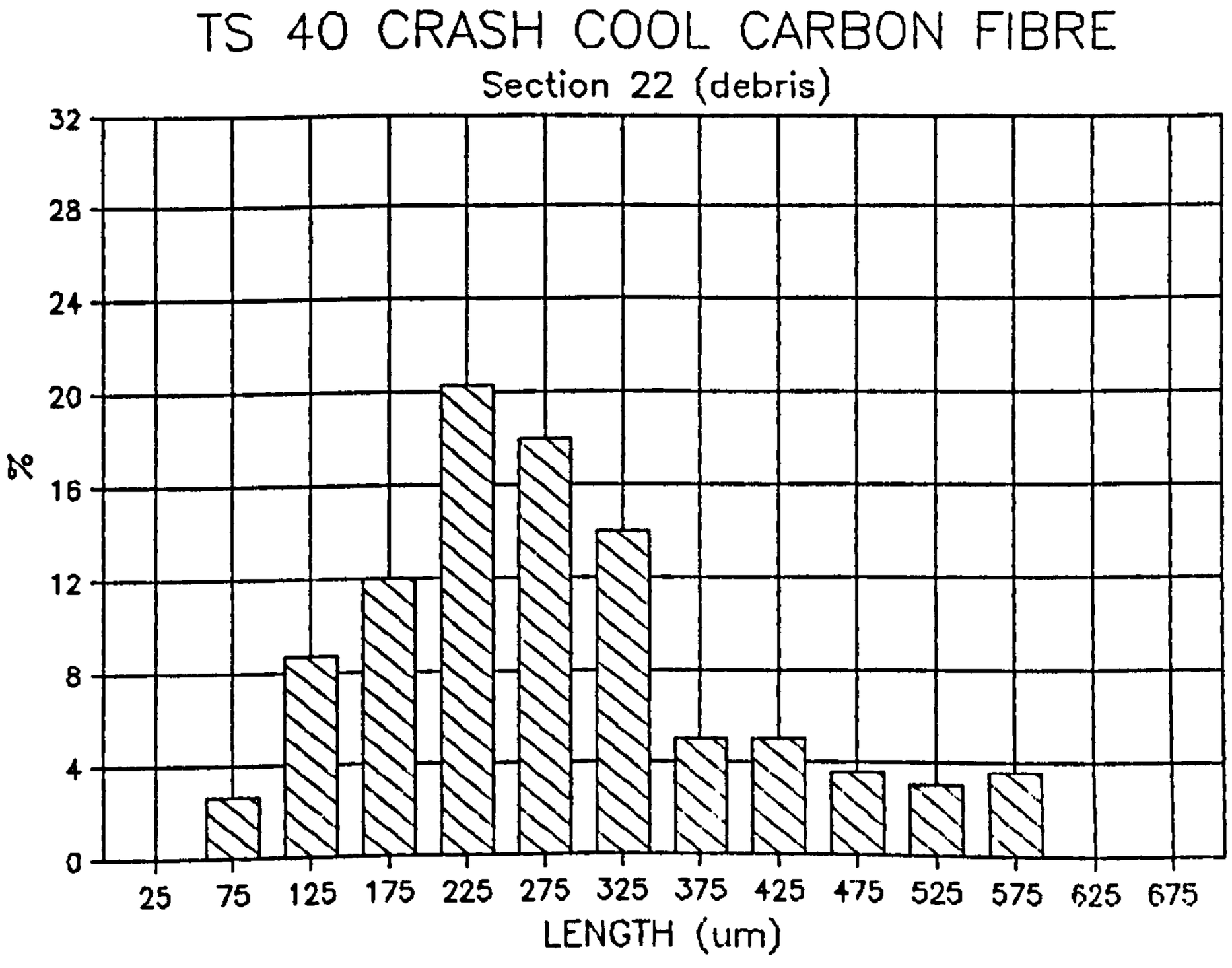
TS 40 CRASH COOL CARBON FIBRE
Section 22 (debris)
%
32
28
24
20
16
12
8
4
0
25
75
125
175
225
275
325
375
425
475
525
575
625
675
LENGTH (um)

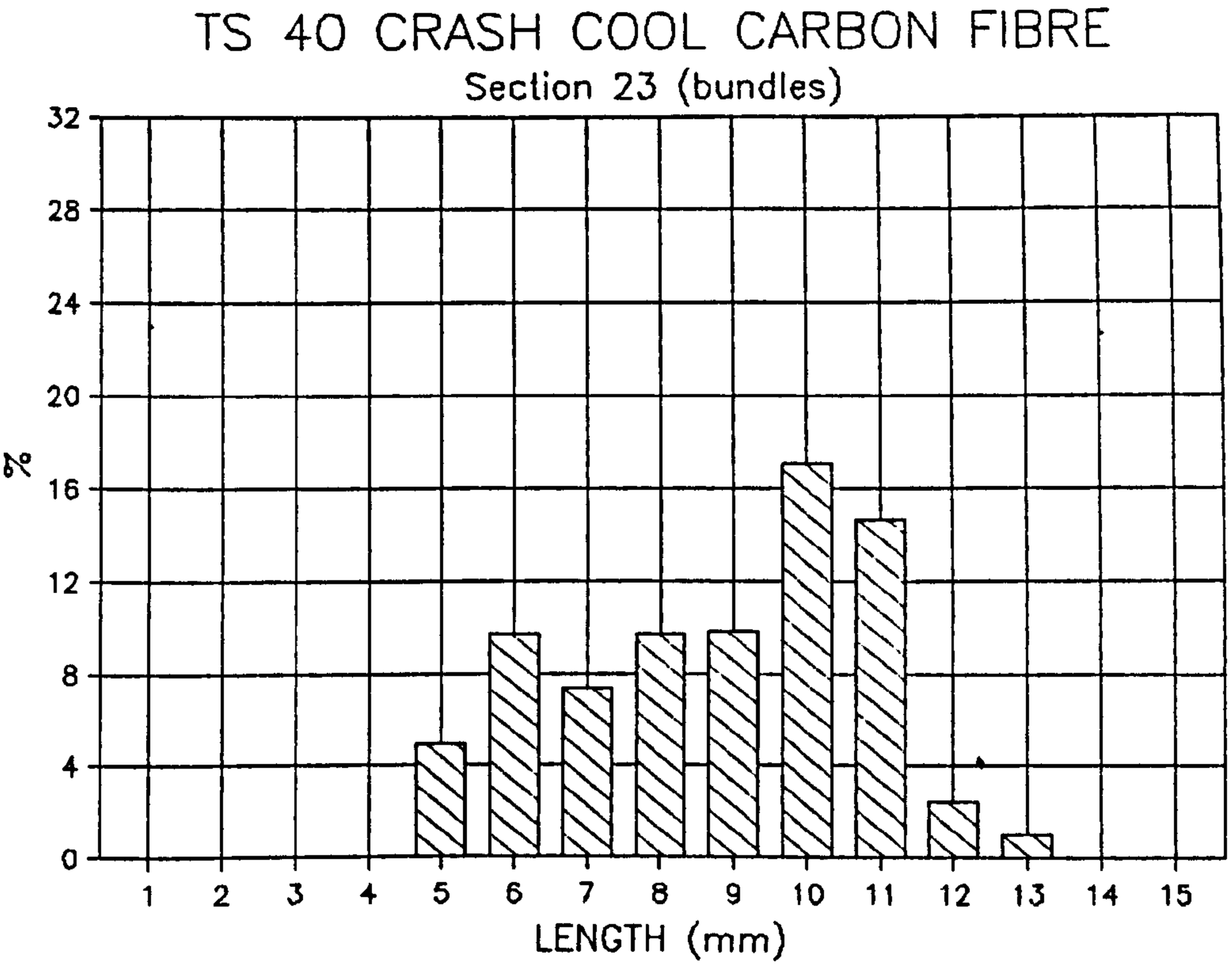
TS 40 CRASH COOL CARBON FIBRE
Section 23 (bundles)
32
28
24
20
16
12
8
4
0
%
1 2 3 4 5 6 7 8 9 10 11 12 13 14 15
LENGTH (mm)

Figure 47

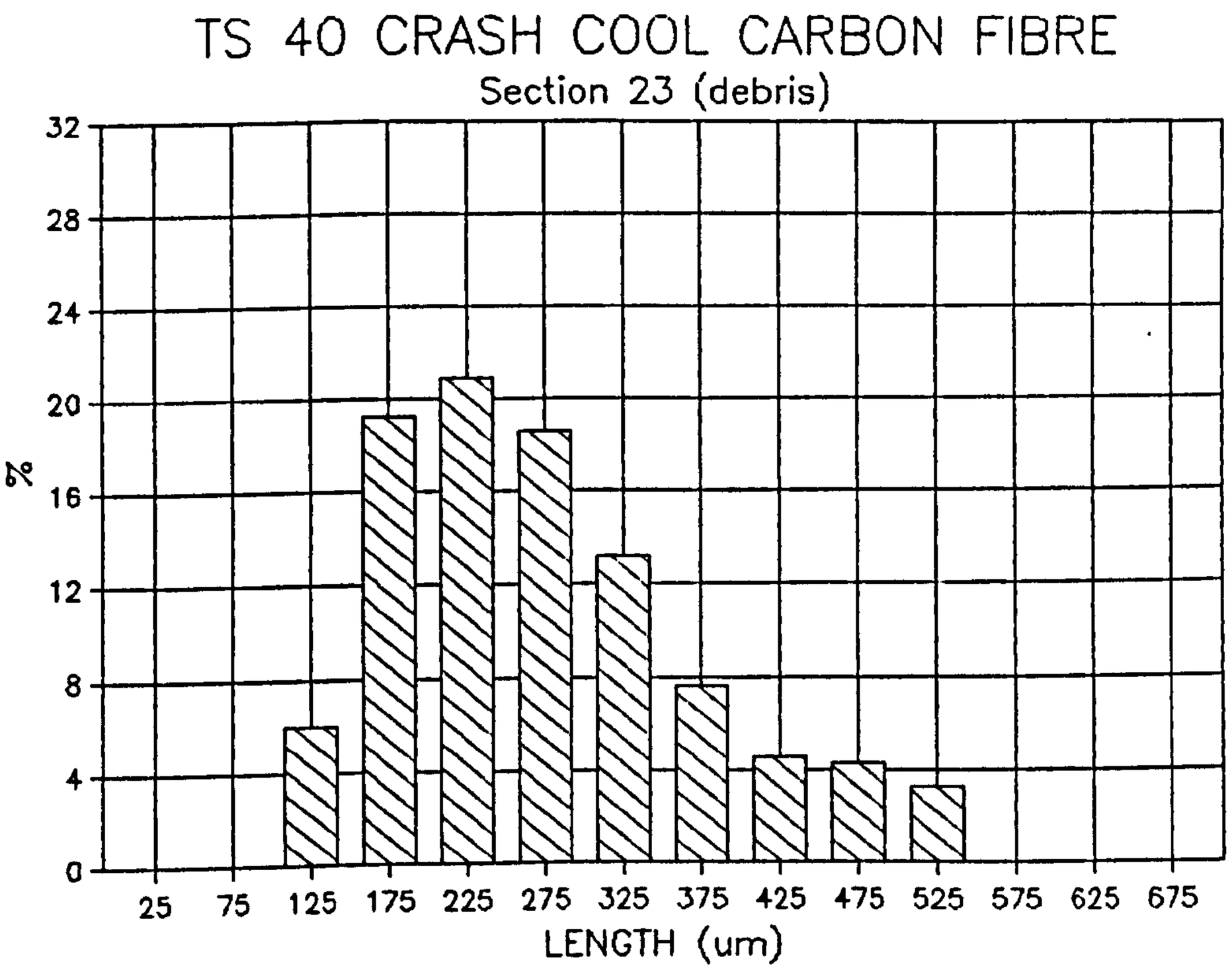
TS 40 CRASH COOL CARBON FIBRE
Section 23 (debris)
32
28
24
20
16
12
8
4
0
%
25 75 125 175 225 275 325 375 425 475 525 575 625 675
LENGTH (um)

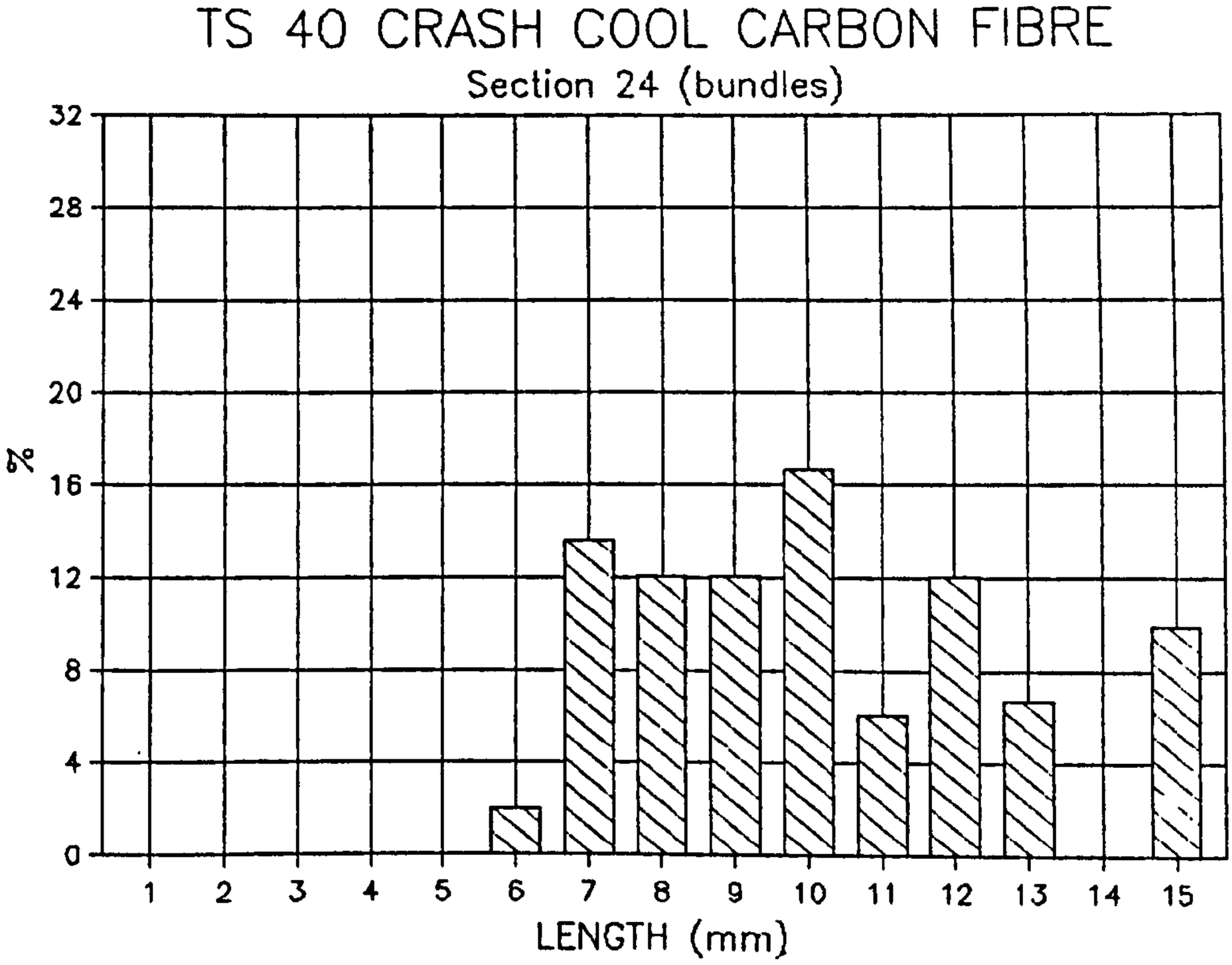
TS 40 CRASH COOL CARBON FIBRE
Section 24 (bundles)
%
32
28
24
20
16
12
8
4
0
1 2 3 4 5 6 7 8 9 10 11 12 13 14 15
LENGTH (mm)

Figure 48

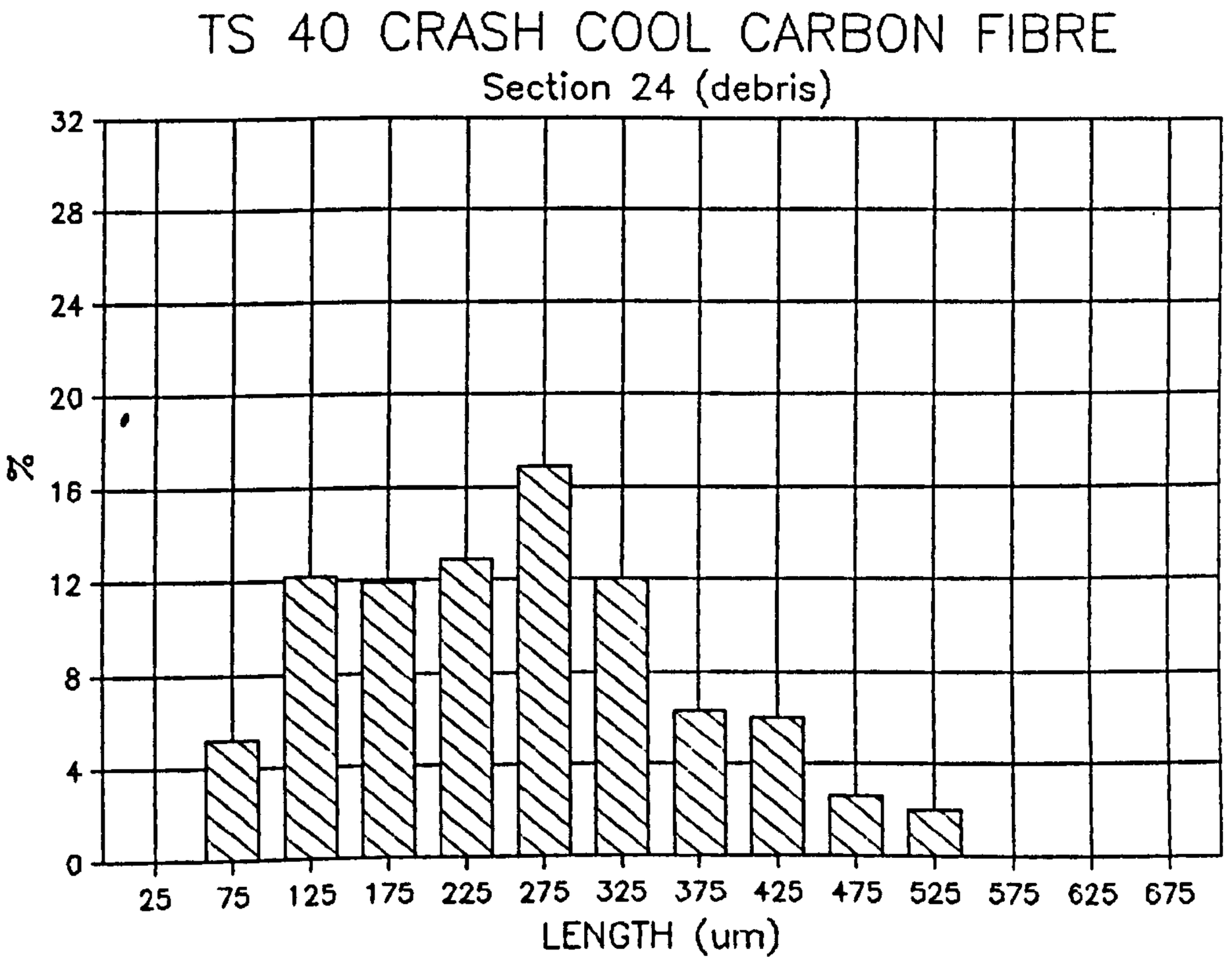
TS 40 CRASH COOL CARBON FIBRE
Section 24 (debris)
%
32
28
24
20
16
12
8
4
0
25 75 125 175 225 275 325 375 425 475 525 575 625 675
LENGTH (um)

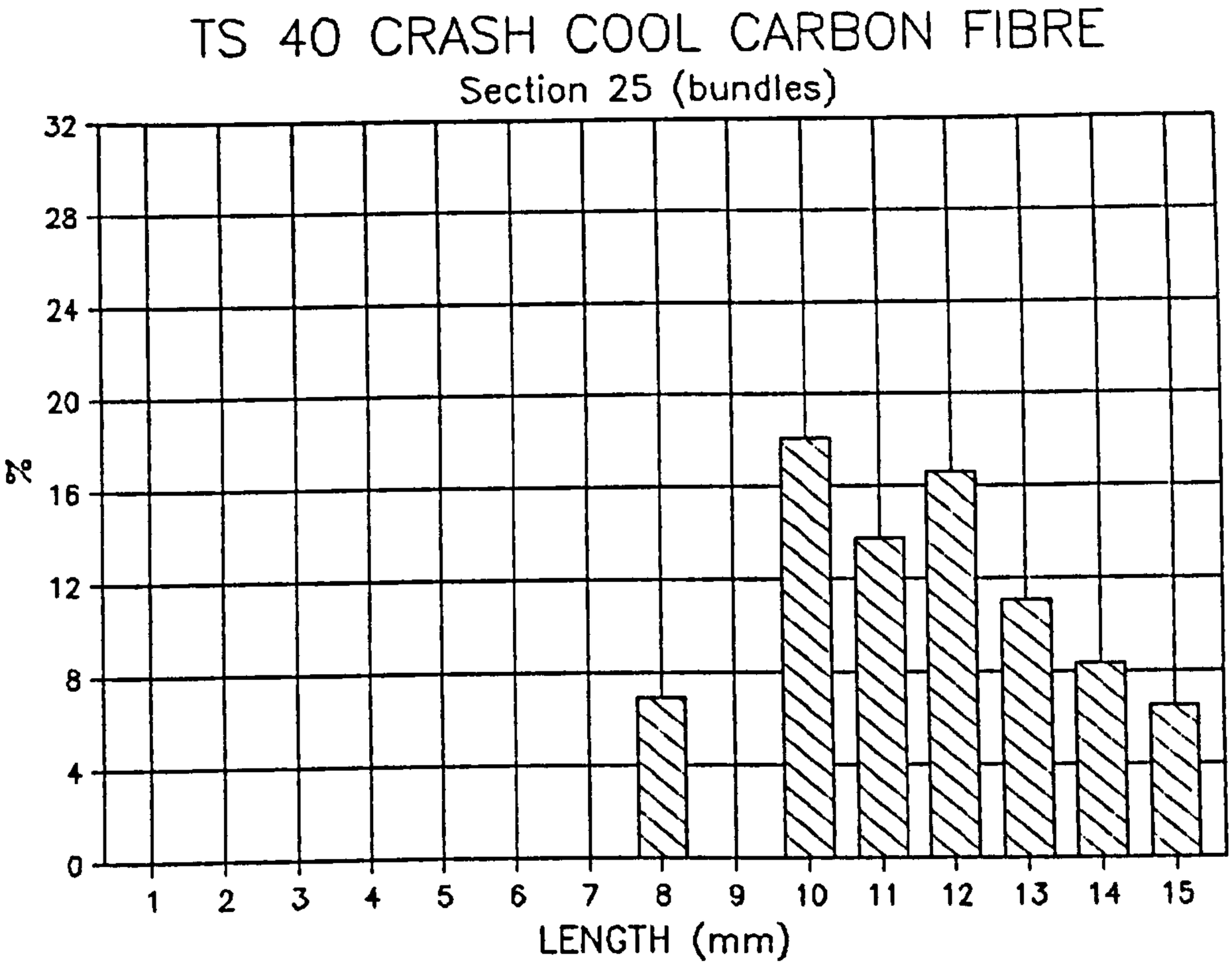
TS 40 CRASH COOL CARBON FIBRE
Section 25 (bundles)
%
32
28
24
20
16
12
8
4
0
1 2 3 4 5 6 7 8 9 10 11 12 13 14 15
LENGTH (mm)

Figure 49

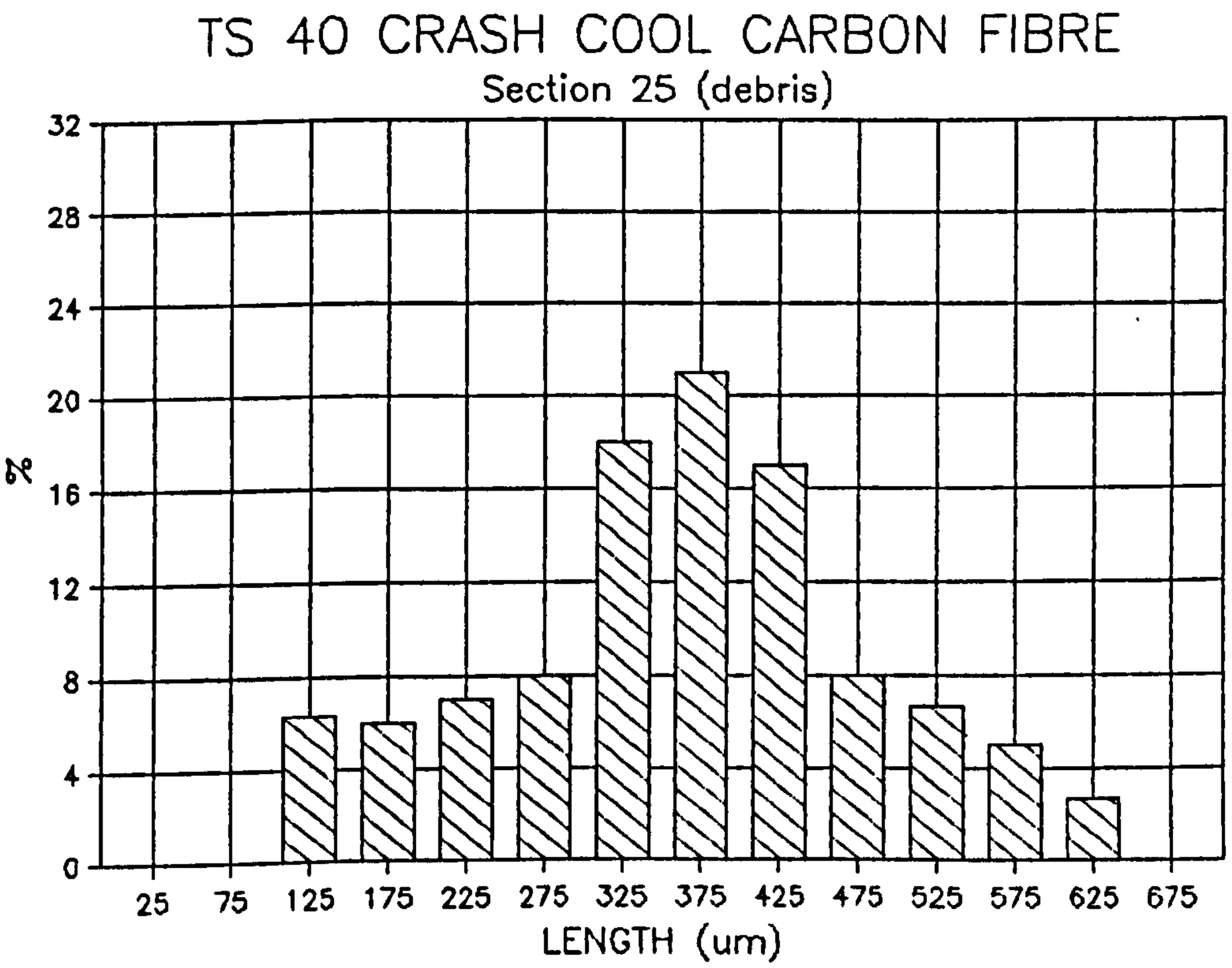
TS 40 CRASH COOL CARBON FIBRE
Section 25 (debris)
%
32
28
24
20
16
12
8
4
0
25 75 125 175 225 275 325 375 425 475 525 575 625 675
LENGTH (um)

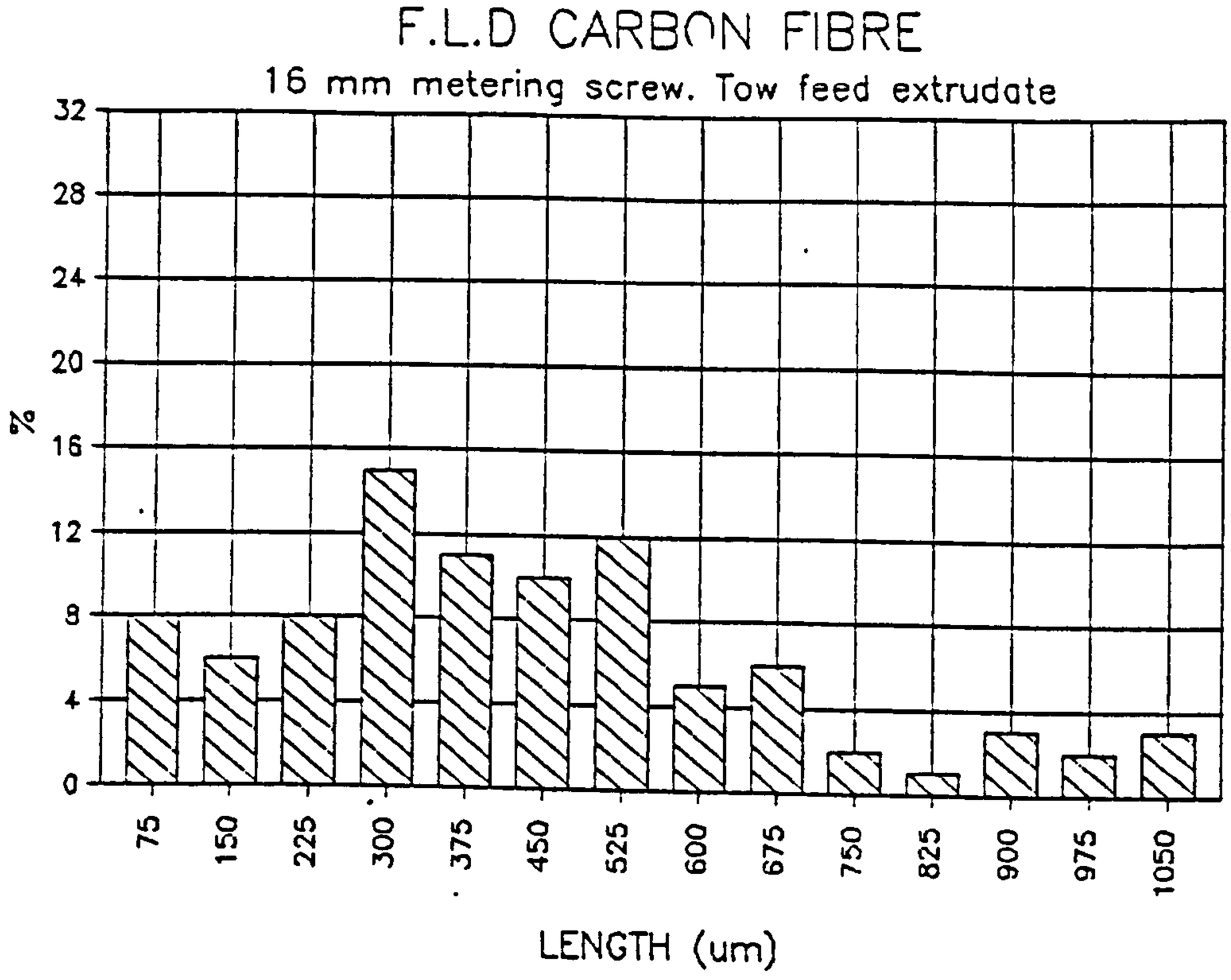

Figure 50

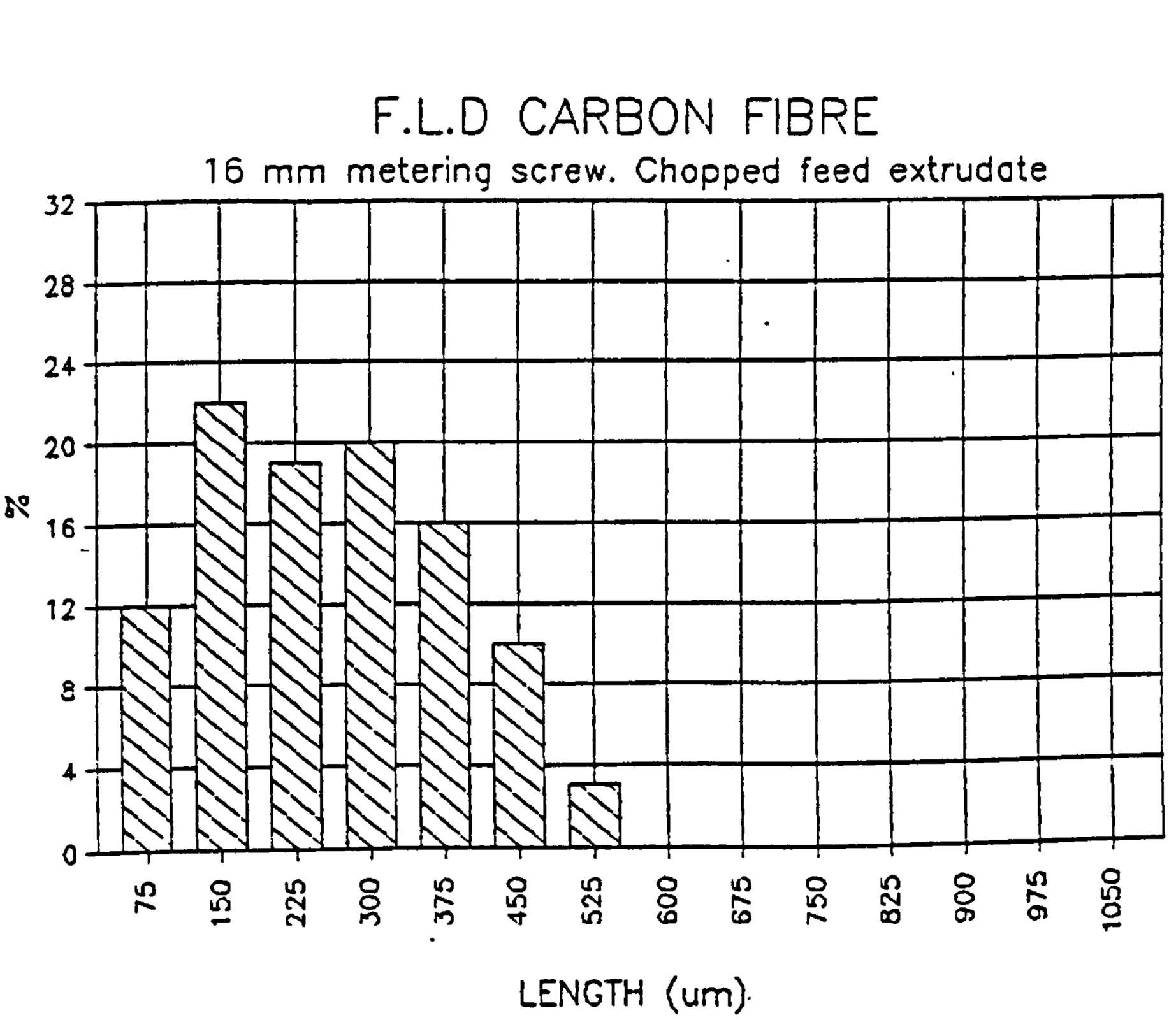

Figure 51

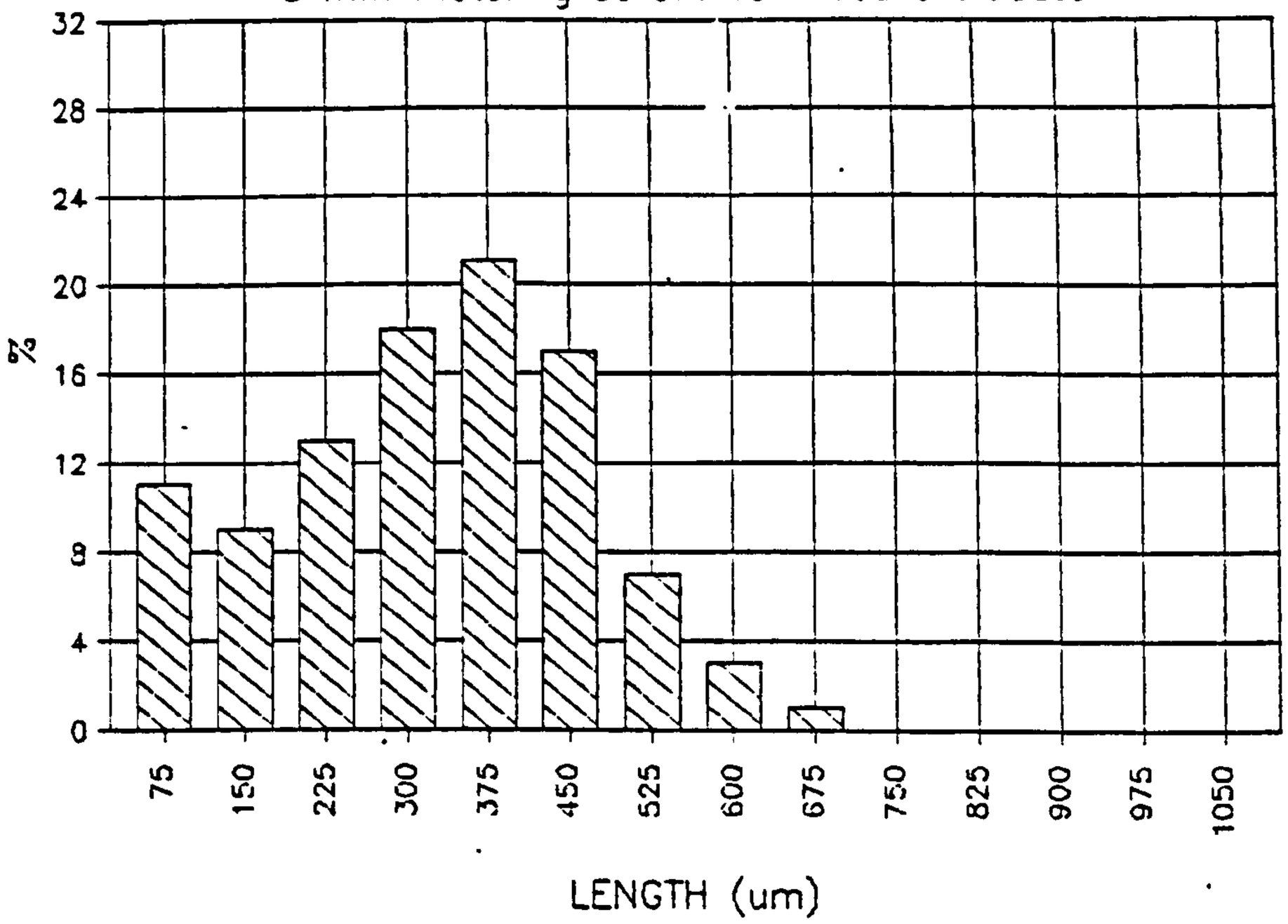

Figure 52

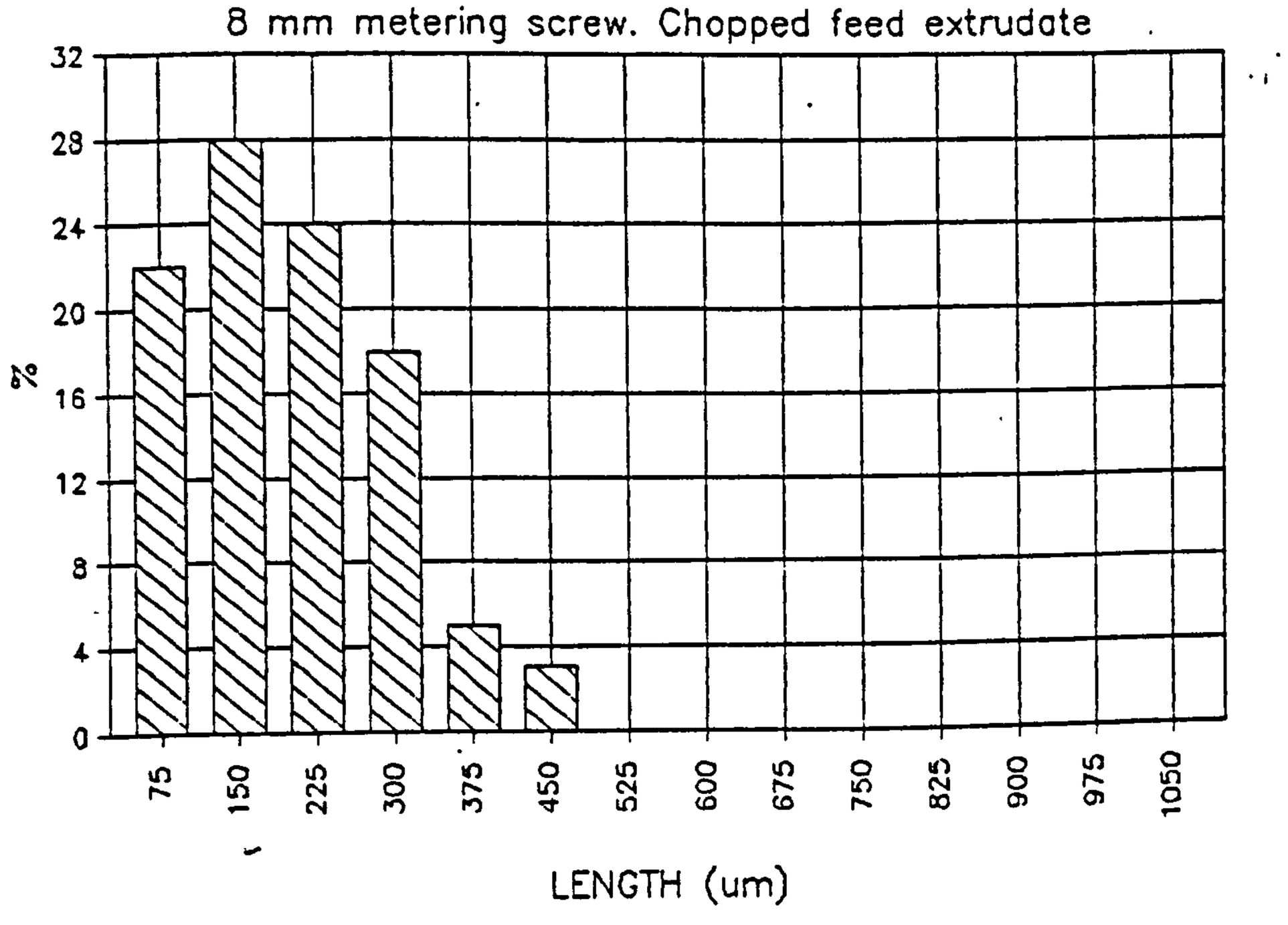

Figure 53

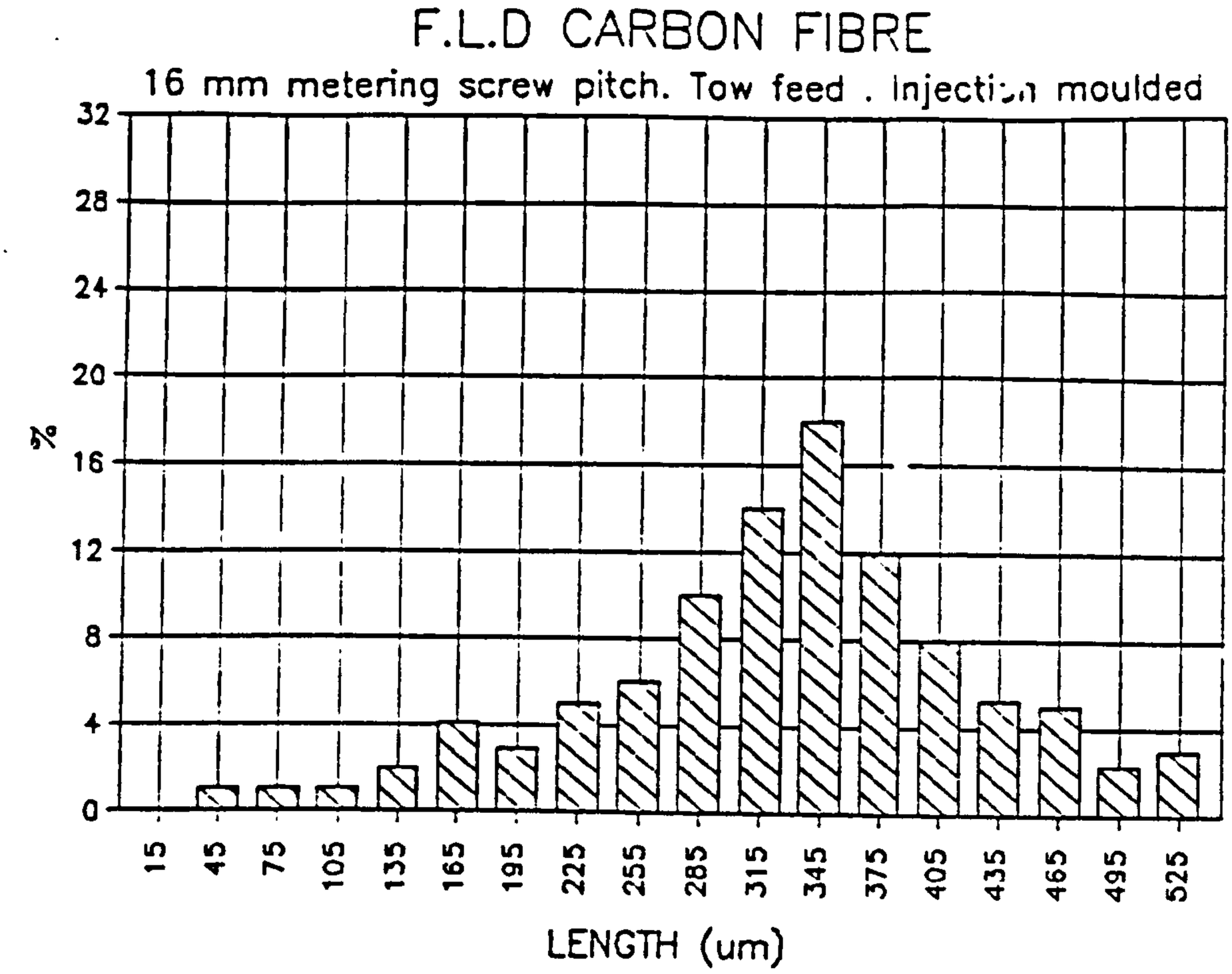

Figure 54

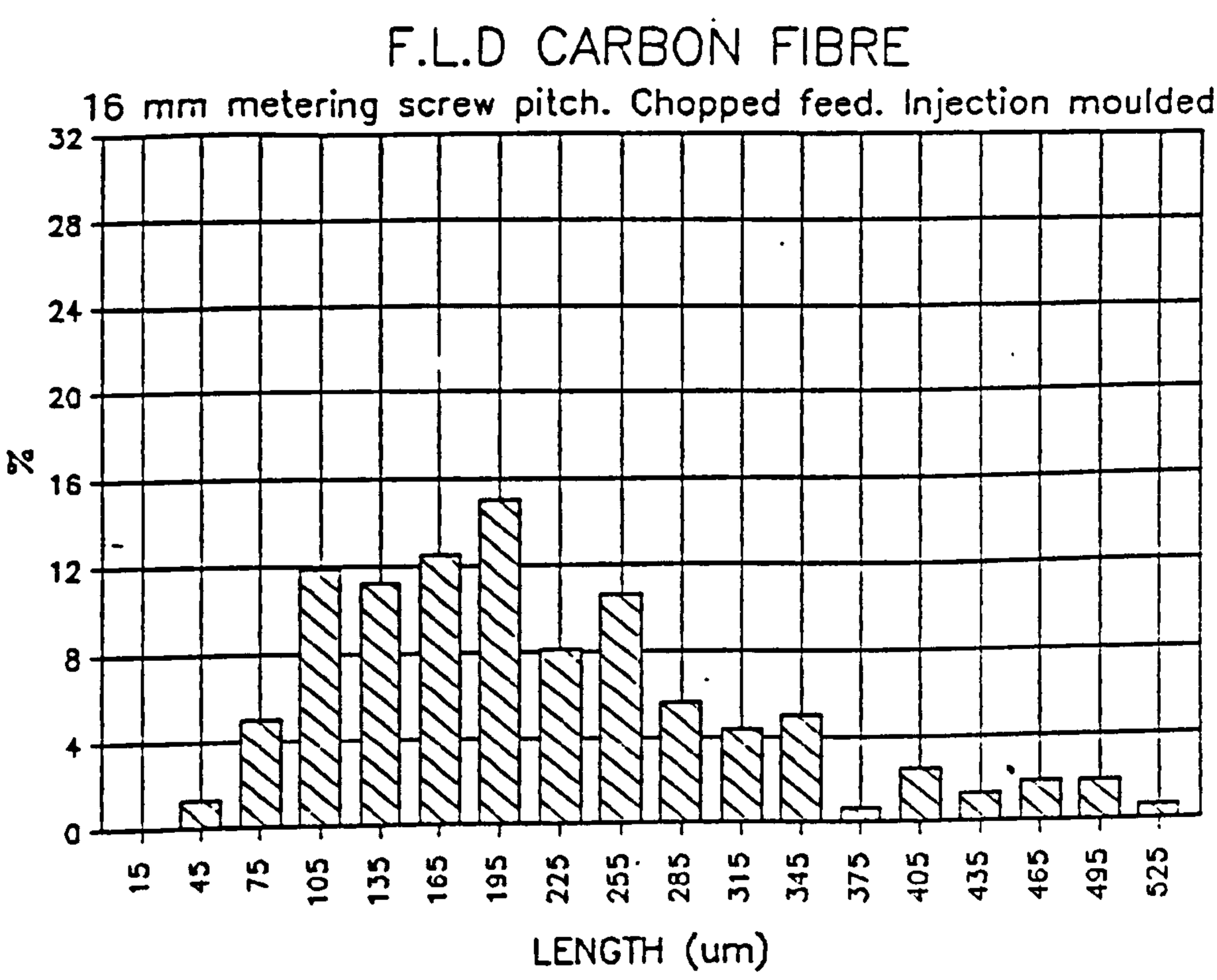

Figure 55

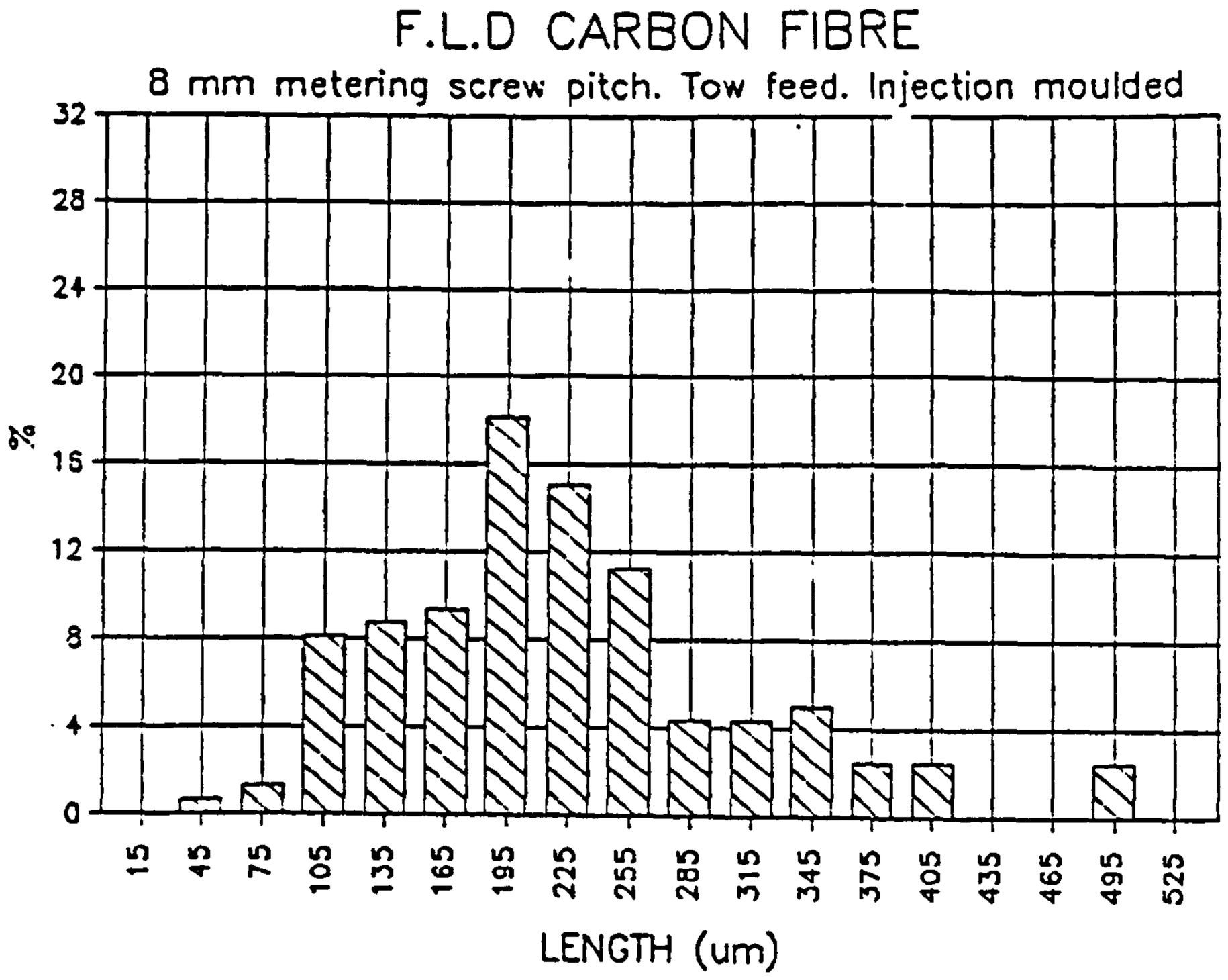

Figure 56

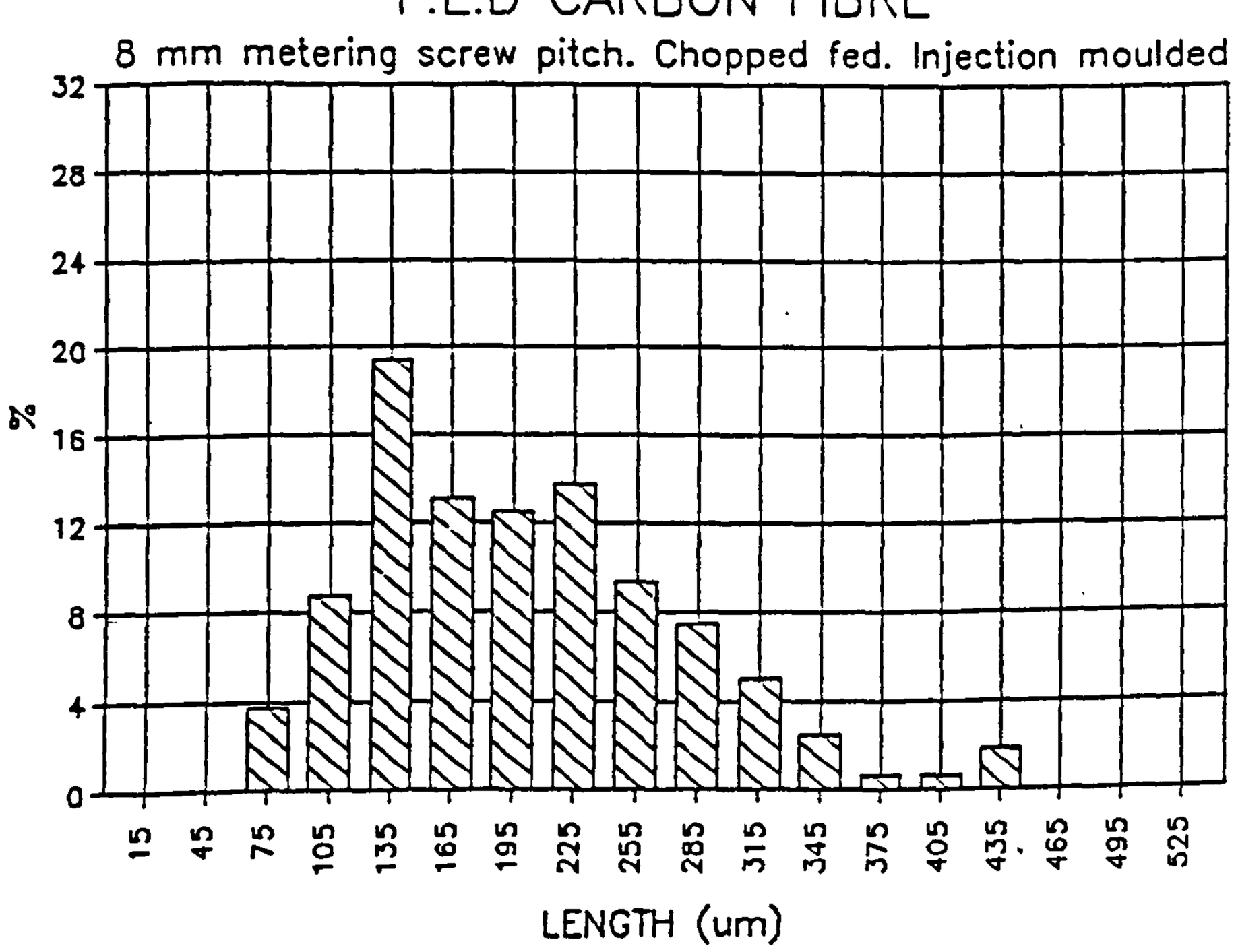

Figure 57

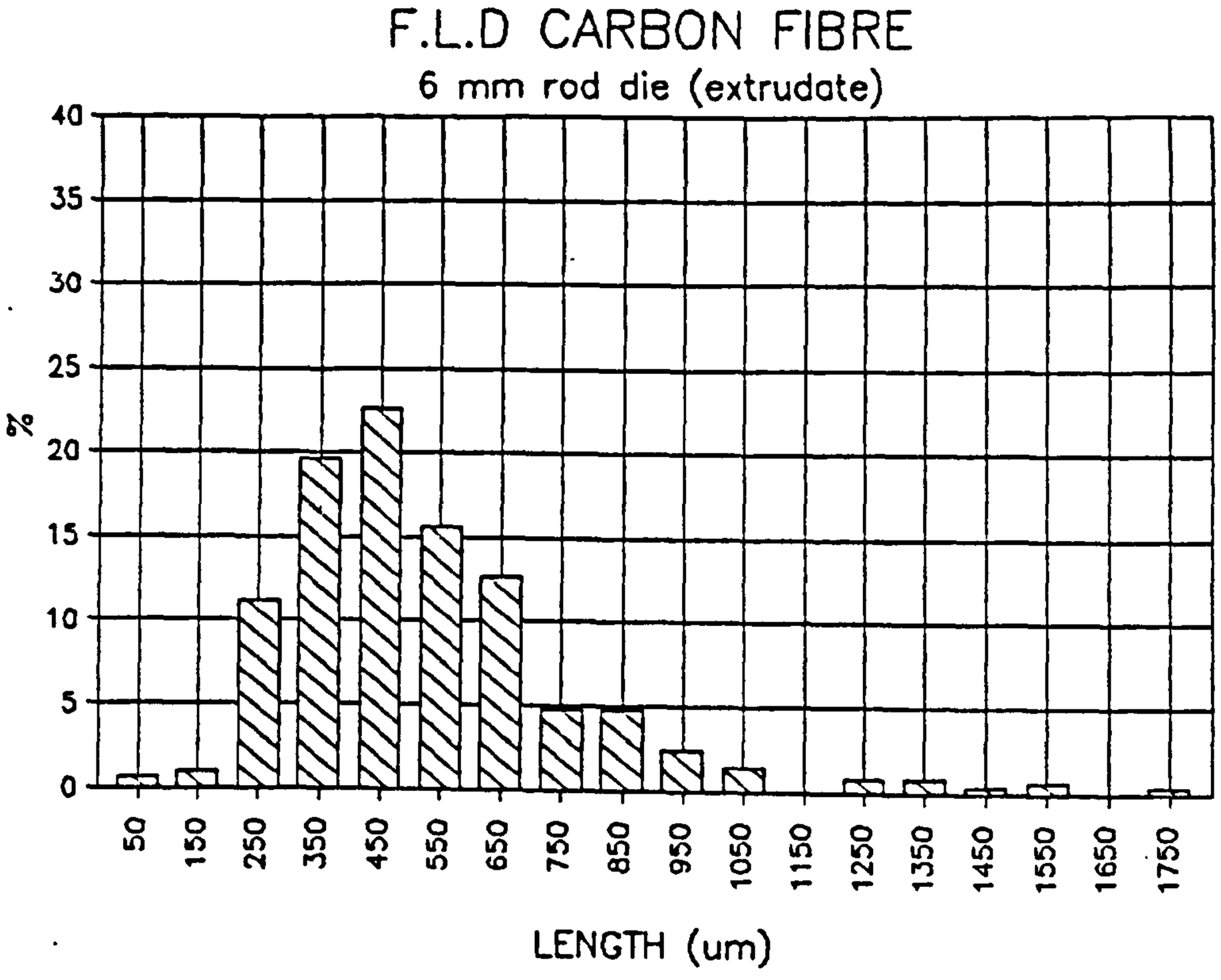

Figure 58

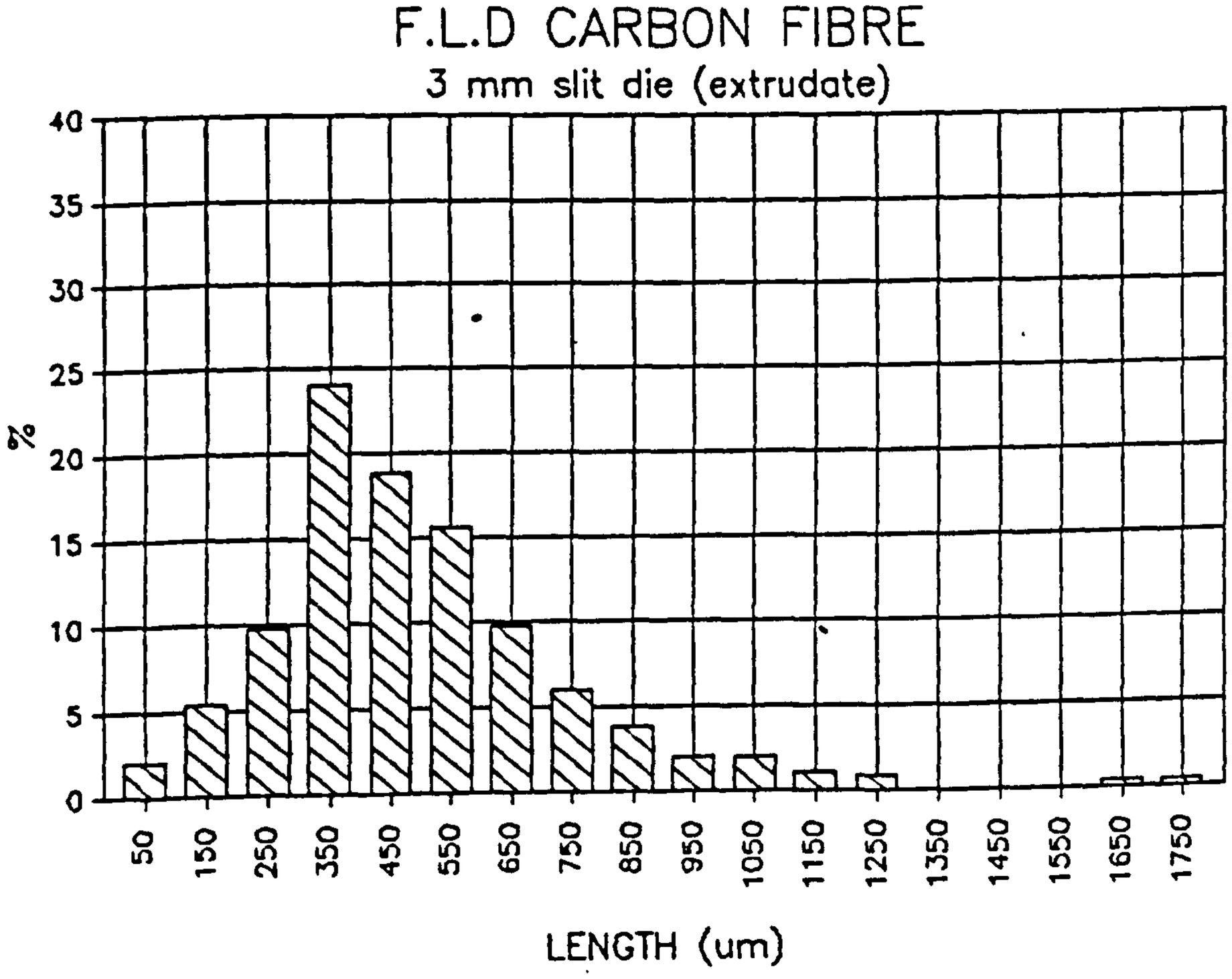

Figure 59

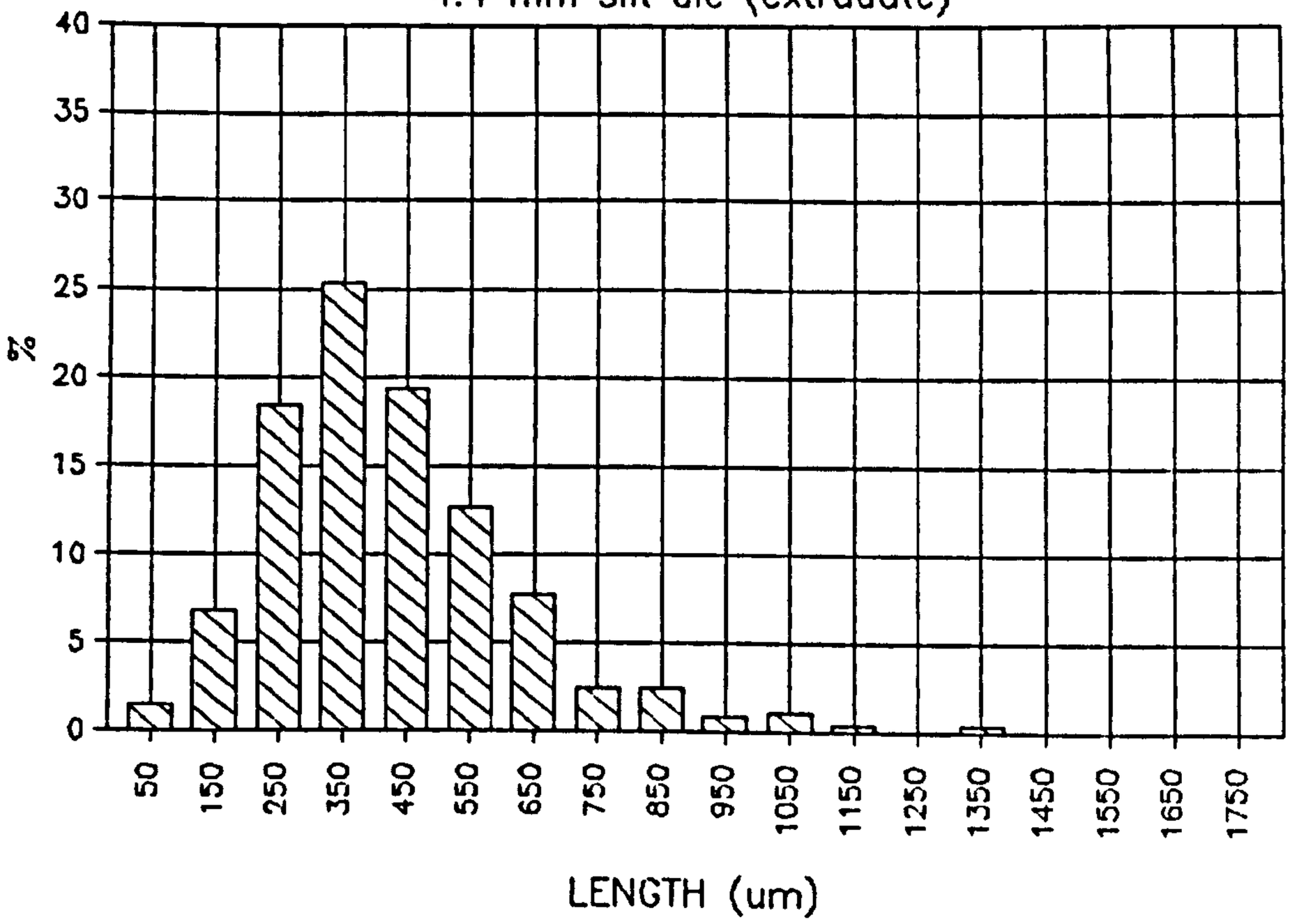
F.L.D CARBON FIBRE
4.4 mm slit die (extrudate)
%
40
35
30
25
20
15
10
5
0
50
150
250
350
450
550
650
750
850
950
1050
1150
1250
1350
1450
1550
1650
1750
LENGTH (um)

Figure 60

Rod die extrudate

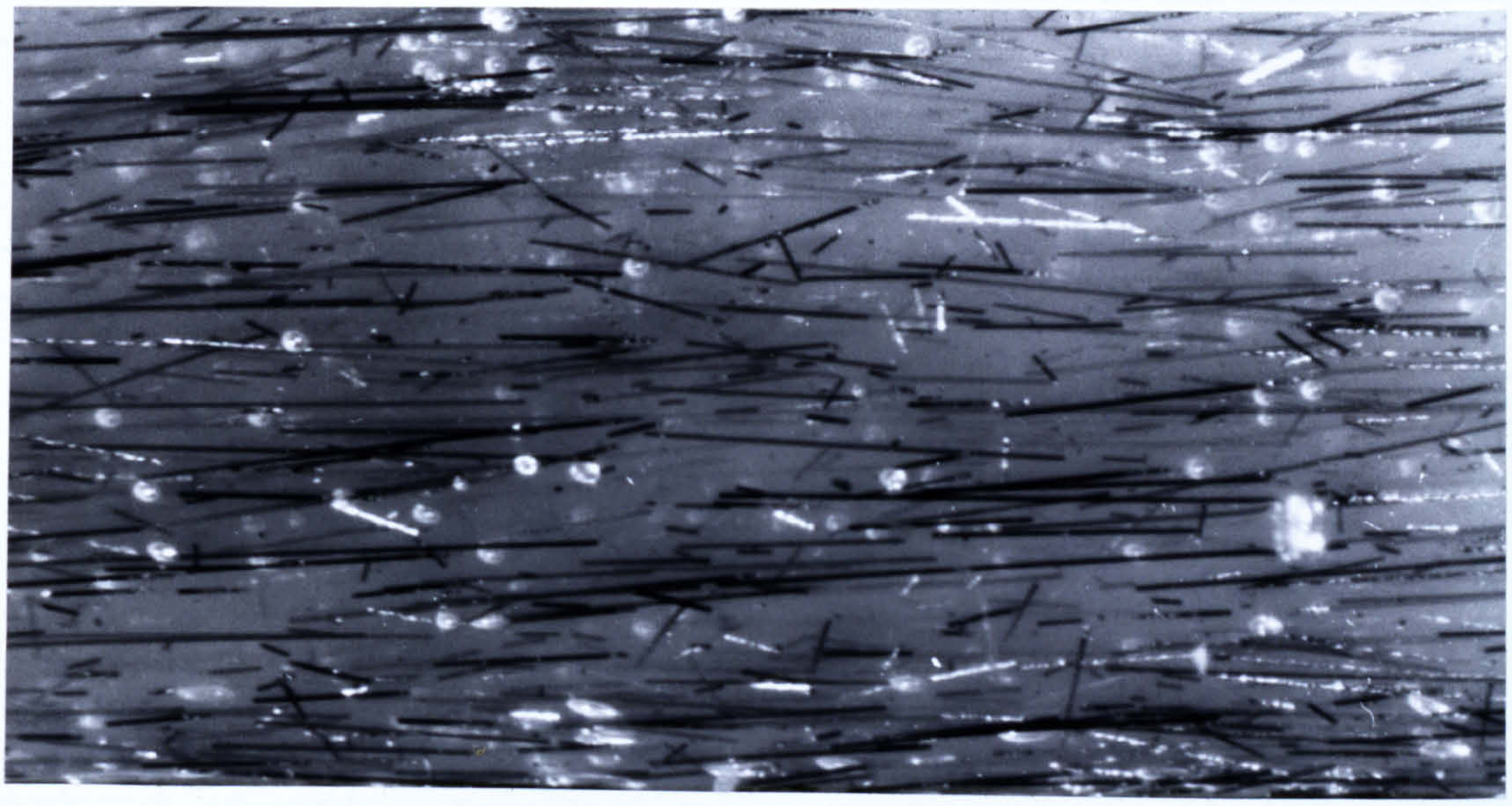

Flow Direction ⟶

0.1mm

Figure 61

Slit die extrudate
(Die set at 4.4mm)

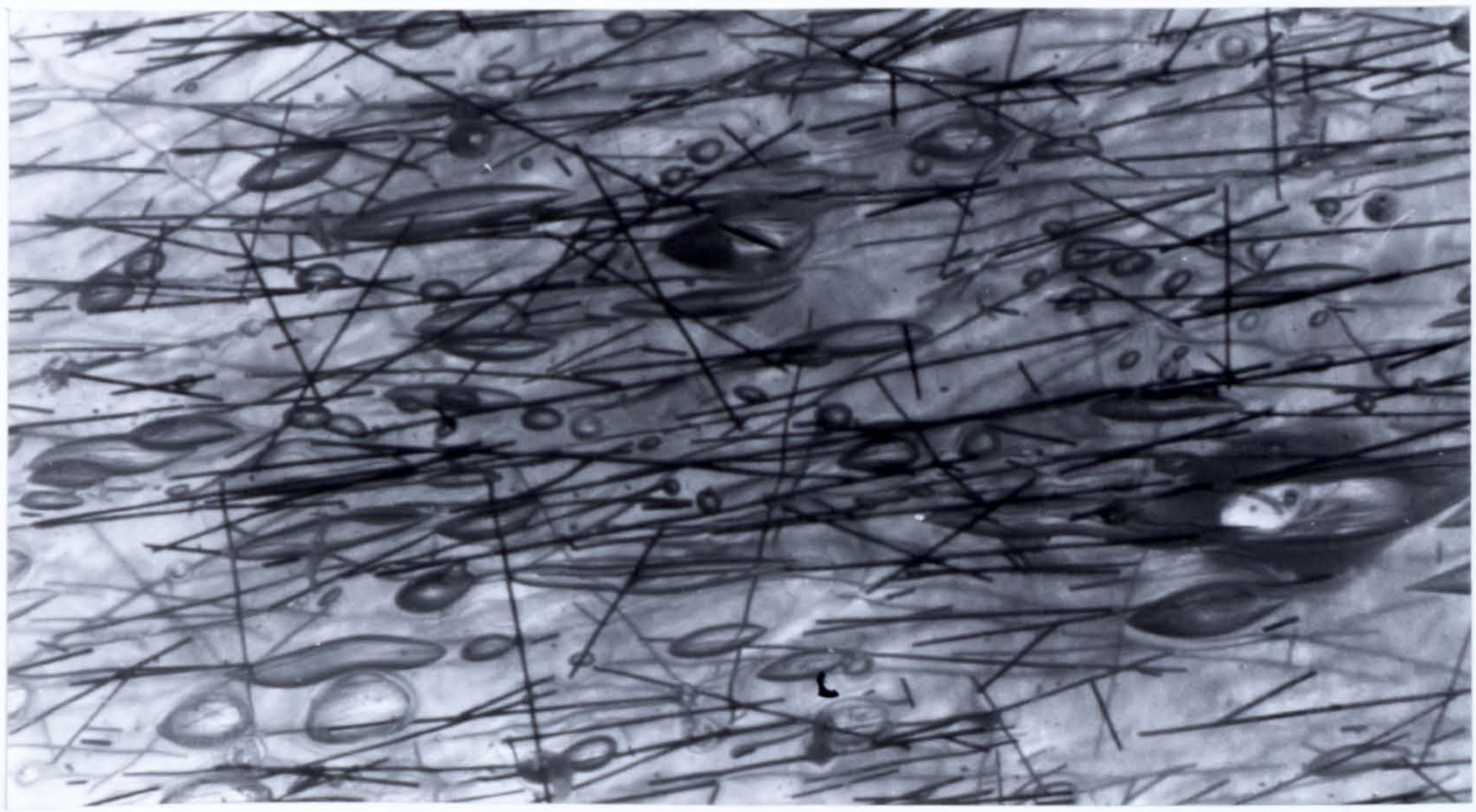

Flow Direction ⟶

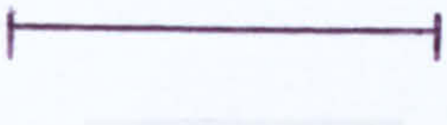

Figure 62

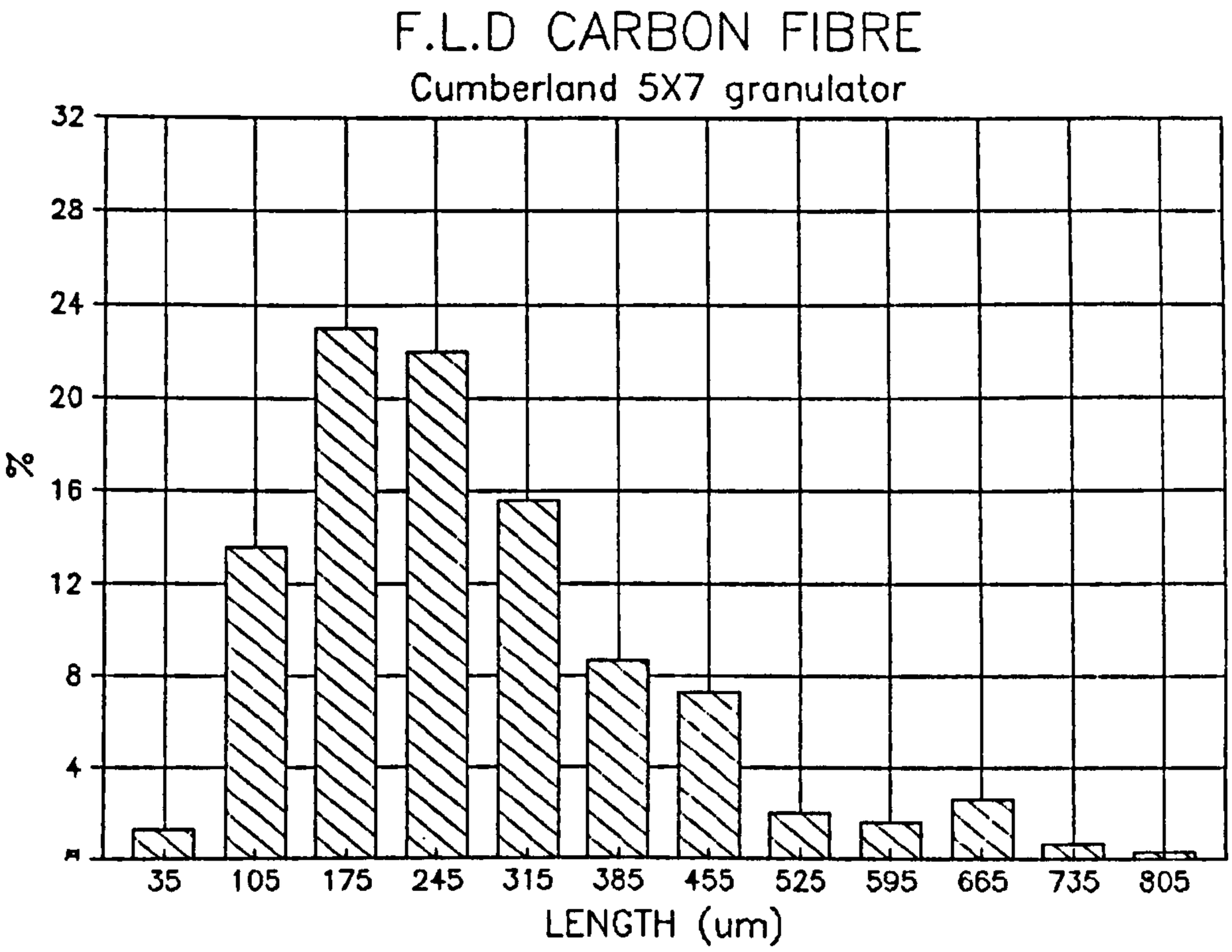

Figure 63

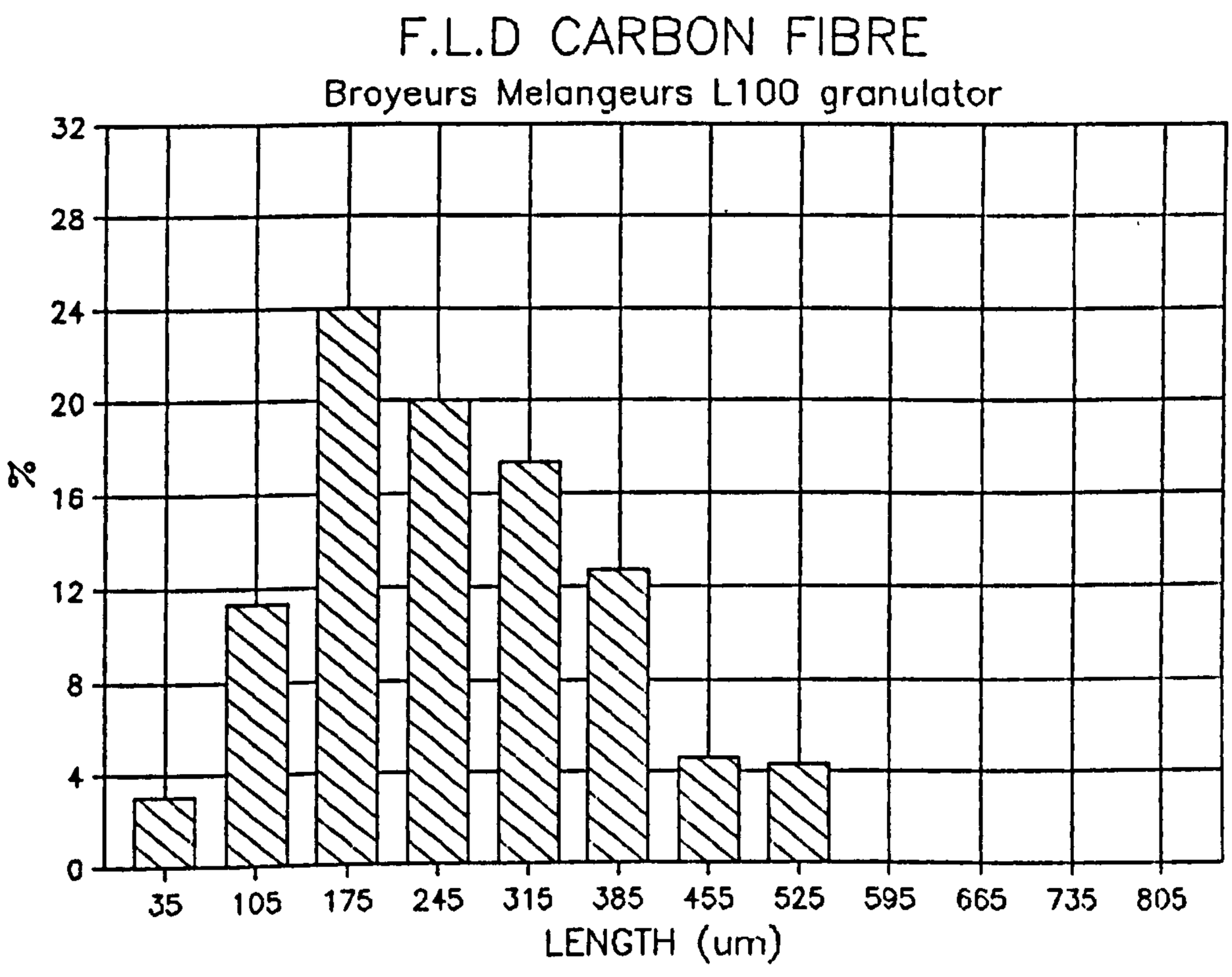

Figure 64

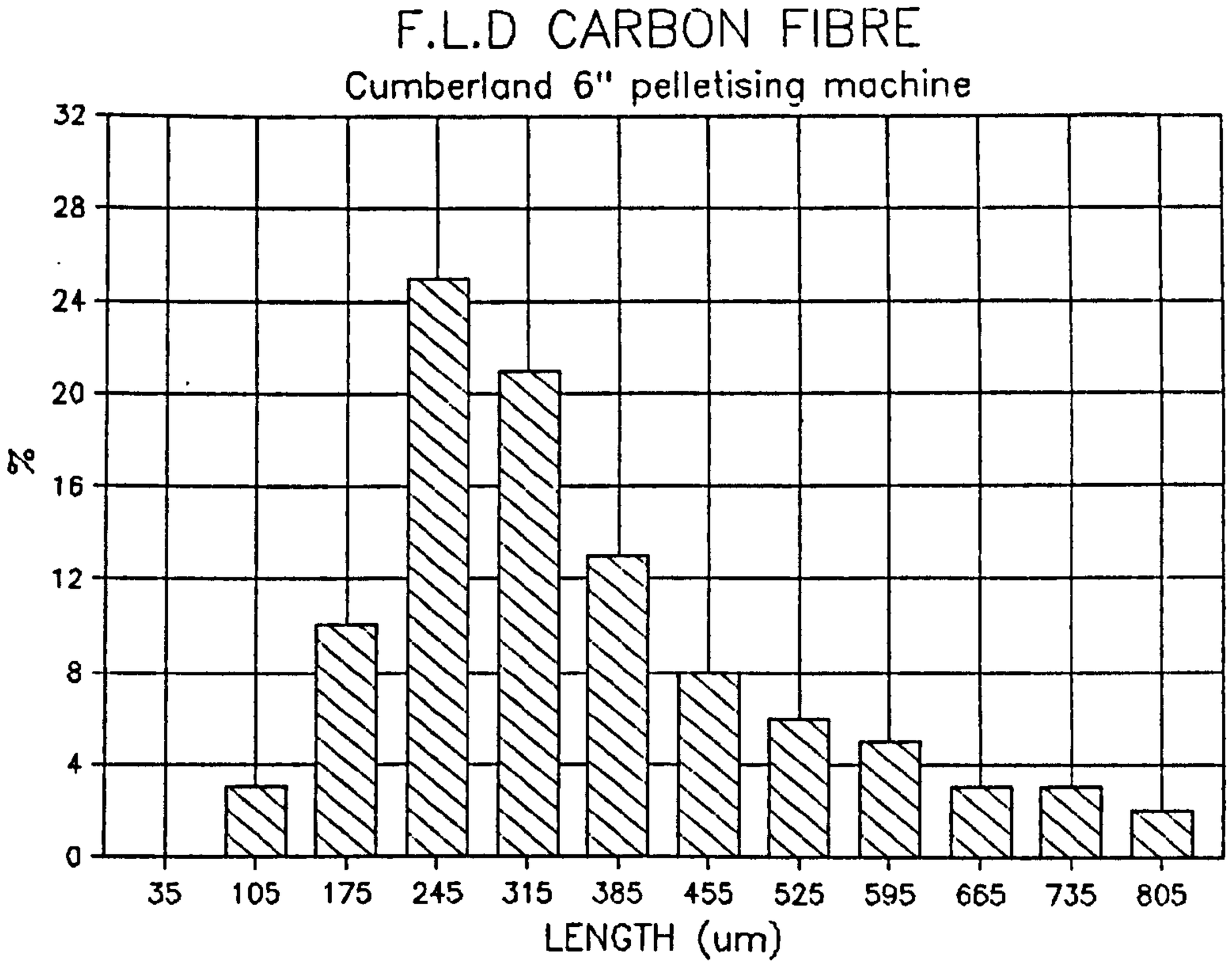
F.L.D CARBON FIBRE
Cumberland 6" pelletising machine
32
28
24
20
16
12
8
4
0
%
35
105
175
245
315
385
455
525
595
665
735
805
LENGTH (um)

Figure 65

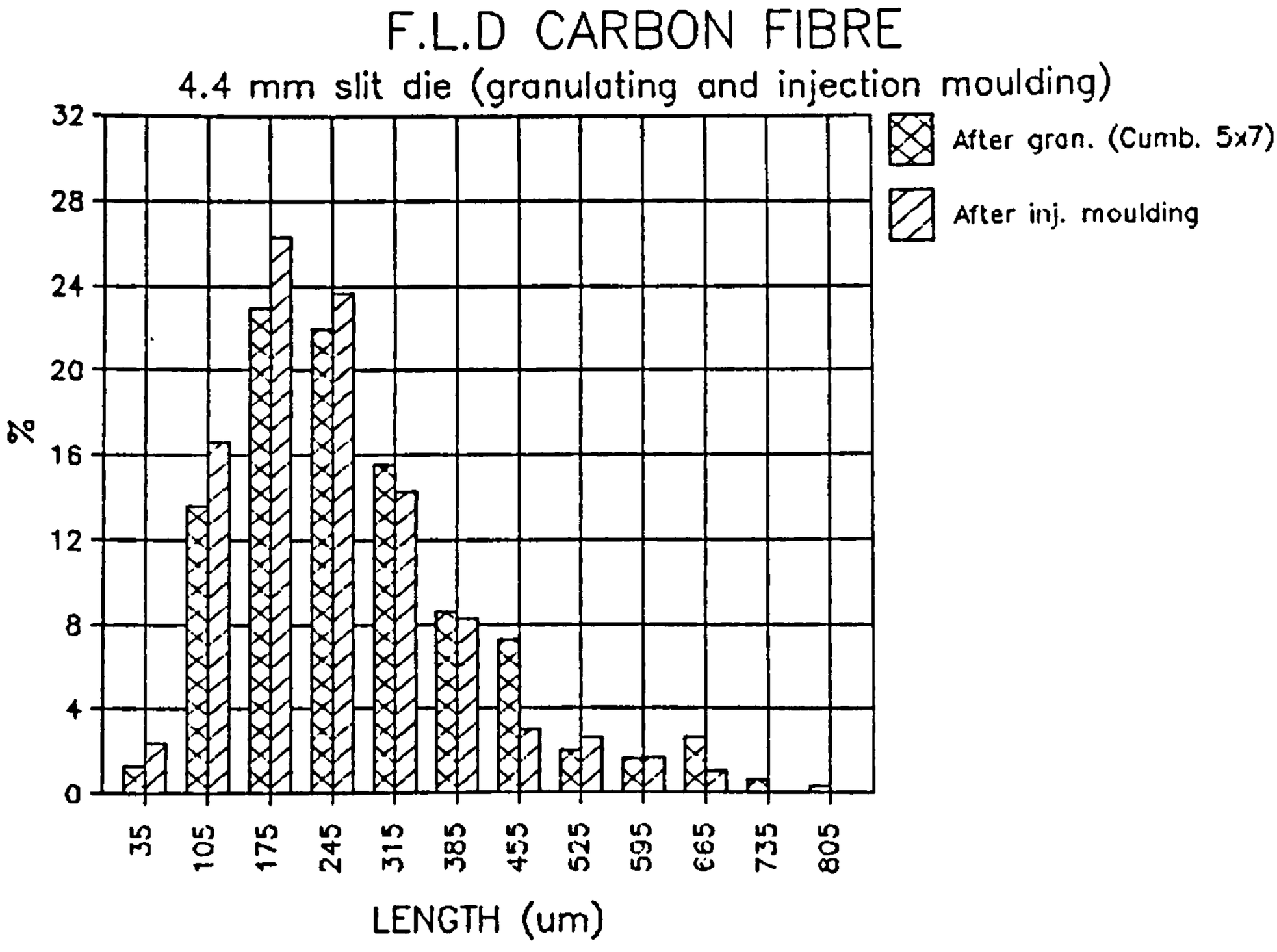
F.L.D CARBON FIBRE
4.4 mm slit die (granulating and injection moulding)
After gran. (Cumb. 5x7)
After inj. moulding
%
32
28
24
20
16
12
8
4
0
35
105
175
245
315
385
455
525
595
665
735
805
LENGTH (um)

Figure 66

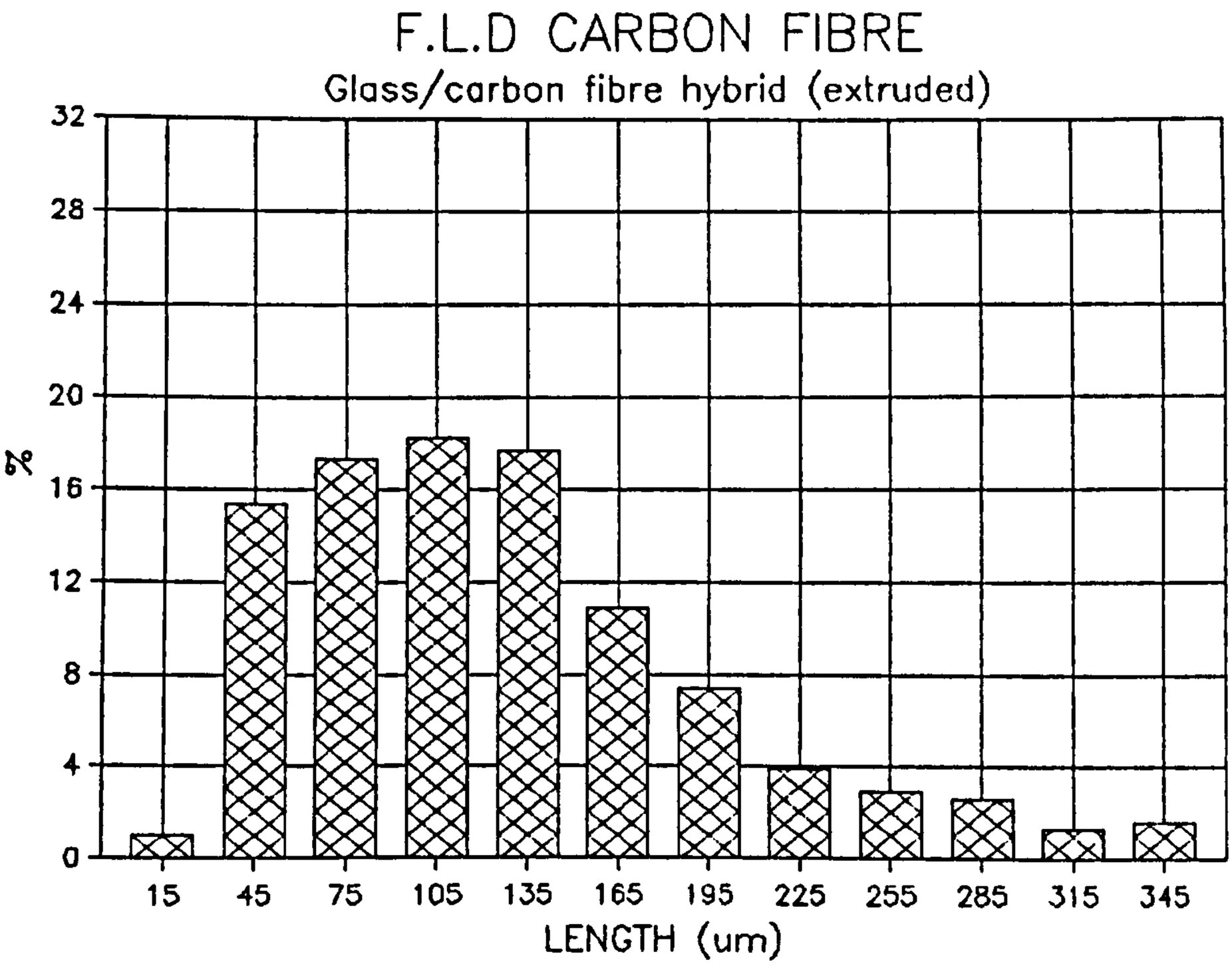
F.L.D CARBON FIBRE
Glass/carbon fibre hybrid (extruded)
%
32
28
24
20
16
12
8
4
0
15
45
75
105
135
165
195
225
255
285
315
345
LENGTH (um)

Figure 67

Pelletiser and granulator design

Figure **68**

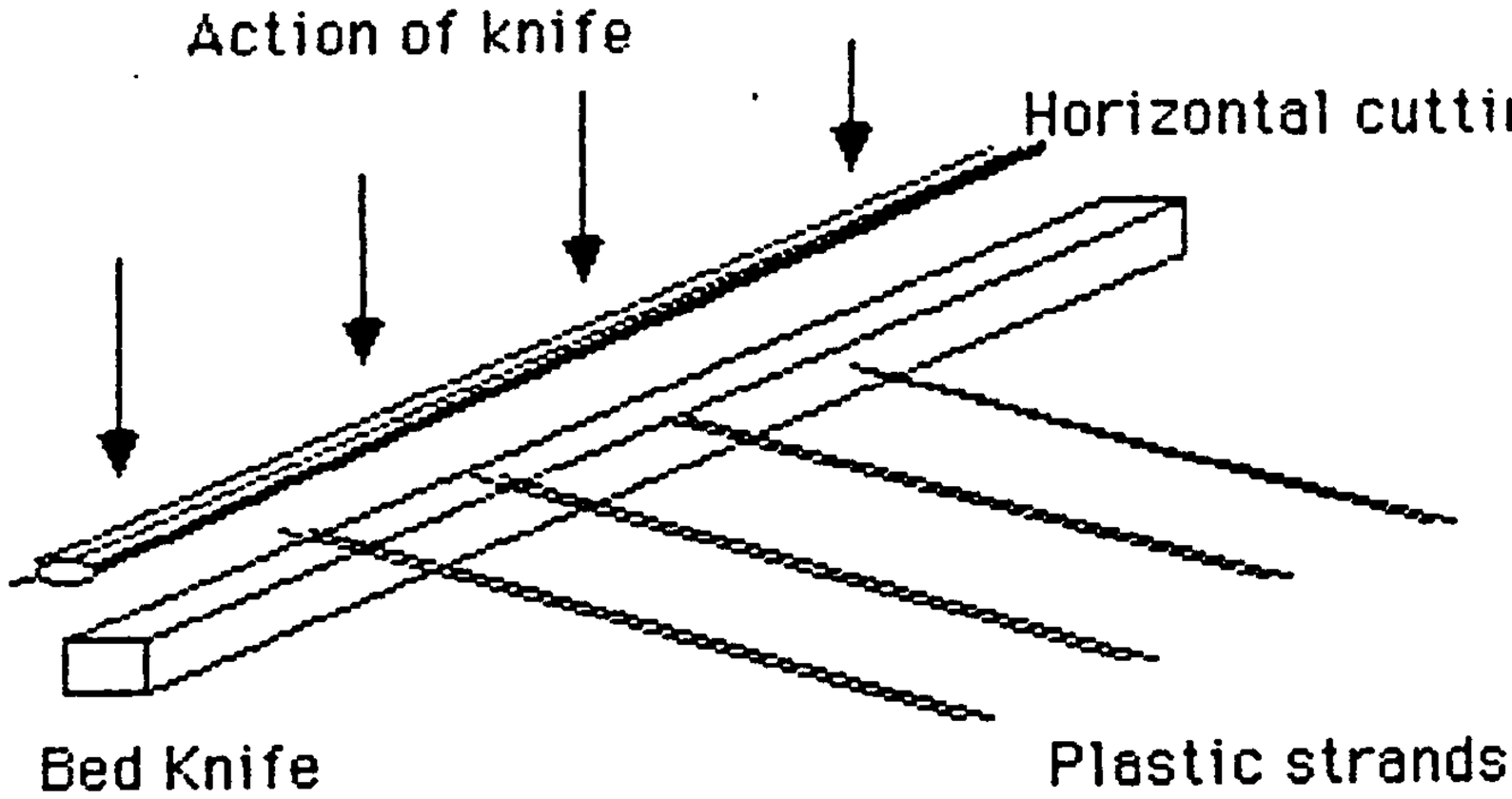

Typical Pelletiser design

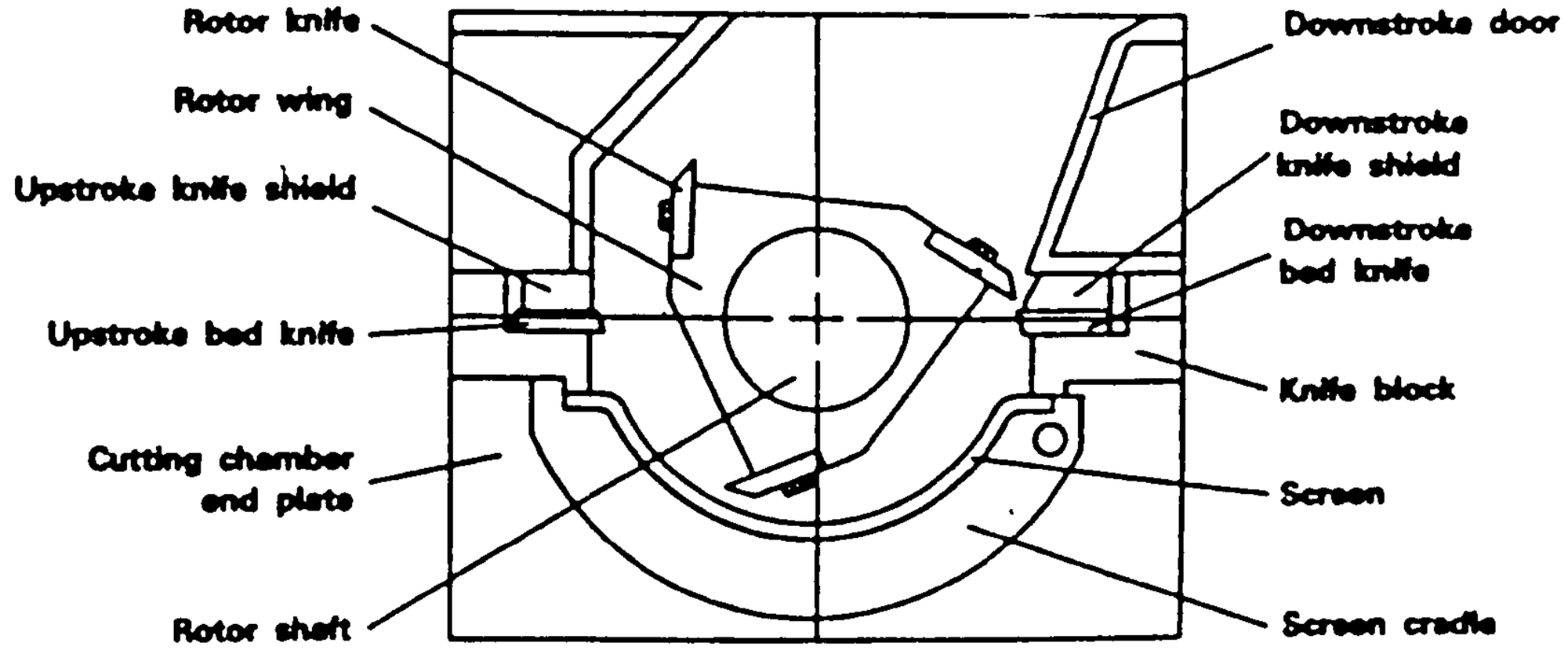

Typical granulator design

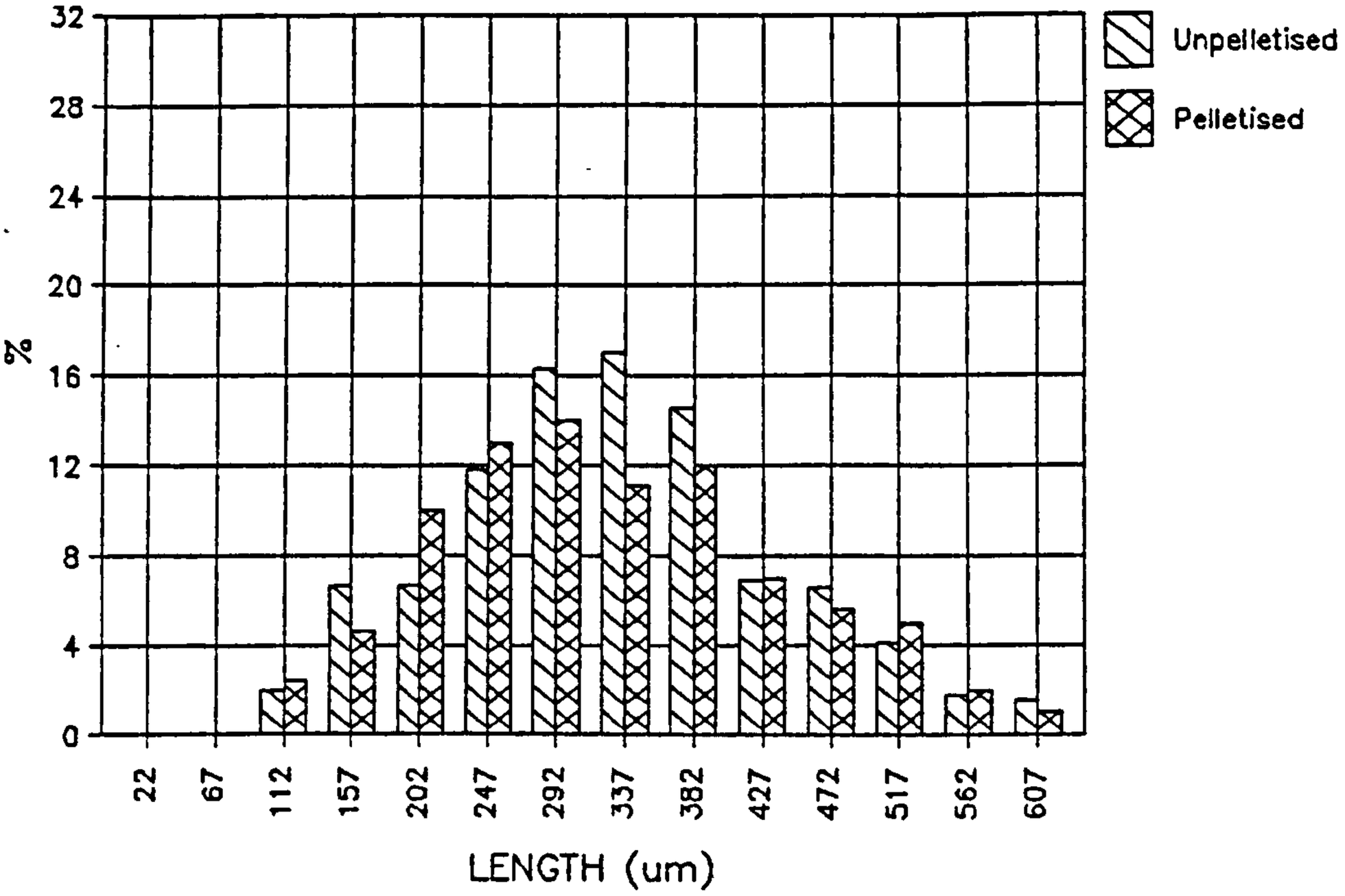

Figure 69

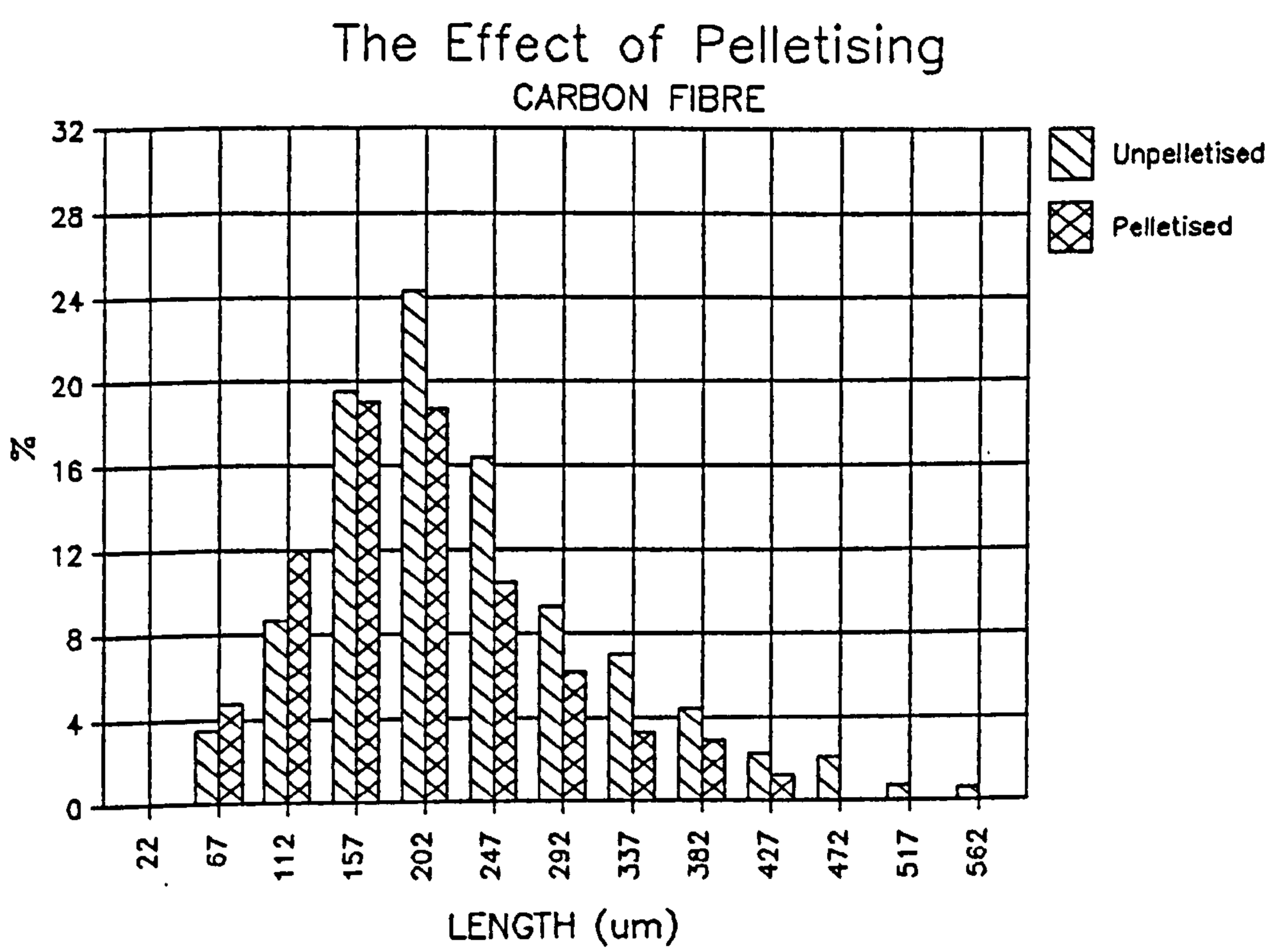

Figure 70

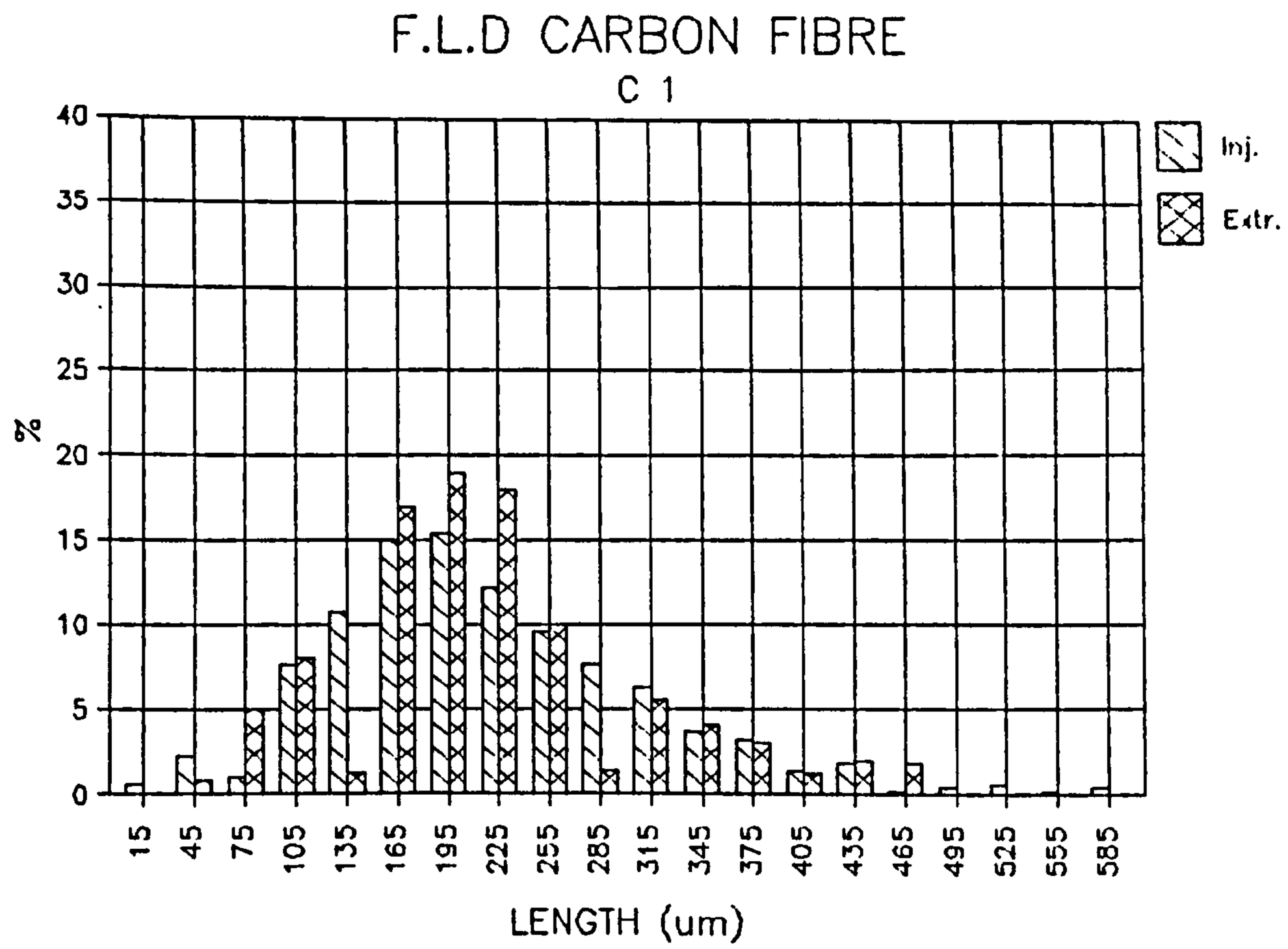

Figure 71

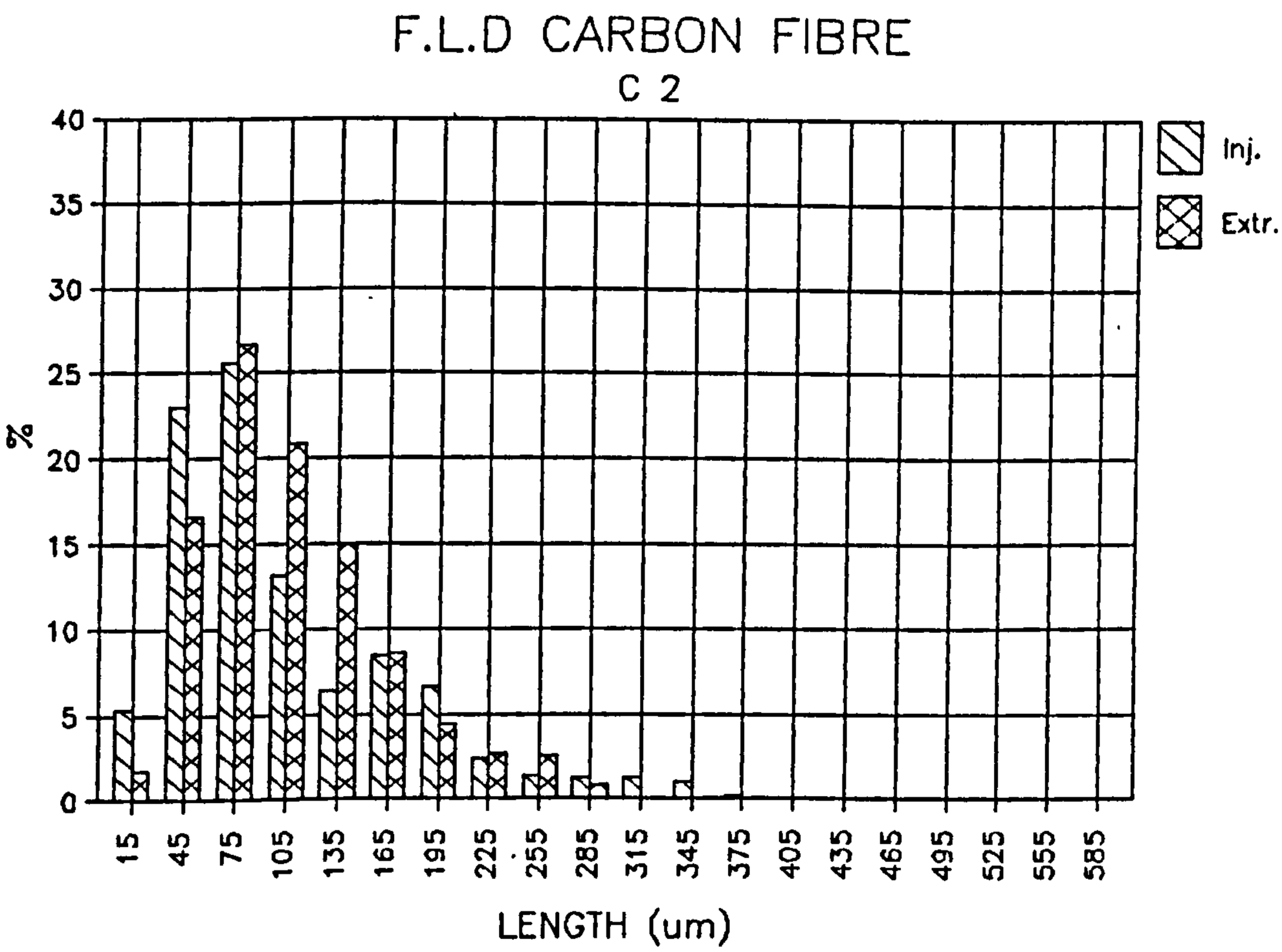

Figure 72

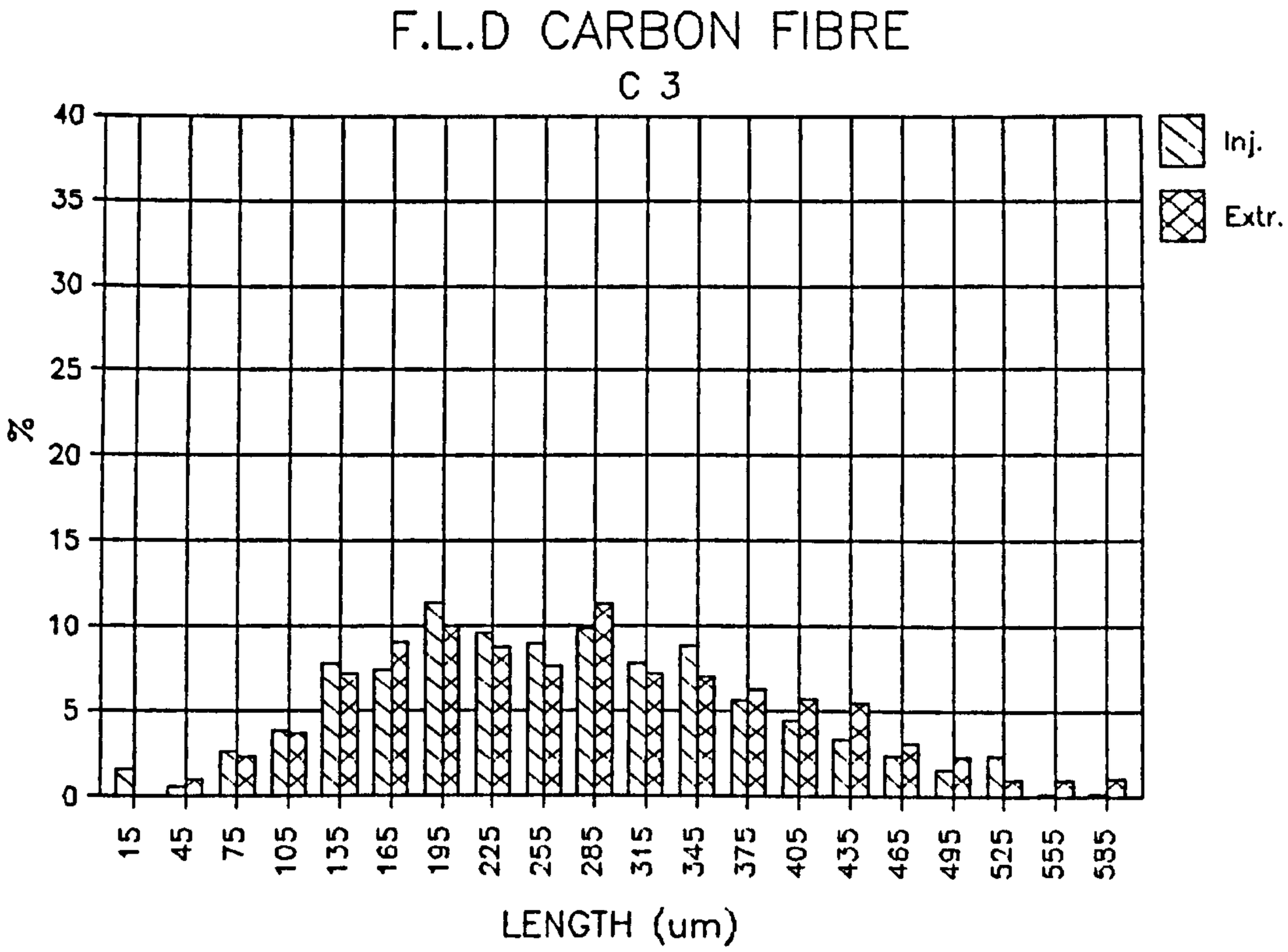

Figure 73

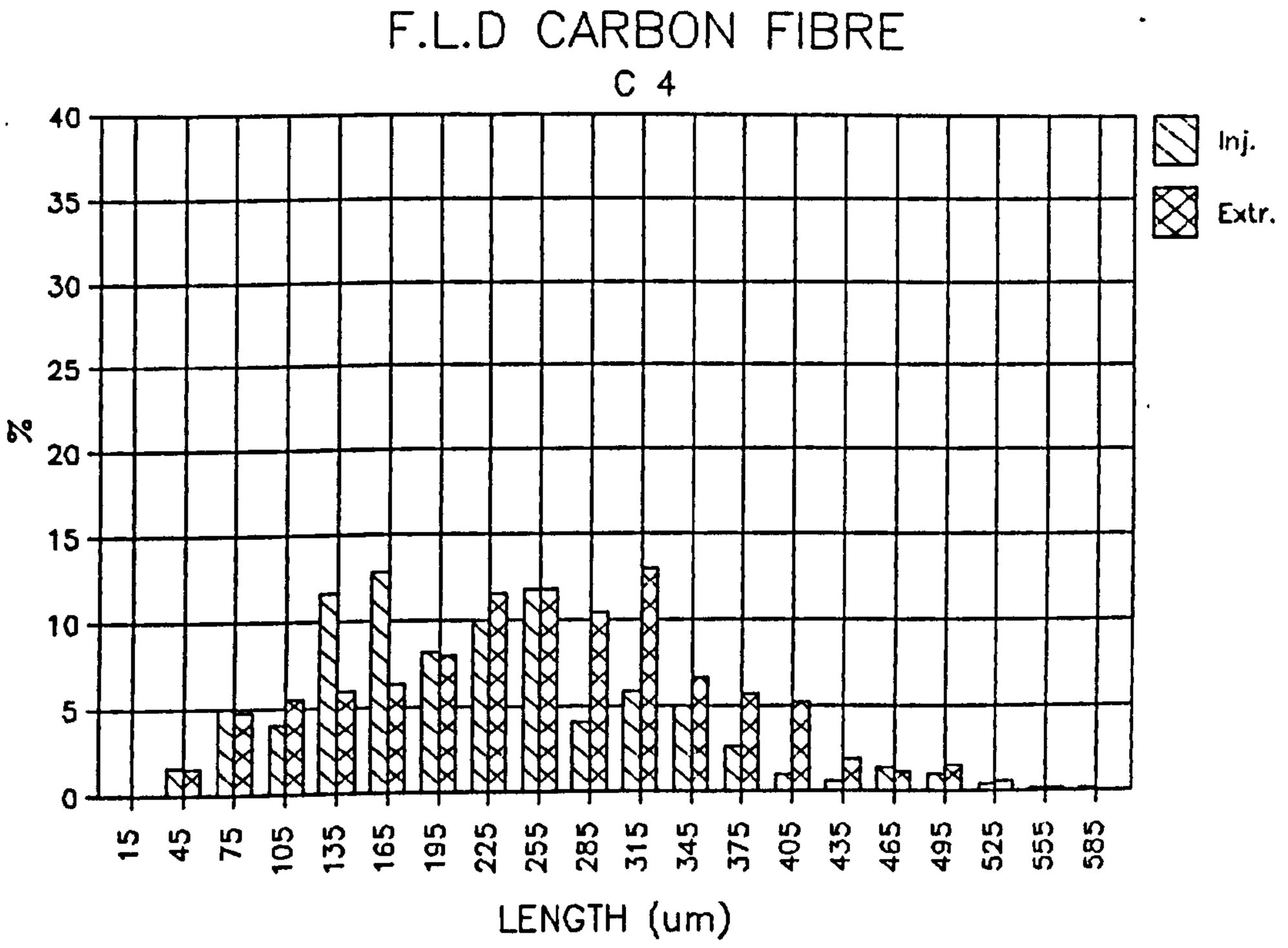

Figure 74

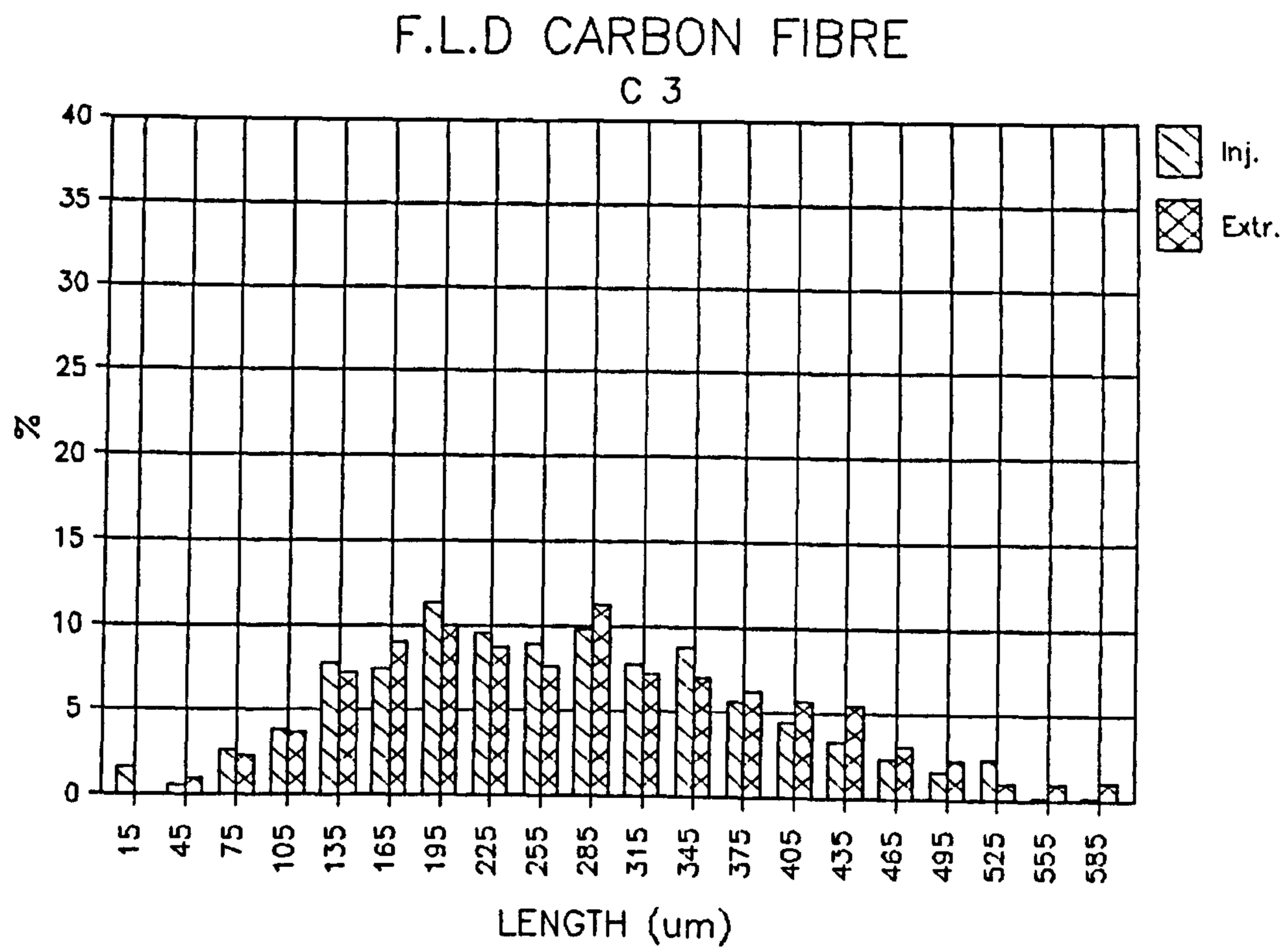

Figure 75

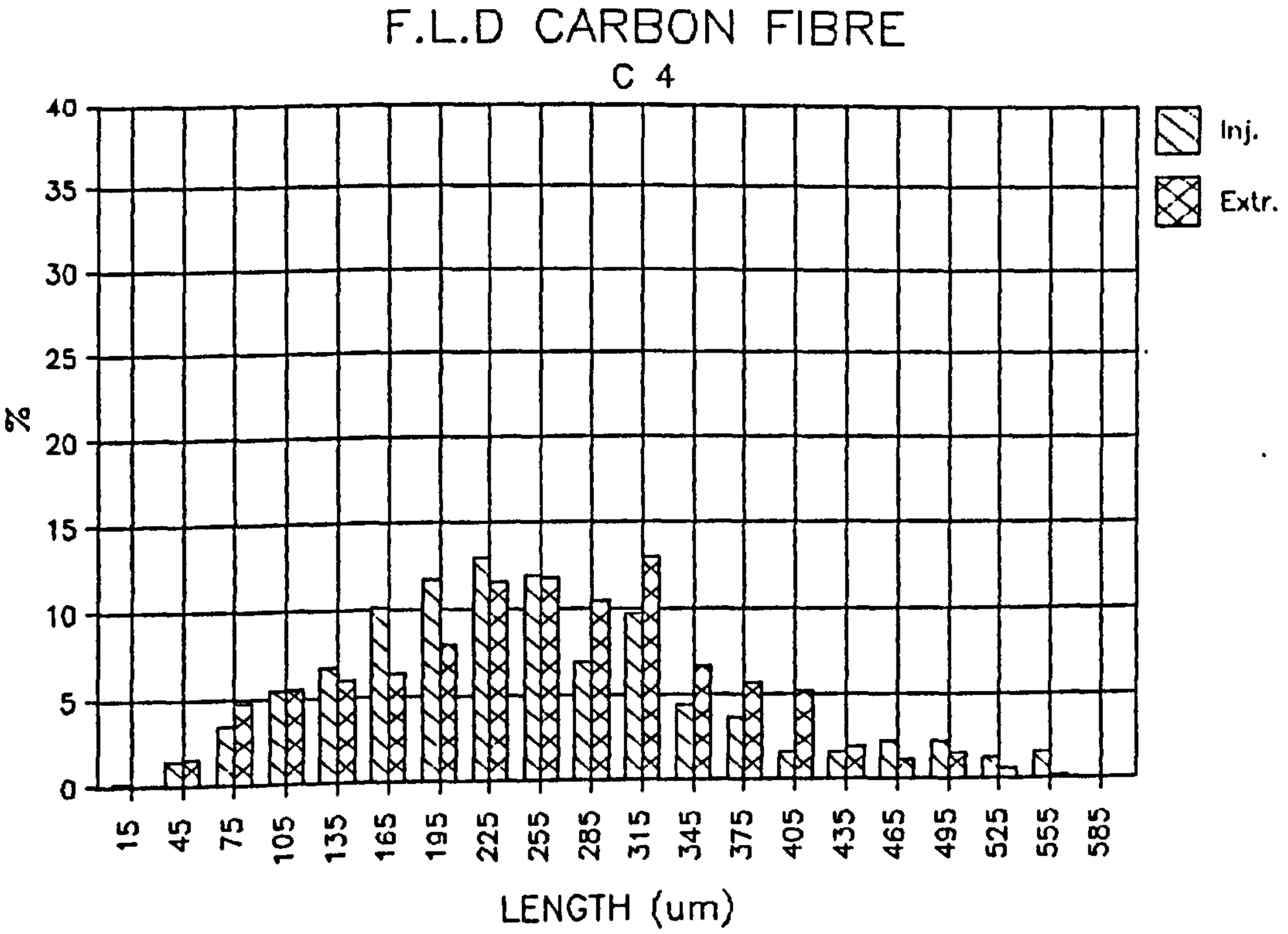

Figure 76

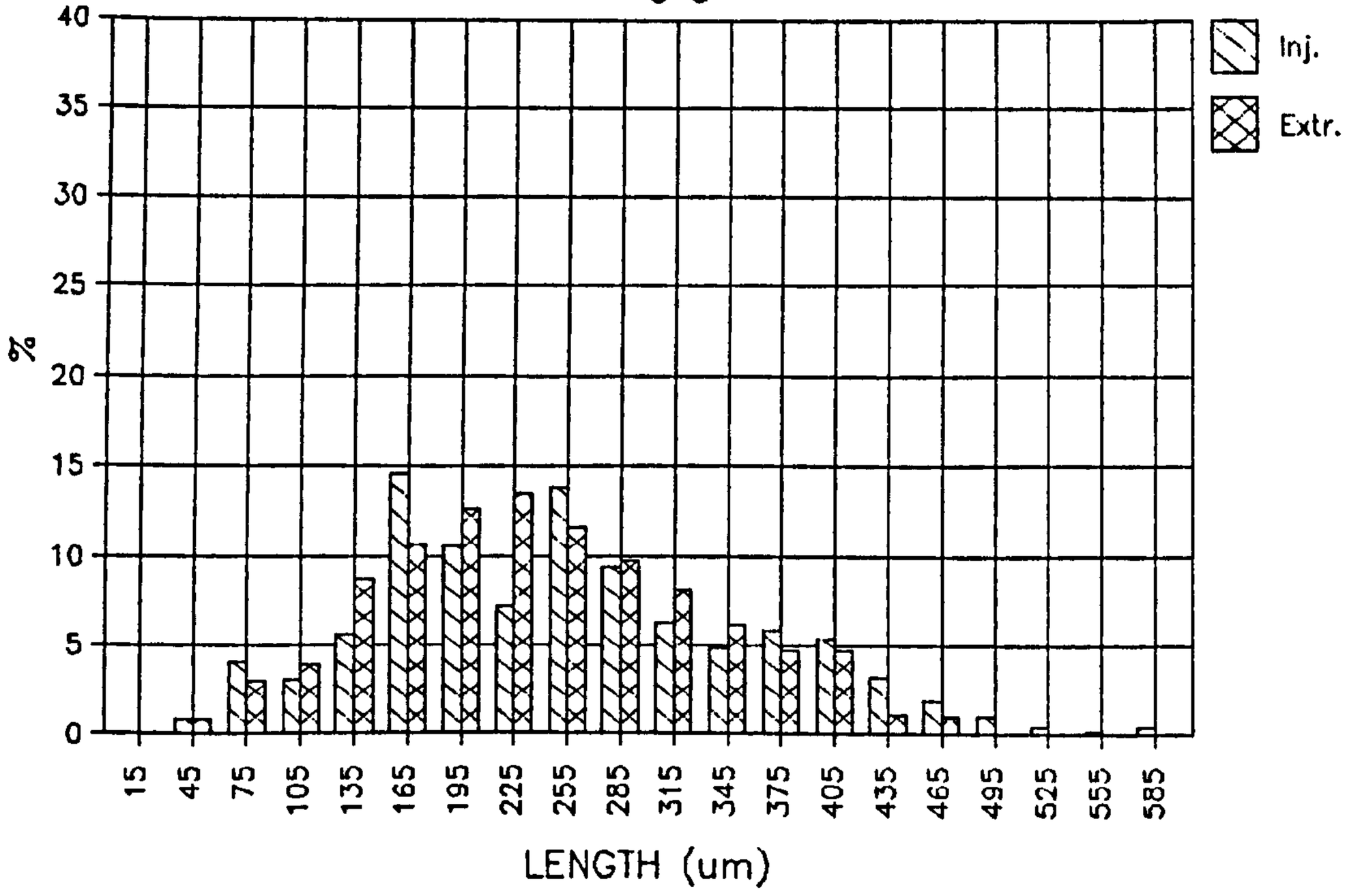

Figure 77

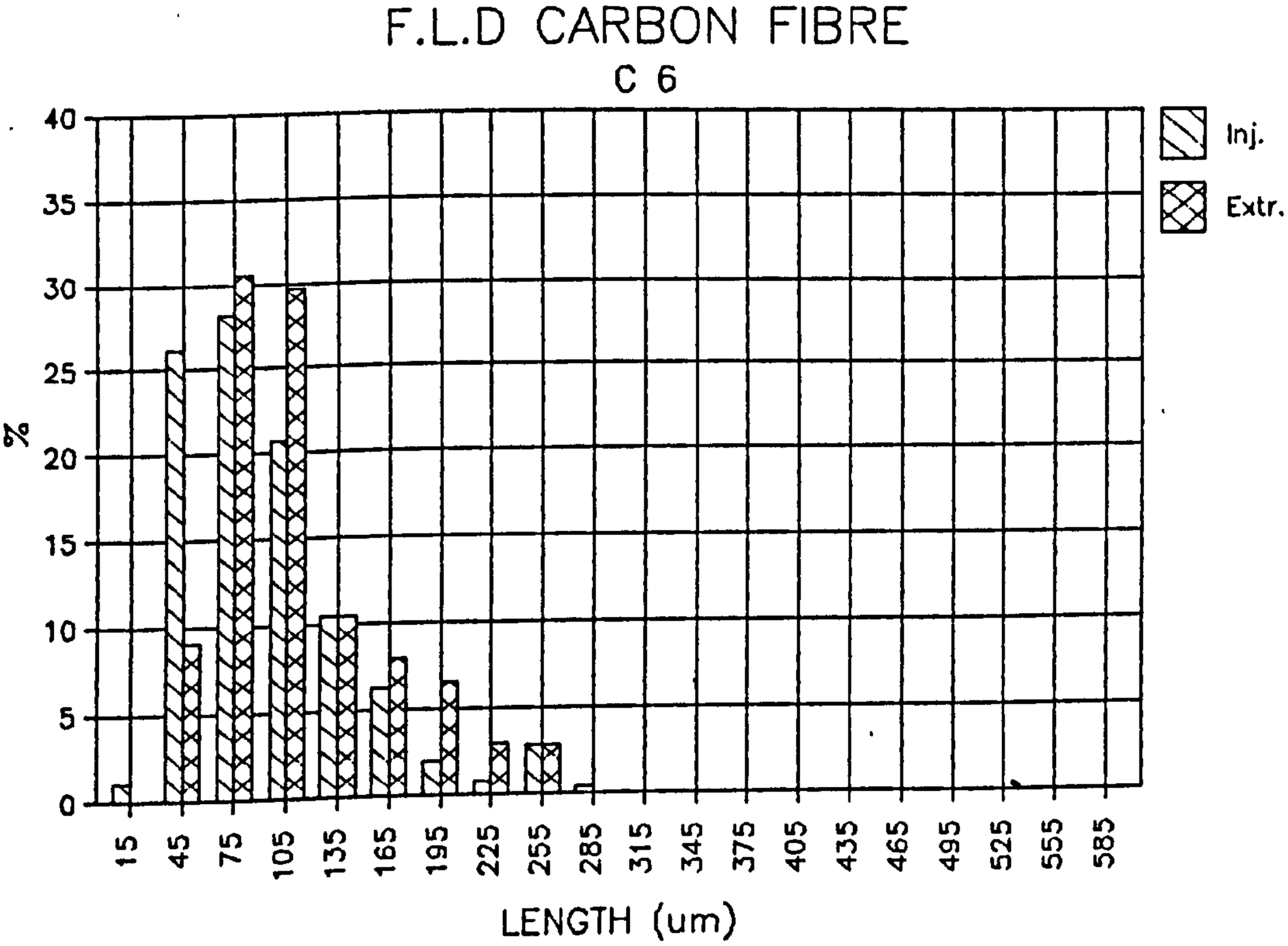

Figure 78

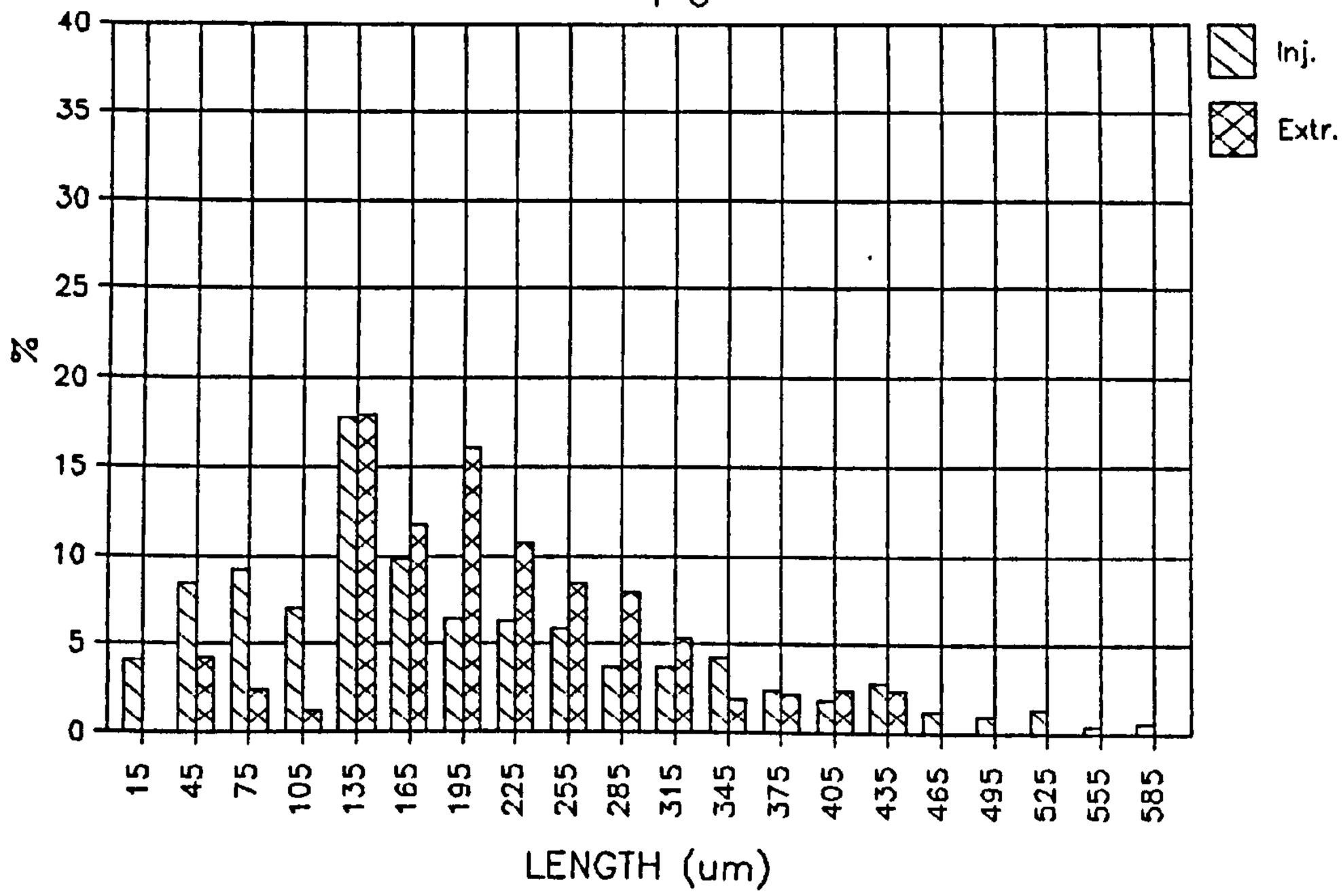

Figure 79

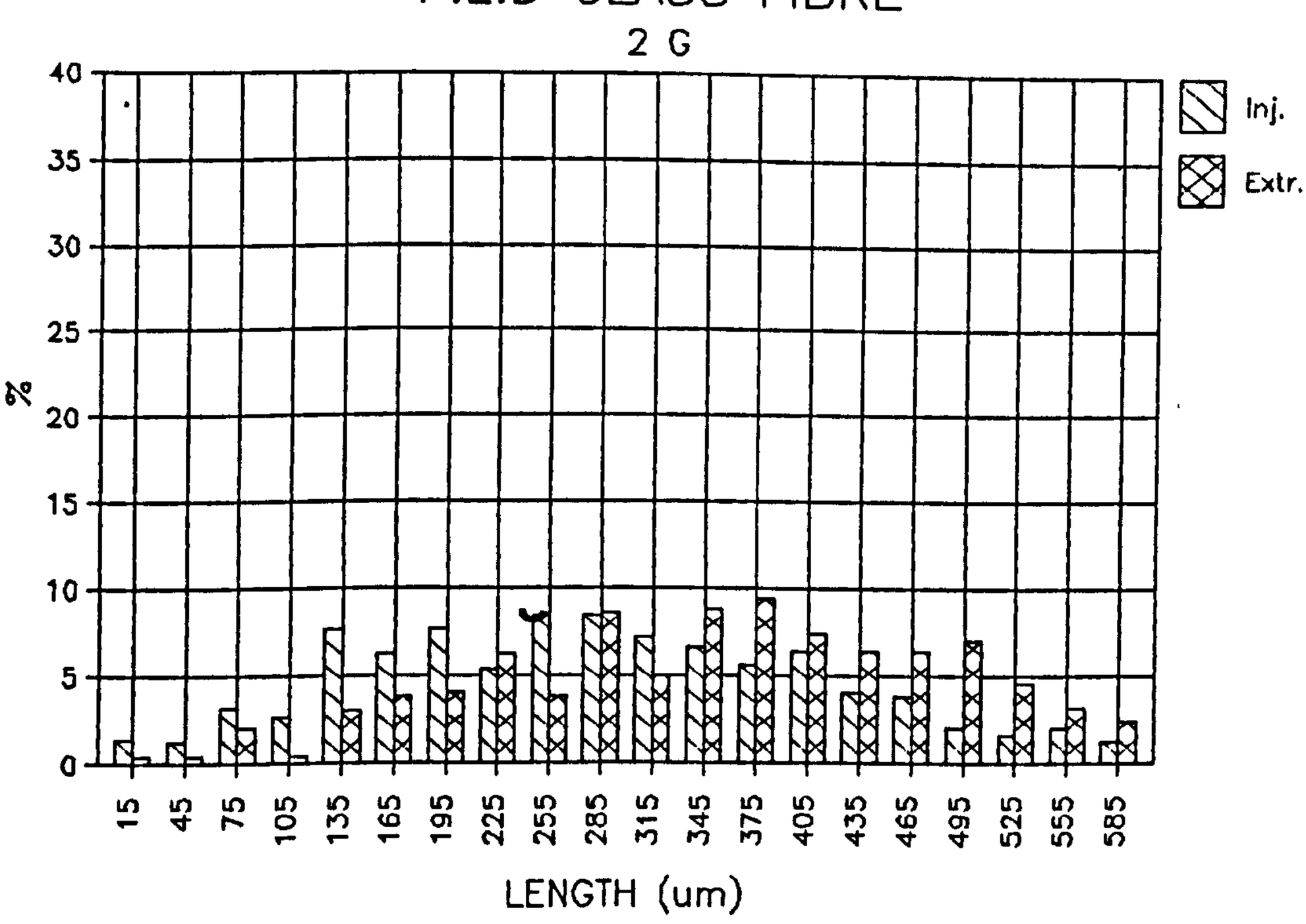

Figure 80

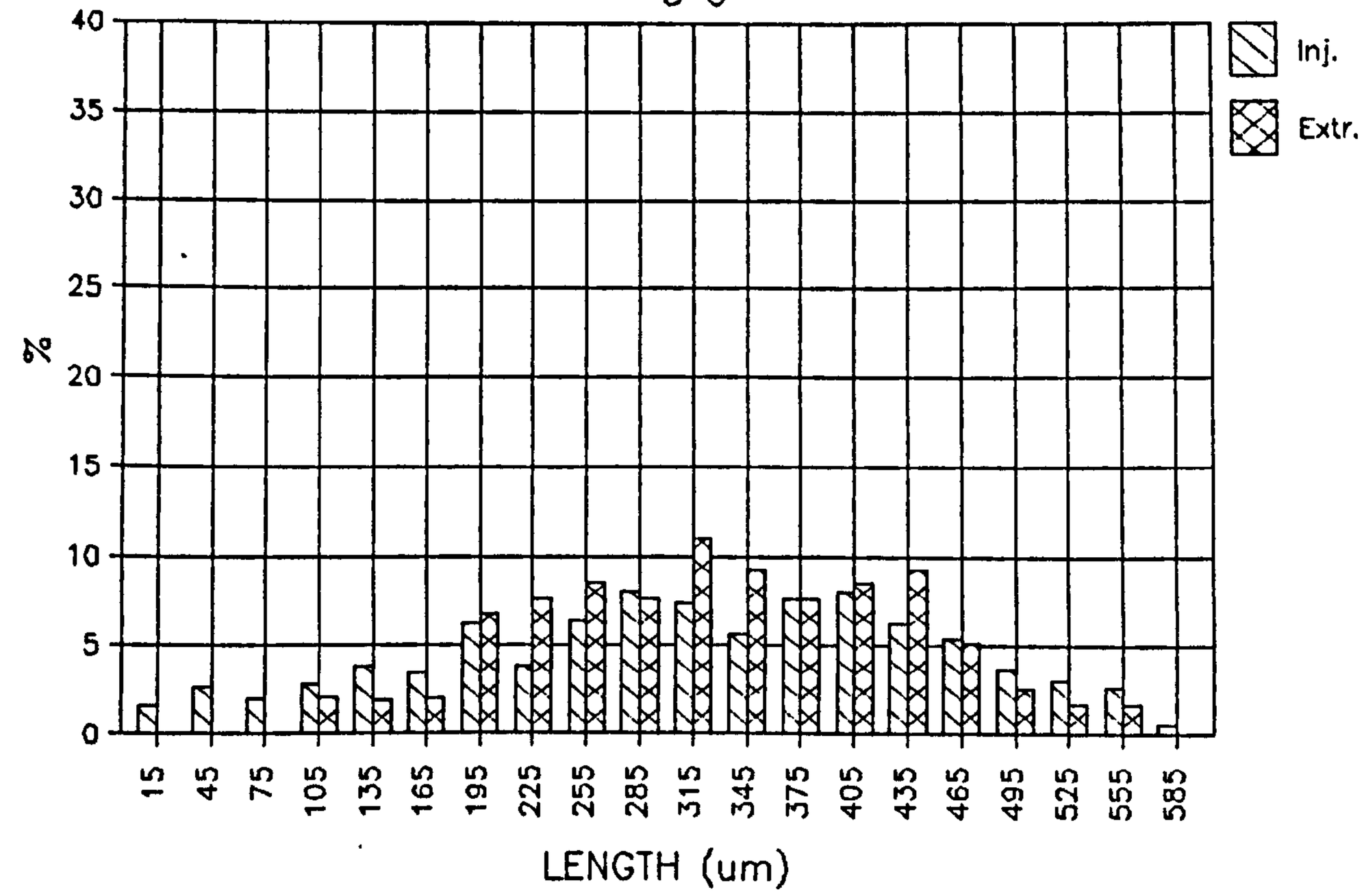

Figure 81

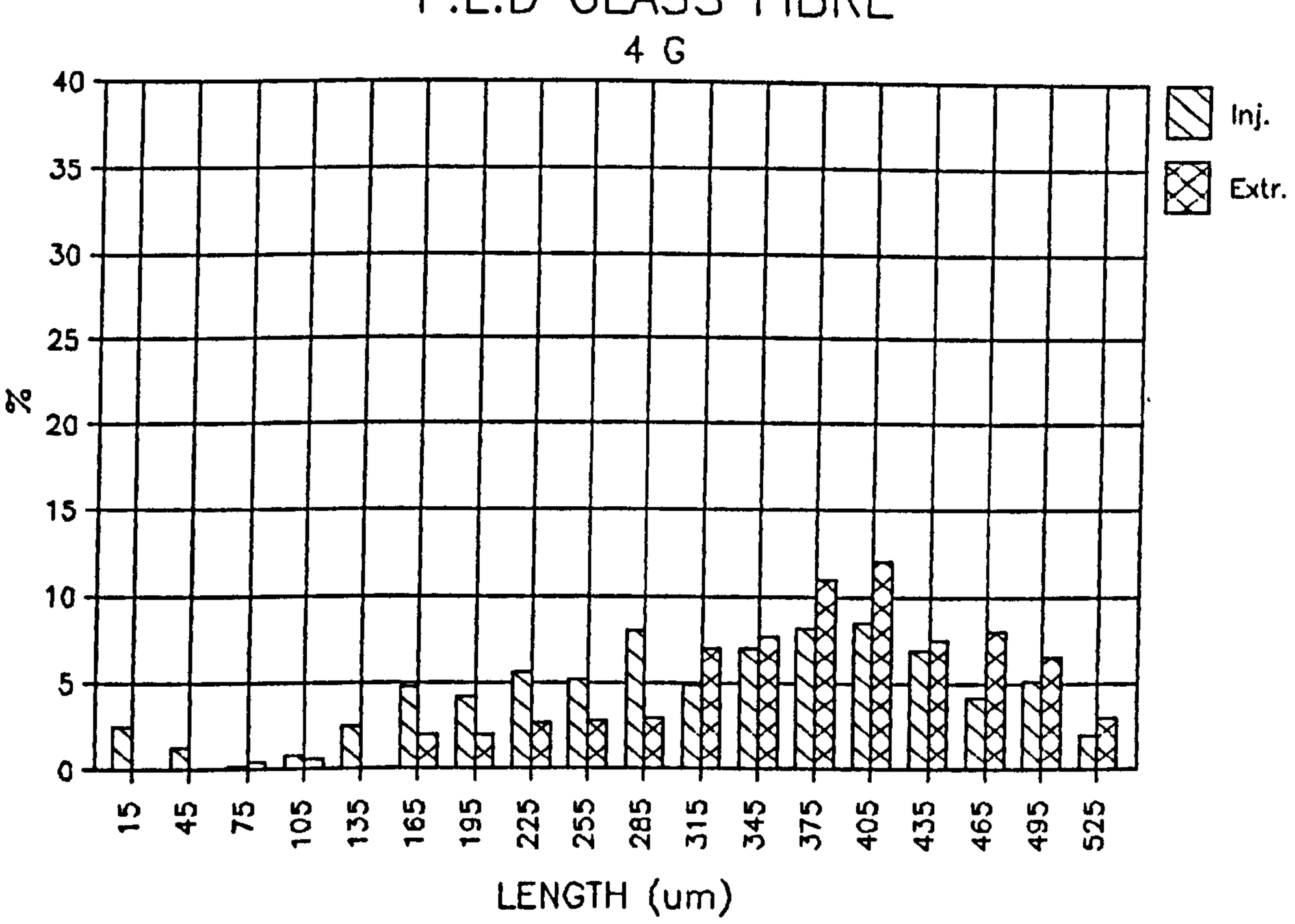

Figure 82

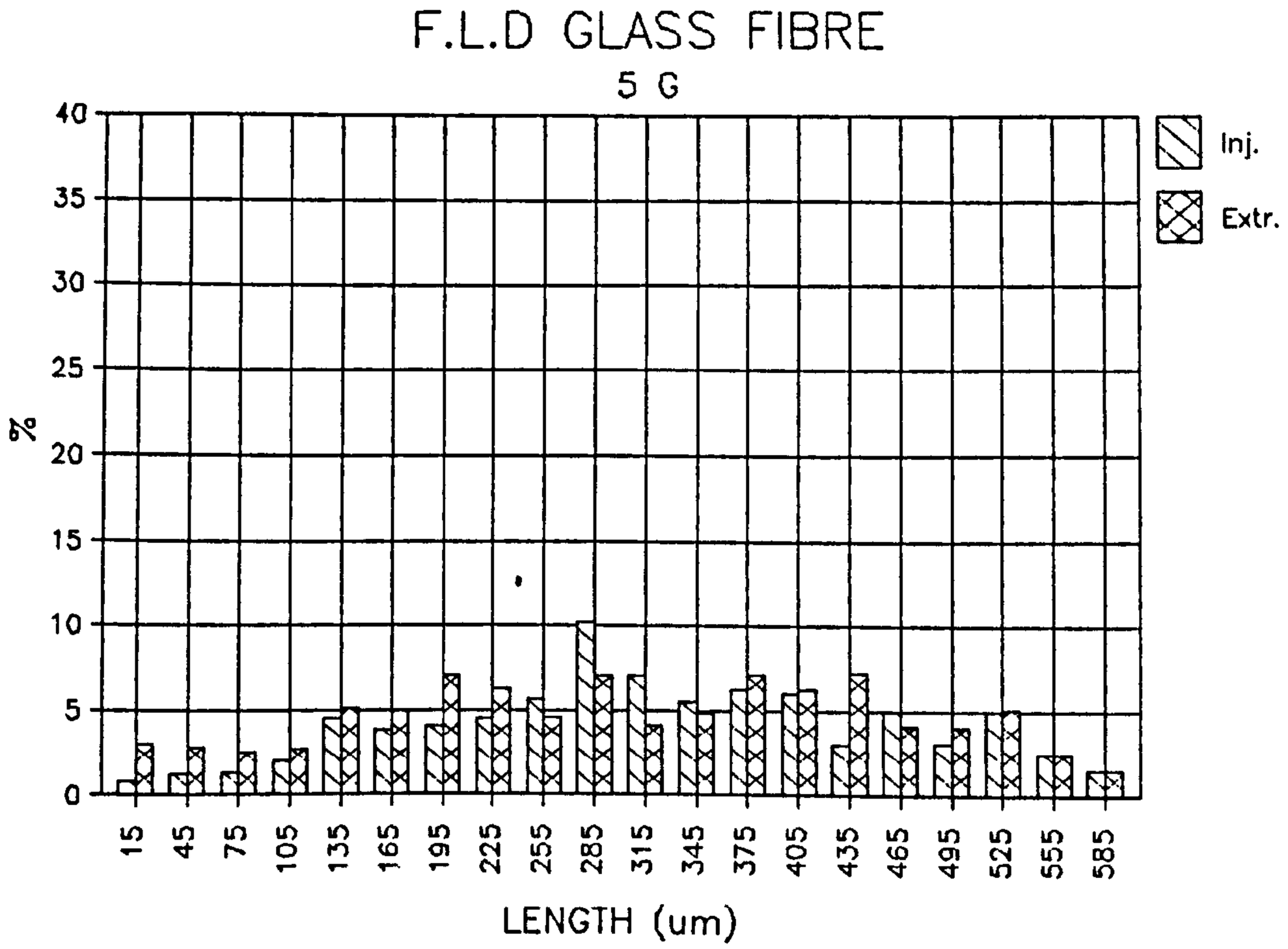

Figure 83

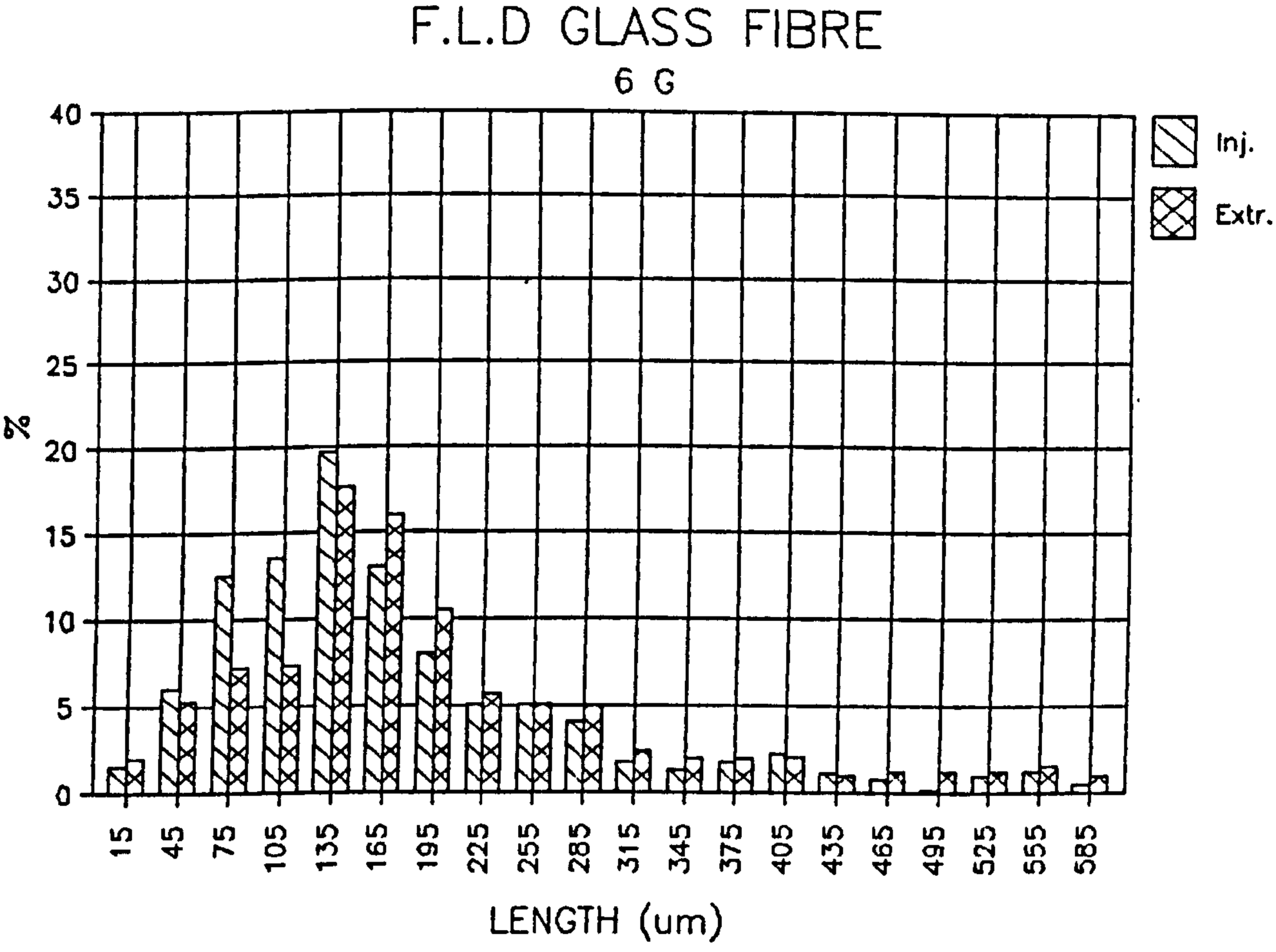

Figure 84

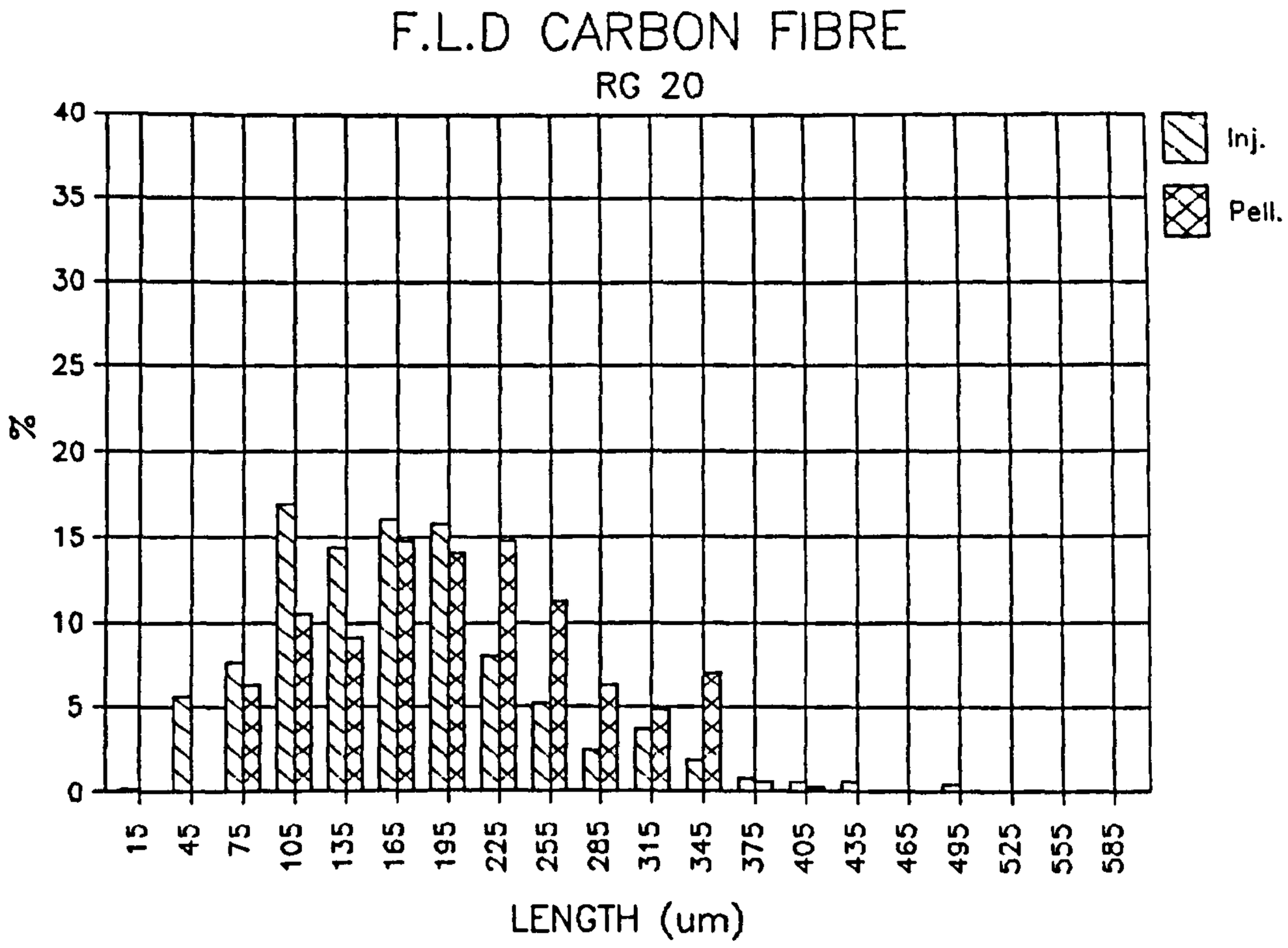
F.L.D CARBON FIBRE
RG 20
40
35
30
25
20
15
10
5
0
%
Inj.
Pell.
15
45
75
105
135
165
195
225
255
285
315
345
375
405
435
465
495
525
555
585
LENGTH (um)

Figure 85

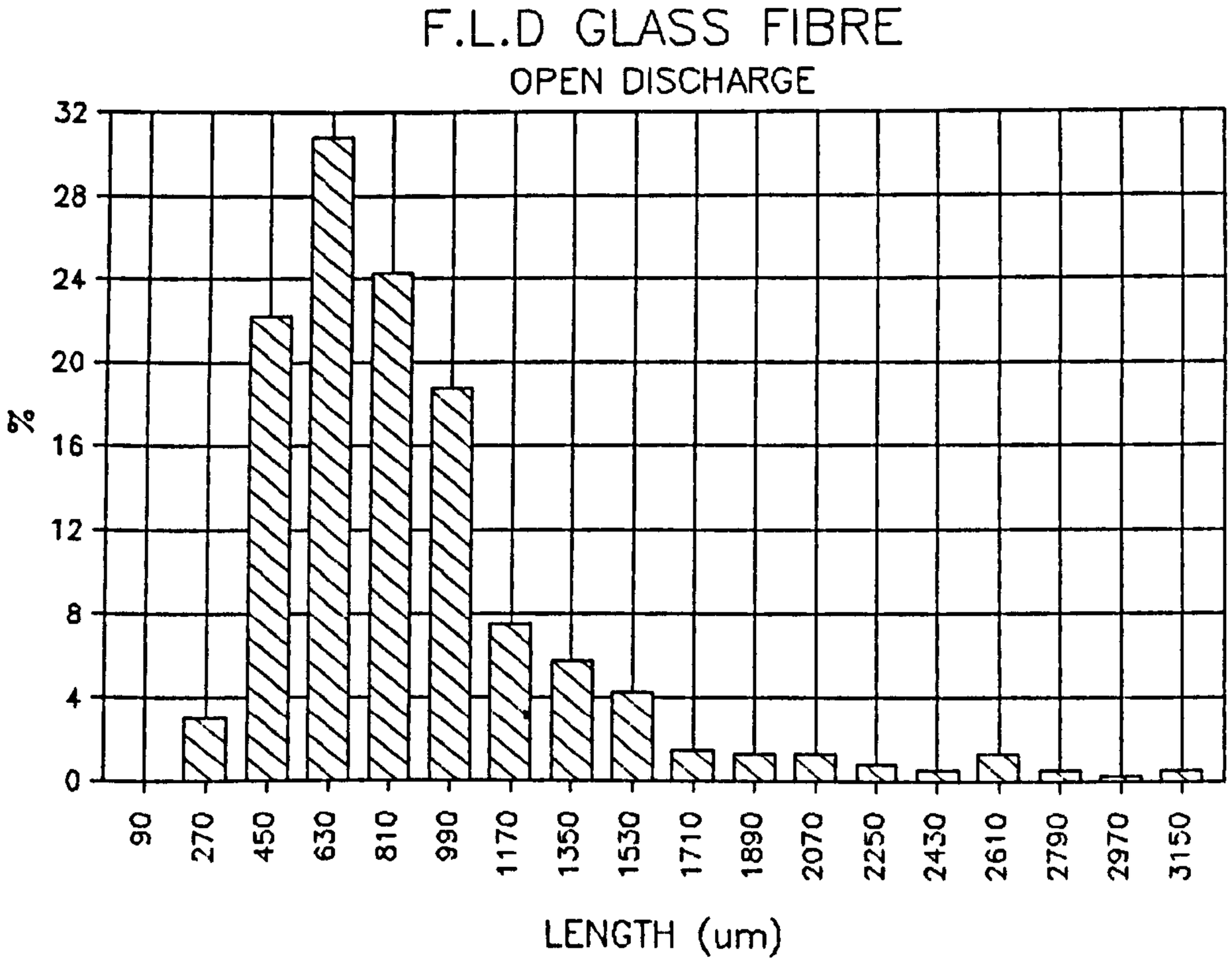
F.L.D GLASS FIBRE
OPEN DISCHARGE
%
32
28
24
20
16
12
8
4
0
90
270
450
630
810
990
1170
1350
1530
1710
1890
2070
2250
2430
2610
2790
2970
3150
LENGTH (um)

Figure 86

Screw profile used for experiment
BRITTLE 5

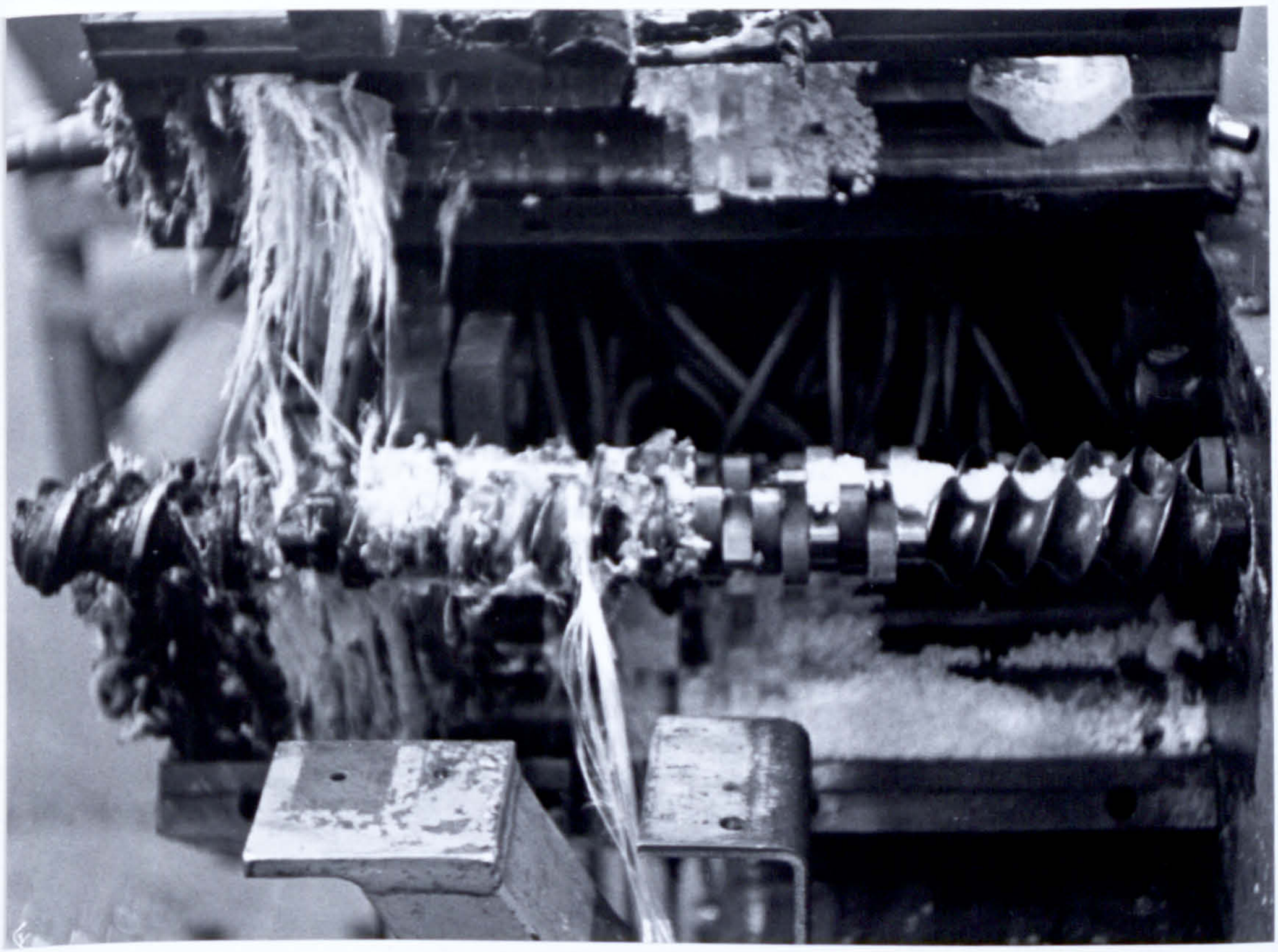

Figure 87

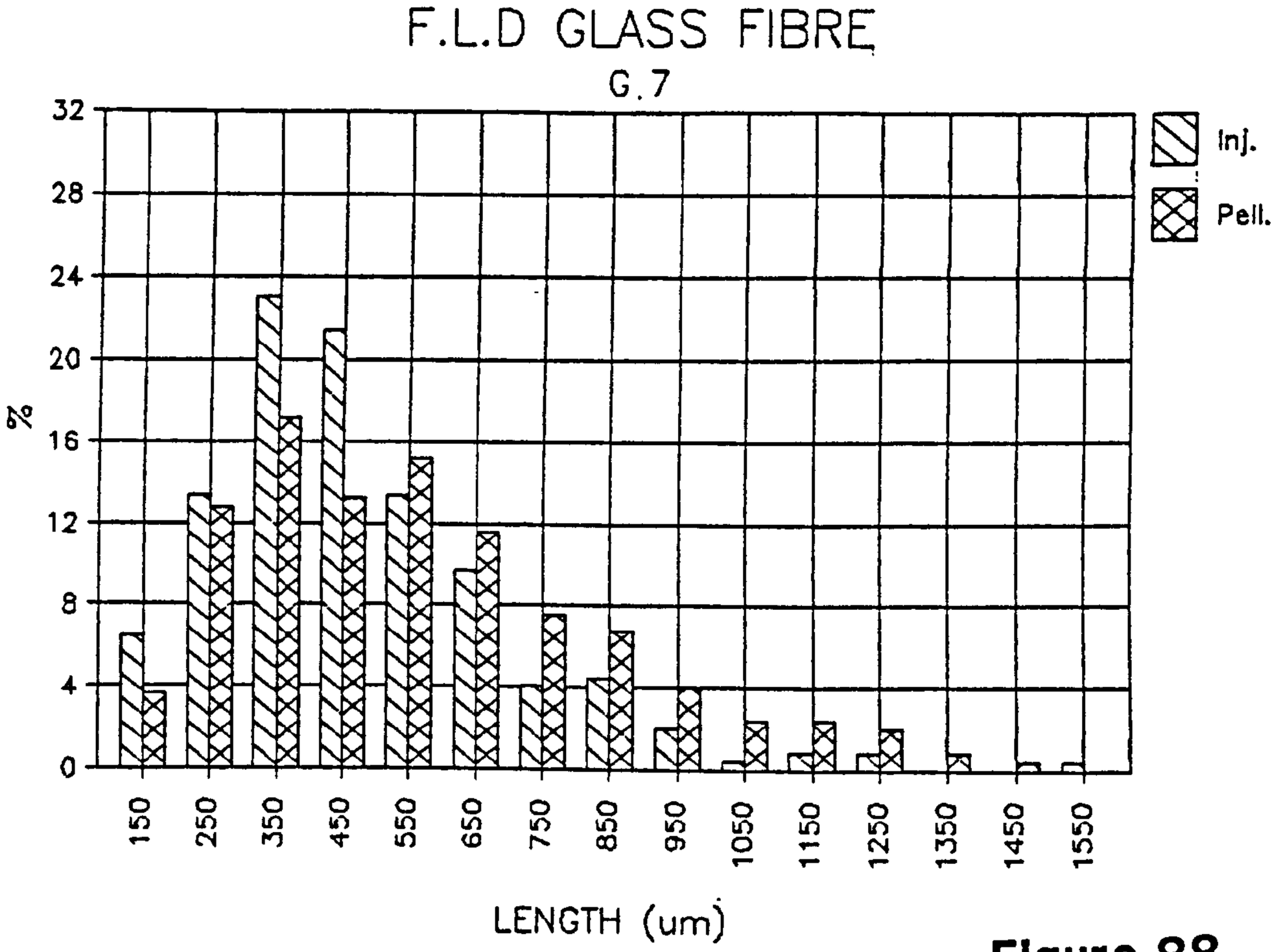
F.L.D GLASS FIBRE
G.7
Inj.
Pell.
%
32
28
24
20
16
12
8
4
0
150
250
350
450
550
650
750
850
950
1050
1150
1250
1350
1450
1550
LENGTH (um)

Figure 88

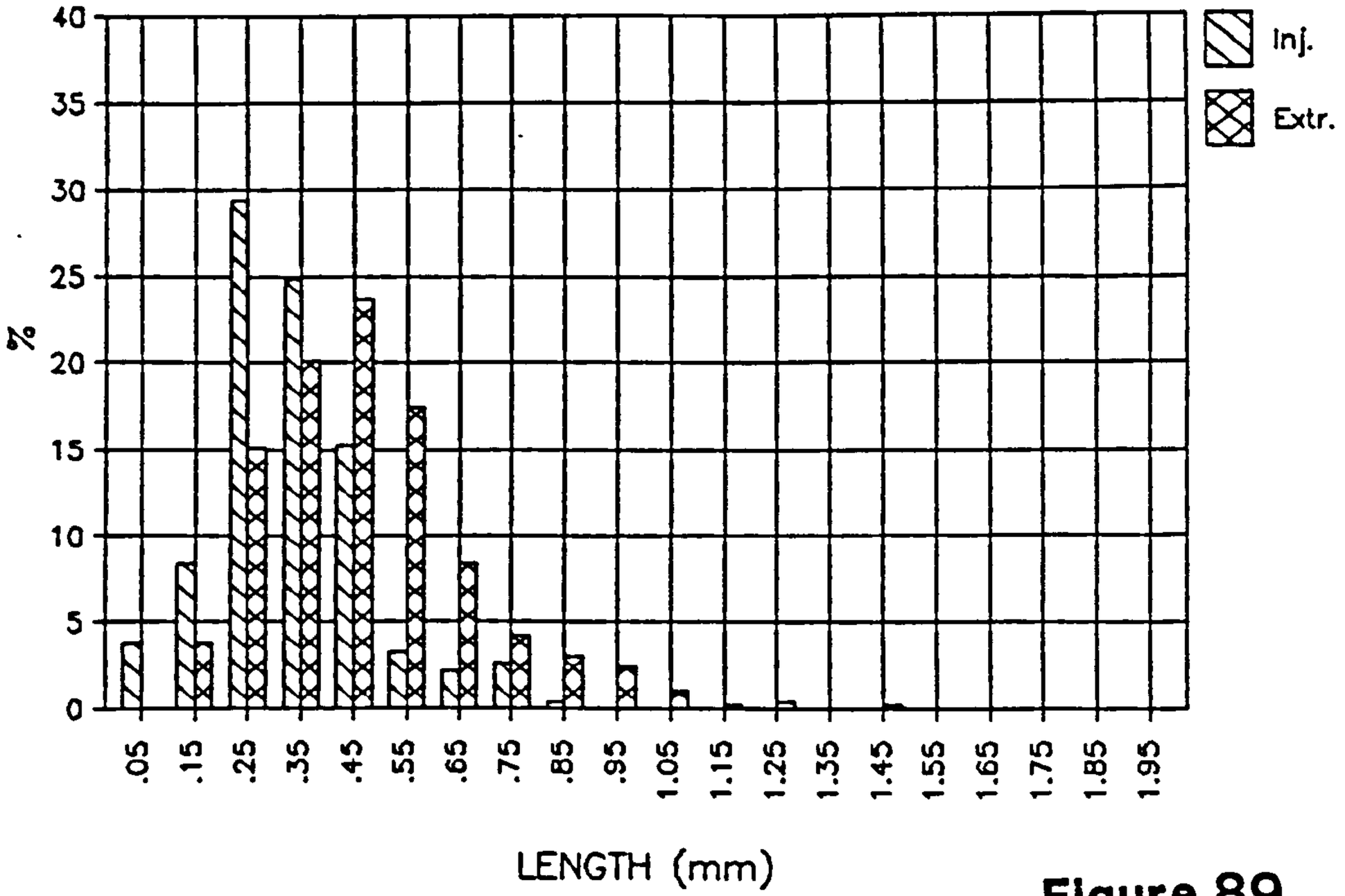

Figure 89

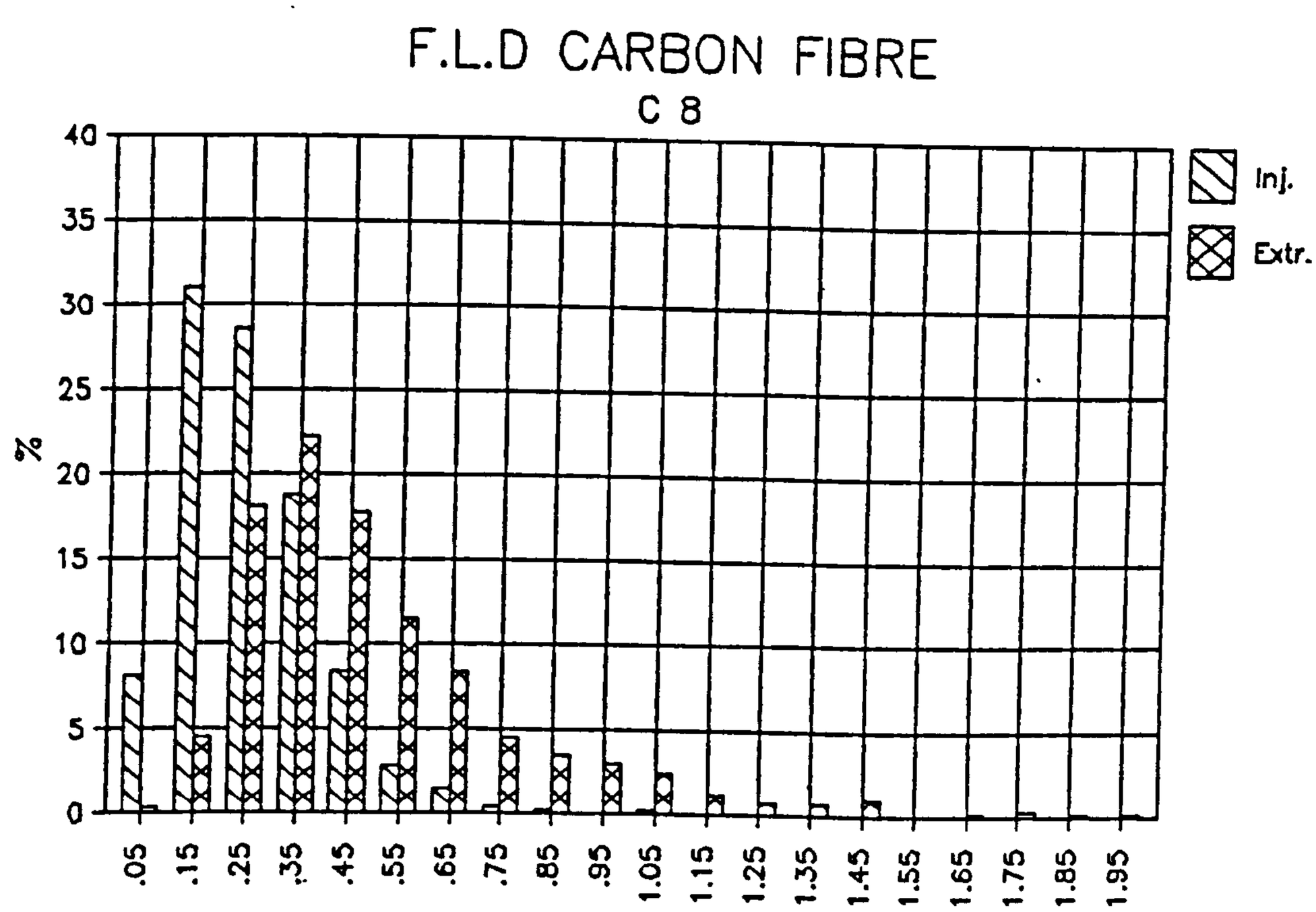

Figure 90

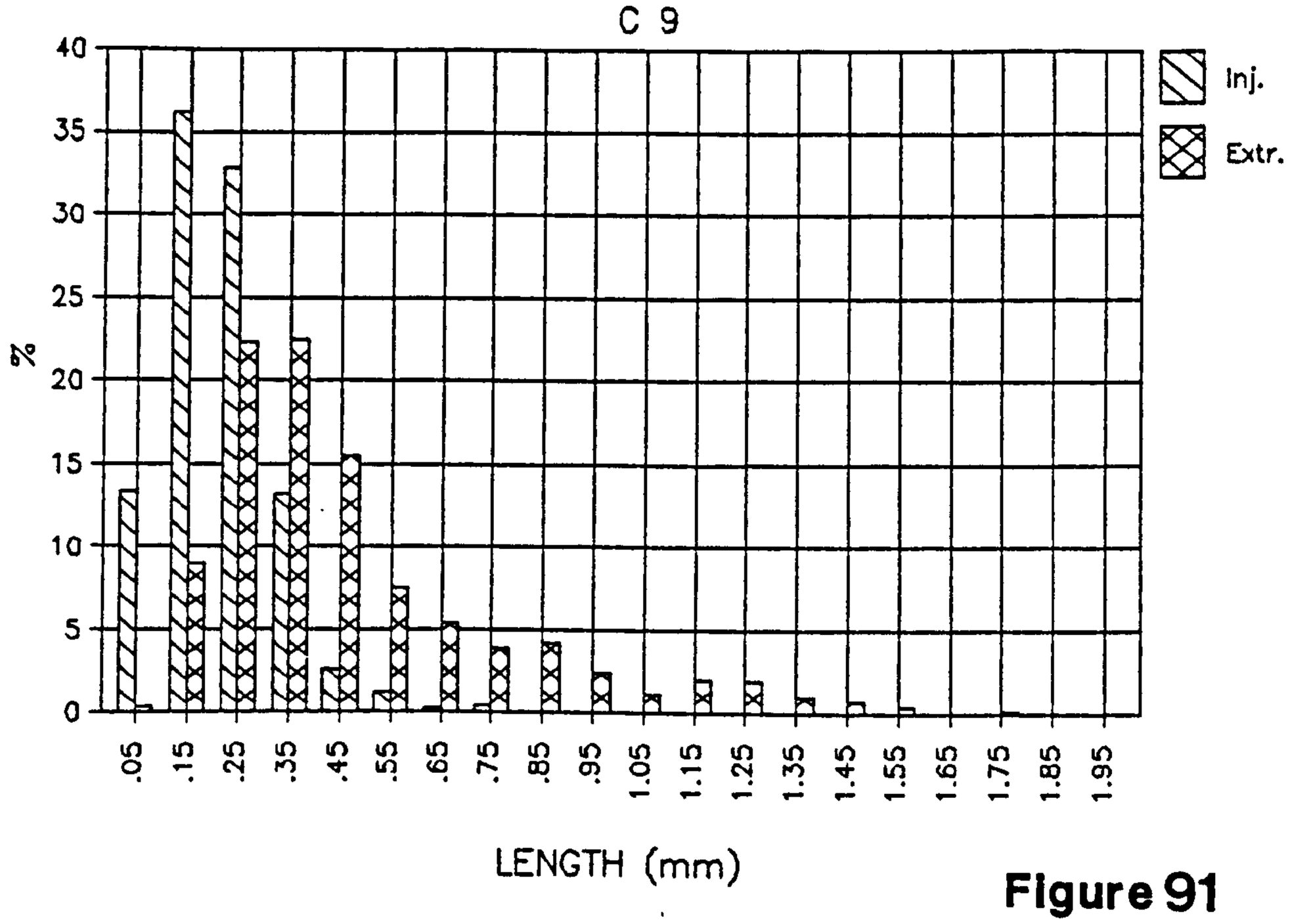

Figure 91

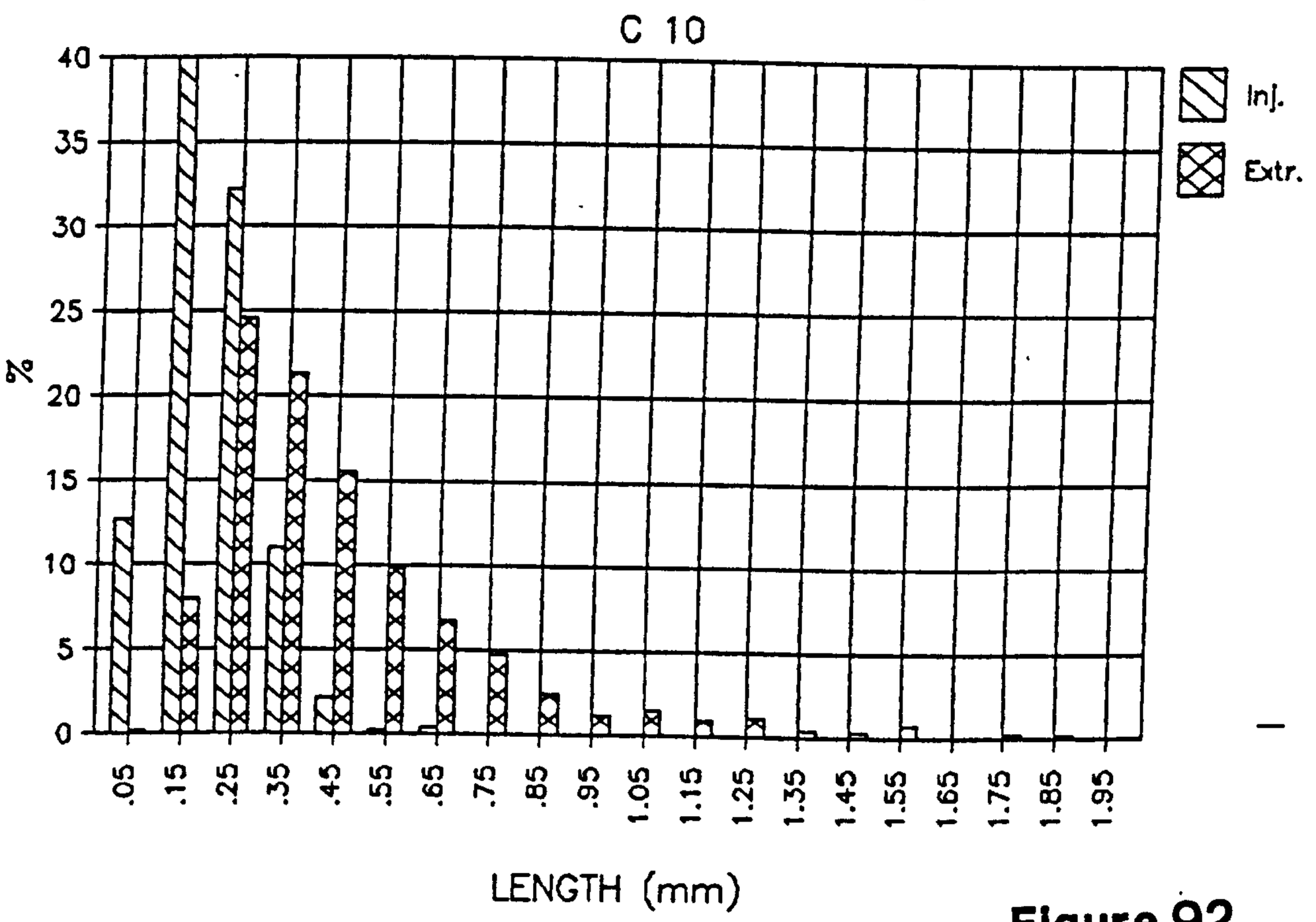

Figure 92

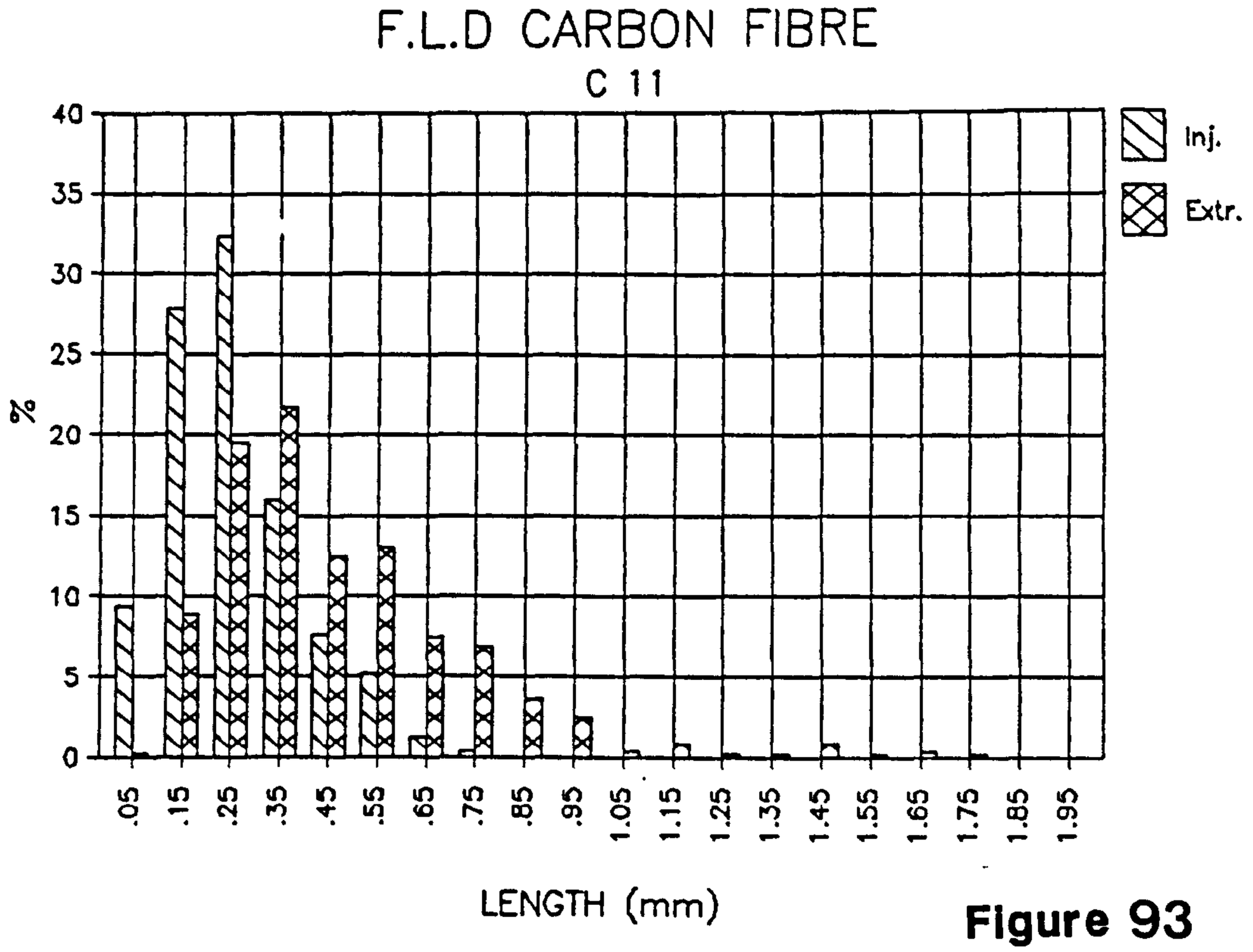

Figure 93

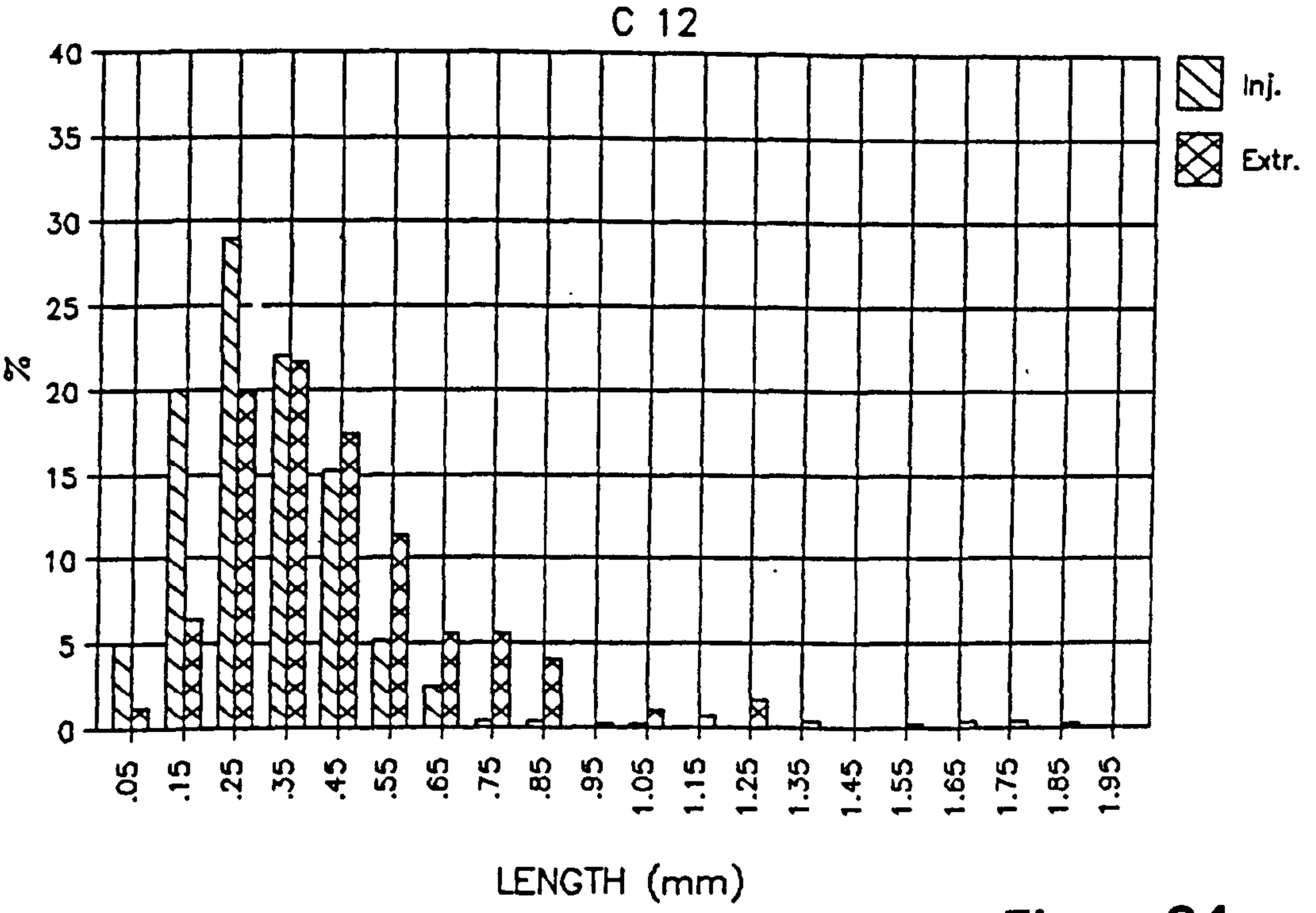

Figure 94

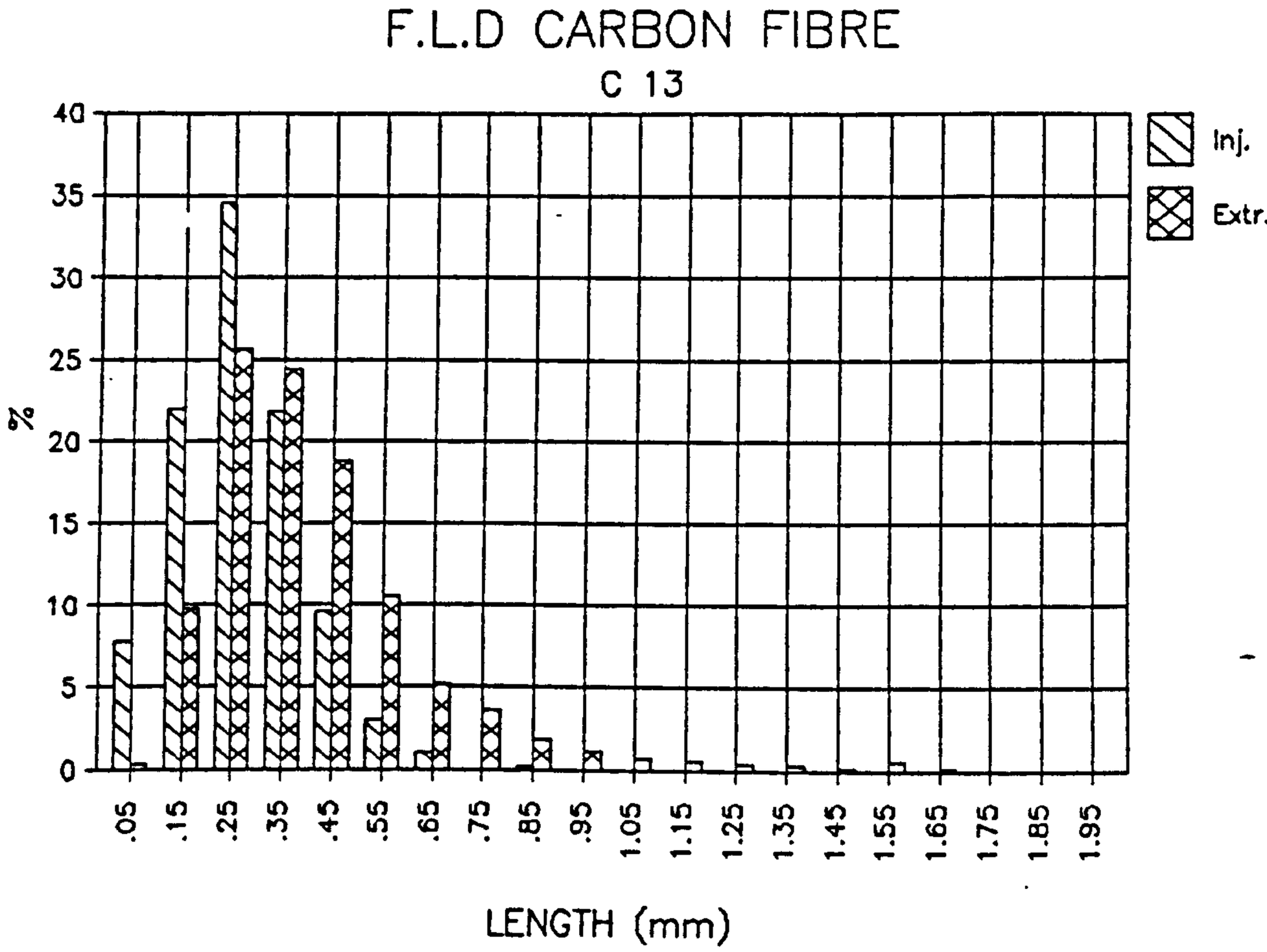
F.L.D CARBON FIBRE
C 13
40
35
30
25
20
15
10
5
0
%
Inj.
Extr.
.05
.15
.25
.35
.45
.55
.65
.75
.85
.95
1.05
1.15
1.25
1.35
1.45
1.55
1.65
1.75
1.85
1.95
LENGTH (mm)

Figure 95

Experiment BRITTLE 6. Influence of fibre content on average fibre length in extrudate and injection mouldings

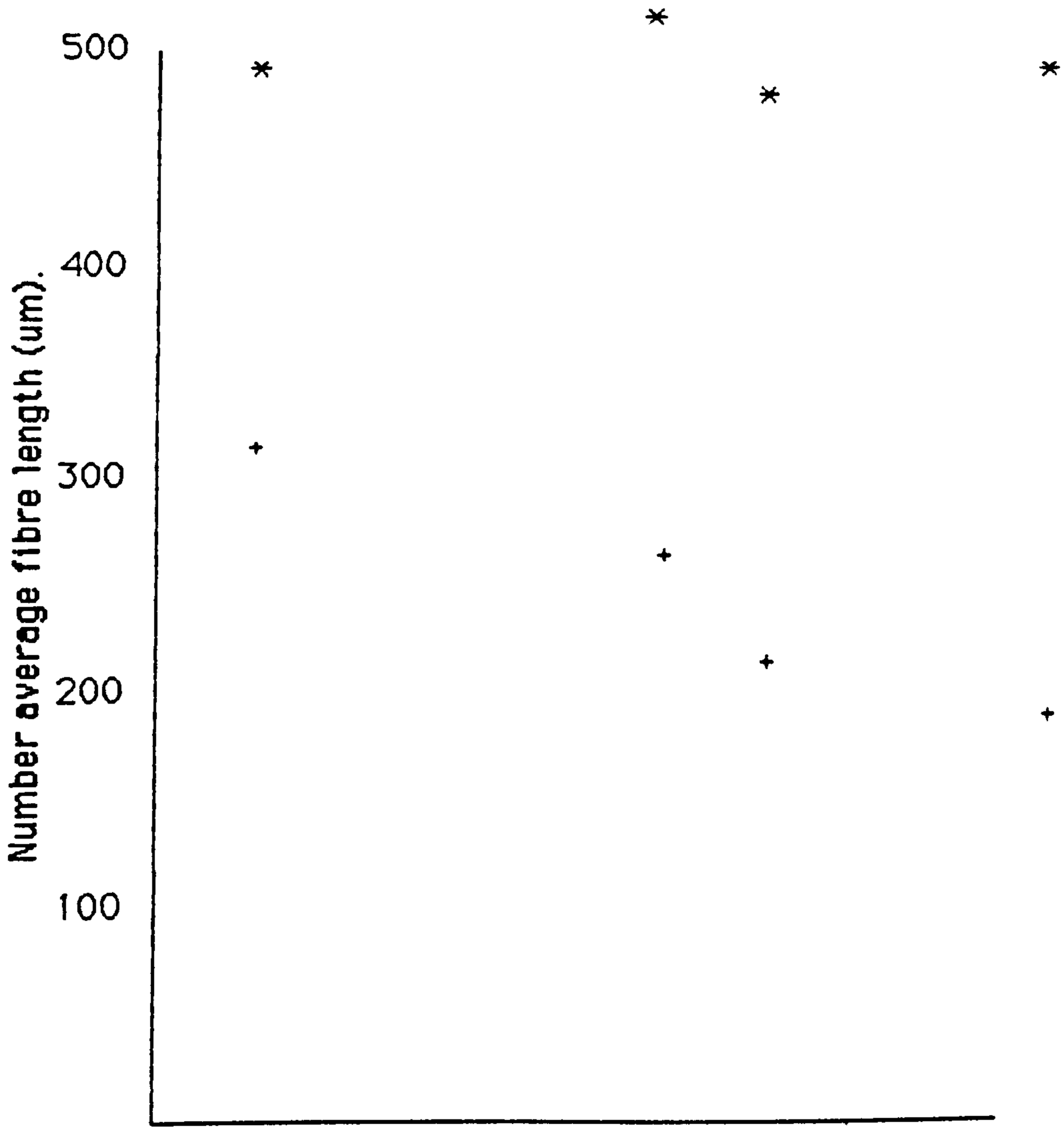

Figure 96

Experiment BRITTLE 6. Influence of screw speed on average fiber length in extrudate

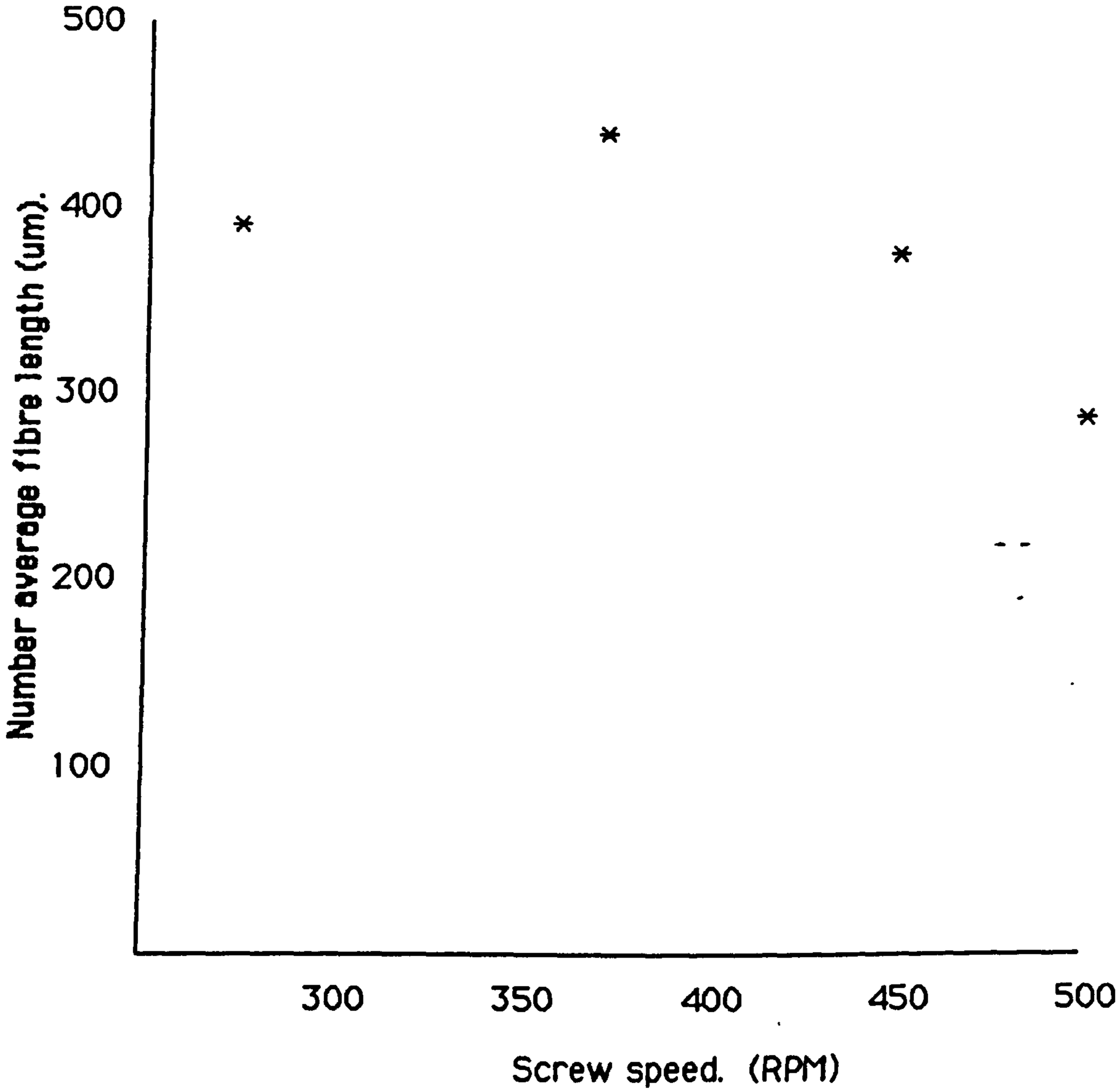

(Volume fraction between 0.0555 and 0.0750)

Figure 97

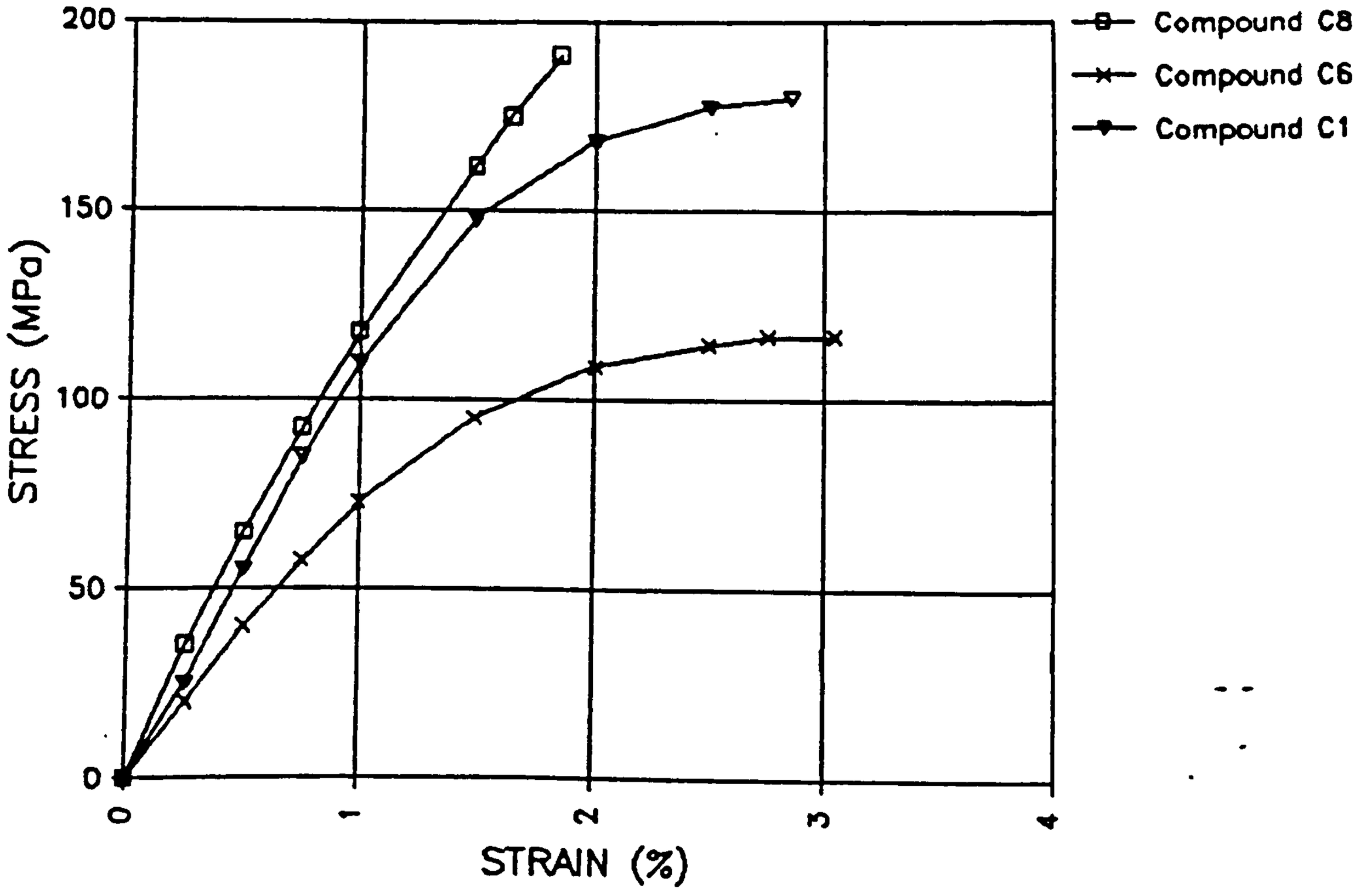

Figure 98

	Fibre Length	
	Number Average (mm)	Weight Average (mm)
Compound C8	0.502	0.670
Compound C6	0.101	0.134
Compound C1	0.246	0.289

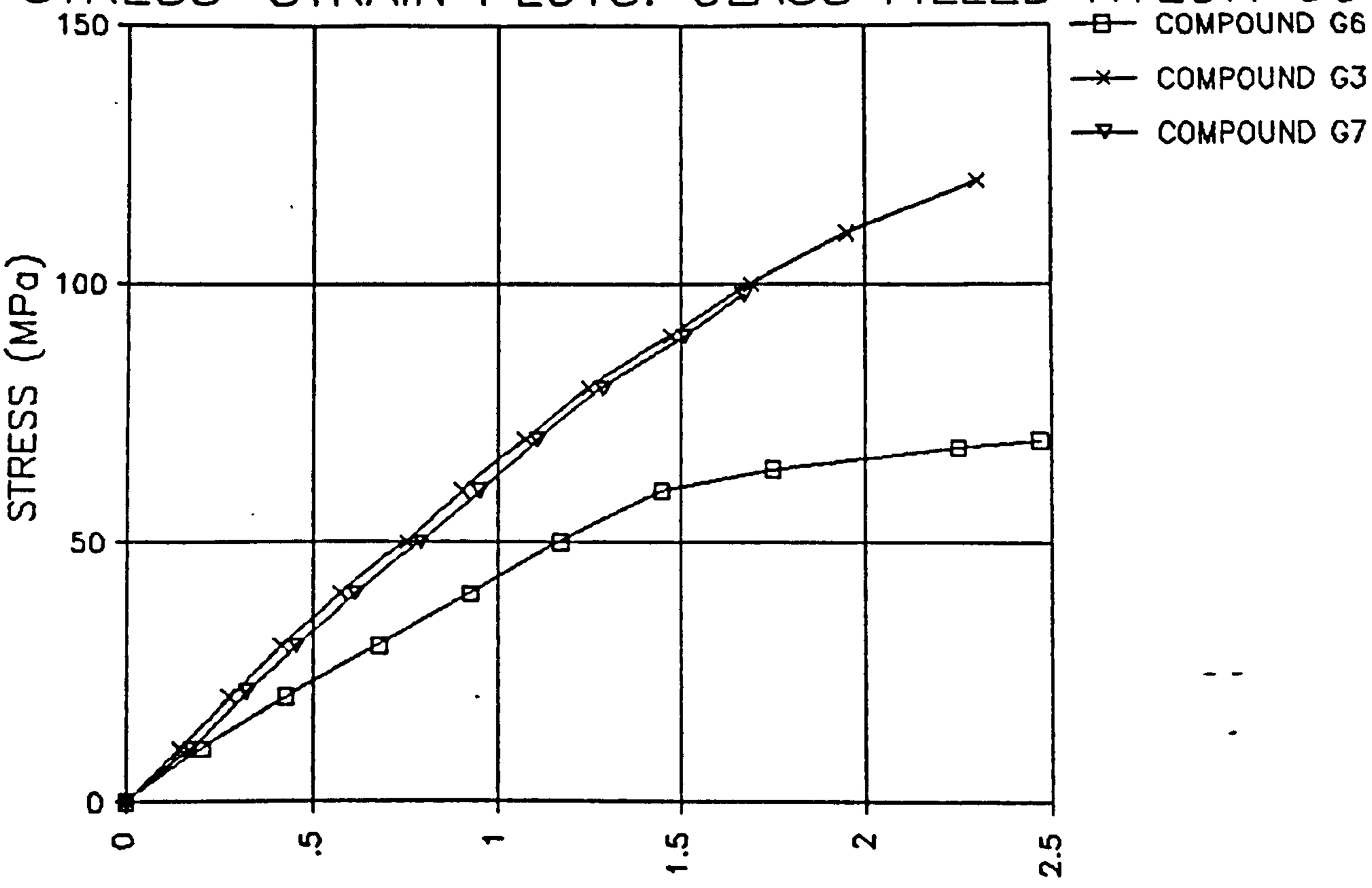
STRESS-STRAIN PLOTS. GLASS FILLED NYLON 66
COMPOUND G6
COMPOUND G3
COMPOUND G7
STRESS (MPa)
150
100
50
0
0
.5
1
1.5
2
2.5
STRAIN (%)

Figure 99

The influence of fibre length on orientation ratio of glass and carbon fibre reinforced nylon 66 compounds

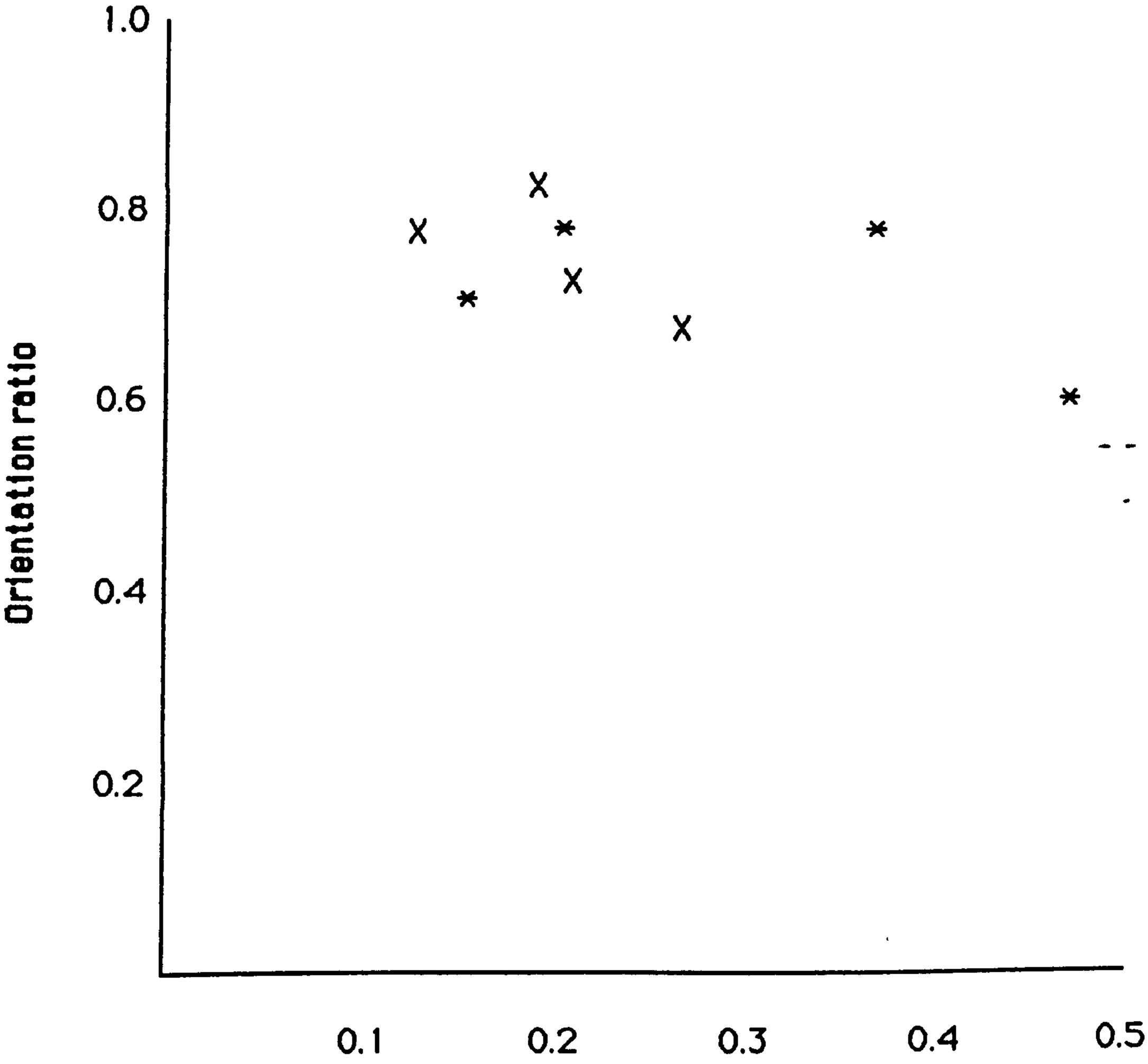

Figure 100

The fracture surface in tensile of injection moulded compound C1

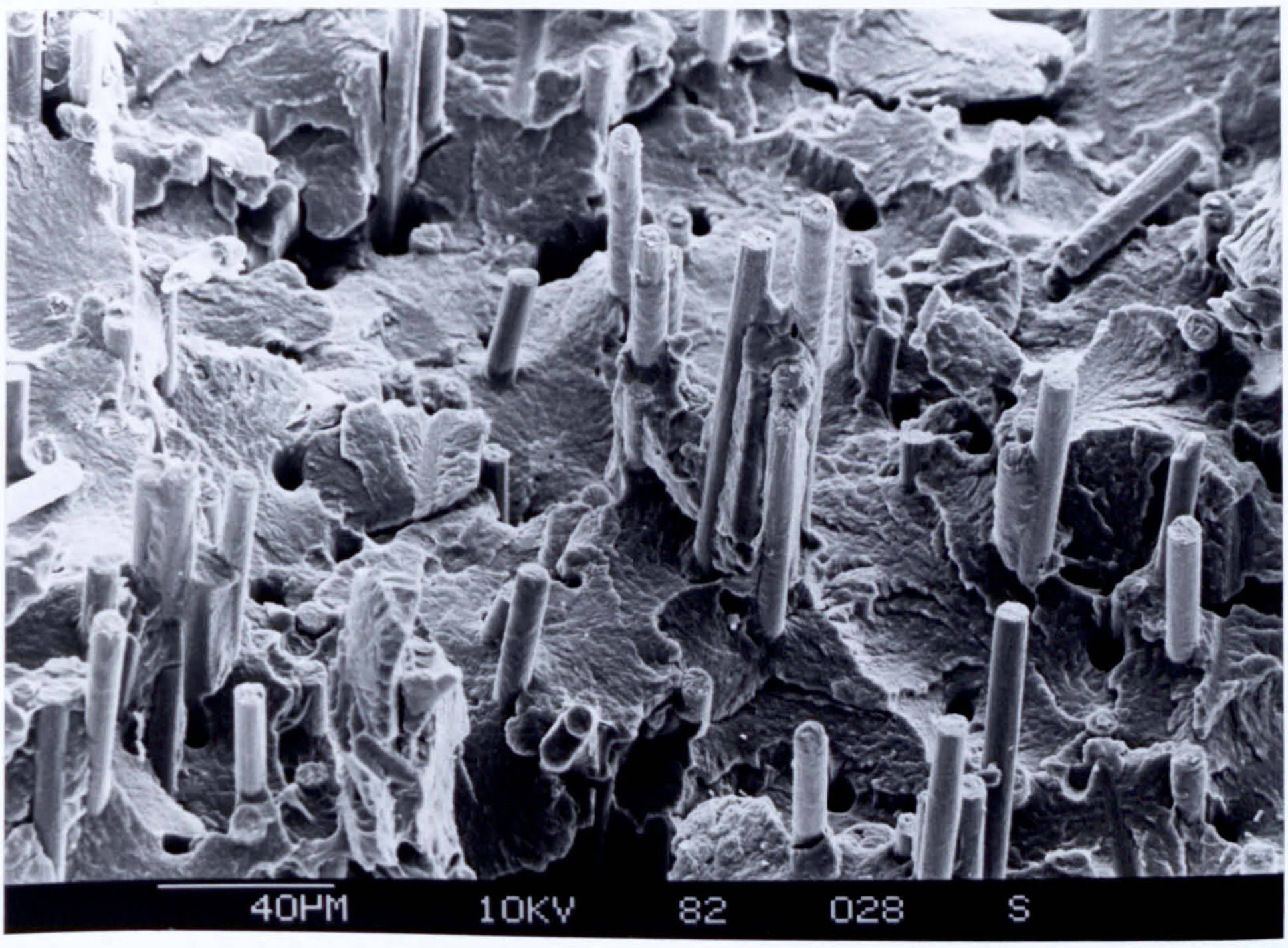

Figure 101

A close study of the fracture surface
in tensile of injection moulded compound C1

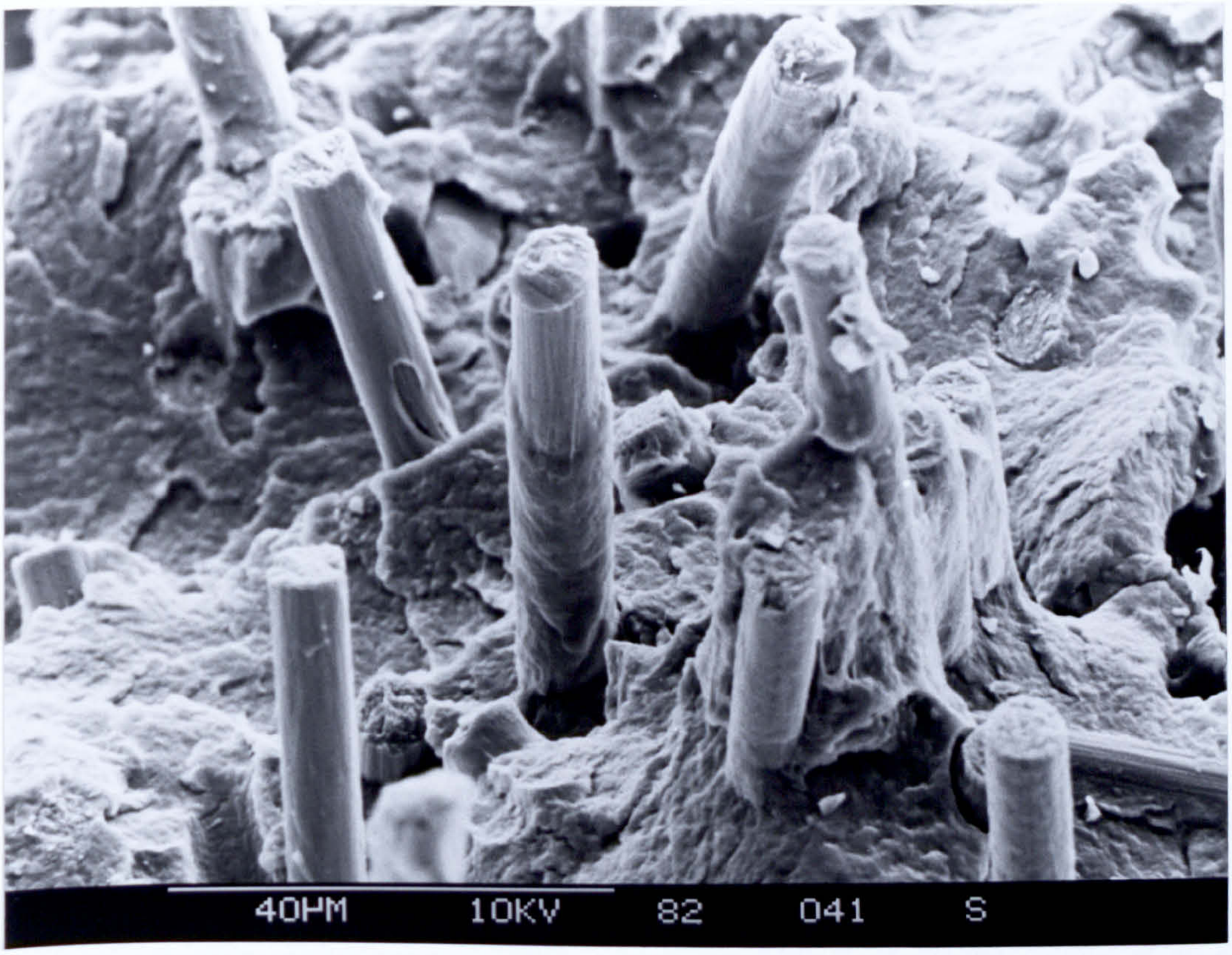

Figure 102

The fracture surface in tensile of injection moulded compound G4

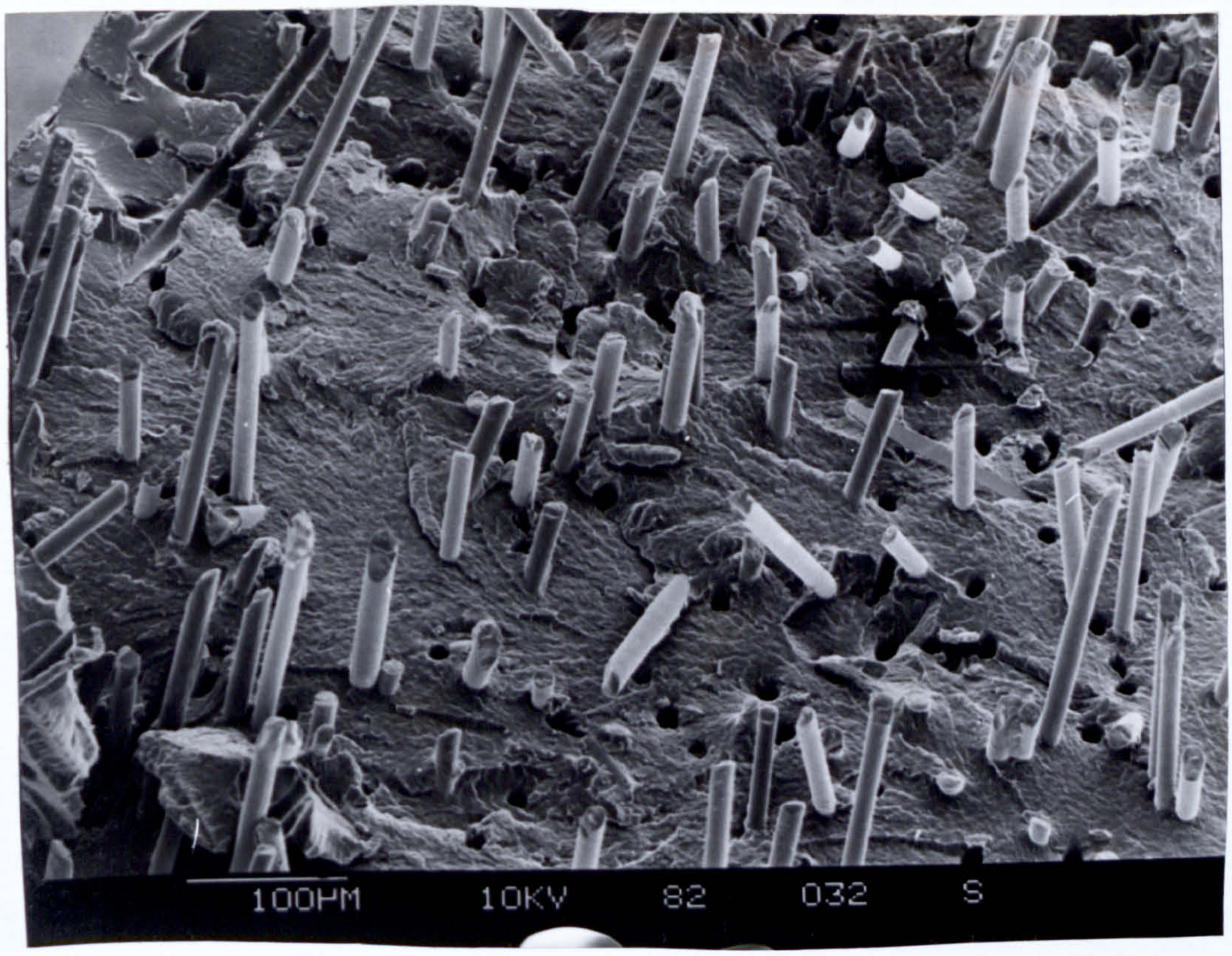

Figure 103

A close study of the fracture surface in
tensile of injection moulded compound G4

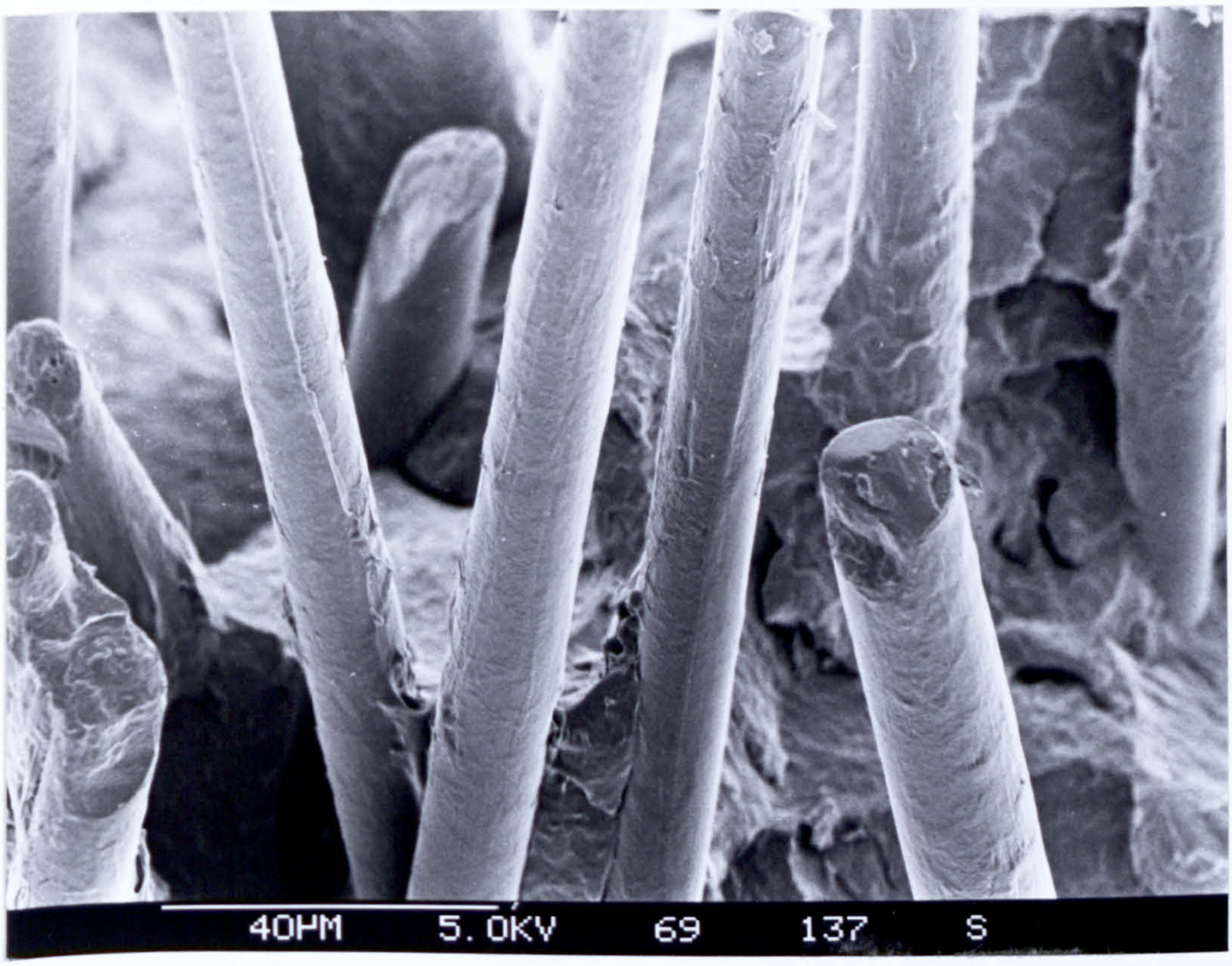

Figure 104

The transcrystallinity produced around two high modulus carbon fibres in nylon 66

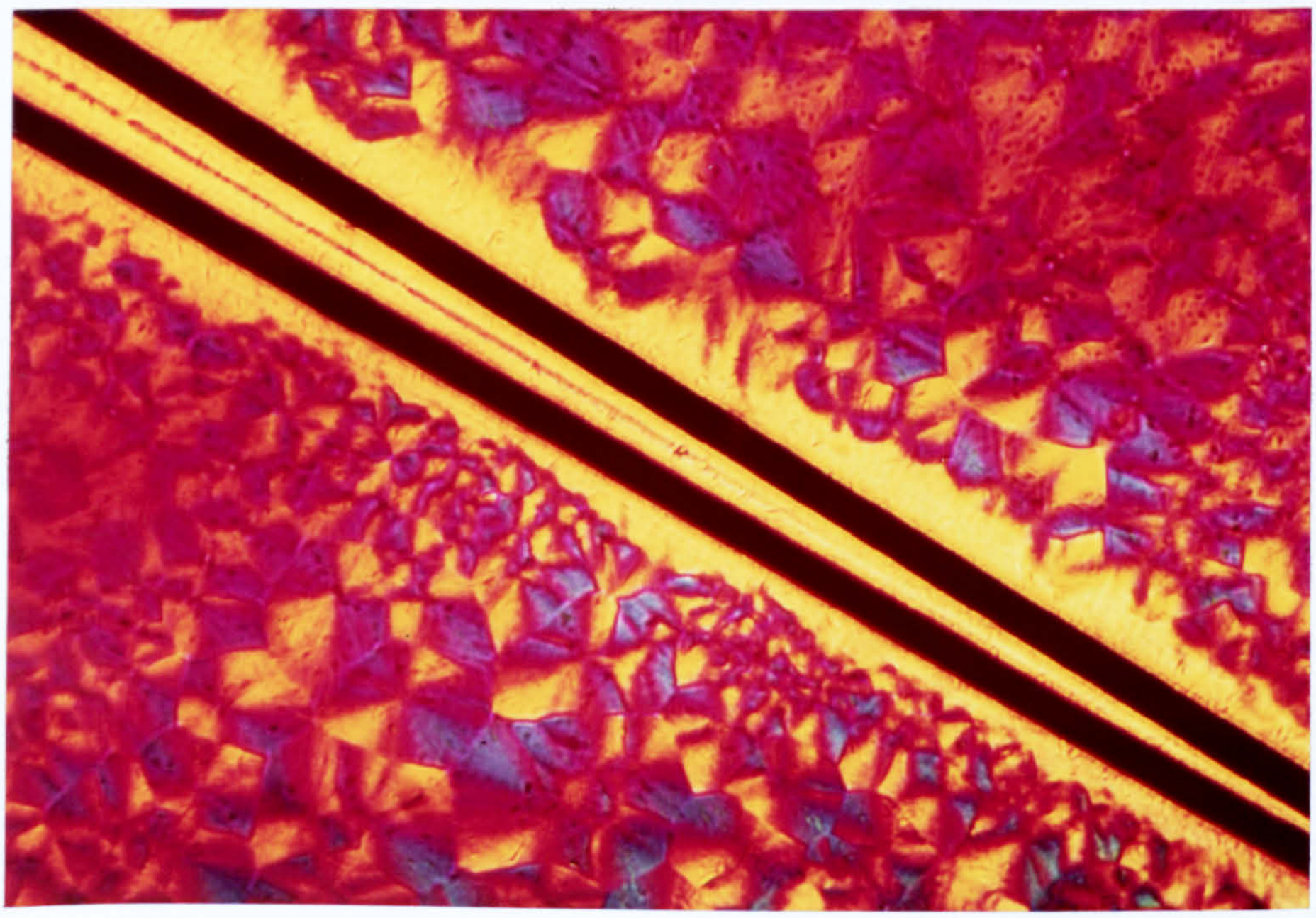

Figure 105

The transcrystallinity produced around two
E glass fibres in nylon 66

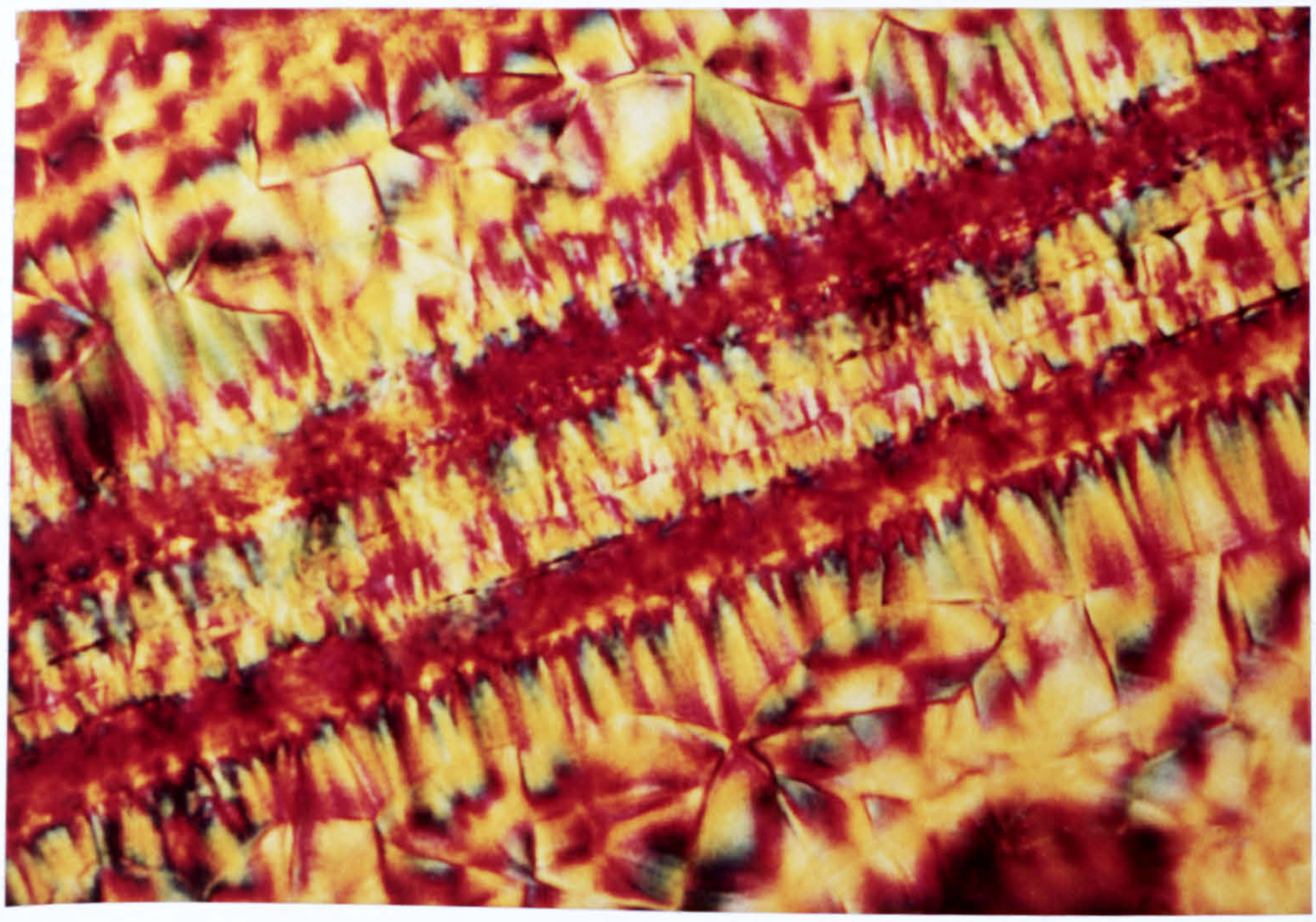

Figure 106

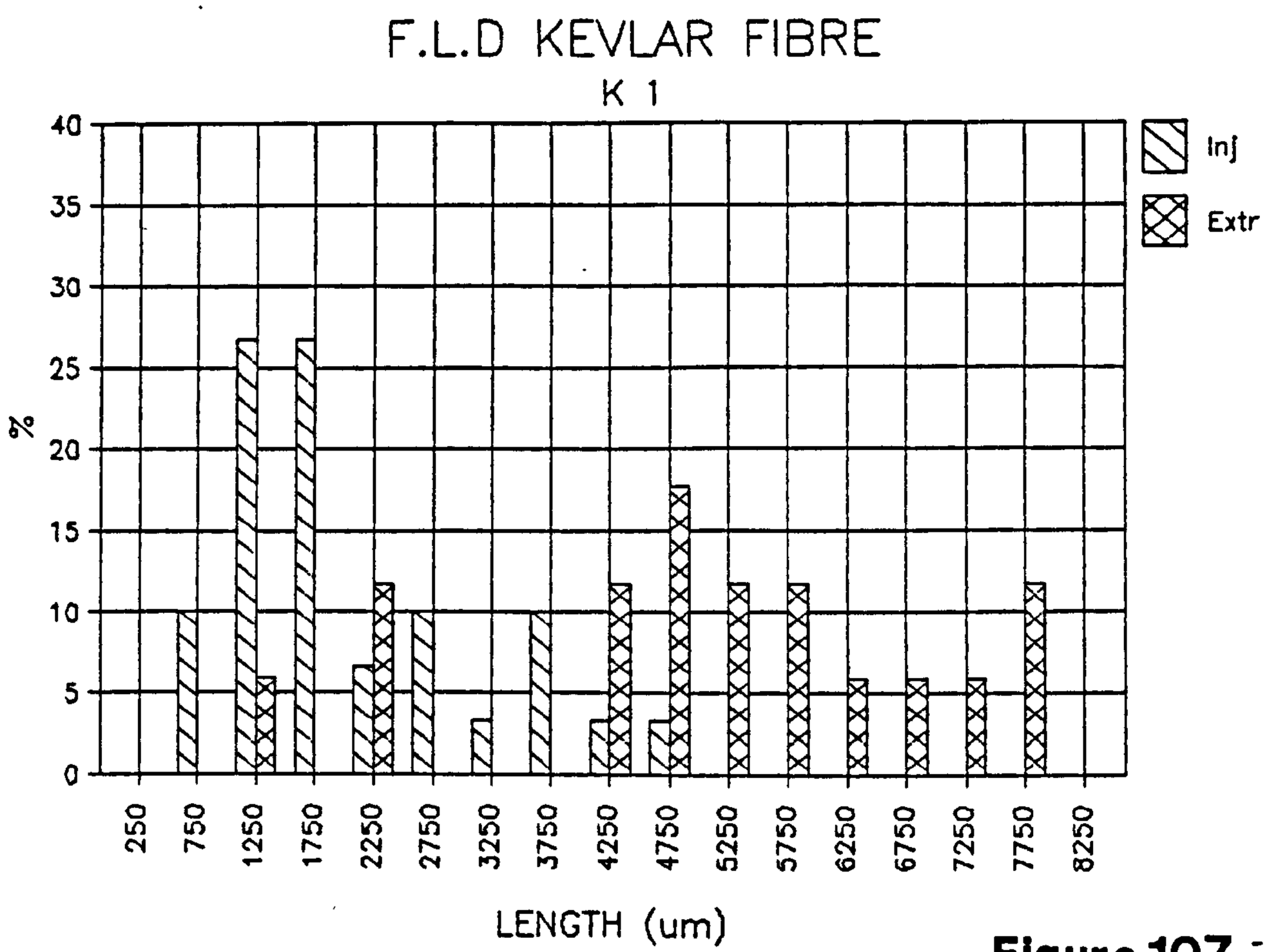

Figure 107

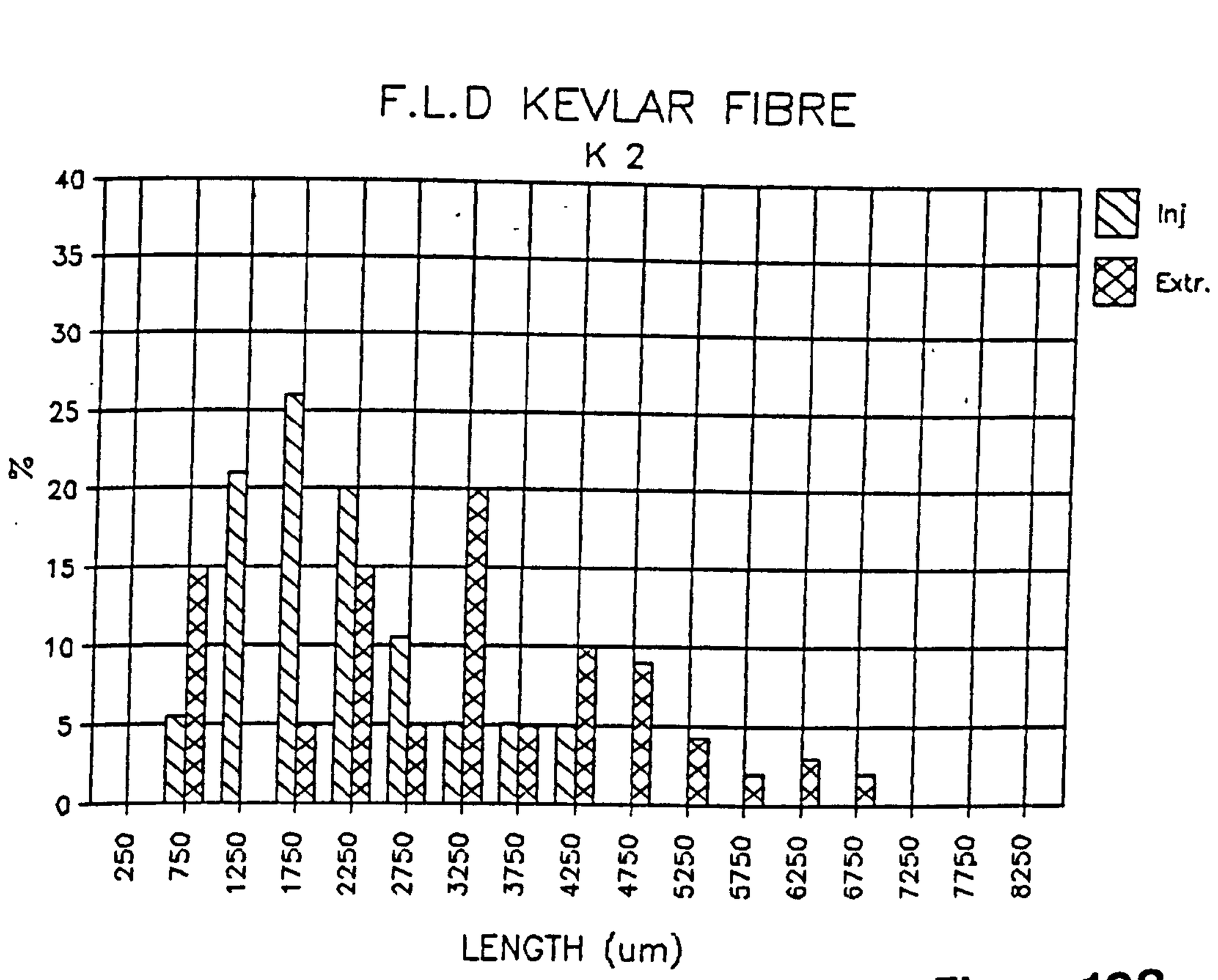

Figure 108

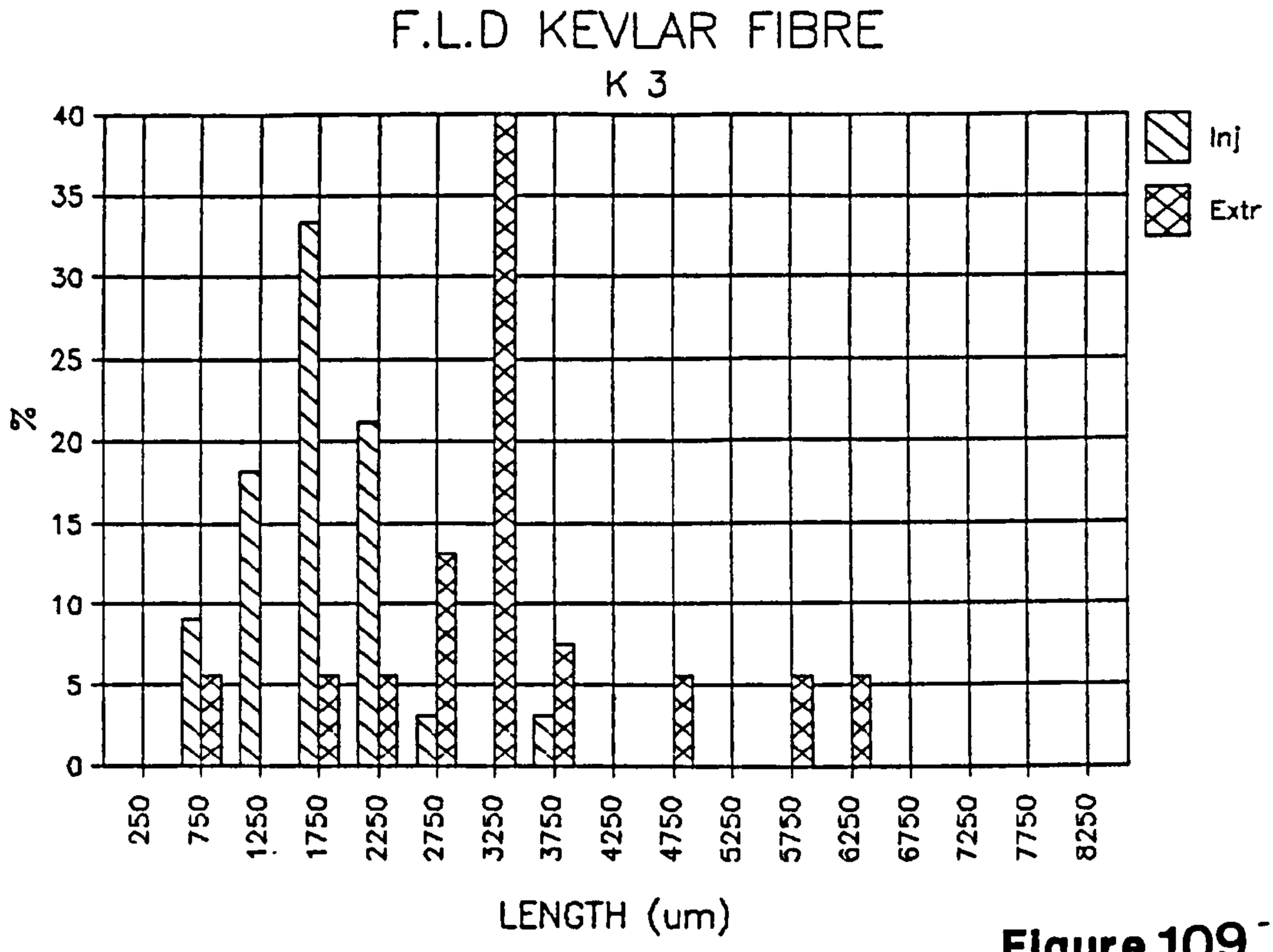

Figure 109

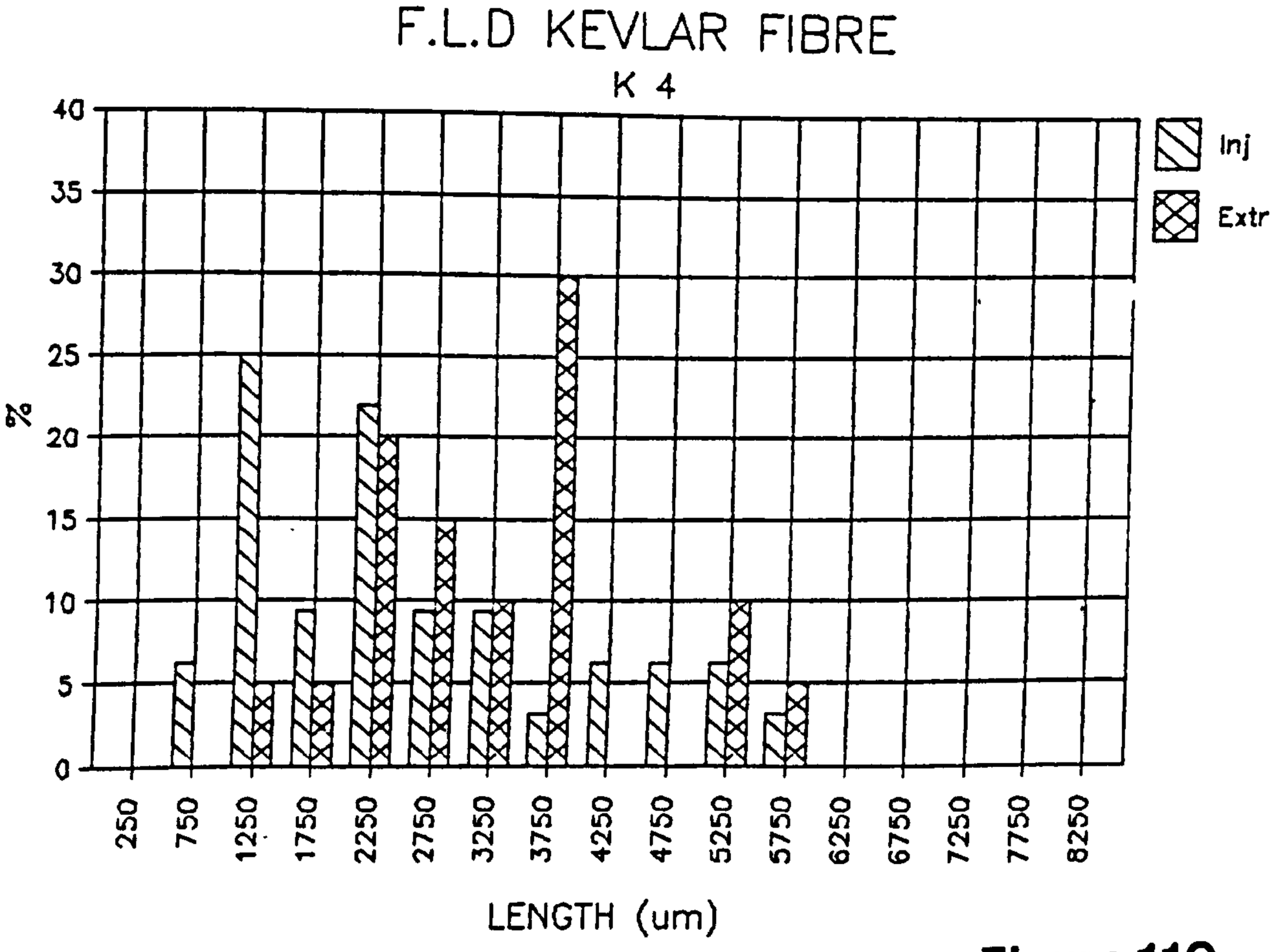

Figure 110

A section removed from injection moulded
Kevlar reinforced polypropylene observed
by polarised light

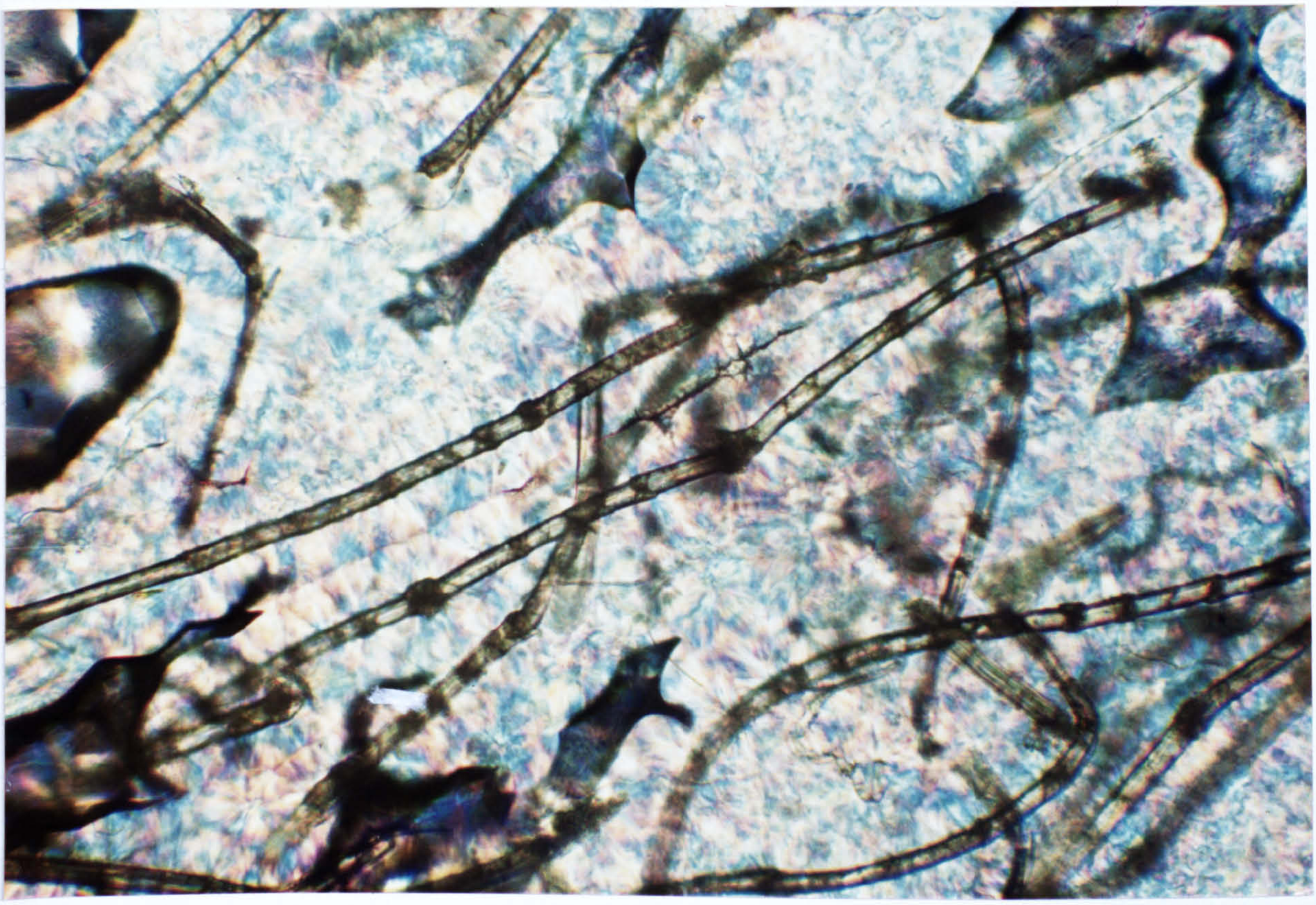

0.1mm

Figure 111

A close study of a kink faults
in compounded Kevlar fibre

0.05mm

Figure 112

A cross section cut from a tensile
test piece of compound K2

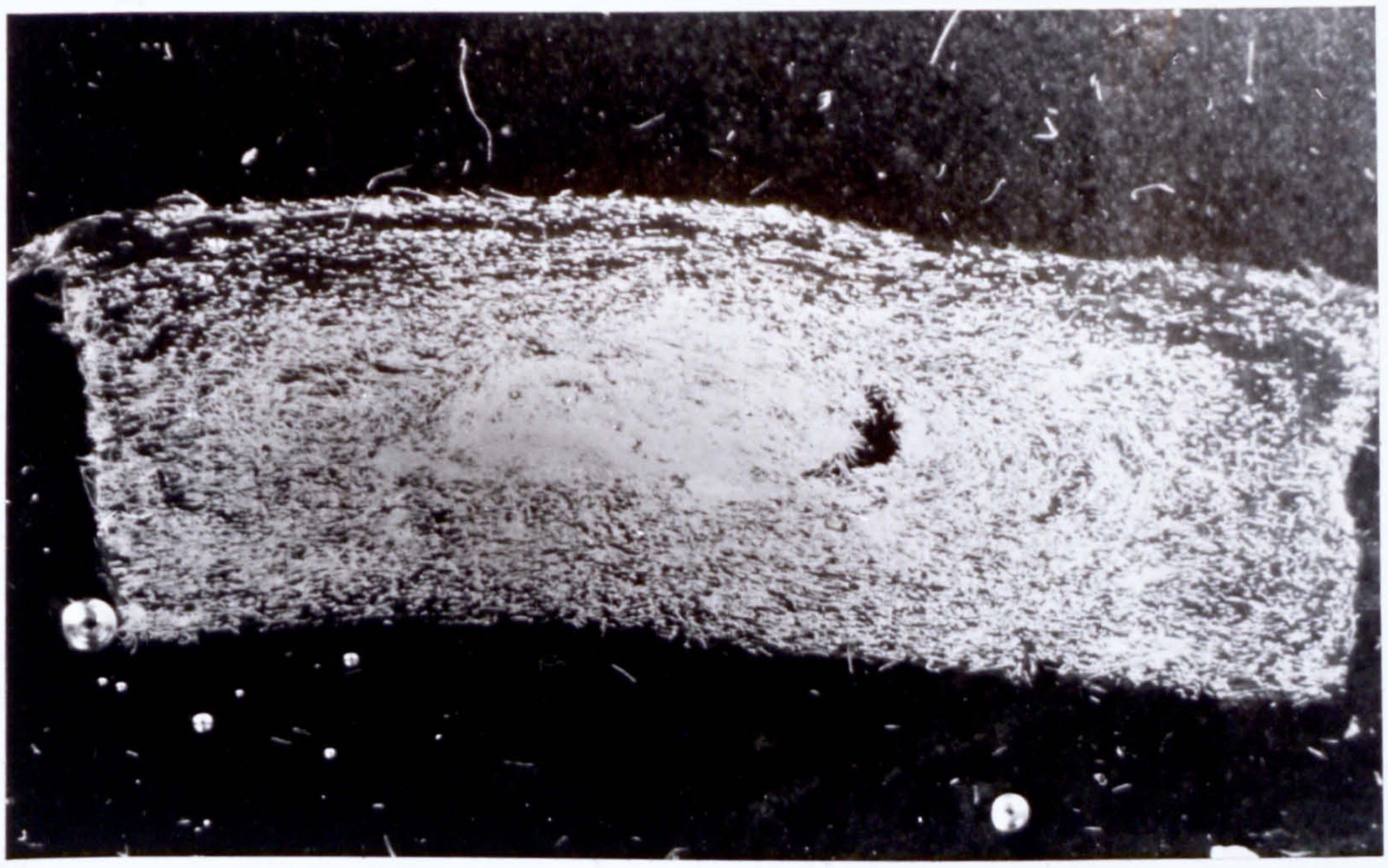

Figure 113

The fracture surface in tensile of injection moulded compound K1

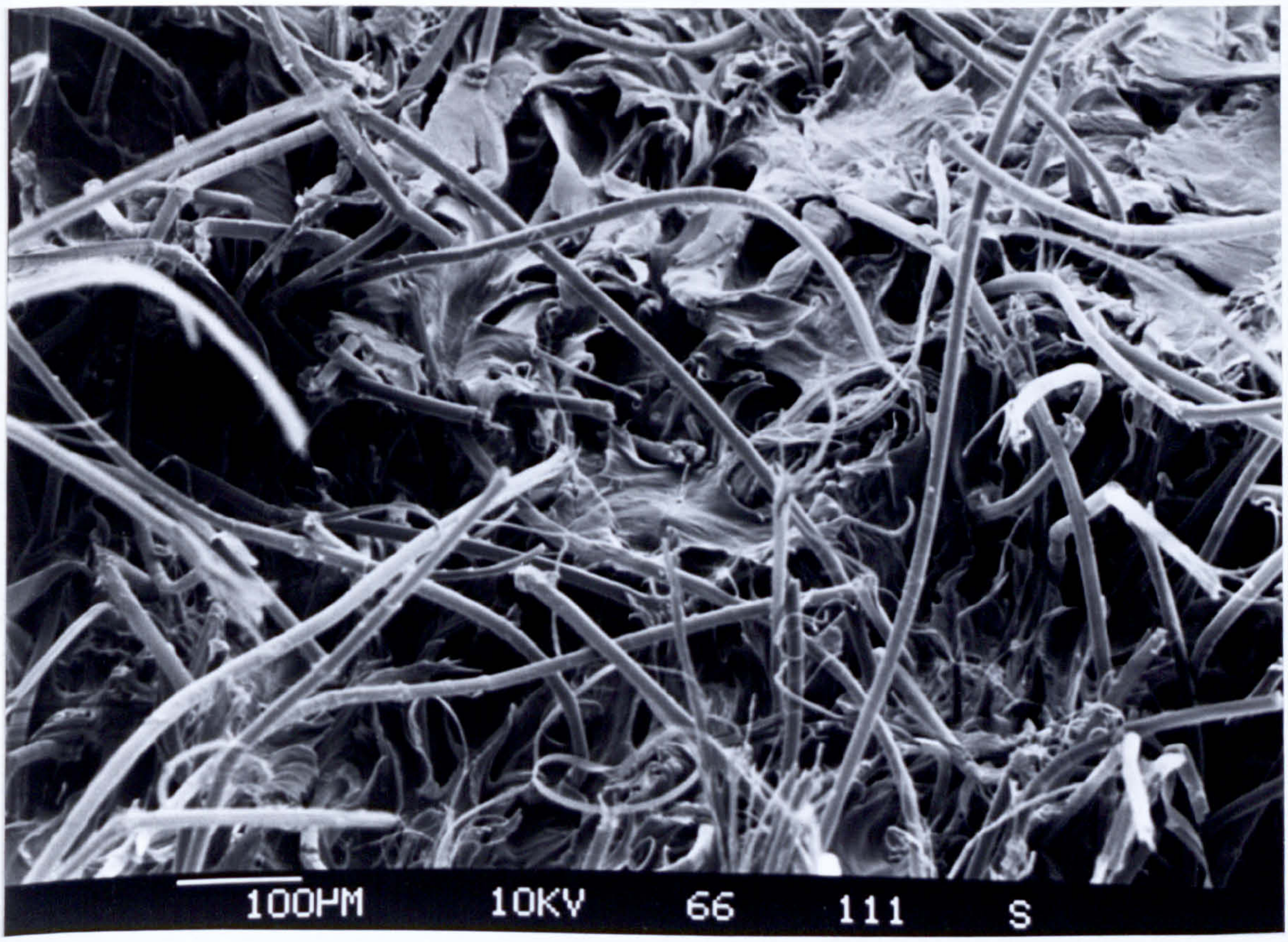

Figure 114

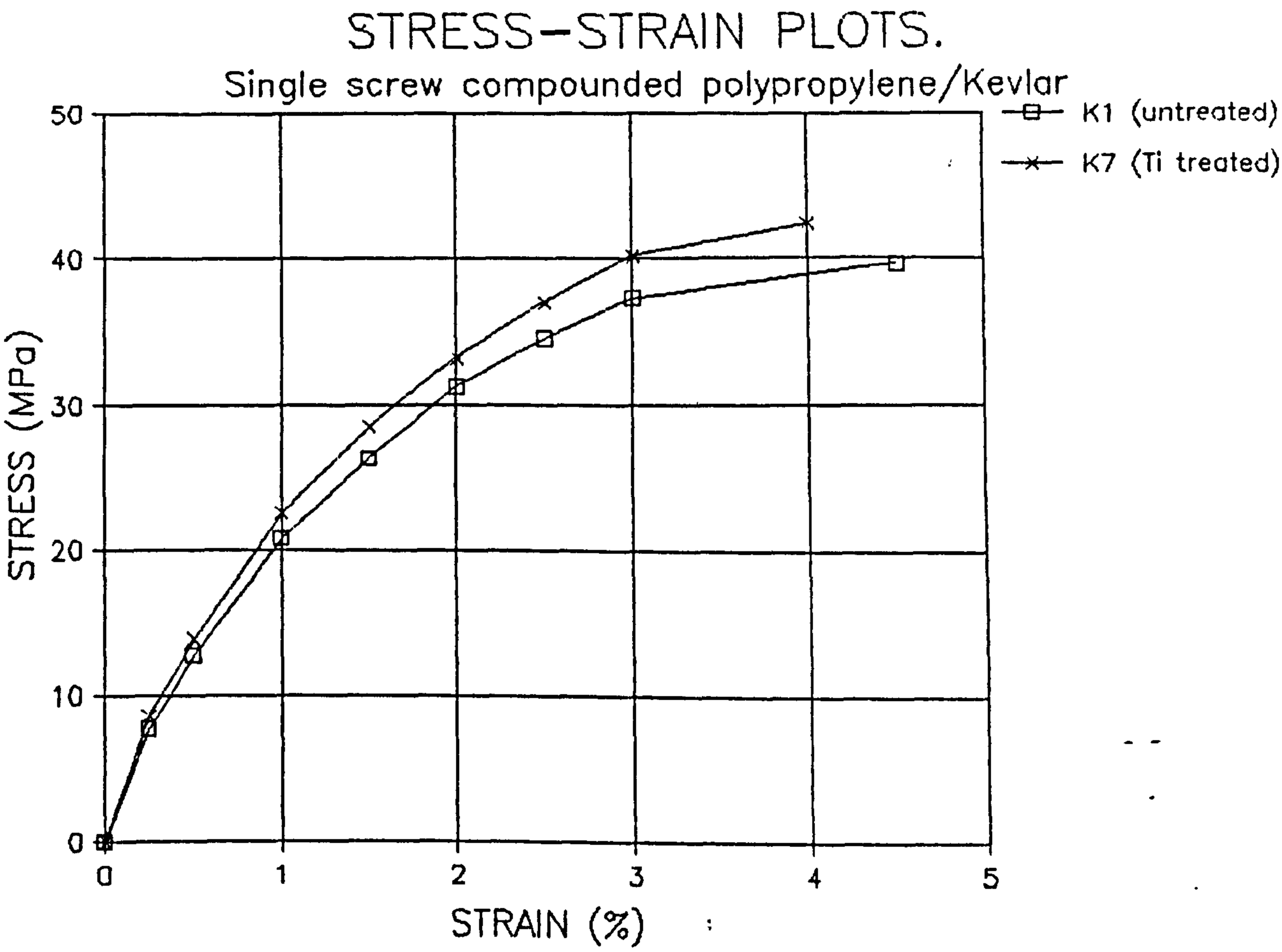
STRESS-STRAIN PLOTS.
Single screw compounded polypropylene/Kevlar
K1 (untreated)
K7 (Ti treated)
STRESS (MPa)
50
40
30
20
10
0
0
1
2
3
4
5
STRAIN (%)

Figure 115

Mechanism of band formation in compressed Kevlar fibres

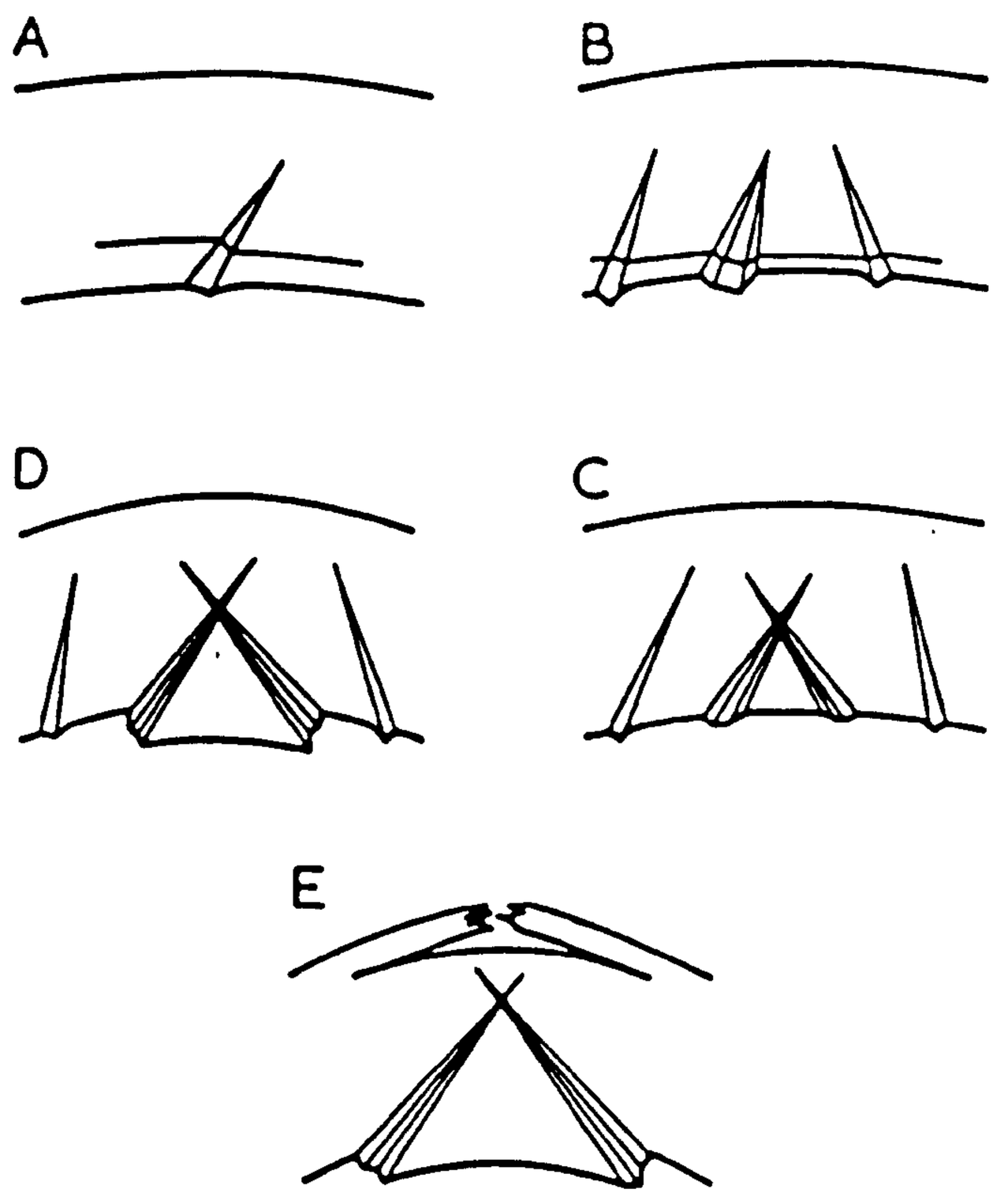

Figure 116

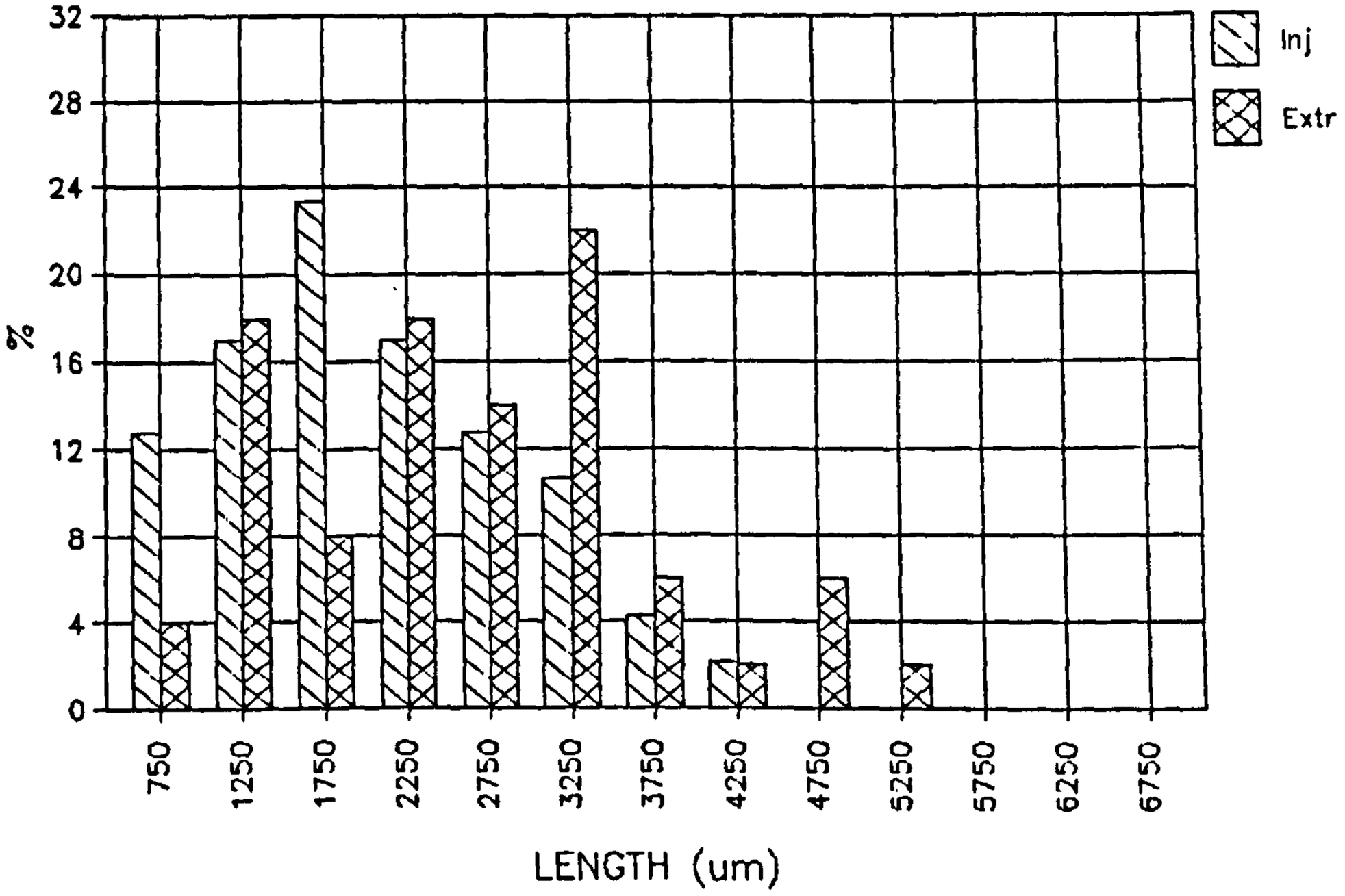

Figure 117

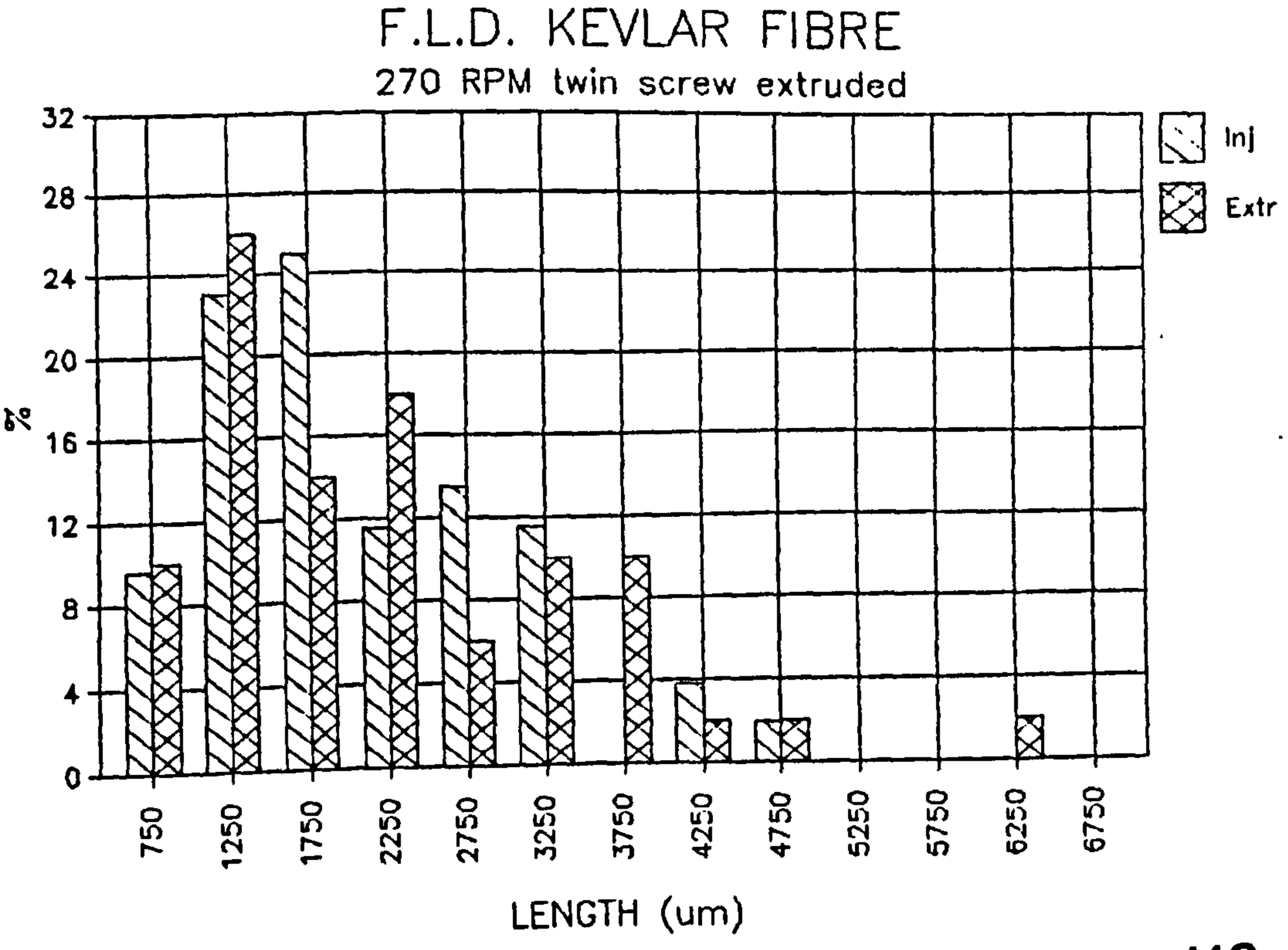

Figure 118

A cross section cut from a tensile test piece of compound K11

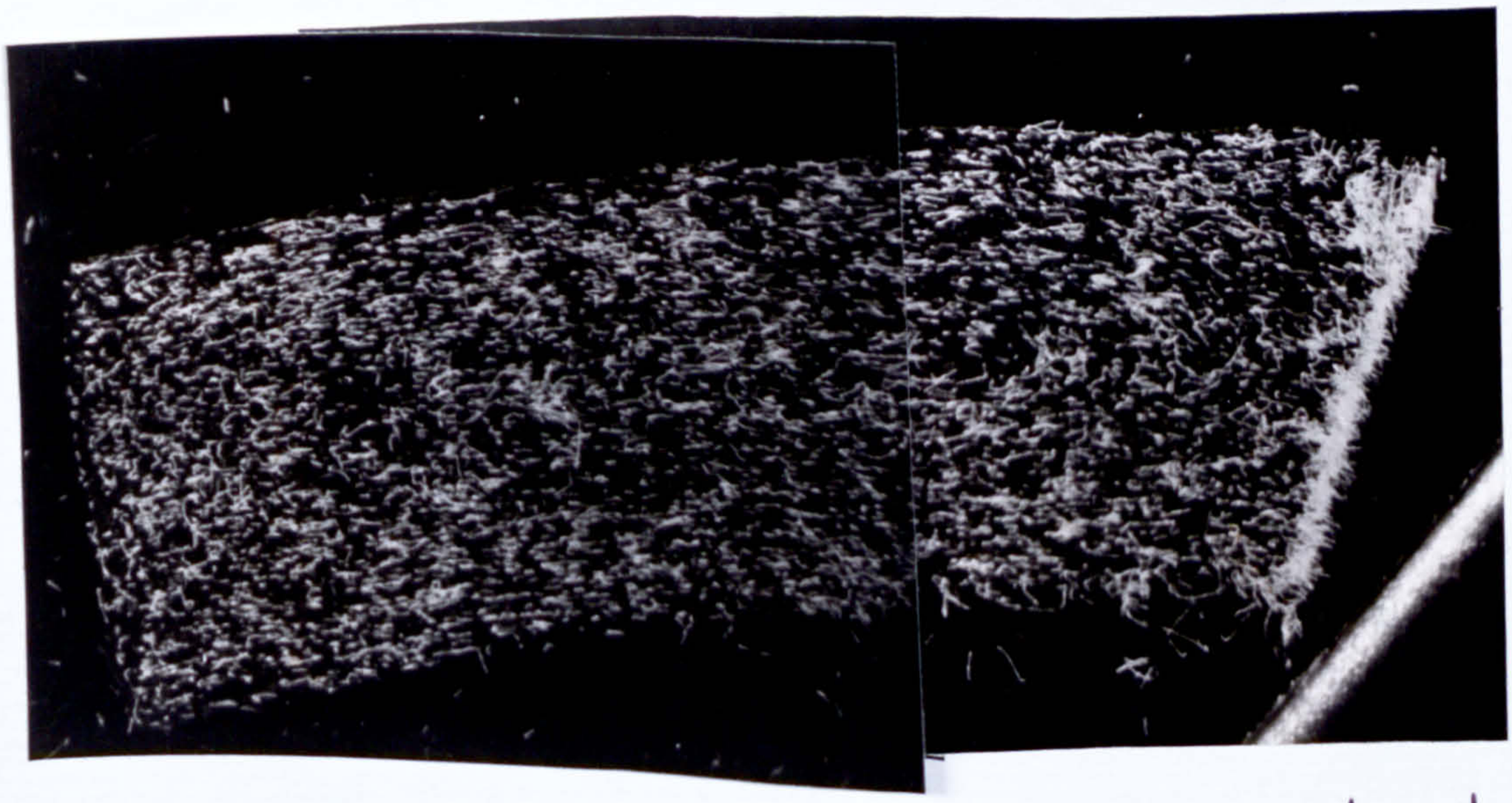

Figure 119

The Baker Perkins compounder screw
profile used for experiment
KEVLAR 4

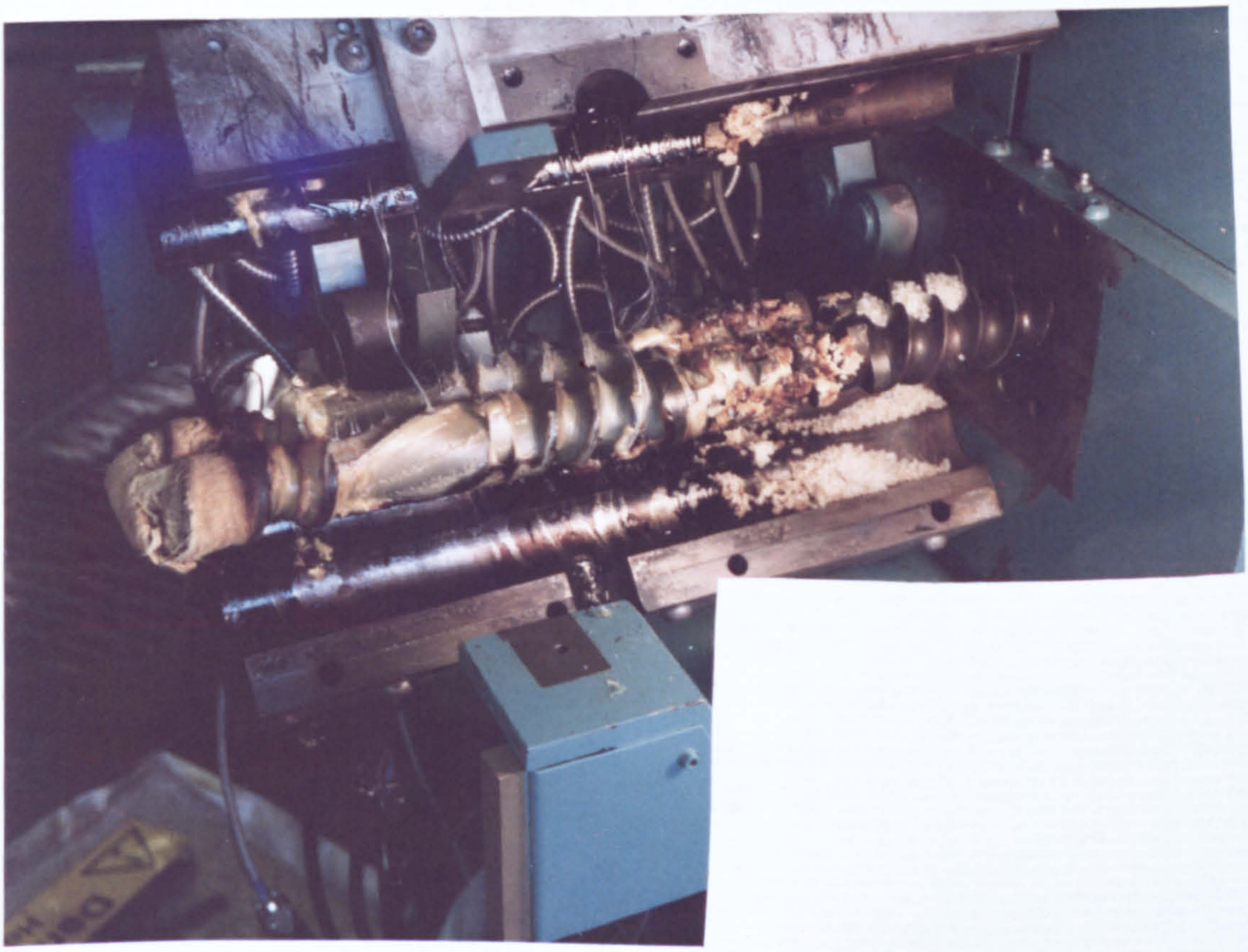

Figure 120

Moulding for mechanical anisotropy investigation

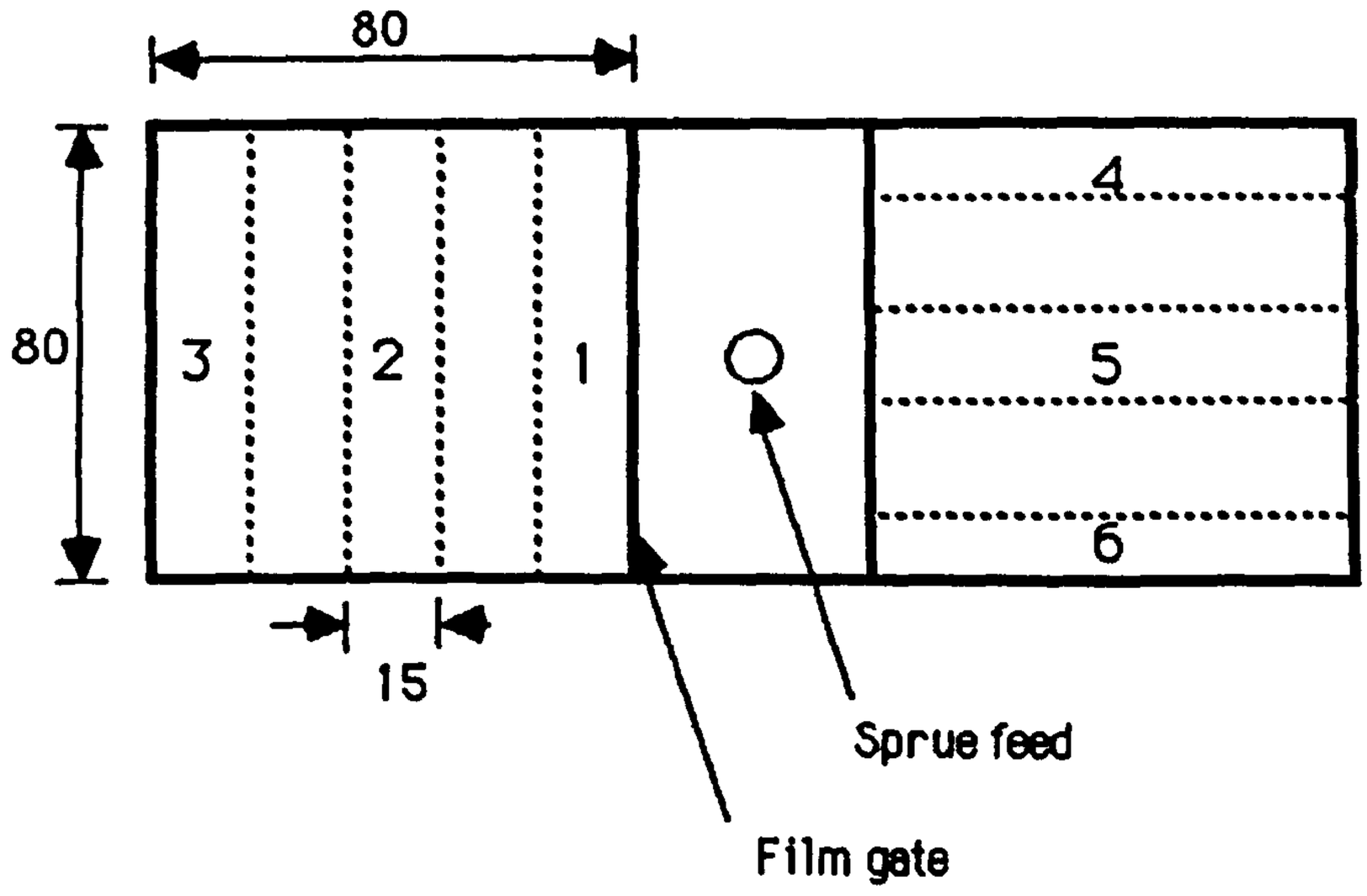

All dimensions in mm.

Sample position numbered.

Figure 121

Damaged Kevlar fibre observed in the
tensile failure of an injection moulding

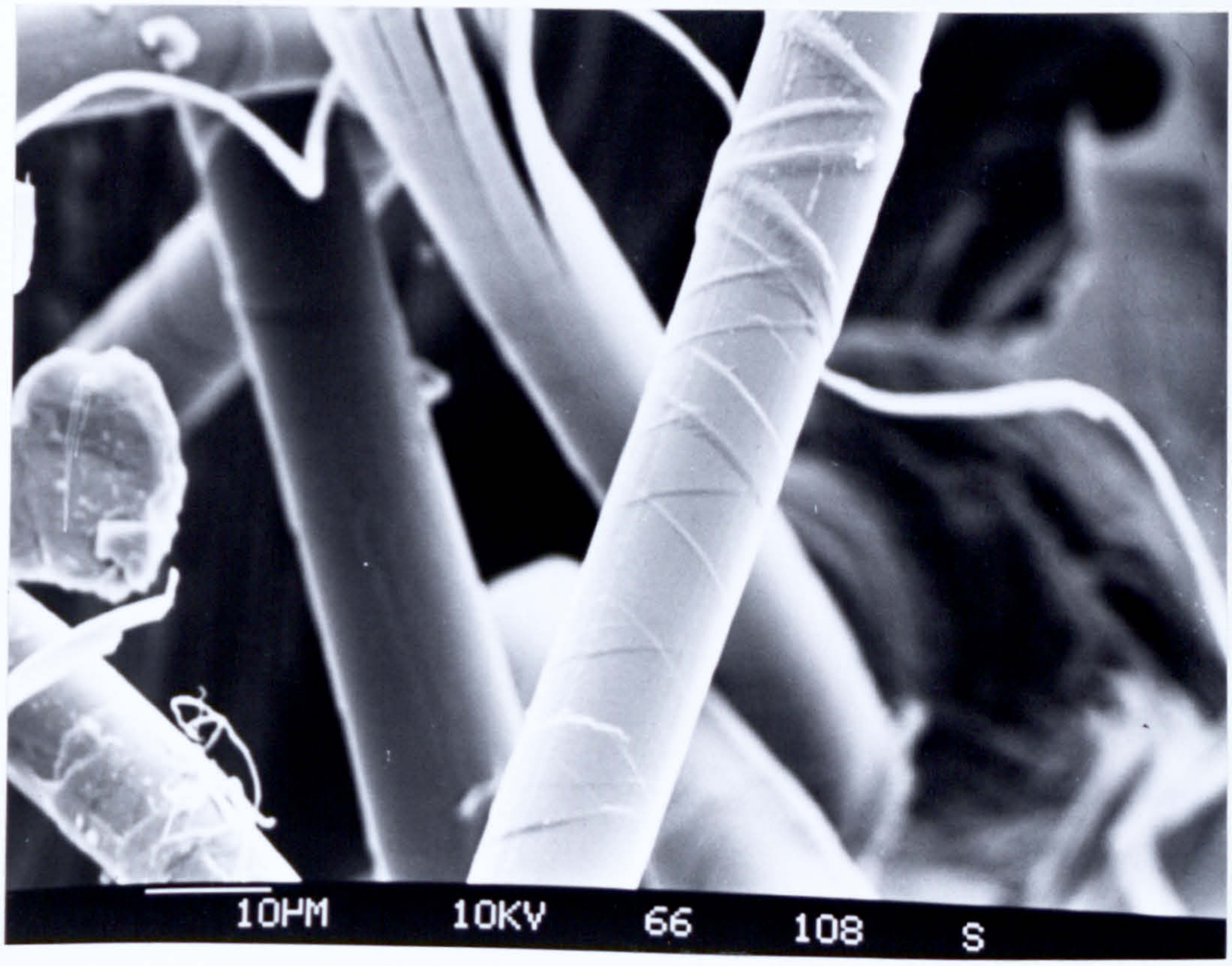

Figure 122

Damaged Kevlar fibre observed in the tensile failure of an injection moulding

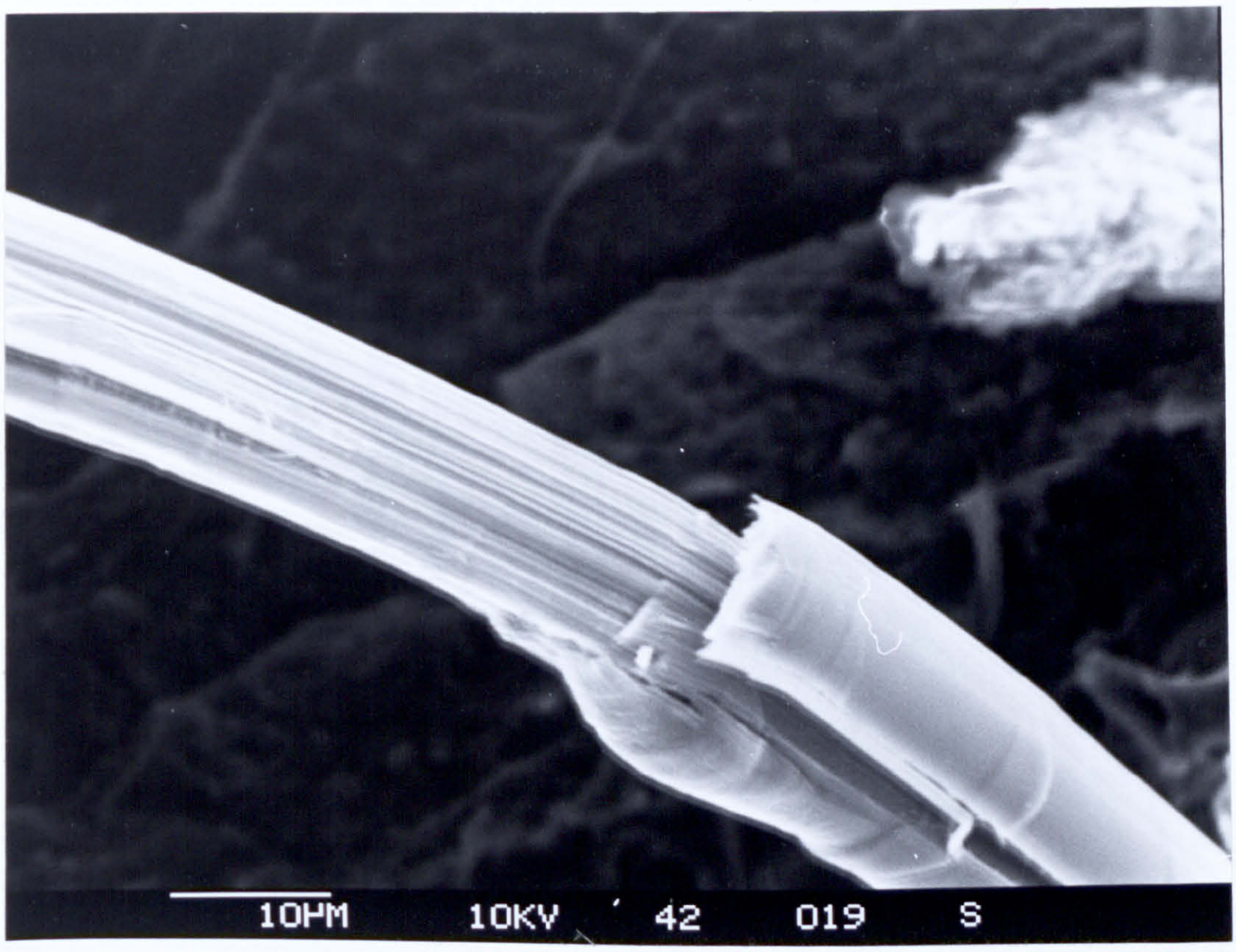

Figure 123

Damaged Kevlar fibre observed in the tensile failure of an injection moulding

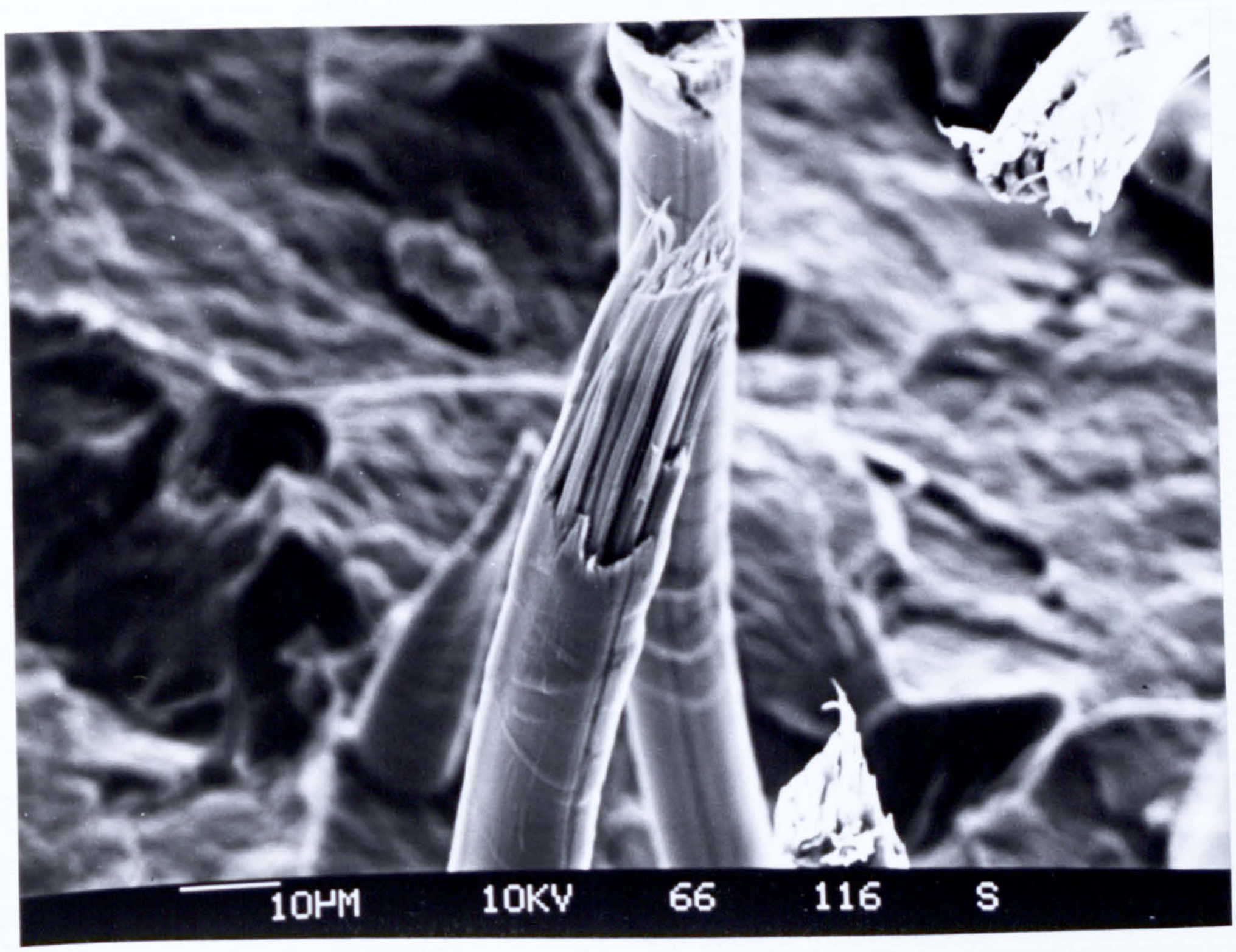

Figure 124

Damaged Kevlar fibre observed in the
tensile failure of an injection moulding

Figure 125

Damaged Kevlar fibres observed in the tensile failure of an injection moulding

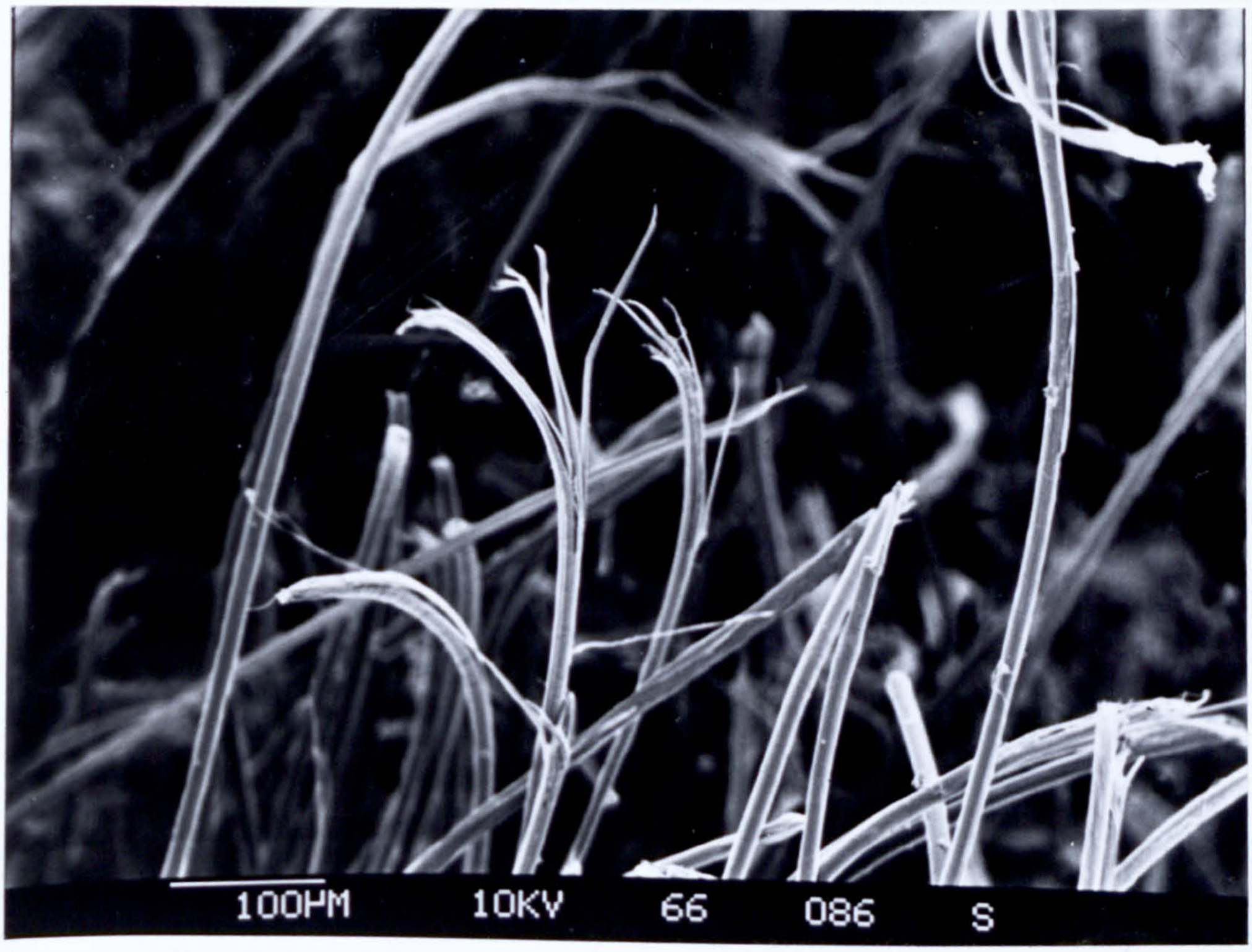

Figure 126

Fracture surface of an extruded rod section

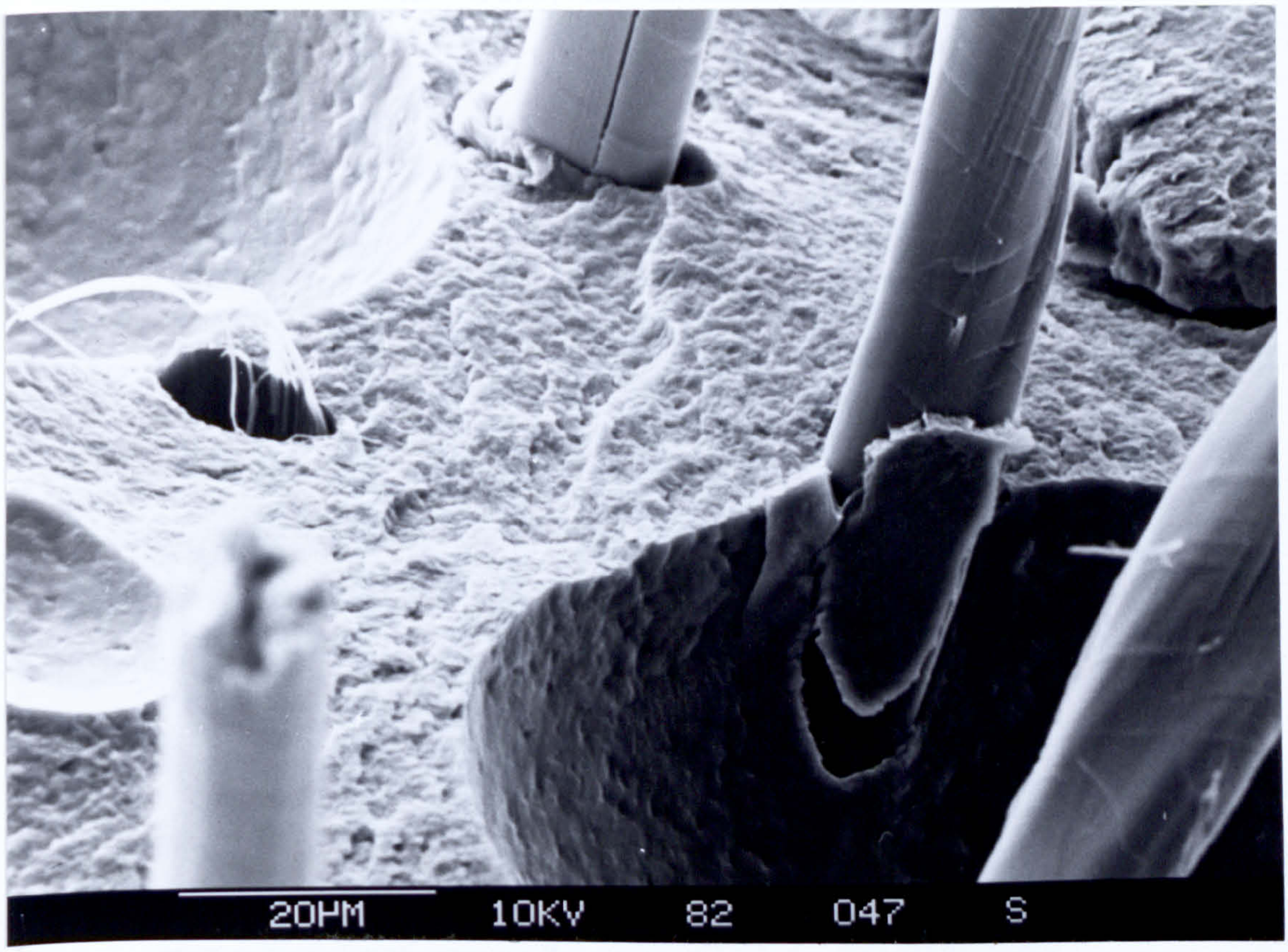

Figure 127

The fracture surface in tensile of injection moulded compound K 11

Figure 128

The fracture surface in tensile of injection moulded compound K 11 showing detail of the bases of pulled out fibres

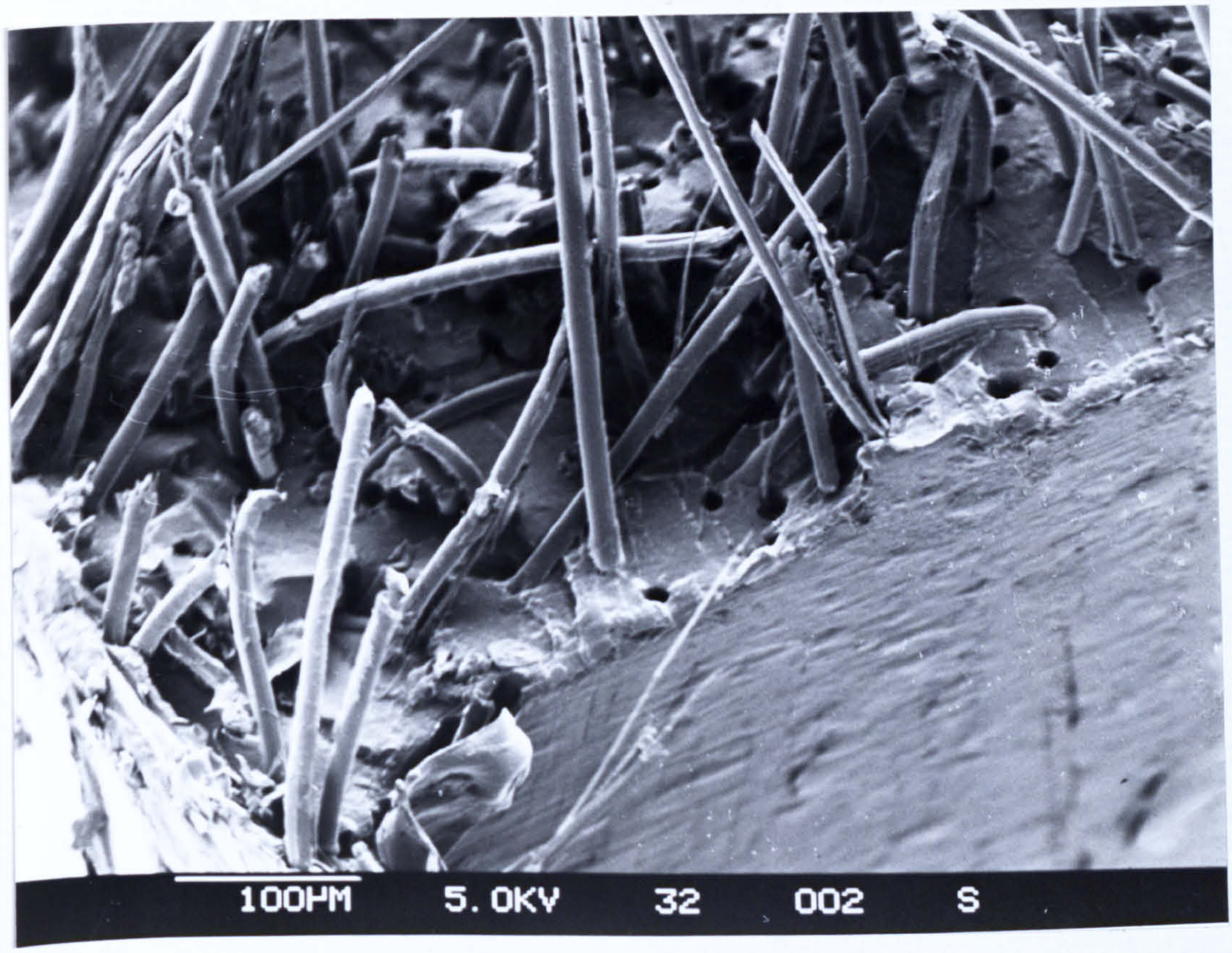

Figure 129

The fracture surface in tensile of injection moulded compound K 11 where fibres are orientated at right angles to the testing direction

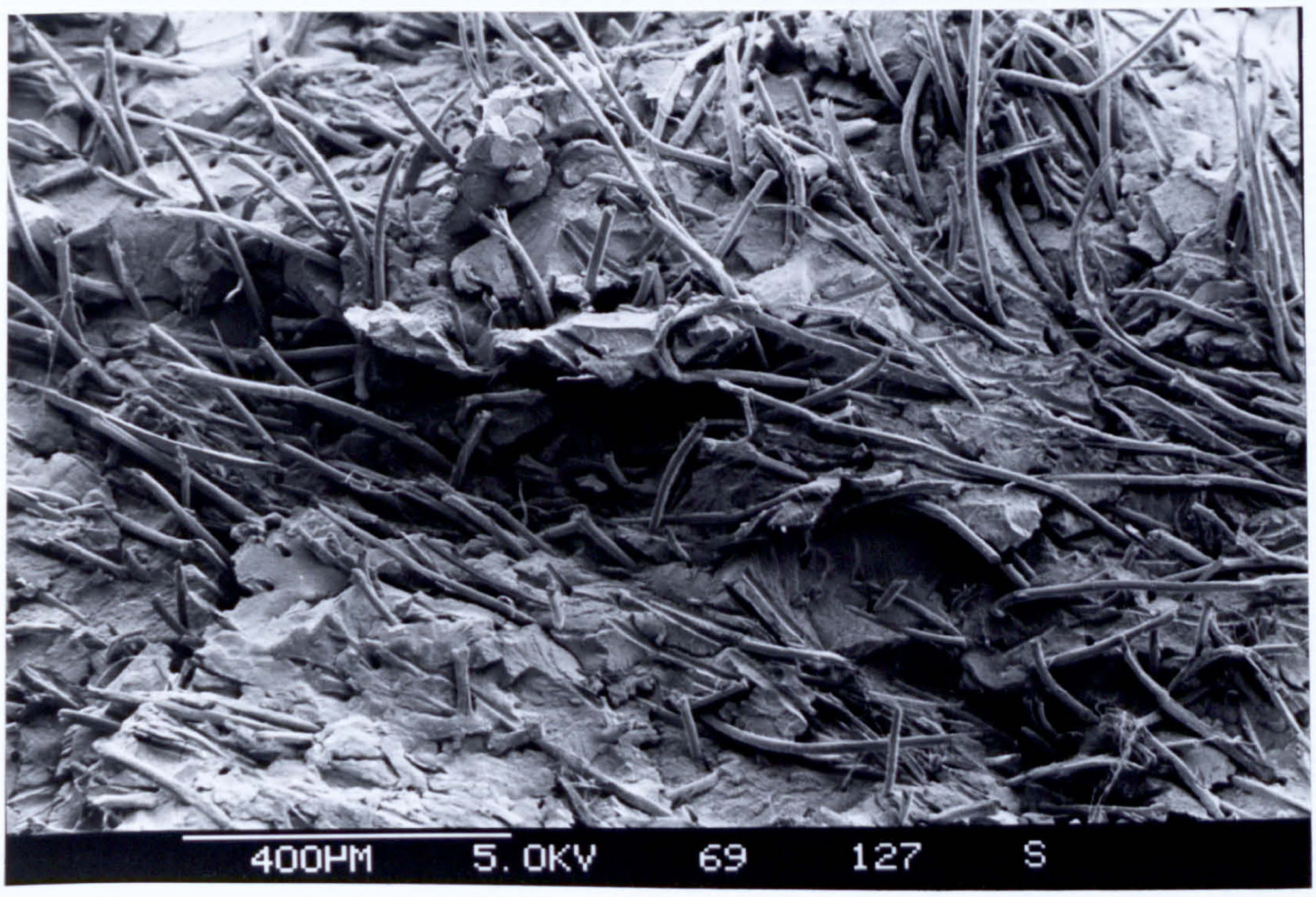

Figure 130

The fracture surface in tensile of injection moulded compound K 13

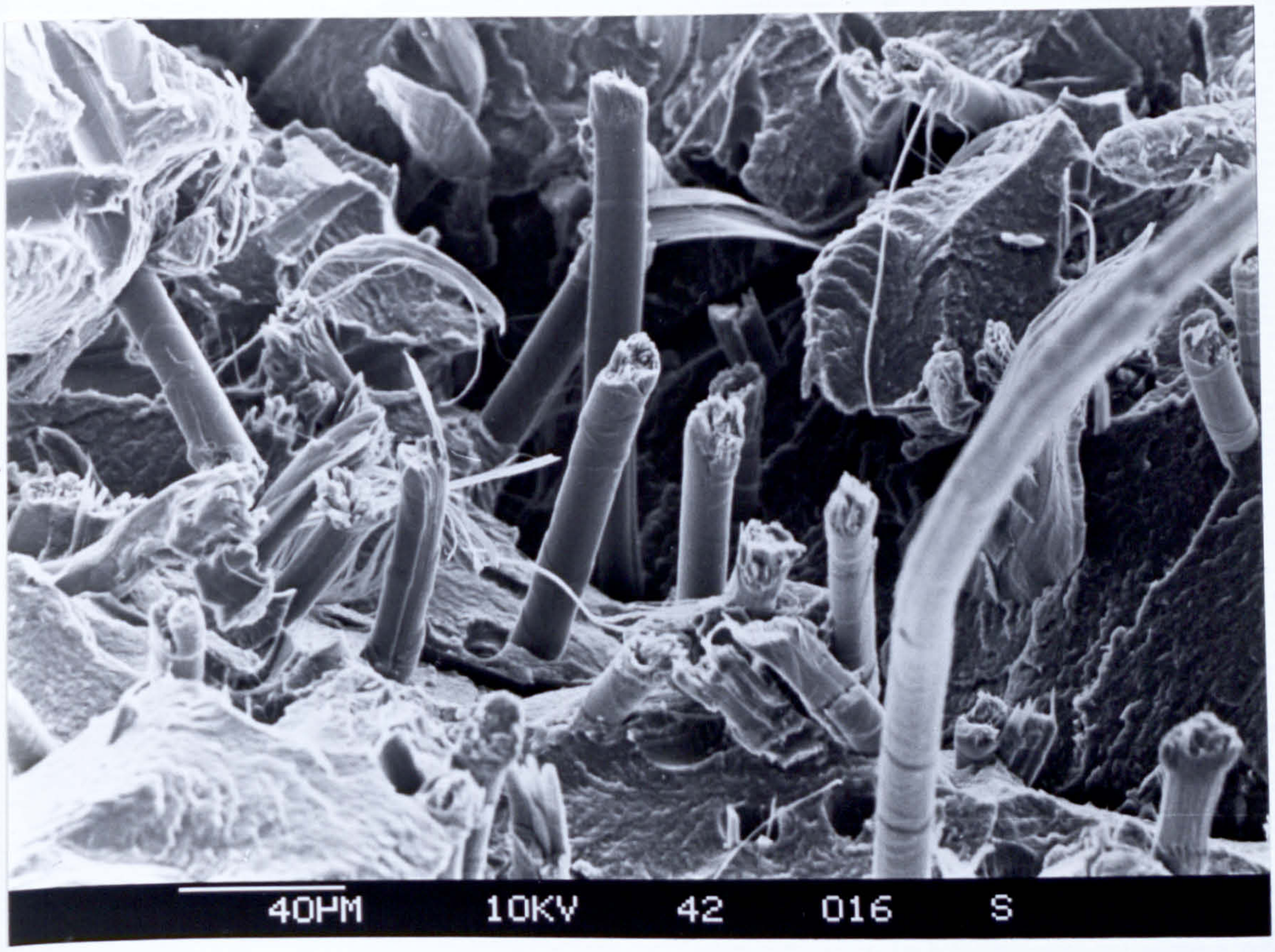

Figure 131

The fracture surface in tensile of injection moulded compound K 13 where fibres are orientated at right angles to the testing direction

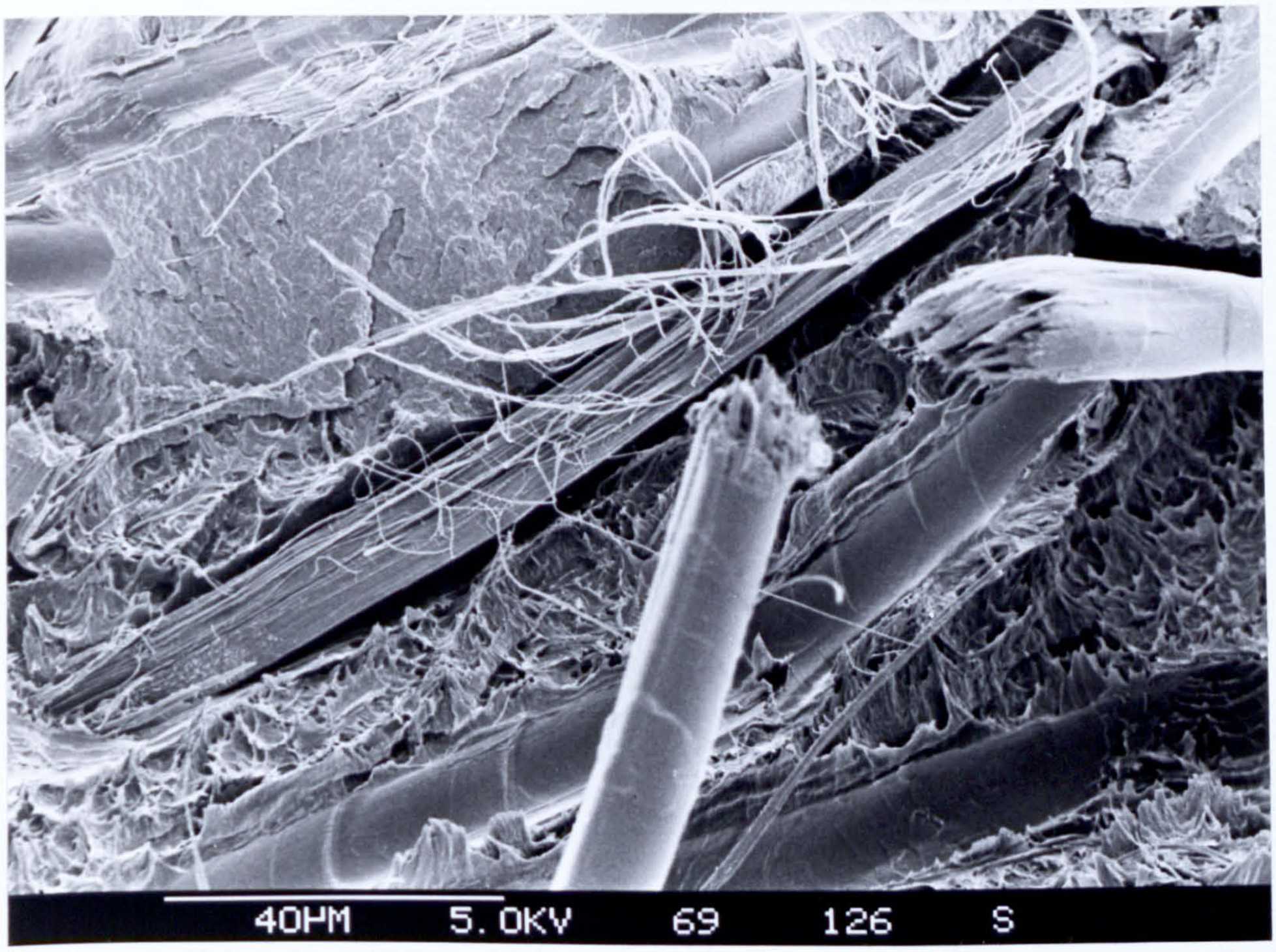

Figure 132

KEV. REINFORCED THERMO. (TWIN SCREW)

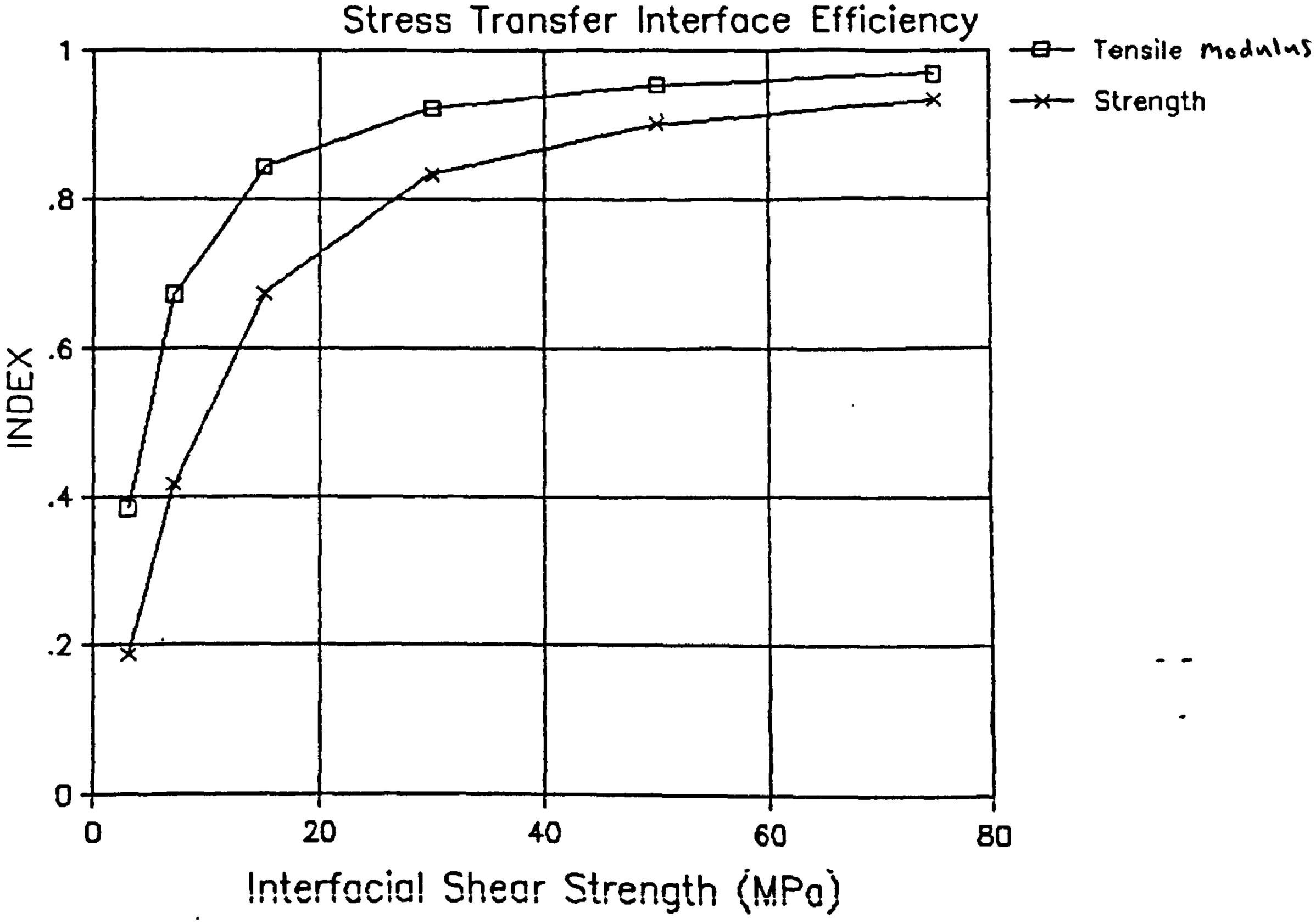

Figure 133

Coefficient of expansion values for fibres and matrices used

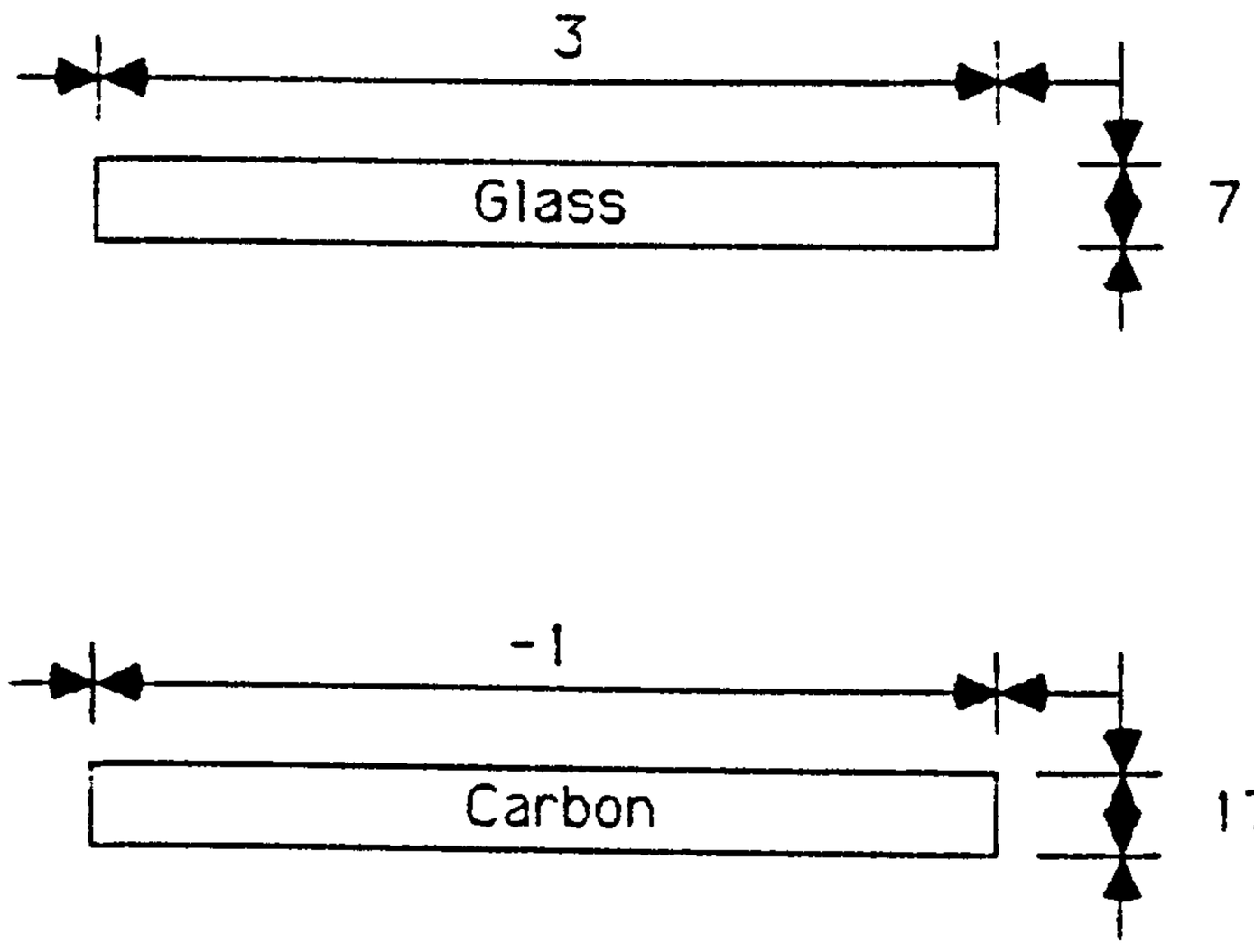

Matrix : Nylon 66. =100
Polypropylene=110
(All values 10*-6/in/in/C)

Figure **134**

A section cut from a tensile test piece of compound K 11 from the location shown in Figure 136

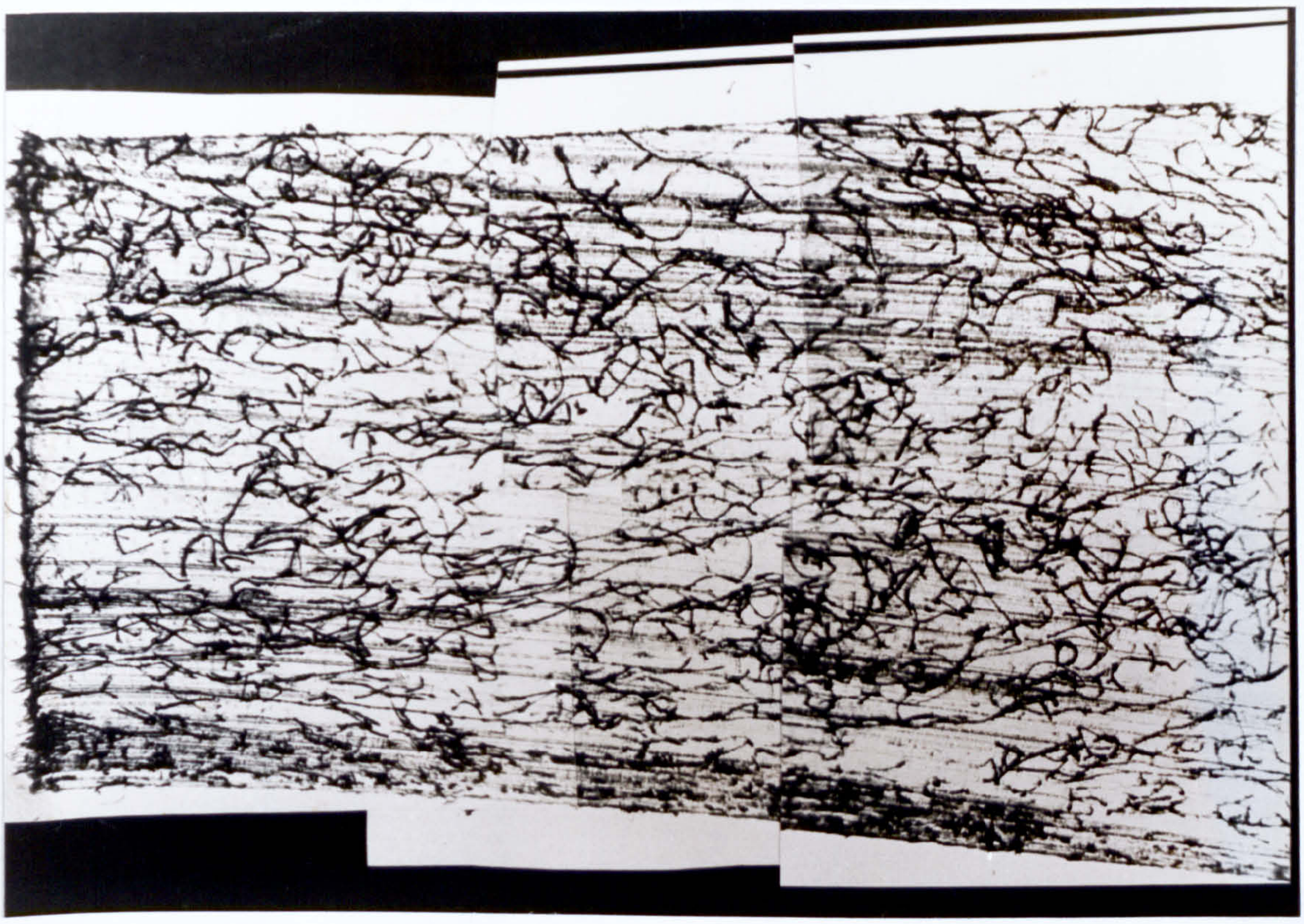

Figure 135

The location in a tensile test bar where a section was removed for the observation of fibre orientation

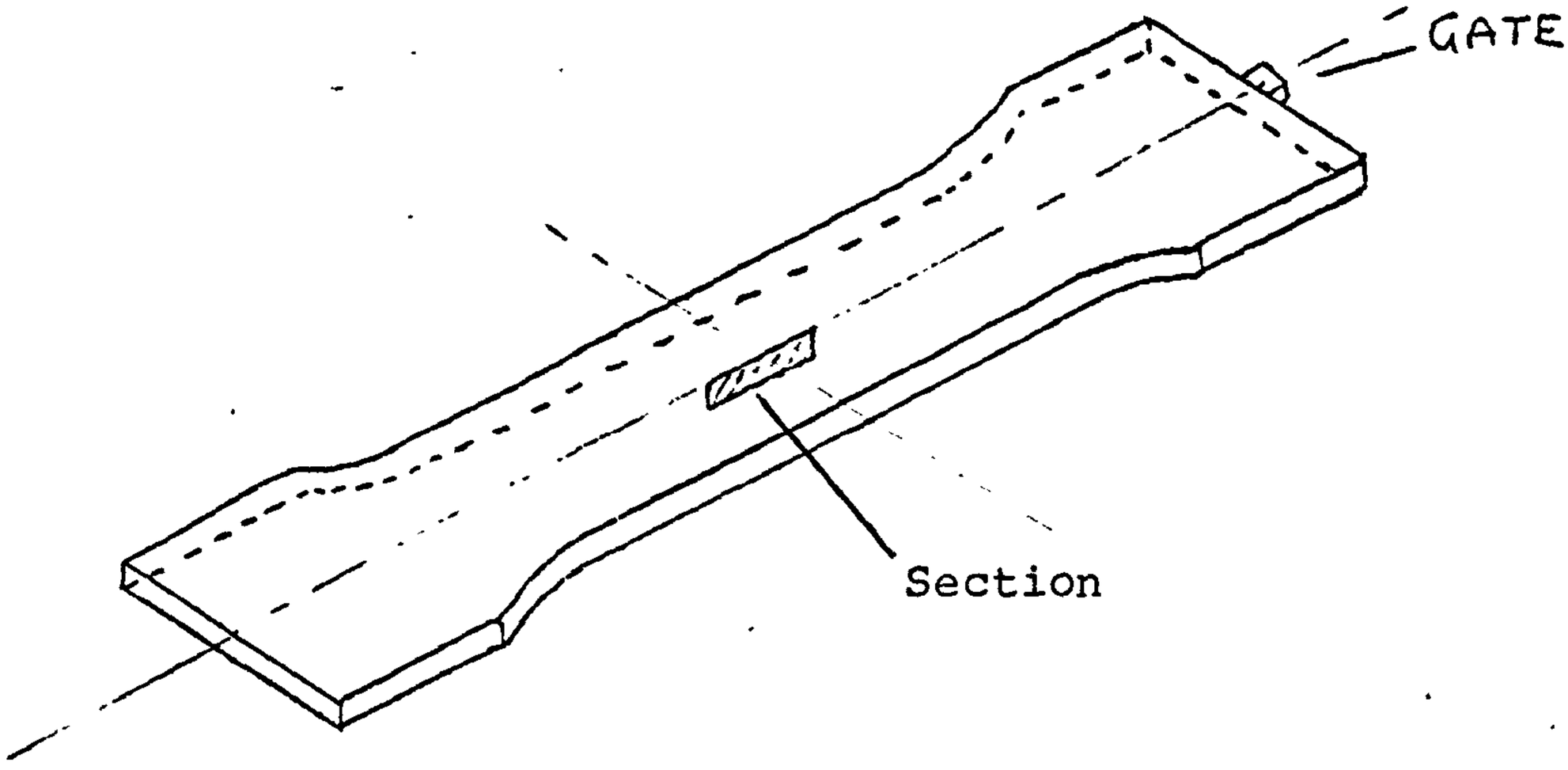

Figure 136

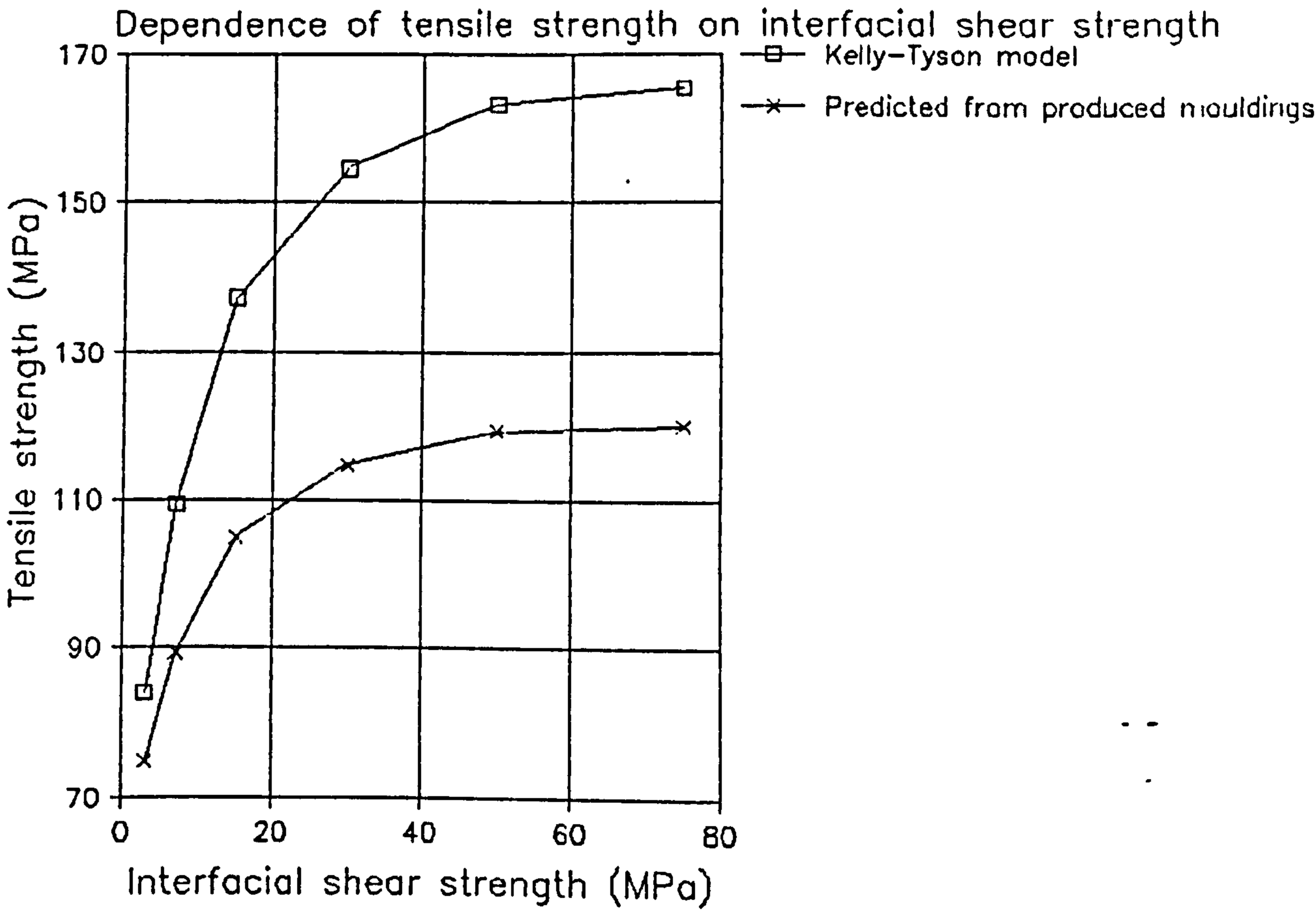
KEVLAR REINFORCED NYLON 66
Dependence of tensile strength on interfacial shear strength
Kelly-Tyson model
Predicted from produced mouldings
Tensile strength (MPa)
170
150
130
110
90
70
0
20
40
60
80
Interfacial shear strength (MPa)

Figure 137

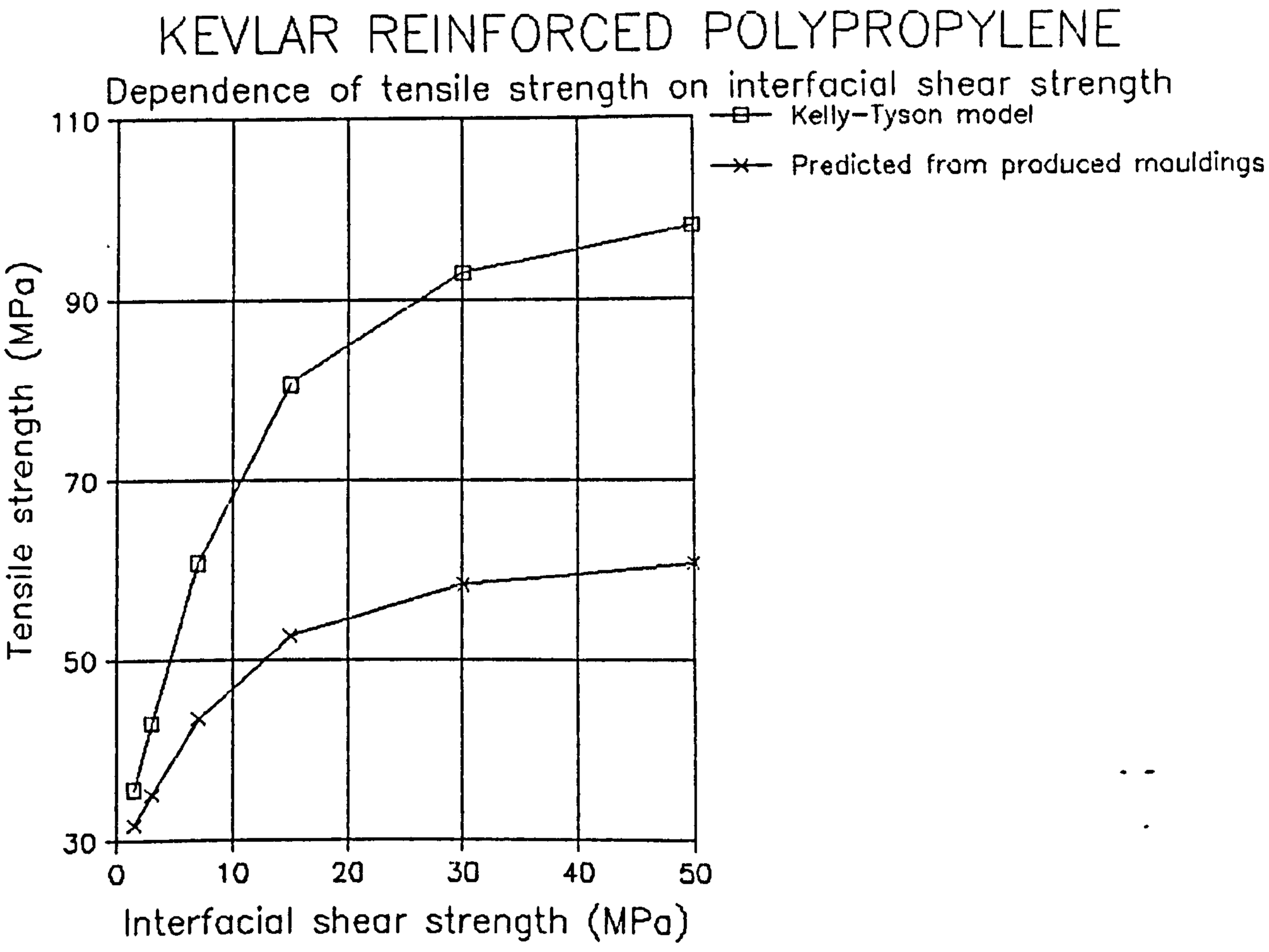
KEVLAR REINFORCED POLYPROPYLENE
Dependence of tensile strength on interfacial shear strength
Kelly-Tyson model
Predicted from produced mouldings
Tensile strength (MPa)
110
90
70
50
30
0
10
20
30
40
50
Interfacial shear strength (MPa)

Figure 138

The various types of feature in a force-deflection curve.

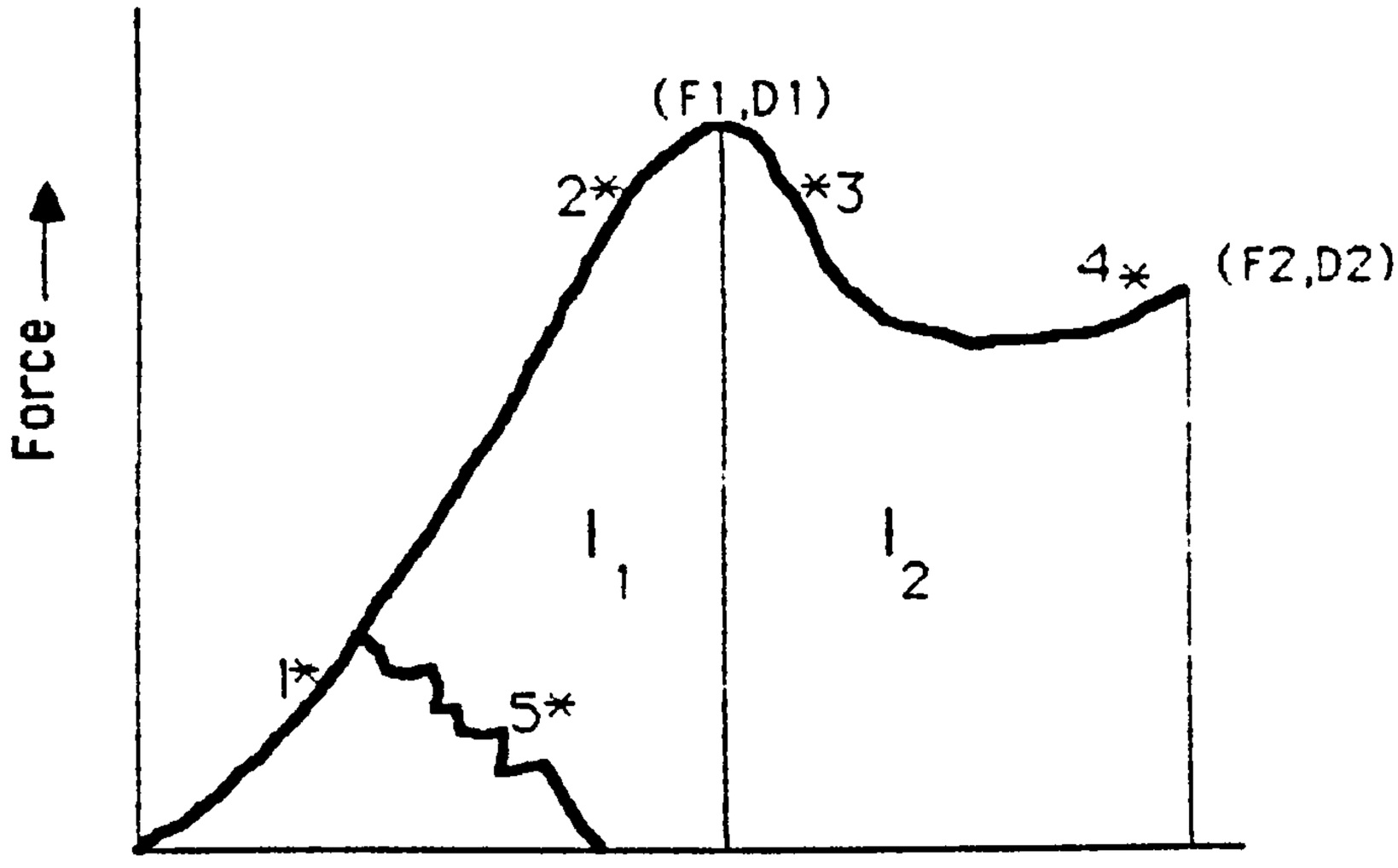

Elements that may be extracted from a force-deflection curve.

-Stiffness, this is related to the slope of a straight line region up to yield (coordinates F1,D1)

-Yield force (F1)

-Yield deflection (D1)

-Energy to yield (I_1) (intergral of curve up to co-ordinates F1,D1)

-Energy to fracture (I_B) ($I_B = I_1 + I_2$)

-Fracture deflection (D2)

-Type of curve (1,2,3,4, or 5 : the figures are the fracture points e.g. the fracture points of the curve) i.e. :

Type 1 Brittle. Type 2 Brittle-Ductile. Type 3 Ductile-Brittle.

Type 4 Ductile. Type 5 Initiation followed by propagation.

Figure 139

Force-deflection impact curves for Kevlar reinforced polypropylene produced in experiment KEVLAR 1.

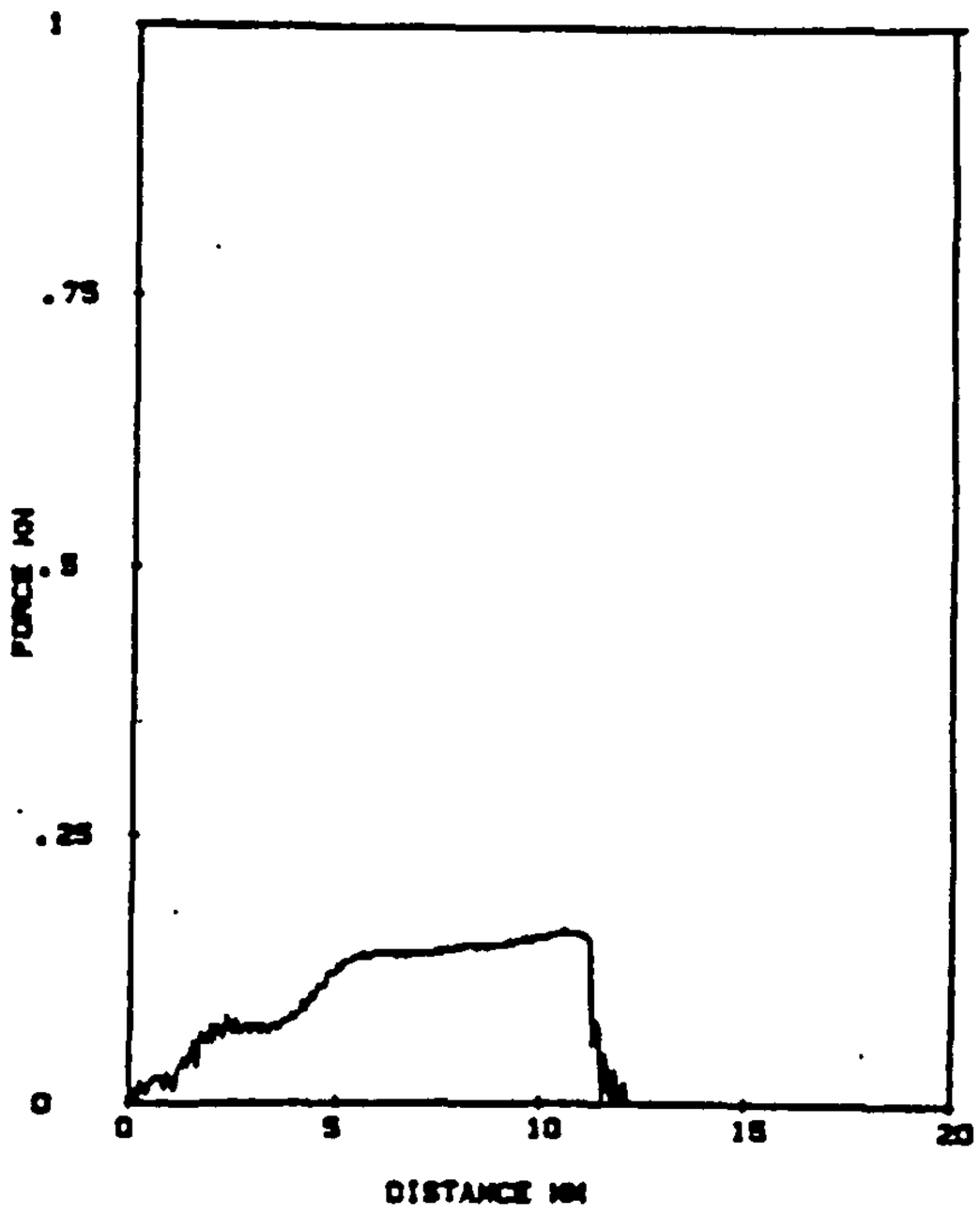

a. 24 % vol. fraction 10 RPM

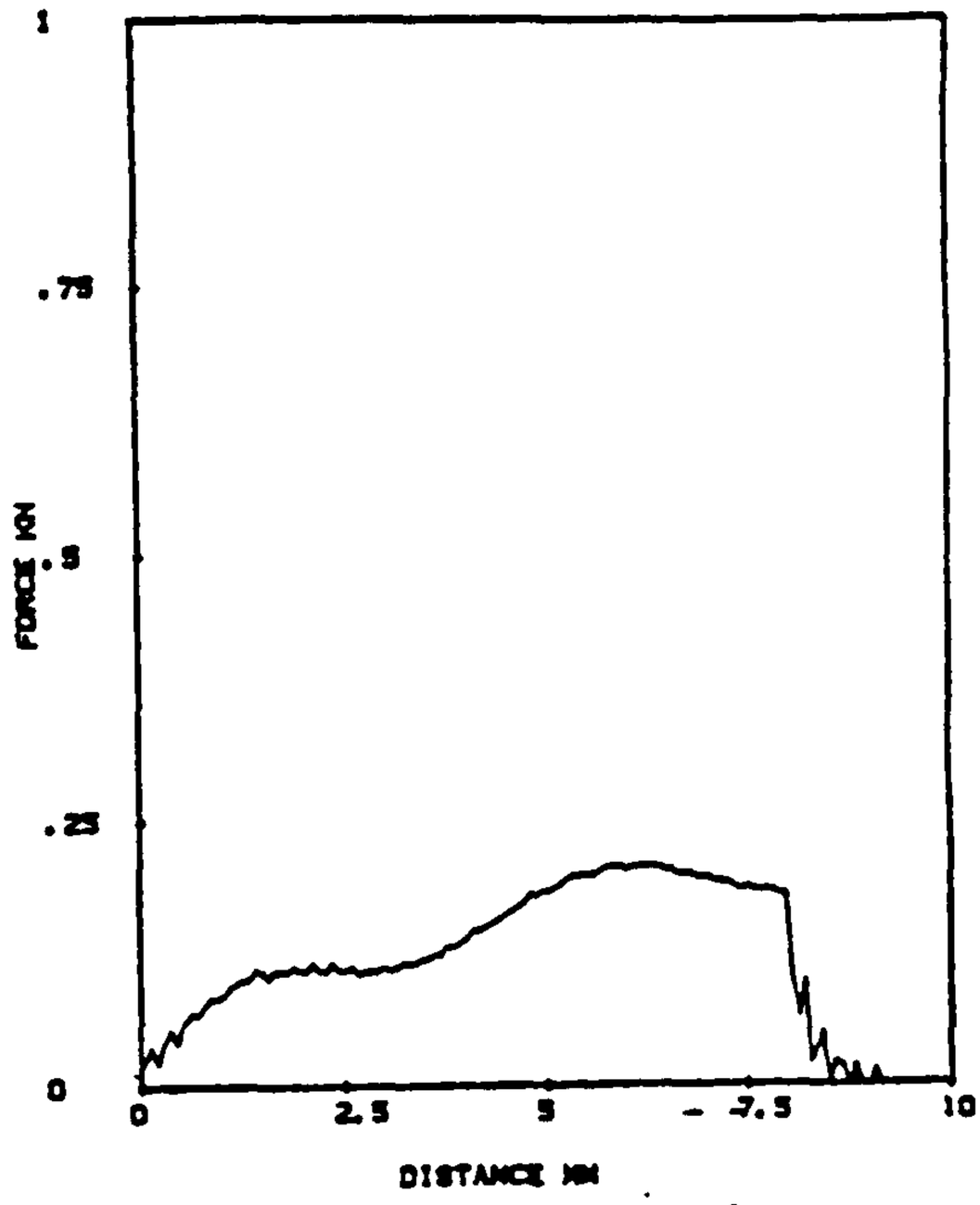

b. 19 % Vol fraction 30 RPM

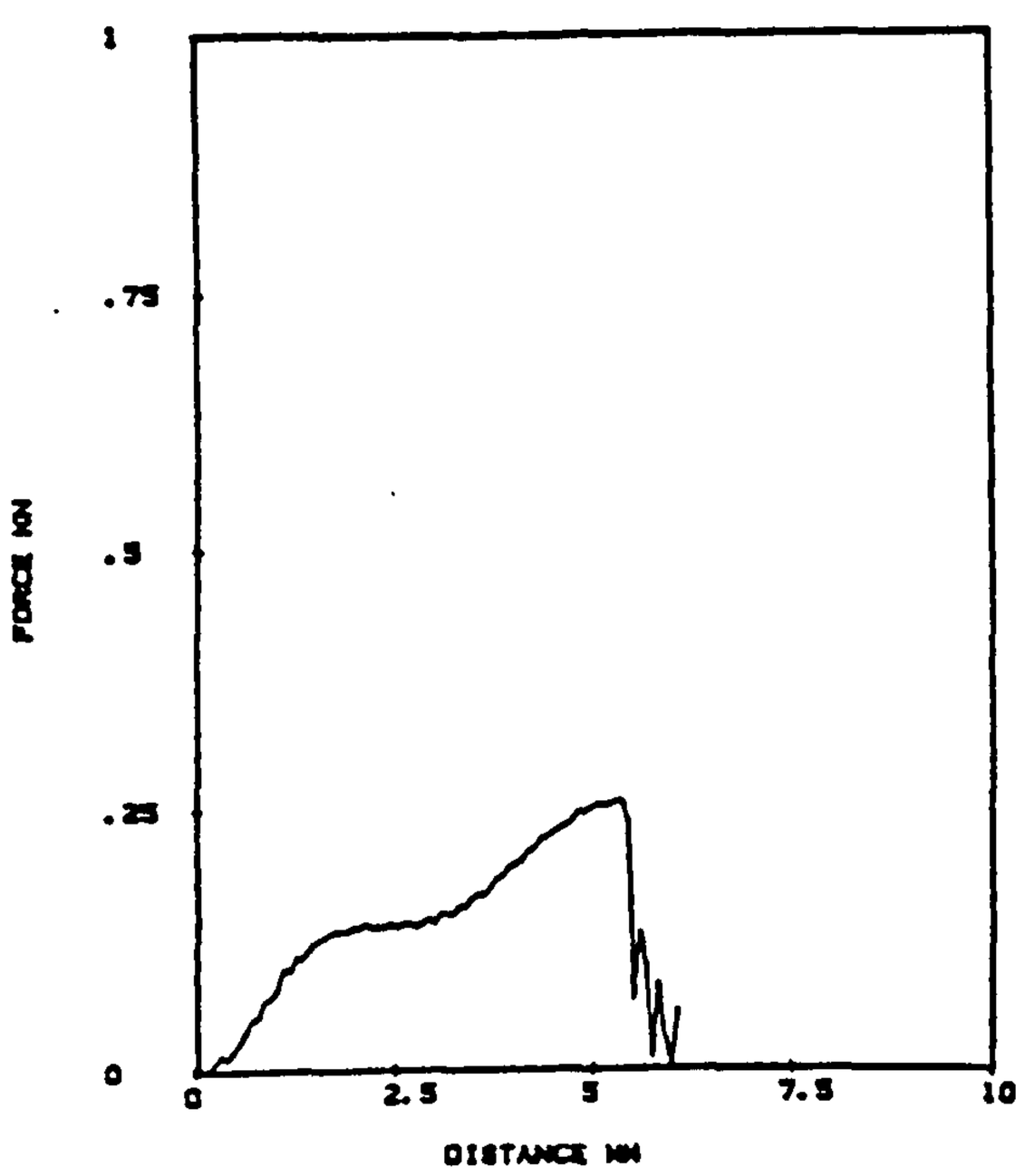

c. 19 % Vol fraction 50 RPM

Figure 140

The fracture surface in impact of an
injection moulded plaque of compound K1

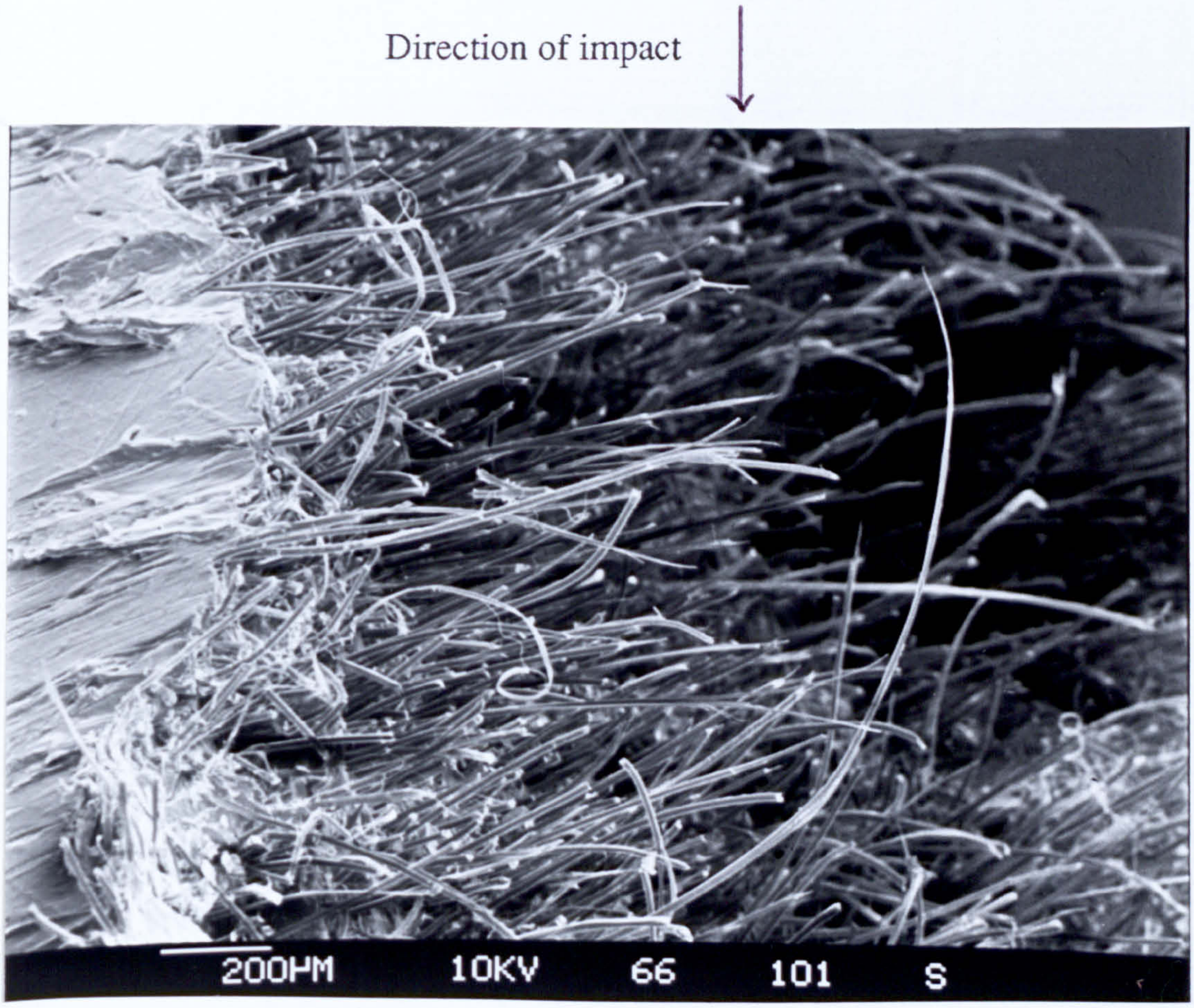

Figure 141

Force-deflection impact curves for polypropylene and glass reinforced polypropylene plaques

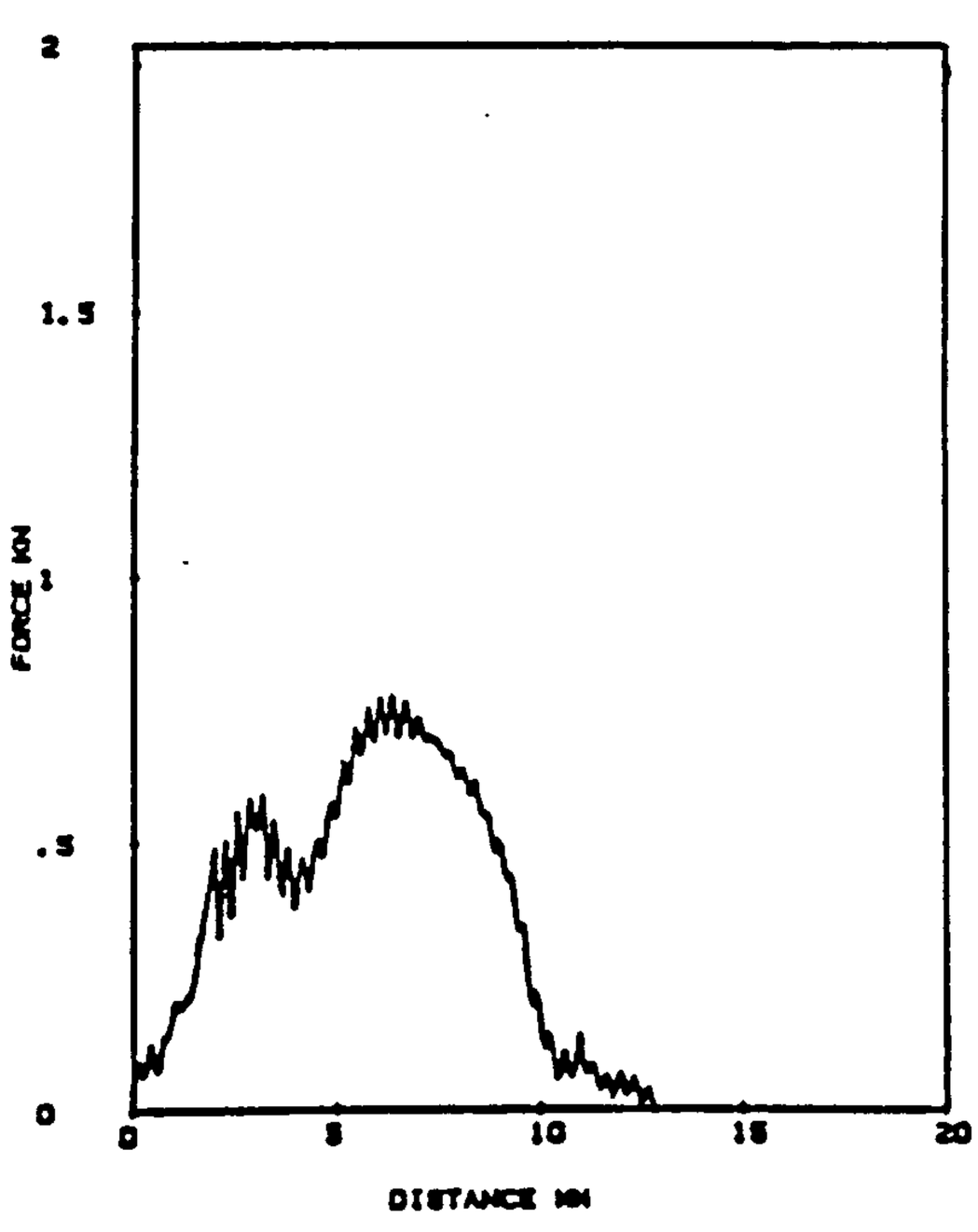

a. 8.1 % Vol. fraction glass

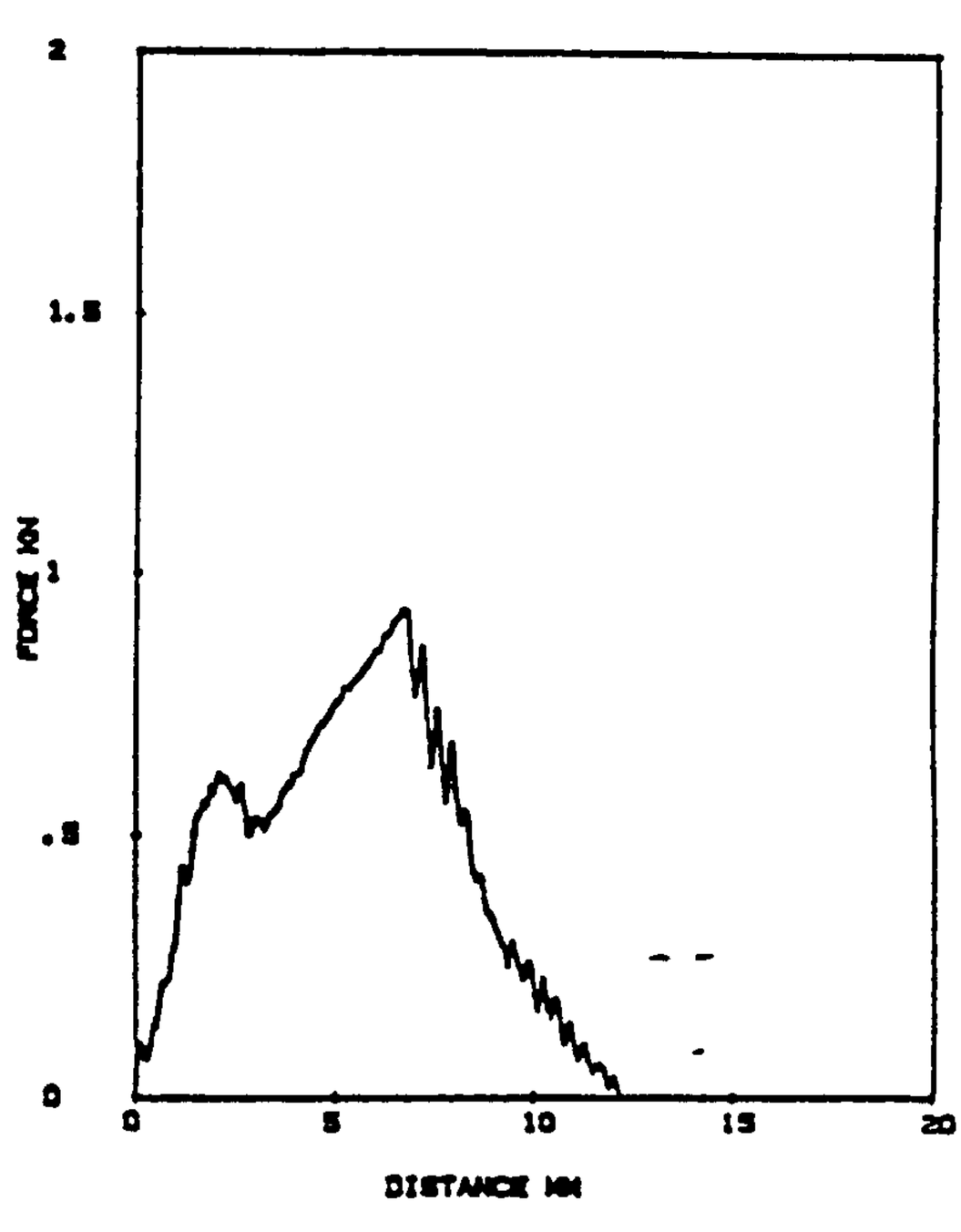

b. 13.2 % vol. fraction glass

Figure 142

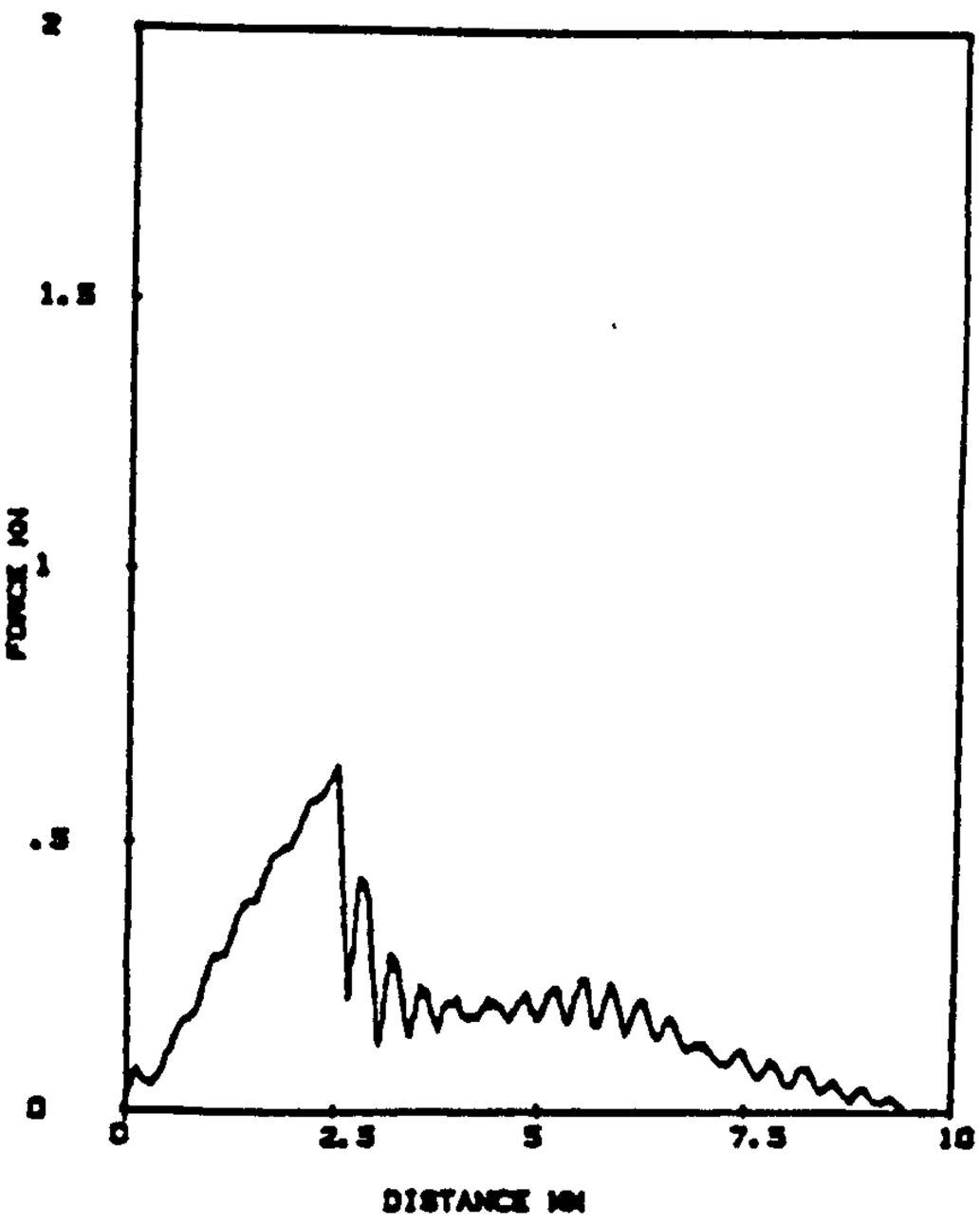

Polypropylene

Force-deflection impact curves for Kevlar reinforced polypropylene plaques

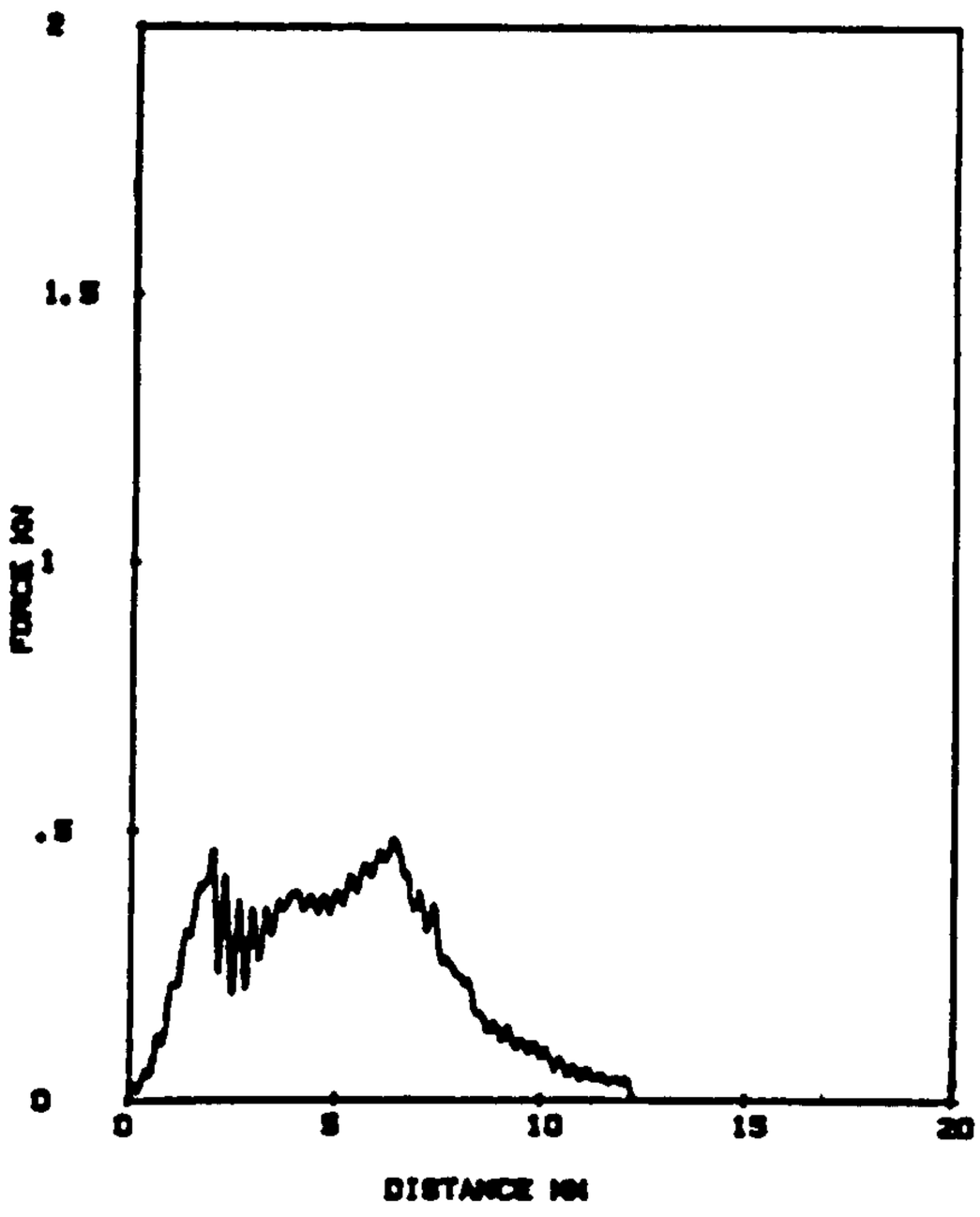

a. 8% Vol. fraction Kevlar

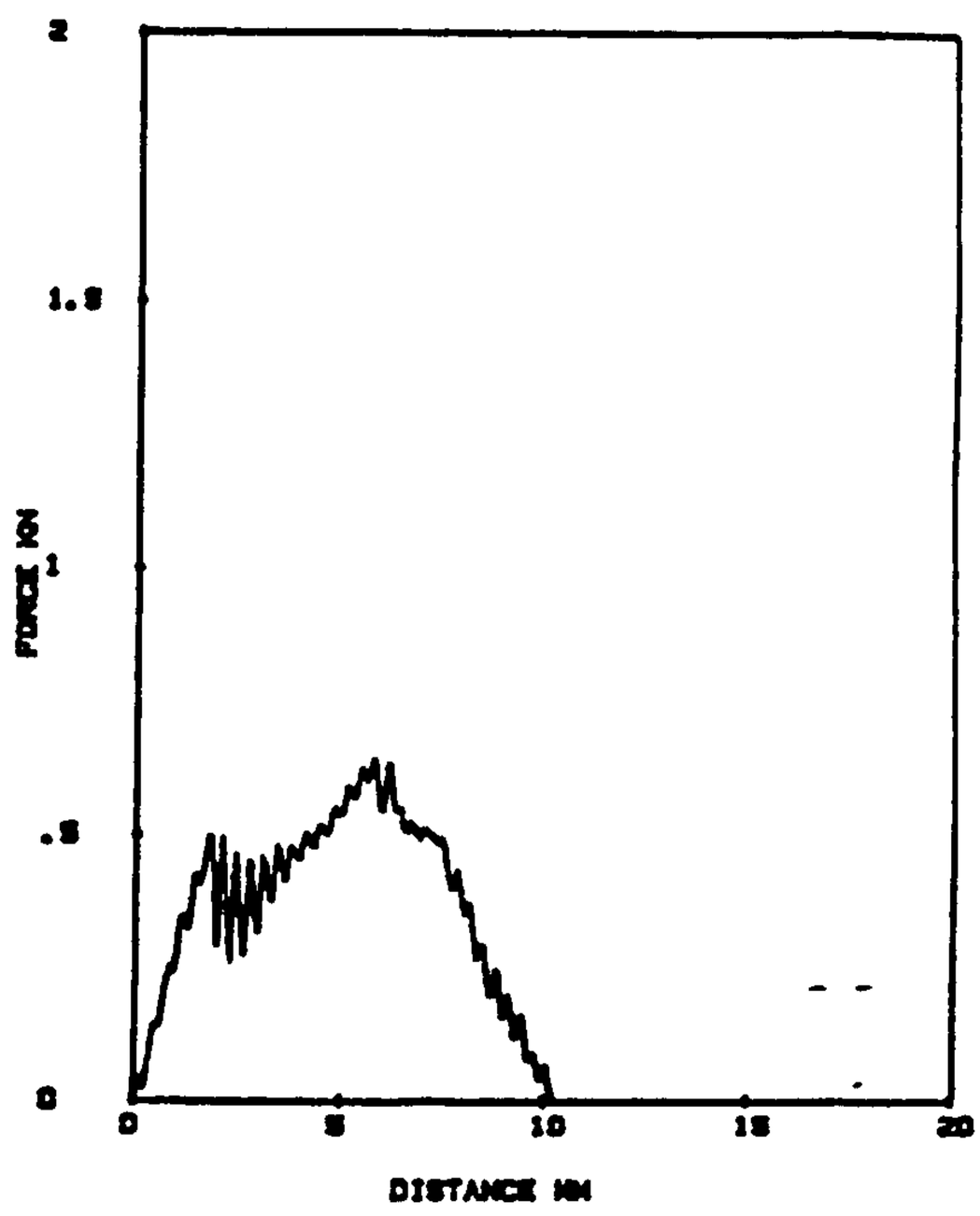

b. 12% vol. fraction Kevlar

Figure 143

The fracture surface in impact of an injection moulded plaque of compound K 11

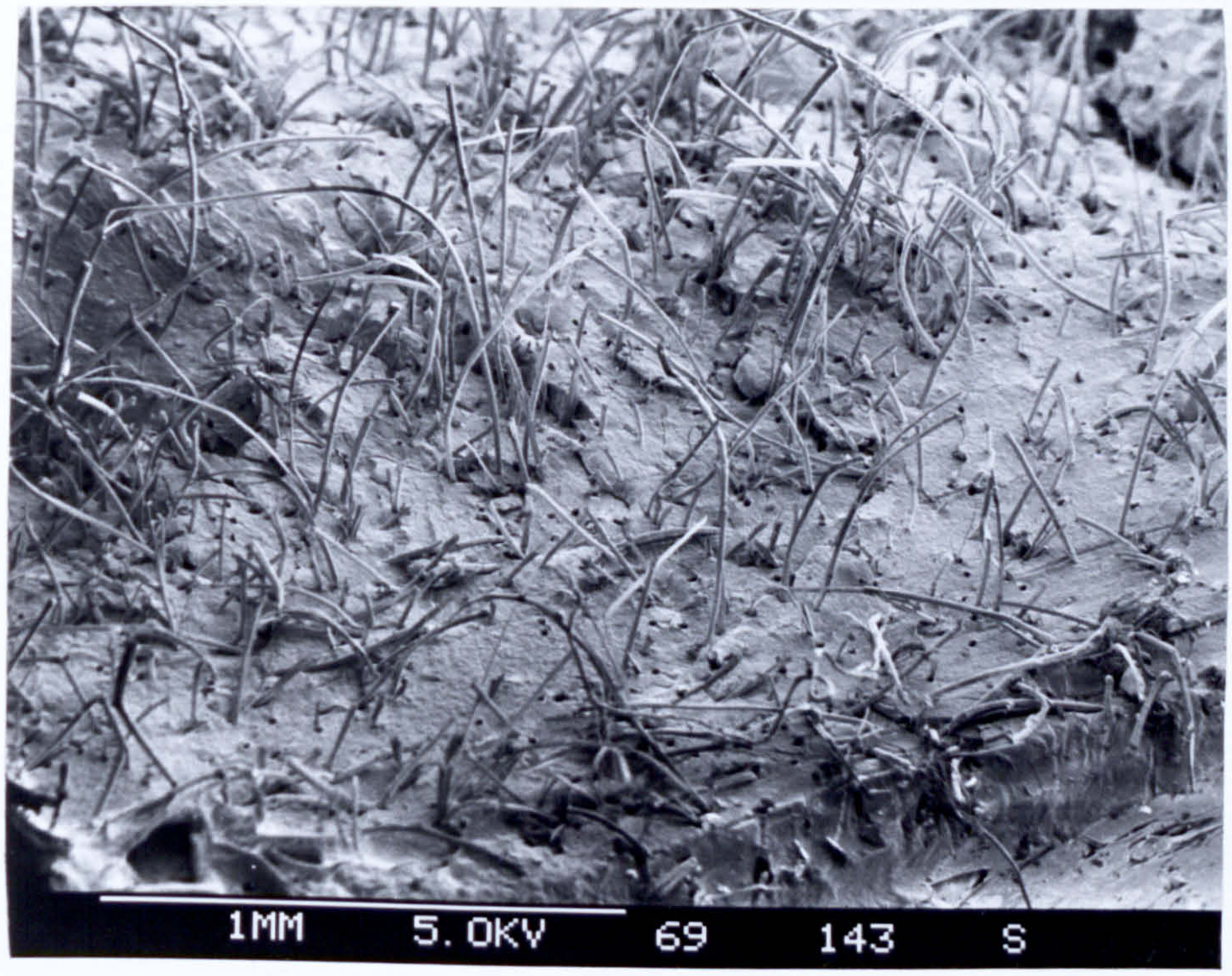

Direction of Impact

Figure 144

Force-deflection impact curves for nylon 66, glass reinforced nylon 66 and Kevlar reinforced nylon 66 plaques.

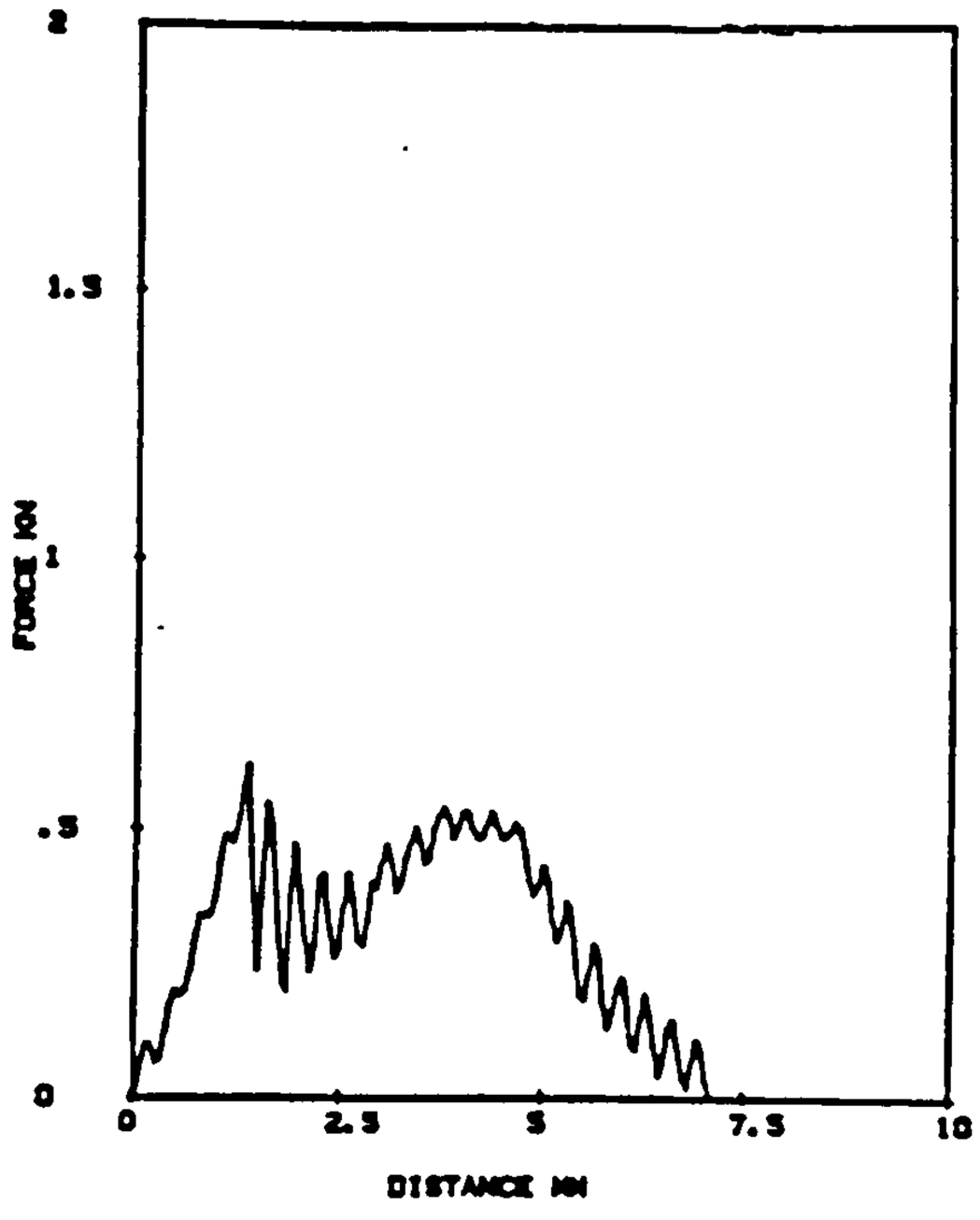

a. 8% Vol. fraction Kevlar

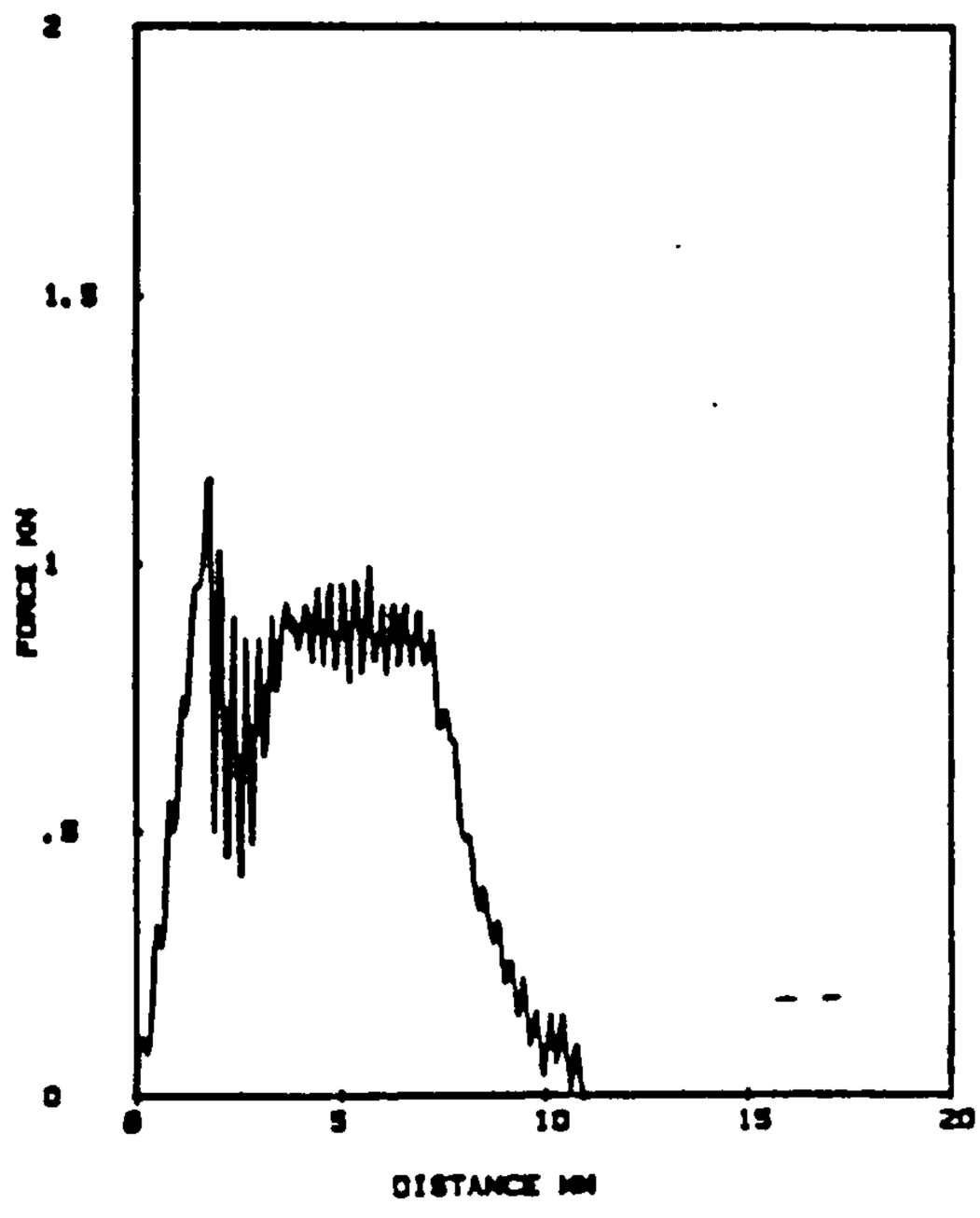

b. 8 % vol. fraction glass

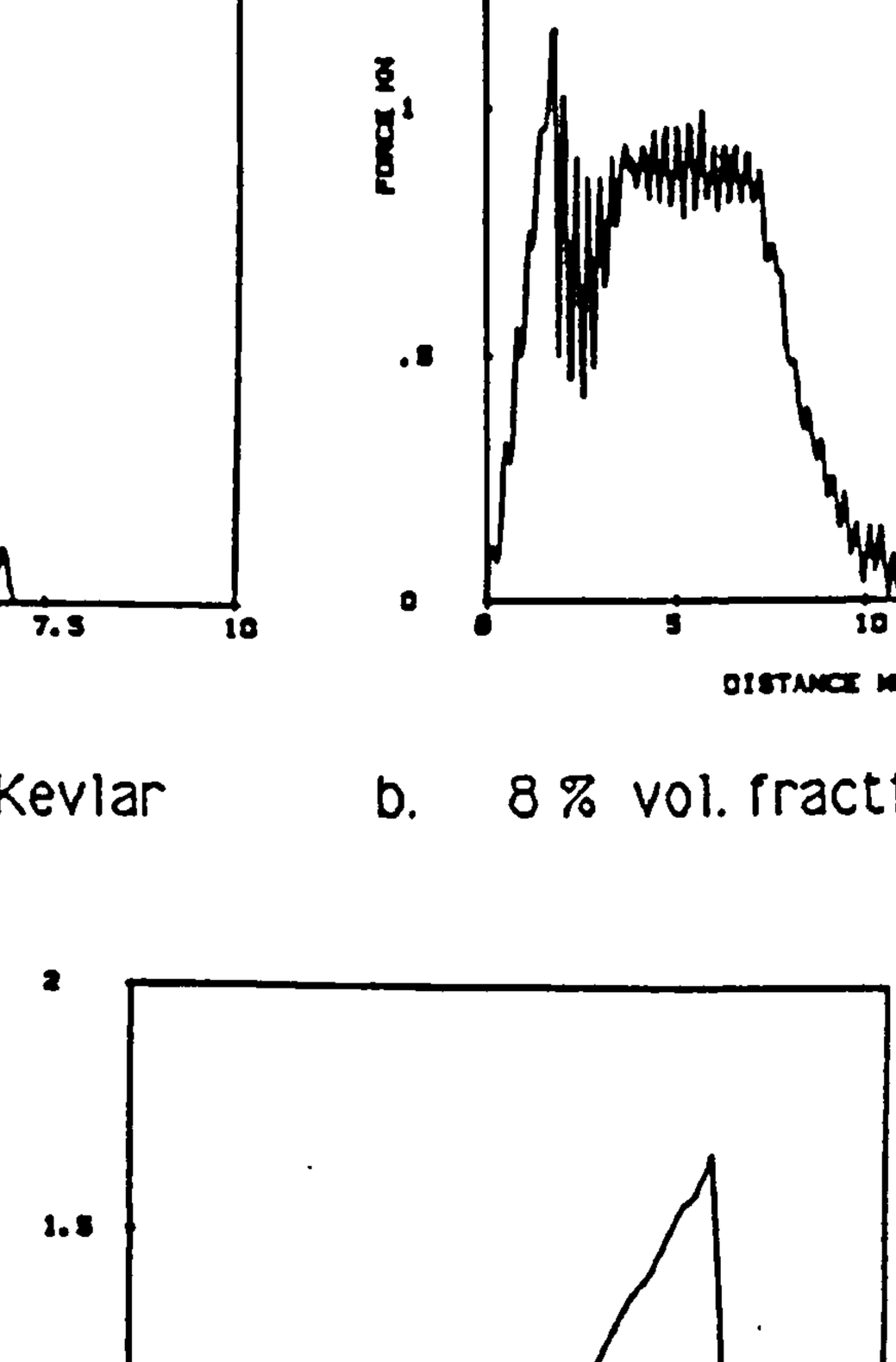

Figure 145

c.. Nylon 66.

The fracture surface in impact of a processed but unreinforced injection moulded plaque of nylon 66

Direction of Impact

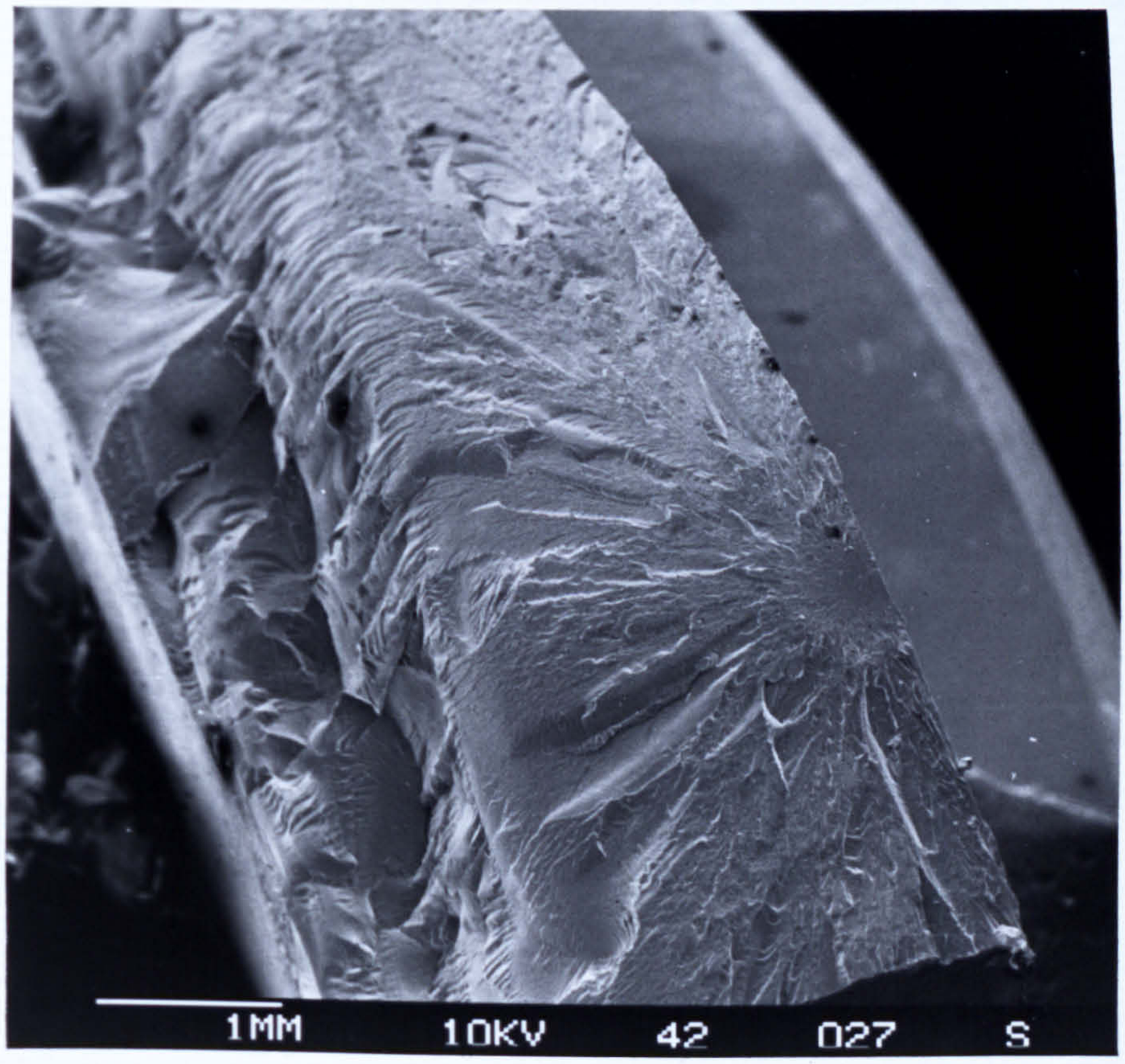

Figure 146

The fracture surface in impact of an injection moulded plaque of compound K 13

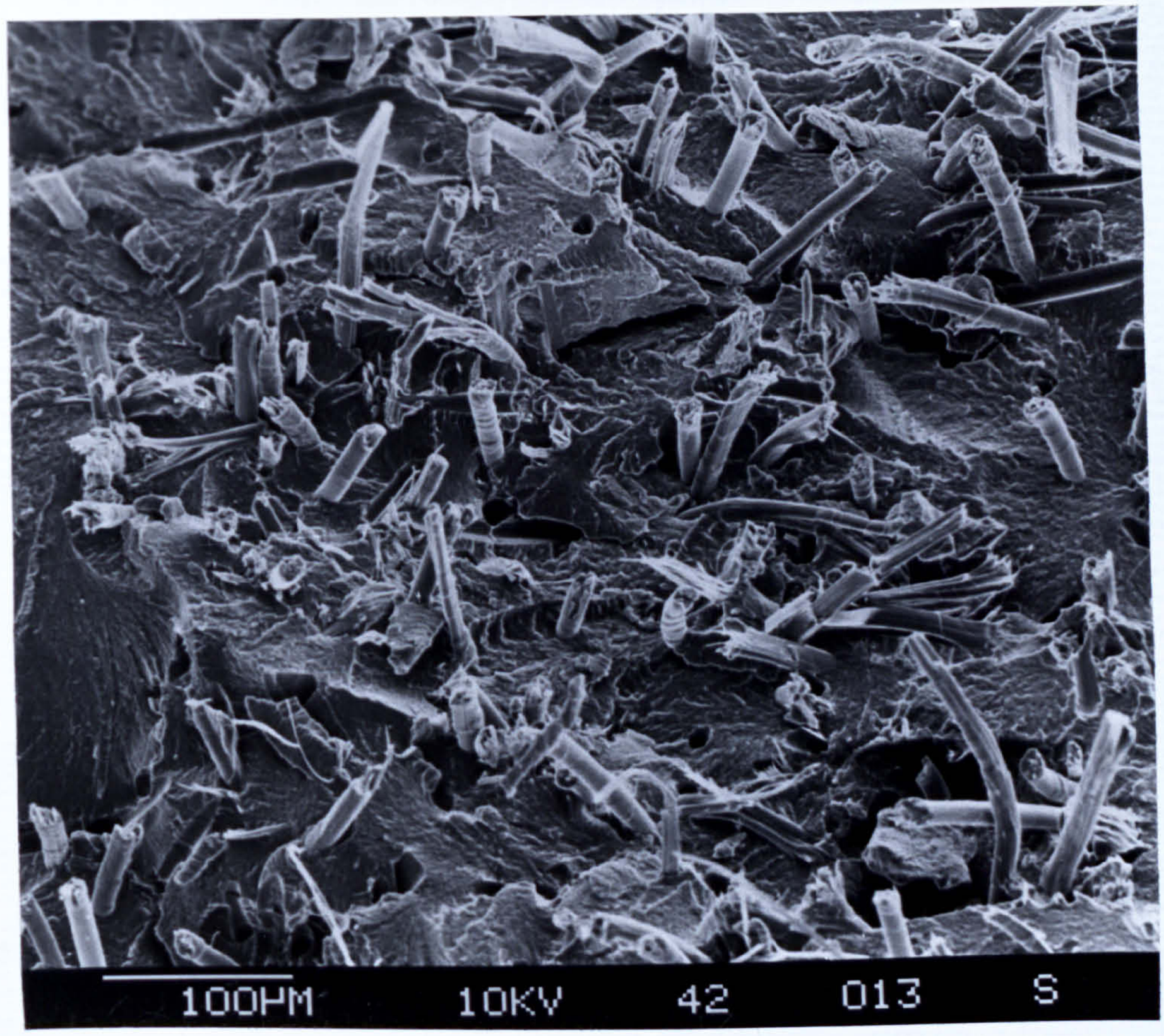

Figure 147

Force-deflection impact curves for G estimations of glass reinforced nylon 66.

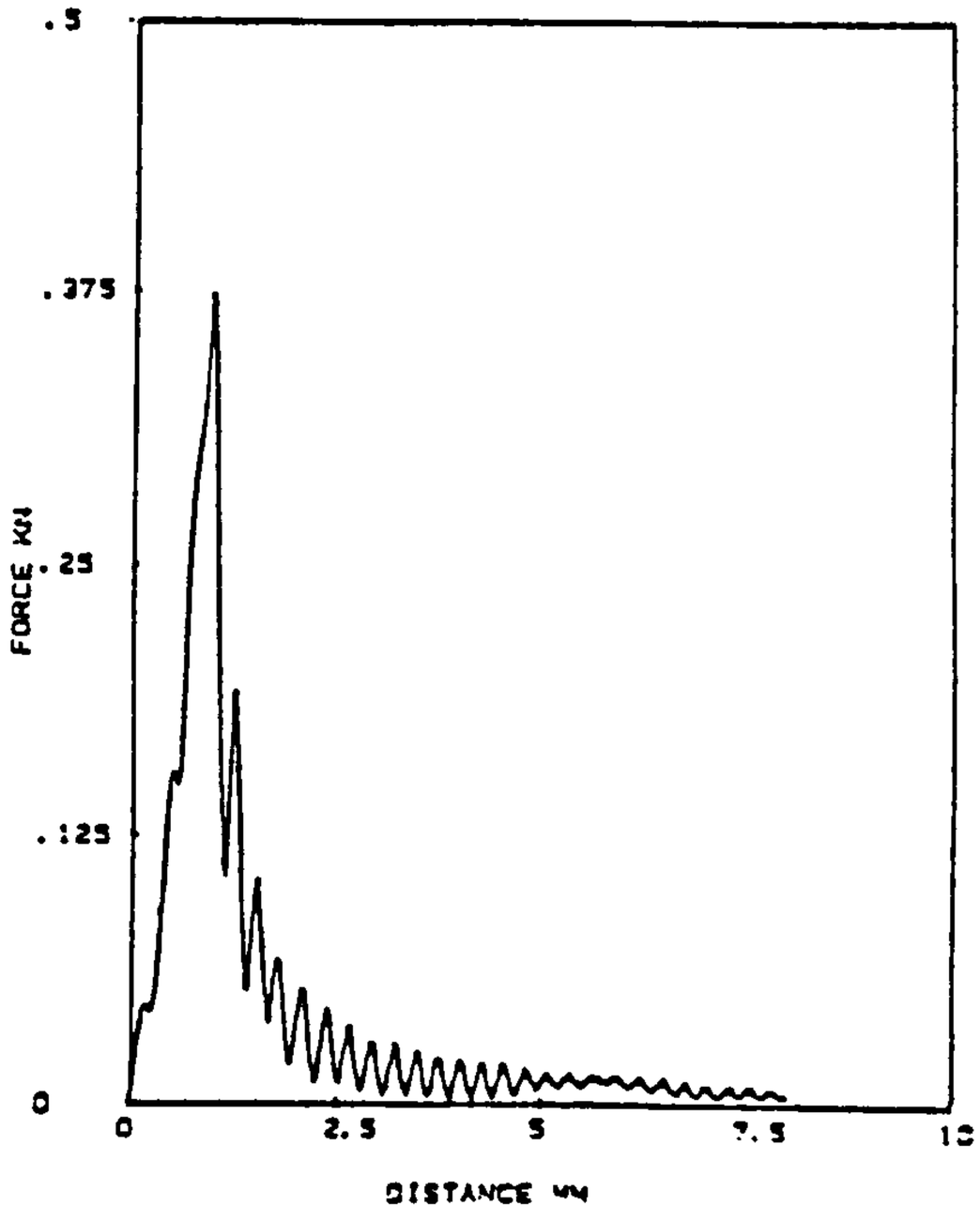

a. Compound G3

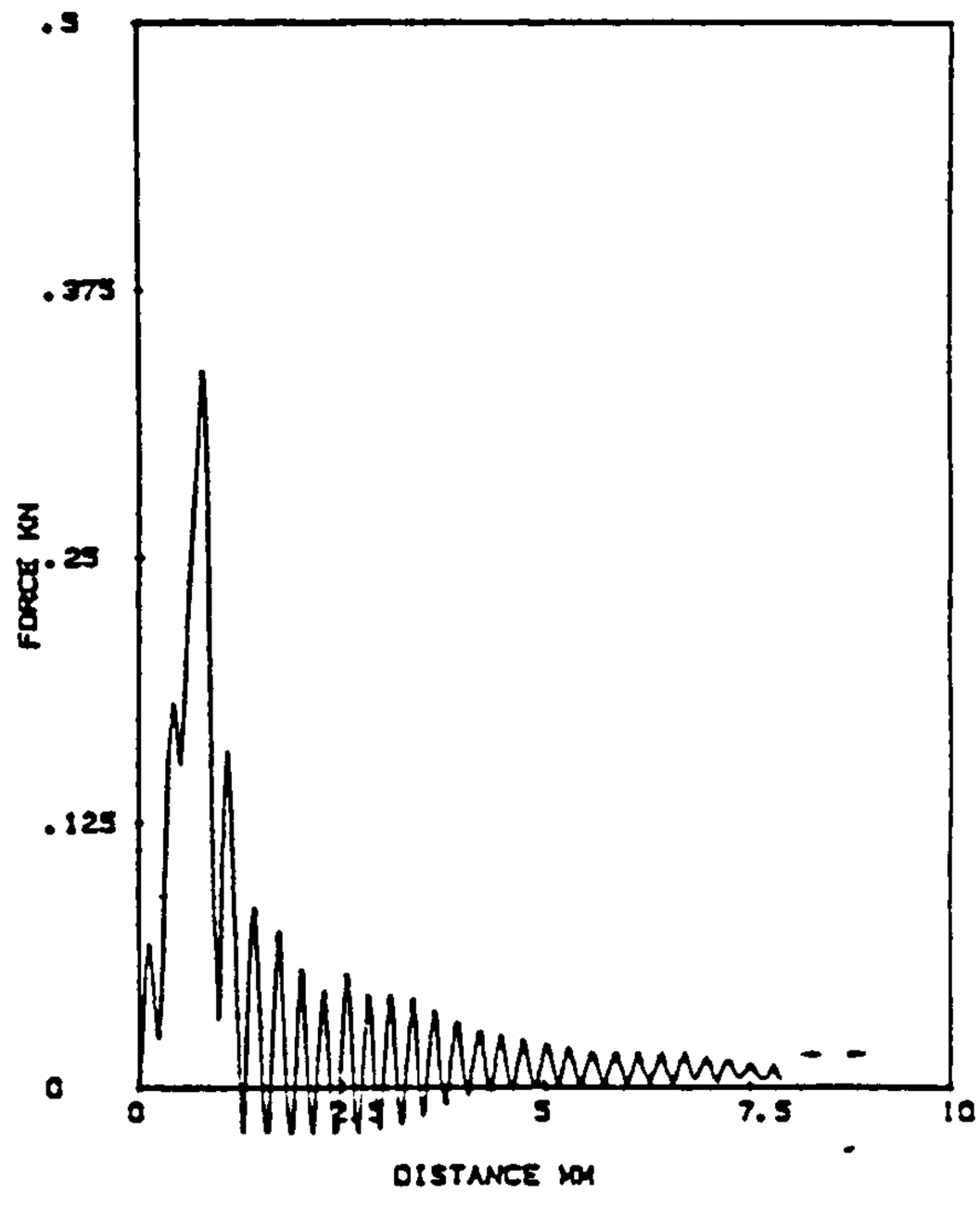

b. Compound G6

Figure 148

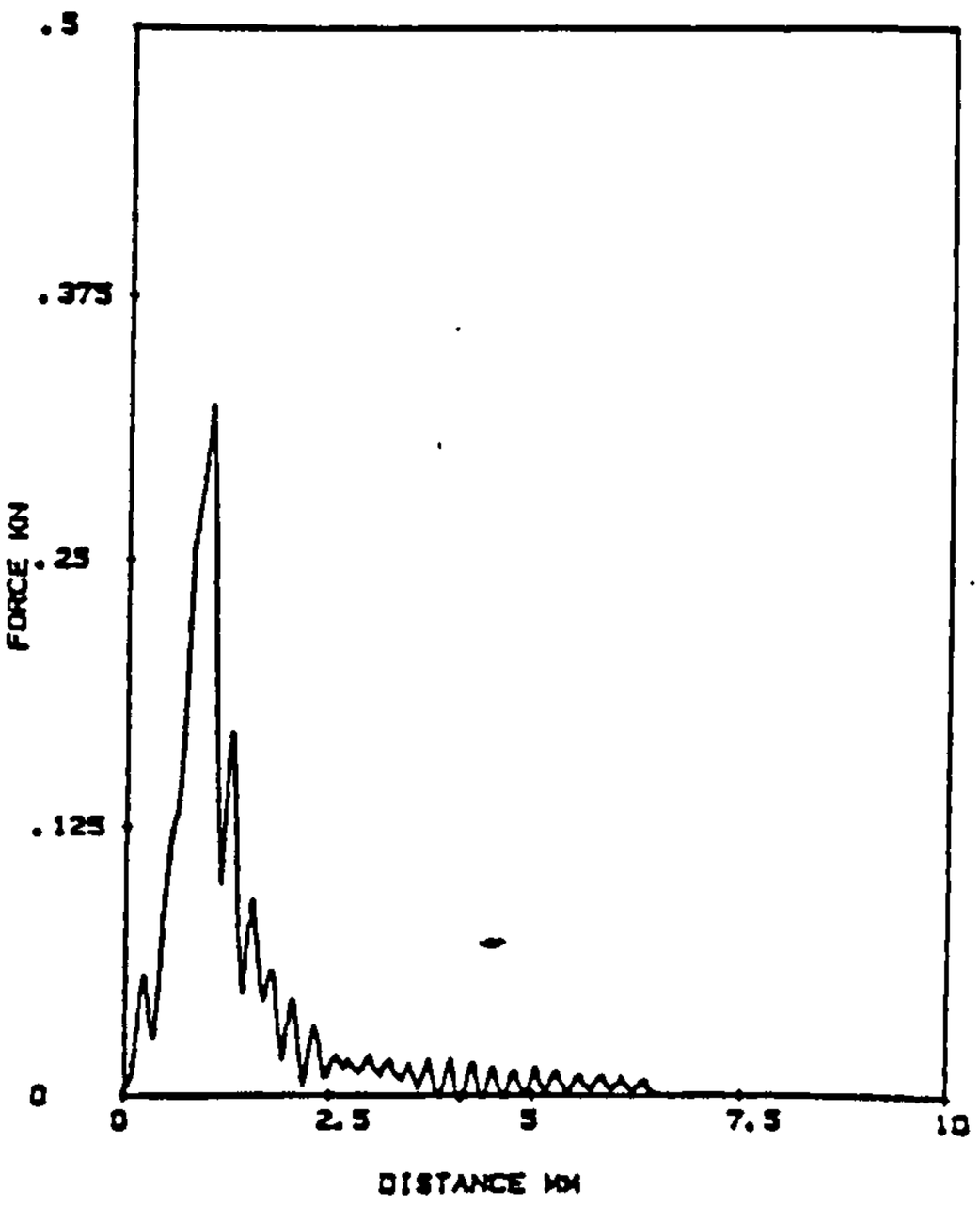

c Compound G7

Analysis of sample points from experiment BRITTLE 1

Section	Die	1	4	7	13	19	21	22	23	24	25	
"Bundles"												
%		0	0	0	0	0	0	51	41	70	72	89
Average Length		--	--	--	--	--	--	7.5	8.2	8.1	10.2	12.5
"Debris"												
%		100	100	100	100	100	100	49	59	30	28	11
Fibre Length (um)												
Wt. Av.		302	374	330	332	395	514	317	328	310	305	405
No. Av.		270	319	290	280	382	508	310	305	264	265	302

Table 26

Experiment BRITTLE 2. Carbon fibre reinforced nylon 66

Material	Extrudate Average fibre length (um) No. av	Wt. av	Inj. Moulded Average fibre length (um) No. av	Wt. av	Tensile strength (MPa)	Tensile modulus (GPa) 1% strain	Property index Tensile modulus	Tensile strength
16mm pitch metering screw Tow feed 8.2 Wt.% 5.3 Vol.%	552	601	380	392	126 S.D 2.12	5.55 S.D. 0.15	1.25	1.58
16mm pitch metering screw chopped feed 2.8 Wt % 1.8 Vol%	265	401	233	265	61 S.D. 0.5	2.85 S.D. 0.21	Below properties of matrix	
8mm pitch metering screw low feed 7.72 Wt % 5.06 Vol %	321	467	243	259	94 S.D. 0.59	4.88 S.D. 0.30	1.17	1.25
8mm pitch metering screw chopped feed 10.1 Wt % 6.67 Vol%	220	400	202	235	82 S.D. 3.21	4.83 S.D. 0.23	0.84	0.90
RG 20 18.85 Wt % 12.88 Vol %	230	257	206	215	183 S.D. 2.60	10.61 S.D. 0.31	1	1

$$\text{Property index} = \frac{\text{property of material/fibre content of material}}{\text{property of RG20/fibre content of RG20}}$$

Table 27

Experiment BRITTLE 3. Carbon fibre reinforced nylon 66.

Material produced using 16mm pitch metering screw
tow feed

Effect of die on fibre length of extruded material

	Average fibre length (um)	
	No. av.	Wt. av
Die used		
Rod 6mm diameter	534	679
3mm slit	492	632
4.4mm slit	424	515

Effect of granulating/ pelletising operation

Rod 6mm diameter die material used

Cumberland 5X7 granulator	290	347
Broyeurs Malangeurs L100 granulator	264	312
Cumberland 6" pelletiser	342	428

Effect of injection moulding operation

4.4mm slit die material used

Cumberland 5X7 granulated	278	348
Injection moulded	260	308

Table 28

Hybrid glass/carbon

Extrudate	141	166

Experiment BRITTLE 4. Properties of carbon fibre compounds

	C1	C2	C3	C4	C5	C6	RG20
Volume fraction (%)	13.95	13.43	6.81	8.25	8.31	13.70	12.12
Extruded average fibre length							
No.Av. (mm)	0.246	0.137	0.282	0.263	0.267	0.101	0.230 *
Wt.AV. (mm)	0.289	0.168	0.313	0.310	0.300	0.134	0.257 *
Injection moulded average fibre length					* Pelletised		
No.Av (mm)	0.219	0.126	0.254	0.251	0.254	0.095	0.193
Wt.Av.(mm)	0.271	0.165	0.302	0.303	0.302	0.127	0.243
Ultimate tensile strength (MPa)	179	112	147	167	149	116	183
S.D.	2.8	2.1	5.8	1.8	5.0	3.6	2.7
Strain at break (%)	2.62	3.15	2.05	2.10	2.04	3.2	2.85
Tensile modulus @ 0.5% strain (GPa)	13.18	8.06	9.36	10.58	10.56	7.93	12.89
S.D.	0.20	0.09	0.37	0.16	0.15	0.10	0.27
Flexural modulus(GPa)	9.94	6.01	8.23	8.64	9.51	5.99	10.09
S.D.	0.24	0.1	0.95	0.91	0.70	0.31	0.35
Cox estimation of tensile modulus (GPa)	15.34	9.58	9.42	10.60	10.66	7.81	12.44
Rule of mixtures estimate of tensile modulus(GPa)	33.23	32.14	17.77	20.9	21.09	32.73	29.30
Interfacial shear strength (MPa)	Assumed to be the shear strength of the matrix (48 MPa)						
Orientation ratio	0.7142	0.778	0.8477	0.7572	0.7733	0.7116	0.817
Stress transfer efficiency (strength)	0.4705	0.2791	0.5351	0.5059	0.5167	0.2124	0.4101
Stress transfer efficiency (modulus) @ 0.5% strain	0.7582	0.5689	0.7789	0.7706	0.7796	0.4667	0.695

Table 29

Experiment BRITTLE 4. Properties of glass fibre compounds

	G1	G2	G3	G4	G5	G6
Volume fraction (%)	9.905	8.904	8.685	9.56	9.06	9.87
Extruded average fibre length						
No.Av. (mm)	0.225	0.380	0.390	0.394	0.380	0.176
Wt.AV. (mm)	0.320	0.451	0.462	0.477	0.480	0.239
Injection moulded average fibre length						
No.Av (mm)	0.204	0.315	0.339	0.377	0.374	0.166
Wt.Av.(mm)	0.314	0.402	0.421	0.455	0.467	0.225
Ultimate tensile strength (MPa)	80	119	120	127	126	74
S.D.	4.2	2.8	2.7	2.1	2.7	5.6
Strain at break (%)	3.64	2.65	2.46	2.55	2.42	3.4
Tensile modulus @ 1.0% strain (GPa)	4.66	6.46	6.53	6.59	6.80	4.61
S.D.	0.19	0.21	0.17	0.24	0.16	0.19
Flexural modulus(GPa)	3.09	4.86	4.88	5.45	5.24	2.82
S.D.	0.12	0.22	0.08	0.45	0.16	0.2
Cox estimation of tensile modulus (GPa)	6.11	6.58	6.57	7.46	6.93	5.30
Rule of mixtures estimate of stiffness (GPa)	9.83	9.14	8.99	9.59	9.26	9.68
Interfacial shear strength (MPa)	23	32.6	28.6	28.5	27.7	26
Orientation ratio	0.7875	0.8121	0.8333	0.7830	0.7677	0.7051
Stress transfer efficiency (strength)	0.1464	0.2818	0.2570	0.2927	0.2866	0.1385
Stress transfer efficiency(modulus) @ 1.0% strain	0.4563	0.7164	0.7045	0.7345	0.7642	0.4484

Table 30

Estimation of interfacial shear strength from stress-strain curve for carbon fibre reinforced compound 1C

	Strain taken (%)	Stress at strain (MPa)	Calculated interfacial shear strength (MPa)
e1	0.25	34.09	
			110
e2	0.50	65.9	
e1	0.50	65.9	
			89
e2	1.0	120.9	
			- -
e1	1.0	120.9	-
			60
e2	2.0	171	
e1	1.3	149.5	
			52
e2	2.6	179.6	

Matrix shear yield strength 48 MPa

Table 31

Experiment BRITTLE 5 properties of glass reinforced nylon 66. compound. G7

Volume fraction (%)	Average fibre length (um)						Tensile strength (MPa)
	On discharge		Pelletised		Injection moulded		
	No av.	Wt av.	No. av	Wt. av	No. av	Wt. av	
							100
7.813	898	1224	567	696	467	576	
							S.D. 1.12

Tensile modulus 1% strain (GPa)	Flexural modulus (GPa)	Stress transfer interface efficency (strength)
5.6	4.7	0.2261
S.D. 0.32	S.D. 0.13	

Stress transfer interface efficency (modulus @ 1%)	Interfacial shear strength (MPa)
0.6794	17.3

Orientation	Cox estimation of tensile modulus (GPa)
0.6042	6.67

Rule of mixtures estimation of tensile modulus (GPa)
8.39

Elongation at break (%)
1.69

Table 32

Experiment BRITTLE 6. Properties of carbon fibre compounds

Table 33

	C7	C8	C9	C10	C11	C12	C13
Volume fraction (%)	0.947	12.60	14.76	22.16	6.25	4.73	3.58
Extruded average fibre length							
No.Av. (mm)	0.482	0.502	0.485	0.484	0.480	0.452	0.430
Wt.AV. (mm)	0.583	0.670	0.646	0.561	0.672	0.644	0.545
Injection moulded average fibre length							
No.Av (mm)	0.312	0.258	0.207	0.198	0.253	0.299	0.264
Wt.Av.(mm)	0.382	0.326	0.265	0.245	0.327	0.368	0.323
Ultimate tensile strength (MPa)	64	181	213	242	99	94	80
S.D.	5.8	2.1	5.3	1.4	7.3	5.6	7.0
Strain at break (%)	2.0	1.85	1.7	1.38	1.78	1.76	1.85
Tensile modulus @ 0.5% strain (GPa)	4.22	13.53	14.62	20.70	8.24	6.50	5.36
S.D.	0.05	0.67	0.23	0.88	0.93	0.15	0.26
Flexural modulus(GPa)	2.98	9.28	12.3	17.98	6.29	5.42	4.04
S.D.	0.1	0.43	0.28	0.48	0.57	0.37	0.22
Cox estimation of tensile modulus (GPa)	3.93	15.82	16.17	23.78	9.34	8.19	6.41
Flexural strength (MPa)	100	252	300	365	200	187	146
Rule of mixtures estimate of tensile modulus (GPa)	5.05	30.35	35.03	51.0	16.56	13.26	10.76
Interfacial shear strength (MPa)	Assumed to be the shear strength of the matrix (48MPa)						
Orientation ratio	———	0.6921	0.7947	0.8120	0.6036	0.6586	0.675
Stress transfer efficiency (strength)	———	0.4996	0.4338	0.4217	0.4989	0.5615	0.522
Stress transfer efficiency (@ 0.5% strain)	———	0.7593	0.7114	0.7044	0.7576	0.7966	0.770

The Influence of volume fraction on the strain to break of carbon fibre reinforced nylon 66.

Compound	Volume fraction (%)	Failure strain (%)	Fibre length (mm) Wt. average	No. average
C3	6.31	2.05	0.302	0.254
C8	12.6	1.89	0.326	0.258
C10	22.2	1.38	0.245	0.198

Table 34

Experiment KEVLAR 1 polypropylene/Kevlar 49 compounds (single screw compounded)

		K1	K2	K3	K4
Volume fraction (%)	0	18.67	18.78	24.22	10.78
Screw speed (RPM)	--	50	30	10	30
Tensile strength (MPa)	26.4	39.6	33.7	34.05	30.8
S.D.	0.61	1.71	0.97	0.69	0.84
Modulus 1% strain (GPa)	1.24	2.175	1.79	1.90	1.45
S.D.	0.12	0.12	0.06	0.09	0.07
Failure strain (%)	>20	4.3	6	7.1	11
Interfacial shear strength (MPa)	—	2.38	2	1.8	1.5
Orientation ratio	—	0.31	0.21	0.156	—

Table 35

Experiment KEVLAR 1 polypropylene/Kevlar 49 compounds (single screw compounded). Fibre properties.

	Compounds			
	K1	K2	K3	K4
Extruded fibre length.				
No. average (mm)	4.8	3.2	3.75	3.76
wt. average (mm)	5.7	4.12	3.82	3.04
Distance between kink faults (mm)	0.383	0.414	0.424	0.473
S.D.	0.174	0.169	0.208	0.192
Injection moulded fibre length				
No. average (mm)	1.84	1.78	1.83	2.17
wt. average (mm)	2.62	2.50	1.98	3.03
Distance between kink faults (mm)	0.248	0.325	0.320	0.335
S.D.	0.110	0.182	0.126	0.127

Table 36

Experiment KEVLAR 2 polypropylene/Kevlar 49 compounds.
(single screw compounded and Ti. coupling agent treated)

	K5	K6	K7	K8	K9	K10
Volume fraction (%)	17.1	13.4	13.4	6.5	14.2	14.1
Screw speed (RPM)	10	30	50	30	30	30
Coupling agent added (%)	1	1	1	1	3	5
Tensile strength (MPa)	40.2	37.9	42.3	34.7	38.5	35.4
S.D.	1.03	0.43	1.13	0.83	0.50	0.64
Modulus 1% strain (GPa)	2.31	1.87	2.25	1.78	2.08	1.94
S.D.	0.05	.041	0.13	0.04	0.067	0.06
Failure strain (%)	6.7	5	6.8	11	6.25	9.7
Interfacial shear (MPa) strength	--	--	3.2	--	--	--
Orientation ratio	--	--	0.12	--	--	--

Table 37

Experiment KEVLAR 3 polypropylene/Kevlar 49 compounds. (twin screw compounded)

	K11	K12	E-glass for comparision
Volume fraction (%)	8.76	12.5	8.78
Screw speed (RPM)	135	270	135
Fibre length			
Extruded:			
No. average (mm)	2.61	2.24	---
Wt. average (mm)	3.06	2.84	---
Injection moulded:			
No. average (mm)	1.95	1.87	---
Wt. average (mm)	2.43	2.49	---
Tensile strength (MPa)	31.04	34.33	57.2
S.D.	0.9	0.4	0.97
Modulus 1% strain (GPa)	1.46	1.60	3.43
S.D.	0.05	0.1	0.09
Flexural modulus (GPa)	2.11	2.25	4.44
S.D.	0.06	0.13	0.16
Cox estimation of tensile modulus (GPa)	6.81	9.77	---
Failure strain (%)	23.3	11.8	6
Interfacial shear strength (MPa)	——	2.21	16
Orientation ratio	0.153	0.2	0.43

Table 38

Experiment KEVLAR 4 nylon 66/Kevlar 49 compounds.(twin screw compounded)

		K13	K14	E-glass for comparision
Volume fraction (%)	0	8.07	12.1	8.86
Screw speed (RPM)	---	135	270	500
Tensile strength (MPa)	72	85	93	120
S.D.	1.4	1.9	3.5	2.7
Modulus 1% strain (GPa)	2.94	4.49	4.56	6.45
S.D.	0.16	0.27	0.16	0.17
Flexural modulus (GPa)	---	3.61	3.92	4.9
S.D.		0.33	0.18	0.08
Cox estimation of tensile modulus (GPa)	---	11.88	16.40	6.57
Failure strain (%)	>10	3.45	2.5	2.3
Interfacial shear strength (MPa)	---	7.05	6.8	28.6
Orientation ratio	---	0.11	---	0.833

Table 39

Mechanical anisoptropy investigation

Kevlar 49/Nylon 66.

Vol fraction (%)	8.07		
	U.T.S. (MPa)	Tens. Mod @1% strain. (MPa)	Strain at failure (%)
Position 1	62.9	3.5	2.45
Position 2	59.92	3.53	2.32
Position 3	63.69	3.67	2.09
Position 4	67.06	3.58	2.38
Position 5	62.07	3.57	2.24
Position 6	77.91	4.01	2.20

Glass (Etype)/Nylon 66.

Volume fraction (%)	8.685		
	U.T.S. (MPa)	Tens. Mod. @1% strain. (MPa)	Strain at failure. (%)
Position 1	77	3.97	2.26
Position 2	82	3.98	2.35
Position 3	80.6	4.96	1.94
Position 4	104.9	6.28	1.85
Position 5	102	5.12	2.23
Position 6	106	6.04	1.90

Table **40**

Experiment KEVLAR 1. Impact properties of polypropylene/Kevlar 49 compounds (impact bars)

Compound	Screw speed (RPM)	Vol fraction (%)	Stiffness	Yield force (N)	Energy to fracture (Nm)	Coefficient of variation energy to fracture (%)
--	--	0	32	110	2.3	5.5
K1	50	19	107	225	1.00	10.4
K2	30	19	74	180	1.13	13
K3	10	24	69	166	1.3	15
K4	30	11	102	222	1.15	12.9

Table 41

Experiment KEVLAR 2. Impact properties of polypropylene/Kevlar 49 compounds Ti. coupling agent treated (impact bars)

Compound	Coupling agent added (%)	Screw speed (RPM)	Vol fraction (%)	Stiffness	Yield force (N)	Energy to fracture (Nm)	Coefficient of variation energy to fracture (%)
K6	1	30	13	63	190	1.33	14.2
K7	1	50	13	69	207	0.96	4.8
K8	1	30	6.5	58	185	1.45	13
K9	3	30	14	61	182	1.07	6.8
K10	5	30	14	58	166	1.03	8.1

Table 42

Experiment KEVLAR 3. Impact properties of polypropylene/Kevlar 49 (twin screw compounded) and commercial polypropylene/glass compounds.

Impact bars

Compound	Screw speed (RPM)	Vol fraction (%)	Stiffness	Yield force (N)	Energy to fracture (Nm)	Coefficient of variation energy to fracture (%)
K11	135	8.8	49	157	1.33	9.7
K12	270	12.5	53.5	150	1.54	9.5
Glass	--	8.1	73	229	1.04	6.5

Impact plaques

--	--	0	363	570	1.73	10.6
K11	135	8.8	378	492	2.98	13
K12	270	12.5	355	542	3.49	20
Glass	--	8.1	478	760	5.00	5.2
Glass	--	13.2	765	960	5.68	15.2

Table 43

Experiment KEVLAR 4. Impact properties of nylon 66/Kevlar 49 (twin screw compounded) and nylon 66/glass compounds.

Impact bars

Compound	Screw speed (RPM)	Vol fraction (%)	Stiffness	Yield force (N)	Energy to fracture (Nm)	Coefficient of variation energy to fracture (%)
Processed	500	0	63	207	1.94	64.52
Unproccesed	--	0	49	185	3.59	30.50
K13	135	8.1	91	212	0.85	6.25
K14	270	12.5	101	222	1.53	4.72
Glass	500	8.86	121	375	1.67	4.8

Impact plaques

--	--	0	848	1986	4.51	50
K13	135	8.1	522	548	2.47	18.5
K14	270	12.1	548	582	2.59	10.4
Glass	500	8.86	500	777	5.9	13

Table 44

Measurement and estimation of G_c of glass reinforced nylon 66

Compound	Vol. fraction	Interfacial shear strength (MPa)	Measured G_c I (kJ)	Measured G_c II (kJ)	Calculated G_c (kJ)	Maximum possible G (kJ)
G3	0.087	28.6	3.35	10.88	5.43	13.66
G6	0.099	26	1.65	5.19	2.28	17.08
G7	0.078	17.3	3.27	9.74	5.83	20.34

Measured G_c I from peak force value
II from total impact energy

Maximum possible G_c calculated when all fibres have length Lc

Table 45

	Fibre Length	
	Number Average (mm)	Weight Average (mm)
Compound G3	0.390	0.462
Compound G6	0.176	0.239
Compound G7	0.467	0.576

5. The Determination of Critical Fibre Length in Short Fibre Reinforced Thermoplastics

5.1 Introduction

The strength of short-fibre reinforced composites depends critically on the bond strength between the fibres and the reinforcing material. The bond strength is infuenced in the compounding operation by the level of fibre wet-out. One method of measuring the bond strength is through the determination of the critical fibre length of the fibre in the matrix. In this chapter an investigation into the values of critical length for the fibre-matrix combinations used in this study is made. A novel method is used to measure directly critical length. The values obtained are compared with estimates based on the derived interfacial shear strengths from the stress-strain curves of injection moulded tensile bars and estimates made from observations of fracture surfaces using a scanning electron microscope.

The development of different techniques for the measurement of critical fibre length in short fibre reinforced thermoplastics is useful for developing suitable size systems or coupling agents to improve bond strength. In the context of this study, a measurement of critical fibre length is useful for assessing the effectiveness of the compounding process.

5.2 Experimental

The Measurement of Critical Fibre Length Directly by the Observation of Fibre Breakage in Extruded Tape

This technique was developed by Folkes and Wong[133] to measure directly critical fibre length. The technique involves preparing specimens of thermoplastic tape containing a small concentration of well aligned fibres by an extrusion process. When stress is applied to the specimen the stress will be transferred from the matrix to the fibres. An increase in applied stress results in a progressive reduction of the fibres into shorter fragments.

Fabrication of the specimens was accomplished using a Betol 2520 single screw extruder with a slit die. The extruder specifications and operating conditions are given in Table 46. Small

quantities of fibre were added to the extruder hopper. On extruding, the semi molten polymer was passed through a series of water cooled nip rollers and pressed into thin tape. Care was taken during the extrusion and cooling operations not to stretch the tape more than necessary to prevent extensive fibre breakage prior to testing.

An area of tape was then selected and cut into a dumbell shaped specimen for the tensile loading operation. The tensile loading was carried out using a type W Monsanto tensometer equipped with grips for holding films. During all stressing operations care was taken to maintain a steady and uniform strain rate. A maximum strain of approximately 10% was applied to each specimen at a loading rate of approximately 1cm/minute.

Fibre fragments were measured using an optical microscope with a graticule eye piece. Only fibres that were closely aligned to the tensile loading axis were measured. The technique was used in this study for the following combination of fibre and matrix:

1. Nylon 6,6 and E glass (standard size)
2. Nylon 6,6 and carbon type II (epoxy size)
3. Nylon 6,6 and carbon type II (polyamide size)
4. Polypropylene and Kevlar 49 (standard size)
5. Nylon 6,6 and Kevlar 49 (standard size)
6. Nylon 6,6 and Kevlar 49 (fibre boiled for 6 days)

Theory

Figure 149 shows schematically a single fibre embedded in a matrix. When an external stress is applied to the specimen parallel to the fibre axis, the tensile load will be transmitted from the matrix to the fibre through the interfacial shear stress. An increase of applied stress will result in a progressive break-up of the fibres into shorter fragments, a knowledge of the distribution of fragment lengths enables a value for the critical length and hence interfacial shear strength to be determined. The tensile stress (σ_f) in the fibre increases from nearly zero at the fibre ends to a maximum value, limited by the ultimate tensile strength of the fibre (σ_{fu}). When this limit is

reached, the fibre should break anywhere between A and B. On the other hand, the interfacial shear stress (τ_u), which has a maximum value at the fibre ends, decreases to nearly zero towards the middle of the fibre. If the external stress is increased, this fibre breakage process should continue until all fibre fragments are less than $2X_o$, in which case the tensile stress in the fibres can not reach σ_{fu}. The minimum fibre length for which the tensile stress can reach the ultimate strength of the fibre is termed the "critical length", l_c.

The Kelly-Tyson model predicts that the fibre fracture process should result in a distribution of fragment lengths $l_c/2$ to l_c. Often, the distribution of fragment lengths obtained is broader than the 2:1 ratio predicted. This has been attributed to the existence of flaws in the fibre thereby causing its strength to depend on length[134].

Different models[135] have been reported which take into account the existence of flaws along the fibre when utilizing the fibre fragment data for the evaluation of l_c. However, if a normal fibre fragment distribution histogram is obtained, the peak of the histogram should equal 3/4 l_c. Also, the mid point (50% point) of the cumulative fibre fragment length distribution curve should also equal 3/4 l_c, if enough fragments are included.

As discussed in Section 1.5.2 Kelly and Tyson have related critical length, l_c to the interfacial shear strength through a force balance around the embedded fibre. They assumed that the shear stress at the interface (τ_u) is constant and equal to the shear yield strength of the matrix, see equation 7.

The Kelly-Tyson model seems to be of relevance to our system in determining interfacial bond strength, from the fragment lengths since the thermoplastic matrix we use has a yield point.

The Kelly-Tyson model indicates that the shear yield strength of the matrix should be large enough to resist the shear stress at the interface, otherwise matrix yielding will occur before the maximum stress can be transferred to the fibre. In general, the shear stress at the interface can never exceed the shear yield strength of the matrix. When utilizing the Kelly-Tyson relationship, the ultimate tensile strength of the fibres can only be used for pristine fibres. The true ultimate strength of the fibre in the moulded component may be different.

5.3 Results

Considered first in this section are the results from the direct method of critical length. After the extension of tapes containing glass and carbon fibres, the fibres were found to break cleanly. The distributions of fibre lengths for E glass in nylon 6,6 is shown in Figure 150. The length distributions for polyamide and epoxy sized carbon fibre in nylon 6,6 are shown in Figure 152. Critical lengths were calculated using the cumulative frequency distributions shown in Figures 151 and 153.

Microscopic examination of tapes prepared with Kevlar fibre revealed that the extrusion operation had produced kink and shear bands in the fibre. After extending tapes of polypropylene containing Kevlar fibres, fibres as long as 5mm were found not to have broken. For Kevlar incorporated in nylon 6,6, microscopic examination before and after stressing revealed that fibre breakage only occurred in areas of the fibre that had been previously damaged by the shear compounding process. These areas included kink bands. As discussed in Section 4.4.3 kink faults are points along a damaged Kevlar fibre where gross deformation of the fibre structure is believed to have occurred. Kink bands are an accumulation of kink faults. The distribution of fibre fracture lengths for the damaged Kevlar fibre in nylon 6,6 is shown in Figure 154. The critical length was calculated using the cumulative frequency distribution shown in Figure 155.

Eagles Blumentritt and Cooper[123] found that by boiling in water, the surface of Kevlar fibres could be roughened to increase their interfacial bond strength with a range of thermoplastics. In order to assess this effect on critical fibre length, Kevlar fibre that had been immersed in boiling water for six days, were incorporated into nylon 6,6 tape and the critical fibre length measured. There was however, no significant difference in the fracture lengths measured compared with the untreated fibre variant. Figure 156 and 157 are scanning electron photomicrographs of Kevlar fibre before and after boiling in water for 6 days.

The estimation of critical fibre lengths from tensile fracture surfaces of injection moulded samples were made from scanning electron photomicrographs. Examples of such photomicrographs are shown in Section 4.2.4, Figure 103 for E glass in nylon 6,6, Section 4.2.4, Figure 101

for carbon in nylon 6,6, Section 4.4.3 Figure 128 for Kevlar in polypropylene and Section 4.4.3, Figure 131 for Kevlar in nylon 6,6.

Table 47 presents the critical length values measured by the three methods. All calculations are based on fibres in their pristine condition.

5.4 Discussion

The value of critical fibre length for E-glass fibre in nylon 6,6 measured by the direct method is significantly shorter than is estimated from calculations based on the stress-strain curves of injection moulded test bars. Consequently the interfacial shear strength is greater in the extruded tape than in the moulded composite. The value of critical length estimated from stress-strain curves can be thought of as an average value, the value of critical fibre length being longer as a result of incomplete fibre dispersion and inadequate fibre wetting. Dividing the value of critical length measured directly by the value derived from actual mouldings allows an estimate of mixing efficiency, complete fibre dispersion and wet-out being obtained when the ratio equals 1. In the case of glass fibre in nylon 6,6 the ratio is equal to 0.65.

In the case of carbon fibre in nylon 6,6 the value of critical length from the direct method is longer for both size treatments than it is estimated from injection mouldings. Consequently the interfacial shear strength appears to be greater in the moulded composite than it is in the extruded tape. This is opposite to the case found for the combination of E-glass and nylon 6,6. In Section 4.2.4, Figure 102, Scanning electron photomicrographs of an injection moulded test piece fracture surface revealed that a thin irregular sheath of matrix surrounds each fibre. One explanation for the increased interfacial shear strength in the injection mouldings may be the increased frictional work that would be have to be overcome in pulling out irregular sheaves from the bulk matrix. Studies of the surfaces of carbon fibres pulled out from extruded tape after being strained uncovered no such sheath of matrix. Bessel and Shortall[114] have shown from fracture surface studies of composites containing 15% volume fraction of uniaxially aligned fibres that when fibre pull-out occurs it is possible for the fibres to be surrounded by sheaths of the matrix material. They suggest that this may be related to the presence of transcrystalline material but were unable

to demonstrate if transcrystallinity had any role in increasing the adhesive bond between fibres and matrix. The effect of transcrystallinity on the bond between a matrix and substrate has been a topic of some controversy. Schonhorn and Ryan[136] reported that the critical surface tension for the wetting of a surface by a transcrystalline matrix to be greater than for a nontranscrystalline one. This implied that the adhesive strength between polymers and substrates may be enhanced by transcrystallinity. Fitchmun et al[137] found that transcrystallinity harms the bond during peel tests. The difference in the matrix morphology surrounding the fibre between injection moulded and tape extruded nylon may be the result of the different flow history experienced by carbon fibres in each processing operation. Fibres that have been injection moulded would be surrounded by matrix that had undergone a high degree of shear. A study by Maxwell[138] of injection moulded melts revealed that processing can and does markedly affect the crystallisation of polymers. In general, sheared regions tend to give rise to very many spherulites.

It is interesting to note using the direct method, that although the nylon size appears to give a shorter critical length and thus have a higher interfacial shear strength compared with the epoxy size, this advantage seems to be lost when comparing values of critical fibre length derived from the injection mouldings of such materials. A possible reason for this is the short residence time in the extruder when producing tape for the direct method. Here it can be envisaged that the low melting point thermoplastic may just have enough time to migrate so the matrix bonds directly on to the carbon fibre surface which has a chemically activated surface. In the case of the extruder the size may remain intact, so the matrix is only allowed to contact with an epoxy shell. In the case of compounded and injection moulded test bars the fibres present would have undergone a relatively long residence time at high shear stresses and high temperatures. It is likely that under these conditions the epoxy size would migrate to leave the uncoated carbon fibre surface which could bond directly to the matrix.

The finding that even weakened Kevlar fibres in polypropylene tape did not break on straining serves to confirm what was discussed in Section 4.4.4 that interfacial bonding between Kevlar and polypropylene is very poor. Better bonding was found between Kevlar fibres and nylon 6,6,

however even in this case undamaged fibres in tape were found not to break. The improvement in properties with a nylon matrix may be partly explained by the presence of hydrogen bonds between the amide groups of Kevlar 49 and nylon 6,6.

As Kevlar fibre is damaged by processing it is not possible to assume an accurate value of tensile strength for the estimation of critical fibre length after processing. For the direct method, the high degree of scatter for the critical length measurement of Kevlar in nylon indicates the wide range in the severity of flaws that exist within the fibres after being incorporated into the tape. On carrying out tensile strength tests on pristine unprocessed Kevlar 49 fibre Bunsell[139] found considerable variability. The calculated percentage variability was 17%. This variation may be a reflection of the faults that are produced in Kevlar fibre during handling. Although Kevlar is flexible and tough, in order to obtain its optimum tensile properties, care is needed in its handling.

The values of critical fibre length obtained through observation of fracture surface can only be considered as an approximate estimate, as fibres observed are not lying normally to the fracture surface. A Scanning electron micrograph shows only a two dimensional projection of the fracture surface. For this reason the values of critical fibre length obtained using this technique are lower than those obtained using the other two approaches. An additional reason why the critical length estimate is likely to be shorter than the direct method is that the compounding and injection moulding processes are likely to have further reduced the strength of the fibres.

Schematic diagram showing the stress distribution along a fibre embedded in a matrix (load parallel to fibre axis)

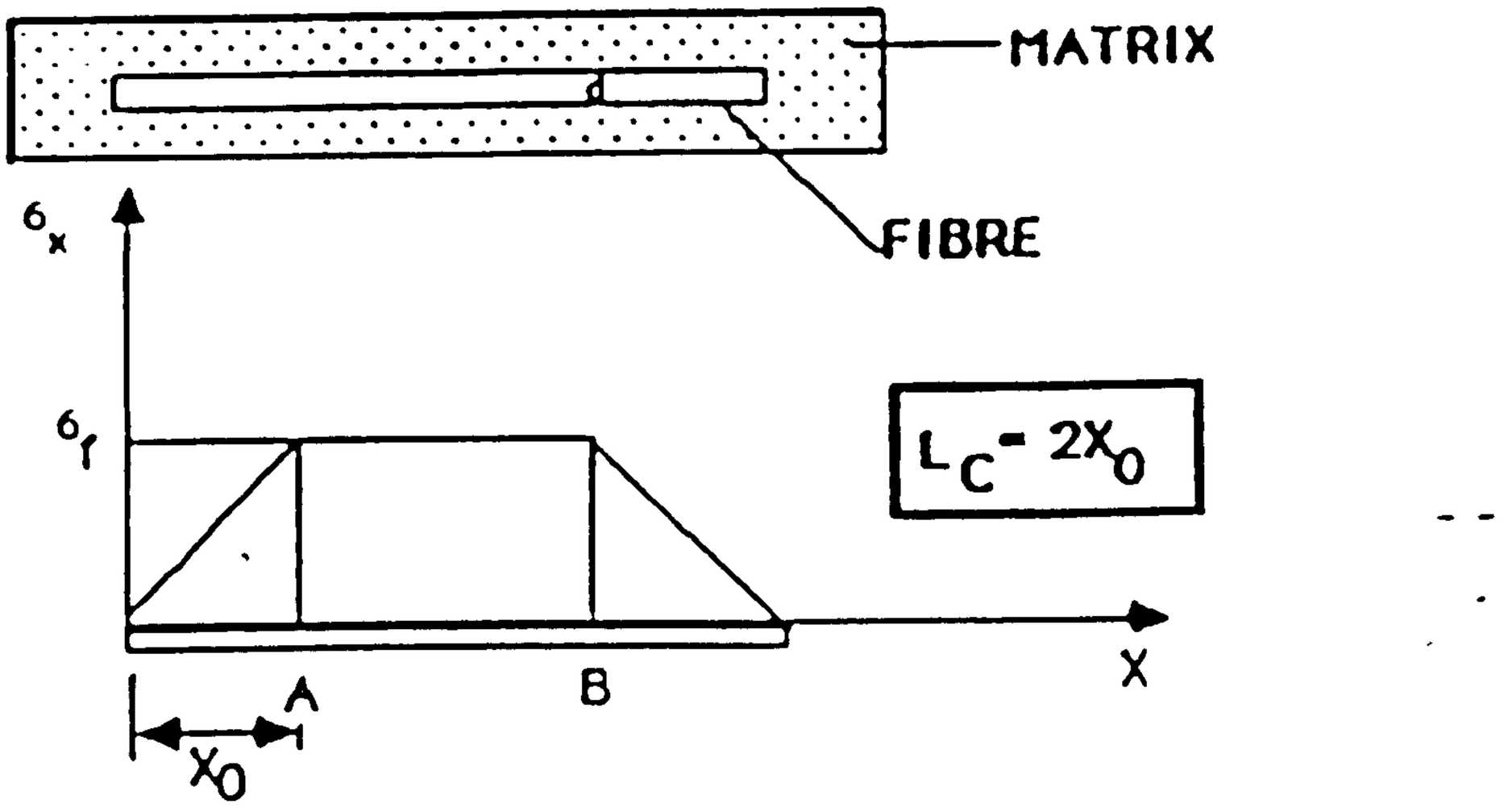

Figure 149

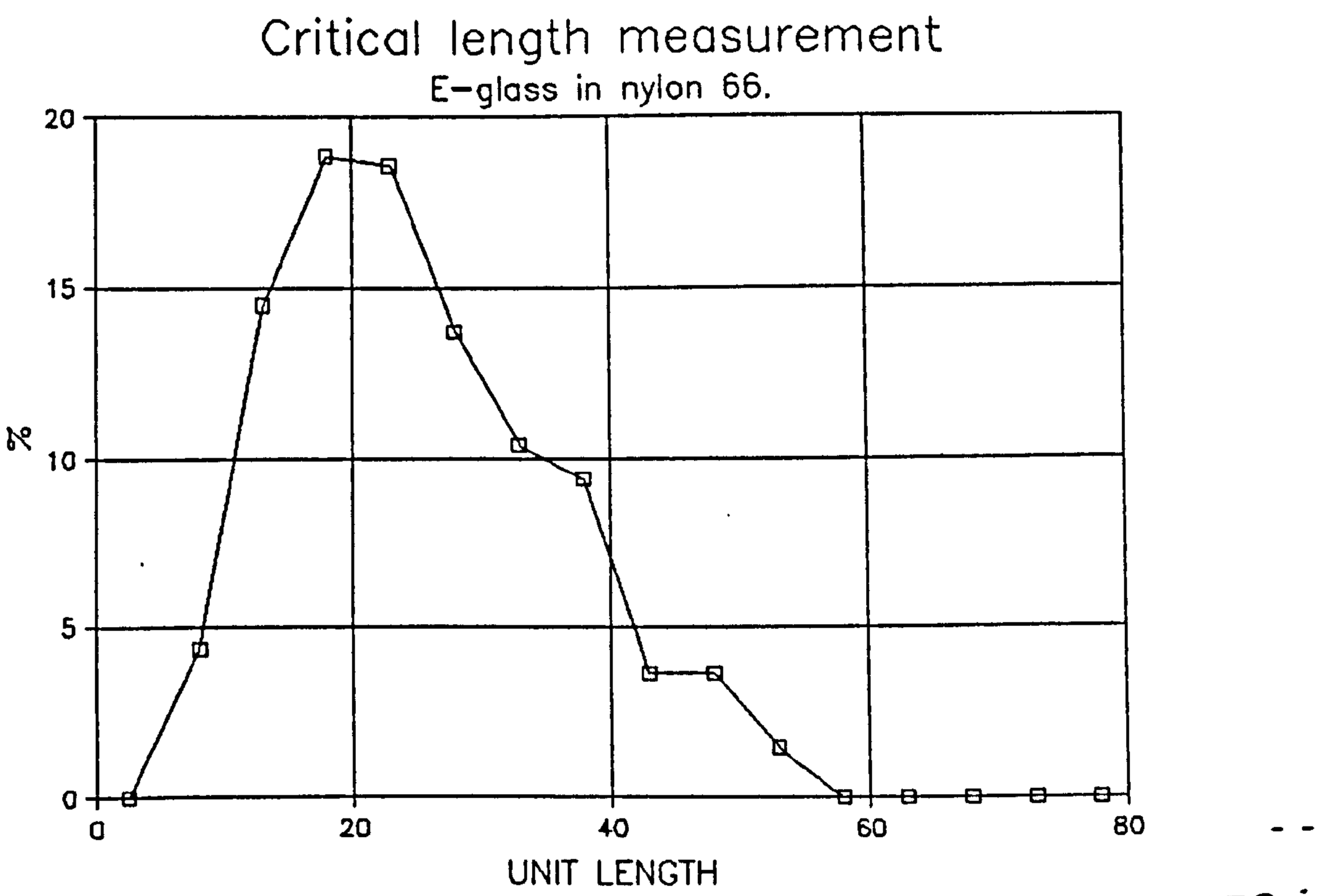

Figure 150

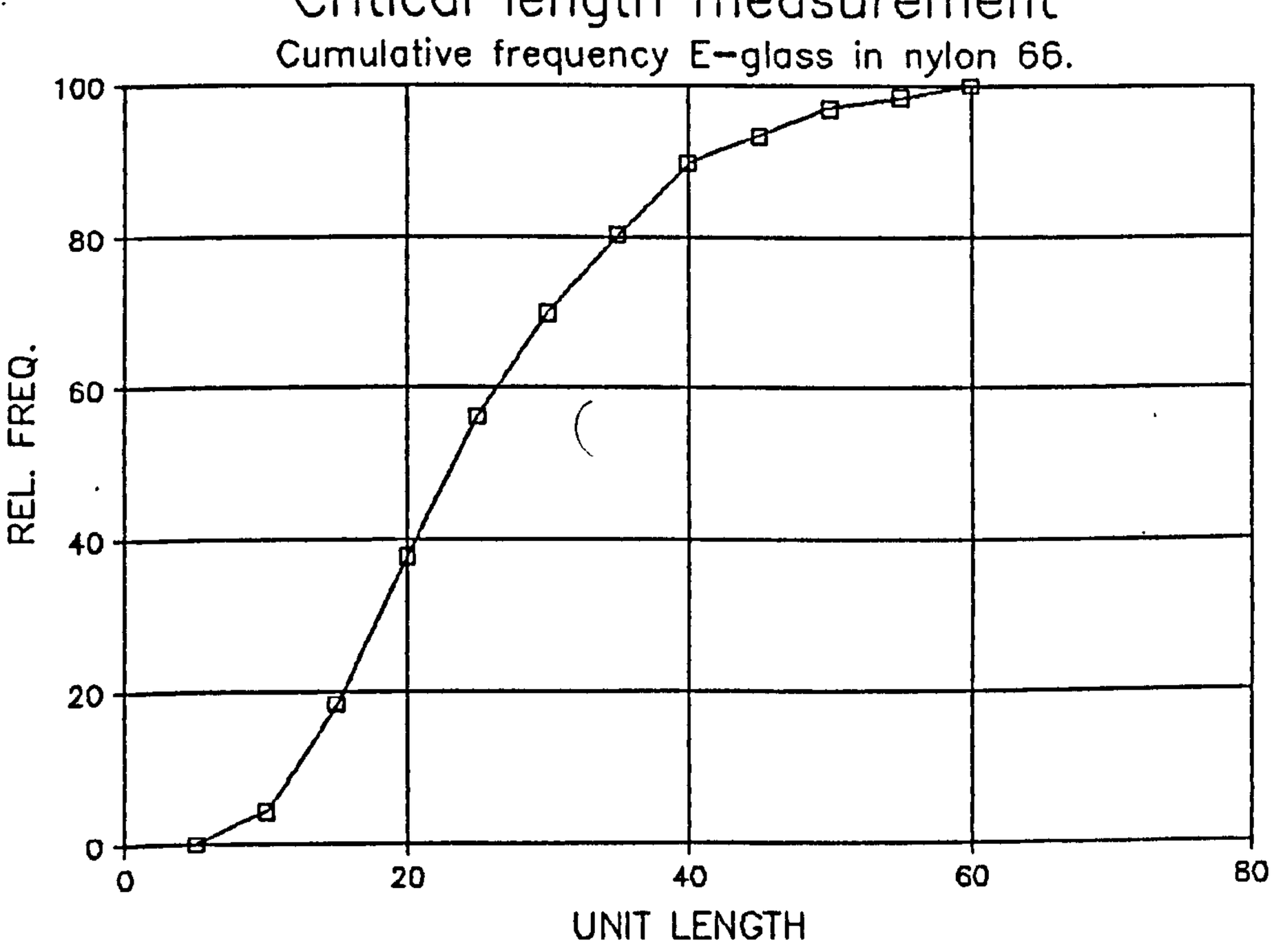

Figure 151

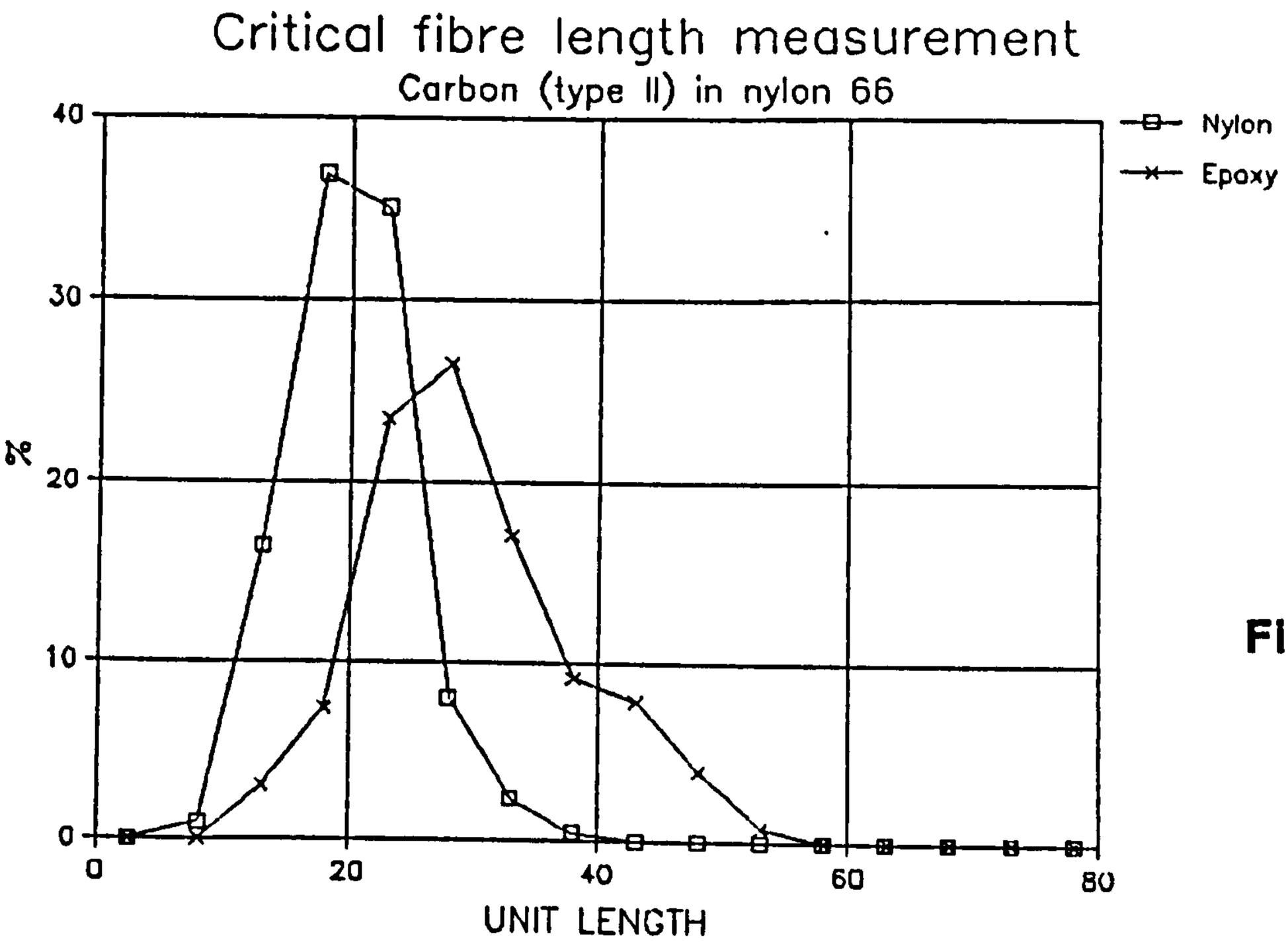

Figure 152

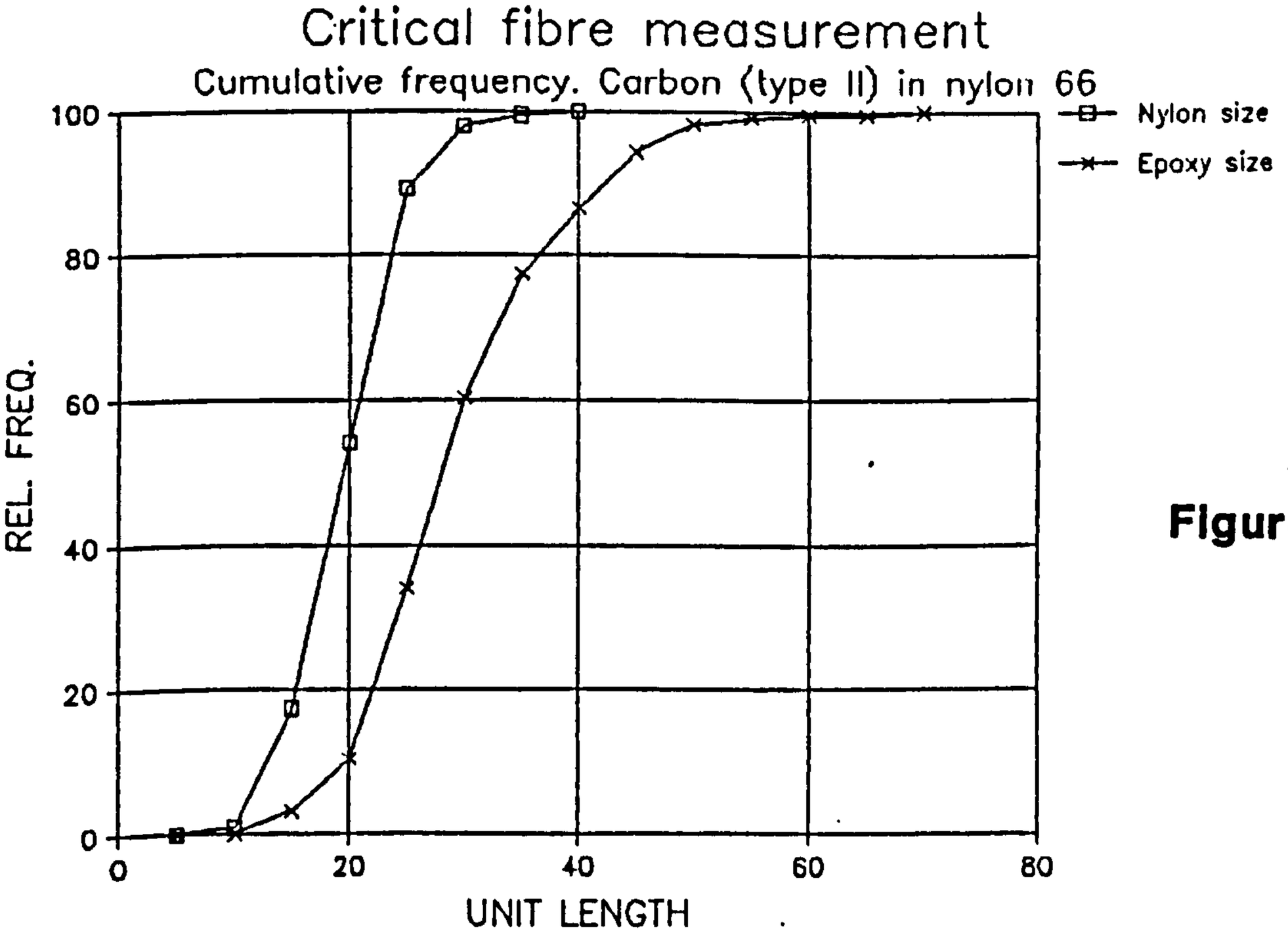

Figure 153

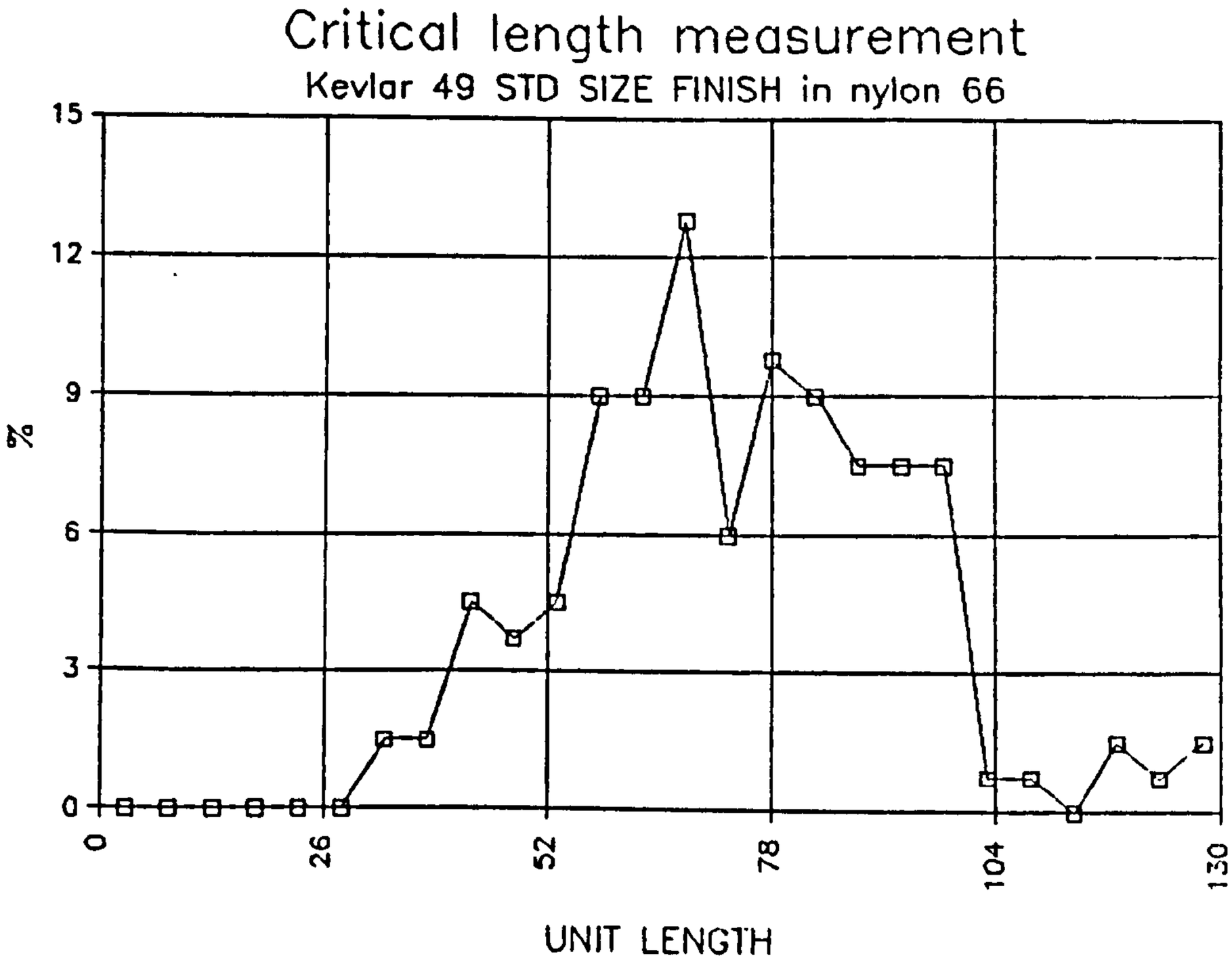

Figure 154

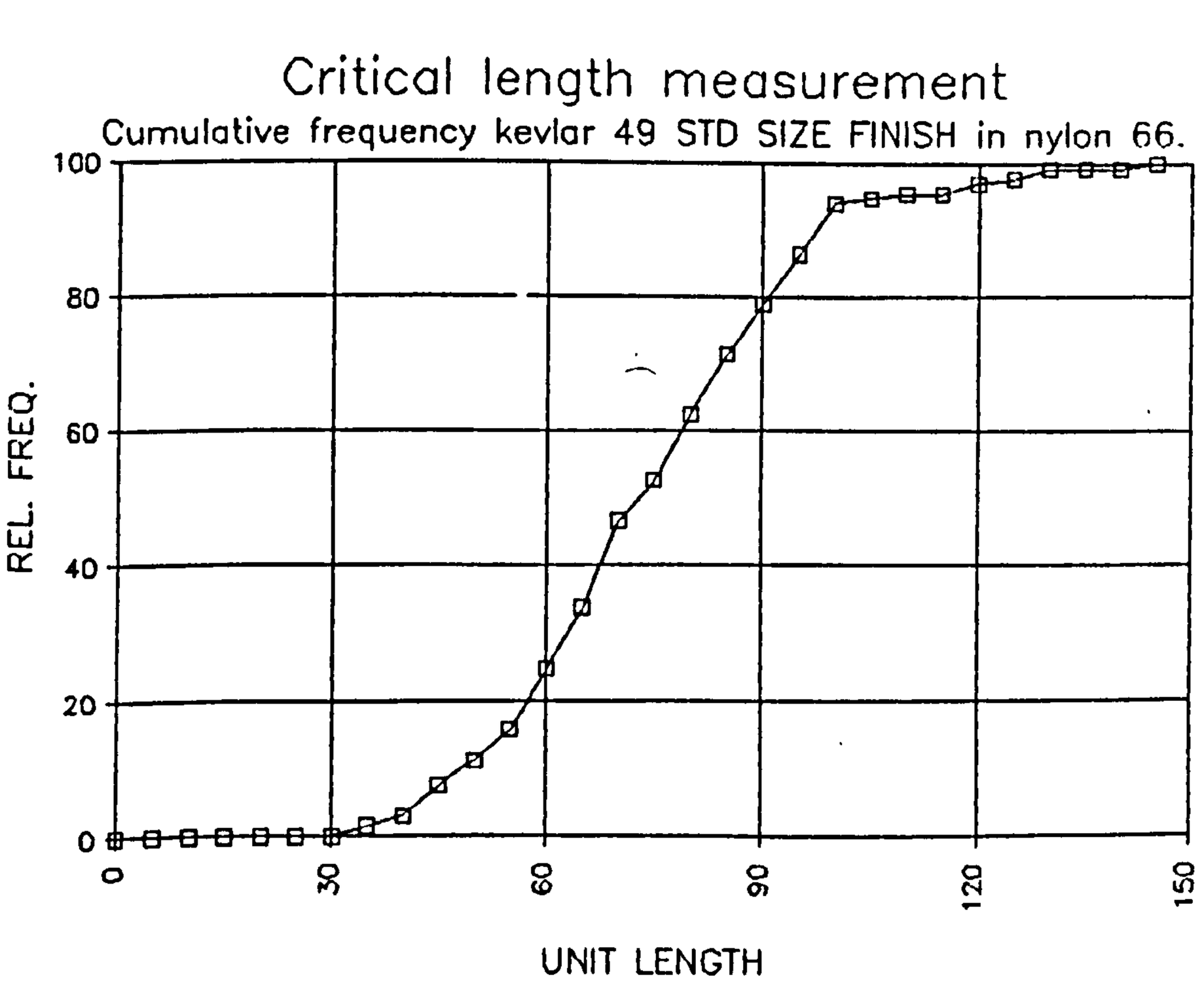

Figure 155

Kevlar fibre before boiling in water for 6 days

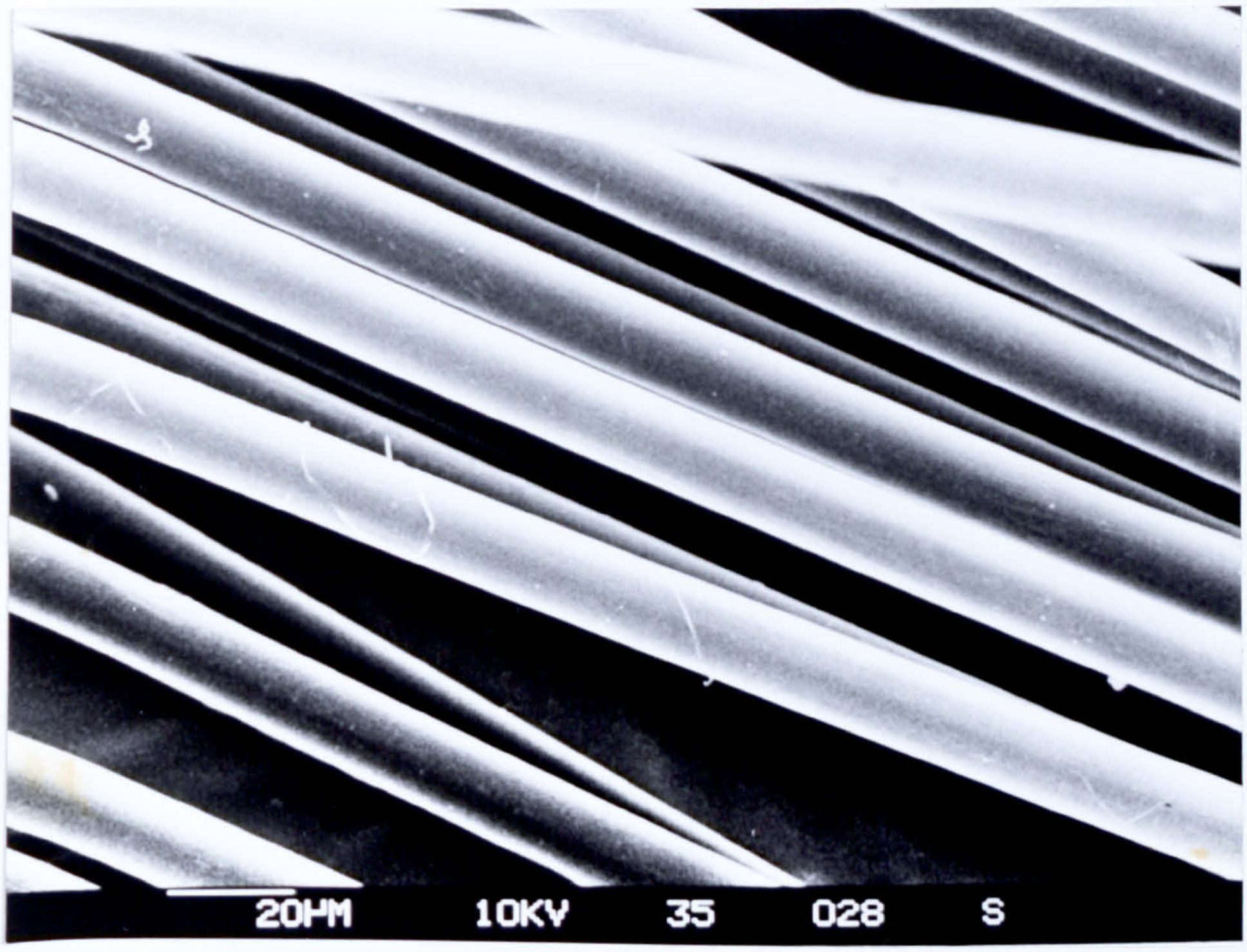

Figure 156

Kevlar fibre after boiling in water for 6 days

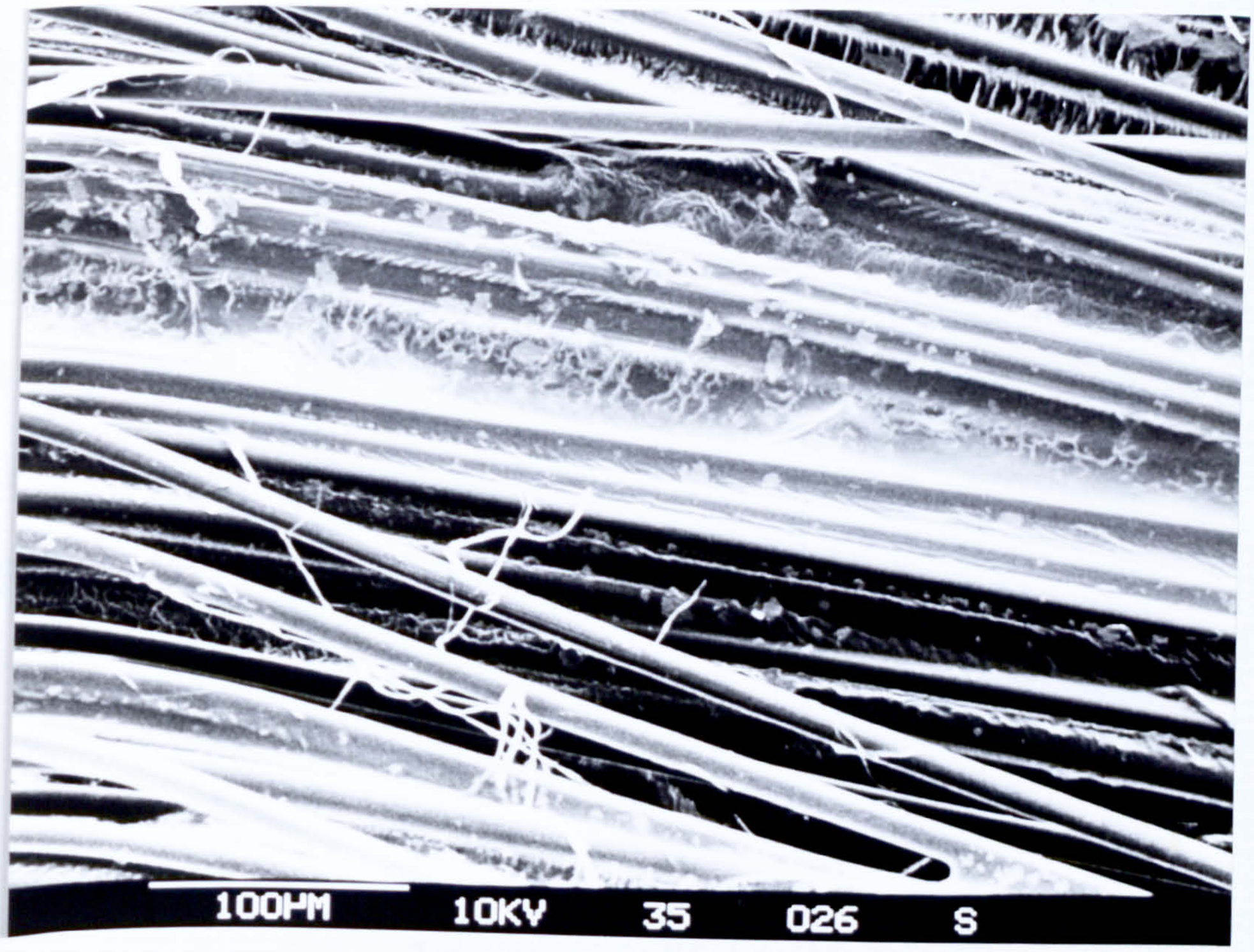

Figure 157

Specifications for Betol 2520 single screw extruder.

Barrel	25mm diameter electrical heated.
Screw speed	0-100 RPM.
Drive	1.5 kW
L/D ratio	20:1
Screw	Polyethylene and Nylon screws used.
Die	Vairable strip.

Temperature settings

Polypropylene experiments

	Temperature (C)	
Feed	175	
Middle	175	Screw speed 20 RPM
Die	250	

Nylon experiments

Feed	280	
Middle	280	Screw speed 20 RPM
Die	285	

Table 46

Measurement and estimation of critical Fibre lengths

	E-glass/ Nylon 66.	Carbon(type II)/ Nylon 66 Epoxy sized	Carbon(type II)/ Nylon 66. Polyamide sized	Kevlar 49/ Polypropylene	Kevlar 49/ Nylon 66.
Critical length from direct method (mm)	0.486	0.559	0.390	VERY LITTLE BREAKAGE	>1.07
Calculated interfacial shear strength (MPa)	46	19.3	27.7	--	<15
Interfacial Shear strength based on Stress-strain curve (MPa)	30.2	48 *	48 *	2.4	7 02
Calculated critical fibre length (mm)	0.586	0.216	0.216	6.75	2.31
Critical length estimate from fracture surface (mm)	0.400	0.100	0.105	2.20	0.550

Table 47

* Result based on shear yield strength of matrix

6 The Production of Fibre Reinforced Thermoplastics Using a Specially Designed Cross-head Die

6.1 Introduction

The experiments BRITTLE 1 to 6 and KEVLAR 1 to 4 have served to highlight the limitations of existing conventional compounding extrusion techniques to produce long fibre materials that exploit the properties of high performance reinforcing fibres. Because of these limitations an alternative approach is required to develop a novel technique where these properties could be realised.

Alternative methods to produce long fibre feed stock involve starting with the continuous tow, impregnating the fibres with the polymer and then cutting the continuous strands to produce pellets that can be used as feed stock for the injection moulding process. In the past, three basic methods have been used for the impregnation step:

a. A solvent based method where a polymer is dissolved in a solvent which is used to impregnate fibres.

b. The dry process, here fine powder is applied to the fibre by the fluidised bed process. Electrostatic charging may aid coating.

c. The melt process, here fibre is drawn through a low viscosity melt.

The solvent based method is limited to thermoplastics that are easily dissolved. The mechanical properties of the polymer are often restricted by the inability to remove all the solvent.

The dry process would seem most elegant in concept. It leads to a high fibre/polymer ratio and good impregnation. This is the basis of a number of patents. The technique is limited by a slow production rate and the expense of using the polymer in a powder form.

The most commercially viable approach would seem to be the melt process. Progress in the last few years has been made in the compounding of fibre reinforced thermoplastics based on pultrusion technology developed in the 1960's. The pultrusion process was originally related to the

production of beams and channel sections using thermosetting resin. It consisted of drawing fibre rovings (usually glass) through a resin bath, followed by passage through a bush of the required shape to remove excess resin and any trapped air. The drawn material was then passed continuously through an oven to crosslink the resin. The main limitations of this process when used to produce long fibre reinforced thermoplastic injection moulding feed stock is poor fibre impregnation.

The technique developed in this study also involved impregnating continuous fibres, but in this case a cross head die that could be attached to a simple melt pump was employed. The design philosophy was initially to well separate the fibres under tension, coat individual fibres with thermoplastic then consolidate the well wetted fibres together to make an extrudate containing undamaged and well dispersed fibres. The continuous strands could then be pelletised to produce pellets containing fibres of the same length as the pellets. These pellets could then be used directly or in a diluted form in the injection moulding operation.

A search was made of United States and United Kingdom patents for a technique of similar design. The only patent found to be similar was assigned to R Brant of the Fiberfil corporation, US Patent number 3042570. In this patent, continuous lengths of reinforcing fibres are passed through a bath of molten thermoplastic cooled to solidify the resin and then cut into pellets of the desired length. The patent describes how impregnating and coating baths are insulated from the feeding mechanism which is illustrated as a single screw extruder. Unlike the technique described in this chapter the impregnating stage does not incorporate a torpedo over which the fibres are drawn in order to be well separated whilst they are impregnated. Other patents sighted relating to the novel production of fibre reinforced thermoplastic composites are shown in Table 48. Patents related to cross head dies are listed in Table 49.

Die Design and Working Principle

It would appear that there is no equipment currently available that can be used with conventional polymer processing equipment which enables the production of well wetted fibre reinforced thermoplastic pellets for injection moulding where the fibres are of the same length as the

pellets. The cross head die was designed to fulfil this role and at the same time overcome the limitations of the previously discussed current solvent, dry and melt processes.

The die assembly is shown in Figure 158. The die consists essentially of four main parts: the inlet assembly, the melt chamber, the torpedo and the outlet assembly. Fibres are drawn through the die from left to right.

It is through the inlet assembly the fibres enter the die. This assembly has a removable inlet orifice (16) which can be replaced with orifices of different size for the production of composites with different concentrations of fibre. The inlet assembly bolts on to the melt chamber and holds the torpedo in position. The torpedo is used to separate the fibres as they are coated with polymer in the melt chamber.

The melt chamber is connected to the melt pump (25) and so is designed that the melt is pumped around the circumference of the torpedo before wetting the fibres. This ensures an even flow of polymer around the torpedo and prevents fibres being swept to one side. Adjustment of melt flow is possible by the regulation of the width of the annular gap. The annular gap allows a local reduction in melt viscosity and hence better potential fibre wetting. Fibres are drawn off the torpedo, drawn together and consolidated by passing through the outlet assembly (5), which contains a replaceable die orifice, of similar design to the inlet orifice. The die orifice dictates the final cross sectional shape and the concentration of the fibre in the matrix. Figures 159 and 160 are photographs of the front and side elevations of the assembled die.

The inlet assembly, melt chamber and die assembly are each heated by their own band heaters. Tension throughout the system is maintained by a caterpillar haul off and braked drum.

6.2 Experimental

The configuration for the production of glass reinforced thermoplastic is shown in Figure 161. As described earlier, fibre was drawn off of a braked drum which was used in combination with a caterpillar haul-off. The braked let-off drum is shown in Figure 162, it was constructed by the author and his father using the spinning drum from the family's old washing machine. A sim-

ple thumb screw was used to tighten a collar around the drums axle and so control the resistance of the drum to be turned. By adjusting the thumb wheel carefully, an acceptable level of tension could be maintained throughout the system.

To ensure the fibres were adequately separated, a series of polished convex aluminium rollers were employed to spread the fibres before they entered the die.

A 30mm screw diameter Betol single screw extruder was used as the melt pump. A D.M.E. temperature controller was used to control the temperatures of two sections of the die, the extruder die temperature controller was used to control the third.

In order to set up the die for operation, fibre was ran from the braked drum through the die and clamped in the tracks of the caterpillar haul-off. A laboratory tripod was used to initially spread fibres around the torpedo before it was loaded into the die.

After extrusion of the composite extrudate from the die, a jet of compressed air was used to cool the semi molten polymer before it entered the caterpillar haul-off tracks.

Extruded lengths of composite were collected and sections examined by optical microscopy.

6.3 Results

To test the operating principle of the cross head die, copper wire was used in combination with polypropylene. Although only 4 strands were used, good separation of individual strands was found (Figure 163). There was however evidence that the tension needed to separate the wires within the cross head produced abrasion damage to the fibres. Flakes of copper abraded from the surface can be seen in the extruded section in Figure 164.

For the production of conventional fibre reinforced composites the cross head die was tested initially with carbon fibre tow sized with a polyamide in conjunction with polypropylene. Problems were encountered with friction and sharp edges within the die. After a few centimeters of composite material were produced the carbon fibres broke within the die producing blockages. The blockage grew worse until eventually all the fibres were broken. Such a problem was

extremely inconvenient, the die had to be dismantled the blockage cleared and the broken tow re-threaded through the cross head die and haul-off system. Despite the torpedo being modified by removing all obvious sharp edges and filing flat some separating pins, fibre breakage was still a major problem within the die. It was found in a small scale experiment that even the movement of discrete carbon fibres over a polished metal surface was enough to produce "fluffing up" and fibre breakage and for this reason E glass and Kevlar 49 were assessed.

The bending of fibres over radii of curvature results in high surface tensile stresses which lead to fibre fracture. According to Hull[40] the minimum radius of curvature which fibres can sustain before fracture occurs is

$$P_{min}=\frac{Ed}{2\sigma f_u}$$

where E = Youngs modulus of fibre

d = fibre diameter

σf_u = fracture strength of the fibre

On this basis, E glass fibre with a lower modulus and higher strength than carbon fibre is less susceptible to fibre breakage by bending than carbon fibre. The first problem encountered with glass was the separation of individual fibres. A level of approximately 10% nylon compatible size was present on the fibres. Initially fibres were separated by hand before being threaded through the cross head die system, on running however, fibres bound together by size jammed and broke on entering the die. An attempt was made to remove the size by washing the fibres in acetone, but the difficulty was not resolved. Recurring blockages in the die caused by broken glass fibre allowed only short lengths of extrudate to be produced.

Owing to the difficulties experienced, the die was finally assessed incorporating Kevlar 49 into polypropylene. Kevlar 49 is a tough ductile fibre with abrasion resistance. The main problem encountered with it was the inherent twist produced in the fibre tow at the manufacturing stage. On running the fibres through the die, the twists got caught in the separating pins.

6.4 Discussion

From the results it is clear that there are major problems to be overcome in order to produce impregnated fibres constantly using the cross head die designed.

Coating the torpedo and the inside of the die with a PTFE film may help to overcome the problem of fibre breakage occurring in the die and also aid the cleaning operation.

Separating the glass fibres efficiently by treating them with a solvent to remove the size is not entirely satisfactory as on removing the size any silane coupling agent present in the size may also be removed. This is likely to produce poor bonding and an interface easily affected by moisture. Clearly specially sized fibres are needed for this application.

An alternative to the polished rolls to spread carbon fibres was suggested by J N Hall in a United States patent[140]. It involves vibrating carbon fibre tow in air which is pulsing at a frequency and intensity sufficient to couple the energy of the pulsating air to the carbon fibre tow. Vibration of the air causes separation and spreading of the filaments in the tow.

The initial experiment performed with a limited number of copper wires in the cross head die has indicated that providing the problem of fibre friction can be overcome, good fibre dispersion should be possible. In the past, problems of insufficient fibre wetting have been a limitation in the development of long fibre reinforced feed stock for injection moulding. Sharp[141] using a development of the cross head wire coating technique successfully produced carbon fibre reinforced nylon 6,6 with a weight averaged fibre length of over 2mm. However poor fibre dispersion and lack of wetting of the fibres by the matrix caused problems when pelletising feed stock for injection moulding. The pelletising operation was found to pull out loose fibres in the pellets. It was suggested that penetration of the fibres could be improved by the adoption of the hot-tube modification (Table 47). Bader and Collins[60] prepared materials by the cross-head route but found that only on injection moulding could acceptable dispersion be achieved. It was observed that for long fibre feed stock high back pressure was needed for adequate dispersion reducing seriously the fibre length in the final moulding. Slow production rate and excessive machine wear have also been found when the injection moulding machine was relied upon to disperse

fibres.

One method to measure the level of consistency of dispersion in fibre reinforced pellets was suggested in an United States patent[142]. Here the force necessary to pass a No.1 sewing needle through a pellet diameter at a constant rate was measured on a standard Instron tester.

Because of the greater problems found in this thesis for compounding Kevlar 49 fibres by shear intensive mixing (Sections 4.3 and 4.4), the cross head die technique would seem a promising method of incorporating this fibre into a thermoplastic matrix. Specially prepared Kevlar tows are needed without an inherent twist.

Once the initial problems found with the novel cross head die are overcome it should be possible to process the resultant long fibre feed stock in much the same way as the ICI long fibre reinforced thermoplastic "Verton" material. According to Gibson[143] these materials can contain 50% by weight glass with fibres of length 5mm or more. These materials are processable on conventional injection moulding machines with little loss in reinforcing integrity. On examination of injection moulded samples it was found that these materials contained domains of parallel ordered fibres. One reason for the absence of serious fibre degradation being very little fibre-fibre interaction. The processing and mechanical properties of Verton are discussed in the next section.

6.5 The Injection Moulding and Mechanical Properties of a "Long Fibre" Glass Reinforced Nylon 6,6 Material (ICIs Verton)

Although difficulties were experienced in preparing sufficient samples of cross head produced material for evaluation by injection moulding, as a final part of the work undertaken on the novel production technique it was decided to investigate the processing and mechanical properties of a commercially available long fibre compound: ICIs Verton CG 1090.

The material was injection moulded using moulding conditions as described in Table 18 with the exception of back pressure and barrel temperatures. Two screw back pressures were used, 0 and 10 MN/m^2. The barrel temperatures were 10°C higher than is listed.

The fibre length distributions measured from injection moulded test bars are presented in Figure 165. Increasing back pressure was found to have a significant effect on fibre length. The fibre length properties are summarised and the mechanical properties of moulded test bars listed in Table 50. The interfacial shear strength values are as calculated from the stress-strain curves of tensile bars tested in tension as described in Section 2.5.

The mechanical properties of these long fibre materials were not found to be improved over the short glass fibre materials produced in this study, see Table 30. One reason for the lack of improvement of mechanical properties may be poorer fibre wet-out producing lower levels of interfacial shear strength. An additional likely reason was evident on examination of the fracture surfaces by scanning electron microscopy. Figures 166 and 167 are scanning electron photomicrographs of the tensile fracture surface. A significant portion of the fracture surface contains fibres orientated transverse to the testing direction, these fibres contribute little to the load bearing process. This effect is important and indicates that optimisation of injection moulding arrangements are necessary in order to obtain the increased mechanical properties that "long fibre" reinforced thermoplastics would seem to promise.

Optimisation of the injection moulding scheme may include modifying gate design, mould flow rate and matrix viscosity but perhaps the greatest attention will be needed in controlling the converging and diverging flows that occur in a moulding by a careful selection of gate location and component geometry.

The crosshead die assembly

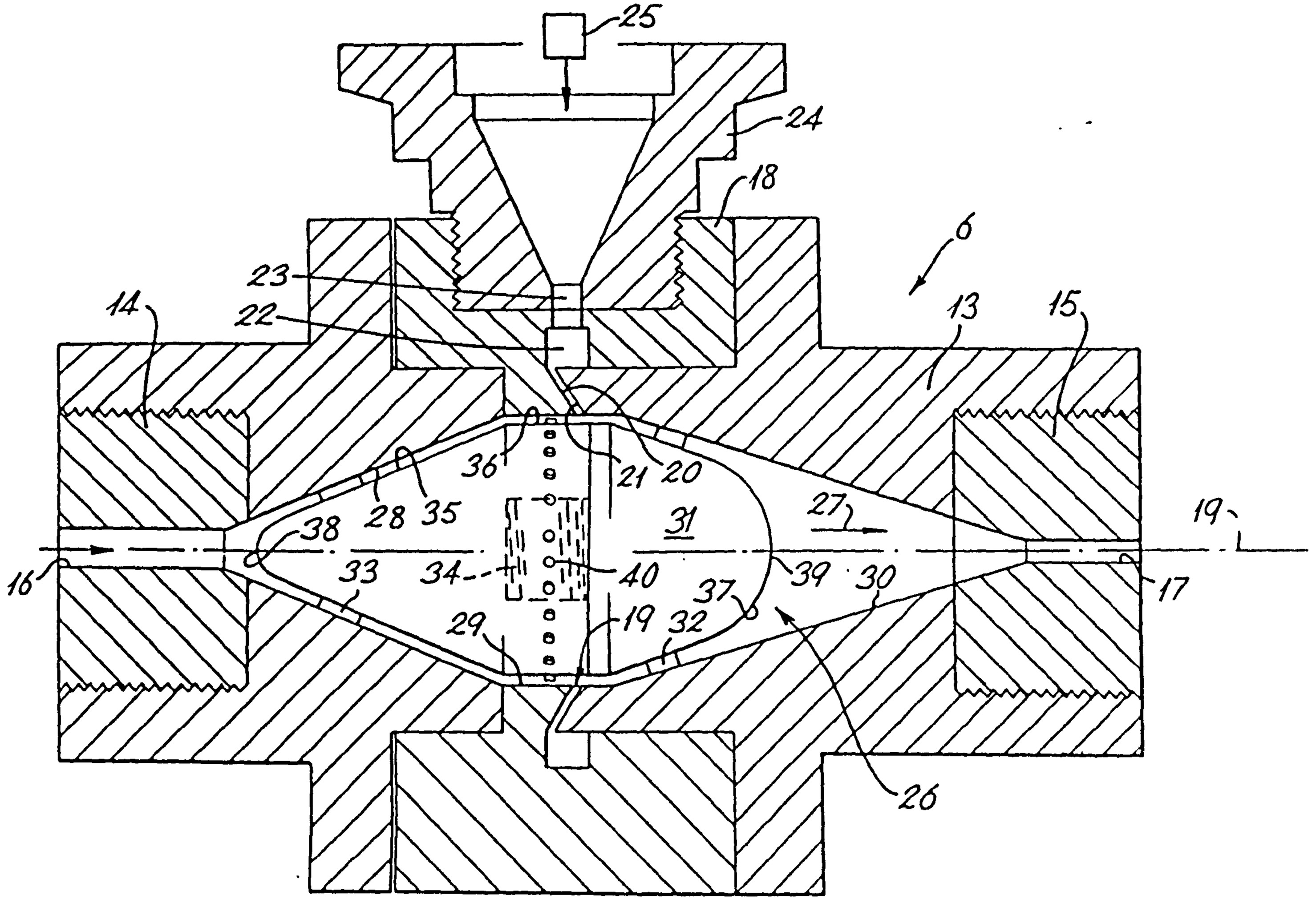

Figure 158

The front elevation of the assembled crosshead die

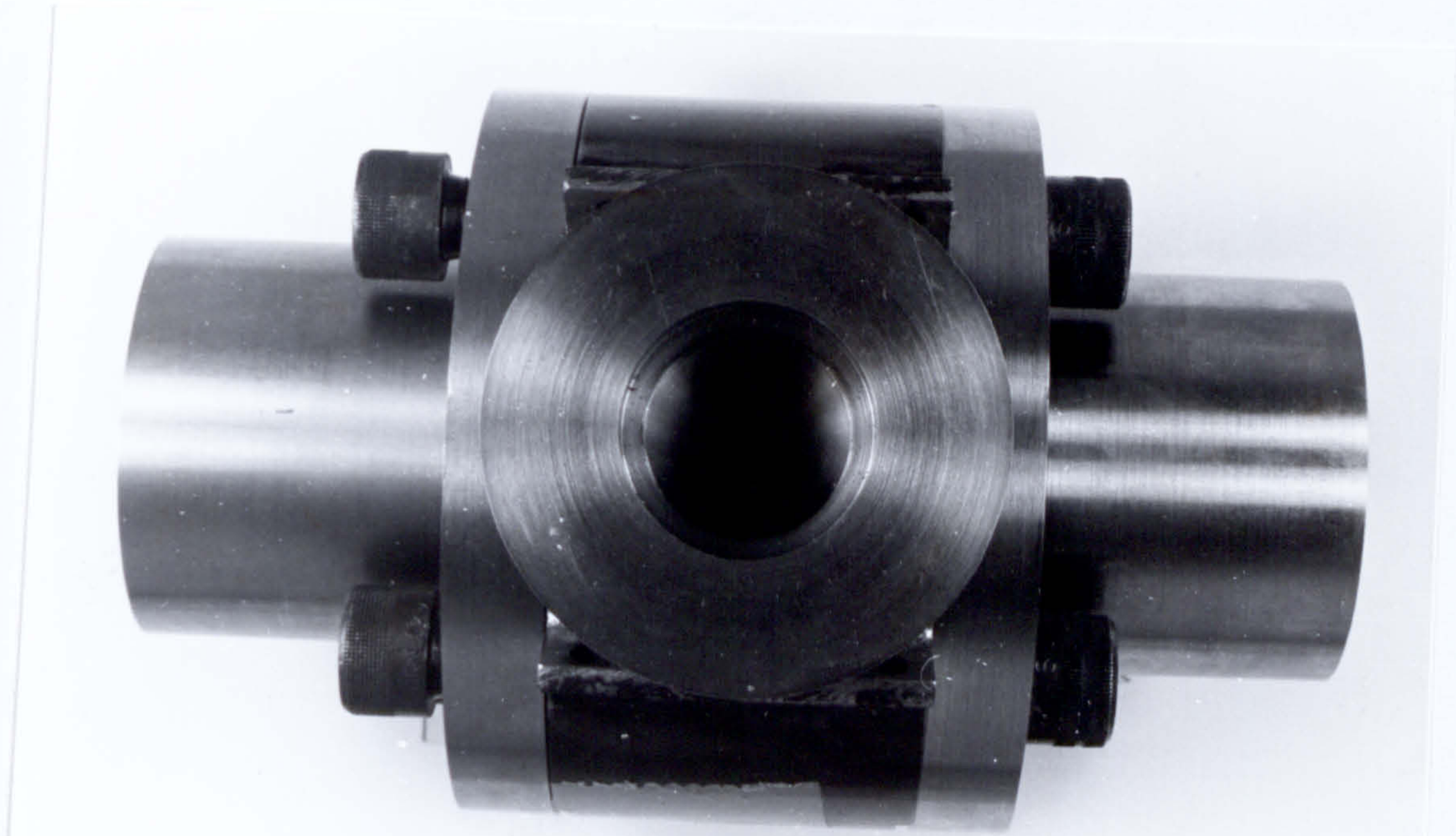

Figure 159

The side elevation of the assembled crosshead die

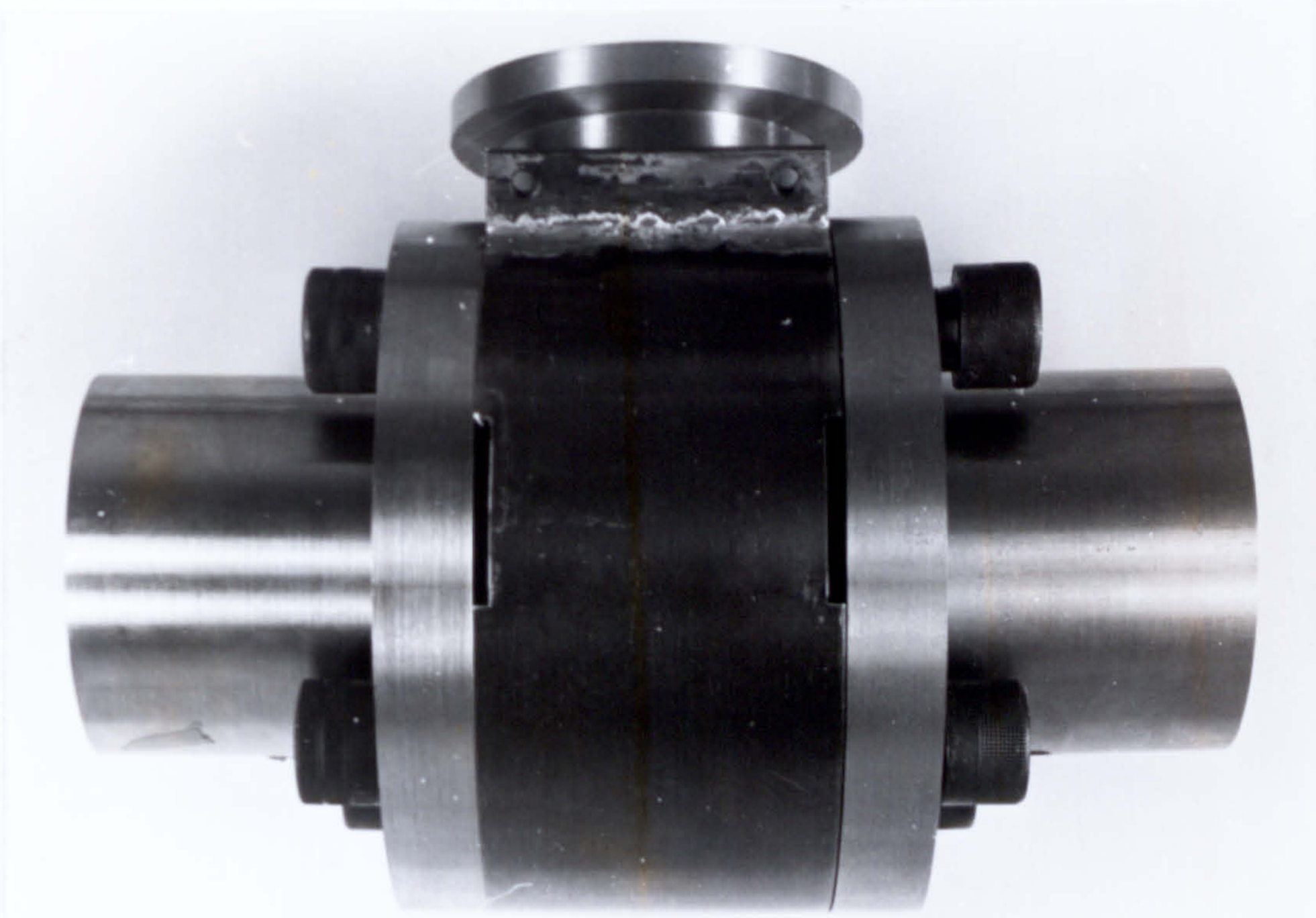

Figure 160

The configuration used for the production
of glass reinforced thermoplastic

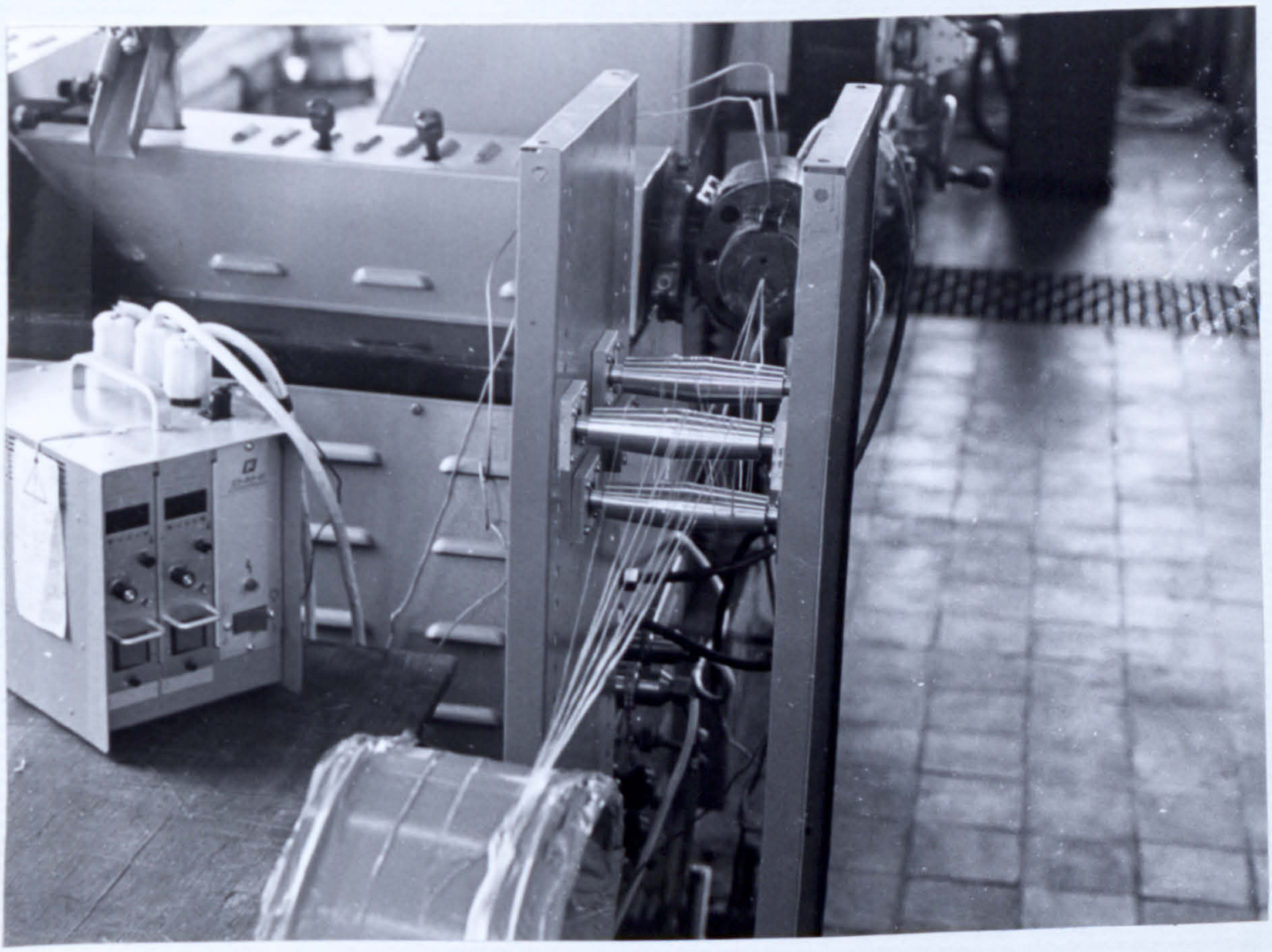

Figure 161

The braked let-off drum

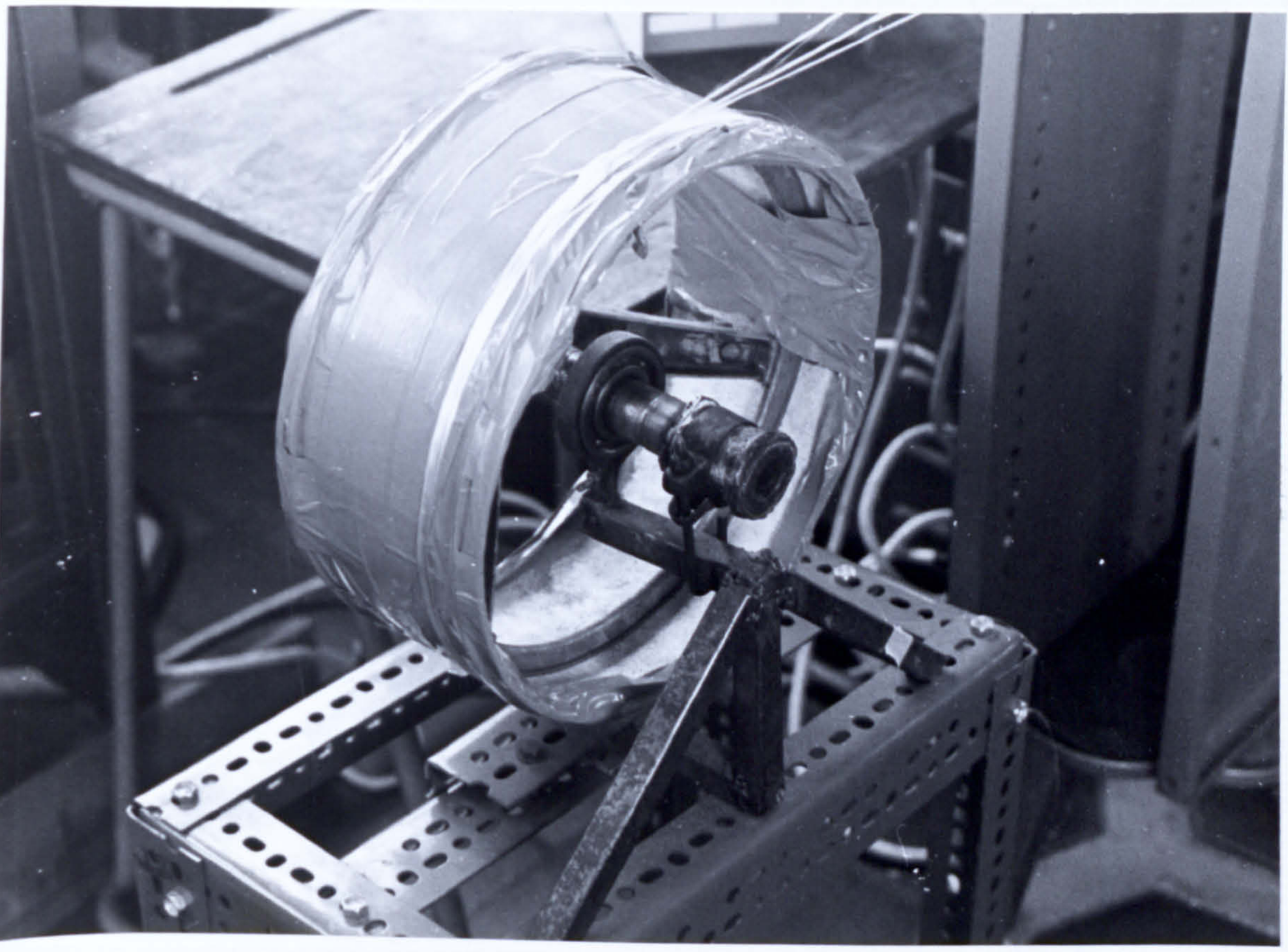

Figure 162

Copper wire incorporated into polypropylene
using the crosshead die

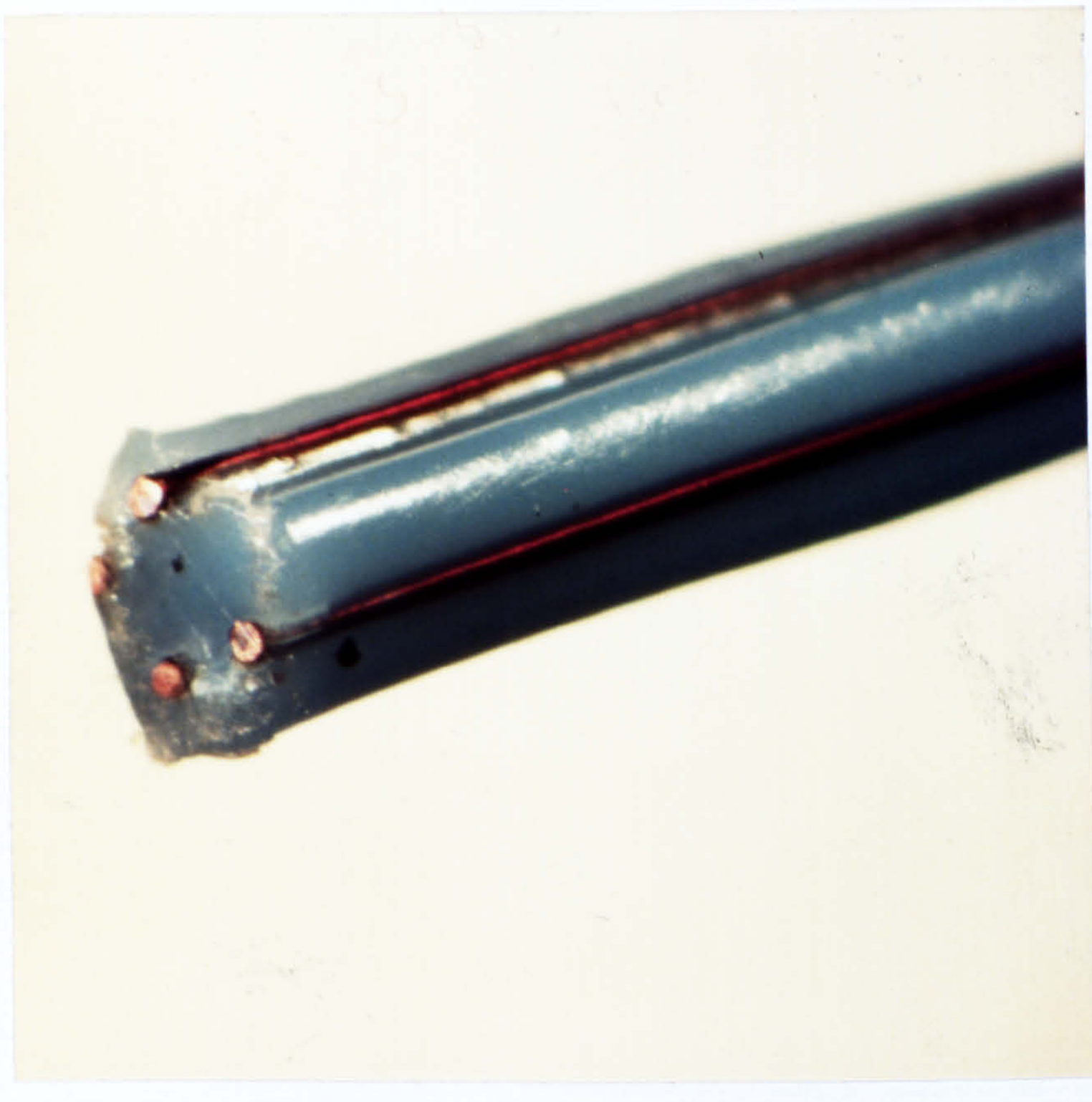

Figure 163

Copper wire with abraded surface on
being incorporated into polypropylene
using the crosshead die

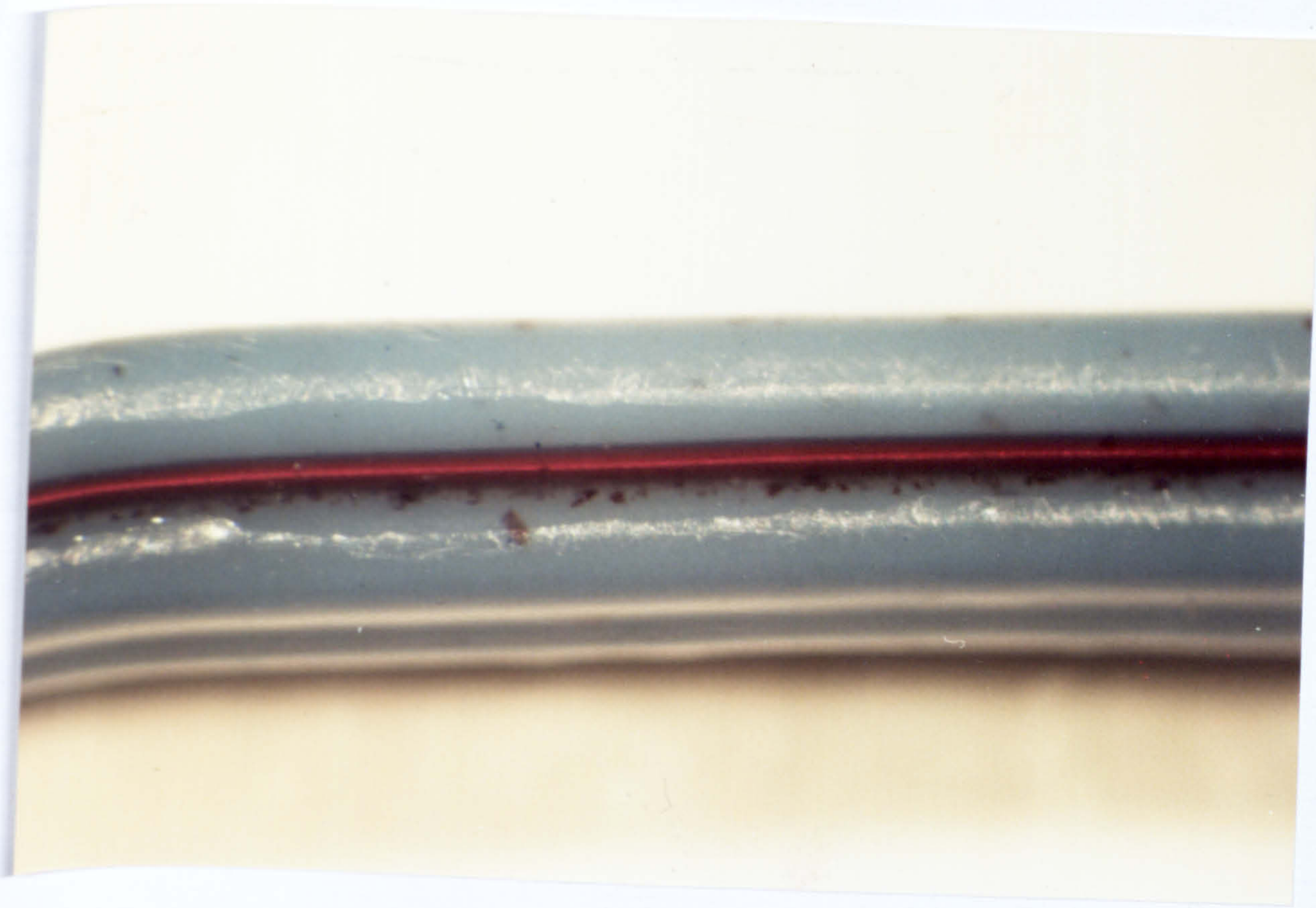

Figure 164

1cm

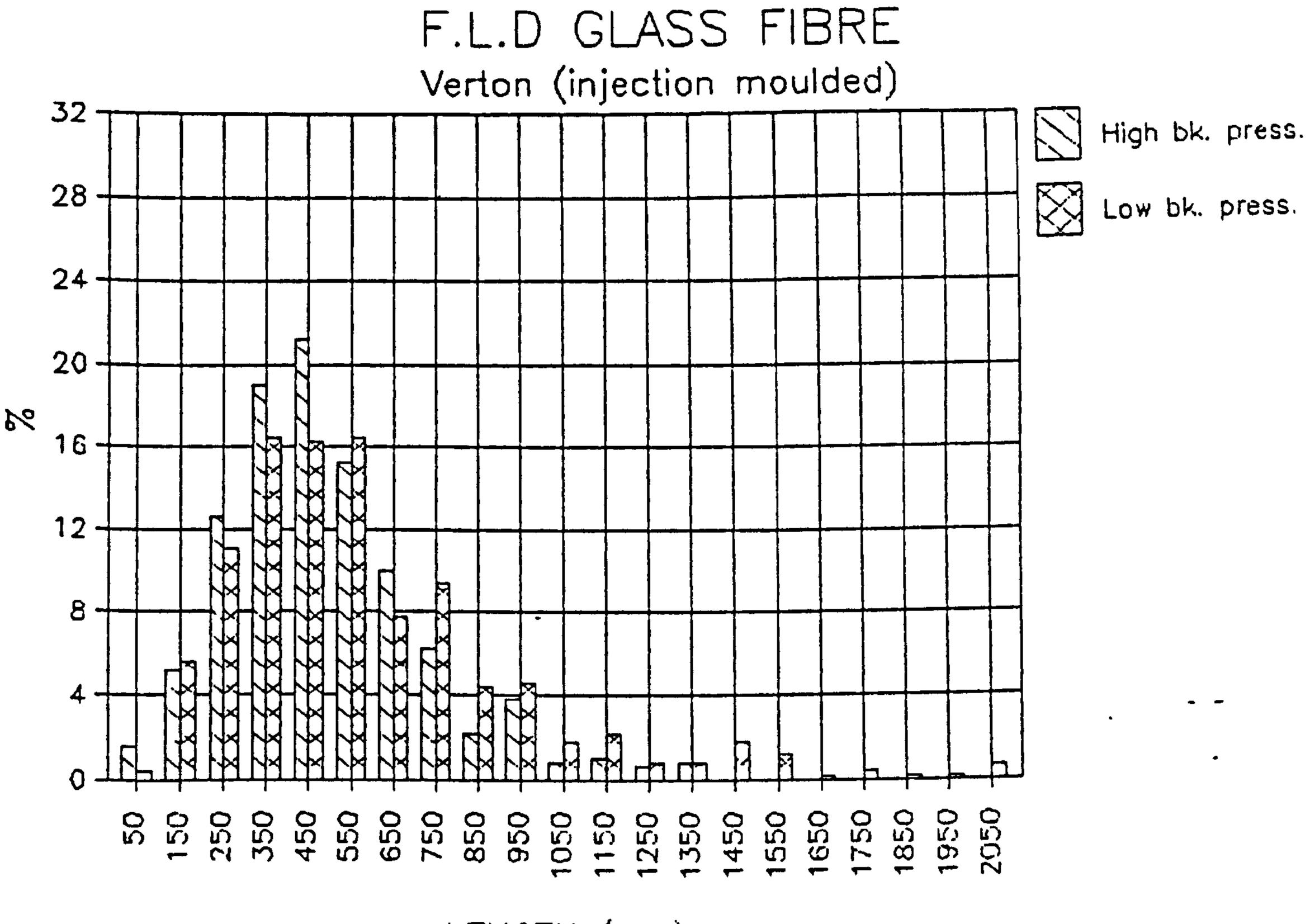
F.L.D GLASS FIBRE
Verton (injection moulded)
High bk. press.
Low bk. press.
%
32
28
24
20
16
12
8
4
0
50
150
250
350
450
550
650
750
850
950
1050
1150
1250
1350
1450
1550
1650
1750
1850
1950
2050
LENGTH (um)

Figure 165

The fracture surface in tensile of
injection moulded Verton CG 1090

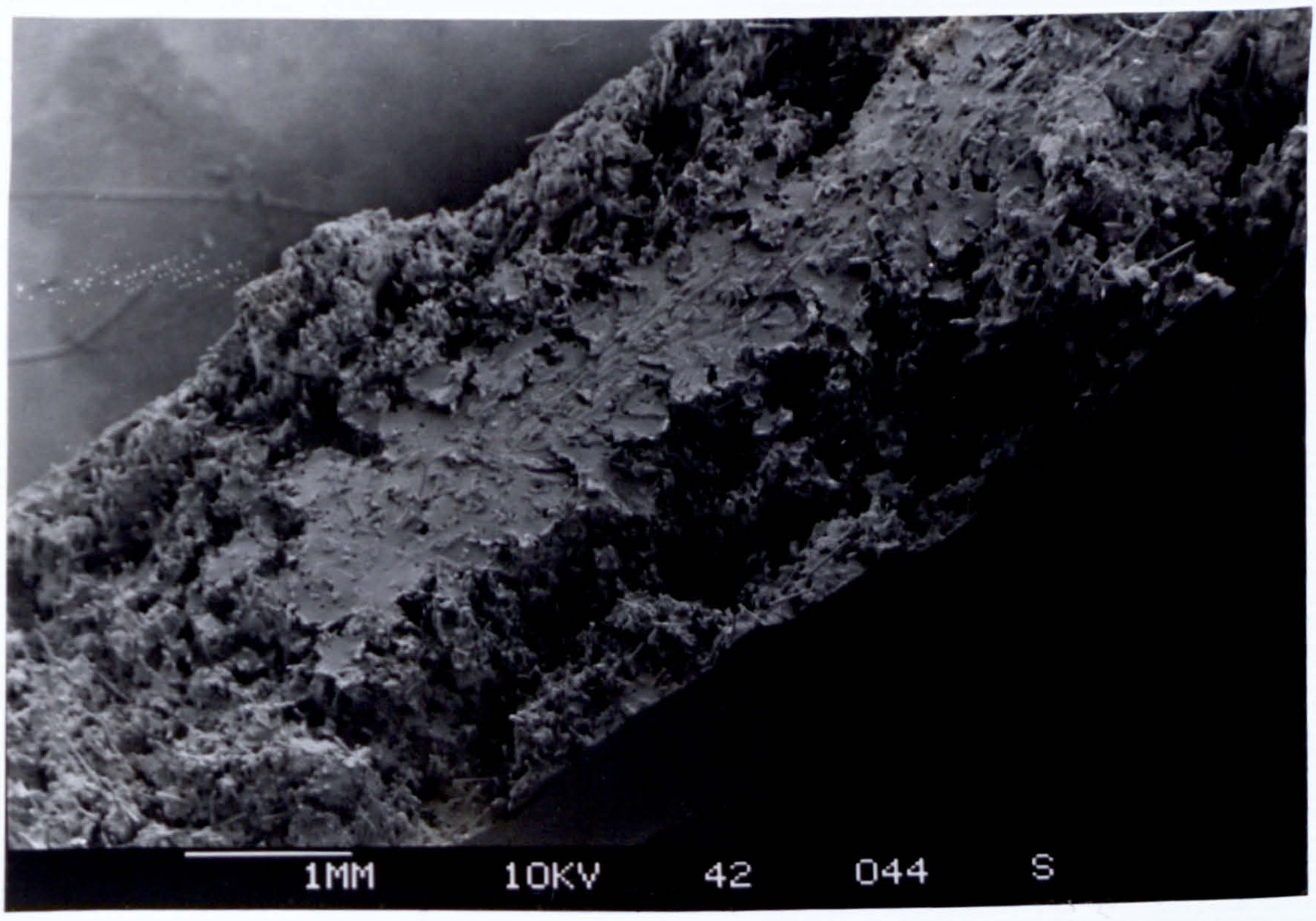

Figure 166

The fracture surface in tensile of
injection moulded Verton CG 1090

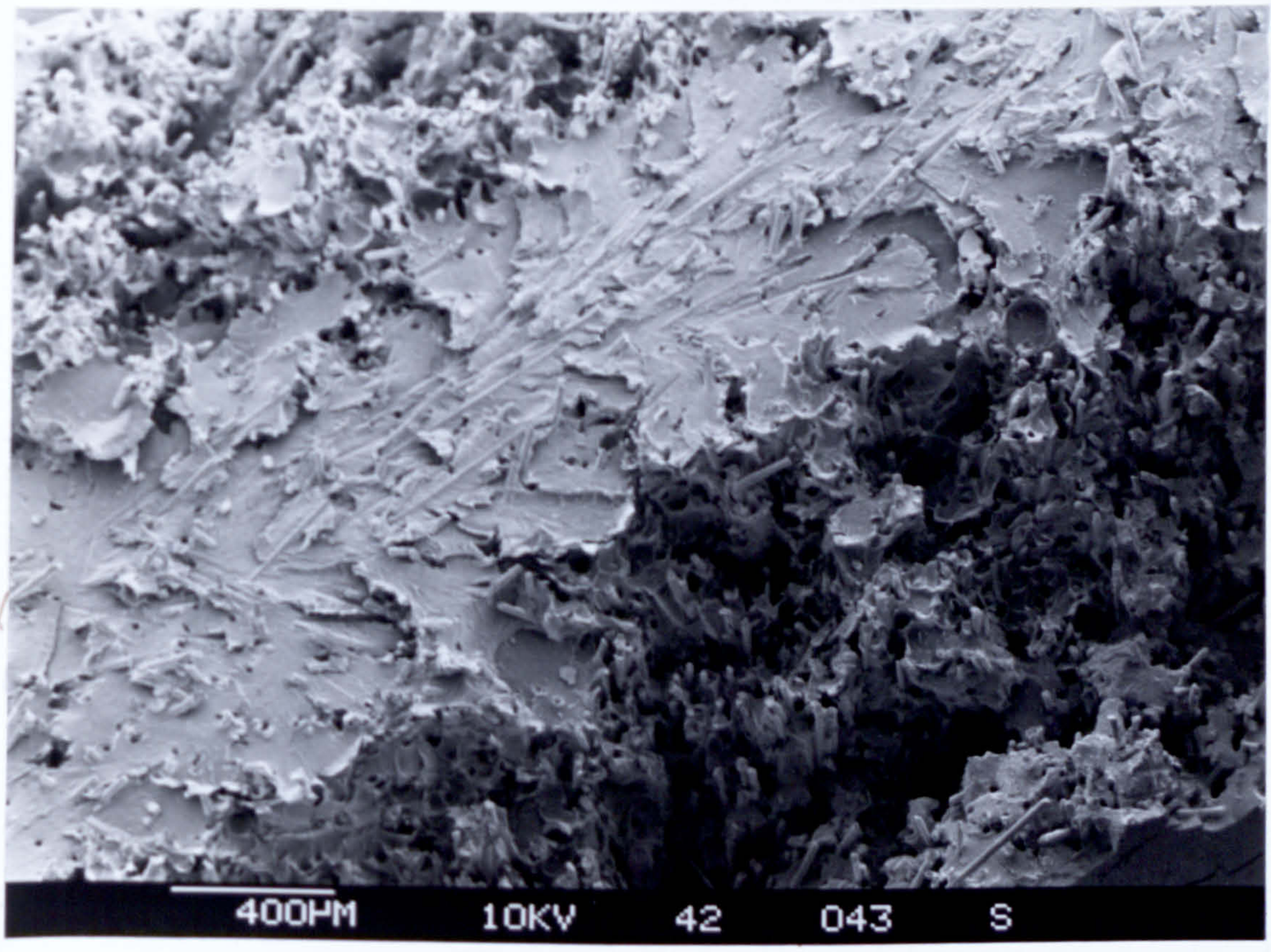

Figure 167

Patents related to the novel production of fibre reinforced thermoplastics composites

Table 48

Patent No	Patentee	Year	Comments
UK 1 200 342	J. H. Davis Imperial Chemical Industries. U.K.	1967	Fibre reinforced plastic initially in mat form produced by fusing lower melting point component around the higher melting point fibre.
UK 1 234 208	C. A. F. Long Courtaulds Ltd U.K.	1967	Involves incorporating carbon fibres or filaments activated caprolactam monomer . The caprolactam is polmerised to form a composite.
UK 1 227 756	W. C. Paterson Courtaulds Ltd U.K.	1967	Carbon fibres are precoated with a thermoplastic polymer deposited from solution and subsequently incorporated in to a molten thermoplastic.
US 4 037 011 UK 1 167 849	K. Kattori. E. L. Lowery W. H. Chadbourne W. M. Boyer Dart industries U.S.A. (formerly Rexall Drug and Chemical Company)	1977 1969	Continuous multi filament strands are impregnated with 10 to 30% by weight of thermoplastic resin by use of a solvent bath.
US 3 742 106 UK 1 334 702	R. V. Price Imperial Chemical Industries U.K.	1973 1970	Method involves spreading rovings out as they pass through a bed of powdered thermoplastic and heated the rovings so that thermoplastic flows to produce a matrix around the fibres.
UK 1 565 195	G. D. Garry A. Cox-Harper B. W. R. Turncliffe Imperial Chemical Industries U.K.	1975	Improved method of above. Controlled tension of roving in the system, to prevent breakages

Patents related to crosshead dies

Patent No	Patentee	Year	Comments
US 3 608 033	N. T. Hall	1969	Use conventional crosshead
US 3 702 356	Liquid Nitrogen	1970	die to coat glass roving.
US 3 709 773	Processing Company.	1972	Polymer may contain short
US 3 834 980		1974	glass fibres and coupling
UK 4 295 812		1970	agent.
US 3 758 247	A.W. Degen International Business Machines Corporation. U.S.A.	1973	Crosshead die technique for covering flat cables in which the melt flow is split into two partial flows and two diversion rollers with helical groves are provided to guide and direct the partial flows after conversion of their cross-section.
US 3 947 172	D.L. Myers Western electric company U.S.A.	1976	Crosshead method of applying a uniform coating around a central core. Able to achieve identical pressure and velocity profiles around core.
US 4 295 812	D.C. Haddinott Crompton and Knowles Corporation U.S.A.	1981	Ribbon cable extrusion crosshead used to coat fine wires. Flow from plastics extruder is into top and bottom distribution channels compensating passages provide an even flow of material.

Table 49

The influence of injection moulding back pressure on the properties of Verton (long glass fibre reinforced nylon 66)

			High back pressure	Low back pressure
Volume fraction		(%)	16.78	19.0
(weight fraction		(%)	31.17	34.51)
Average fibre length	No.Av (mm)		0.495	0.581
	Wt.Av(mm)		0.609	0.808
Tensile modulus @1% strain		(GPa)	6.81	8.86
Tensile strength		(MPa)	144	157
Strain at break		(%)	3.31	2.47
Flexural strength		(MPa)	240	249
Flexural modulus		(GPa)	7.22	7.82
Cox estimate of tensile modulus		(GPa)	12.9	14.3
Interfacial shear strength		(MPa)	21.8	23.32

Table 50

7. Conclusions and Suggestions for Further Work

7.1 Conclusions

7.1.1 Carbon and glass fibre undergo considerable fracture during the twin screw compounding and injection moulding processes used to manufacture short fibre reinforced thermoplastic components.

7.1.2 Compounding screw design and processing variables show significant effects on extrusion compounding performance and degree of fibre fracture observed in the initial compounding stage. Other factors that influence fibre length are compounding die design and the method used to pelletise extrudate.

7.1.3 The optimum compounding arrangement for compounding carbon fibres into nylon involves adding fibre whilst the nylon is in its molten state and employing non aggressive screw elements.

7.1.4 Carbon fibre length reduction in the compounding operation can be minimised to the point that the limitation of fibre length in the final component is imposed by the injection moulding operation.

7.1.5 The incorporation of fibres with increased fibre length does not increase the ultimate tensile strength of the composite proportional to the increase in tensile modulus observed at low strains. This can be attributed to the effect that longer fibre compounds exhibit a lower strain at failure.

7.1.6 With a knowledge of the variables of fibre length distribution, mechanical properties of fibre and matrix and stress-strain characteristics of injection mouldings, it is possible to employ computer programs to predict properties, assess compound quality and estimate fibre-matrix bond strengths. From this analysis the optimum compounding arrangement can be derived.

7.1.7 The potential properties of long fibre reinforced thermoplastics are limited by unfavourable fibre orientation. Comparing end-gate tensile bars, as average length is increased

the orientation of the fibre are less well aligned in the loading direction.

7.1.8 Using a twin-screw compounding extruder it is possible to produce well dispersed short fibre Kevlar reinforced thermoplastics. The mechanical properties of these materials are poor. This is a result of fibres in mouldings being in a randomly coiled state, the degradation characteristics of the fibre under shear and the poor intrinsic interfacial bond strength. The calculated critical length at Kevlar in polypropylene is 6.75mm, and for Kevlar in nylon 6,6 2.3mm. During even low intensity compounding slip bands are formed which are incipient forms of weakness. They can lead to the formation of kinks and subsequent fibre breakage or fibrillation.

7.1.9 Kevlar reinforced thermoplastic mouldings have more isotropic mechanical properties than glass reinforced thermoplastic mouldings. The mechanical properties of Kevlar fibre reinforced polypropylene sections cut from different points of fan gated plaque mouldings differed by 13% compared to 36% for a glass reinforced polypropylene equivalent.

7.1.10 In contrast to continuously reinforced thermosets, short fibre reinforced thermoplastics rely on a good bond between the fibre and matrix to produce good impact resistance. Because of a combination of poor interfacial bonding and fibre degradation properties after compounding, short Kevlar fibre reinforced thermoplastics have inferior impact properties to short glass fibre reinforced thermoplastics.

7.1.11 A technique has been used which enables the direct determination of the critical fibre length of reinforcing fibres in thermoplastics.

For glass reinforced nylon materials the value of interfacial bond strength determined in this way can be compared with values derived from an analysis on injection moulding specimens to give an overall fibre wet-out efficiency estimate. A value of 65% was typical for glass reinforced nylon compounds produced.

The direct measurement technique has revealed the differences in the nature of the carbon fibre-nylon 6,6 bond produced by an alternative melt shear and thermal history to the processes of compounding and injection moulding.

7.1.12 A novel crosshead die method for the production of long fibre has been produced and evaluated. The design allows fibres to be well wetted. Several minor modifications are necessary to enable the die to produce feed stock reliably.

7.2 Suggestions for Further Work

7.2.1 In order to exploit the progress made in the development of long fibre compound feed stock, long fibre compounds must be moulded in manner that allows for maximal retention of fibre length. Work is required to redesign conventional parts of the injection moulding machine and review mould design to enable fibre lengths to be retained. The basic concept required would be to eliminate or enlarge any restriction the melt must flow through.

Suitable candidates for redesigning include the nozzel check valve which must allow the free-flow of melt and the gate and runners which must be as large as possible.

7.2.2 In order to exploit the benefits of increased fibre length, control of overall fibre orientation is an important parameter that requires investigation. A better understanding is required of the influence of component shape, gate position and moulding parameters such as injection speed on overall fibre orientation.

Acknowledgements

The author wishes to express his gratitude to his supervisors Dr M J Folkes and Dr P R Hornsby. This is especially with regard to Dr Folkes's technical help from his encyclopaedic knowledge of composites and Dr Hornsby's help with polymer processing aspects of this study. The help of Mr R.H. Burton is acknowledged for Figures 105 and 106.

Thanks are extended to members of the department of Materials Technology at Brunel. Especially Professor M J Bevis for his encouragement, Mr K Batchelor for his help in computing, Messrs Johns, Mellet and Felgate for help in the practical aspects of the study.

The author is indebted to his parents, for their moral support over his time spent at Brunel and his wife Helen for putting up with him whilst writing up.

A special thanks is owed to Mrs Buxton who so competently typed the thesis.

REFERENCES

1. Parrat, N.J. "Fibre Reinforced Materials Technology", Van Nostrand Reinhold (1972)

2. Encyclopedia of Science and Technology, "Composite Materials" McGraw Hill **13**, 225, (1971)

3. Holister, G.S. and Thomas, C. "Fibre Reinforced Materials" Elsevier (1966)

4. Cox, H.L., Brit. J. App. Phys. **3**, 72 (1952)

5. Outwater, J.O.(Jr), Modern Plastics **1**, 56 (1956)

6. Dow, N.F., GEC Missile and Space Division Report No. R 63SD61 (1963)

7. Rosen, W.B., Fibre Composite Materials, Chapter 3 A.S.T.M. publication (1964)

8. Kelly, A. and Tyson, W.R., J. Mech. Phys. Solids **13**, No.6, 329 (1965)

9. Piggot, M.R., J. Mat. Sci. **13**, 1709 (1978)

10. Chen, P.E., Poly. Eng. Sci. **11**, 51 (1971)

11. Tyson, W.R. and Davis G.J. Brit. J., Appl. Phys. **16**, 199 (1965)

12 Chen, P.E. and Lavengood, R.E., Proceedings of the International Conference on Solid Mechanics and Engineering Design in Civil Engineering Materials. Southampton, England, April 1969

13 Bader, M.G. and Bower W.H., Composites, 150 July (1973)

14. Nielson, L.E. and Chen, P.E., J. Mat. Sci. **3**, 352 (1969)

15. Riley, V.R., J. Composite Mat. **2**, No.4, 436 (1968)

16. Krenchel, H., "Fibre Reinforcement" Academisk Forlay, Copenhagen (1964)

17. Jerina, K.L., Halpin, J.C. and Nicolas, L., Ing. Chim Ital. **9**, 94 (1973)

18. Brody, H. and Ward, I.M., Poly. Eng. Sci **11**, 139 (1971)

19. Stowell, E.Z. and Lin, T.S., J. Mech. Phys. Solids. **9**, 242 (1961)

20. Hill, R., Proc. Roy. Soc. A193, 281 (1948)

21. Azzi, V.D. and Tsai, SW., Exp. Mech. 5, 282 (1965)

22. Lees J.K., Poly. Eng. Sci. 8, No.3, 195 (1968)

23. Chen, P.E. Poly. Eng. Sci. 11, No.1, 51 (1971)

24. Folkes, M.J., "Short Fibre Reinforced Thermoplastics" Research Studies Press. (1982)

25. Cook, J. and Gordon, J.E., Proc. Roy. Soc. A282, 508 (1964)

26. Outwater, J.O. (Jr) and Murphy, M.C., Mod. Plastics 7, 160 (1970)

27. McGarry, F.J. and Mandle, J.F., Proc. of the 27th An. Tech. Conf. Reinforced Plast/Comps Institute of S.P.I. Paper 9-A.

28. Beaumont, P.W.R. and Phillips, D.C., J. Mat. Sci. 7, 682 (1972)

29. Cottrell, A.H., Proc. Roy. Soc. A282, 1 (1964)

30. Cooper, G.A. and Kelly, A. "Mechanics of Composite Materials" Ed. F.W. Wendt, Pergamon (1970)

31. Cooper, G.A., J. Mat. Sci. 5, 645 (1970)

32. Helfer, J.L. and Harris, B., J. Mat. Sci. 7, 494 (1972)

33. Kelly, A., "Strong Solids" Oxford, (1973)

34. Beaumont, P.W.R., Harris, B. and Ferran, E. J., Mat. Sci. 6, 238 (1971)

35. Bader, M.G., Bailey, J.E. and Bell, I., Mat Sci. Res. 5 245 (1971)

36. Encyclopedia of Polymer Science and Technology 12 Interscience (1979)

37. Maxwell, J., Plastics and Rubber International, 18, 2 (1983)

38. Shindu, A., Fujii, K. and Senyoka, M. Japanese Bureau of Industrial Technics Jap. Pat. 4405/1962, 13.6.62

39. Watt, W., Phillips, L.N. and Johnson, W., Engineer, Lond., 221, No.5757, 815 (1966)

40. Hull, D. "An Introduction to Composite Materials" Cambridge University Press (1981).

41. Cluley, A.P., Trewin, E.M. and Turner, R.F., I.C.C.M.3, Paris, (1980)

42. Rose, P.G. "Processing and Uses of Carbon fibre reinforced plastics" 5th pub, V.D.I.-Verlang Dusseldorf (1981)

43. Patrick, A.J. and Hood, J.H. 20th Ann. Tech. Conf. S.P.I. Reinforced Plastics Div. Sec 9-D (1965)

44. Metcalfe, A.G. and Schmitz, G.K., A.S.T.M. Proc. 1075 (1964)

45. River, J.T., Shell Polymer, 8, No.3, 84 (1984)

46. Dobb, M.G., Johnson, D.J., and Saville, B.P., J. Poly. Sci. (Symp.), **58**, 287 (1977)

47. Dobb, M.G., Johnson, D.J., and Saville, B.P., J. Poly. Sci. (Poly. Phys. Edn), **15**, 2201 (1977)

48. Dobb, M.G., Johnson, D.J., and Saville, B.P., Phil. Trans. R. Soc. Lond. A294 463 (1980)

49. Li, L.S., Allard, L.F. and Bigelow, W.C., J. Macromul. Sci - Phys. B22 (2), 269 (1983)

50. Moore, J.W. and Sturgeon D.L.G., Composites 4, 34 (1973)

51. Greenwood, J.H. and Rose, P.G., J. of Mat. Sci. 9, 1809 (1974)

52. Dobb, M.G., Johnson, D.J. and Saville, B.P., Polymer 22, 960 (1981)

53. Ferns, A.W.D., Plastics and Polymer, 149 Aug (1974)

54. Moore W.C., P.I. Trans. and J. 32, 247 (1964)

55. Tadmor, Z. and Gogos, C.G., "Principles of Polymer Processing" Wiley Interscience (1979)

56. Charrier, J.M., Poly. Eng. Sci. 15, 731 (1975)

57. Milewski, J.V., "Packing concepts in the utilisation of filler and reinforcement combinations". Handbook of fillers and reinforcements for plastics, Van Nostrand Reinhold (1978)

58. Gibson, A.G., Fibre reinforced composites. PRI Conference, Liverpool (1984)

59. Folkes, M.J. and Kells, D., Plast. and Rubber Proc. and Apps. 5, No.2 (1985)

60. Bader, M.E. and Collins, J.F., Fibre Sci. and Tech 18, 217 (1983)

61. Cloud, P.J. and Schulz, R.E., Plastics World 22, 26 Sept (1975)

62. Baer, M. J., App. Poly. Sci. 19, 1323 (1975)

63. Hollingsworth, B.L. and Sims, D., Composites 80 Dec. (1969)

64. Stade, K., Poly.Eng. Sci. 17, 50 (1977)

65. Lunt, J.M. and Shortall, J.B., Plast. and Rubber Proc. 108 Sept. (1979)

66. Lunt, J.M. and Shortall, J.B., Plast. and Rubber Proc. 37 June (1980)

67. Fenner, R.T. "Principles of Polymer Processing" Macmillan London (1979)

68. Folkes, M.J. and Stuart, T., Internal report, Brunel University (1979)

69. Kashfi, K., MSc thesis, Cranfield Institute of Technology (1976)

70. Murphy, T.P., Modern Plastics 129 June (1965)

71. Filbert, W.C., S.P.E. Journal 25, 65 (1969)

72. Yung, W.H., Farris, R. and Chien, J.C.W., J. App. Poly. Sci. 23, 3375 (1979)

73. Mack, W.A., 29th Antec S.P.E. Conference 29th May (1971)

74. Adams, R.L., S.P.E. Technical Paper 20, 479 (1974)

75. Martelli, F., "Twin Screw Extruders, a basic understanding" Van Nostrand Reinhold (1983)

76. Jankopin, S., 37th Antec S.P.E. Conference Session 13-A (1979)

77. Henson, J.H.L. and Whelan, A. "Development in PVC Technology" Proceedings of the Symposium, Polytechnic North London Applied Science (1973)

78. Anon, 39th Antec S.P.E. Conference (1981)

79. Mack, W.A. Modern Plastics International, 70 Nov (1973)

80. Grass, D., Plastics Technology, 40 Feb (1972)

81. Janssen, L.P.B.M. and Smith, J.M., Plast. and Rubber Proc., 1, No.2 90 (1976)

82. Hermann, H. and Burkhardt, U., Plast. and Rubber Proc., 5 No.3,4 101 (1980)

83. Martelli, F., S.P.E. Journal 27, 70 (1971)

84. Rauwendaal, C.J., 39th Antec S.P.E. Conference, 618 (1981)

85. Janssen, L.P.B.M. and Smith J.M., Plast. and Rubber Proc. Sept/Dec (1980)

86. Anon, Engineering and Processing News, Jun (1981)

87. Chiao, T.T. and Moore, R.J., Composites 31 Jan. (1973)

88. "Handbook of Fillers and Reinforcement for Plastics" Ed. Katz, H.S. and Mileswski, J.V., Chapter 27 Van Nostrand Reinhold (1978)

89. Whitney, W. and Kimmel, R.M., Nat. Phys. Sci. **237**, 93 (1972)

90. Bader, M.G. and Bowyer, W.H., J. Phys. D. Appl. Phys. **5**, 2215 (1972)

91. Blumentritt, B.F., Vu, B.T. and Cooper S.L., Poly. Eng. Sci. No.9, **14**, 633 (1977)

92. Blumentritt, B.F., Vu, B.T. and Cooper S.L., Poly. Eng. Sci. No.6, **15**, 428 (1975)

93. Blumentritt, B.F., Vu, B.T. and Cooper, S.L., Composites 105 May (1975)

94. Farre, J.P., and Merienne M.C., Int. J. Adhesion and Adhesives **6**, 311 (1981)

95. Takayanayi, M. Kajiyama and Katayose, T. J., App. Poly. Sci. **27**, 3903 (1982)

96. Theberge, J., Crossby, J. and Hutchins, M., 40th Ann. Conference Reinforced Plastics/Composite Institute S.P.I. (1985)

97. Hancox, N.L. and Wells, H., Fibre Sci. and Tech. **10**, 9 (1977)

98. Bader, M.G. and Bowyer W.H., J. of Mat. Sci. **7**, 1315 (1972)

99. McNally, D., Freed, W.T., Shaner, J.R. and Sell, H.W., Poly. Eng. and Sci **18**, No.5, 392 (1978)

100. The Davenport R.P.D. Instrumented falling weight Impact tester, Rosand Technical Leaflet (1984)

101. Brown, W.F. and Scrawley, J.E., A.S.T.M. Special Publication No. 410, 1749 (1966)

102. Bucknall, C. "Toughened Plastics" Applied Science,(1977)

103. Steroscan 250 Scanning electron microscope operating instructions Issue 2 Cambridge *Instruments Ltd.* (1981)

104. Monte S.J. and Sugarmann G., Poly. Eng. and Sci. **24**, No.18, 1376 (1984)

105. Curtis, P.T, Bader, M.G. and Bailey, J.E., J. Mat. Sci. **13**, 377 (1978)

106. Schweizer, R.A., Plastics Compounding 59, Nov/Dec, (1981)

107. Turner, S., "Mechanical Testing of Plastics" George Godwin-PRI (1983)

108. Vincent, P.I., Br. J. App. Phys. **13**, 578 (1962)

109. McNally, D., Poly. Plastics Techn. and Eng. **8**, No.2, 101 (1977)

110. Darlington M.W. and McGinley, P.L., J. Mat. Sci., **10**, 906 (1975)

111. Bright, P.F. Crowson, R.J. and Folkes, M.J., J. Mat. Sci. **13**, 2497 (1978)

112. Sanou, M. Chung, B. and Cohen, C., Poly. Eng. and Sci. **25**, No.16, 1008 (1985)

113. Bessell,, T. Hull, D. and Shortall J.B. Faraday Special Discussions Chem. Soc. No.2, 137 (1972)

114. Bessel, T. and Shortall, J.B., J. of Mat. Sci. **10**, 2035 (1975)

115. Burton R.H. and Folkes, M.J,. Plast. and Rubb. Proc. and Apps. **3**, 129 (1983)

116. Pristavka, L.V. Evdokimov, E.I., Zlobina, V.A. Kerber M.L. and Rumytantsera, E.I., International Pol. Sci. and Tech. **11**, No.9, 62 (1984)

117. Greenwood, J.H. and Rose, P.G., J. Mat. Sci. **9**, 1809 (1974)

118. Dobb, M.G. Johnson, D.J. and Saville, B.P., Polymer. **22**, 960 (1981)

119. Czarnecki, L. and White, J.L., J. App. Poly. Sci. **25**, 1217 (1980)

120. Forgacs, O.L. and Mason, S.G., J. Colloid Science **14**, 457 (1959)

121. DeTersa, S.J. Farris, R.J. and Porter, R.S., Polymer Composites **3**, No.2, 57 (1982)

122. Pruneda, C.O., Steel, W.J., Kershaw, R.P. and Morgan, R.J., Composites Review (Polymer Preprints American Chemical Society **22**, No.2 103 (1981))

123. Eagles, D.B. Blumentritt, B.F. and Cooper, S.L., J. App. Poly. Sci. 20, 435 (1976)

124. Bowden, P.B., J. Mat. Sci. 5, 517 (1970)

125. Friedrich K., Comp. Sci and Tech. 22, 43 (1985)

126. Piggot, M.R., J. Mat. Sci. 9, 494 (1974)

127. Mandle, J.F. Darwish, A.Y., McGarry F.J., ASTM, STP 734 73 (1981)

128. Leach, D.,C., and Moore, D.R. Composites 16, No.2, 113 (1985)

129. Ramsteiner, F. and Theysohn, K., Composites April, 111 (1979)

130. Atkins, A.G., J of Mat. Sci., 10, 819 (1975)

131. Handcock, N.L. and Wells, H., Fibre Science and Technology 10, 9 (1977)

132. Sung, N.H., Jones, T.J. and Sun, N.P., J. Mat Sci. 12, 239 (1977)

133. Folkes, M.J. and Wong, W.K., Polymer 28, 1309 (1987)

134. Fraser, W.A., Ancker F.H., Di Benedetto A.T. and Elbirli B., Poly. Composites 4, 238 (1983)

135. Miwa, M., Ohsuwa, T., and Tahara K.J., J. App. Poly. Sci. 25. 795 (1980)

136. Schonhorn, H. and Ryan F.W., J. Poly. Sci. Part A-2 6, 231 (1968)

137. Fitchmun D.R., Hewman S. and Wiggle, R. J., App. Poly. Sci. 14, 2441 (1970)

138. Maxwell, B. J., Poly. Sci. Part C, 9, 43 (1965)

139. Bunsell, A.R., J. Mat. Sci. 10, 1300 (1975)

140. Hall, J.H., US Patent 3,704,485

141. Sharp J.R., PhD Thesis, Brunel University (1983)

142. Kattori, K., Lowery, E.L., Chadbourne, W.H. and Boyer, W.M., US Patent 4, 037, 011

143. Gibson, A.G., Fibre Reinforced Composites, P.R.I. Conference Liverpool (1984)

Fibre volume fraction V_f in a composite was calculated from the weight fraction W_f using the following equation:

$$V_f = \frac{W_f (\rho m/\rho f)}{1 - W_f [1-(\rho m/\rho f)]}$$

where

ρm = Density or matrix g/cm^3

ρf = Density of fibre g/cm^3

Appendix 1

G_C estimation for discontinuous reinforced composites

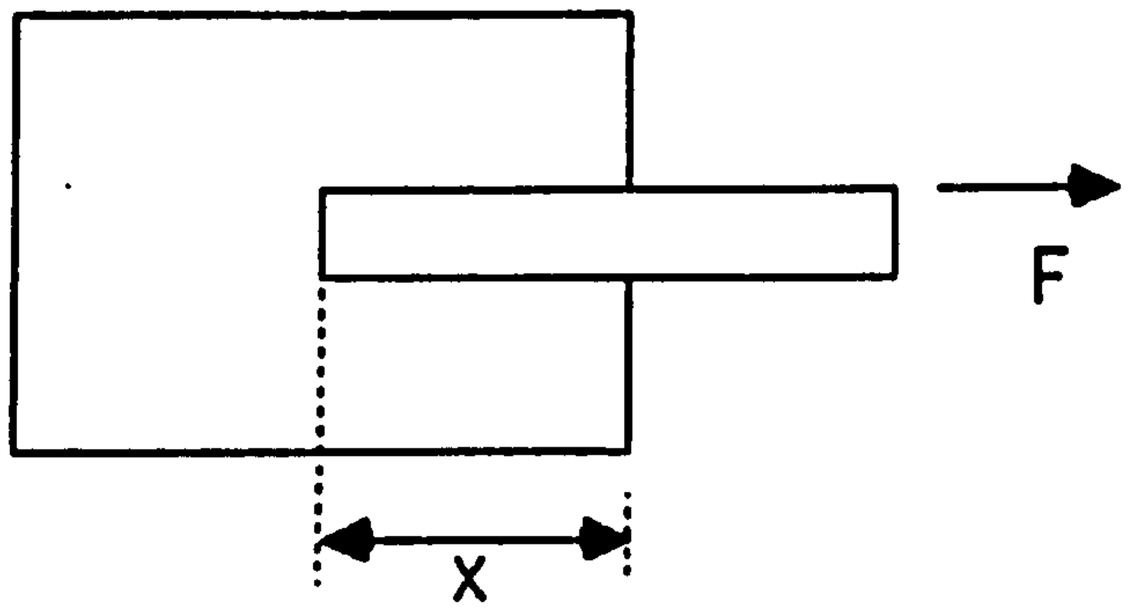

Force to pull-out F
$= 2.\pi.r.\tau_u.X$

work required to move a fibre a distance ∂X

$\partial w = F.\partial X = 2.\pi.r.\tau_u.X.\partial X$

Total energy to completely pull-out fibre =

$$W = \int_0^{L/2} \partial w = 2.\pi.r. \int_0^{L/2} X.\partial X = 1/4.\pi.r.\tau_u.L^{*}2$$

Average work done $WA = 1/L \int_0^{L} W.\partial L$

$$= 1/L.\pi/4.r. \int_0^{L} L^{*}2.\partial L = 1/L.\pi/4.r.\tau_u.(L^{*}3/3)$$

$$WA = (\pi.r.\tau_u.L^{*}2)/12$$

For an aligned fibre composite $Vf = N.\pi.r^{*}2$, where N is no of fibres crossing unit area of crack

On average N/2 fibres will pull-out on one side of the fracture

if $8 = N/2.WA$ or $G_c = 2.8 = N.WA$

$G_c = 1/12.\pi.\tau_u.L^{*}2.N = 1/12.\pi.r.\tau_u.L^{*}2.(Vf./\pi.r^{*}2)$

$= 1/12.(\tau_u.L^{*}2/r).Vf$

$G_c = 1/6.(\tau_u.L^{*}2/D).Vf$

Appendix 2

The estimation of interfacial shear strength

```
10 PRINT"■ ESTIMATION OF SHEAR STRENGTH ■":PRINT
50 DIMV(20),X(20),P(20),Y(20),S(30),K(30),B(30),D(30),L(30),O(30),F(30),H(30)
60 OPEN1,4
70 INPUT"NO OF FIBRE GROUPS";W
100 INPUT"RADIUS OF FIBRE (UM) ";RI:RE=RI*10↑-6
110 INPUT"STRAIN OF COMP E1 ";E1:E2=2*E1
120 INPUT"TOTAL VOL FRACTION ";VF
130 INPUT"STIFF OF FIBRE (GPA)";SF:EF=SF*10↑9
140 INPUT"STIFF OF MATRIX (GPA)";SM:EM=SM*10↑9
150 Z1=EM*E1*(1-VF):Z2=EM*E2*(1-VF)
160 INPUT"STRESS AT STRAIN 1 (MPA)";SA:S1=SA*10↑6
170 INPUT"STRESS AT STRAIN 2 (MPA)":SB:S2=SB*10↑6
180 INPUT"ASSUMED VAL OF SHEAR ST (MPA) ";TM:T=TM*10↑6
190 LA=(EF*E1*RE)/T:LB=(EF*E2*RE)/T
200 PRINT:PRINT"LA=";LA,"LB=";LB
210 IFF=1THEN500
220 PRINT:PRINT"■ SHEAR STRENGTH FOR LA ■":PRINT
230 FORI=1TOW
240 INPUT"AVERAGE LENGTH OF FIB GROUP (MM)";O(I):L(I)=O(I)*10↑-3
250 INPUT"VOLUME FRACTION OF FIB GROUP";V(I)
260 IFL(I)=>LATHENP(I)=(EF*E1*RE)/(2*L(I)*T):Y(I)=E1*EF*(1-P(I))*V(I)
265 Y=Y+Y(I)
270 IFL(I)<LATHENX(I)=(T*L(I)*V(I))/(2*RE):X=X+X(I)
275 NEXT
280 PRINT"■ SHEAR STRENGTH FOR LB ■":PRINT
290 FORI=1TOW
300 INPUT"AVERAGE LENGTH OF FIB GROUP (MM)";F(I):H(I)=F(I)*10↑-3
310 INPUT"VOLUME FRACTION OF FIB GROUP";S(I)
320 IFH(I)=>LBTHENK(I)=(EF*E2*RE)/(2*H(I)*T):B(I)=E2*EF*(1-K(I))*S(I)
330 B=B+B(I)
340 IFH(I)<LB THENO(I)=(T*H(I)*S(I))/(2*RE):D=D+D(I)
345 NEXT
350 R1=(X+Y)/(B+D):R=(S1-Z1)/(S2-Z2)
360 PRINT:PRINT"R="R,"R1="R1
370 PRINT#1,"R= "R,"R1= "R1
380 INPUT"■ASSUMED VAL OF SHEAR ST (MPA) ";TM:T=TM*10↑6:F=1:REM SET FLAG
390 GOTO190
400 END
500 Y=0:X=0:B=0:D=0
502 FORI=1TOW
505 IFL(I)=>LATHENP(I)=(EF*E1*RE)/(2*L(I)*T):Y(I)=E1*EF*(1-P(I))*V(I)
510 Y=Y+Y(I)
520 IFL(I)<LATHENX(I)=(T*L(I)*V(I))/(2*RE):X=X+X(I)
522 NEXT
525 FORI=1TOW
530 IFH(I)=>LB THENK(I)=(EF*E2*RE)/(2*H(I)*T):B(I)=E2*EF*(1-K(I))*S(I)
540 B=B+B(I)
550 IFH(I)<LBTHEND(I)=(T*H(I)*S(I))/(2*RE):D=D+D(I)
555 NEXT
560 R1=(X+Y)/(B+D):R=(S1-Z1)/(S2-Z2)
570 PRINT"R="R,"R1="R1
580 PRINT#1,"R= "R,"R1= "R1
585 PRINT#1,"SHEAR ST="TM
587 PRINT#1,"                "
590 INPUT"■ASSUMED VAL OF SHEAR ST (MPA) ";TM:T=TM*10↑6:F=1:REM SET FLAG
600 GOTO190
```

Appendix 3

The assessment of stress transfer interface efficiency - strength

```
10 PRINT"☐ STRESS TRANS. INTER. EFF.(STENGTH) ■":PRINT
20 DIMX(20),N(20),Y(20),K(20)
30 INPUT"RADIUS OF FIBRE (UM) ";RI:RE=RI*10↑-6
60 INPUT"NO OF FIBRE GROUPS";W
70 INPUT "INTERFACIAL SHEAR STREN (MPA)";TM:T=TM*10↑6
80 INPUT"STRENGTH OF FIBRE (GPA) ";P:B=P*10↑9
90 INPUT"TOTAL NO OF FIBRES";M
120 LC=(B*RE)/T
130 FORI=1TOW
140 INPUT"AVERAGE LENGTH OF FIB GROUP (MM)";LI:L=LI*10↑-3
150 INPUT"NO. OF FIBRES OF THIS LENGTH":N(I)
160 IFL=>LCTHENX(I)=LC/(2*L):Y(I)=(1-X(I))*B*N(I)
170 IFL=>LCTHENY1=Y1+Y(I):NEXT
180 IFL<LCTHENK(I)=(T*L)/(2*RE)*N(I):K1=K1+K(I):NEXT
190 V=K1+Y1
195 Z=V/(M*B)
200 PRINT "S.T.I. EFFICIENCY IS "  Z
220 END
```

Appendix 4

The assessment of stress transfer interface efficiency - modulus

```
10 PRINT"□■ STRESS TRANS. INTER. EFF.(MODULUS) ■':PRINT
20 DIMX(20),N(20),Y(20),K(20)
30 INPUT"RADIUS OF FIBRE (UM) ";RI:RE=RI*10↑-6
60 INPUT"NO OF FIBRE GROUPS";W
70 INPUT "INTERFACIAL SHEAR STREN (MPA)";TM:T=TM*10↑6
80 INPUT"STRAIN OF COMPOSITE";ES
85 INPUT"STIFFNESS OF FIBRE(GPA)";G:GF=G*10↑9
90 INPUT"TOTAL NO OF FIBRES";M
120 LC=(ES*GF*RE)/T
130 FORI=1TOW
140 INPUT"AVERAGE LENGTH OF FIB GROUP (MM)";LI:L=LI*10↑-3
150 INPUT"NO. OF FIBRES OF THIS LENGTH";N(I)
160 IFL=>LCTHENX(I)=LC/(2*L):Y(I)=(1-X(I))*ES*GF*N(I)
170 IFL=>LCTHENY1=Y1+Y(I):NEXT
180 IFL<LCTHENK(I)=(T*L)/(2*RE)*N(I):K1=K1+K(I):NEXT
190 V=K1+Y1
195 Z=V/(M*ES*GF)
200 PRINT "S.T.I. EFFICIENCY IS "  Z
220 END
```

Appendix 5

The estimation of composite strength

Kelly-Tyson model

```
10 PRINT"□□ ESTIMATION OF COMPOSITE STENGTH ■":PRINT
20 DIMX(20),K(20),Y(20),V(20)
30 OPEN1,4
40 INPUT "ORIENTATION FACTOR";C
50 INPUT"RADIUS OF FIBRE (UM) ";RI:RE=RI*10↑-6
60 INPUT"NO OF FIBRE GROUPS";W
70 INPUT "INTERFACIAL SHEAR STREN (MPA)";TM:T=TM*10↑6
80 INPUT"STRAIN OF COMPOSITE AT FAILURE";ES
90 INPUT"STIFF OF FIBRE (GPA)";ET:EF=ET*10↑9
100 INPUT"STIFF OF MATRIX (GPA)";EU:EM=EU*10↑9
110 INPUT"TOTAL VOL FRAC OF FIB ";VF
120 LC=(EF*ES*RE)/T
130 FORI=1TOW
140 INPUT"AVERAGE LENGTH OF FIB GROUP (MM)";LI:L=LI*10↑-3
150 INPUT"VOLUME FRACTION OF FIB GROUP";V(I)
160 IFL=>LCTHENX(I)=(EF*ES*RE)/(2*L*T):Y(I)=ES*EF*(1-X(I))*V(I)
170 IFL=>LCTHENY1=Y1+Y(I):NEXT
180 IFL<LCTHENK(I)=(T*L*V(I))/(2*RE):K1=K1+K(I):NEXT
190 P=(C*(K1+Y1))+EM*ES*(1-VF)
195 Z=P*10↑-6
200 PRINT "ESTIMATED COMPOSITE STRENGTH (MPA)  =" Z
220 END
```

Appendix 6

The estimation of composite modulus

Cox Shear lag model

```
10 PRINT"  COX ESTIMATION OF COMPOSITE MODULUS "
20 OPEN 1,4
25 DIMX(20),S(20),V(20),L(20),O(20),T(40),D(20)
30 INPUT"POISSONS RATIO OF MATRIX";VM
40 INPUT "DIAMETER OF FIBRE (UM)";O:D=O*10↑-6:R=D/2
45 AF=π*R*R
50 INPUT "MODULUS OF FIBRE (GPA)";E:EF=E*1019
60 INPUT "MODULUS OF MATRIX (GPA)";EN:EM=EN*10↑9
65 GM=EM/(2*(1+VM))
70 INPUT "TOTAL VOLUME FRACTION OF FIBRE GROUP";VF
80 INPUT "NO OF FIBRE GROUPS";W
90 Q=SQR(2*π/(SQR(3)*VF))*R
100 B=SQR((2*π*GM)/(EF*AF*((LOG(Q/R))*2.3026)))
120 FOR I=1 TO W
122 INPUT "AVERAGE LENGTH OF FIBRE GROUP (MM)";O(I):L(I)=O(I)*10↑-3
124 INPUT "VOL FRA OF FIB GRP ";V(I)
125 T(I)=(EXP(B*L(I)/2)-EXP(-B*L(I)/2))/(EXP(B*L(I)/2)+EXP(-B*L(I)/2))
130 D(I)=T(I)/(B*L(I)/2)
150 S(I)=V(I)*EF*(1-D(I))
160 Y1=Y1+S(I):NEXT
170 EC=Y1+(1-VF)*EM
180 PRINT EC
190 PRINT"SAMPLE"
200 INPUT      Z
210 PRINT#1,"SAMPLE "      Z
220 PRINT#1,"COMPOSITE MODULUS IS "
230 PRINT#1,EC
240 STOP
```

Appendix 7

The estimation of composite modulus

Rule of mixture model

```
10 PRINT"□ SIMPLE RULE OF MIXTURES"
20 INPUT "MODULUS OF FIBRE (GPA)";F:EF=F*10↑9
30 INPUT "VOL FRA OF FIBRES";VF
40 INPUT "MODULUS OF MATRIX (GPA)";M:EM=M*10↑9
50 EC=EF*VF+EM*(1-VF)
60 PRINT"          "
80 PRINT EC
100 END
```

Appendix 8

PAGE/PAGES EXCLUDED UNDER INSTRUCTION FROM UNIVERSITY